2008

# Compaction models for predicting moisture-density-energy relationships for earth materials

John Puls
*Iowa State University*

# Compaction models for predicting moisture-density-energy relationships for earth materials

by

**John Michael Puls**

A thesis submitted to the graduate faculty

in partial fulfillment of the requirements for the degree of

MASTER OF SCIENCE

Major: Civil Engineering (Geotechnical Engineering)

Program of Study Committee:
David White, Major Professor
Charles Jahren
Max Morris
Vernon Schaefer

Iowa State University

Ames, Iowa

2008

## TABLE OF CONTENTS

## LIST OF FIGURES

## LIST OF TABLES

# ABSTRACT


## Research Summary

The Compaction Forecasting Expert Database (CFED) analysis tool developed by Caterpillar was analyzed and compared to traditional approaches for predicting a family of laboratory soil compaction curves for a given soil. Classification, laboratory compaction, and field compaction data for forty-two soils collected from seven states (Iowa, Illinois, Minnesota, North Carolina, Colorado, Maryland, Florida) and China were input into CFED to evaluate its performance. Five other methods for prediction of all or part of the laboratory compaction curve were determined from the literature review. The performance of CFED was determined both absolutely and relative to these five prediction techniques.

Soil samples were compacted in the laboratory using impact compaction at standard, modified and intermediate compaction energies. Lab compaction curves were interpreted by hand as well as by the six other methods of prediction. 763 compaction tests were completed as part of this study. The deviation of predicted values to interpreted values was compared to determine how the performance of CFED compared to the other five prediction models found in the literature.

Another aspect of the research was to link relationships between laboratory compaction energy and machine pass. Field compaction data was available for some soils input into CFED. These field data included density, dynamic cone penetration index (DCPI), Clegg impact value (CIV), light-weight deflectometer (LWD), and plate load testing (PLT) data versus machine pass for various machine configurations. Field data was available for the CP-533, CS-533, CS-683, CS-563 and CAT825H roller for use in the research. Curve fitting methods were applied to field and laboratory data in an attempt to determine a relationship between the two.

**Research Conclusions**

CFED performs as well as methods from the literature in predicting the family of compaction curves for a given soil. One advantage that CFED has over other methods is that its model includes compaction energy, whereas other methods are only suitable for one compaction curve prediction. An analysis of the difference between actual and predicted maximum dry density values for a given soil showed that the average difference for CFED was on the order of 1.2 $lb/ft^3$ and 1.0% for optimum moisture content. In general, all methods tend to over-predict maximum density and optimum water content.

CFED is not without its limitations, however. CFED can model a laboratory compaction curve with a relatively small amount of error. However, the model relies upon laboratory data (minimum 3 points per energy level) to create its curves and is not able to predict the curve in the absence of laboratory data. Also, at this point in time, the CFED database is not sufficiently populated with field data to allow for prediction of field compaction performance for a wide variety of soils. This issue will be less problematic as more soils and field data become available to the CFED database. Also, as with other models, CFED does not predict compaction curves for granular soils in the range of bulking moisture contents. This is one major limitation of the model and should be viewed as an opportunity for CFED to excel where other models have not.

A first-order rate equation analysis was performed on soils with both laboratory and field compaction data in an attempt to establish a relationship between laboratory impact and field compaction energy. However, it was determined that this method did not accurately represent the data for either the field or the laboratory. It was determined that a hyperbolic curve fit the data more accurately. More analysis is needed to determine the validity of this model.

CFED has high potential to provide a unique tool to earthwork professionals (both contractor and engineer). As with any software applied to engineering projects, CFED should not be

used blindly and the results of software predictions should always be subject to professional judgment.

**Recommendations for Implementation**

CFED provides an opportunity to limit required field testing and a means to make field compaction of soils more efficient. By predicting the number of passes required for desired compaction levels, the number of field tests to verify adequate compaction can be substantially decreased. Also, CFED has the potential to be a basis of scientific (numerical) selection of a compaction machine for a given soil type/project. Selection of machines need not be based solely upon field experience.

CFED, as a tool, can provide the earthwork contractor and engineer a channel through which the optimal machine(s) and method(s) may be determined for any given project. These new methods of compaction forecasting offer the ability to more accurately determine the time, effort and budget required for completion of an earthworks project. The ultimate goal of CFED is to provide the means to achieve the best possible product from inception to completion.

**Future Research**

CFED's performance should be evaluated as new soils are added to the database. Anytime a new soil is available, it should be added to the database so that any unknown limitations to CFED may be discovered. Special attention should be paid to the ability of CFED to predict curves for granular soils. The models of the literature have not been able to accurately predict lab compaction curves for granular soils; this would be an opportunity for CFED to achieve something which has been otherwise undetermined.

More research into establishing a relationship between laboratory compaction energy and number of machine passes is needed. A compaction study is proposed to evaluate how machine type, moisture content, and lift thickness affect field compaction for a given soil type. This relationship is imperative to establishing a link between laboratory and field

compaction. If a valid link can be established, it will be invaluable to the ability of CFED to predict machine performance for a given soil type and will only increase the success of the software.

# CHAPTER 1. INTRODUCTION

## Problem Statement

Caterpillar is developing new technologies and analytical models to improve compaction efficiency for earthwork projects. One of the developments of this effort is the Compaction Forecasting Expert Database (CFED). The specific goals of the CFED technology are to a) predict the capability of compaction machines to meet compaction specifications, b) predict productivity for specific machines, c) evaluate sensitivity of compaction and productivity to soil moisture, and d) recommend soil lift thickness with anticipated number of machine passes to meet compaction specifications.

The purpose of the technology is for both pre-bid and operation on earthworks construction. The pre-bid application is to assist contractors and project owners to determine cost and probability to meet compaction requirements based on available soils, whether those soils are in-situ or from borrows. The operational application is for construction management, particularly for analysis and solutions when compaction requirements are not achieved, or when productivity is unacceptable.

The technology is site and soil specific. It requires standard and specialized testing of the actual earthworks construction soils. Results from the soil testing are then input to unique software that converts the input data to the four predictions for a) capability of available machines to meet the desired specification, b) productivity of selected machinery for a given soil type, c) sensitivity of the soil to changes in site (e.g. moisture) conditions, and d) the process by which a through c may be achieved (i.e. number of passes required). This output is considered a recipe for successful and cost effective earthworks construction.

## Research Tasks

A. Obtain soil samples and complete lab testing as prescribed for the compaction forecasting technology (determination of relationships between compaction energy,

dry density and moisture content). Soil index properties including Atterberg limits and particle-size analysis will be performed for all samples.

B. Perform a detailed literature review to determine other applicable methods to predict laboratory compaction.
C. Exercise the forecasting algorithms to predict the laboratory compaction curve.
D. Compare CFED forecast to other methods determined from task B.
E. Recommend improvements and/or changes to be made to CFED software based upon tasks A-D.

**Project Scope**

The scope of the project is to evaluate CFED with respect to its ability to predict a family of compaction curves for a given soil and determine its validity in use. Updating the CFED database is important to determine how CFED performs for a variety of soils. The evaluation of CFED is to be based upon its ability to predict the compaction curves compared to other methods in the literature. While it is important to predict the entire compaction curve special emphasis is put upon the model's ability to predict the optimum moisture content and maximum dry density for a given soil.

**Thesis Organization**

Chapter 2 gives background to the reader regarding parameters which affect field compaction of soils including: machine type, soil type, lift thickness, moisture content, etc. Also, methods of compaction prediction from the literature review are presented and discussed in detail. Chapter 3 outlines research methodology for both laboratory and field investigations while Chapter 4 describes field testing performed at several sites around the country. Chapters 5 and 6 present data collected and discussion of the results obtained from testing and analytical analyses. Finally, Chapter 7 gives conclusions and recommendations in regard to the performance of CFED compared to other forecasting methods.

# CHAPTER 2. BACKGROUND

This section provides background information for the reader with respect to the perceived need for CFED. It is meant to give the reader insight into why CFED has been created and why it is important to continue to improve the software. Also, a user overview of CFED and specifications for Caterpillar compaction machinery used in the research are provided.

## Compaction Forecasting Expert Database (CFED)

CFED, when complete, will be a tool for the earthwork contractor and owner to save time and money in earthwork projects. Most state DOTs have requirements of the contractor for completion of an earthwork project (e.g. 90%, 95%, 100% Standard Proctor density). Currently, once the site and contractor are known, soil samples are collected and tested in the laboratory to determine the optimum soil characteristics for compaction. Then, the soil is compacted in the field with whatever compaction machines the contractor may have available. Regular density testing is completed to determine if and when the soil has reached the required density. However, much time can be wasted testing the soil when it is far from its maximum density. Or, in a more extreme case, improper machine selection may prevent the contractor from ever being able to compact the soil to its required density.

CFED would save time and money by providing the owner/contractor a recommendation of the most proper machine for a given soil and also a forecast of expected results for a given project. Just as money is lost from under-compacting soil, money can also be wasted by over-compacting a soil after it has already reached its density requirements.

An important aspect of implementation of CFED is to establish a relationship between laboratory and field compaction. To be effective CFED should provide a link so that compaction in the laboratory can be correlated directly to compaction in the field. Once this link is established, CFED will become an invaluable tool to any earthwork contractor seeking to save time and money using Caterpillar machines.

**User Overview of Compaction Forecast Expert Database (CFED)**

This section is included to provide an overview of how CFED works. Screenshots are included to give the reader a visual aid to understand the program-user interface of each step. Figure 1 shows the home screen of CFED which appears when the program is opened.


**Figure 1: CFED Home screen**


**Figure 2: CFED Home screen options**

Upon opening CFED, the user can either use the program to enter soils into the data via the

"Data Management" tab or employ the prediction models of the program via the "Prediction" tab (See Figure 2).

Clicking on the "Data Management" tab allows the user to enter new soils into the database or modify a pre-existing record. These options, shown in Figure 3 include: Add a New Soil Record, Display Data of an Existing Soil Record, Add Test Data to an Existing Soil Record, Modify the Data of an Existing Soil Record, and Delete an Existing Soil Record. Users of the program would be allowed to enter new soils into the database. This will be especially useful for contractors and/or engineers who have experience with, and data for, a given soil in which they work with on a regular basis.

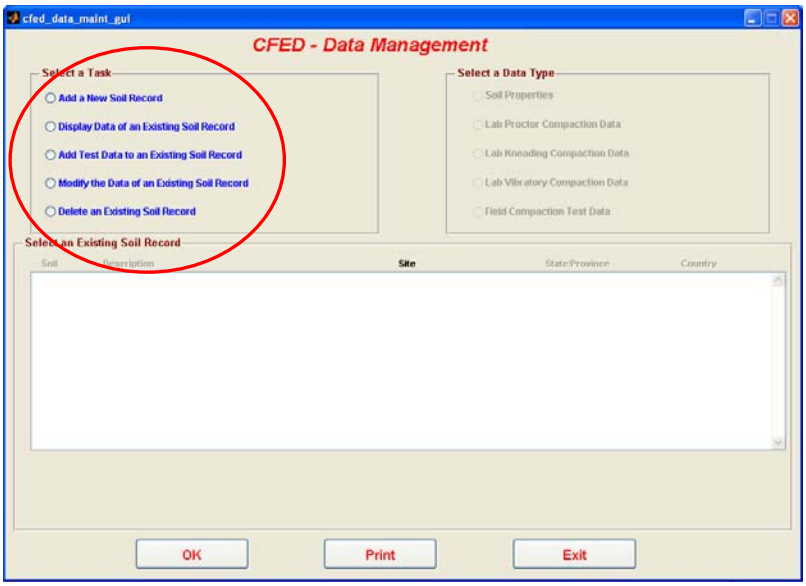


**Figure 3: CFED Data management options**

To add a new soil record, the user may simply click this option and then "OK" at the bottom of the screen. This will give the user a screen to enter data for the soil including soil classification data as well as project data (See Figure 4).

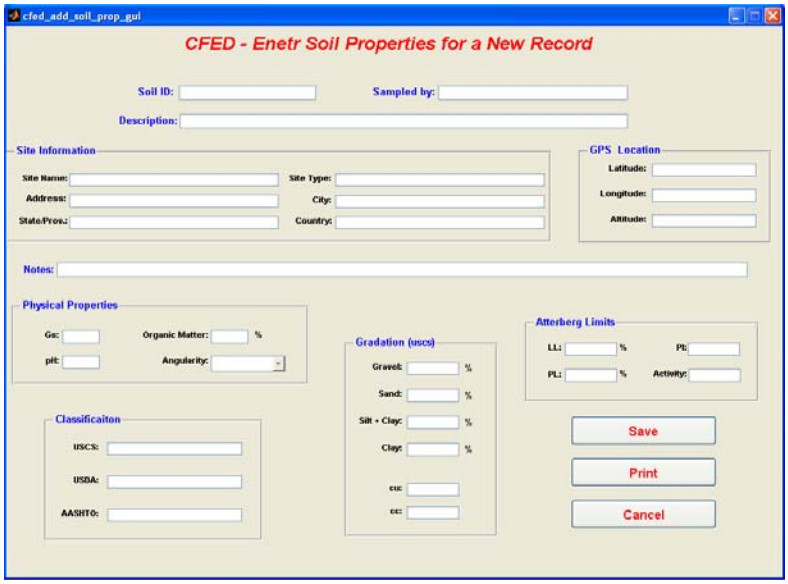


**Figure 4: CFED Adding a new soil record**

Upon adding the soil to the CFED database, the user then has the option to add test data to the soil record including field and lab proctor compaction data. By clicking the "Lab Proctor Compaction Data" tab, the user may enter information about the proctor data as well as the data itself. The data is input via a Microsoft Excel spreadsheet or text file which is made by the user prior to entering the soil into the CFED database. The data must be organized in the spreadsheet or text file such that there are no headings or zeros in any of the columns. If either of these is included in the columns, CFED will not accept the data. The data should be arranged to include columns, in order, of: water content (percent), compaction energy (foot pound force per square foot), and density (pounds per cubic foot). See Figure 5 through Figure 7 for screenshots.

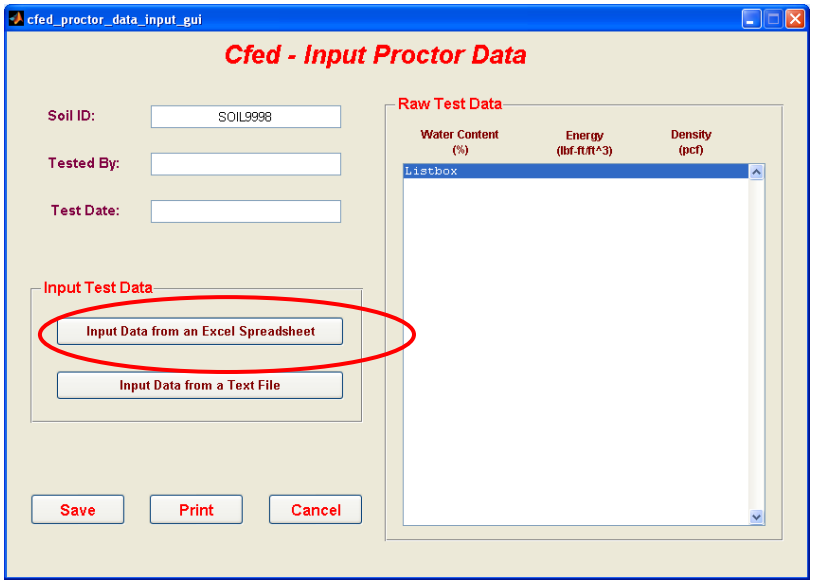


**Figure 5: CFED Input proctor data**

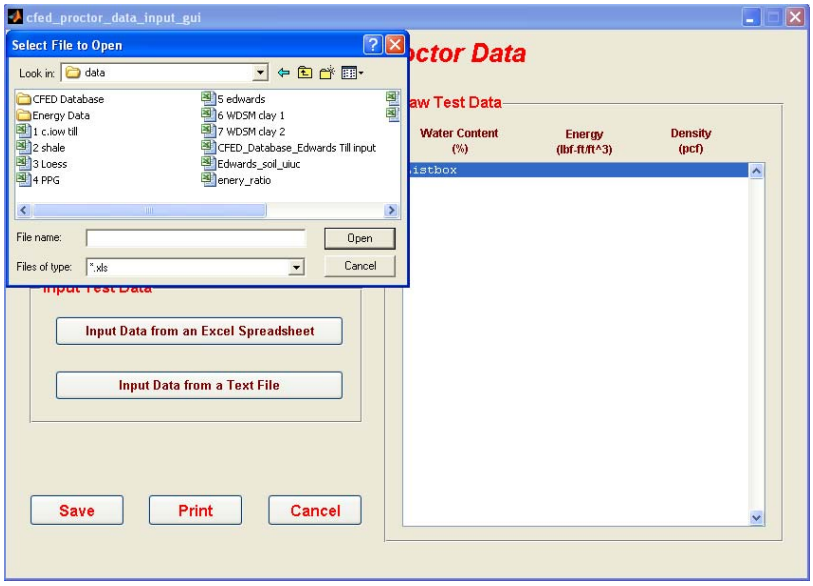


**Figure 6: CFED Selecting Excel spreadsheet with data**

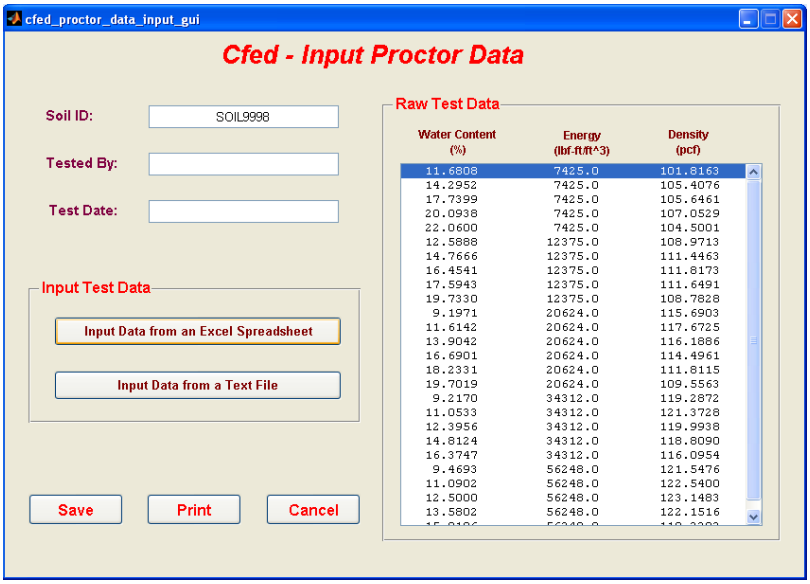


**Figure 7: CFED Proctor data has been input**

Field data from the project site may also be entered into CFED using a similar process. Returning to the "Add Test Data to an Existing Soil Record" option and clicking "Field Compaction Test Data" CFED will open a screen which allows the user to input all field data relevant to the project including information about the roller type and settings used (See Figure 8).

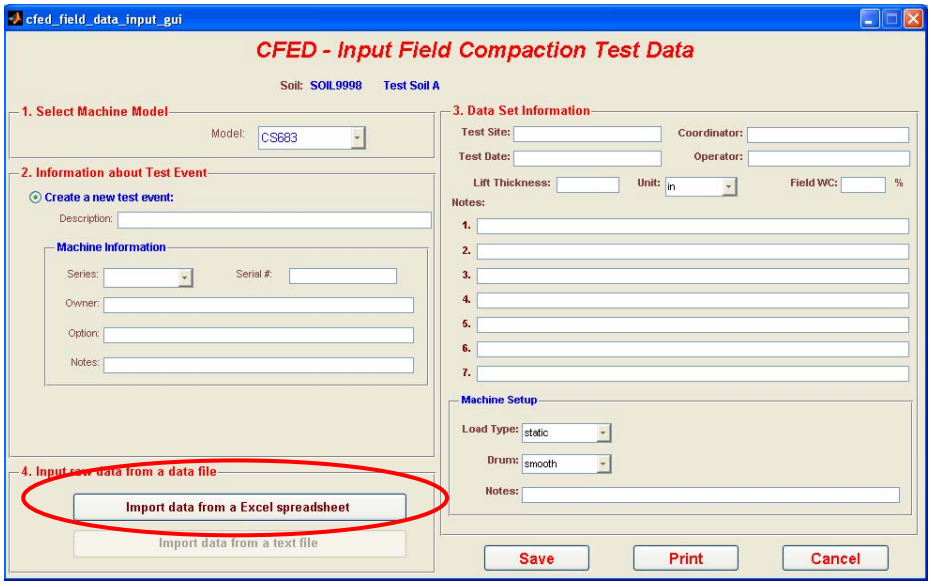


**Figure 8: CFED Input field compaction test data**

Upon inputting all information, the user may import the field testing data from an Excel spreadsheet, similar to the process used for the lab proctor data. Data must be arranged in columns within the Excel file and headings may be included in the cells. The user may enter the appropriate column heading and choose between varying units to input the field data so that conversions are minimized. Again, no zeros may be entered into the cells; otherwise, CFED will not accept the data (See Figure 9 and Figure 10). The current version of CFED (v3.5a) allows the following field data to be entered these are provided in Table 1.

**Table 1: Available field input parameters for CFED v3.5a**

| Field Input Parameter | CFED Abbreviation/Symbol |
|---|---|
| Measurement location | MeasLoc |
| Measurement depth | MeasDepth |
| Machine pass number | Pass |
| Gross power | GrsPower |
| Net power | NetPower |
| Density | Density |
| Moisture content | WC |
| Drum vibration amplitude | Amplitude |
| Drum vibration frequency | Frequency |
| Net energy | NetEnergy |
| Gross Energy | GrsEnergy |
| Accumulated net energy | AccuNetEng |
| Accumulated gross energy | AccuGrsEng |
| Compaction meter value | CMV |
| Machine speed | Speed |
| Dynamic Cone Penetration Index | DCPI |
| Clegg impact value | CIV |
| Soil stiffness gauge modulus | $E_{SSG}$ |
| Soil stiffness gauge stiffness | $k_{SSG}$ |
| Plate load modulus | Ev1 |
| Plate re-load modulus | Ev2 |
| Lightweight deflectometerd modulus | $E_{LWD}$ |

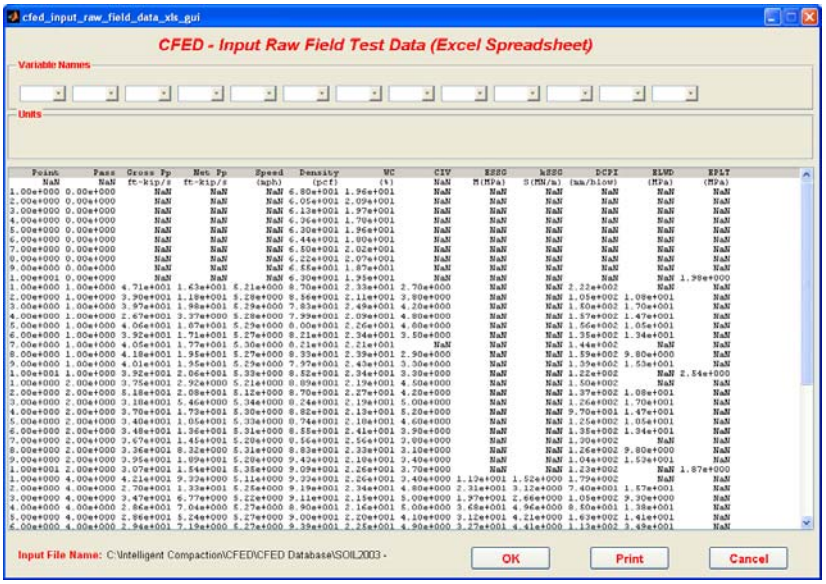


**Figure 9: CFED Field data after input**

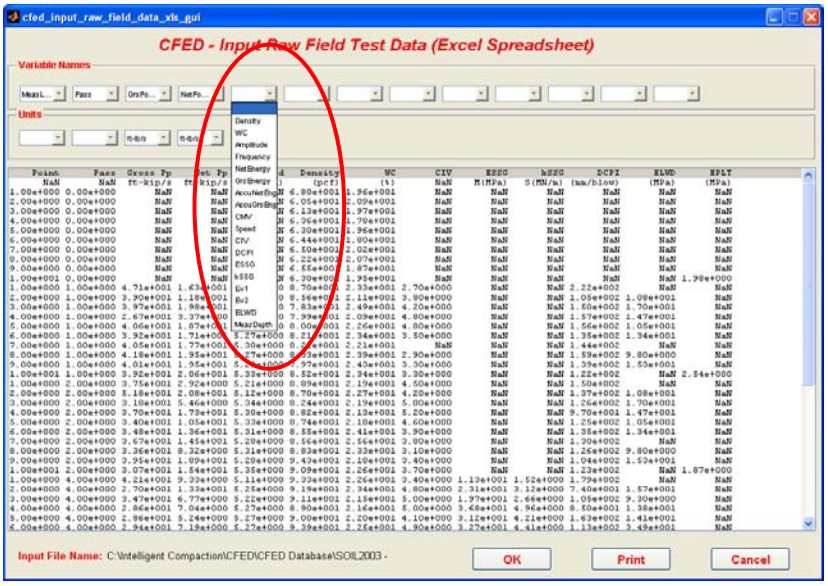


**Figure 10: CFED Selection of heading and units for field compaction data**

Once a field event has been entered into CFED, several additional events may be added to this field event so that several strips with the same machine may be organized under one event.

With all data for a given soil entered into the database CFED will produce several plots derived from the data. These plots are shown in Figure 11 through Figure 18.

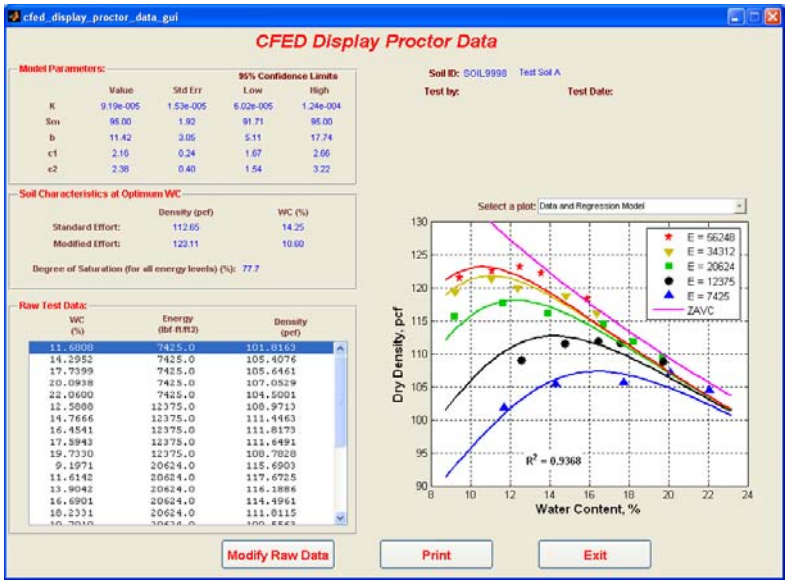


**Figure 11: CFED Data and regression model**

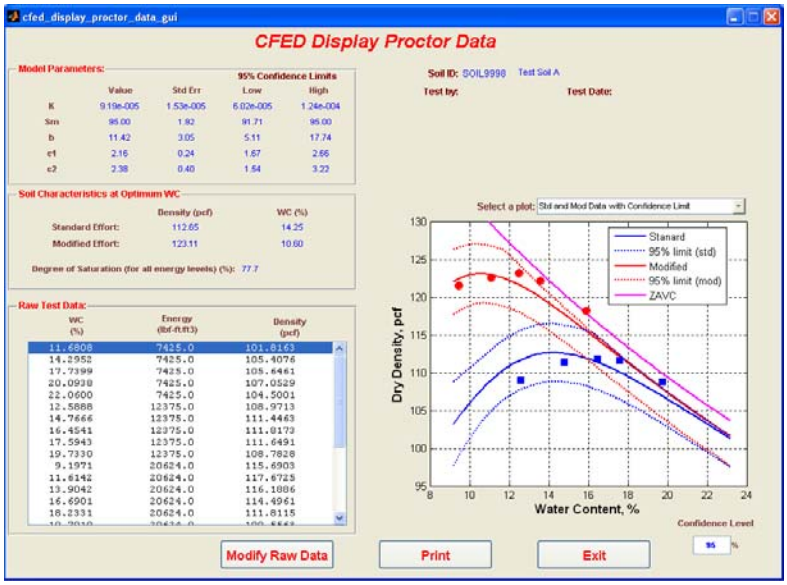


**Figure 12: CFED Std and Mod Data with Confidence Limit**

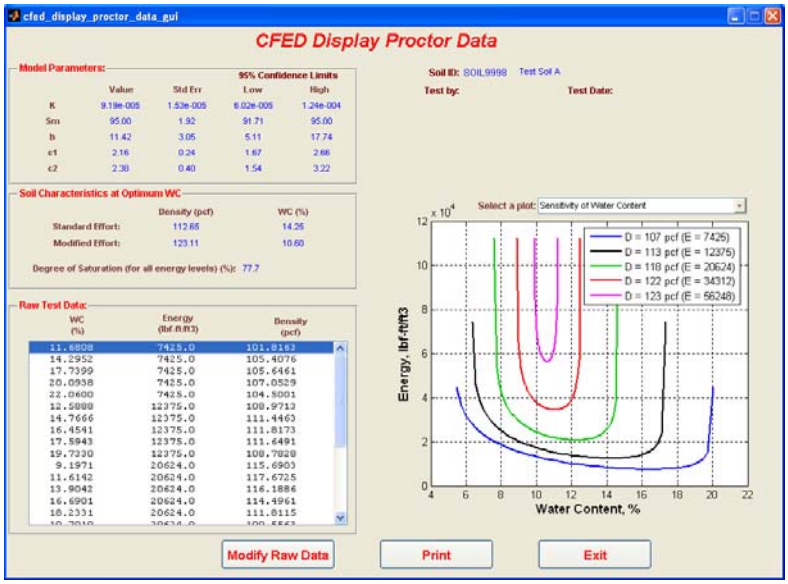


**Figure 13: CFED Sensitivity of Water Content**

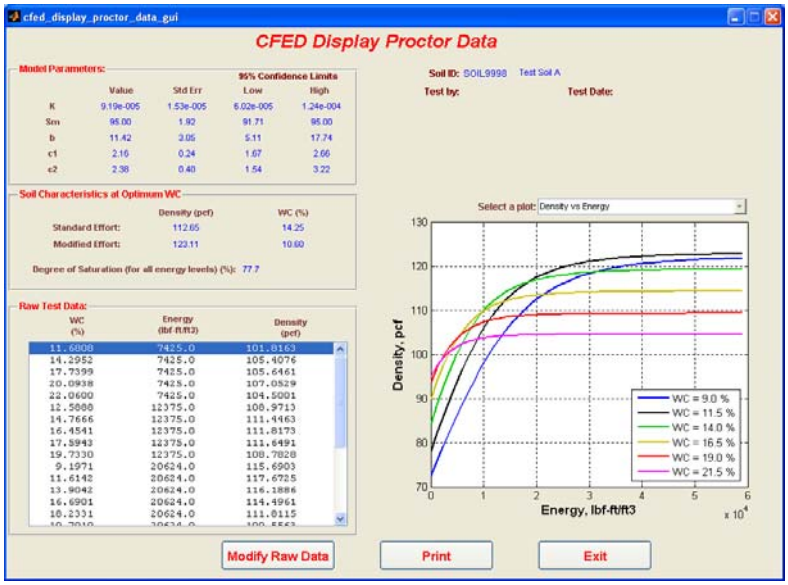


**Figure 14: CFED Density vs Energy**

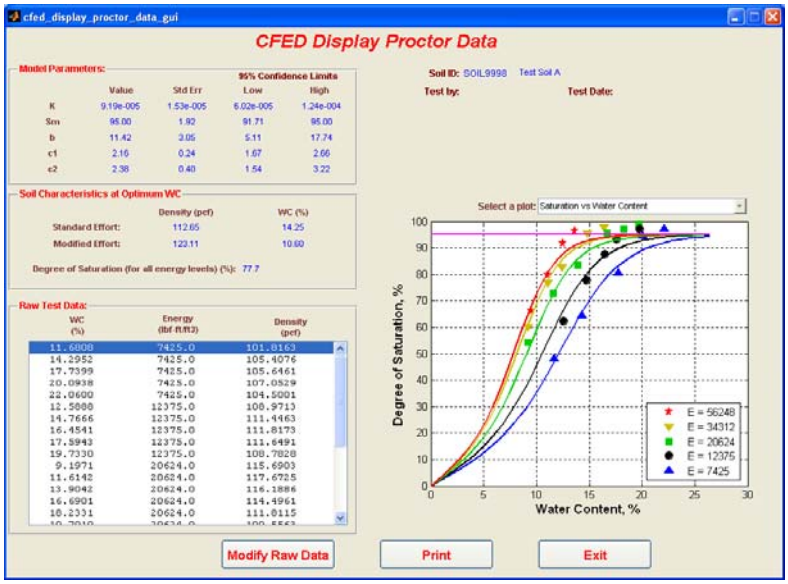


**Figure 15: CFED Saturation vs Water Content**

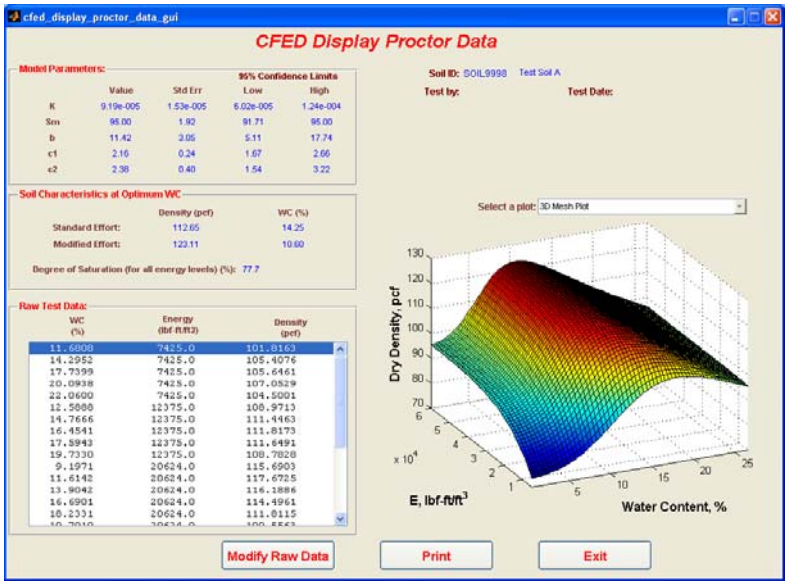


**Figure 16: CFED 3D Mesh Plot**

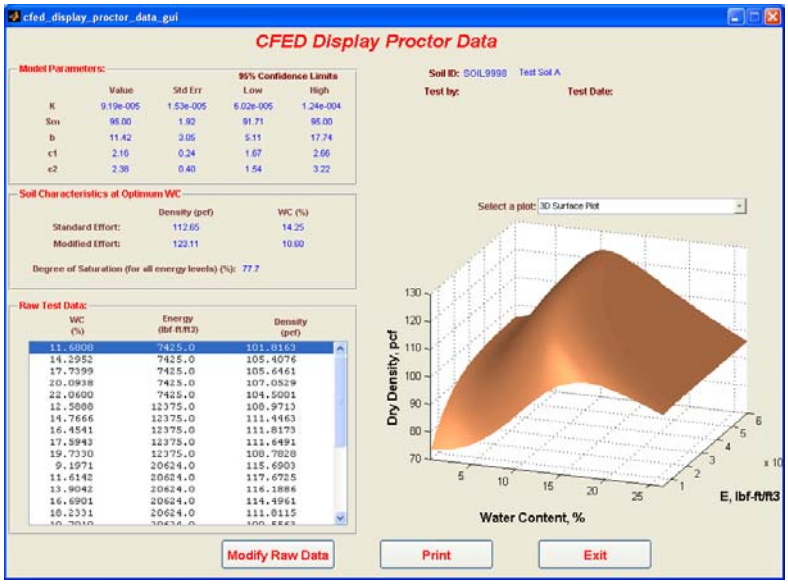


**Figure 17: CFED 3D Surface Plot**

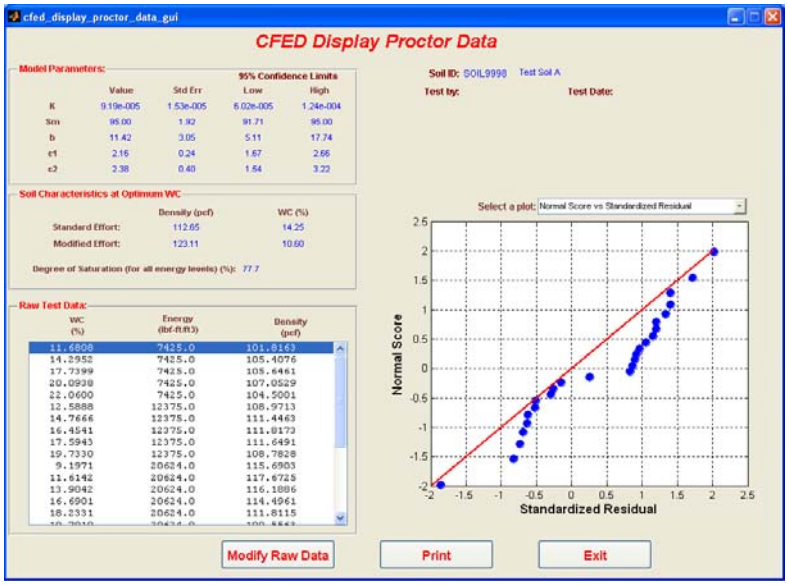


**Figure 18: CFED Normal Score vs Standardized Residual**

Once the database has been sufficiently built, CFED may be used to predict compaction information for a target soil. The user must enter information about the target soil into the CFED database, select a reference soil, and CFED will predict the optimum moisture content and maximum dry density as well as display roller pass versus dry density data from the reference soil. This is shown in Figure 19 and Figure 20.

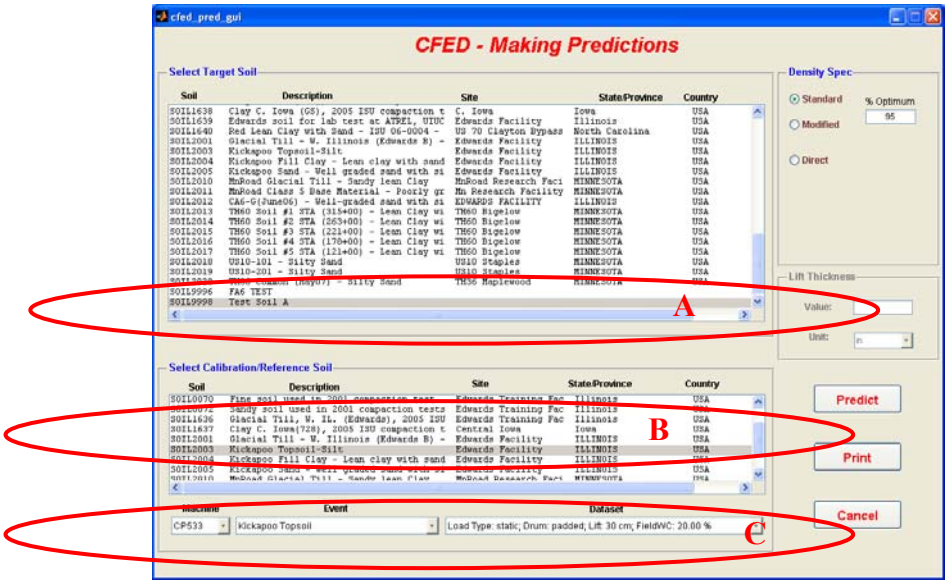


**Figure 19: CFED Prediction selection of target soil (A), reference soil (B) and reference event (C)**

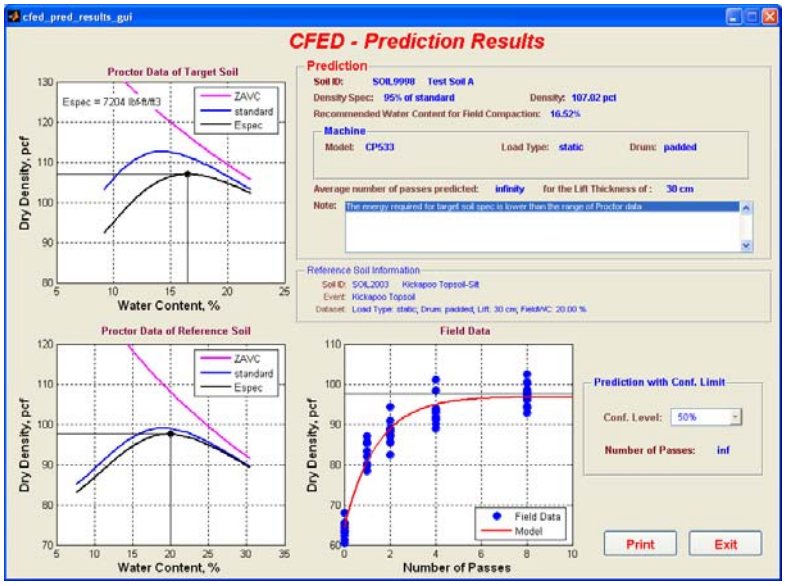


**Figure 20: CFED Prediction Results**

**Caterpillar Compaction Equipment**

Caterpillar rollers were used in performing field research. Several different models were used including: CS533E, CS-563E, CP533E, CS683E, and CAT825. A photo of each and an accompanying table are listed below which give the standard specifications for each machine. The specifications provided here are as described in Caterpillar (2003).


**Figure 21: CS-533E**

**Table 2: CS-533E Standard Specifications**

| | | |
|---|---|---|
| **Gross Power** | 97 kW | 130 hp |
| **Rated Engine RPM** | 2200 | |
| **No. Cylinders** | 4 | |
| **Displacement** | 4.4 L | 269 $in^3$ |
| **Engine Model** | 3054C | |
| **Speeds** | 2 forward/2 reverse | |
| **Max. Speed (For./Rev.)** | 12 km/h | 7.5 mph |
| **Working Speed** | 8 km/h | 4.9 mph |
| **Operating Weight** | 10,485 kg | 23,120 lb |
| **Shipping Weight** | 10,405 kg | 22,945 lb |
| **Drive** | Drum/Rear Wheel | |
| **Steering:** | | |
| Inside Radius | 3680 mm | 12'1" |
| Outside Radius | 5810 mm | 19'1" |
| Steering Angle | ±34° | |
| **Vibratory System:** | | |
| Ecc. Weight Drive | Hydraulic | |
| Frequency | 31 Hz | 1860 vpm |
| Amplitude | 2 | |
| High Amplitude | 1.80 mm | 0.071" |
| Low Amplitude | 0.85 mm | 0.033" |
| Centrifugal Force | | |
| Maximum | 234 kN | 52,600 lb |
| Minimum | 133 kN | 30,000 lb |
| **General Dimensions:** | | |
| Overall Width w/Blade | 2430 mm | 8'0" |
| Overall Width w/o Blade | 2286 mm | 7'6" |
| Drum Width | 2130 mm | 7'0" |
| Drum Diameter | 1534 mm | 5'0" |
| Tires | 23.1 x 26-8 ply flotation | |
| Overall Height* | 3070 mm | 10'1" |
| Wheel to Drum | 2900 mm | 9'6" |
| Overall Length | 5510 mm | 18'1" |
| Curb Clearance | 521 mm | 20.5" |
| **Service Refill Capacities:** | | |
| Fuel Tank | 180 L | 47 U.S. gal |
| Crankcase | 9 L | 2.4 U.S. gal |
| Hydraulic Fluid | 60 L | 16 U.S. gal |

*With ROPS/FOPS Canopy


**Figure 22: CS-563E**

**Table 3: CS-563E Standard Specifications**

| | | |
|---|---|---|
| **Gross Power** | 112 kW | 150 hp |
| **Rated Engine RPM** | 2200 | |
| **No. Cylinders** | 6 | |
| **Displacement** | 5.98 L | 365 $in^3$ |
| **Engine Model** | 3056E ATAAC | |
| **Speeds** | 2 forward/2 reverse | |
| **Max. Speed (For./Rev.)** | 11.4 km/h | 7 mph |
| **Working Speed** | 5.7 km/h | 3.5 mph |
| **Operating Weight** | 11,120 kg | 24,520 lb |
| **Shipping Weight** | 11,040 kg | 24,345 lb |
| **Drive** | Drum/Rear Wheel | |
| **Steering:** | | |
| Inside Radius | 3680 mm | 12'1" |
| Outside Radius | 5810 mm | 19'1" |
| Steering Angle | ±34° | |
| **Vibratory System:** | | |
| Ecc. Weight Drive | Hydraulic | |
| Frequency | 31.9 Hz | 1914 vpm |
| Amplitude | 2 | |
| High Amplitude | 1.70 mm | 0.067" |
| Low Amplitude | 0.85 mm | 0.033" |
| Centrifugal Force | | |
| Maximum | 266 kN | 60,000 lb |
| Minimum | 133 kN | 30,000 lb |
| **General Dimensions:** | | |
| Overall Width w/Blade | 2500 mm | 8'2" |
| Overall Width w/o Blade | 2290 mm | 7'6" |
| Drum Width | 2130 mm | 7'0" |
| Drum Diameter | 1524 mm | 5'0" |
| Tires | 23.1 x 26-8 ply flotation | |
| Overall Height* | 3070 mm | 10'1" |
| Wheel to Drum | 2900 mm | 9'6" |
| Overall Length | 5760 mm | 18'11" |
| Curb Clearance | 497 mm | 19.6" |
| **Service Refill Capacities:** | | |
| Fuel Tank | 300 L | 79 U.S. gal |
| Crankcase | 12.1 L | 3.2 U.S. gal |
| Hydraulic Fluid | 64 L | 16.9 U.S. gal |

*With ROPS/FOPS Canopy

**Figure 23: CP-533E**

**Table 4: CP-533E Standard Specifications**

| | | |
|---|---|---|
| **Gross Power** | 97 kW | 130 hp |
| **Rated Engine RPM** | 2200 | |
| **No. Cylinders** | 4 | |
| **Displacement** | 4.4 L | 269 $in^3$ |
| **Engine Model** | 3054C | |
| **Speeds** | 2 forward/2 reverse | |
| **Max. Speed (For./Rev.)** | 12 km/h | 7.5 mph |
| **Working Speed** | 8 km/h | 4.9 mph |
| **Operating Weight** | 11,320 kg | 24,960 lb |
| **Shipping Weight** | 11,240 kg | 24,785 lb |
| **Drive** | Drum/Rear Wheel | |
| **Steering:** | | |
| Inside Radius | 3680 mm | 12'1" |
| Outside Radius | 5810 mm | 19'1" |
| Steering Angle | ±34° | |
| **Vibratory System:** | | |
| Ecc. Weight Drive | Hydraulic | |
| Frequency | 31.9 Hz | 1914 vpm |
| Amplitude | 2 | |
| High Amplitude | 1.70 mm | 0.067" |
| Low Amplitude | 0.85 mm | 0.033" |
| Centrifugal Force | | |
| Maximum | 266 kN | 60,000 lb |
| Minimum | 133.5 kN | 30,000 lb |
| **General Dimensions:** | | |
| Overall Width w/Blade | -- | |
| Overall Width w/o Blade | 2286 mm | 7'6" |
| Drum Width | 2130 mm | 7'0" |
| Drum Diameter | 1549 mm | 5'1" |
| Tires | 23.1 x 26-8 ply flotation | |
| Overall Height* | 3070 mm | 10'1" |
| Wheel to Drum | 2900 mm | 9'6" |
| Overall Length | 5510 mm | 18'1" |
| Curb Clearance | 521 mm | 20.5" |
| **Service Refill Capacities:** | | |
| Fuel Tank | 180 L | 47 U.S. gal |
| Crankcase | 9 L | 2.4 U.S. gal |
| Hydraulic Fluid | 60 L | 16 U.S. gal |

*With ROPS/FOPS Canopy


**Figure 24: CS-683E**

**Table 5: CS-683E Standard Specifications**

| | | |
|---|---|---|
| **Gross Power** | 129 kW | 173 hp |
| **Rated Engine RPM** | 2200 | |
| **No. Cylinders** | 6 | |
| **Displacement** | 5.98 L | 365 $in^3$ |
| **Engine Model** | 3056E | |
| **Speeds** | 2 forward/2 reverse | |
| **Max. Speed (For./Rev.)** | 11.3 km/h | 7 mph |
| **Working Speed** | 5.7 km/h | 3.5 mph |
| **Operating Weight** | 18,500 kg | 40,785 lb |
| **Shipping Weight** | 18,420 kg | 40,610 lb |
| **Drive** | Drum/Rear Wheel | |
| **Steering:** | | |
| Inside Radius | 3680 mm | 12'1" |
| Outside Radius | 5810 mm | 19'1" |
| Steering Angle | ±34° | |
| **Vibratory System:** | | |
| Ecc. Weight Drive | Hydraulic | |
| Frequency | 30 Hz | 1800 vpm |
| Amplitude | 2 | |
| High Amplitude | 1.80 mm | 0.071" |
| Low Amplitude | 0.90 mm | 0.035" |
| Centrifugal Force | | |
| Maximum | 332 kN | 74,600 lb |
| Minimum | 166 kN | 37,300 lb |
| **General Dimensions:** | | |
| Overall Width w/o Blade | 2460 mm | 8'1" |
| Drum Width | 2130 mm | 7'0" |
| Drum Diameter | 1524 mm | 5'0" |
| Tires | 23.1 x 26-12 ply flotation | |
| Overall Height* | 3020 mm | 9'11" |
| Wheel to Drum | 2900 mm | 9'6" |
| Overall Length | 6000 mm | 19'8" |
| Curb Clearance | 495 mm | 19.5" |
| **Service Refill Capacities:** | | |
| Fuel Tank | 300 L | 79 U.S. gal |
| Crankcase | 12.1 L | 3.2 U.S. gal |
| Hydraulic Fluid | 64 L | 16.9 U.S. gal |

*With ROPS/FOPS Canopy


**Figure 25: CAT 825H**

**Table 6: CAT 825H Standard Specifications**

| | | |
|---|---|---|
| **Gross Power** | 299 kW | 401 hp |
| **Displacement** | 15.2 L | 983 $in^3$ |
| **Engine Model** | Cat C15 ACERT | |
| **Speeds** | 3 forward/3 reverse | |
| **Max. Speed (For./Rev.)** | 17.2 km/h | 10.7 mph |
| **Operating Weight** | 32,723 kg | 72,164 lb |
| **Shipping Weight** | 31,200 kg | 68,796 lb |
| **Steering:** | | |
| Inside Radius | 7417 mm | 24.3 ft |
| Outside Radius | 3362 mm | 11 ft |
| **Wheel Dimensions:** | | |
| Drum Width | 1125 mm | 3.69 ft |
| Drum Diameter | 1311 mm | 4.3 ft |
| Outside Diameter | 1677 mm | 5.5 ft |
| Wheel Weight | 1766 kg | 3893 lb |
| **Machine Dimensions:** | | |
| Height to Top of Cab | 3755 mm | 12.3 ft |
| Center Line of Rear Axel to Edge of Counterweight | 2687 mm | 8.8 ft |
| Wheelbase | 3700 mm | 12.1 ft |
| Ground Clearance | 414 mm | 1.4 ft |
| **Service Refill Capacities:** | | |
| Fuel Tank | 603 L | 159 gal |
| Crankcase | 34 L | 9 gal |

**Figure 26: Compactor used for TH60 project (specifications unknown)**

# CHAPTER 3. LITERATURE REVIEW

The purpose of the literature review was to determine what factors influence the compaction of soils in the field. These factors include: machine type, soil type, moisture content and lift thickness. A particular focus of the review was to find multiple field compaction curves. These relationships are important in establishing relationships between laboratory impact and field compaction. Two references: Johnson and Sallberg (1960) and Parsons (1992) were particularly useful as resources for field compaction curves.

## Factors That Influence Field Compaction of Soils

### *Machine Type*

#### Smooth Drum Rollers

Smooth drum rollers are typically described by a cylindrical drum with a smooth surface; these may be self-propelled with one, two, or three drums and/or pulled by another piece of machinery (See Figure 27). These rollers compact the soil in a method similar to static compaction. The smooth drum-soil interface coupled with the weight of the roller achieves compaction by applying a force sufficient enough to cause individual particles to break their natural bonds and assist compaction. If the moisture content of the soil is appropriate (near optimum), particles will slide past each other, smaller particles will move into the pore spaces, and the density of the soil will increase. Primary factors which influence the ability of a smooth drum to achieve soil compaction are: axle load, drum width, drum diameter, and rolling speed (Caterpillar 2000).


**Figure 27: Caterpillar CS-563 smooth drum roller**

A numerical representation of the potential of a smooth-drum roller to compact soil is referred to as the "static compaction potential." It is calculated by dividing the weight of the drum (i.e. axle load) by the width of the drum and is expressed as pounds per linear inch (PLI) or kilograms per centimeter (kg/cm) (Caterpillar 2000). Parsons (1992) found that maximum relative compaction (to British Standard Compaction Test) decreased and the optimum relative moisture content increased as the static compaction potential decreased. If force imparted to the ground by the compactor is a function of weight of the machine, this means that for a given drum width the energy input from the machine will increase as the weight of the machine increases. As energy input increases, the optimum moisture content decreases and maximum dry density increases.

Smooth drum rollers have difficulty compacting soils which are exceptionally wet or where lift thicknesses have been applied excessively thick. In these conditions the roller is susceptible to rutting or plowing of the soil. If this is the case, the soil may need to be dried, spread into a thinner lift with a dozer or a different, and a lighter type of compacting machine may be used to "pre-compact" the soil. Also, if lifts are applied too thick, the smooth-drum roller may compact only the top portion of the lift leaving the lower portion of the lift loose. Assuming the prior lift was compacted properly, this will result in an intermediate soft layer between two compacted layers. Settlement may occur with repeated traffic loading causing failure of the overlying pavement.

Another issue with smooth-drum rollers is the bridging across depressions which may occur during compaction. If a depressed spot is present and smaller than the width of the drum, the drum may not come into contact with the soil across the entire width of the drum; thus, preventing uniform compaction (See Figure 28).

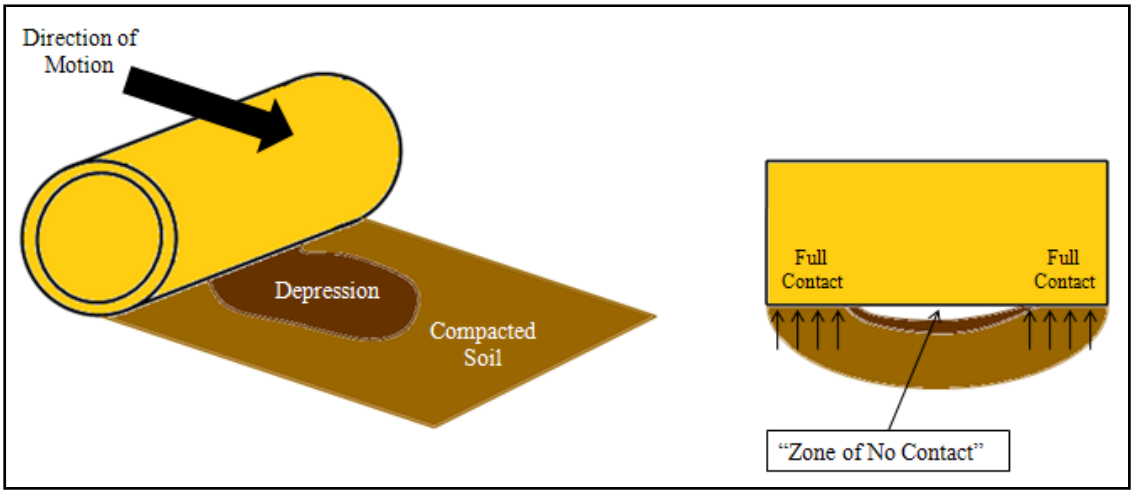


**Figure 28: Bridging effect of smooth-drum rollers**

Johnson and Sallberg (1960) investigated the ability of smooth-drum rollers to compact five soil types. The roller used was a 9.5-ton 3-wheel roller; the compacted soils were placed in 9-inch loose lifts and near optimum moisture content for field compaction. The field compaction curves are shown in Figure 29 and Figure 30; the soil properties are shown in Table 7.

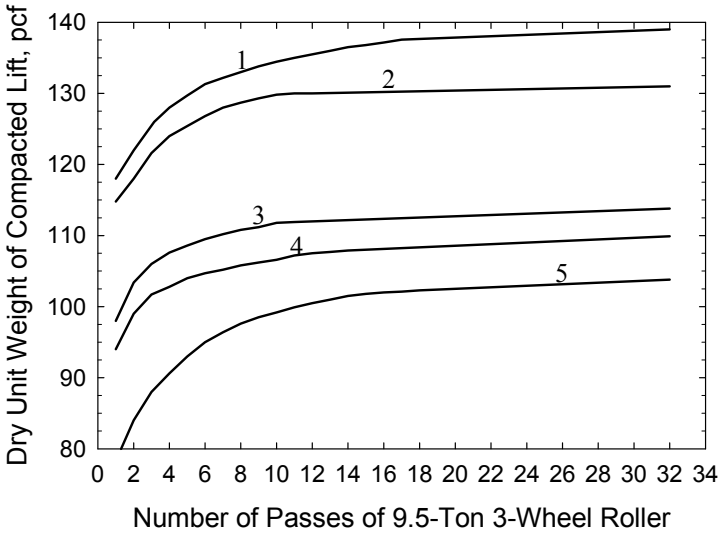


**Figure 29: Effect of number of passes on unit weights for 9.5-ton 3-wheel roller from Johnson and Sallberg (1960)**

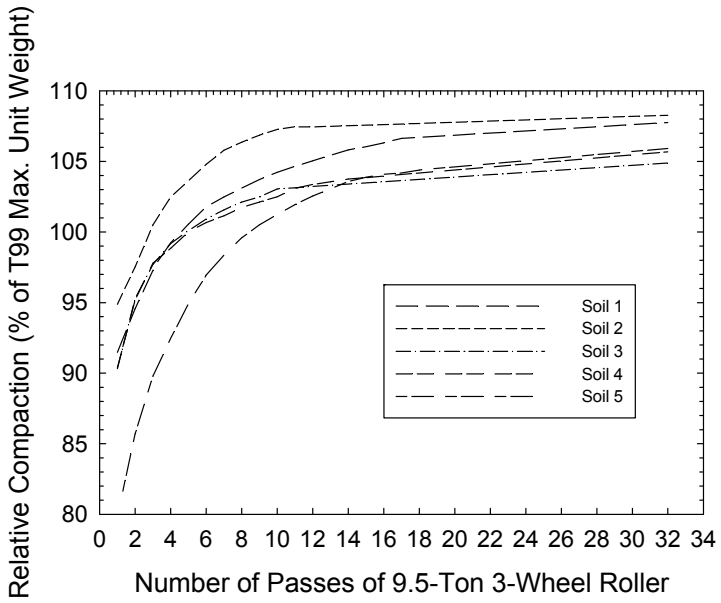


**Figure 30: Effect of number of passes on relative compaction for 9.5-ton 3-wheel roller from Johnson and Sallberg (1960)**

**Table 7: Soil properties from Johnson and Sallberg (1960)**

| Soil Number - Type | LL | PI | Sp. Gr ($G_s$) |
|---|---|---|---|
| 1 – Gravel-Sand-Clay | NP | NP | 2.68 |
| 2 – Well-Graded Sand | NP | NP | 2.70 |
| 3 – Sandy Clay | 27 | 8 | 2.70 |
| 4 – Silty Clay | 43 | 19 | 2.69 |
| 5 – Heavy Clay | 75 | 52 | 2.77 |

From Figure 29 it is evident that smooth-drum rollers are able to compact varying types of soil; although at different degrees. In all cases, the roller compacted density exceeded 100% of AASHTO T99 maximum unit weight (See Figure 30). The most dramatic increase of dry unit weight was in the case of the heavy clay where the roller increased dry density from 80 pcf to approximately 103.8 pcf; a increase of nearly 25% relative compaction.

Parsons (1992) experienced the same general relationship with an 8.6-ton smooth-drum roller when compacting 3 soils (See Figure 31). These three soils (sandy clay, well-graded sand, and gravel-sand-clay) were compacted dry of their respective optimums which is shown in Figure 31. In general, the results from each soil are similar with the well-graded sand having the best relative compaction. In all three cases the roller compacted the soil to more than 100% relative compaction value. These relative compaction values correspond to the British Standard Compaction test.

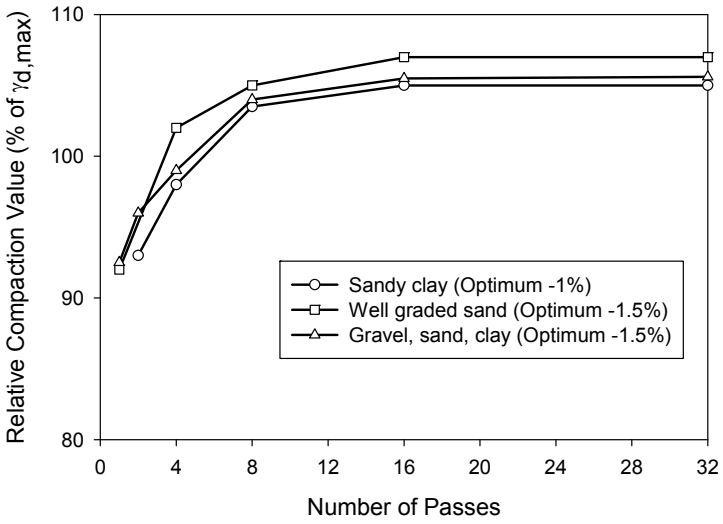


**Figure 31: Relationship between relative compaction value and roller passes for 8.6-ton smooth-drum roller from Parsons (1992)**

Natrajan (1983) compacted three soils with an 8-10 ton conventional three wheel roller. The soils were compacted in strips with lifts of 30 cm; no moisture information was given. The field compaction curves are shown in Figure 32 and the soil index properties are shown in Table 8 (Note that properties for the clayey sand (PI=15) were not provided in the original reference). The fully compacted dry density was much larger for the gravel (~136 pcf) compared to that of the clayey sand (PI=15) which reached a maximum value of approximately 121 pcf. However, each of the three soils achieved more than 100% relative compaction of Modified AASHTO laboratory compaction. Natrajan (1983) concluded that more passes are required to achieve 100% relative compaction in clayey soils versus gravels for the 8-10 ton conventional three wheel roller.

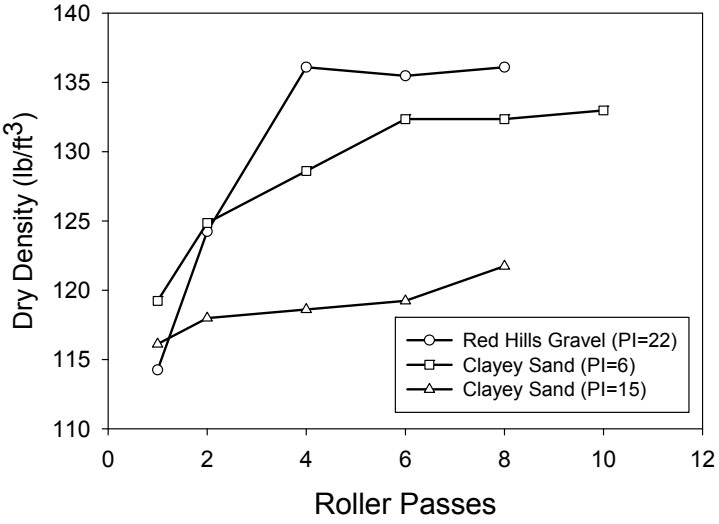


**Figure 32: Relationship between machine pass and dry density for 8-10 ton conventional three wheel roller from Natrajan (1983)**

**Table 8: Soil index properties from Natrajan (1983)**

| | | | | Index Test | | | Sieve Analysis | | | | Sedimentation Analysis | | | Proctor Test | | C.B.R. @ Proctor density O.M.C | | |
|---|---|---|---|---|---|---|---|---|---|---|---|---|---|---|---|---|---|---|
| Serial Number | Description of soil | Unified soil classification | P.R.A. soil classification | Liquid limit % | Plastic limit % | Plasticity index | Percent passing 15200 | Percent passing 1540 | Percent passing 158 | Specific gravity | Sand % | Silt % | Clay % | Maximum density (gm/cc) | Optimum % moisture content | Immediate % | After 4 day soaking % | Moisture after 4 day soaking % |
| 1 | Foundation soil (H.R.S. Clay) | CL | A.6 | 35 | 15 | 20 | 99 | 79 | 52 | 2.44 | 35 | 34 | 31 | 1.74 | 17 | 8 | 3 | 24 |
| 2 | Gravel | GC | A.2.6 | 37 | 15 | 22 | 42 | 31 | 23 | 2.74 | 47 | 22 | 31 | 2.11 | 11 | 19 | 18 | 13 |
| 3 | Silty Sand | -- | -- | -- | -- | -- | 100 | 74 | 10 | 2.52 | 92 | 8 | -- | 1.89 | 11 | 32 | 27 | 12 |
| 4 | Clayey Sand | SM, SC | A.2.4 | 19 | 13 | 6 | 99 | 77 | 26 | 2.64 | 76 | 19 | 5 | 2.12 | 10 | 16 | 9 | 10 |
| 5 | Red Earth | -- | -- | 22 | 14 | 8 | 95 | 71 | 30 | -- | -- | -- | -- | 1.93 | 12 | 21 | 10 | -- |

Pneumatic-Tired Rollers

Pneumatic compactors are typically used on relatively small-scale work including finishing work or compaction of smooth, granular base materials. These rollers use both static and kneading action to achieve compaction. The pressure of the tires helps to compact the soil while the tire treads knead the soil and create some lift bonding. Characteristics of these machines which are important to compaction are the wheel load, tire pressure, and wheel/surface contact area.


**Figure 33: Caterpillar PS/PF-360C pneumatic-tire compactor (from product brochure Sept., 2004)**

The compaction energy supplied to the soil by these machines is determined by tire pressure; the higher the pressure, the higher the compactive effort. Rodriguez (1988) cautions against very high tire pressures, however, because too high of tire pressure will cause bearing capacity failure beneath the tires. This will induce rutting and little compaction may occur. Also, increasing tire pressure reduces the surface contact area of the tires thereby reducing compaction efficiency. According to Rodriguez (1988), it is not advisable to increase tire pressure unless the load per wheel is increased. This should be done to maintain contact pressure and confinement so that the entirety of a lift is compacted. Pneumatic-tire rollers can usually compact soil in less time and at a lower cost than sheepsfoot rollers (Fang 1991).

With sheepsfoot rollers only a percentage of the area of the drum is in contact with the ground at any given time, hence, it would take more coverages and more time to completely compact a given lift when compared to a pneumatic-tire roller.

Pneumatic-tire rollers may have the "bridging" problem similar to that shown in Figure 28; this will occur if the tires are all on the same axle. If the tires lie upon independent axles, a pneumatic-tire roller may not experience this problem. Though these rollers apply some kneading compaction to the soil they generally will create a smooth, hard surface, post-compaction (similar to the smooth-drum roller). It may be necessary for the surface to be scarified by disking before another lift is applied. The pneumatic-tire rollers have a tendency to plow loose soil or experience excessive rutting when lifts have been applied too thick or too moist; similar, also, to smooth-drum rollers.

One study, published by Johnson and Sallberg (1960), showed that pneumatic-tire rollers are suitable to compact a wide variety of soil types. Three pneumatic-tire rollers were used on four soil types shown in Figure 34 through Figure 37; the data for the three rollers used is shown in Table 9. These curves show that for most soils a large portion of the compaction is completed in four passes or less. Also, in each case the heavier roller achieved greater compaction than the two lighter rollers. Even in the case of roller 3, which compacted a layer approximately 3 inches thinner than the other two rollers, less compaction was achieved.

It is important to note that the roller optimum moisture content, determined by Johnson and Sallberg (1960), is less than the laboratory optimum moisture content for all soils investigated. The compaction energy relationship developed by Proctor (1933a, b, d) stated that as compaction energy is increased maximum dry density increases and optimum moisture content decreases. Therefore, it is reasonable to state that the pneumatic-tire rollers in this study applied compaction energy greater than the AASHTO T99 laboratory compaction (12,375 lb-ft/ft$^3$).

**Table 9: Roller specifications for compaction study from Johnson and Sallberg (1960)**

| Curve Number | Roller Rating (tons) | Wheel Load (lb) | Tire Inflation Pressure (psi) | Loose Lift Thickness (in.) |
|---|---|---|---|---|
| 1 | 46.8 | 22,400 | 140 | 12 |
| 2 | 46.8 | 11,200 | 90 | 12 |
| 3 | 13.44 | 2,985 | 36 | 9 |

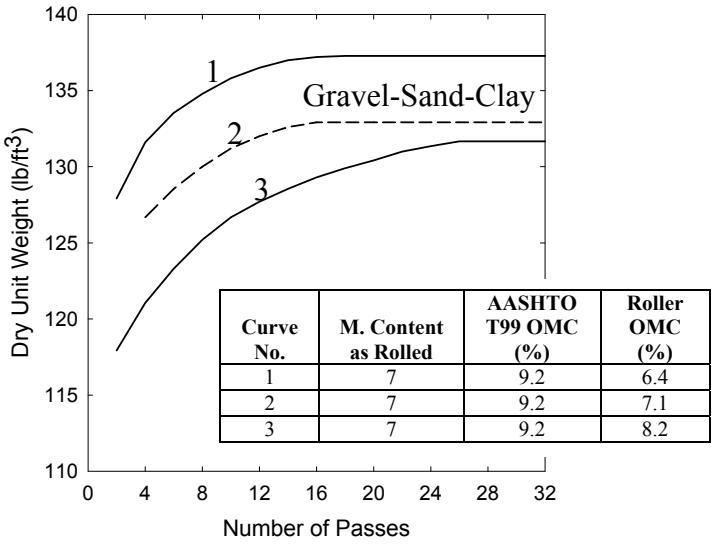


| Curve No. | M. Content as Rolled | AASHTO T99 OMC (%) | Roller OMC (%) |
|---|---|---|---|
| 1 | 7 | 9.2 | 6.4 |
| 2 | 7 | 9.2 | 7.1 |
| 3 | 7 | 9.2 | 8.2 |

**Figure 34: Relationship between dry unit weight and roller passes for pneumatic-tire roller in gravel-sand-clay from Johnson and Sallberg (1960)**

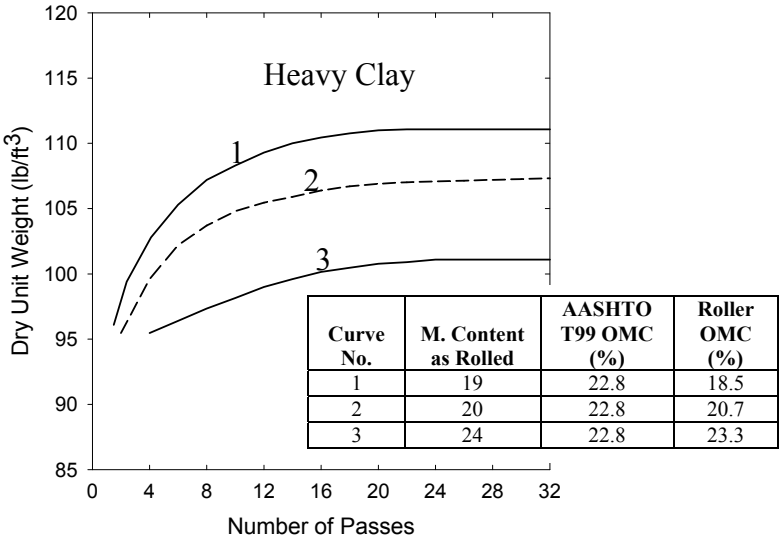


| Curve No. | M. Content as Rolled | AASHTO T99 OMC (%) | Roller OMC (%) |
|---|---|---|---|
| 1 | 19 | 22.8 | 18.5 |
| 2 | 20 | 22.8 | 20.7 |
| 3 | 24 | 22.8 | 23.3 |

**Figure 35: Relationship between dry unit weight and roller passes for pneumatic-tire roller in heavy clay from Johnson and Sallberg (1960)**

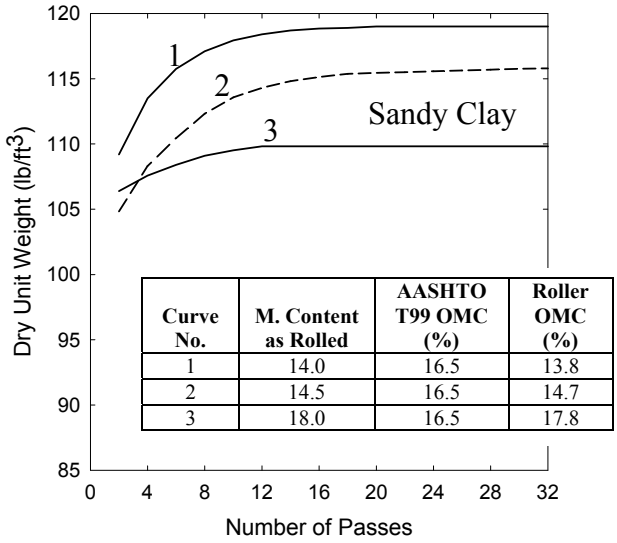


| Curve No. | M. Content as Rolled | AASHTO T99 OMC (%) | Roller OMC (%) |
|---|---|---|---|
| 1 | 14.0 | 16.5 | 13.8 |
| 2 | 14.5 | 16.5 | 14.7 |
| 3 | 18.0 | 16.5 | 17.8 |

**Figure 36: Relationship between dry unit weight and roller passes for pneumatic-tire roller in sandy clay from Johnson and Sallberg (1960)**

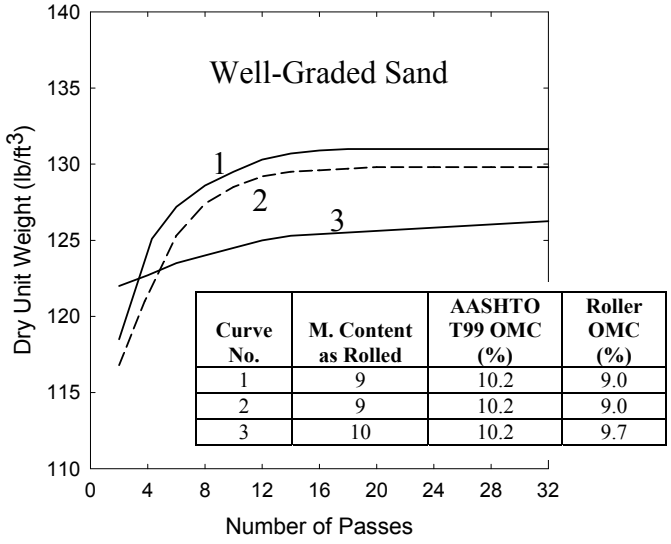


| Curve No. | M. Content as Rolled | AASHTO T99 OMC (%) | Roller OMC (%) |
|---|---|---|---|
| 1 | 9 | 10.2 | 9.0 |
| 2 | 9 | 10.2 | 9.0 |
| 3 | 10 | 10.2 | 9.7 |

**Figure 37: Relationship between dry unit weight and roller passes for pneumatic-tire roller in well-graded sand from Johnson and Sallberg (1960)**

One factor which influences soil compaction for pneumatic-tire rollers and is unique from other machines is tire inflation pressure; Figure 38 supports this statement. The Waterways Experiment Station (1956) study was performed on a lean clay (LL=36, PI=15) at a moisture content of 16.3% and a lift thickness of 6 inches. The roller used in this study was a towed,

dual-wheel, pneumatic-tire roller. Information on the compacting machine is shown in Table 10. From Figure 38, as tire inflation pressure and number of coverages increase, so does the dry unit weight of the soil. It is known from the laboratory (Proctor 1933a, b, d) that the dry unit weight of a soil will increase as compaction energy increases for a given moisture content. From Waterways Experiment Station (1956), it is apparent that tire inflation pressure and number of coverages influence field compaction energy for pneumatic-tire rollers. Turnbull and Foster (1957) had results very similar to that of the Waterways Experiment Station (1956). The same tire inflation pressure-number of coverages-dry unit weight relationship was observed for a soil compacted at 3 separate moisture contents.

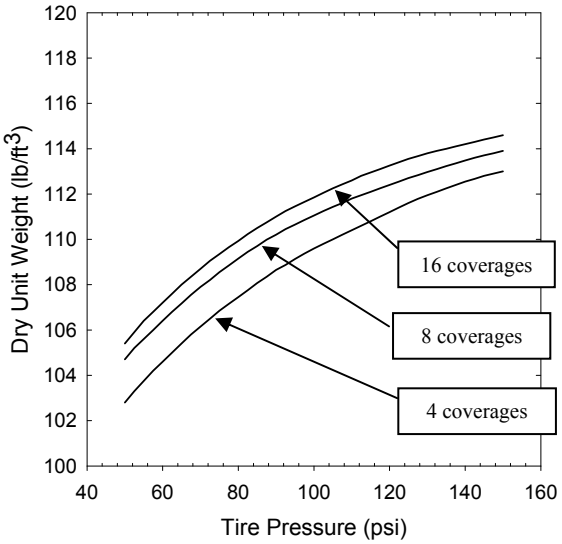


**Figure 38: Relationship between tire inflation pressure, number of coverages and dry density for pneumatic-tire roller from Waterways Experiment Station (1956)**

**Table 10: Roller specifications from Waterways Experiment Station (1956)**

| Tire Size (in.) | C-to-C Wheel Spacing (in.) | Free Space between Tire Prints (in.) | No. of Tires | Tire-inflation Pressure (psi) | Gross Roller Weight (lb) | Average Contact Tire Area ($in^2$) | Computed Contact Pressure (psi) |
|---|---|---|---|---|---|---|---|
| 18.00x24 | 28-7/8 | 12 | 4 | 50 | 63,500 | 305 | 52 |
| 18.00x24 | 28-7/8 | 12 | 4 | 90 | 100,000 | 305 | 82 |
| 16.00x21 | 26 | 11 | 4 | 150 | 125,000 | 260 | 120 |

Sheepsfoot, Padfoot, and Tamping Rollers

Sheepsfoot, padfoot and tamping rollers can generally be described as a roller, similar to a smooth-drum roller in configuration, but in which compacting feet protrude outward and are spread throughout the drum; they may be self-propelled or towed behind other machinery (See Figure 39). These feet can vary in length and contact area, but are generally approximately 8 inches long with pads that range in diameter from 3 to 5 inches (Caterpillar 2000). In all cases, the end of the pad will be smaller than the base; this allows the feet to be properly cleared of soil by the scraping device attached to the compacting machine.

**Figure 39: Caterpillar CP-533E padfoot roller**

Compaction of the soil is achieved via bearing capacity failures beneath the feet of the roller. This is commonly referred to as "kneading compaction." Rather than simply compressing the soil, the feet on the drum work to break natural bonds and increase density. Where other compactors compact the soil from the surface layer down, sheepsfoot rollers compact the soil from the bottom up. In the initial stages of compaction, the soil layer is loose with low density and high void ratio. For the initial passes of the machine, the feet will penetrate deep within the lift. As the number of passes increase the lower layers become compacted and the feet will not penetrate as deeply within the lift. When high amounts of compaction have been achieved, the roller feet will penetrate only fractions of an inch below the surface; at

this time the roller is said to “walk-out.”

Rodriguez (1988) stated that the sheepsfoot compactor produces two desirable results: 1) a reasonably uniform distribution of the compaction effort within each layer and 2) irregular dimpled surface from the remaining foot penetration which prevents a smooth, weak surface between successive layers. This statement is also true of tamping and padfoot rollers.

Tamping foot compactors produced by Caterpillar, Inc. have four steel padded wheels and a dozer blade. They are capable of high speeds of 16 – 32 km/h (10 – 20 mph). Because these machines travel at such high speeds, they are capable of all four forces of compaction: pressure, impact, vibration, and kneading. These rollers tend to leave a relatively smooth surface which allows them to achieve compaction high speeds. Because these rollers are equipped with a dozer blade, the contractor is able to spread and compact the soil with one machine; this can greatly reduce the time and number of machines require for compaction (Caterpillar 2000). These machines are, however, quite expensive and only economical when used on large projects. Large uninterrupted distances are required for these machines to build up the proper speed to achieve efficient compaction. Therefore, these machines are only applicable to a certain scale of project. Tamping rollers are different from sheepsfoot rollers in that the feet have a larger surface area. The contact pressure under a tamping roller is reduced in comparison with the sheepsfoot roller and as a result the tamping roller can be expected to be better suited for wetter soil conditions (Parsons 1992).


**Figure 40: Caterpillar 825G tamping foot roller**

Sheepsfoot rollers are effective in a variety of soil types, but are generally most effective in cohesive soils. Where pneumatic-tire or smooth drum rollers tend to plow or push the soil, the feet of the sheepsfoot roller break apart large clumps of soil which better aids in compaction. Figure 41 shows the ability of a 10,010 lb club-style sheepsfoot roller to compact four soil types for a large number of passes. The relative compaction values are not shown on this plot, but the roller achieved 100 percent relative compaction in fewer passes for the fine-grained soils. For the heavy clay and silty clay, 100% relative compaction was achieved in approximately 13 passes. The sandy clay and gravel-sand-clay required 41 and 63 passes to achieve 100% relative compaction, respectively. Parsons (1992) observed the effectiveness of tamping rollers in three soil types and found that, similar to sheepsfoot, they are most effective in fine-grained soils (See Figure 42).

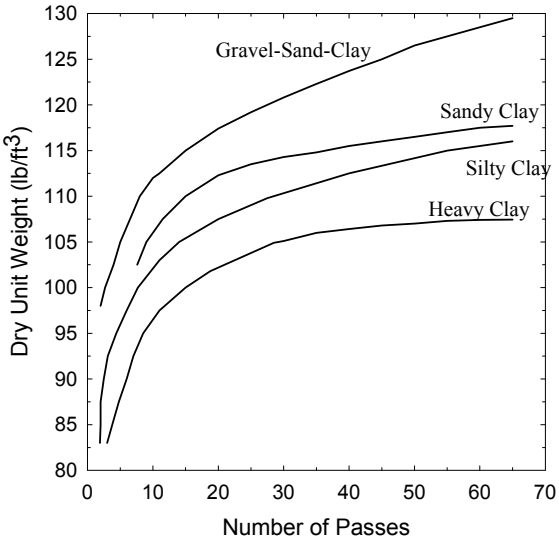


**Figure 41: Relationship between number of passes and dry unit weight for sheepsfoot roller in four soil types from Johnson and Sallberg (1960)**

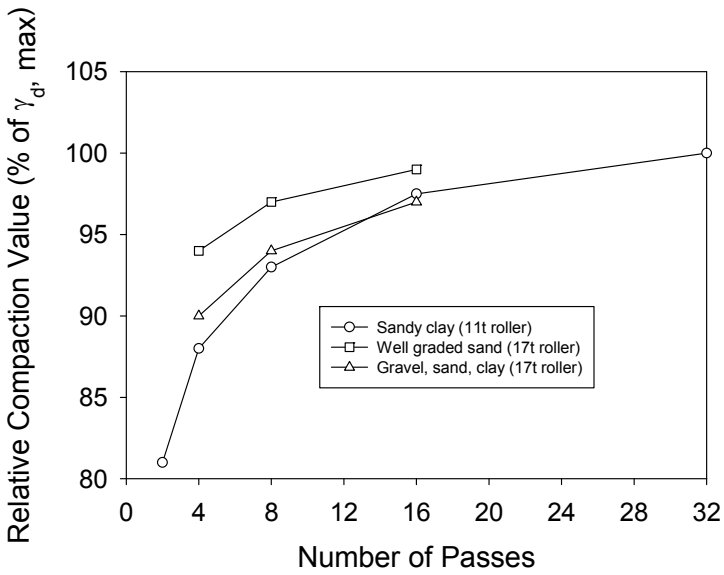


**Figure 42: Relationship between dry unit weight and number of passes for tamping rollers on three soil types from Parsons (1992)**

One important characteristic of these types of rollers is the pad type and configuration. Sheepsfoot, tamping, and padfoot compactors differ in the pad configuration on the drum. Sheepsfoot rollers contain pads which are straight with a circular end ranging from 76 – 127 mm (3 – 5") in diameter (Caterpillar 2000). Tamping and padfoot rollers have pads which

are tapered and usually have an oval or rectangular shape. Increasing the size or number of pads on a drum will increase the efficiency of the roller to cover a given area, however it will decrease the pressure under the pad thereby increasing the number of passes required to achieve desired compaction on a certain lift. Figure 43 shows the influence of foot contact area on soil compaction for a sheepsfoot roller. In this study from Johnson and Sallberg (1960) a silty clay was compacted with three rollers each with a different contact area (7 $in^2$, 14 $in^2$ and 21 $in^2$) to a total of 24 passes. It is evident from Figure 43 that as the contact area is increased for a given contact pressure, the maximum dry density increases and the optimum moisture content decreases. It is intuitive, then, that contact area and number of passes are related to field compaction energy. Parsons (1992) stated that the greater the contact area and the greater the number of passes, the greater the compactive effort applied.

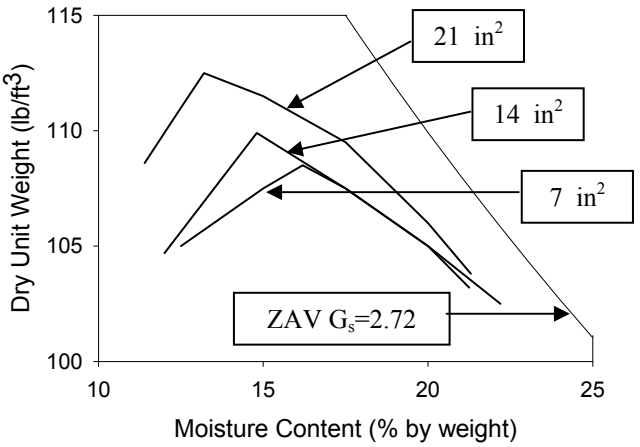


**Figure 43: Relationship between moisture content, dry unit weight and foot contact area for sheepsfoot roller from Johnson and Sallberg (1960)**

One disadvantage of sheepsfoot rollers is that they must travel at relatively low (compared to 10 – 20 mph for tamping) speeds 6 – 10 km/h (4 -6 mph) to achieve compaction (Caterpillar 2000). This reduced speed lowers the effects of impact compaction to the soil. Also, the dimples left in the soil after compaction will increase penetration of rainwater into the soil and may slow or even halt construction after a rain event (Rodriguez 1988). If lifts are applied excessively thick, these rollers may only compact the upper portion of the lift, as described with other roller types. Standard density tests are performed only near the top 6

inches of soil and therefore may not highlight the loose, underlying layers. Dynamic Cone Penetrometer (DCP) tests, modulus testing, or proof rolling methods may better highlight the presence of a soft, underlying layer.

Vibratory Rollers

These compactors use vibration to break bonds (frictional and to some degree, natural) between soil particles. This results in a rearranging of soil particles, thereby decreasing void ratio and increasing density. Many types of vibratory rollers are available including vibrating sheepsfoot or padfoot machines as well as vibrating plate compactors for small working environments. However, typical vibratory compactors are similar in characteristic to the smooth-drum rollers; with the exception of their vibration capability (See Figure 44). The vibration action of the drum is generally achieved via eccentrically mounted weights within the drum. As these weights oscillate, their momentum causes the drum to oscillate up and down; thus, causing the drum to vibrate.


**Figure 44: Caterpillar CS-563E vibratory smooth-drum roller**

A general rule of field compaction is to only use vibratory rollers in cohesionless (sandy) soils. All soils, regardless of type, respond to vibrations induced by mechanical oscillations (Johnson and Sallberg 1960). Figure 45 shows the field compaction curves for a pan-type vibratory compactor on three soil types. They soil types and corresponding curves are: 1-

Gravel, water content = 9.5%, 2 – Crushed gravel, water content =8.0%, 3 – Gravel, water content = 6.2%, and 4 – Sand, water content = 11.5%. Overall, the machine was able to compact each soil type well. However, the most efficient compaction was the sand in which full compaction was achieved after approximately 2 passes. The gravel at the higher moisture content continued to increase in density even after 5 passes of the machine. Similar results from Parsons (1992) for two vibratory towed rollers on three soil types are shown in Figure 46. It should be noted that the vertical axis from Figure 46 is the relative compaction value, not dry density. This relative compaction value is expressed as a percentage of the maximum dry density achieved from the standard laboratory (Proctor) compaction test.

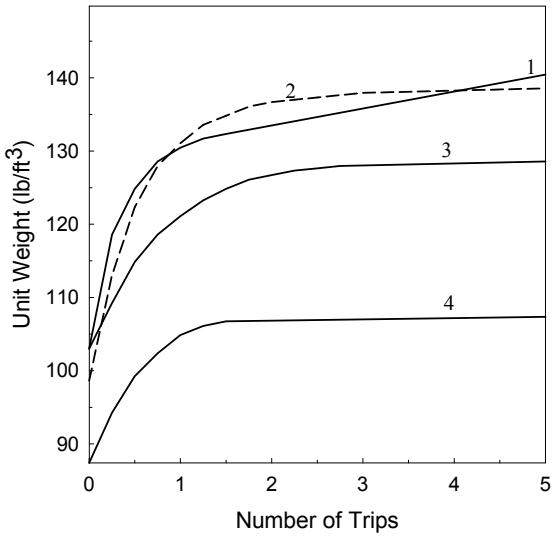


**Figure 45: Relationship between number of passes and unit weight for a single-unit heavy pan-type vibratory compactor for three soil types from Johnson and Sallberg (1960)**

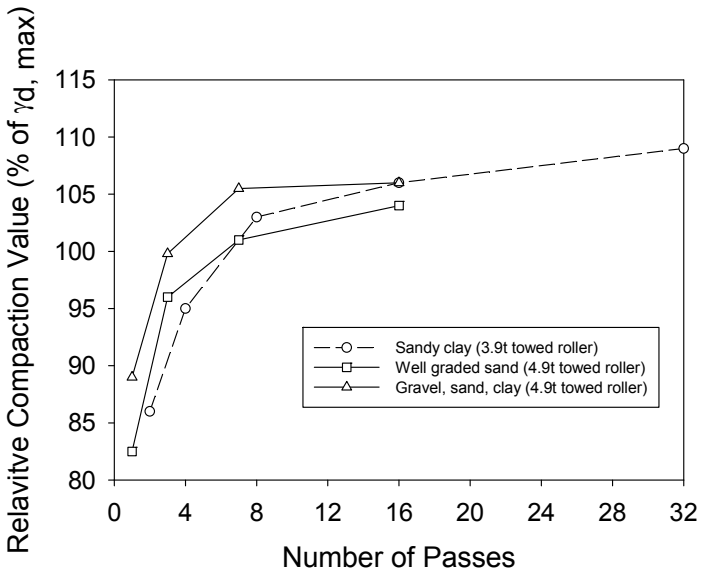


**Figure 46: Relationship between relative compaction value and number of passes for two vibratory rollers in three soils from Parsons (1992)**

Two factors which influence compaction with vibratory rollers which are unique to the machine are vibration frequency and amplitude.

Frequency is a measure of the number of complete cycles or revolutions of the weights around the axis of rotation over a given period of time. A relationship exists between frequency and working speed such that proper combination of the two can yield better results. If too high of working speed is used "wash boarding" may result, soil will not be uniformly compacted and may require more passes. If one were to use too low of a working speed, machine productivity will be negatively impacted. For each compaction application, there exists an optimum speed and frequency. Caterpillar suggests a general rule which states that frequency and/or working speed should be adjusted to yield approximately one impact per 25mm (1") of travel (Caterpillar 2000).

Amplitude is the measure of total peak-to-peak vertical movement of a vibrating drum per complete cycle. Energy is a function of amplitude; higher amplitude will result in higher energy supplied to the soil, all other things being equal (Caterpillar 2000). Therefore, in soils which require more energy applied to the soil (i.e. cohesive) it may be more efficient to use

high amplitude and low frequency settings. In soils with high amounts of sand, low amplitude and high frequency may yield better results. The frequency and dead-weight of vibratory rollers must be matched to the material being compacted: heavyweight rollers with low-frequency for gravel or rockfill, light- to medium-weight rollers with high-frequency vibrations for sands, and heavyweight rollers with low-frequency vibrations for clays (Fang 1991)

Speed is important for vibratory compaction; more so than other compactor types. The frequency of the machine determines the number of vibratory tamps in a given period of time and the speed of the machine determines the area covered by the machine for a given period of time. Therefore, if the speed of the machine is excessive relative to the frequency of vibration, the effect of vibration to the soil will be minimal; i.e. less vibration cycles per a given distance. Hall (1968), using vibratory rollers on 3 types of soils, found that in sands frequency was most important, but in clays the deadweight of the roller was of most importance.

Because a relationship exists between operating speed, frequency, and resultant compaction, slower working speeds are required for vibratory compactors. Caterpillar suggests a working speed of 3.2 – 6.4 km/h (2 – 4 mph) to provide the best results (Caterpillar 2000). As would be expected, the compactive effort of these machines is influenced by the vibrations. Tests on 3 soils (silty clay, sand, and gravel-sand-clay) using a 5,400 lb vibrating tandem roller with and without vibration found that maximum dry unit weight was increased and optimum moisture content decreased when the vibration was turned on (Johnson and Sallberg 1960).

Smooth drum vibratory compactors are most effective on granular materials such as large rocks to fine sands; they can also be used on somewhat cohesive materials which may contain up to 50 percent cohesive soil content. As with any type of machine, lift thicknesses will vary according to the machine size. However, lift thicknesses on granular materials should be relatively small (<24”) (Caterpillar 2000).

*Soil Type*

There does not yet exist one machine which can provide the best, most efficient and cost-effective compaction for any given soil type. The compaction curves presented in the previous section show the ability of different machine types to compact different types of soil. It is apparent from these curves that a given machine type will perform better in some soil types than others. However, as has been stated, at least some compaction is achieved in each soil type with each type of roller. The efficiency and degree of compaction, however, can vary greatly with machine type.

The compaction which can be achieved can vary greatly across many soil types. Clayey soils of volcanic origin may only reach 60 lb/ft$^3$ or less when completely compacted. In contrast, a well-graded sand may achieve densities on the order of 130 lb/ft$^3$ at 100% compaction (Johnson and Sallberg 1960). Figure 47 shows the laboratory compaction data for 8 different soils using the same compaction energy from Johnson and Sallberg (1960). Classification data for these eight soils is shown in Table 11. The maximum density for these soils ranges from 135 lb/ft$^3$ to 100 lb/ft$^3$ for the well graded loamy sand and poorly graded sand, respectively. Optimum moisture contents range from 7.0% for the well graded loamy sand to 21.0% for the heavy clay. It is possible (and likely) to have a combination of soil types on a given earthwork project. Therefore, it is important to select the compaction machine which will provide the most efficient results for the soils which are present for a given a site.

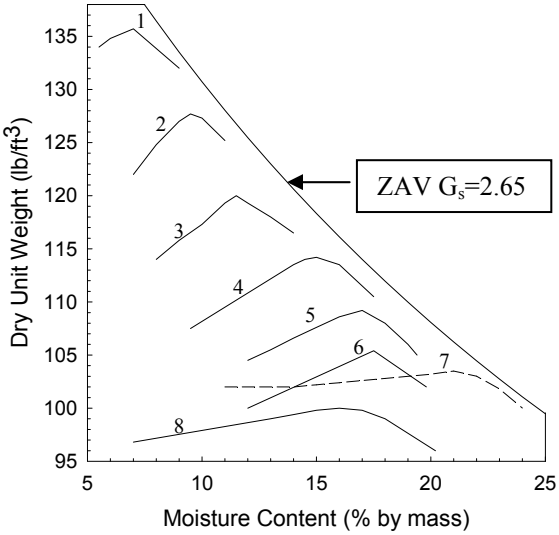


**Figure 47: Moisture content-unit weight relationships for eight soils compacted according to AASHTO Method T99 from Johnson and Sallberg (1960)**

**Table 11: Soil texture and plasticity data from Johnson and Sallberg (1960)**

| No. | Description | Sand (%) | Silt (%) | Clay (%) | LL | PI |
|---|---|---|---|---|---|---|
| 1 | Well graded loamy sand | 88 | 10 | 2 | 16 | N.P. |
| 2 | Well graded sandy loam | 72 | 15 | 13 | 16 | N.P. |
| 3 | Med. graded sandy loam | 73 | 9 | 18 | 22 | 4 |
| 4 | Lean sandy silty clay | 32 | 33 | 35 | 28 | 9 |
| 5 | Lean silty clay | 5 | 64 | 31 | 36 | 15 |
| 6 | Loessial silt | 5 | 85 | 10 | 26 | 2 |
| 7 | Heavy clay | 6 | 22 | 72 | 67 | 40 |
| 8 | Poorly graded sand | 94 | 6 | | N.P. | N.P. |

Because soils can vary through the entirety of a given project or area to be compacted it is difficult to determine the most suitable compaction machine for a given project. A standard method of machine selection has yet to be developed. Often, the selection of the machine to be used on a job is based upon engineer experience, field conditions, and/or available equipment. Rodriguez (1988) provided a table to use in the selection of compaction machines. Shown in Table 12, this provides a guide as to which types of compactors perform best in a variety of soil types; 1 is the best rating for the scale used. Caterpillar (2000) also provided a chart which provided some guidance to the selection of compaction equipment (See Figure 48).

**Table 12: Guide to the choice of compaction equipment from Rodriguez (1988)**

| Usage | Group symbol U.S.C.S. | Material | Self-driven tamper | Tractor-drawn tamper | Self-driven sheepsfoot | Tractor-drawn sheepsfoot | Small smooth vib. roller | Heavy smooth vib. roller | Small vib. sheepsfoot | Heavy vib. sheepsfoot | Light tired roller | Heavy tired roller |
|---|---|---|---|---|---|---|---|---|---|---|---|---|
| Base | | Clean granular | -- | -- | -- | -- | 1 | 1 | -- | -- | 3 | 2 |
| Sub base | | Granular-few fines | 1 | 1 | -- | -- | 1 | 1 | 2 | 2 | -- | 2 |
| Earth fill | | Rock | 2 | 2 | -- | -- | -- | 4 | -- | 5 | -- | -- |
| | GW, SP, SW | Sands, gravels | 2 | 2 | -- | -- | 1 | 1 | 2 | 2 | -- | 2 |
| | SP | Uniform sand | -- | -- | -- | -- | 1 | 1 | 2 | 2 | -- | 2 |
| | SM, GM | Silty sands or gravels | 1 | 1 | 4 | 4 | 3 | 3 | 2 | 2 | -- | 2 |
| | ML, MH | Silts | 1 | 1 | 2 | 2 | -- | -- | 3 | 3 | -- | 2 |
| | GC, SC | Clayey sands or gravels | 1 | 1 | 2 | 2 | -- | -- | 3 | 3 | -- | 2 |
| | CH, CL | Clays | 1 | 1 | 2 | 2 | -- | -- | -- | 3 | -- | 3 |

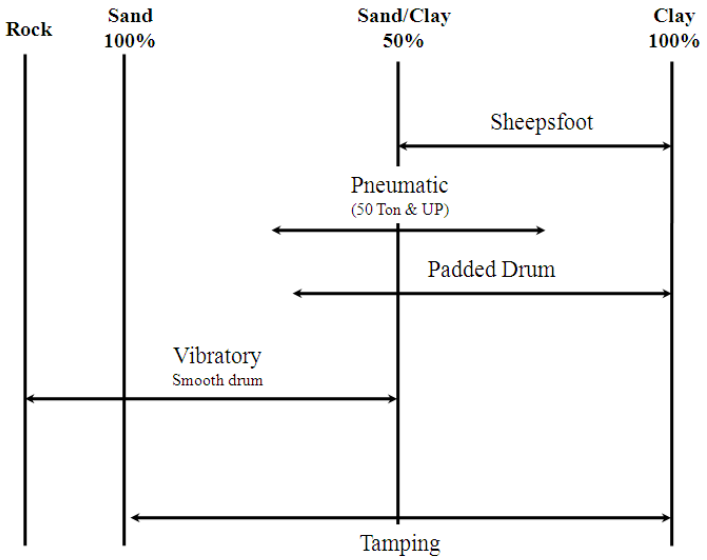


**Figure 48: Range of soil types for soil compaction equipment from Caterpillar (2000)**

*Moisture Content*

It can be argued that moisture content is the most important factor in soil compaction due to its effects on compaction and the difficultly with which it is controlled in the field. In nearly all earthwork projects, a maximum dry density and optimum moisture content are determined from laboratory testing and specified. Large deviations from the optimum moisture content may cause compaction productivity to become extensively diminished. Too little water makes it difficult for the compaction machine to overcome the frictional and chemical bonds between soil particles; too much water greatly reduces shear strength of soils and results in rutting and poor compaction. Of all the factors which the engineer/contractor has control, moisture content is of prime significance. Figure 49 and Figure 50 show the influence in moisture content for a pneumatic-tire roller in two soil types.

In Figure 49 the soil wet of optimum achieved compaction in fewer passes than the conditions near and dry of optimum. These relationships are apparent in curves from Johnson and Sallberg (1960) as well as Parsons (1992). This indicates that the field optimum moisture content may be different from that of the laboratory optimum because great compaction (dry density) was achieved with fewer passes at 18.9% moisture versus 14.4% which was close to the laboratory optimum. This does not suggest that 18.9% is the field optimum moisture content, but rather, greater compaction is achieved at a moisture content higher than that of the laboratory optimum. If decreasing compaction energy increases optimum moisture content, this would indicate that the machine is supplying less compaction energy to the soil than the laboratory compaction test.

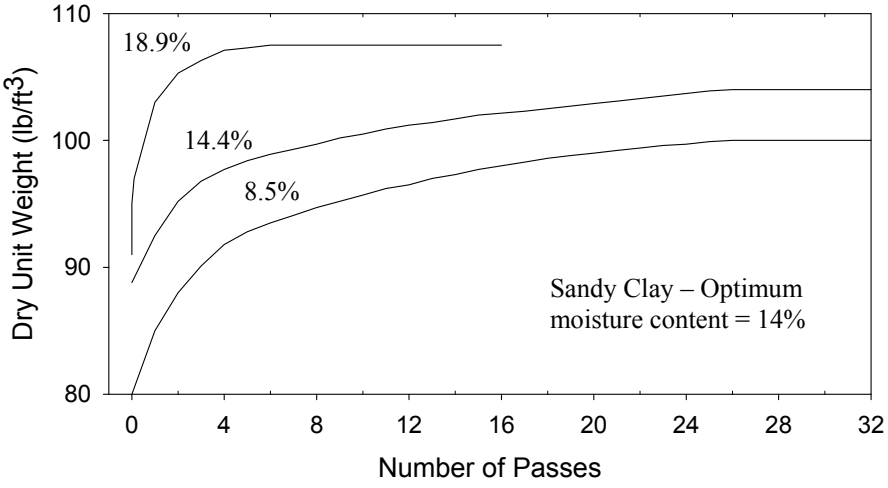


**Figure 49: Influence of moisture content on number of passes needed to obtain maximum unit weight for 13.44-ton pneumatic-tired roller on sandy clay from Johnson and Sallberg (1960)**

In Figure 50 it is the condition closest to laboratory optimum that produces the most efficient compaction. In both soils the dry of optimum condition hindered compaction; both required more passes to reach an asymptotic state and also did not achieve a density as high as the conditions for wet and near optimum. Laboratory maximum density for these soils was not given in the literature.

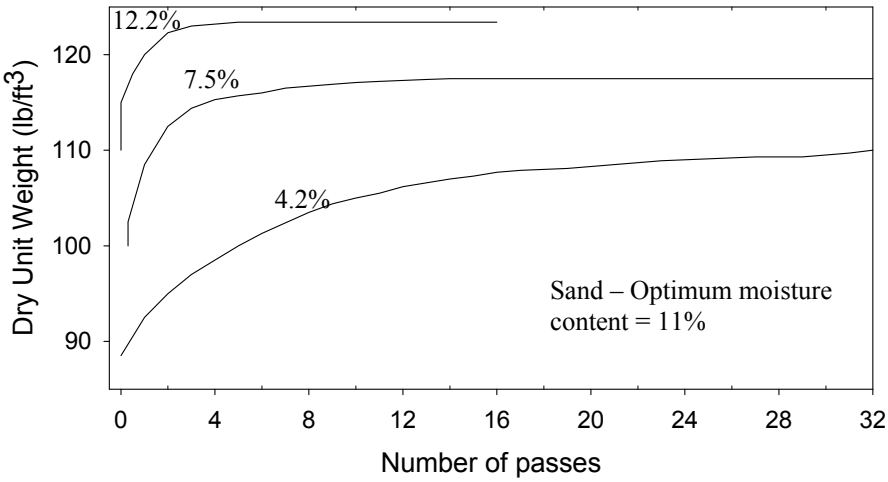


**Figure 50: Influence of moisture content on number of passes needed to obtain maximum unit weight for 13.44-ton pneumatic-tired roller in sand from Johnson and Sallberg (1960)**

*Lift Thickness*

Another factor which the engineer/contractor can control is the lift thickness or thickness of uncompacted soil which is spread in the field. In the laboratory, compaction energy is calculated in part by using the volume of soil being compacted. In the field, therefore, if a thicker lift is to be compacted, it will decrease the overall compaction energy applied to the volume of soil. If a lift is applied too thin the compactive effort will continue to be applied to the underlying layer and thus result in inefficient compaction. If the lift is applied too thick, the compaction energy may become exceptionally low and thus the entire lift may not be compacted. In some cases, the weight of the machine can cause it to rut and potentially get stuck in the uncompacted soil; the machine may also being to push or "plow" the material in front of the drum rather than compacting it. As described in the "Roller Type" section, some rollers may only compact the upper-most portion of the lift. If specific testing is not used to determine if loose underlying layers are present, this phenomena may go unnoticed.

Natrajan (1983) studied the effect of lift thickness for one roller on three soil types (See Figure 51 through Figure 53). The roller was described as an "8-10 ton conventional three-wheel roller" and the soils were a clayey sand (PI=6), a clayey sand (PI=15) and a gravel (PI=22); more information on these soils may be found in Table 8. The soils were laid in lift thicknesses varying from 10 to 45 cm (3.9 in. to 17.7 in.); density measurements were made at the top of the thin layers and at the bottom of the thick layers.

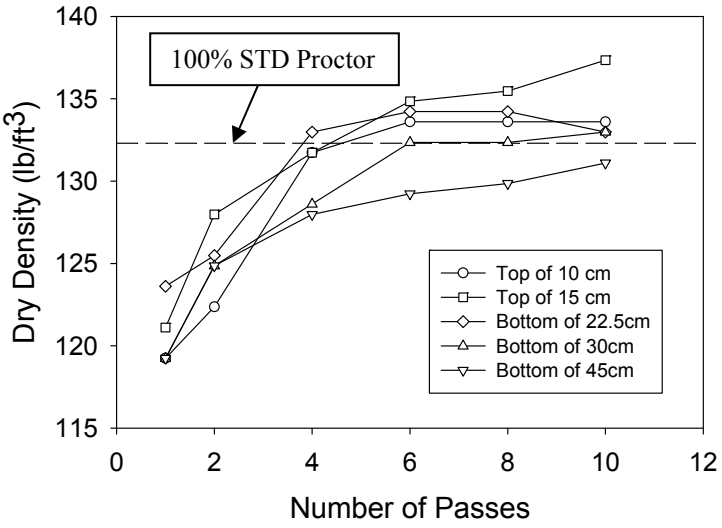


**Figure 51: Influence of lift thickness on compaction of clayey sand (PI=6) using 8-10 ton conventional three-wheel roller from Natrajan (1983)**

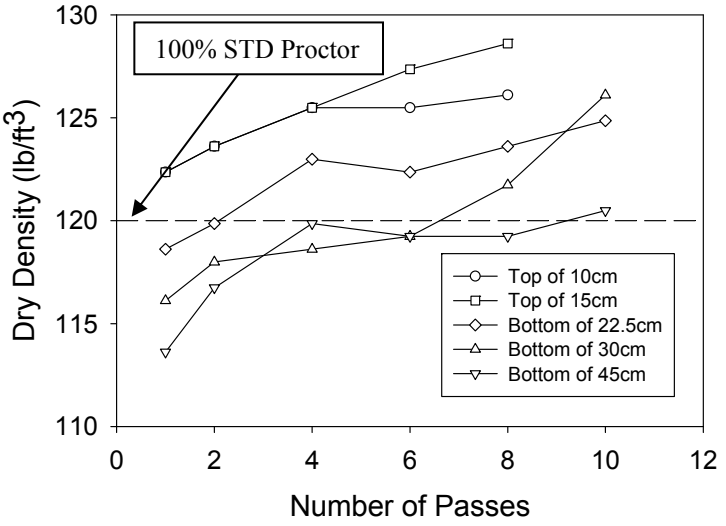


**Figure 52: Influence of lift thickness on compaction of clayey sand (PI=15) using 8-10 ton conventional three-wheel roller from Natrajan (1983)**

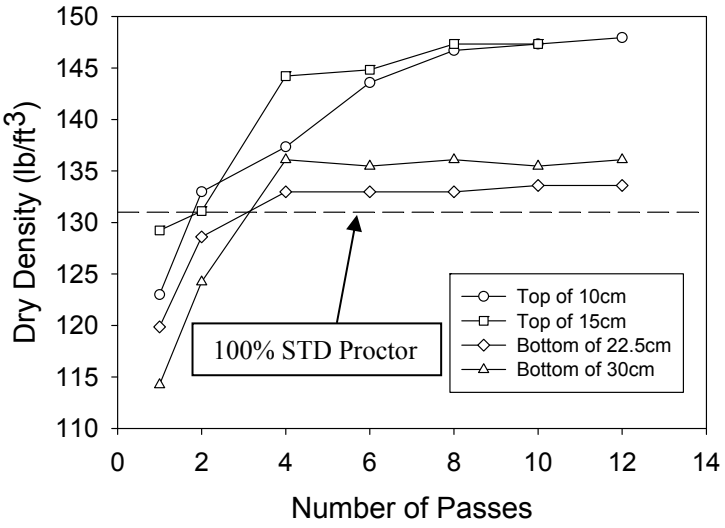


**Figure 53: Influence of lift thickness on compaction of gravel (PI=22) using 8-10 ton conventional three-wheel roller from Natrajan (1983)**

It is apparent from Figure 51 through Figure 53 that lift thickness does play a role in field compaction. In all cases, it was the thinnest lift thickness which produced the best compaction (relative to laboratory). In the case of both clayey sands the lift thickness of 45 cm did not reach 100% relative compaction at the bottom of the layer. This is indicative of the condition described earlier in which only the top-most layer is compacted in lifts which are applied too thick. Natrajan (1983) concluded that when the thickness of a soil layer is greater, the energy input by the roller per unit weight of soil will be less compared to a soil layer of smaller thickness. In each case, more passes of the machine were required for thicker lifts to achieve 100% relative compaction. Waterways Experiment Station (1957) found similar results when compacting a lean clay with a pneumatic-tire roller. In this study, it was determined that as compacted lift thickness increased, the difficulty of the roller to compact increased as well.

Therefore, it can be said that lift thickness influences field compaction of soils. As lift thickness increases, the difficulty to compact the soil will increase. However, it would seem that a balance does exist between soil type, lift thickness, and compaction machinery. In the interest of time and efficiency, the thickest lift possible should be used for a given soil and

machine in which compaction may still be achieved throughout the newly applied lift.

**Compaction Prediction Techniques**

In order to properly evaluate the ability of CFED to predict the laboratory compaction curve, it was important to review the literature to determine all available methods available which make similar predictions. Those methods found in the literature are discussed and their equations presented.

*Quadratic Model*

SoilVision 4.0 (2006) software was used to evaluate some of the methods found in the literature. This software includes a quadratic fit equation to predict the compaction curve for a given soil. As described in the SoilVision (2006) User's Manual the quadratic fit of the compaction curve is included due to the frequency of its presentation in research literature. Equation 1 displays the form used:

$$\rho_d(w) = a_q + b_q w + c_q w^2 \quad (1)$$

Where $\rho_d$ is the dry density as a function of gravimetric water content, $w$ is the gravimetric water content, and $a_q$, $b_q$, and $c_q$, are fitting parameters for the equation. SoilVision applies the quadratic fit to the given data adjusting the fitting parameters to increase the $R^2$ value to its maximum. The optimum water content and maximum dry density are determined with mathematical equations that determine the local maxima of quadratic equations. A minimum of 3 inputted points are required to use this method in SoilVision.

*Ohio Curves - Woods Model (1938)*

In 1924 the Ohio State University Engineering Experiment Station, The United States Bureau of Public Roads, and the Ohio Department of Highways began collaboration to study the various properties and characteristics of soils. Part of this investigation was the application of R. R. Proctor's (1933a, 1933b, 1933d) compaction control methods. The Ohio Department of Highways adopted the Proctor test as a quality control method for moisture and compaction of earth embankments in mid-1935. The method of testing was in accordance with ASTM D698-00a and is the same method of testing used today.

The research included density tests for 461 Ohio soil samples or approximately 1900 density tests. The researchers made note of the characteristic shape of each of the compaction curves and sought to create typical density curves for different soil types needing only one point from the laboratory compaction testing. The soil samples were divided into groups by the maximum dry unit weight achieved from testing. Divisions were made at 5-lb intervals starting with 90 $lb/ft^3$. The samples within each division were then averaged to determine a representative curve from each division. The curves which were created can be seen in Figure 54.

Woods (1938) directly states in his report that these "type curves" should not be used in place of laboratory curves actually made for the soil being used. However, he does state that they can provide an excellent method by which one may gather an estimation of values to control the placing of embankment.

For the purposes of this research, SoilVision 4.0 (2006) was again employed to determine the best fit curve. From the laboratory data the point closest to optimum moisture content and maximum density was entered into SoilVision (2006) which returned a best-fit curve. This was performed for all soils, but because the method was developed using only the Standard Proctor energy effort, only this level was estimated. It has not yet been determined how SoilVision chooses the Woods fit for a given set of data. It would seem likely that this fit is

based entirely on the regression coefficient; however, this has not been proven. Contact has been made with SoilVision to answer this query, but no response has been received at this time.

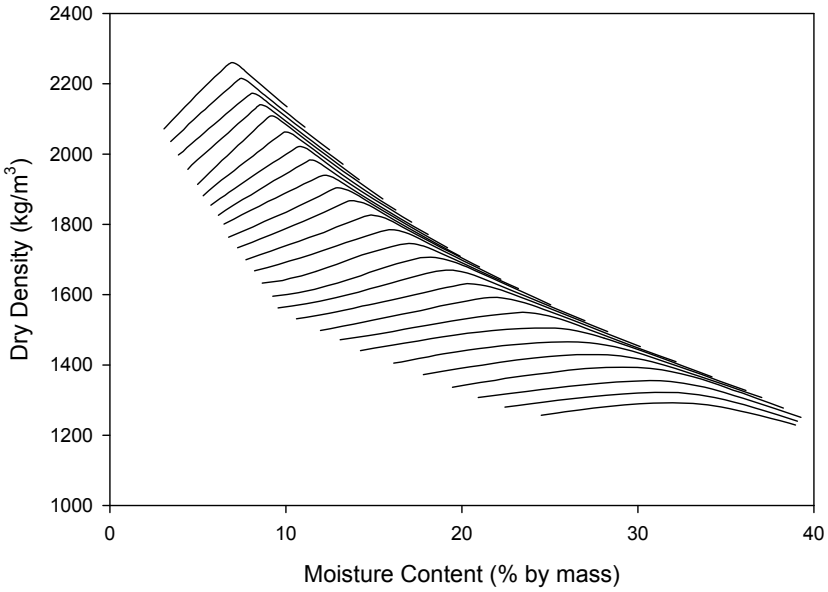


**Figure 54: Ohio Curves reproduced from SoilVision 4.0**

*Li and Sego Model*

A detailed description of Li and Sego's curve model may be found in the reports *Soil Compaction Parameters and Their Relationship with Soil Physical Properties* and also *Equation for Complete Compaction Curve of Fine-grained Soils and Its Applications*. A summary of this method is provided in this report.

Li and Sego (1999, 2000a, and 2000b) developed an equation which could be used to predict a family of compaction curves for a given fine-grained soil. This approach uses the relationship between degree of saturation and water content. The model predicts the compaction curve from dry to very wet conditions. This relationship is shown in Equation 2:

$$S = f(w) \tag{2}$$

The equation to predict the compaction curve is shown in Equation 3:

$$\gamma_d = \frac{G\gamma_w}{1 + \frac{wG}{f(w)}} \tag{3}$$

Where $\gamma_d$ is the dry density of the soil, G is the specific gravity of the soil, $\gamma_w$ is the density of water and *w* is the moisture content of the soil.

The relationship between saturation and water content is rewritten by Li and Sego in Equation 4 as:

$$S = S_m - S_m \times \left( \frac{w_m - w}{w_m} \right)^{n+1} \times \left( \frac{{w_m}^n + p^n}{(w_m - w)^n + p^n} \right) \quad \text{for } w < w_m \tag{4}$$

Where $S_m$ is the maximum saturation, $w_m$ is the moisture content at $S_m$, *n* and *p* are parameters which determine the shape and width of the compaction curve.

$S_m$ is the boundary of the model on the wet side of optimum. It can be determined from the water content vs. degree of saturation curve or from the wet side of the compaction curve running parallel to the zero air void curve as shown in Figure 55. $S_m$ usually remains constant and does not change as the compactive effort changes (Seed et al 1960, Lee and Haley 1968). The boundary on the dry side of optimum is the dry density ($\gamma_{dd}$). Because the dry density at very dry conditions remains nearly constant it is assumed that $\gamma_{dd}$ is the lowest density possible for a given soil. The dry density remains approximately constant until it reaches a value referred to as the compaction sensitivity threshold (CST). As shown in Figure 56, the CST occurs at a point where the saturation versus moisture curve departs from its initial linear growth and begins to curve toward a new linear slope. Figure 55 also

displays a technique to locate the CST point on a compaction curve for a given soil proposed by Li and Sego. The slope of the approach line has been defined as:

$$k = \frac{1}{\frac{\gamma_w}{\gamma_{dd}} - \frac{1}{G}} \tag{5}$$

The CST point is determined by drawing a line from point M (the point of maximum dry density), tangent to the initial portion of the curve to the origin O. Another line is drawn tangent to the upper portion of the S-*w* curve. A line drawn parallel to the X-axis to intersect with the curve; this is the CST point. This point is used to predict the family of curves as the $S_{CST}$ value appears to remain constant for a given soil compacted with different energy efforts (Faure 1994, Li and Sego 1998). $S_{CST}$ can also be derived from the following, Equation 6:

$$S_{CST} = S_m - kp \cdot \left(\frac{n+1}{n-1}\right)^{\frac{n+1}{n}} \tag{6}$$

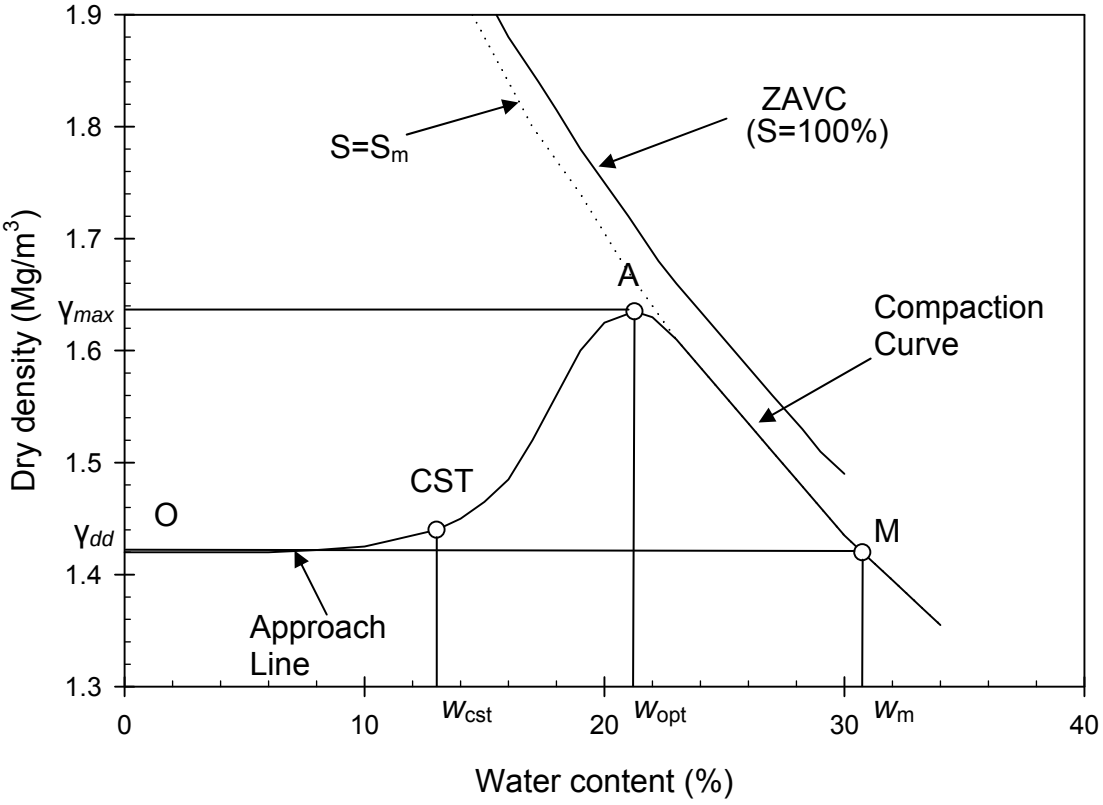


**Figure 55: Density curve reproduced from Li and Sego (1999)**

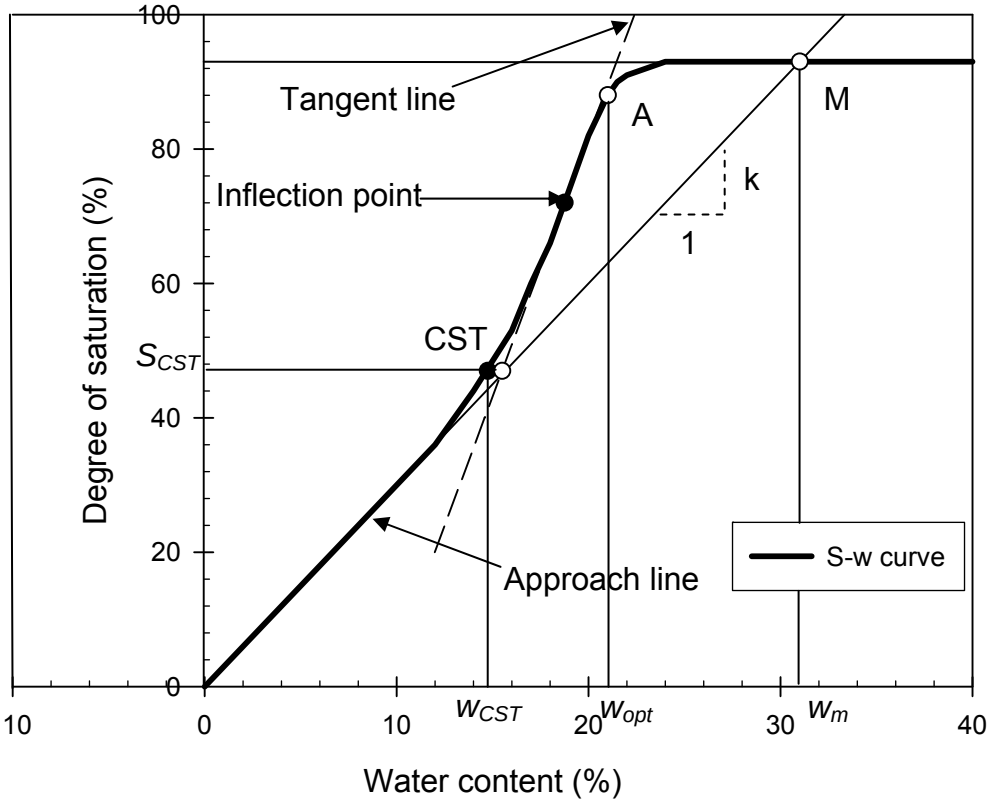


**Figure 56: Saturation vs. moisture curve reproduced from Li and Sego (1999)**

The parameter *n* is referred to as the shape factor. The shape factor affects the dome portion of the compaction curve; as *n* is increased the dome of the curve becomes sharper whereas when *n* is decreased the curve tends to flatten and become less exaggerated. When a given soil is compacted using the same method at different energy levels a series of curves is created. Generally, each of these curves maintains the same shape. Because a series of curves maintains a given shape the same value of *n* can be used for the entire family of curves.

The parameter *p* influences the width of the upper portion of the curve, also referred to as the index of the compactable moisture range. Parameter *p* allows the equation to define the size of this range without changing its shape factor (*n*) and boundary conditions (defined by $S_m$

and $\gamma_{dd}$). Parameter $p$ is directly related to $w_{CST}$ of a soil through the following relationship: $p = w_m - w_{CST}$. Because the maximum degree of saturation does not generally change for a given fine-grained soil, assumptions can be made which can permit simple calculation of $p$. Given Equation 7, only one test is necessary to create the entire compaction curve for a given soil and compactive effort:

$$kp = \frac{S_m}{w_m} \cdot p = const. \tag{7}$$

Li and Sego (1999) suggested a graphical method to determine both $n$ and $p$. Parameter $n$ is determined as shown in Figure 57. The procedure is as follows: from origin O, draw a tangent line on the S-$w$ curve to point A (point of maximum dry density), or use the optimum water content ($w_{opt}$) obtained from the compaction curve. Extend the line MA to cross the X-axis at point B. The calculation then becomes:

$$n = \frac{nw_{opt}}{w_{opt}} = \frac{BM'}{OA'} \tag{8}$$

Parameter $p$ is determined by a similar method shown in Figure 58. Point C has coordinates $(0,S_m/2)$. A line (MC) is drawn from point C to point M (point of maximum dry density). Parameter $p$ is the distance between point D, which intersections the S-$w$ curve, and point M. It is important to note that to determine both $n$ and $p$, both axes for each graph must be the same scale. Parameter $n$ is unit less and parameter $p$ is expressed as a percentage; for the soil shown, $n$ is 5 and $p$ is 12%.

Employing Equations 1 through 7, a family of prediction curves can be created with only one Proctor test at each energy level desired. First, four parameters ($n$, $p$, $S_m$, and $w_m$) can be found for the family of curves. Assuming $n$ and $S_m$ remain constant for all levels of compaction a compaction test on an air-dried sample are required to determine $\gamma_{dd}$ at a given energy level. From this, $k$ and $w_m$ can be calculated. Parameter $p$ can then be obtained using

Equation 6. With all the parameters for the family of curves known, Equation 3 can be used to create the entire family of curves.

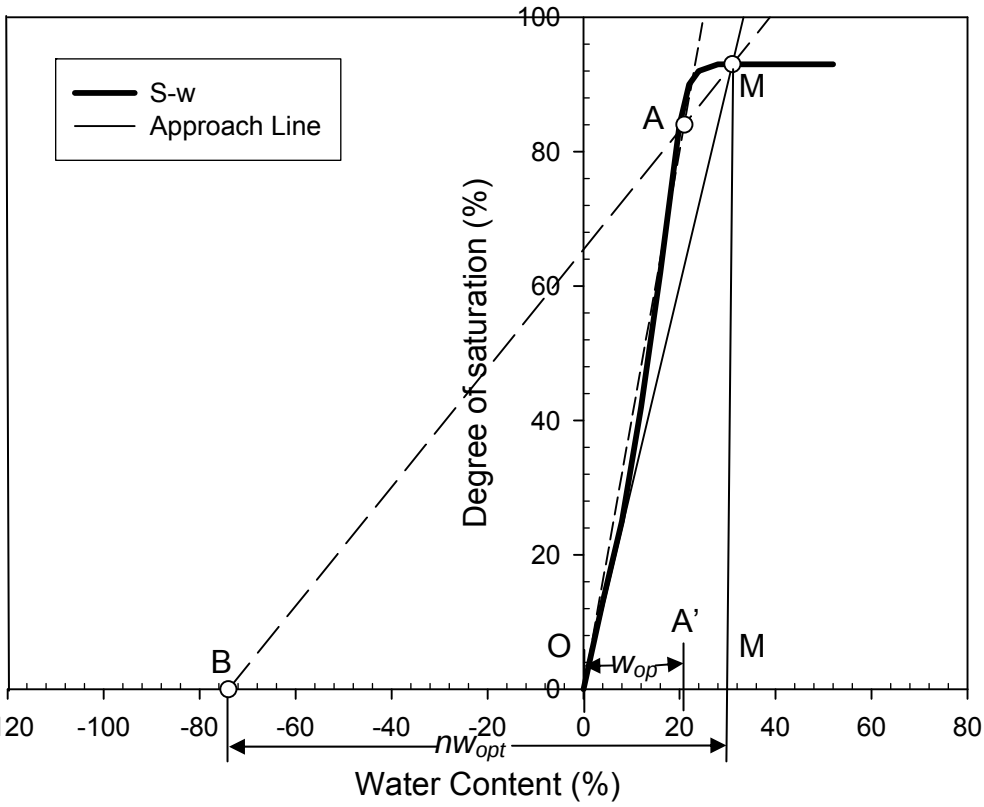


**Figure 57: Determination of parameter *n* reproduced from Li and Sego (2000)**

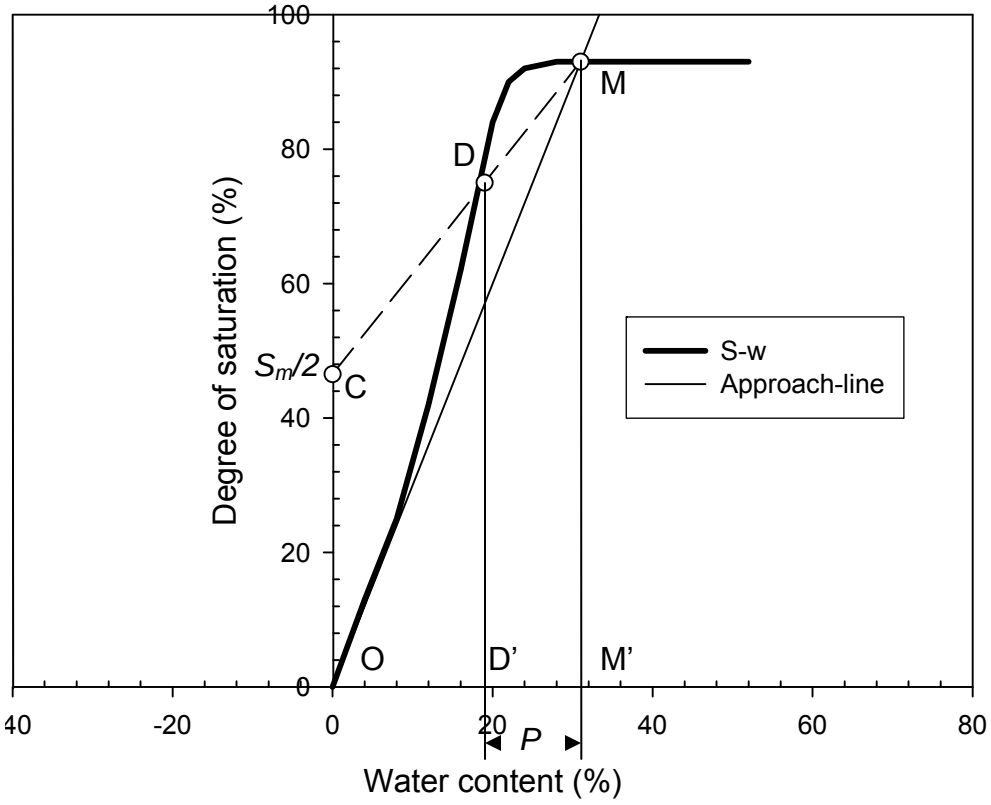


**Figure 58: Determination of parameter p reproduced from Li and Sego (2000)**

For the purposes of this study the program SoilVision 4.0 was used to create the Li and Sego prediction curves. By inputting the Proctor test data (ASTM D698-00a) into the program, a best-fit curve is created using a nonlinear regression method; a minimum of 4 points are required to create the compaction curve for a given soil in SoilVision. The form of Li and Sego's prediction is a combination of Equations 1, 2, and 3 and is shown here as Equation 9:

$$\rho_d(w) = \frac{G_s \rho_w}{\left(1 + \frac{wG_s}{S_m - S_m \cdot \left(\frac{w_m - w}{w_m}\right)^{n+1} \cdot \left(\frac{w_m^n + p^n}{(w_m - w) + p^n}\right)}\right)} \tag{9}$$

All parameters in Equation 9 are the same as described previously. However, rather than determine the actual values of *n* and *p*, SoilVision uses the regression analysis to determine the values of *n* and *p* which create the best fit for the data given. The SoilVision program allows the user to output the data from the prediction curve, but requires that at minimum of 4 points be input into the program. This is a contradiction to the literature; Li and Sego require only one point to per energy level to create a family of compaction curves. All curves obtained using the Li and Sego approach were created using the SoilVision program.

*Caterpillar's Liqun Model*

Liqun Chi, a senior engineering specialist with the Caterpillar Inc. company, recently developed a method to predict a family of compaction curves. His method is employed in the Compaction Forecasting Expert Database (CFED) program. The model itself is similar to Li and Sego's method with some differences. In this method, saturation is also determined as a function of water content and dry density is determined using an equation similar to Li and Sego's. Equations 10 through 14 display the equations used in the CFED model for a constant energy level.

$$S = \frac{S_m w}{w + f_w(w)} \tag{10}$$

where $f_w(w) = \frac{(1 + b_2^2)}{c(e^{cw} + b_2)}$

$$\rho = \frac{G_s \rho_w}{1 + G_s \frac{(w + f_w(w))}{S_m}} \tag{11}$$

where $f_w(w) = \frac{(1 + b^2)}{c(e^{cw} + b)}$

$$w_{opt} = \frac{\ln(b^2)}{c} \tag{12}$$

$$S_{opt} = \frac{S_m b \ln(b^2)}{1 + b + b\ln(b^2)} \tag{13}$$

$$\rho_{opt} = \frac{G_s \rho_w S_m bc}{G_s\left[1 + b + b\ln(b^2)\right] + S_m bc} \tag{14}$$

Similar to SoilVision, CFED uses a nonlinear regression method to fit parameters b, $b_2$, and c to create the best fit curve for the given data. Proctor lab data are input into CFED with corresponding compaction energies for the tests performed (standard, modified, sub-standard, etc). CFED determines the best fit prediction curve and it is displayed with the lab data to present the accuracy of the model. For determination of curves with multiple energy levels Equation 15 and 16 are used for 3 or more energy levels and only 2 energy levels, respectively.

$$c = \frac{1}{c_1 + c_2 e^{-KE}} \tag{15}$$

$$c = c_1 + c_2 E \tag{16}$$

*Blotz's Atterberg Limits Model*

Blotz et al. (1998) developed a method to predict the maximum dry density and optimum moisture content using the Atterberg limits for clayey soils. Their research used the linear relationship between maximum dry density ($\gamma_{d\,max}$) and log *E* (Energy) and also found a linear relationship between optimum moisture content ($w_{opt}$) and log *E*. Using these relationships, two sets of equations (referred to here as Method A and Method B) were created to predict $\gamma_{d\,max}$ and $w_{opt}$ for a given soil at four energy levels. Method A requires the liquid limit (LL) of the soil as well as $\gamma_{d\,max}$ and $w_{opt}$ for one energy level (most commonly,

the standard Proctor level 592 kJ/m$^3$). Equation 17 and 18 show the two prediction equations for Method A:

$$\gamma_{d\,\max,E} = \gamma_{d\,\max,k} + [2.27\log(LL) - 0.94]\log\left(\frac{E}{E_k}\right) \quad (17)$$

$$w_{opt,E} = w_{opt,k} + [12.39 - 12.21\log(LL)]\log\left(\frac{E}{E_k}\right) \quad (18)$$

In Method A, the maximum dry density of a soil at any energy level, E, can be predicted using LL, maximum dry density at a known energy level ($\gamma_{d\,max,k}$) and the energy at that level ($E_k$). The same method is used to predict optimum moisture content with known LL, optimum moisture content ($w_{opt,k}$) and the energy at that level ($E_k$).

Method B uses similar equations, but only the LL is required to predict $\gamma_{d\,max}$ and $w_{opt}$; shown in Equation 19 and 20. Only the energy at the level desired, E, and LL are input to prediction $\gamma_{d\,max}$ and $w_{opt}$.

$$\gamma_{d\,\max,E} = [2.27\log(LL) - 0.94]\log E - 0.16LL + 17.02 \quad (19)$$

$$w_{opt,E} = [12.39 - 12.21\log(LL)]\log E + 0.67LL + 17.02 \quad (20)$$

Blotz et al. (1998) found that the errors associated with Method A to be ±1% for $w_{opt}$ and ±2% for $\gamma_{dmax}$. Method B, as suggested by the authors, should only be used to obtain a rough estimate of $\gamma_{d\,max}$ and $w_{opt}$. The authors also suggested some limitations on Equations 15 through 18; these equations should only be used for a range of LL similar to the soils within the study ($17 \leq LL \geq 70$) and only for the following energy levels: supermodified Proctor (5386.4 kJ/m$^3$), modified Proctor (2693.6 kJ/m$^3$), standard Proctor (592.5 kJ/m$^3$), and reduced Proctor (355.5 kJ/m$^3$).

**Connecting Lab Compaction to Field Compaction**

Since Proctor's essays in 1933, the maximum density and optimum moisture content determined from laboratory testing has become a standard for specification in earthwork projects. Many times, however, compaction achieved in the laboratory is not indicative of what is achieved in the field. Efforts have been made to find some connection between compaction energy applied in the laboratory to compaction energy applied in the field.

Proctor (1948) attempted to connect his standard laboratory compaction test to field compaction. He used drawbar pull, number of passes, depth of fill and width of roller to calculate field compaction energy in lb-ft/ft$^3$ for a towed sheepsfoot roller. He then compared the compaction energy required in the laboratory versus that required in the field to achieve a given density for six soils. He found that in all cases, the compaction energy required to achieve a given density was equal to or higher in the field than in the lab. He concluded, therefore, that more compaction energy is supplied to the soil by machines in the field than in the laboratory compaction test.

**Table 13: Relationship between laboratory and field compaction for a towed sheepsfoot roller from Proctor (1948).**

| Soil | Relationship |
|---|---|
| Light brown silty sand | $E_{FIELD}=E_{LAB}$ |
| Brown clay | $E_{FIELD}=1.27\ E_{LAB}$ |
| Red sand mixed with silty clay-pebbles and gravel | $E_{FIELD}=1.10\ E_{LAB}$ |
| Silty clay and sand | $E_{FIELD}=1.12\ E_{LAB}$ |
| Reddish-brown-silty clay and sand | $E_{FIELD}=1.01\ E_{LAB}$ |

Johnson and Sallberg (1960) compacted five soil types (heavy clay, silty clay, sandy clay, sand and gravel-sand-clay) and found that for a three-wheel smooth-drum roller, the greatest differences between maximum roller and maximum laboratory dry unit weights were for sand and gravel-sand-clay. For this same study, it was determined that the greatest differences between roller optimum and laboratory optimum moisture content were found in the clayey soils. In this case, the roller optimum was 6 to 7 percent less than corresponding values. This would indicate that the compaction energy in the field is greater than that in the laboratory.

Johnson and Sallberg (1960) had similar results with sheepsfoot rollers compacting four soil types similar to that in the smooth-drum study. Field values for "full compaction" were greater than laboratory values which indicated a higher compactive effort from the roller than from laboratory testing. These authors also studied this effect for pneumatic-tire and vibratory rollers. Similar to other tests, it was determined that the maximum densities and optimum moisture contents were higher for the pneumatic-tire field roller than for the laboratory compaction test. Results for the vibratory roller were, however, inconclusive. This may be largely due to the different modes of compaction. In the previous case of smooth-drum, pneumatic-tire and sheepsfoot rollers, the mode of compaction, while different, is still somewhat similar to the laboratory mode. For vibratory compactors, the mode in which compaction energy is applied to the soil is greatly dependent upon frequency and amplitude and therefore can be expected to bare little relationship to laboratory impact compaction.

The calculation of field compaction energy has proved to be a very difficult task. Caterpillar (2001) received a patent for the calculation of field compaction energy. The calculation is shown in Equation 21:

$$\text{CE}=\frac{\text{T}}{\text{R x W}} \quad CE=\frac{R}{TxW} \quad CE=\frac{R}{T*W} \tag{21}$$

Where CE is compaction energy, T is the lift thickness, R is machine rolling resistance, and W is the compaction width. This method of calculating compaction energy makes use of machine-mounted measuring systems to calculate both the rolling resistance and the lift thickness. However, this technology is still in the development stage and has yet to be applied to field compaction.

Selig (1971) published an extensive essay meant to quantitatively evaluate compactor performance. The purpose of the research was to develop a method in which different

compaction machines (smooth-drum, pneumatic-tire, tamping (sheepsfoot) and vibratory) could be evaluated, their performance predicted and a more precise method of machine selection made. Similar to earlier discussion, often machine selection is based upon experience and availability. Equations developed by Selig for each machine type are shown in Table 14 and the description of parameters is provided in Table 15.

**Table 14: Machine compaction energy equations from Selig (1971)**

| Roller Type | Equation |
|---|---|
| Smooth Wheel | $E=\frac{f\,W\,P}{B\,t}$ |
| Pneumatic-Tire | $E=\frac{f\,W\,P}{h\,t}$ or<br>$E=\frac{f\,W\,P}{B\,t}$ if $d < 2b$ |
| Tamping | $E=\frac{f\,W\,\Pi\,(D+2l)}{k_o\,t\,c\,N\,A}$ or<br>$E=\frac{f\,W\,P}{B\,t}$ (if average compaction is specified) |
| Vibratory | $E=\frac{375\,H_v\,P}{S\,B\,t}$ or<br>$E=\frac{f\,W\,P}{B\,t}$ with $f=\frac{375\,H_v}{W\,S}$ |

**Table 15: Symbol description and units from Selig (1971)**

| Symbol | Description (Dimension) |
|---|---|
| A | Contact area of tamping foot ($ft^2$) |
| B | Roller width (ft) |
| b | Width of tire (ft) |
| c | Foot area correction factor (>1.0) |
| D | Roller drum diameter (ft) |
| d | Center-to-center tire spacing (ft) |
| E | Compactive effort per unit volume ($ft\text{-}lb/ft^3$) |
| f | Coefficient of compaction |
| H | Horsepower |
| $H_v$ | Horsepower of vibrator engine |
| h | n b for d > 2b<br>B = b+(n-1)d for d<2b |
| $k_o$ | Overlap correction factor (<1.0) |
| l | Tamping foot length (ft) |
| N | Number of tamping feet |
| n | Number of tires |
| P | Number of passes |
| S | Forward speed (mph) |
| t | Compacted lift thickness (ft) |
| W | Total weight (lb) |

Difficulty with developing direct correlations between lab and field compaction energy has been an issue since the implementation of Proctor's (1933a) method for lab compaction. This correlation is difficult because there are many variables in both lab and field compaction that cannot be completely accounted for. These include: boundary condition, method of compaction and calculation of energy among others. Figure 59 and Table 16 show some of these parameters and how they affect the correlation.

In the lab, the boundary condition is well-defined; energy is applied to a known volume of soil. In the field, however, this influence is unknown and very difficult to define. Another issue with the boundary condition in the lab is how much energy is actually input into the soil. For example, in very wet tests, the hammer will penetrate completely through the soil and impact the bottom of the mold. In this case energy is being applied to the mold and not to the soil.

The method of compaction is also different between lab and field. In the lab, compaction energy is typically applied via impact, although, it can be applied through static, vibratory, kneading, or gyratory action. The focus of this document is, however, impact compaction. In the field, compaction is achieved via any combination of impact, kneading and/or vibratory methods. Therefore, it is difficult to directly correlate lab compaction to field compaction because the way in which the soil is being compacted is completely different. It is rare that field compaction is ever achieved simply by impact; as is almost always the case in the laboratory.

Finally, the actual calculation of compaction energy is different for lab and field compaction. Lab compaction is very controlled and compaction energy can be calculated from known parameters. In the field, however, a proven method is yet to be developed in which machine compaction energy can be absolutely determined. This issue is highly dependent upon the boundary conditions; the volume of soil over which field compaction energy is applied will change dependent up roller type, moisture content, lift thickness, etc. Therefore, if a direct correlation is to be made for lab and field compaction, an absolute method of field compaction energy calculation must be developed.

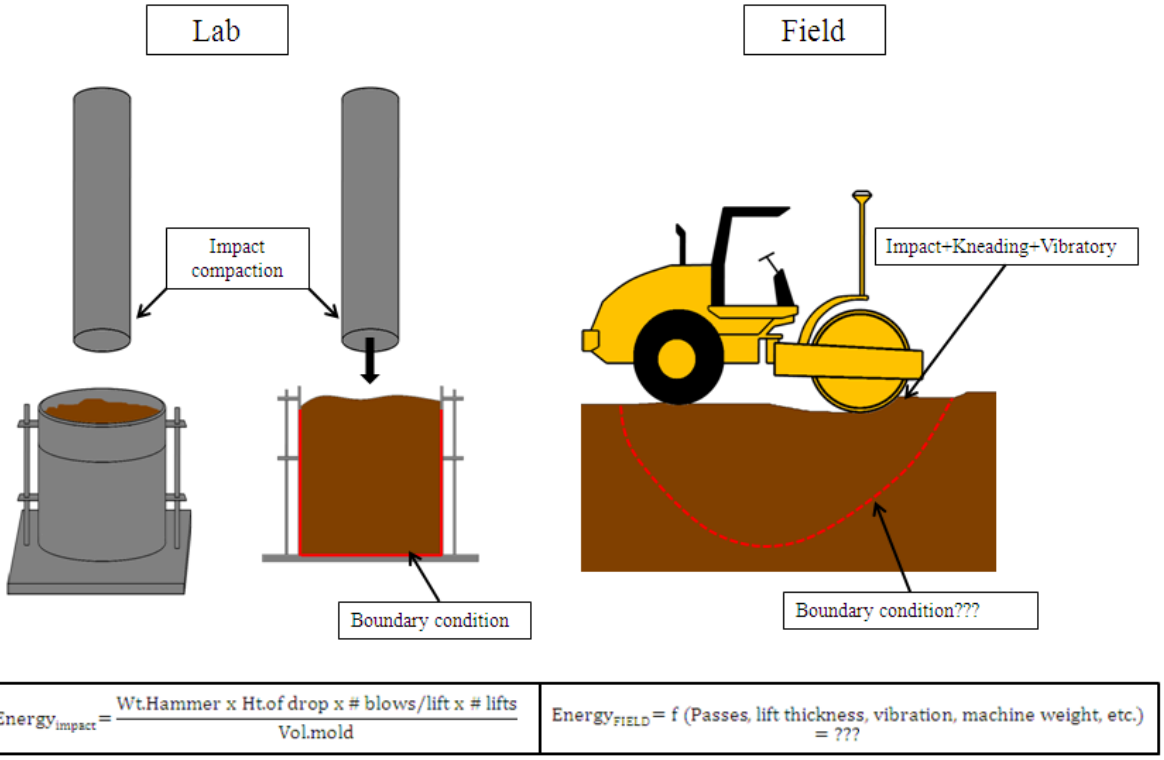


**Figure 59: Complexity with developing correlation between lab and field compaction**

**Table 16: Lab and field compaction parameters**

| Parameter | Laboratory | Field |
|---|---|---|
| Method of compaction | Impact (typical) | Impact, Kneading, and/or Vibratory |
| Compaction energy | Known | Unknown |
| Boundary condition | Known | Unknown |
| Scale of compaction | 1/30 $ft^3$ | 1000 $ft^3$+ |
| Moisture Content | Controlled | Somewhat controlled |
| Lift thickness | Controlled | Somewhat controlled |
| Soil variability | Limited | Unlimited |

# CHAPTER 4. RESEARCH METHODOLOGY

## Laboratory Testing Methods

Description of standard laboratory and field testing provided here is adopted from White et. al (2007d,e).

*Soil Index Properties*

Particle-size analysis was conducted in accordance with ASTM D422-63(2002). Coarse grained particle-size analysis was performed by washing about 2000 grams of air-dried soil over a No. 10 sieve, oven drying the retained soil, and sieving through the 1 inch, 0.75 inch, 0.375 inch, and No. 4 sieve sizes. Fine-grained particle-size analysis was performed using the hydrometer method with an air dried sample of about 70 grams passing the No. 10 sieve. After completing the hydrometer test, the suspended material was washed through the No. 200 sieve. The material retained on the No. 200 sieve was then oven dried and sieved through the No. 40 and No. 100 sieve sizes.

Atterberg limits were determined in accordance with ASTM D4318-05. Representative samples for the Liquid Limit and Plastic Limit tests were prepared using the "wet preparation" method by screening the sample through the No. 40 sieve using a spatula. Liquid limit tests were performed according to Method A (multi-point liquid limit method).

Based on the Atterberg limits and particle size analysis test results, the soils were classified according to AASHTO and Unified Soil Classification System (USCS).

Specific gravity was determined in accordance with ASTM D 854-06. Representative samples for the test were prepared and tested according to Method A – Procedure for oven-dried specimens.

*Soil Compaction Characteristics*

**Impact Compaction.**

Laboratory impact compaction tests were performed in accordance with the ASTM D 698–00, and the ASTM D 1557–02 standard test procedures. The appropriate test method (i.e. mold size) was identified from particle size distribution criteria. In addition to standard compaction energy (592 kN-m/m$^3$) and modified compaction energy (2693 kN-m/m$^3$), compaction tests on some soils were performed at lower and intermediate compaction energy levels (Table 17). The impact compaction energy is determined using Equation 22 (Proctor 1948). The purpose of performing tests at multiple energies is to derive relationships between moisture content, dry unit weight, and compaction energy. An automated, calibrated mechanical rammer (See Figure 60) was used to perform these tests.

**Figure 60: Automated mechanical rammer for impact compaction test**

$$\text{Energy}_{\text{impact}} = \frac{\left(\begin{matrix}\text{number of blows}\\ \text{per layer}\end{matrix}\right)\times\left(\begin{matrix}\text{number of}\\ \text{layers}\end{matrix}\right)\times\left(\begin{matrix}\text{weight of}\\ \text{hammer}\end{matrix}\right)\times\left(\begin{matrix}\text{height of}\\ \text{drop hammer}\end{matrix}\right)}{\text{Volume of mold}} \quad (22)$$

**Table 17: Laboratory Compaction Methods**

| Energy Name | Compaction Energy (kN-m/m$^3$) | Lifts | Blows/ Lift | Hammer Weight (kN) | Drop Height (m) |
|---|---|---|---|---|---|
| Sub-Standard (SS) | 355 | 3 | 15 | 0.024 | 0.305 |
| Standard (S) | 592 | 3 | 25 | 0.024 | 0.305 |
| Super-Sub-Modified (SSM) | 987 | 5 | 25 | 0.024 | 0.305 |
| Sub-Modified (SM) | 1481 | 5 | 25 | 0.024 | 0.457 |
| Modified (M) | 2693 | 5 | 25 | 0.044 | 0.457 |

**Field Testing Methods**

The calibrated nuclear moisture-density gauge provided a rapid measurement of soil dry unit weight and moisture content. The Humboldt HS-5001B122 device is shown in Figure 61. Following ASTM WK218, two measurements of moisture and dry unit weight at a particular location were averaged.

**Figure 61: Nuclear moisture density gauge**

The dynamic cone penetrometer (DCP), shown in Figure 62, is a testing device that provides the stability characteristics of pavement layers. The test involves dropping an 8-kg hammer 575 mm (i.e. drop height) and measuring the penetration rate of a 20-mm-diameter cone. Penetration index, which typically has units of mm per blow, is inversely related to penetration resistance (i.e. soil strength). DCP testing is discussed in literature (Burnham and

Johnson 1993; Gabr *et al*. 2000; Livneh *et al*. 2000; Siekmeier *et al*. 2000; Gabr *et al*. 2001; Konrad and Lachance 2001; Amini 2004; Ampadu and Arthur 2006) with a general focus of correlating DCP index to other measures of pavement performance (e.g. CBR, modulus). The following relationships have previously been proposed in ASTM D 6951-03:

$$CBR = \frac{292}{(DCPI)^{1.12}}, \text{ all soils except for CH and CL soils with CBR} < 10 \quad (23)$$

$$CBR = \frac{1}{(0.017019 \cdot DCPI)^2}, \text{ CL soils with CBR} < 10 \quad (24)$$

$$CBR = \frac{1}{(0.002871 \cdot DCPI)}, \text{ CH soils} \quad (25)$$

**Figure 62: Strength determination using dynamic cone penetrometer**

Clegg impact hammers, which were developed by Clegg during the late 1970's and later standardized as ASTM D 5874-02 for evaluating compacted fill and pavement materials, are shown in Figure 63. The Clegg impact value is derived from the peak deceleration of a 4.5-kg or 20-kg hammer free falling 450 mm in a guide sleeve for four consecutive drops. Clegg impact values ($CIV_{4.5\text{-kg}}$ or $CIV_{20\text{-kg}}$) have been correlated to CBR (Clegg 1986).

$$CBR = (0.24IV + 1)^2 \quad (26)$$

**Figure 63: Strength determination using Clegg Impaction testers: 4.5-kg (left) and 20-kg (right)**

Two light weight deflectometers (LWDs) were used to determine elastic modulus. In performing the tests with the Keros model, a 10-kg weight is dropped to produce a dynamic load on a plate. A load sensor measures the load pulse, and a geophone at the center of the plate measures the corresponding soil deflection. For the Zorn ZFG model, a plate stress is assumed based on calibration of the falling weight, and plate deflection is obtained from an accelerometer. For both devices, soil modulus is then calculated as:

$$E_{LWD\text{-}K2(DH)} \text{ or } E_{LWD\text{-}Z2(DH)} = \frac{f\,(1-\nu^2)\cdot\sigma_0\cdot r}{h_0} \quad (27)$$

where $E_{LWD\text{-}K2}$ = elastic modulus from 200-mm Keros device, $E_{LWD\text{-}Z2}$ = elastic modulus from 200-mm Zorn device, DH = drop height in cm, $\nu$ = Poisson's ratio ($\nu$ = 0.40), $\sigma_0$ = peak applied stress at surface, $r$ = plate radius, $h_0$ = peak plate deflection, and $f$ is a factor that depends on the stress.

**Figure 64: 300-mm light weight deflectomoeters: Zorn ZFG (left) and Keros (right)**

The soil stiffness gauge (see Figure 65) may be the least destructive device for obtaining the in-situ deformation characteristics of soil. The device, which is also referred to as the GeoGauge, rests on the soil surface and vibrates at 25 frequencies ranging from 100 to 196 Hz. The vibrating device produces small dynamic forces and soil deflections, from which soil modulus can be calculated as (Humboldt Mfg. Co. 2000):

$$E_{SSG} = \frac{F}{\delta} \cdot \frac{(1-\nu^2)}{(1.77R)} \qquad (28)$$

where F is a dynamic force caused by the vibrating device, □ is the deflection measured with a geophone, $\nu$ is Poisson's ratio, and R is the radius of the annular ring. Only modulus from the soil stiffness gauge ($E_{SSG}$) was used for developing correlations with other soil properties, because stiffness and modulus from the SSG are related through a linear relationship, dependent on Poisson's ratio ($\nu = 0.40$) and the diameter of the annular ring of the device (Humboldt Mfg. Co. 2000).

**Figure 65: Modulus determination using soil stiffness gauge**

Displacement-controlled static plate load tests were performed for soil modulus ($E_{PLT}$) using a 300-mm plate, a 90-kN load cell, and three 50-mm linear voltage displacement transducers (LVDT). Elastic modulus ($E_{PLT}$) was calculated with equation 29. The soil modulus was determined using the straight-line portion of the test data. (See Figure 67).

**Figure 66: Static plate load test performed for modulus determination using 300-mm plate, load cell, and three displacement transducers**

$$E_{PLT} = \frac{f\,(1-\nu^2)\cdot\Delta\sigma\ \cdot r}{\Delta h} \qquad (29)$$

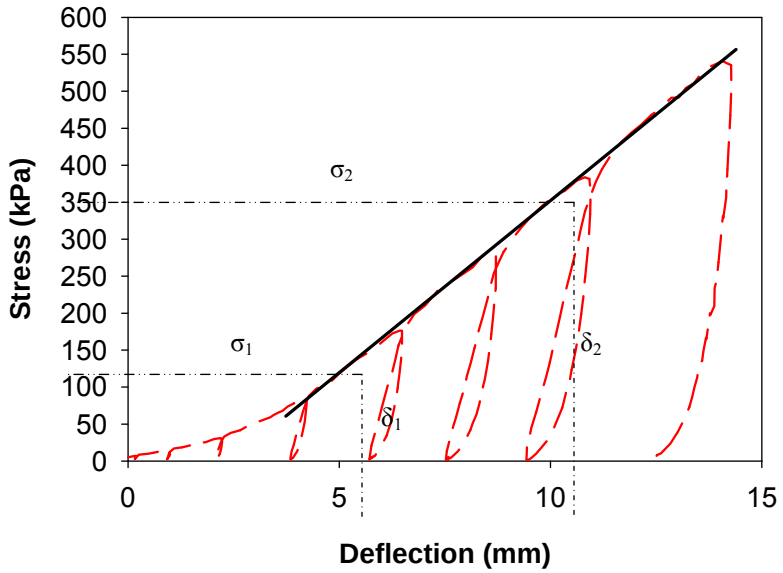


**Figure 67: Determination of $E_{PLT}$**

# CHAPTER 5. OVERVIEW OF FIELD INVESTIGATIONS

This section provides a brief overview of each field project summarizing construction operations, type of rollers, in-situ tests, soil conditions, etc. Some of the descriptions provided are not yet published works. However, they are the result of project reports and personal communication with Dr. David White and Pavana Vennapusa. References, when known, are provided.

## Field Evaluation of Compaction Monitoring Technology: Phase I (Sep. 2003 to Jul. 2004) (White et al. 2004)

*Proving Ground (PPG) Field Test, Peoria, IL*

Six test strips constructed at the PPG field test site were identified as 1A through 3B. The number represents the number of passes by the compactor that each test strip experienced, and the letters indicate A for reverse direction and B for forward direction. Preparation for the site consisted of aerating the soil with a dozer ripper to a loose lift thickness of 20 to 25 cm. Test strips were then compacted at 1, 2, and 3 roller passes with the CAT CP-533E roller. There was very little variation in moisture content between test strips.

Table 18 summarizes the average values of in situ properties and machine energy data at each test strip. Because the computer program was not set to record data for test strips 1A and 1B, machine energy values are not reported.

**Table 18: Summary of compaction monitoring output and in-situ measurements (PPG)**

| | | Average Values For Final Roller Pass | | | | | | |
|---|---|---|---|---|---|---|---|---|
| Test Strip | Number of Roller Passes | Machine Energy (kJ) | Dry Unit Weight ($kN/m^3$) | Moisture Content (%) | DCP Index (mm/blow) | Clegg Impact Value | Stiffness (MN/m) | Modulus (MPa) |
| 1 | 1 | -- | 16.3 | 8.6 | 24.4 | 6.6 | 7.8 | 67.9 |
| 2A | 2 | 8.4 | 16.7 | 9.2 | 23.2 | 6.0 | 6.9 | 63.9 |
| 2B | 2 | 6.2 | 17.3 | 8.3 | 24.2 | 6.4 | 6.4 | 56.1 |
| 3A | 3 | 7.2 | 17.5 | 9.6 | 17.8 | 6.5 | 8.2 | 71.5 |
| 3B | 3 | 3.8 | 18.5 | 9.1 | 6.9 | 7.0 | 9.2 | 80.1 |

Ten test points were established on 10-foot intervals in the middle of each test strip. At each test point, dry unit weight (nuclear gauge), water content (nuclear and oven methods), strength (dynamic cone penetrometer), and stiffness (Clegg impact hammer and GeoGauge) were determined. Bag samples were collected at each test location to determine water contents using the oven method. GPS coordinates were assigned to each test point. They were determined with a hand-held GPS unit and with a base-station GPS Trimble unit. The coordinates obtained by the Trimble unit allowed for direct comparison with GPS data from the compaction monitoring system.

One CFED soil was collected from this project: Glacial Till W. IL. (PPG) CFED #1638.

**Figure 68: Compaction being performed by CAT CP533E roller in reverse for test strip 2A**

*Edwards Facility Field Test, Edwards, IL*

Eight test strips, identified as A through H, were constructed and tested. Construction operations consisted of the following steps: (1) aerate/till existing soil with an RR350, (2) moisture condition soil with water truck, (3) remix with 1 to 2 additional passes of the RR350, (4) blade to level surface, and (5) compact with 6 to 10 passes of the CAT CP-533E roller. The test strips varied in loose lift thickness and water content. Table 19 summarizes the average values of lift thickness, number of passes, in situ test results, and machine energy values for each test strip.

**Table 19: Summary of compaction monitoring output and in-situ measurements (Edwards Test Facility)**

| | | | Average Values For Final Roller Pass | | | | |
|---|---|---|---|---|---|---|---|
| Test Strip | Loose Lift Thickness (cm) | Number of Roller Passes | Machine Energy (kJ) | Dry Unit Weight ($kN/m^3$) | Moisture Content (%) | DCP Index (mm/blow) | Clegg Impact Value |
| A | 30 | 6 | 33.3 | 17.48 | 9.5 | 24 | 13.0 |
| B | 40 | 6 | 36.1 | 17.24 | 13.6 | 47 | 9.0 |
| C | 40 | 6 | 33.4 | 17.87 | 15.4 | 80 | 5.7 |
| D | 40 | 6 | 39.6 | 17.67 | 15.7 | 81 | 5.1 |
| F | 68 | 10 | 30.4 | 18.11 | 15.6 | 60 | 7.6 |
| G | 68 | 10 | 26.1 | 18.53 | 12.8 | 41 | 11.6 |
| H | 30 | 10 | 20.5 | 19.09 | 12.8 | 25 | 13.0 |

Test strips A through D were compacted first. Test strips F through G were compacted in the forward and reverse directions, and test strip H was compacted with 10 passes in the forward direction only.

To evaluate changes in soil properties with compaction, 5 to 10 test points were randomly identified within each test strip and measured for density (nuclear and drive core methods), water content (nuclear, oven, and time-domain reflectometry methods), strength (dynamic cone penetrometer), and stiffness (Clegg impact hammer). At each test point, it was noted if the test location was within or out of the rear roller wheel paths. Drive core and/or bag samples were collected at each test location to determine water contents, using the oven method. Density comparisons were also made by comparing the drive core density values with the in situ nuclear density measurements. The drive core samples generally yielded a higher density. The drive core samples were taken in the top 5 to 13 cm, whereas the nuclear tests averaged a measurement over the top 20 to 30 cm. Shallower nuclear tests (i.e., 10, 15, 20 cm) also show higher density values near the surface. This finding suggests that the compaction effort was not reaching the full depth of the loose lift.

**Figure 69: Test strips A through D after compaction**

One CFED soil was collected from this project: Edwards Till A CFED #1636.

**Field Evaluation of Compaction Monitoring Technology: Phase II (Feb. 2005 to Jul. 2005) - White et al. (2007a)**

Test Project 1 was conducted at the indoor Caterpillar Inc. Edwards Demonstration Arena from February 7–18, 2005. The testing program used four soils, variable moisture content, and variable loose lift thickness and was designed to include a relatively wide yet representative range of field conditions encountered during earthwork construction operations. In all, 19 test strips were constructed, compacted using a CP-533 static padfoot roller, and tested. The testing schedule is provided in Table 20.

**Table 20: Phase II Testing Program**

| Soil Type | Strip # | Loose lift thickness (cm) | Moisture content (%) | Moisture deviation [a] (%) |
|---|---|---|---|---|
| Topsoil | 1 | 30 | 8 | -11 |
| | 2 | 20 | 8 | -11 |
| | 3 | 30 | 16 | -3 |
| | 4 | 20 | 16 | -3 |
| | 5 | 30 | 12 | -7 |
| | 6 | 20 | 12 | -7 |
| Fill clay | 1 | 25 | 24 | +4 |
| | 2 | 25 | 16 | -4 |
| | 3 | 25 | 20 | 0 |
| Till | 1 | 15 | 8 | -4 |
| | 2 | 25 | 8 | -4 |
| | 3 | 15 | 16 | +4 |
| | 4 | 25 | 16 | +4 |
| | 5 | 25 | 12 | 0 |
| | 6 | 15 | 12 | 0 |
| Sand | 1 | 25 | 5 | -4 |
| | 2 | 36 | 5 | -4 |
| | 3 | 36 | 10 | +1 |
| | 4 | 25 | 10 | +1 |

[a] Moisture deviation from optimum, based on standard Proctor test ($w - w_{opt}$)

Within the indoor facility, two parallel test pits were established. The existing Edwards till of the arena was excavated, and the pit bases were stabilized with liberal compaction to create a relatively uniform and stable base. With the exception of DCP measurements, the engineering properties of the stabilized bases were not determined using in situ test methods. Testing materials (topsoil, fill clay, till, and sand) were placed in the pits and mixed in situ with a road reclaimer or tiller to achieve uniform, relatively homogeneous soil conditions. The specified moisture content was verified by drying soil samples using a microwave. The moisture was accepted for testing, provided the moisture content was within about 2% of the desired moisture for each strip. Water and/or wet soil were added to test strips containing soil too dry for testing. Soil too wet for testing was air-dried and occasionally mixed.

**Figure 70: CP-533 static padfoot roller**

For testing the soil, ten test points were established at 1.5 m intervals in the center of the strip, between the paths of the roller tires. At these points, the density and moisture content of the uncompacted soil were determined using a nuclear moisture-density gauge. Following the first pass of the roller over the strip, in situ test measurements of density, moisture content, strength, and stiffness were obtained at each test point. Laser positioning measurements were additionally collected to facilitate later correlations of field measurement results with machine power data. Considering the relative influence of soil disturbance on test results and the tests' sensitivity to soil disturbance, the order in which tests were performed was determined as follows: (1) nuclear moisture and density, (2) GeoGauge, (3) PFWD, (4) Clegg impact, (5) DCP, and (6) time domain reflectometry (TDR) and Duff moisture sensing equipment. A single plate load test was conducted at the end of the test strip next to the tenth test point. Following subsequent passes of the CP-533 padfoot roller (e.g., one, two, four, eight), the same measurements were obtained for the increasingly compact material. Following the final roller pass, drive core samples were excavated for a direct measurement of density and moisture.

Four CFED soils were collected from this project and they include (CFED# in parenthesis): Kickapoo Topsoil (2003), Kickapoo Fill Clay (2004), Kickapoo Sand (2005), and Edwards Till B (2001).

**Field Study of Compaction Monitoring Systems – Tamping Foot 825 and Vibratory Smooth Drum CS-533E Rollers (June 2005 to June 2006) – White et al. (2007c)**

*Project No. 1 – Edwards Facility – 825 Roller*

**Table 21: Project 1 Testing Program**

| Soil Type | Strip No. | Loose Lift Thickness (mm) | Moisture Content (%) | Moisture Deviation [a] (%) |
|---|---|---|---|---|
| Till | 1 | 200 | 12 | -1 |
| [a] Moisture deviation from optimum, based on standard Proctor test ($w - w_{opt}$) | | | | |

One CFED soil was collected from this project: Edwards Till B CFED #2001.

*Project No. 2 – Edwards Facility – CS-533 Vibratory Smooth Drum*

Project 2 was conducted from 8/1/05 to 8/4/05 to evaluate both machine drive power (MDP) and compaction meter value (CMV) for vibratory compaction of five cohesionless soil types. The experimental testing plan of this study, comprised of five test strips for the respective soils, is provided in Table 22. The specific objective of experimental testing and subsequent analyses was to investigate relationships between MDP, CMV, and soil properties, including soil density, moisture content, strength and deformation characteristics.

The roller used for this project was a prototype CS-533 vibratory smooth drum roller. The 9,960-kg roller had a drum diameter of 1.52 m, a drum width of 2.13 m and a rear wheel-to-drum length of 2.90 m. The roller was additionally fitted with a GPS system, such that coverage (i.e. history of the roller location), MDP, and CMV were each mapped and viewed in real time during compaction operations.

**Table 22: Testing Program**

| Soil Type | Strip No. | Loose Lift Thickness (mm) | Moisture Content (%) | Moisture Deviation [a] (%) |
|---|---|---|---|---|
| RAP | 1 | 350 | 8 | 0 |
| CA6-C | 2 | 280 | 4 | +4 [b] |
| CA5-C | 3 | 300 | 4 | --- |
| FA6 | 4 | 360 | 6 | -2 |
| CA6-G | 5 | 340 | 8 | -2 |

[a] Moisture deviation from optimum, based on standard Proctor test ($w - w_{opt}$)

[b] Within bulking moisture range

Five 30-m-long test strips were constructed using five different cohesionless subbase materials. The test strips were constructed with widths of approximately 3.0 m, slightly wider than the roller drum. The soils were placed on well-compacted subgrade at approximately natural moisture content – varying by soil type – with loose lift thicknesses ranging from 280 to 360 mm between test strips. Additional material was placed at the ends of the test strips to transition from the existing ground surface to the test strip elevations. Constructed test strips are shown in Figure 71.

Soil was compacted using the prototype CS-533 vibratory roller at the "high" amplitude (1.70 mm) setting. The frequency of drum vibration (31.9 Hz) was also constant throughout the field study. During this compaction operation, machine power and CMV measurements were collected approximately every 20 cm along the test strip. Near-continuous roller location information was also obtained from GPS measurements.

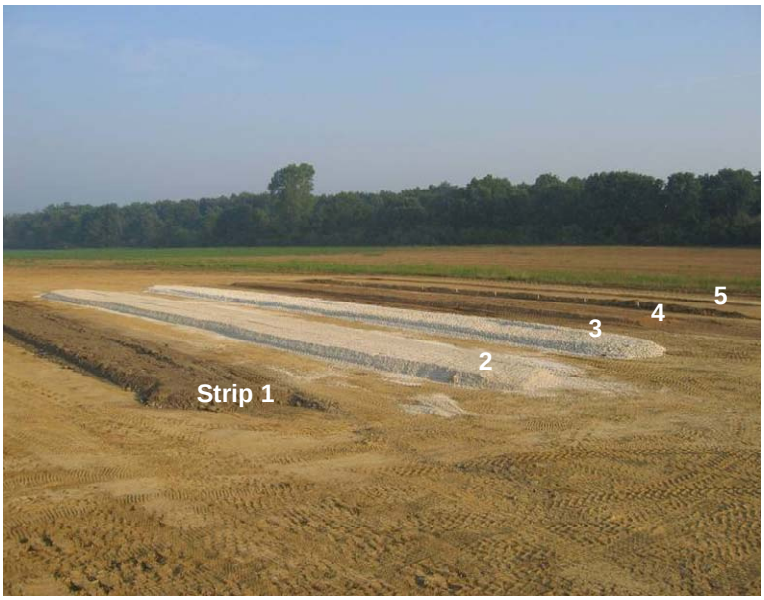


**Figure 71: Test Strips**

For determining the properties of the compacted soil, field measurements were obtained at each of ten 2.5-m-spaced test points. Field measurements of density, moisture content, strength, and modulus were obtained for the uncompacted material and following 1, 2, 4, 8, and 12 roller passes over the test strip. GPS measurements were additionally collected at each test location using a rover to allow pairing of the field measurement results with spatially-nearest intelligent compaction data. Considering the relative influence and sensitivity of soil disturbance on test results, the order in which tests were performed was predetermined as follows: (1) nuclear moisture and density using a calibrated nuclear moisture-density gauge, (2) soil stiffness gauge, (3) portable falling weight deflectometer, (4) Clegg impact test, and (5) dynamic cone penetrometer. As for Project No. 1, the mean DCP index at the bottom of the compaction layer was calculated using Equation 27 and subsequently used for analysis. A single 300-mm-diameter plate load test was conducted at the end of the test strip next to the tenth test point. Upon completion of testing, the characteristics of the compacted subbase materials, defined using MDP, CMV, and in-situ measures of soil density, strength, and stiffness, were available for the full range of soil compaction states. Five CFED soils were collected from this project. They are as follows

(CFED # in parenthesis): RAP (2006), CA6-C (2007), FA6 (2008), and CA6-G (2009).

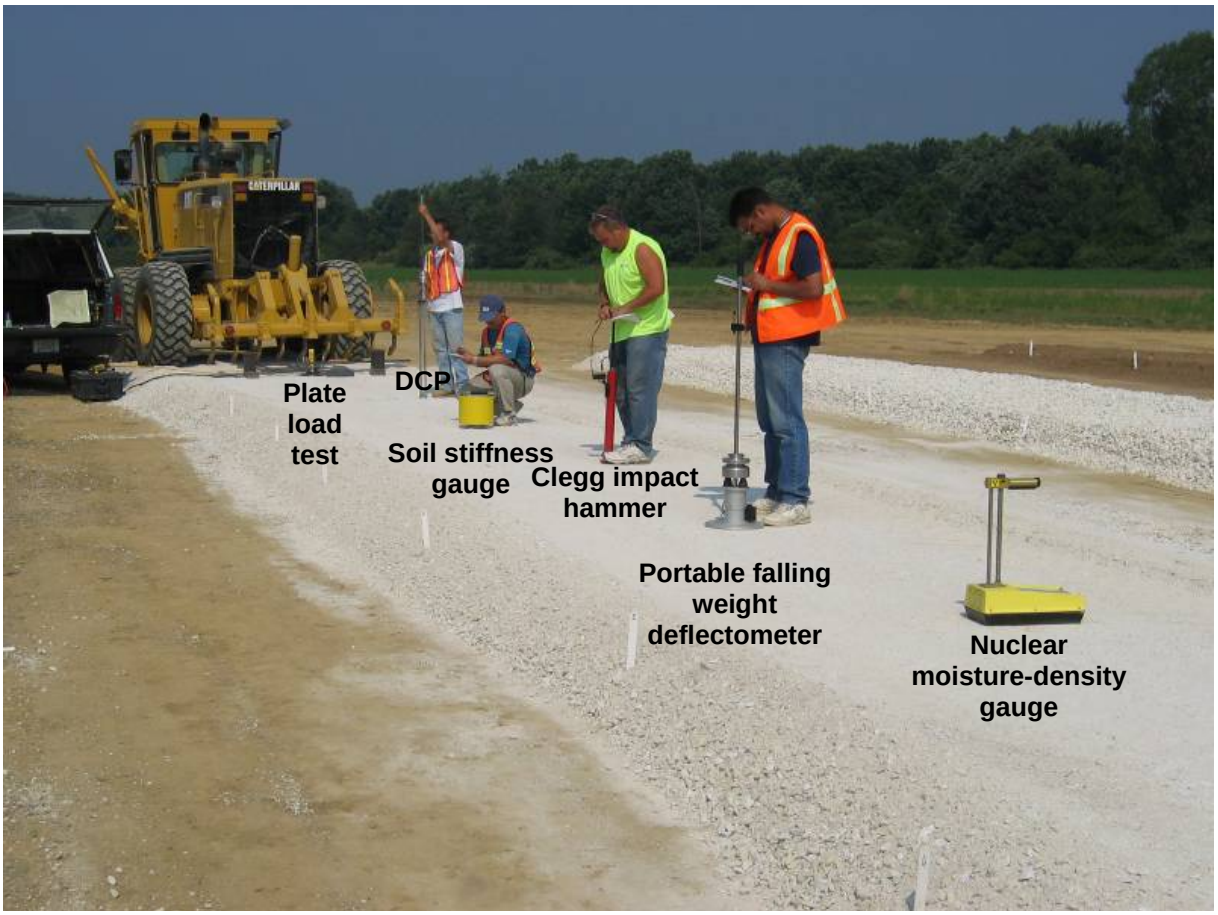


**Figure 72: In situ testing, Strip 2**

*Project No. 3 – Edwards Facility – CS-533 Vibratory Smooth Drum*

This project was conducted from 6/12/06 to 6/15/06, experimental testing and results are described for establishing the applicability of using averaged roller data from one-dimensional calibration test strips to assess compaction of a two-dimensional (i.e. spatial) area. Such an evaluation is necessary for verifying the reliability of one-dimensional test strip calibrations as a component of specifications (see ISSMGE (2005)) for use of compaction monitoring technologies. The specific objectives of this project included: (1) collection of compaction monitoring results over a two-dimensional area that incorporates

variable lift thickness and stiffness properties, (2) documentation of how the result from two different compaction monitoring technologies are related considering spatial variability of soil properties and also measurement variability, (3) evaluation of how accurately two different compaction monitoring technologies predict soil properties compared with using in-situ compaction control tests, and (4) evaluation of previous research findings, such as using moisture content in concert with machine compaction monitoring values to predict soil properties, for implementing the findings into quality statements or specifications.

The MDP and CMV compaction monitoring technologies were used for the project. The technologies were applied to a CS-533 vibratory smooth drum roller. The 10,240-kg roller has a drum diameter of 1.55 m, a drum width of 2.13 m, and a rear wheel-to-drum width of 2.90 m. The roller was additionally fitted with a global positioning system (GPS) to track roller coverage and apply compaction monitoring results to discrete locations over the project area (i.e. mapping).

Field calibration testing of the roller was performed using four 30-m test strips. The initial test strips were comprised of uniformly placed and moisture-conditioned material. To identify the influence of moisture content on machine response during compaction, the first test strip was compacted, tested, and then reconstructed at two additional moisture contents. For each of these test strips, five tests were conducted with each test device following 1, 2, 4, 8, and 12 roller passes. This compaction curve testing was used to develop statistical regressions relating MDP, CMV, and moisture content to the various in-situ soil properties. The second test strip, which was constructed using well-graded subbase material at optimum moisture content, incorporated variable lift thickness (127 to 508 mm). Roller data from this test strip indicated the effect of lift thickness on machine response. The calibration strip testing program is shown in Figure 73.

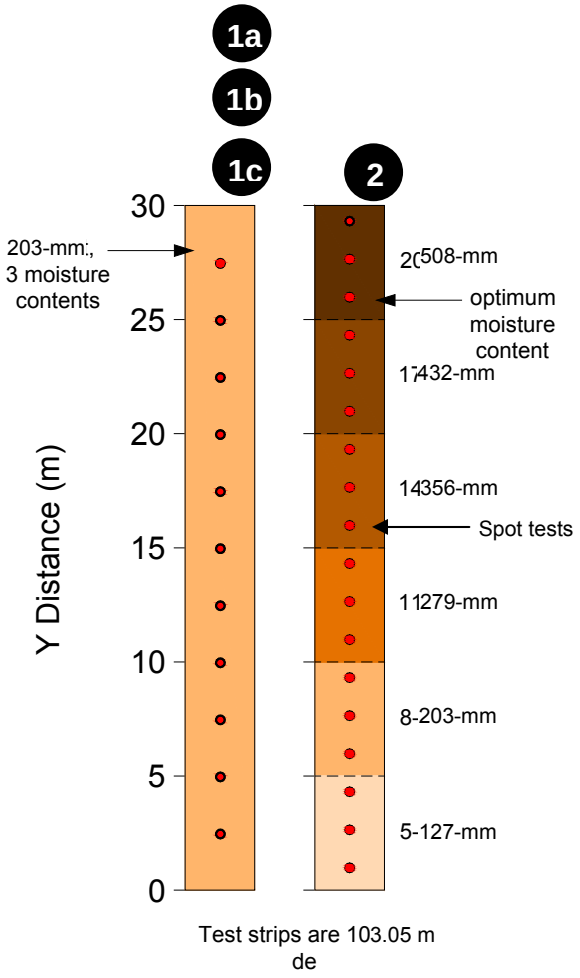


**Figure 73: Calibration strip testing program from White et al. (2007c)**

The second spatial testing plan (Spatial 2) was designed with dimensions of 30 m by 17.1 m with increasing x-coordinates oriented at the testing site in the North direction. The plan area, which is shown in Figure 73, was subdivided into eight roller widths. The testing used only one soil type and one nominal moisture content (optimum), but incorporated variable lift thickness (either 200 or 510 mm) to artificially achieve variation in stiffness properties of the soil.

The third spatial testing plan (Spatial 3) was designed with dimensions of 15 m by 17.1 m with increasing x-coordinates oriented at the testing site in the North direction. The plan area was also subdivided into eight roller widths. The testing area used the first 10 m of Spatial 1 (CA6-G material), but incorporated relatively stiff subgrade material to artificially achieve variation in stiffness properties of the soil.

**Mn/DOT Intelligent Compaction Study – TH 36, Maplewood, MN (May 2007 to July 2007) – White et al. (2007e)**

The Caterpillar CS-563 smooth drum roller equipped with compaction meter value (CMV) IC measurement technology and AccuGrade compaction mapping system was used on the project. The IC measurement output on the machine is referred to as CCV (Caterpillar Compaction Value). The pavement foundation layers on the project consisted of recycled granular base material (SM) underlain by select granular fill material (SP-SM) and common subgrade material (SM).


**Figure 74: Field compaction using CS-563 roller**

In-situ testing involved determination of: (a) in-situ moisture and density using nuclear

density gauge, (b) dynamic cone penetration index (DCP Index), (c) light weight deflectometer modulus ($E_{LWD}$) using Zorn, and Dynatest devices, (d) falling weight deflectometer (FWD) modulus using truck mounted Dynatest FWD, and (e) plate load test initial and reload modulus ($E_{V1}$ and $E_{V2}$).

One CFED soil was collected from this project: TH36 Common CFED #2020.

**Mn/DOT Intelligent Compaction Study – US 10, Staples, MN (July 2007) – White et al. (2007e)**

The Caterpillar CS-563 smooth drum roller equipped with compaction meter value (CMV) IC measurement technology and AccuGrade compaction mapping system was used on the project. The IC measurement output on the machine is referred to as CCV (Caterpillar Compaction Value). Project consisted of granular subgrade fill materials classified as SP-SM, SM, and SW-SM according to the USCS classification system. One CFED soil was collected from this project: US10-101 CFED #2018.

**Figure 75: Field compaction using CS-563 roller**

In-situ testing involved determination of: (a) in-situ moisture and density using nuclear

density gauge, (b) dynamic cone penetration index (DCP Index), (c) light weight deflectometer modulus ($E_{LWD}$) using Zorn, Keros, and Dynatest devices, and (d) plate load test initial and reload modulus ($E_{V1}$ and $E_{V2}$).

**Mn/DOT Intelligent Compaction Study – TH60, Bigelow, MN (August 2007) – White et al. (2007e)**

The Caterpillar CP-563 padfoot roller equipped with machine drive power (MDP) IC measurement technology and AccuGrade compaction mapping system was used on the project. The IC measurement output on the machine is referred to as CCV (Caterpillar Compaction Value) and is calculated using MDP. The project involved construction of subgrade fill sections typically with depth of about 4 to 8 feet and with depth of about 20 to 30 feet at some locations. The subgrade fill on the project mostly consisted of cohesive glacial till material (lean clay to sandy lean clays) classified as CL according to the USCS classification system. Three CFED soils were collected from this project: TH60 Soil 1, TH60 Soil 2, and TH60 Strip 2 soils; CFED #2013, 2014, and 2021, respectively.

In-situ testing involved determination of: (a) in-situ moisture and density using nuclear density gauge and drive cylinders, (b) dynamic cone penetration index (DCP Index), (c) light weight deflectometer modulus ($E_{LWD}$) using Zorn, Keros, and Dynatest devices, (d) undrained shear strength measurements from shelby tube samples. Photos from the project are provided below.


**Figure 76: TH60 strip compaction**

**Figure 77: TH60 Calibration strip**

**I-70 Maryland Testing (October 2007) – Vennapusa (personal communication)**

The ISU research team conducted field testing at the I-70 widening and reconstruction project in Frederick, Maryland from October 22 to November 2, 2007. In review, a subgrade test bed with plan dimensions of about 200 ft x 50 ft consisting of variable moisture

conditions and isolated locations of underlying fractured rock and boulders (see Figure 78 and Figure 79) was prepared. The subgrade was divided in to four lanes, compacted using the Dynapac padfoot roller for several passes, and then mapped using Bomag and Sakai smooth drum rollers. Later, two 0.5 ft thick base layers were placed on top of the subgrade and compacted using different rollers for each lane as shown in Figure 78.

Two CFED soils, #2030 and #2031, were collected from this project.

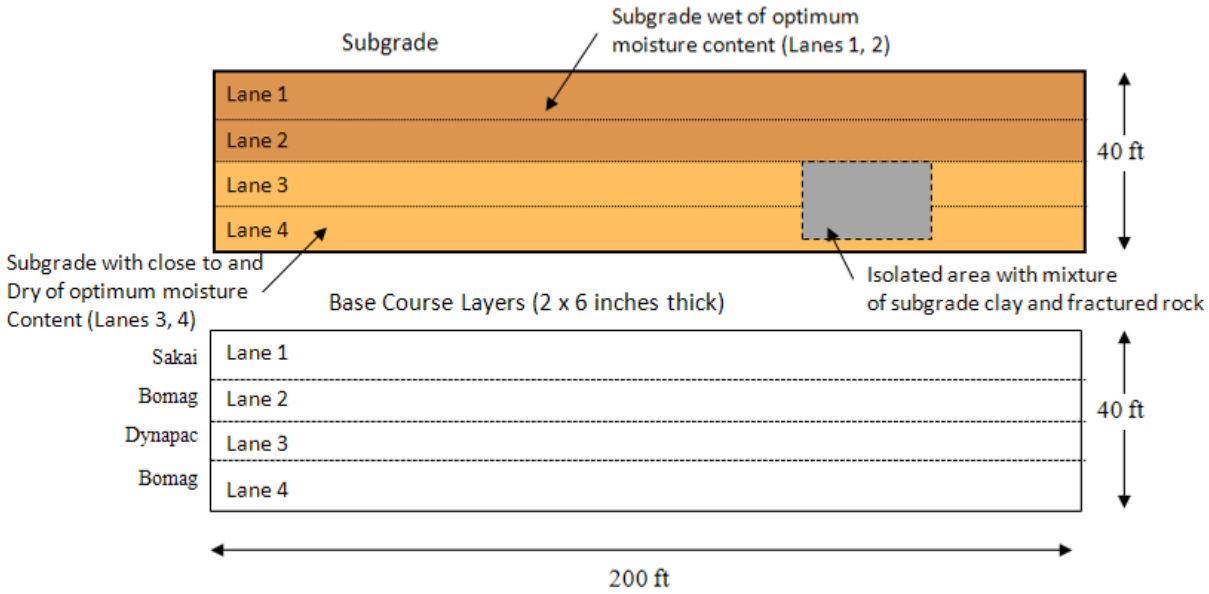


**Figure 78: Plan view of test bed construction at the I-70 Maryland project**

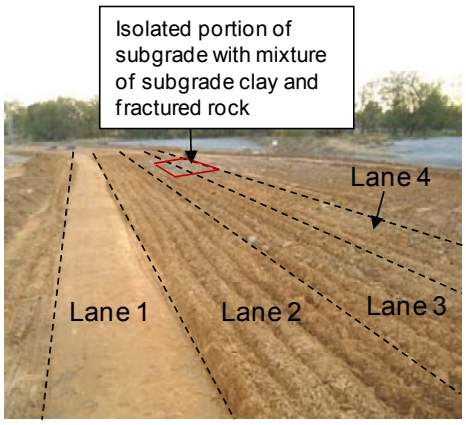


**Figure 79: Picture of subgrade test bed - Maryland**

**I-25 Colorado Testing (August 2007) - Vennapusa (personal communication, quarterly progress report 10/1/07)**

The ISU research team conducted field testing at the I-25 Longmont, CO project site from August 20, 2007 to August 29, 2007. In summary, the subgrade work consisted of three 50 feet long sections with variable moisture conditions as shown in Figure 80. One subgrade section (section 4) was left un-compacted with relatively wet moisture conditions prior to placing subsequent subbase/base layers. The remaining three subgrade sections (sections 1 to 3) were compacted using all three rollers (Bomag, CAT, Dynapac) in four lanes (see Figure 80) in conjunction with in-situ spot test measurements (nuclear gauge, LWD, DCP, and plate load test). Two 1 ft thick subbase layers and one 0.5 ft thick base layer were placed over the subgrade and compacted using the three rollers.

Four CFED soils, #2025, 2026, 2027 and 2029, were collected from this project.

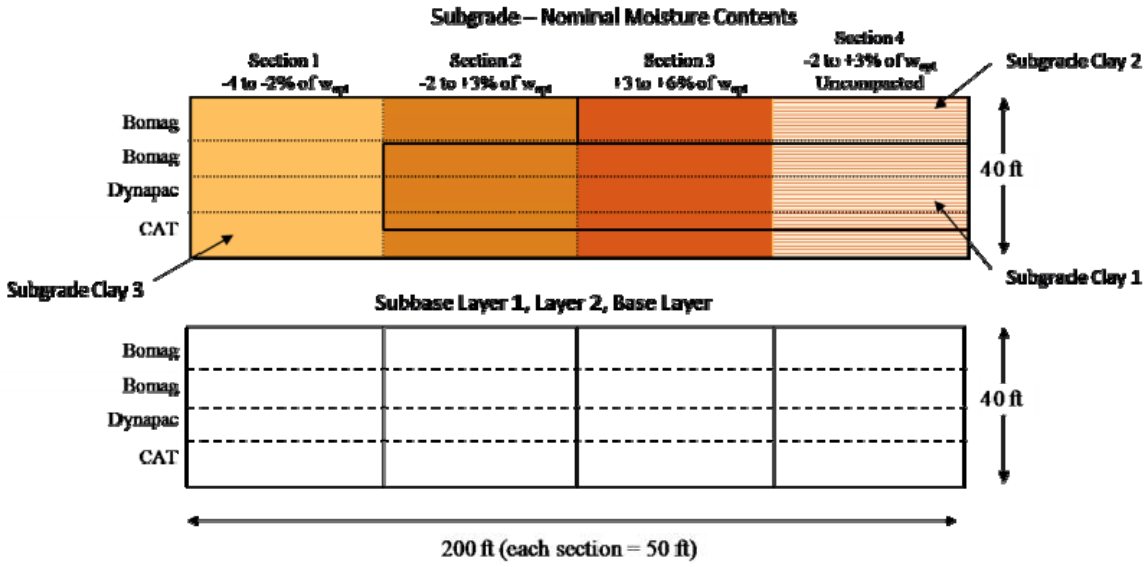


**Figure 80: Plan view of test bed construction at the I-25 Colorado project**


**Figure 81: Picture of subgrade lanes prepared for compaction and testing - Colorado**

**Florida I-10 (April 2008) – Vennapusa (personal communication)**

The ISU research team was on site from April 16 to April 24, 2008. Dynapac, Case/Ammann, and Sakai smooth drum rollers were available at this site. After some investigation and trial runs, it was determined that the Sakai machine had GPS hardware problems and was not used.

Test bed construction involved compacting and testing calibration test strips to develop target roller MVs in relationship with target QA values, and compacting and testing production areas. Samples of embankment subgrade and aggregate base material were reconstituted for laboratory resilient modulus ($M_r$) testing. Results are being used to develop empirical relationships between roller MVs and laboratory $M_r$ for specification. A total of seven test beds were constructed. Of these, four test beds consisted of aggregate base material (6 to 12 inches thick) over compacted stabilized subgrade, two test beds consisted of embankment subgrade materials, and one test bed consisted of stabilized embankment subgrade material. In-situ tests included static plate load, light weight deflectometer, nuclear moisture-density gauge, and dynamic cone penetrometer tests.

Six CFED soils, #2023, 2033, 2034, 2035, 2036, and 2037, were collected from this project.

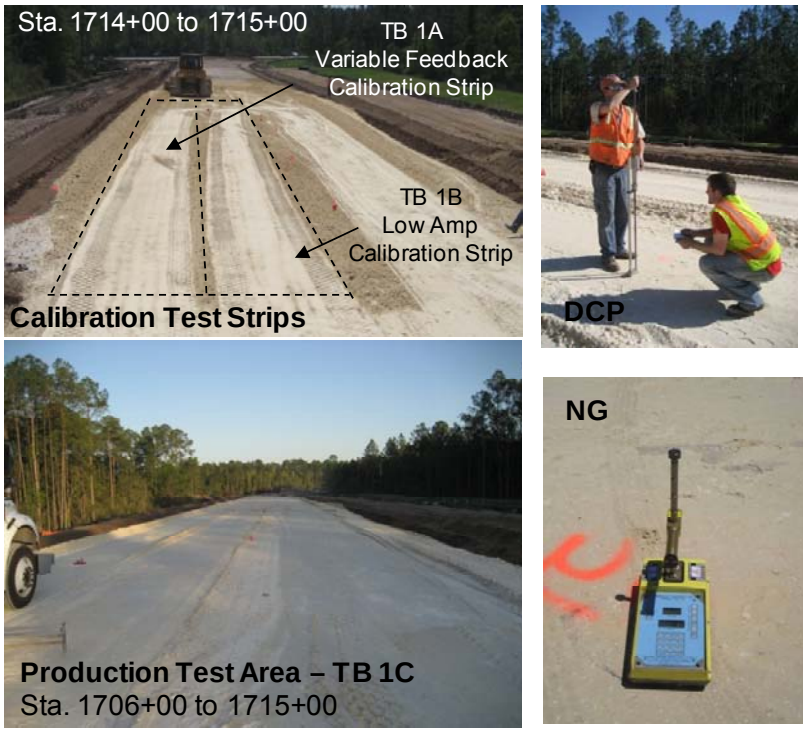


**Figure 82: Field conditions and in-situ testing from Florida I-10 project**

**North Carolina Hwy 311 (May 2008) – Vennapusa (personal communication)**

The ISU research team was on site from May 19 to 27, 2008. Case/Ammann, Bomag, and Sakai smooth drum rollers, and a Caterpillar pad foot roller were available at this project site. The Sakai machine had similar GPS hardware problems as in Florida and was not used. A detailed work plan was developed for evaluating specification options 1 through 5 with three test beds on embankment subgrade material, two test beds on stabilized subgrade, and three test beds on aggregate base material.

Due to a weather delay and some site restrictions, the field testing focused on three test beds with subgrade material and one test bed with aggregate base material. In-place embankment subgrade and aggregate base layers were scarified to a depth of about 6 to 8 inches in

preparation of the test beds.

Samples of embankment subgrade and aggregate base material were reconstituted for laboratory $M_r$ testing. Results will be used to develop empirical relationships between roller MVs and laboratory $M_r$ for specification options. Test bed construction involved compacting and testing calibration test strips for developing target MVs (in relationship with QA target values) and compacting and testing production areas. In-situ tests included static plate load, light weight deflectometer, nuclear moisture-density gauge, and dynamic cone penetrometer tests. Results are expected to help populate correlations between roller MVs and in-situ spot tests for the specification options. The Caterpillar pad foot roller equipped with the machine drive power (MDP) based CCV measurement system was used to compact embankment subgrade material in an area with variable slope conditions. The CCV data indicated that the measurements were sensitive to slope angle, i.e., high CCV-values uphill and low CCV-values downhill. The results are being analyzed by the manufacturer to re-evaluate calibration input parameters. Since the CCV-data did not appear reliable, additional spot test measurements were not performed.

Three CFED soils, #2038, 2039, and 2040, were collected from this project.

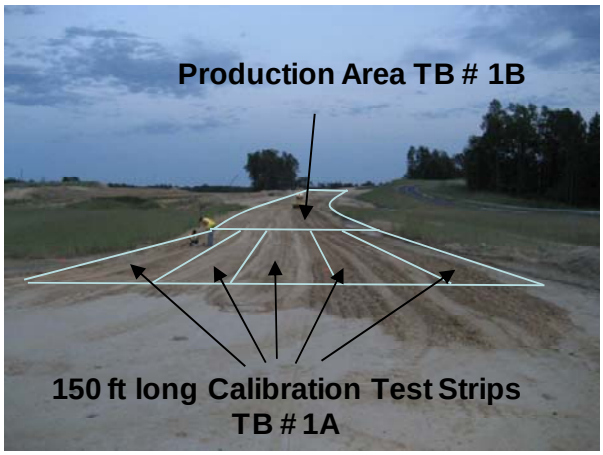


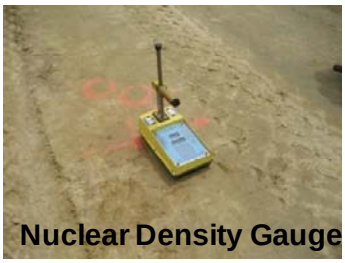



**Figure 83: Field conditions and in-situ testing from North Carolina Hwy 311 project**

# CHAPTER 6. TEST RESULTS AND ANALYSIS

Forty-two soils have been stored in the CFED database to date. Each of these soils was used in the analysis of modeling techniques. All available lab and field data were compiled and input into CFED. The index properties of each soil are shown in Table 23 through Table 26. The results of the analysis are discussed below.

## Index Properties of Soils in CFED

**Table 23: CFED Database Soils**

| Properties | Glacial Till C. Iowa | Weathered Shale C. Iowa | Loess W. Iowa | Glacial Till W. Illinois (PPG)+ | Glacial Till W. Illinois (Edwards A) |
|---|---|---|---|---|---|
| CFED Database ID | SOIL 1632 | SOIL1633 | SOIIL1634 | SOIL1635 | SOIL1636 |
| USCS Description (Symbol) | Sandy lean clay (CL) | Lean clay (CL) | Silt (ML) | Sandy lean clay (CL) | Sandy lean clay (CL) |
| Liquid Limit (LL) [1] | 24 | 35 | 29 | 19 | 29 |
| Plastic Limit (PL)[2] | 15 | 24 | 23 | 11 | 16 |
| Plasticity Index (PI) | 9 | 11 | 6 | 8 | 13 |
| Specific Gravity ($G_s$) | 2.66 | 2.77 | 2.72 | 2.72 | 2.70 |
| Optimum moisture content, $W_{opt}$(%) [3]* | 13.9 | 16.2 | 18.6 | 8.1 | 12.1 |
| Dry Unit Weight $\gamma_{d\ max}$ (kN/m$^3$) [4]* | 18.0 | 17.7 | 15.9 | 21.0 | 19.0 |
| Gravel Size (%) (> 4.75 mm) | 1.4 | 0.0 | 0.0 | 14 | 4.2 |
| Sand Size (%) (4.75 to 0.075 mm) | 46.3 | 9.1 | 2.9 | 42.5 | 26.9 |
| Silt Size (%) (0.075 to 0.002 mm) | 37.7 | 51.7 | 90.6 | 34.6 | 43.8 |
| Clay Size (%) (≤ 0.002 mm) | 14.6 | 39.2 | 6.5 | 8.9 | 25.1 |
| Lab compaction energies | 5 | 5 | 5 | 5 | 5 |
| Field compaction curves | No | No | No | Yes | Yes |

1 – ASTM reported standard deviation 0.98 – 1.07 (2 soils tested by different operators in same lab)
2 – ASTM reported standard deviation 1.07 – 1.21 (2 soils tested by different operators in same lab)
3 – ASTM reported standard deviation ± 0.86 (Multilaboratory precision)
4 – ASTM reported standard deviation ± 0.26 (Multilaboratory precision)
* - Standard Proctor Compaction Energy (592 kJ/m$^3$)
** - Relative Density Compaction Energy
NP – non-plastic
NA – not available

**Table 24: CFED Database Soils (cont.)**

| Properties | Clay C. Iowa (728) | Clay C. Iowa (GS) | Red Soil North Carolina (06-0004)◊ | Glacial Till W. Illinois (Edwards B) | Kickapoo Topsoil |
|---|---|---|---|---|---|
| CFED Database ID | SOIL1637 | SOIL1638 | SOIL1640 | SOIL2001 | SOIL2003 |
| USCS Description (Symbol) | Lean Clay (CL) | Lean clay (CL) | Lean clay with sand (CL) | Sandy lean clay (CL) | Silt (ML) |
| Liquid Limit (LL) [1] | 42 | 49 | 45 | 29 | 38 |
| Plastic Limit (PL)[2] | 32 | 30 | 24 | 17 | 25 |
| Plasticity Index (PI) | 10 | 19 | 21 | 12 | 13 |
| Specific Gravity ($G_s$) | 2.70 | 2.77 | -- | 2.75 | 2.65 |
| Optimum moisture content, $W_{opt}$(%) [3]* | 19.6 | 22.4 | 22.1 | 13.9 | 19.3 |
| Dry Unit Weight $\gamma_{d\,max}$ (kN/m$^3$) [4]* | 16.3 | 15.5 | 15.1 | 18.5 | 16.0 |
| Gravel Size (%) (> 4.75 mm) | 0.4 | 0.0 | 8 | 3.1 | 0.2 |
| Sand Size (%) (4.75 to 0.075 mm) | 1.2 | 2.8 | 25 | 28.9 | 7.9 |
| Silt Size (%) (0.075 to 0.002 mm) | 69.1 | 63.8 | 23 | 45.5 | 73.9 |
| Clay Size (%) (≤ 0.002 mm) | 29.3 | 33.4 | 40 | 22.5 | 18 |
| Lab compaction energies | 5 | 5 | 8 | 2 | 2 |
| Field compaction curves | Yes | Yes | No | Yes | Yes |

1 – ASTM reported standard deviation 0.98 – 1.07 (2 soils tested by different operators in same lab)
2 – ASTM reported standard deviation 1.07 – 1.21 (2 soils tested by different operators in same lab)
3 – ASTM reported standard deviation ± 0.86 (Multilaboratory precision)
4 – ASTM reported standard deviation ± 0.26 (Multilaboratory precision)
* - Standard Proctor Compaction Energy (592 kJ/m$^3$)
** - Relative Density Compaction Energy
◊ - ASTM D4718 warranted but not yet applied
NP – non-plastic
NA – not available

**Table 25: CFED Database Soils (cont.)**

| Properties | Kickapoo Fill Clay | Kickapoo Sand◊ | RAP◊ | CA6-C (August 2005) ◊ | CA5-C◊ |
|---|---|---|---|---|---|
| CFED Database ID | SOIL2004 | SOIL2005 | SOIL2006 | SOIL2007 | TBE |
| USCS Description (Symbol) | Lean clay with sand (CL) | Well graded sand with silt (SW-SM) | Silty gravel with sand (GM) | Silty sand with Gravel (SM) | Poorly graded gravel (GP) |
| Liquid Limit (LL) [1] | 47 | NP | 15 | 14 | NP |
| Plastic Limit (PL)[2] | 25 | NP | NP | NP | NP |
| Plasticity Index (PI) | 22 | NP | NP | NP | NP |
| Specific Gravity ($G_s$) | 2.85 | 2.70 | 2.52 | 2.69 | 2.75 |
| Optimum moisture content, $W_{opt}$(%) [3]* | 16.9 | 4.8 | 9.0 | 9.8 | NA |
| Dry Unit Weight $\gamma_{d\,max}$ (kN/m$^3$) [4]* | 17.8 | 18.3 | 19.4 | 19.6 | NA |
| Gravel Size (%) (> 4.75 mm) | 1.2 | 8.9 | 44 | 37 | 97 |
| Sand Size (%) (4.75 to 0.075 mm) | 20.3 | 84.6 | 42 | 52 | 2 |
| Silt Size (%) (0.075 to 0.002 mm) | 58.6 | 3.3 | 11 | 9 | 1 |
| Clay Size (%) (≤ 0.002 mm) | 20 | 3.2 | 3 | 2 | 0 |
| Lab compaction energies | 2 | 2 | 1 | 1 | 1** |
| Field compaction curves | Yes | Yes | Yes | Yes | Yes |

1 – ASTM reported standard deviation 0.98 – 1.07 (2 soils tested by different operators in same lab)
2 – ASTM reported standard deviation 1.07 – 1.21 (2 soils tested by different operators in same lab)
3 – ASTM reported standard deviation ± 0.86 (Multilaboratory precision)
4 – ASTM reported standard deviation ± 0.26 (Multilaboratory precision)
* - Standard Proctor Compaction Energy (592 kJ/m$^3$)
** - Relative Density Compaction Energy
+ - ASTM D4718 warranted and applied
◊ - ASTM D4718 warranted but not yet applied
NP – non-plastic
NA – not available

**Table 26: CFED Database Soils (cont.)**

| Properties | FA6◊ | CA6-G (August 2005) ◊ | Glacial Till MnRoad | Class 5 Base MnRoad+ | CA6-G (June 2006) ◊ |
|---|---|---|---|---|---|
| CFED Database ID | SOIL2008 | SOIL2009 | SOIL2010 | SOIL2011 | SOIL2012 |
| USCS Description (Symbol) | Silty sand (SM) | Clayey gravel with sand (GC) | Sandy lean clay (CL) | Poorly graded sand with silt and gravel (SP-SM) | Well-graded sand with silt |
| Liquid Limit (LL) [1] | 17 | 26 | 32 | NP | NP |
| Plastic Limit (PL)[2] | NP | 14 | 13 | NP | NP |
| Plasticity Index (PI) | NP | 12 | 19 | NP | NP |
| Specific Gravity ($G_s$) | 2.68 | 2.67 | 2.69 | 2.71 | 2.75 |
| Optimum moisture content, $W_{opt}$(%) [3]* | 7.9 | 9.5 | 15.0 | 7.1 | 8.0 |
| Dry Unit Weight $\gamma_{d\ max}$ (kN/m$^3$) [4]* | 19.9 | 19.9 | 17.3 | 21.3 | 21.4 |
| Gravel Size (%) (> 4.75 mm) | 9 | 37 | 3 | 30 | 29.5 |
| Sand Size (%) (4.75 to 0.075 mm) | 70 | 31 | 37 | 60 | 61.0 |
| Silt Size (%) (0.075 to 0.002 mm) | 16 | 22 | 38 | 7 | 4.2 |
| Clay Size (%) (≤ 0.002 mm) | 5 | 10 | 22 | 3 | 5.3 |
| Lab compaction energies | 5 | 1 | 5 | 5 | 2 |
| Field compaction curves | Yes | Yes | Yes | Yes | Yes |

1 – ASTM reported standard deviation 0.98 – 1.07 (2 soils tested by different operators in same lab)
2 – ASTM reported standard deviation 1.07 – 1.21 (2 soils tested by different operators in same lab)
3 – ASTM reported standard deviation ± 0.86 (Multilaboratory precision)
4 – ASTM reported standard deviation ± 0.26 (Multilaboratory precision)
* - Standard Proctor Compaction Energy (592 kJ/m$^3$)
** - Relative Density Compaction Energy
† - Material Reused in Compaction Testing
◊ - ASTM D4718 warranted but not yet applied
NP – non-plastic
NA – not available

**Table 27: CFED Database Soils (cont.)**

| Properties | Edwards Till (2008) | TH60-Soil#1† | TH60-Soil#2† | US10-#101 Staples◊ | TH36 Common†◊ |
|---|---|---|---|---|---|
| CFED Database ID | SOIL2024 | SOIL2013 | SOIL2014 | SOIL2018 | SOIL2020 |
| USCS Description (Symbol) | Lean Clay (CL) | Lean Clay with Sand (CL) | Lean Clay with Sand (CL) | Silty Sand (SM) | Silty Sand (SM) |
| Liquid Limit (LL) [1] | 32 | 27 | 30 | NP | 13 |
| Plastic Limit (PL)[2] | 15 | 19 | 18 | NP | NA |
| Plasticity Index (PI) | 17 | 8 | 12 | NP | NA |
| Specific Gravity ($G_s$) | 2.75 | 2.69 | 2.70 | 2.57 | 2.71 |
| Optimum moisture content, $W_{opt}$(%) [3]* | 13.3 | 11.7 | 13.3 | 9 | 7.4 |
| Dry Unit Weight $\gamma_{d\,max}$ (kN/m$^3$) [4]* | 18.8 | 18.7 | 18.6 | 19.7 | 20.8 |
| Gravel Size (%) (> 4.75 mm) | 1 | 0 | 0 | 14 | 12 |
| Sand Size (%) (4.75 to 0.075 mm) | 16 | 35 | 37 | 68 | 61 |
| Silt Size (%) (0.075 to 0.002 mm) | 42 | 44 | 39 | 7 | 15 |
| Clay Size (%) (≤ 0.002 mm) | 32 | 20 | 22 | 11 | 12 |
| Lab compaction energies | 2 | 5 | 5 | 5 | 5 |
| Field compaction curves | No | No | No | No | Yes |

1 – ASTM reported standard deviation 0.98 – 1.07 (2 soils tested by different operators in same lab)
2 – ASTM reported standard deviation 1.07 – 1.21 (2 soils tested by different operators in same lab)
3 – ASTM reported standard deviation ± 0.86 (Multilaboratory precision)
4 – ASTM reported standard deviation ± 0.26 (Multilaboratory precision)
* - Standard Proctor Compaction Energy (592 kJ/m$^3$)
** - Relative Density Compaction Energy
† - Material Reused in Compaction Testing
◊ - ASTM D4718 warranted but not yet applied
NP – non-plastic
NA – not available

**Table 28: CFED Database Soils (cont.)**

| Properties | TH60-Strip 2 (Aug07) | China Red Clay | China Yellow Clay | FLA FL19 | CO Subgrade Clay 1 |
|---|---|---|---|---|---|
| CFED Database ID | SOIL2021 | SOIL2022 | SOIL2023 | SOIL2032 | SOIL2025 |
| USCS Description (Symbol) | Sandy Silt (ML) | Silty Clay (CL-ML) | Silty Sand with Gravel (SM) | Silty Sand with Gravel (SM) | Sandy lean Clay (SC-SM) |
| Liquid Limit (LL) [1] | 43 | 26 | 19 | NP | 30 |
| Plastic Limit (PL)[2] | 27 | 20 | NP | NP | 17 |
| Plasticity Index (PI) | 16 | 6 | NP | NP | 13 |
| Specific Gravity ($G_s$) | 2.71 | 2.71 | 2.71 | 2.72 | 2.63 |
| Optimum moisture content, $W_{opt}$(%) [3]* | 18.7 | 14.9 | 11.0 | 13.1 | 11.8 |
| Dry Unit Weight $\gamma_{d\ max}$ (kN/m$^3$) [4]* | 16.3 | 17.2 | 18.8 | 17.9 | 18.7 |
| Gravel Size (%) (> 4.75 mm) | 0 | 5 | 25 | 30 | 1 |
| Sand Size (%) (4.75 to 0.075 mm) | 18 | 27 | 29 | 49 | 31 |
| Silt Size (%) (0.075 to 0.002 mm) | 47 | 54 | 40 | 18 | 39 |
| Clay Size (%) (≤ 0.002 mm) | 35 | 14 | 6 | 3 | 29 |
| Lab compaction energies | 5 | 5 | 5 | 2 | 2 |
| Field compaction curves | Yes | No | No | No | No |

1 – ASTM reported standard deviation 0.98 – 1.07 (2 soils tested by different operators in same lab)
2 – ASTM reported standard deviation 1.07 – 1.21 (2 soils tested by different operators in same lab)
3 – ASTM reported standard deviation ± 0.86 (Multilaboratory precision)
4 – ASTM reported standard deviation ± 0.26 (Multilaboratory precision)
* - Standard Proctor Compaction Energy (592 kJ/m$^3$)
** - Relative Density Compaction Energy
† - Material Reused in Compaction Testing
◊ - ASTM D4718 warranted but not yet applied
NP – non-plastic
NA – not available

**Table 29: CFED Database Soils (cont.)**

| Properties | CO Subgrade Clay 2 | CO Subgrade Clay 3 | CO Base Layer | MD Subgrade Clay | MD Base Material |
|---|---|---|---|---|---|
| CFED Database ID | SOIL2026 | SOIL2027 | SOIL2029 | SOIL2030 | SOIL2031 |
| USCS Description (Symbol) | Silty Clayey Sand (SC-SM) | Sandy lean Clay (CL) | Poorly graded Sand with Silt and Gravel (SP-SM) | Silty Sand (SM) | Poorly graded Sand with Silt and Gravel (SP-SM) |
| Liquid Limit (LL) [1] | 30 | 27 | NP | 22 | NP |
| Plastic Limit (PL)[2] | 23 | 17 | NP | NP | NP |
| Plasticity Index (PI) | 7 | 20 | NP | NP | NP |
| Specific Gravity ($G_s$) | 2.57 | 2.74 | 2.65 | 2.65 | 2.70 |
| Optimum moisture content, $W_{opt}$(%) [3]* | 14.2 | 17.8 | 8.0 | 11.9 | 5.9 |
| Dry Unit Weight $\gamma_{d\ max}$ (kN/m$^3$) [4]* | 15.8 | 16.5 | 21.3 | 18.9 | 22.5 |
| Gravel Size (%) (> 4.75 mm) | 11 | 1 | 44 | 6 | 42 |
| Sand Size (%) (4.75 to 0.075 mm) | 47 | 30 | 49 | 65 | 46 |
| Silt Size (%) (0.075 to 0.002 mm) | 28 | 37 | 4 | 14 | 12 |
| Clay Size (%) (≤ 0.002 mm) | 14 | 22 | 3 | 15 | 0 |
| Lab compaction energies | 2 | 2 | 2 | 2 | 2 |
| Field compaction curves | No | No | No | No | No |

1 – ASTM reported standard deviation 0.98 – 1.07 (2 soils tested by different operators in same lab)
2 – ASTM reported standard deviation 1.07 – 1.21 (2 soils tested by different operators in same lab)
3 – ASTM reported standard deviation ± 0.86 (Multilaboratory precision)
4 – ASTM reported standard deviation ± 0.26 (Multilaboratory precision)
* - Standard Proctor Compaction Energy (592 kJ/m$^3$)
** - Relative Density Compaction Energy
† - Material Reused in Compaction Testing
◊ - ASTM D4718 warranted but not yet applied
NP – non-plastic
NA – not available

**Table 30: CFED Database Soils (cont.)**

| Properties | FLA FL20-22 | FLA FL23 | FLA FL24 | FLA FL25-1 | FLA FL25-2 |
|---|---|---|---|---|---|
| CFED Database ID | SOIL2033 | SOIL2034 | SOIL2035 | SOIL2036 | SOIL2037 |
| USCS Description (Symbol) | Silty Sand with Gravel (SM) | Poorly graded Sand with Silt (SP-SM) | Silty Sand (SM) | Silty sand (SM) | Poorly graded Sand with Silt (SP-SM) |
| Liquid Limit (LL) [1] | NP | NP | NP | NP | NP |
| Plastic Limit (PL)[2] | NP | NP | NP | NP | NP |
| Plasticity Index (PI) | NP | NP | NP | NP | NP |
| Specific Gravity ($G_s$) | 2.72 | 2.64 | 2.74 | 2.67 | 2.70 |
| Optimum moisture content, $W_{opt}$(%) [3]* | 14.2 | 8.3 | 18.0 | 17.3 | 12.5 |
| Dry Unit Weight $\gamma_{d\,max}$ (kN/m$^3$) [4]* | 18.4 | 15.9 | 16.1 | 16.4 | 15.6 |
| Gravel Size (%) (> 4.75 mm) | 28 | 1 | 6 | 0 | 1 |
| Sand Size (%) (4.75 to 0.075 mm) | 48 | 94 | 81 | 94 | 85 |
| Silt Size (%) (0.075 to 0.002 mm) | 19 | 4 | 13 | 5 | 14 |
| Clay Size (%) (≤ 0.002 mm) | 5 | 1 | 0 | 1 | 0 |
| Lab compaction energies | 2 | 2 | 2 | 2 | 2 |
| Field compaction curves | No | No | No | No | No |

1 – ASTM reported standard deviation 0.98 – 1.07 (2 soils tested by different operators in same lab)
2 – ASTM reported standard deviation 1.07 – 1.21 (2 soils tested by different operators in same lab)
3 – ASTM reported standard deviation ± 0.86 (Multilaboratory precision)
4 – ASTM reported standard deviation ± 0.26 (Multilaboratory precision)
* - Standard Proctor Compaction Energy (592 kJ/m$^3$)
** - Relative Density Compaction Energy
† - Material Reused in Compaction Testing
◊ - ASTM D4718 warranted but not yet applied
NP – non-plastic
NA – not available

**Table 31: CFED Database Soils (cont.)**

| Properties | NC1 | NC2 | NC4 |
|---|---|---|---|
| CFED Database ID | SOIL2038 | SOIL2039 | SOIL2040 |
| USCS Description (Symbol) | Silty Sand (SM) | Silty Sand (SM) | Poorly graded Sand with Silt and Gravel (SP-SM) |
| Liquid Limit (LL) [1] | 20 | 28 | NP |
| Plastic Limit (PL)[2] | NP | NP | NP |
| Plasticity Index (PI) | NP | NP | NP |
| Specific Gravity ($G_s$) | 2.73 | 2.67 | 2.74 |
| Optimum moisture content, $W_{opt}$(%) [3]* | 11.0 | 12.8 | 6.2 |
| Dry Unit Weight $\gamma_{d\,max}$ (kN/m$^3$) [4]* | 19.1 | 17.4 | 21.2 |
| Gravel Size (%) (> 4.75 mm) | 5 | 1 | 42 |
| Sand Size (%) (4.75 to 0.075 mm) | 69 | 61 | 47 |
| Silt Size (%) (0.075 to 0.002 mm) | 18 | 34 | 10 |
| Clay Size (%) (≤ 0.002 mm) | 8 | 4 | 1 |
| Lab compaction energies | 2 | 2 | 2 |
| Field compaction curves | No | No | No |

1 – ASTM reported standard deviation 0.98 – 1.07 (2 soils tested by different operators in same lab)
2 – ASTM reported standard deviation 1.07 – 1.21 (2 soils tested by different operators in same lab)
3 – ASTM reported standard deviation ± 0.86 (Multilaboratory precision)
4 – ASTM reported standard deviation ± 0.26 (Multilaboratory precision)
* - Standard Proctor Compaction Energy (592 kJ/m$^3$)
** - Relative Density Compaction Energy
† - Material Reused in Compaction Testing
◊ - ASTM D4718 warranted but not yet applied
NP – non-plastic
NA – not available

## Lab Compaction Data

The lab compaction data for each sample was plotted and the data analyzed manually. Each lab compaction curve is shown with the corresponding maximum dry density ($\gamma_{dmax}$) and optimum moisture content ($w_{opt}$) for each energy level. Limitations associated with quantity of material and time for testing permitted only one or two energy levels for some soils; all other soils contain five energy levels. Recall the compaction energy nomenclature definitions from Table 17.

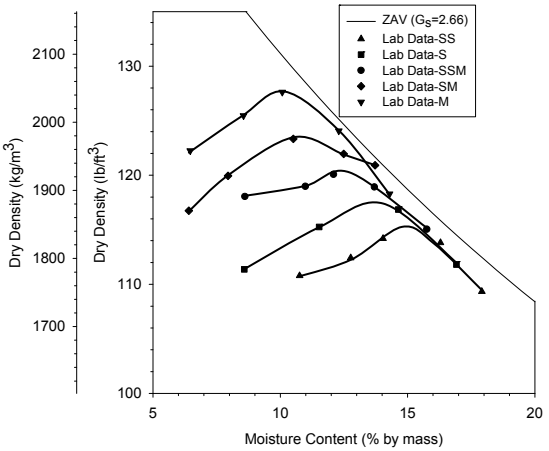


**Figure 84: Glacial Till C. Iowa (Soil 1632) hand curves**

**Table 32: Glacial Till C. Iowa lab compaction results**

| Soil | Glacial Till C. Iowa | |
|---|---|---|
| CFED # | 1632 | |
| Energy Level | $w_{opt}$ (%) | $\gamma_{d,max}$ (lb/ft$^3$) |
| SS | 15.1 | 114.8 |
| S | 13.9 | 117.4 |
| SSM | 12.5 | 120.1 |
| SM | 10.8 | 123.5 |
| M | 10.0 | 127.5 |

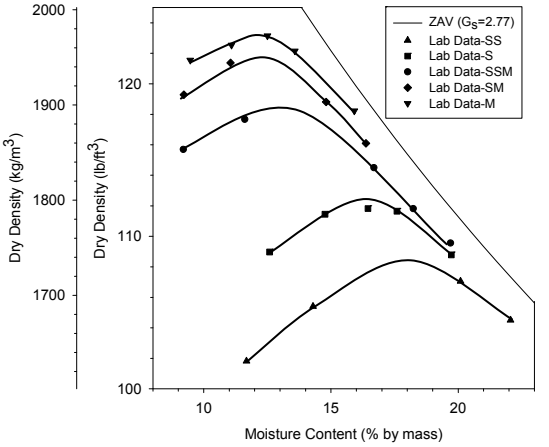


**Figure 85: Weathered Shale C. Iowa (Soil 1633) hand curves**

**Table 33: Weathered Shale C. Iowa lab compaction results**

| Soil | Weathered Shale C. Iowa | |
|---|---|---|
| CFED # | 1633 | |
| Energy Level | $w_{opt}$ (%) | $\gamma_{d,max}$ (lb/ft$^3$) |
| SS | 18.0 | 108.3 |
| S | 16.2 | 112.4 |
| SSM | 13.0 | 118.5 |
| SM | 12.6 | 121.7 |
| M | 12.4 | 123.3 |

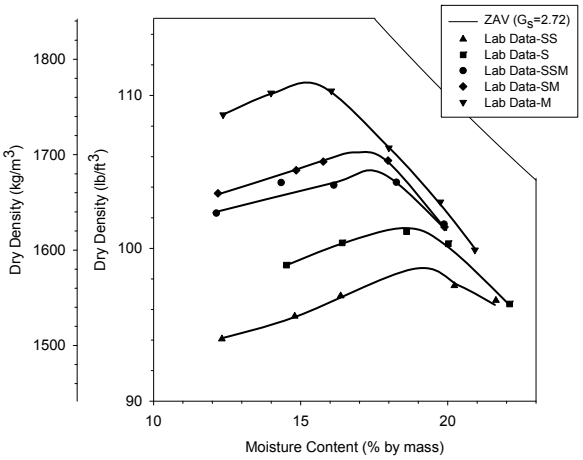


**Figure 86: Loess W. Iowa (Soil 1634) hand curves**

**Table 34: Loess W. Iowa lab compaction results**

| **Soil** | Loess W. Iowa | |
|---|---|---|
| **CFED #** | 1634 | |
| **Energy Level** | $w_{opt}$ (%) | $\gamma_{d,max}$ (lb/ft$^3$) |
| SS | 19.1 | 98.4 |
| S | 18.6 | 101.3 |
| SSM | 17.4 | 104.9 |
| SM | 17.0 | 106.6 |
| M | 15.1 | 110.6 |

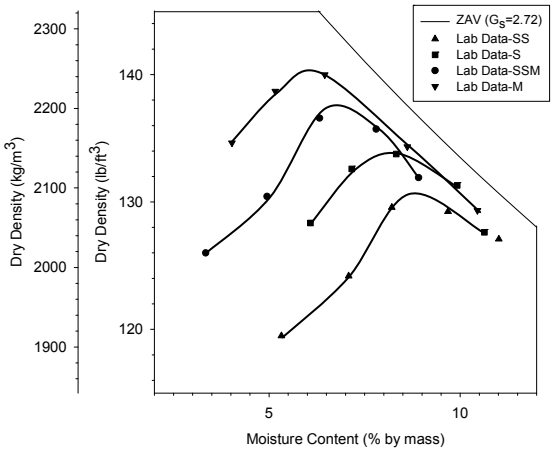


**Figure 87: Glacial Till W. Illinois (PPG) (Soil 1635) hand curves**

**Table 35: Weathered Shale C. Iowa (PPG) lab compaction results**

| **Soil** | Weathered Shale C. Iowa | |
|---|---|---|
| **CFED #** | 1635 | |
| **Energy Level** | $w_{opt}$ (%) | $\gamma_{d,max}$ (lb/ft$^3$) |
| SS | 8.8 | 130.4 |
| S | 8.1 | 133.7 |
| SSM | 6.8 | 137.3 |
| M | 6.0 | 140.0 |

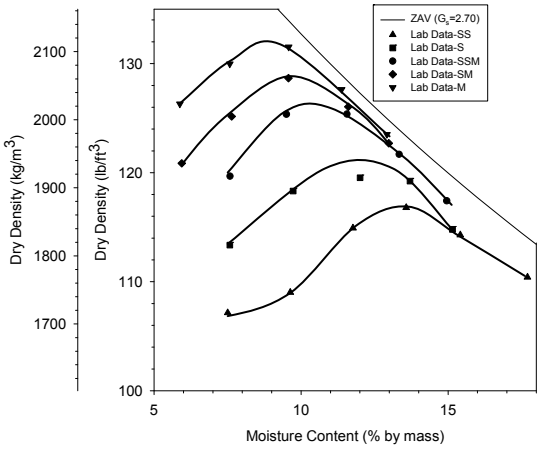


**Figure 88: Glacial Till W. Illinois (Edwards A) (Soil 1636) hand curves**

**Table 36: Glacial Till W. Illinois (Edwards A) lab compaction results**

| **Soil** | Glacial Till W. Illinois | |
|---|---|---|
| **CFED #** | 1636 | |
| **Energy Level** | $w_{opt}$ (%) | $\gamma_{d,max}$ (lb/ft$^3$) |
| SS | 13.5 | 116.7 |
| S | 12.1 | 121.0 |
| SSM | 10.4 | 126.2 |
| SM | 9.8 | 128.6 |
| M | 9.1 | 132.2 |

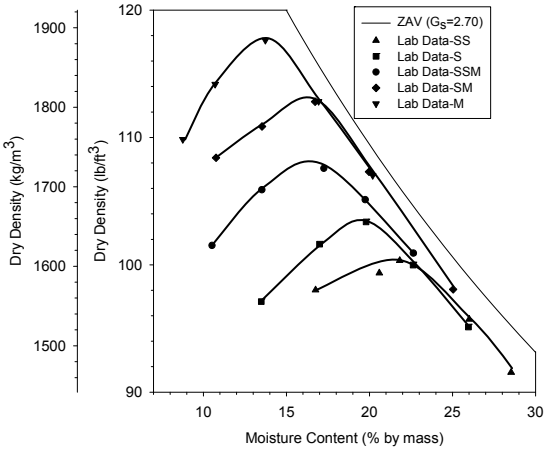


**Figure 89: Clay C. Iowa (728) (Soil 1637) hand curves**

**Table 37: Clay C. Iowa (728) lab compaction results**

| **Soil** | Clay C. Iowa | |
|---|---|---|
| **CFED #** | 1637 | |
| **Energy Level** | $w_{opt}$ (%) | $\gamma_{d,max}$ (lb/ft$^3$) |
| SS | 21.2 | 100.5 |
| S | 19.6 | 103.6 |
| SSM | 16.1 | 108.1 |
| SM | 15.8 | 113.4 |
| M | 13.4 | 117.7 |

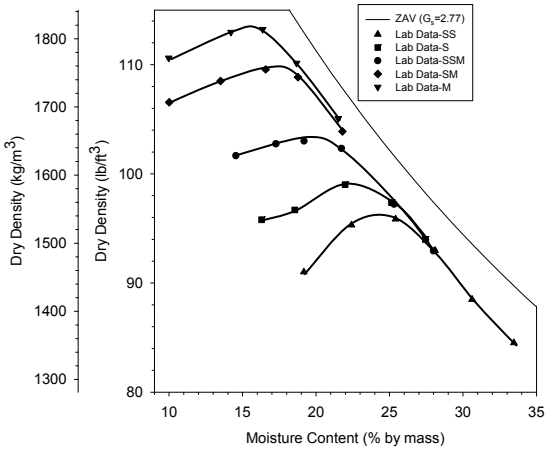


**Figure 90: Clay C. Iowa (GS) (Soil 1638) hand curves**

**Table 38: Clay C. Iowa (GS) lab compaction results**

| **Soil** | Clay C. Iowa (GS) | |
|---|---|---|
| **CFED #** | 1638 | |
| **Energy Level** | $w_{opt}$ (%) | $\gamma_{d,max}$ (lb/ft$^3$) |
| SS | 24.8 | 96.1 |
| S | 22.4 | 98.9 |
| SSM | 20.3 | 103.3 |
| SM | 17.1 | 109.9 |
| M | 15.9 | 113.6 |

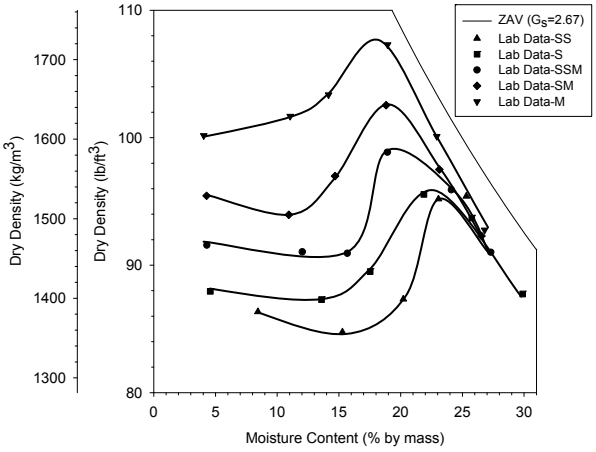


**Figure 91: Red Soil North Carolina (Soil 1640) hand curves**

**Table 39: Red Soil North Carolina lab compaction results**

| **Soil** | Red Soil North Carolina | |
|---|---|---|
| **CFED #** | 1640 | |
| **Energy Level** | $w_{opt}$ (%) | $\gamma_{d,max}$ (lb/ft$^3$) |
| SS | 23.1 | 95.2 |
| S | 22.1 | 96.0 |
| SSM | 20.0 | 99.3 |
| SM | 18.9 | 102.4 |
| M | 17.9 | 108.0 |

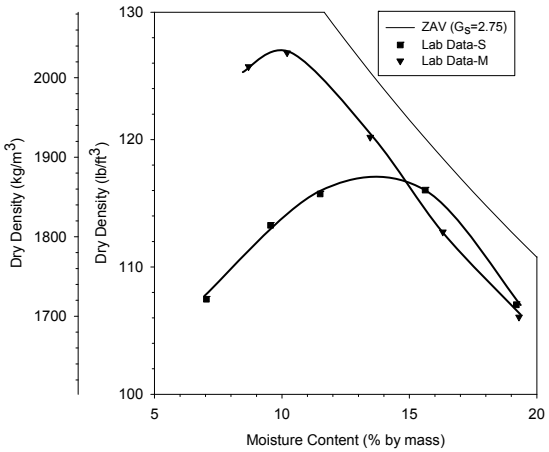


**Figure 92: Glacial Till W. Illinois (Edwards B) (Soil 2001) hand curves**

**Table 40: Glacial Till W. Illinois (Edwards B) lab compaction results**

| **Soil** | Glacial Till W. Illinois | |
|---|---|---|
| **CFED #** | 2001 | |
| **Energy Level** | $w_{opt}$ (%) | $\gamma_{d,max}$ (lb/ft$^3$) |
| S | 13.9 | 117.7 |
| M | 10.0 | 127.2 |

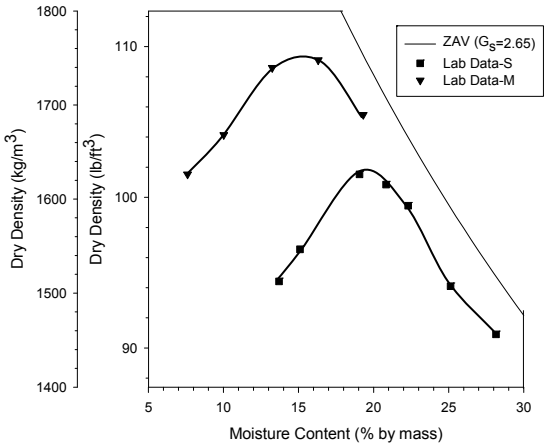


**Figure 93: Kickapoo Topsoil (Soil 2003) hand curves**

**Table 41: Kickapoo Topsoil lab compaction results**

| **Soil** | Kickapoo Topsoil | |
|---|---|---|
| **CFED #** | 2003 | |
| **Energy Level** | $w_{opt}$ (%) | $\gamma_{d,max}$ (lb/ft$^3$) |
| S | 19.3 | 101.6 |
| M | 14.9 | 109.6 |

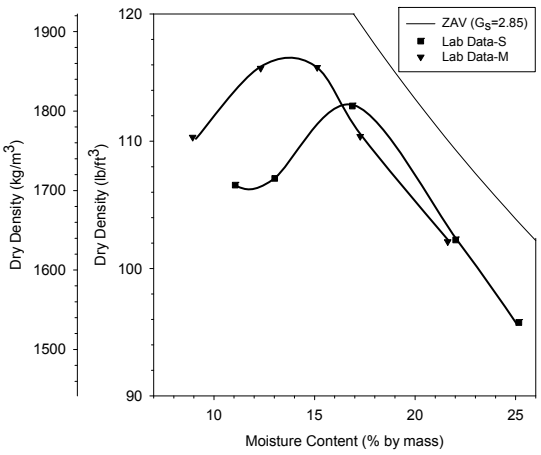


**Figure 94: Kickapoo Fill Clay (Soil 2004) hand curves**

**Table 42: Kickapoo Fill Clay lab compaction results**

| **Soil** | Kickapoo Fill Clay | |
|---|---|---|
| **CFED #** | 2004 | |
| **Energy Level** | $w_{opt}$ (%) | $\gamma_{d,max}$ (lb/ft$^3$) |
| S | 16.9 | 113.0 |
| M | 14.0 | 116.4 |

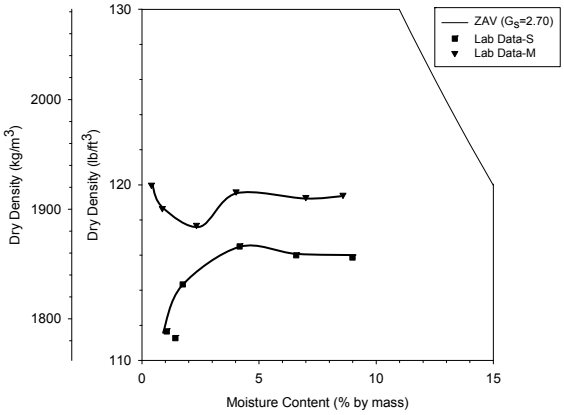


**Figure 95: Kickapoo Sand (Soil 2005) hand curves**

**Table 43: Kickapoo Sand lab compaction results**

| **Soil** | Kickapoo Sand | |
|---|---|---|
| **CFED #** | 2005 | |
| **Energy Level** | $w_{opt}$ (%) | $\gamma_{d,max}$ (lb/ft$^3$) |
| S | 4.8 | 116.7 |
| M | 4.0 | 119.7 |

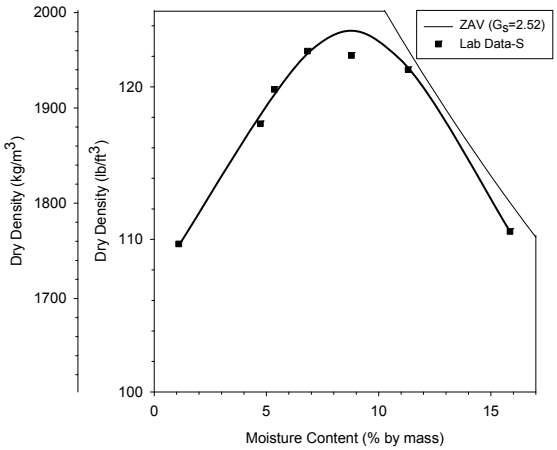


**Figure 96: RAP (Soil 2006) hand curve**

**Table 44: RAP lab compaction results**

| **Soil** | RAP | |
|---|---|---|
| **CFED #** | 2006 | |
| **Energy Level** | $w_{opt}$ (%) | $\gamma_{d,max}$ (lb/ft$^3$) |
| S | 9.0 | 123.5 |

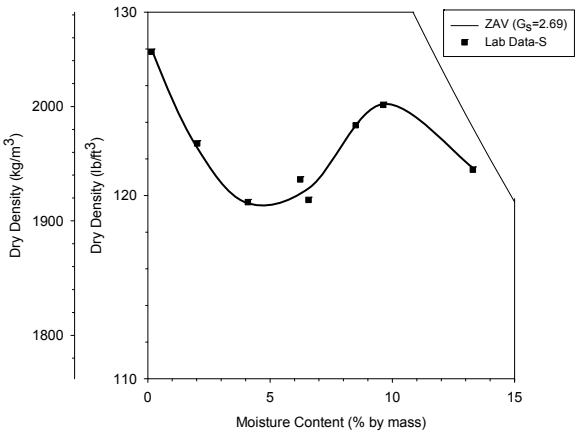


**Figure 97: CA6-C (Aug05) (Soil 2007) hand curve**

**Table 45: CA6-C (Aug05) lab compaction results**

| **Soil** | CA6-C (Aug05) | |
|---|---|---|
| **CFED #** | 2007 | |
| **Energy Level** | $w_{opt}$ (%) | $\gamma_{d,max}$ (lb/ft$^3$) |
| S | 9.8 | 125.0 |

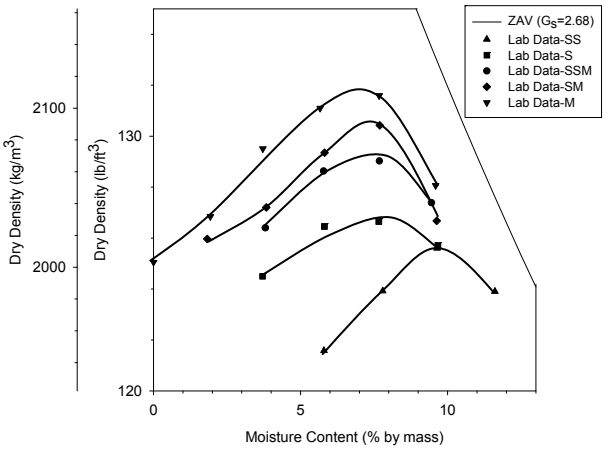


**Figure 98: FA6 (Soil 2008) hand curve**

**Table 46: FA6 lab compaction results**

| **Soil** | FA6 | |
|---|---|---|
| **CFED #** | 2008 | |
| **Energy Level** | $w_{opt}$ (%) | $\gamma_{d,max}$ (lb/ft$^3$) |
| SS | 9.8 | 125.5 |
| S | 7.9 | 126.9 |
| SSM | 7.5 | 129.2 |
| SM | 7.4 | 130.8 |
| M | 6.9 | 132.0 |

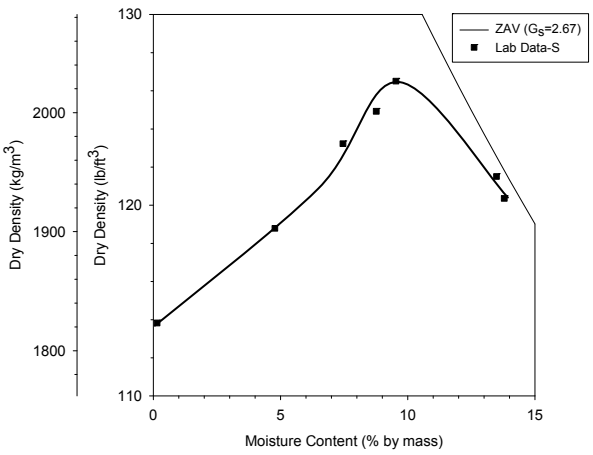


**Figure 99: CA6-G (Aug05) (Soil 2009) hand curve**

**Table 47: CA6-G (Aug05) lab compaction results**

| **Soil** | CA6-C (Aug05) | |
|---|---|---|
| **CFED #** | 2007 | |
| **Energy Level** | $w_{opt}$ (%) | $\gamma_{d,max}$ (lb/ft$^3$) |
| S | 9.5 | 126.4 |

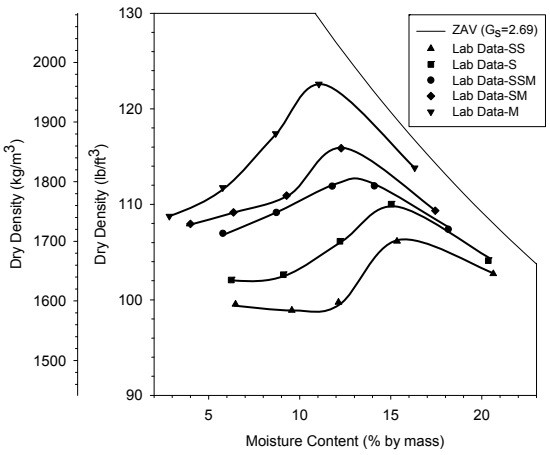


**Figure 100: MnRoad Glacial Till (Soil 2010) hand curves**

**Table 48: MnRoad Glacial Till lab compaction results**

| **Soil** | MnRoad Glacial Till | |
|---|---|---|
| **CFED #** | 2010 | |
| **Energy Level** | $w_{opt}$ (%) | $\gamma_{d,max}$ (lb/ft$^3$) |
| SS | 15.6 | 106.1 |
| S | 15.0 | 109.9 |
| SSM | 13.0 | 112.4 |
| SM | 12.1 | 116.0 |
| M | 11.0 | 122.5 |

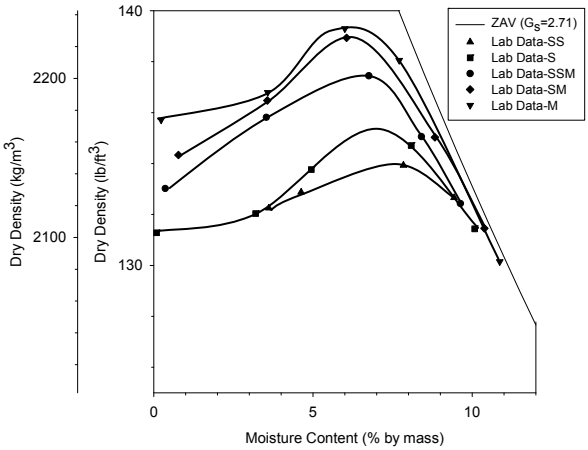


**Figure 101: MnRoad Class 5 Base (Soil 2011) hand curves**

**Table 49: MnRoad Class 5 Base lab compaction results**

| **Soil** | MnRoad Class 5 Base | |
|---|---|---|
| **CFED #** | 2011 | |
| **Energy Level** | $w_{opt}$ (%) | $\gamma_{d,max}$ (lb/ft$^3$) |
| SS | 7.8 | 134.0 |
| S | 7.1 | 135.4 |
| SSM | 6.7 | 137.6 |
| SM | 6.1 | 138.9 |
| M | 6.0 | 139.3 |

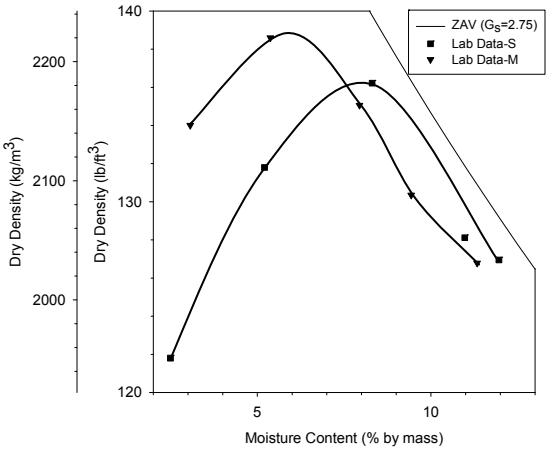


**Figure 102: CA6-G (June06) (Soil 2012) hand curves**

**Table 50: CA6-G (June06) lab compaction results**

| **Soil** | CA6-G (June06) | |
|---|---|---|
| **CFED #** | 2012 | |
| **Energy Level** | $w_{opt}$ (%) | $\gamma_{d,max}$ (lb/ft$^3$) |
| S | 8.0 | 136.3 |
| M | 5.7 | 138.7 |

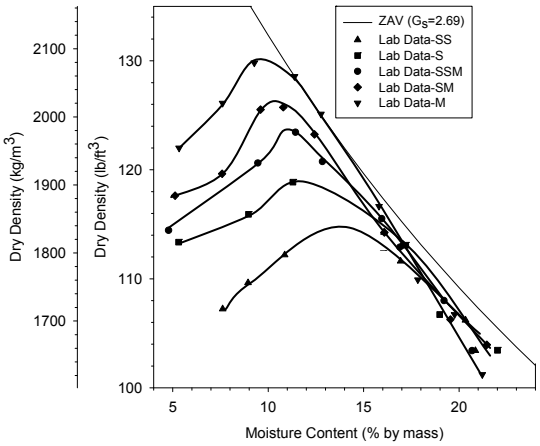


**Figure 103: TH60 Soil #1 (Soil 2013) hand curves**

**Table 51: TH60 Soil #1 lab compaction results**

| **Soil** | TH60 Soil #1 | |
|---|---|---|
| **CFED #** | 2013 | |
| **Energy Level** | $w_{opt}$ (%) | $\gamma_{d,max}$ (lb/ft$^3$) |
| SS | 13.5 | 114.6 |
| S | 11.7 | 119.2 |
| SSM | 11.0 | 123.6 |
| SM | 10.1 | 126.1 |
| M | 9.5 | 129.9 |

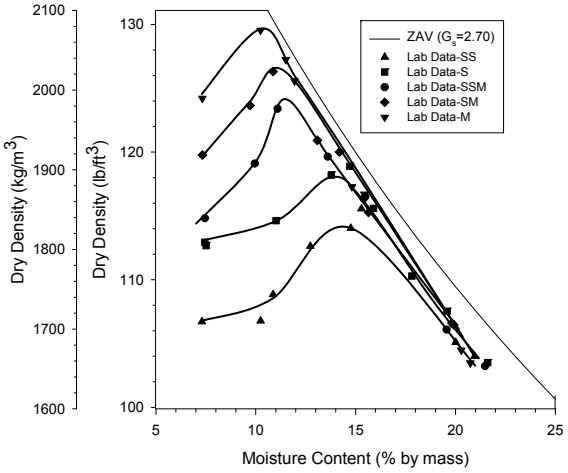


**Figure 104: TH60 Soil #2 (Soil 2014) hand curves**

**Table 52: TH60 Soil #2 lab compaction results**

| **Soil** | TH60 Soil #2 | |
|---|---|---|
| **CFED #** | 2014 | |
| **Energy Level** | $w_{opt}$ (%) | $\gamma_{d,max}$ (lb/ft$^3$) |
| SS | 14.7 | 114.1 |
| S | 13.3 | 118.6 |
| SSM | 11.5 | 123.6 |
| SM | 10.9 | 126.2 |
| M | 10.2 | 129.7 |

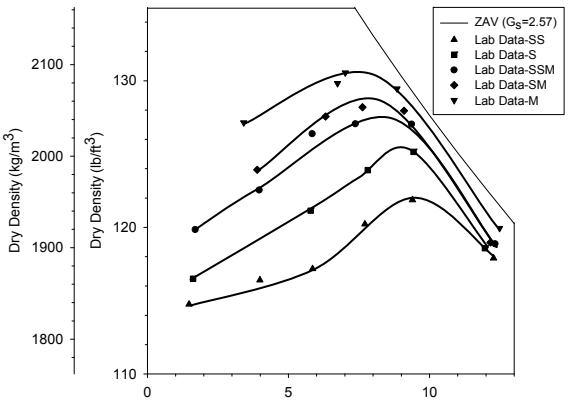


**Figure 105: US10-101 (Soil 2018) hand curves**

**Table 53: US10-101 lab compaction results**

| **Soil** | US10-101 | |
|---|---|---|
| **CFED #** | 2018 | |
| **Energy Level** | $w_{opt}$ (%) | $\gamma_{d,max}$ (lb/ft$^3$) |
| SS | 9.7 | 121.9 |
| S | 9.0 | 125.5 |
| SSM | 8.3 | 127.7 |
| SM | 8.0 | 128.7 |
| M | 7.5 | 130.5 |

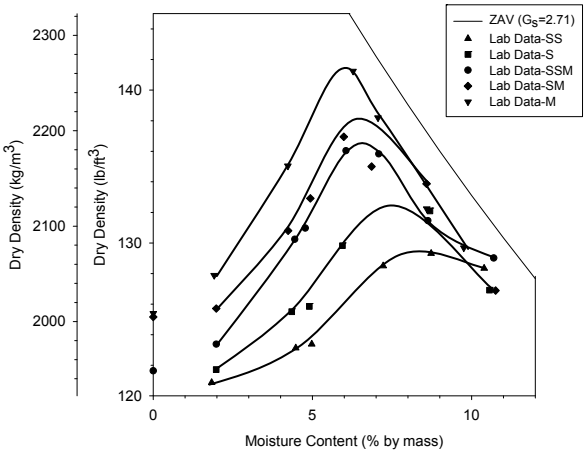


**Figure 106: TH36 Common (Soil 2020) hand curves**

**Table 54: TH36 Common lab compaction results**

| **Soil** | TH36 Common | |
|---|---|---|
| **CFED #** | 2020 | |
| **Energy Level** | $w_{opt}$ (%) | $\gamma_{d,max}$ (lb/ft$^3$) |
| SS | 8.2 | 129.5 |
| S | 7.4 | 132.6 |
| SSM | 6.5 | 136.4 |
| SM | 6.4 | 138.0 |
| M | 5.9 | 141.4 |

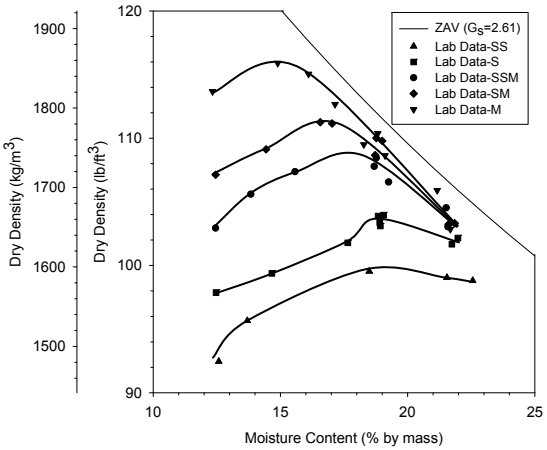


**Figure 107: TH60 Strip 2 (Soil 2021) hand curves**

**Table 55: TH60 Strip 2 lab compaction results**

| **Soil** | TH60 Strip 2 | |
|---|---|---|
| **CFED #** | 2021 | |
| **Energy Level** | $w_{opt}$ (%) | $\gamma_{d,max}$ (lb/ft$^3$) |
| SS | 19.3 | 99.9 |
| S | 18.7 | 103.9 |
| SSM | 17.8 | 108.6 |
| SM | 16.7 | 111.2 |
| M | 14.9 | 116.1 |

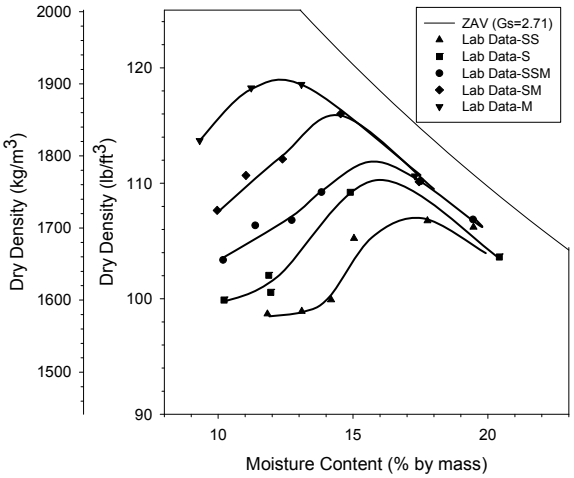


**Figure 108: China Red Clay (Soil 2022) hand curves**

**Table 56: China Red Clay lab compaction results**

| **Soil** | China Red Clay | |
|---|---|---|
| **CFED #** | 2022 | |
| **Energy Level** | $w_{opt}$ (%) | $\gamma_{d,max}$ (lb/ft$^3$) |
| SS | 17.1 | 107.1 |
| S | 16.1 | 110.2 |
| SSM | 15.8 | 112.0 |
| SM | 14.2 | 116.0 |
| M | 12.3 | 119.2 |

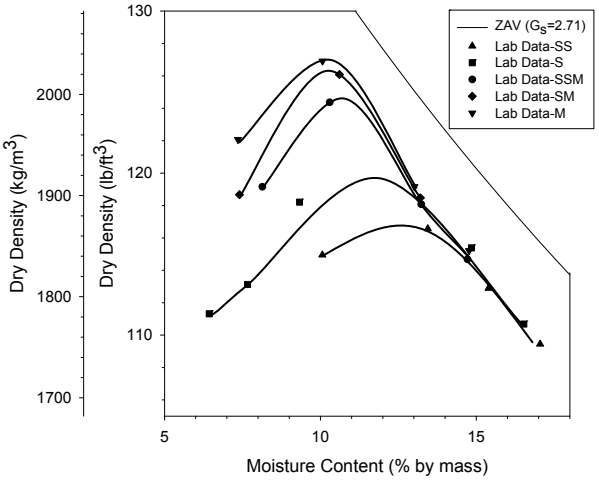


**Figure 109: China Yellow Clay (Soil 2023) hand curves**

**Table 57: China Yellow Clay lab compaction results**

| **Soil** | China Yellow Clay | |
|---|---|---|
| **CFED #** | 2023 | |
| **Energy Level** | $w_{opt}$ (%) | $\gamma_{d,max}$ (lb/ft$^3$) |
| SS | 12.7 | 116.8 |
| S | 11.8 | 119.9 |
| SSM | 10.8 | 124.7 |
| SM | 10.2 | 126.4 |
| M | 10.1 | 127.0 |

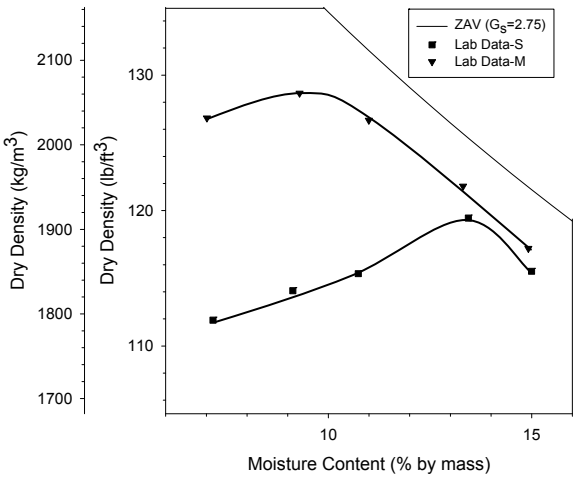


**Figure 110: Edwards Till 2008 (Soil 2024) hand curves**

**Table 58: Edwards Till 2008 lab compaction results**

| **Soil** | Edwards Till (2008) | |
|---|---|---|
| **CFED #** | 2024 | |
| **Energy Level** | $w_{opt}$ (%) | $\gamma_{d,max}$ (lb/ft$^3$) |
| S | 13.3 | 119.5 |
| M | 9.5 | 128.9 |

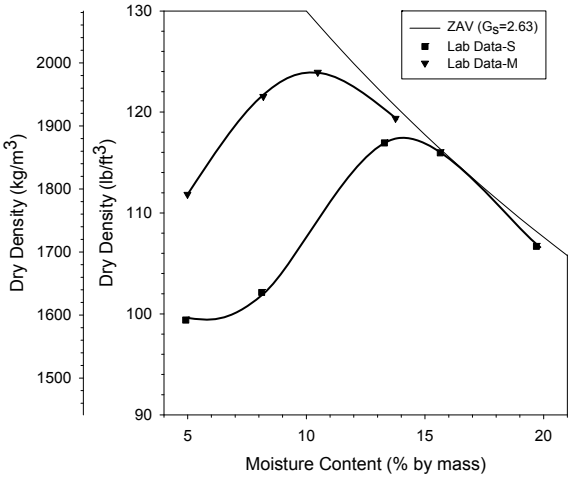


**Figure 111: CO Subgrade Clay 1 (Soil 2025) hand curves**

**Table 59: CO Subgrade Clay 1 lab compaction data**

| **Soil** | CO Subgrade Clay 1 | |
|---|---|---|
| **CFED #** | 2025 | |
| **Energy Level** | $w_{opt}$ (%) | $\gamma_{d,max}$ (lb/ft$^3$) |
| S | 14.1 | 116.8 |
| M | 10.5 | 124.0 |

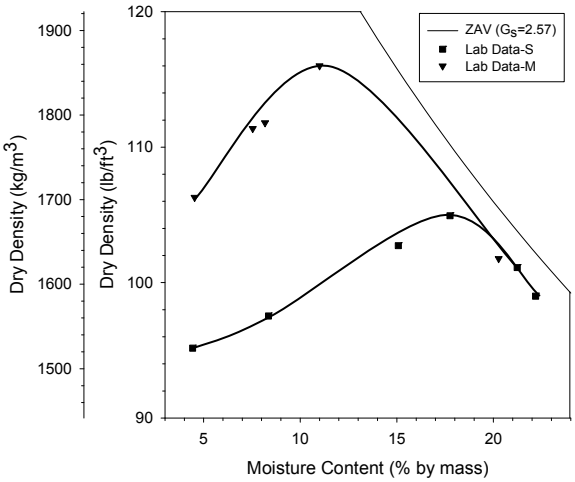


**Figure 112: CO Subgrade Clay 2 (Soil 2026) hand curves**

**Table 60: CO Subgrade Clay 2 lab compaction data**

| **Soil** | CO Subgrade Clay 2 | |
|---|---|---|
| **CFED #** | 2026 | |
| **Energy Level** | $w_{opt}$ (%) | $\gamma_{d,max}$ (lb/ft$^3$) |
| S | 17.8 | 105.1 |
| M | 11.0 | 116.1 |

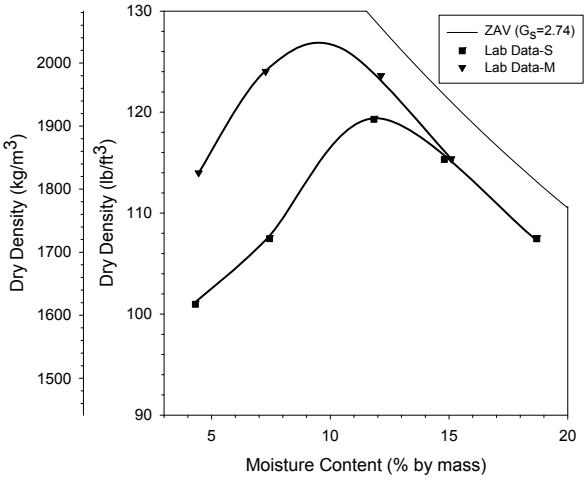


**Figure 113: CO Subgrade Clay 3 (Soil 2027) hand curves**

**Table 61: CO Subgrade Clay 3 lab compaction data**

| **Soil** | CO Subgrade Clay 3 | |
|---|---|---|
| **CFED #** | 2027 | |
| **Energy Level** | $w_{opt}$ (%) | $\gamma_{d,max}$ (lb/ft$^3$) |
| S | 11.9 | 119.8 |
| M | 9.4 | 127.0 |

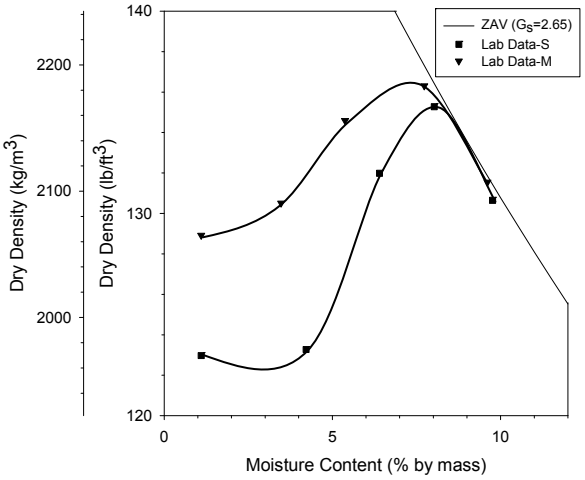


**Figure 114: CO Base Layer (Soil 2029) hand curves**

**Table 62: CO Base Layer lab compaction data**

| **Soil** | CO Base Layer | |
|---|---|---|
| **CFED #** | 2029 | |
| **Energy Level** | $w_{opt}$ (%) | $\gamma_{d,max}$ (lb/ft$^3$) |
| S | 8.0 | 135.2 |
| M | 7.2 | 136.4 |

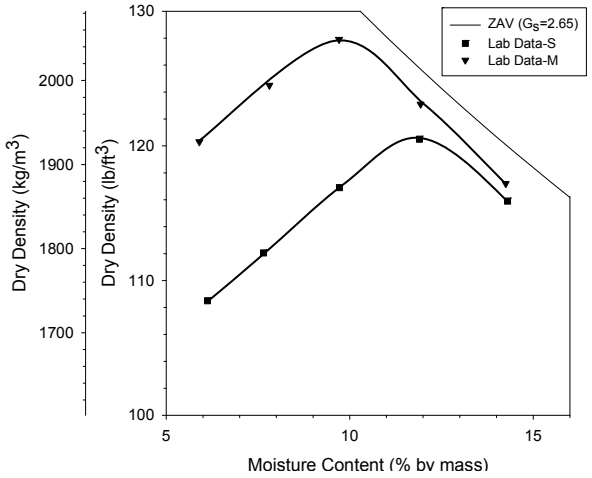


**Figure 115: MD Subgrade Clay (Soil 2030) hand curves**

**Table 63: MD Subgrade Clay lab compaction data**

| **Soil** | MD Subgrade Clay | |
|---|---|---|
| **CFED #** | 2030 | |
| **Energy Level** | $w_{opt}$ (%) | $\gamma_{d,max}$ (lb/ft$^3$) |
| S | 11.9 | 120.8 |
| M | 9.7 | 128.0 |

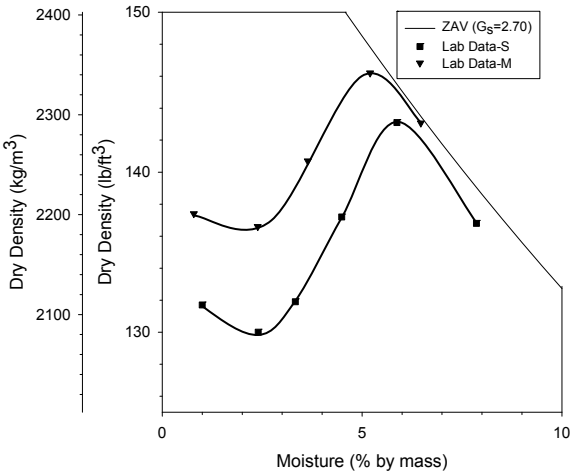


**Figure 116: MD Base Material (Soil 2031) hand curves**

**Table 64: MD Base Material lab compaction data**

| **Soil** | MD Base Material | |
|---|---|---|
| **CFED #** | 2031 | |
| **Energy Level** | $w_{opt}$ (%) | $\gamma_{d,max}$ (lb/ft$^3$) |
| S | 5.9 | 143.1 |
| M | 5.2 | 146.2 |

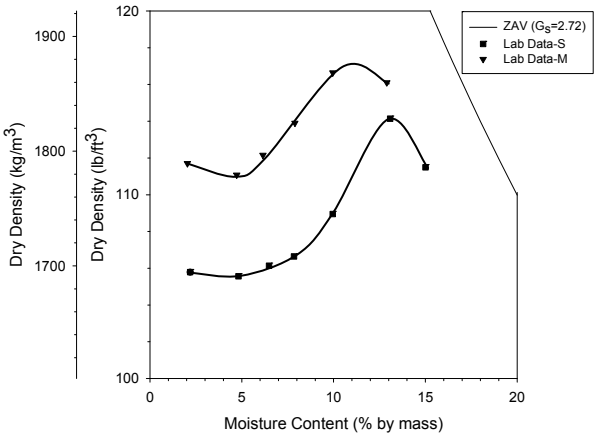


**Figure 117: FLA FL19 (Soil 2032) hand curves**

**Table 65: FLA FL19 lab compaction data**

| **Soil** | FLA FL19 | |
|---|---|---|
| **CFED #** | 2032 | |
| **Energy Level** | $w_{opt}$ (%) | $\gamma_{d,max}$ (lb/ft$^3$) |
| S | 13.0 | 114.2 |
| M | 11.0 | 117.1 |

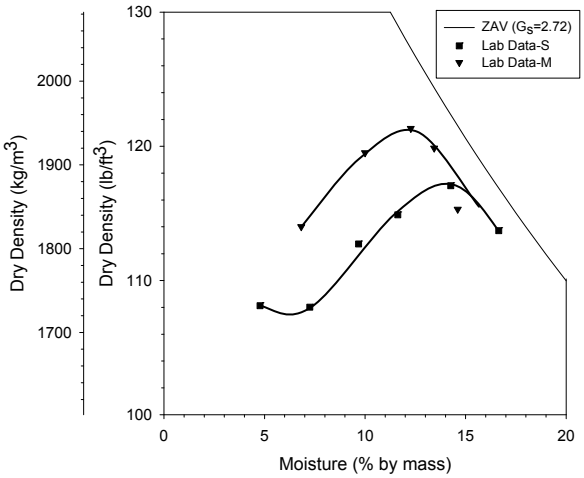


**Figure 118: FLA FL20-22 (Soil 2033) hand curves**

**Table 66: FLA FL20-22 lab compaction data**

| **Soil** | FLA FL20-22 | |
|---|---|---|
| **CFED #** | 2033 | |
| **Energy Level** | $w_{opt}$ (%) | $\gamma_{d,max}$ (lb/ft$^3$) |
| S | 14.1 | 117.0 |
| M | 12.3 | 121.2 |

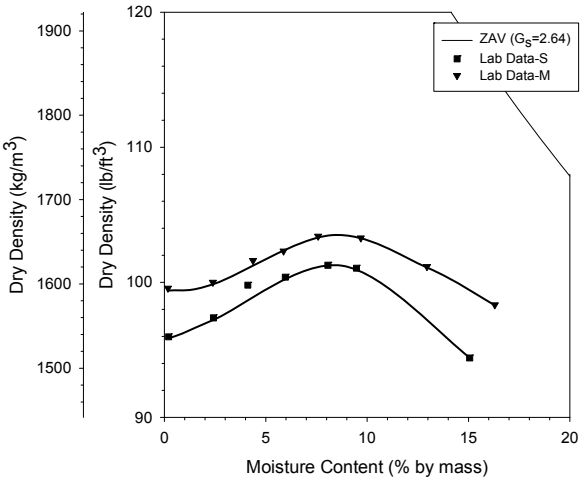


**Figure 119: FLA FL23 (Soil 2034) hand curves**

**Table 67: FLA FL23 lab compaction data**

| **Soil** | FLA FL23 | |
|---|---|---|
| **CFED #** | 2034 | |
| **Energy Level** | $w_{opt}$ (%) | $\gamma_{d,max}$ (lb/ft$^3$) |
| S | 8.6 | 101.5 |
| M | 8.5 | 103.7 |

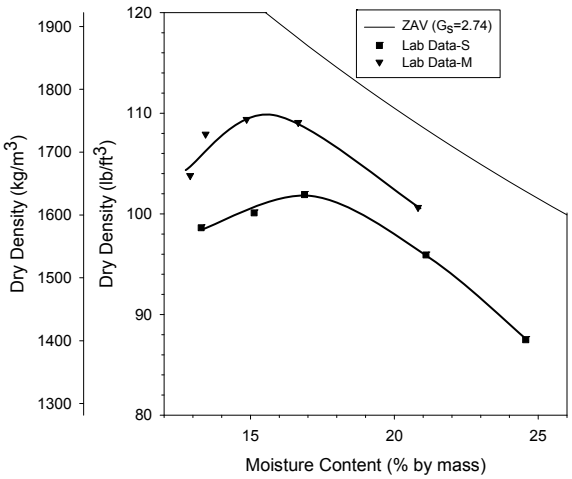


**Figure 120: FLA FL24 (Soil 2035) hand curves**

**Table 68: FLA FL24 lab compaction data**

| **Soil** | FLA FL24 | |
|---|---|---|
| **CFED #** | 2035 | |
| **Energy Level** | $w_{opt}$ (%) | $\gamma_{d,max}$ (lb/ft$^3$) |
| S | 16.9 | 102.0 |
| M | 15.6 | 110.0 |

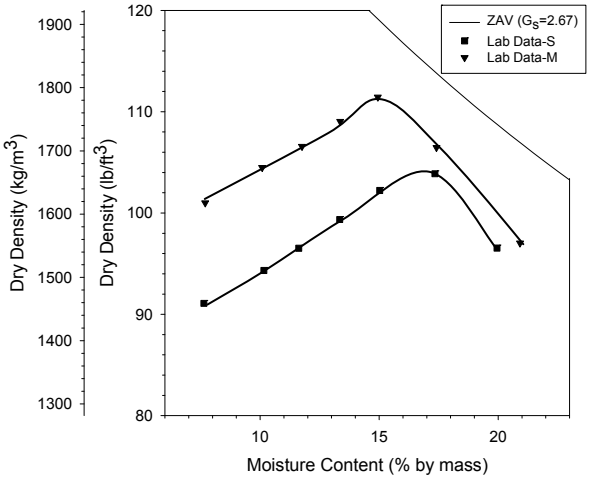


**Figure 121: FLA FL25-1 (Soil 2036) hand curves**

**Table 69: FLA FL25-1 lab compaction data**

| **Soil** | FLA FL25-1 | |
|---|---|---|
| **CFED #** | 2036 | |
| **Energy Level** | $w_{opt}$ (%) | $\gamma_{d,max}$ (lb/ft$^3$) |
| S | 17.0 | 104.2 |
| M | 15.0 | 101.8 |

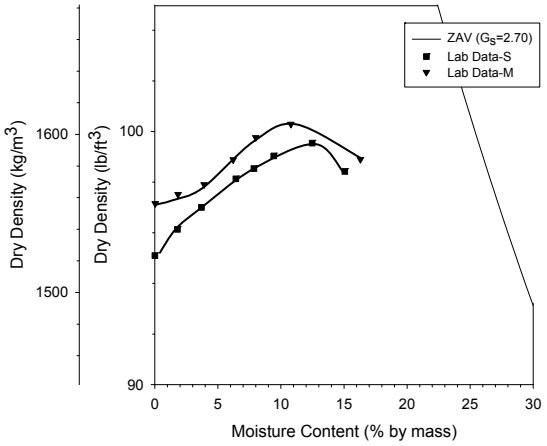


**Figure 122: FLA FL25-2 (Soil 2037) hand curves**

**Table 70: FLA FL25-2 lab compaction data**

| **Soil** | FLA FL25-2 | |
|---|---|---|
| **CFED #** | 2037 | |
| **Energy Level** | $w_{opt}$ (%) | $\gamma_{d,max}$ (lb/ft$^3$) |
| S | 12.5 | 99.7 |
| M | 10.8 | 100.2 |

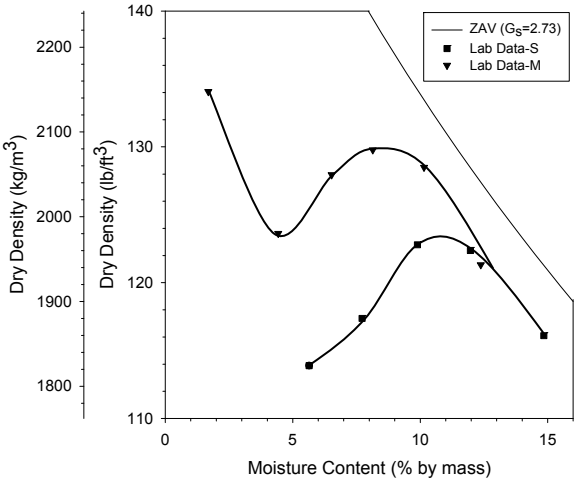


**Figure 123: NC1 (Soil 2038) hand curves**

**Table 71: NC1 lab compaction data**

| **Soil** | NC1 | |
|---|---|---|
| **CFED #** | 2038 | |
| **Energy Level** | $w_{opt}$ (%) | $\gamma_{d,max}$ (lb/ft$^3$) |
| S | 10.9 | 123.6 |
| M | 8.5 | 130.0 |

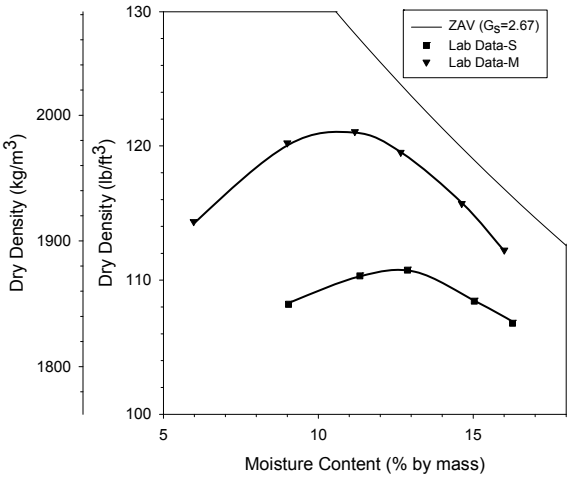


**Figure 124: NC2 (Soil 2039) hand curves**

**Table 72: NC2 lab compaction data**

| **Soil** | NC2 | |
|---|---|---|
| **CFED #** | 2039 | |
| **Energy Level** | $w_{opt}$ (%) | $\gamma_{d,max}$ (lb/ft$^3$) |
| S | 12.8 | 110.8 |
| M | 10.7 | 121.2 |

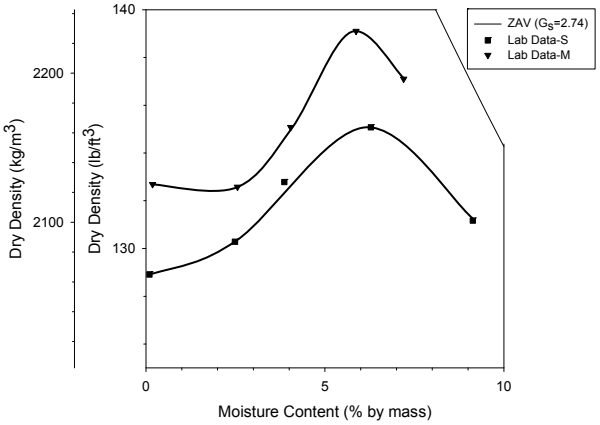


**Figure 125: NC4 (Soil 2040) hand curves**

**Table 73: NC4 lab compaction data**

| **Soil** | NC4 | |
|---|---|---|
| **CFED #** | 2040 | |
| **Energy Level** | $w_{opt}$ (%) | $\gamma_{d,max}$ (lb/ft$^3$) |
| S | 6.2 | 135.1 |
| M | 5.9 | 139.1 |

**Laboratory Compaction Curve Predictions**

Each soil was entered into SoilVision 4.0 (2006) to determine the model prediction for quadratic, Woods, and Li & Sego methods. These predictions have been plotted and are compared with the CFED prediction for each soil. The figures and tables below summarize the maximum dry density ($\gamma_{d,max}$), optimum water content ($w_{opt}$) and coefficient of determination ($R^2$) for each soil and energy level for the four prediction methods. Included in these tables are the Blotz (1998) Atterberg prediction method; however, this data is not shown graphically. For Blotz (1998) method A, the maximum density/optimum moisture content from the standard Proctor test was used to predict other energy levels. Therefore, the prediction for standard energy level was omitted because the model simply output the input parameters. The model prediction was always equal to the hand-curve interpretation because the hand-curve interpretation was used to create the prediction.

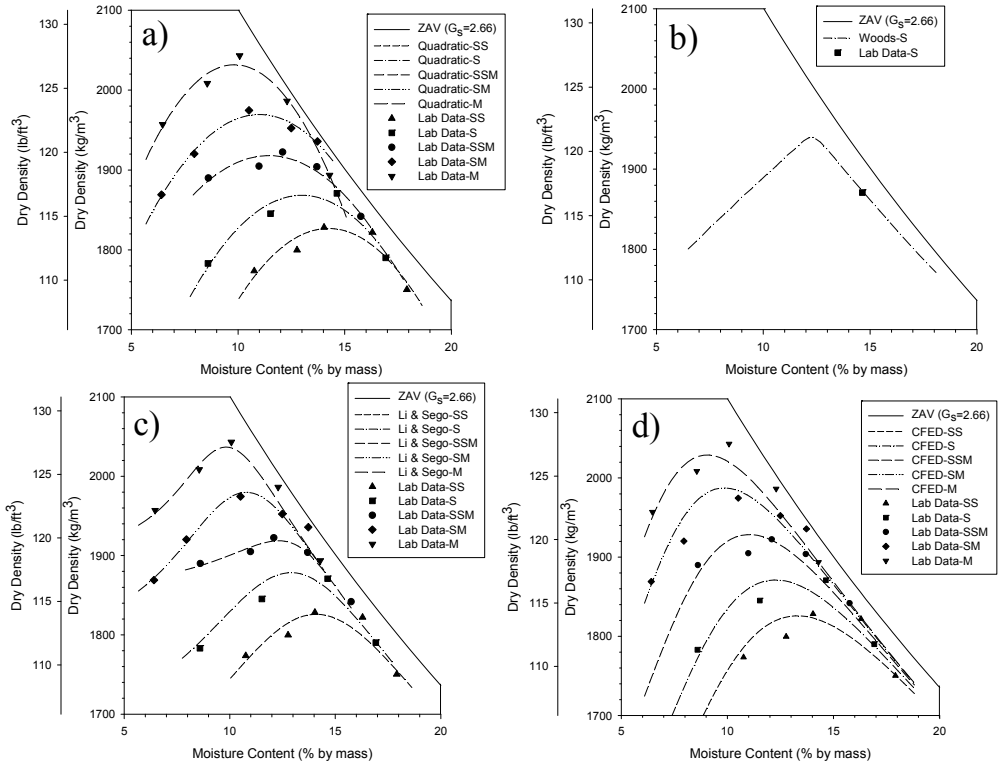


**Figure 126: Glacial Till C. Iowa (Soil 1632) a) Quadratic, b) Woods c) Li & Sego, d) CFED**

**Table 74: Soil 1632 Prediction Values**

| | | Quadratic | | | Woods | | | Blotz A | |
|---|---|---|---|---|---|---|---|---|---|
| Soil CFED # | Energy | $w_{opt}$ (%) | $\gamma_{d\ max}$ (lb/ft$^3$) | $R^2$ | $w_{opt}$ (%) | $\gamma_{d\ max}$ (lb/ft$^3$) | $R^2$ | $w_{opt}$ (%) | $\gamma_{d\ max}$ (lb/ft$^3$) |
| 1632 | SS | 14.2 | 114.0 | 0.85 | -- | -- | -- | 14.9 | 111.5 |
| | S | 13.0 | 116.6 | 0.91 | 11.9 | 121.7 | 1.00 | -- | -- |
| | SSM | 11.4 | 119.7 | 0.93 | -- | -- | -- | -- | -- |
| | SM | 11.0 | 122.9 | 0.98 | -- | -- | -- | -- | -- |
| | M | 9.8 | 126.8 | 0.98 | -- | -- | -- | 11.0 | 123.8 |

| | | Blotz B | | Li & Sego | | | | CFED | | |
|---|---|---|---|---|---|---|---|---|---|---|
| Soil CFED # | Energy | $w_{opt}$ (%) | $\gamma_{d\ max}$ (lb/ft$^3$) | $S_m$ | $w_{opt}$ (%) | $\gamma_{d\ max}$ (lb/ft$^3$) | $R^2$ | $w_{opt}$ (%) | $\gamma_{d\ max}$ (lb/ft$^3$) | $R^2$ |
| 1632 | SS | 13.9 | 91.6 | 93 | 14.1 | 114.0 | 0.80 | 13.2 | 114.0 | 0.94 |
| | S | 13.0 | 122.6 | 93 | 13.4 | 118.2 | 1.00 | 12.3 | 116.8 | |
| | SSM | -- | -- | 93 | 12.3 | 119.8 | 0.97 | 10.9 | 120.4 | |
| | SM | -- | -- | 93 | 10.8 | 123.6 | 0.88 | 9.8 | 124.0 | |
| | M | 10.0 | 131.8 | 93 | 9.8 | 127.2 | 0.96 | 9.0 | 126.7 | |

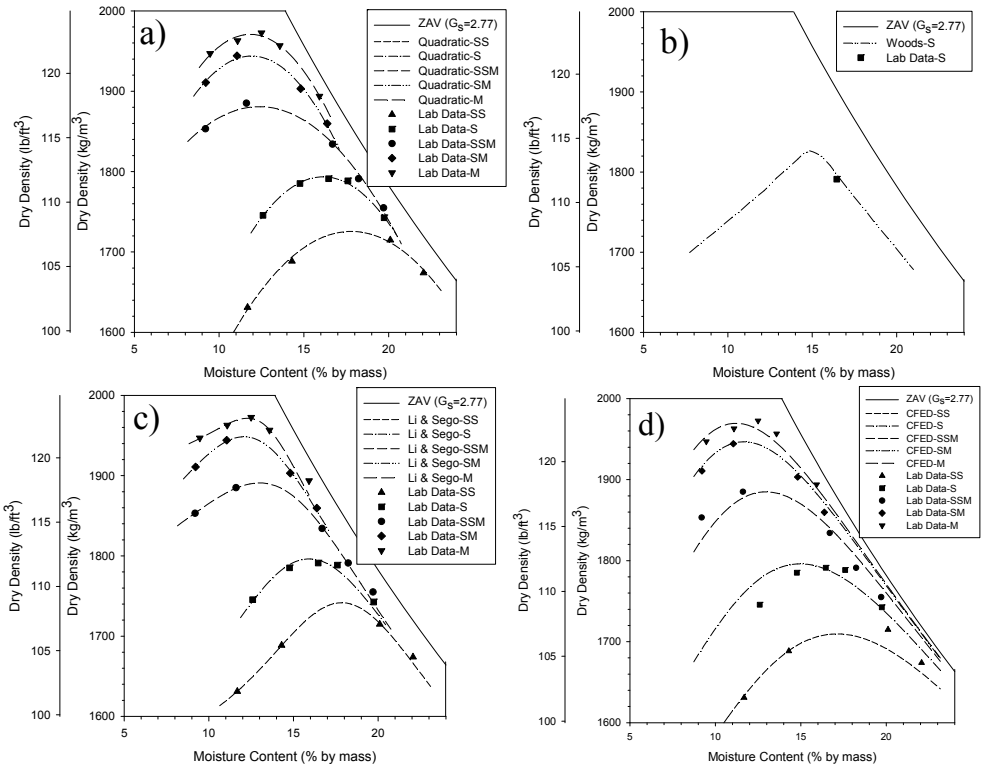


**Figure 127: Weathered Shale Central Iowa (Soil 1633) a) Quadratic, b) Woods, c) Li & Sego, d) CFED**

**Table 75: Soil 1633 Prediction Values**

| | | Quadratic | | | Woods | | | Blotz A | |
|---|---|---|---|---|---|---|---|---|---|
| Soil CFED # | Energy | $w_{opt}$ (%) | $\gamma_{d\ max}$ (lb/ft$^3$) | $R^2$ | $w_{opt}$ (%) | $\gamma_{d\ max}$ (lb/ft$^3$) | $R^2$ | $w_{opt}$ (%) | $\gamma_{d\ max}$ (lb/ft$^3$) |
| 1633 | SS | 17.8 | 107.7 | 0.99 | -- | -- | -- | 17.6 | 109.1 |
| | S | 16.1 | 112.0 | 0.99 | 14.6 | 114.2 | 1.00 | -- | -- |
| | SSM | 12.4 | 117.4 | 0.99 | -- | -- | -- | -- | -- |
| | SM | 11.9 | 121.3 | 0.99 | -- | -- | -- | -- | -- |
| | M | 11.8 | 123.0 | 0.99 | -- | -- | -- | 11.9 | 123.4 |

| | | Blotz B | | Li & Sego | | | | CFED | | |
|---|---|---|---|---|---|---|---|---|---|---|
| Soil CFED # | Energy | $w_{opt}$ (%) | $\gamma_{d\ max}$ (lb/ft$^3$) | $S_m$ | $w_{opt}$ (%) | $\gamma_{d\ max}$ (lb/ft$^3$) | $R^2$ | $w_{opt}$ (%) | $\gamma_{d\ max}$ (lb/ft$^3$) | $R^2$ |
| 1633 | SS | 16.2 | 81.7 | 93 | 17.8 | 108.7 | 0.99 | 17.0 | 106.5 | 0.98 |
| | S | 14.8 | 118.0 | 93 | 15.9 | 110.5 | 0.94 | 15.0 | 112.1 | |
| | SSM | -- | -- | 93 | 13.0 | 118.0 | 0.98 | 12.8 | 117.7 | |
| | SM | -- | -- | 93 | 12.1 | 121.6 | 0.99 | 11.6 | 121.2 | |
| | M | 10.5 | 128.7 | 93 | 12.3 | 123.1 | 0.92 | 11.2 | 113.0 | |

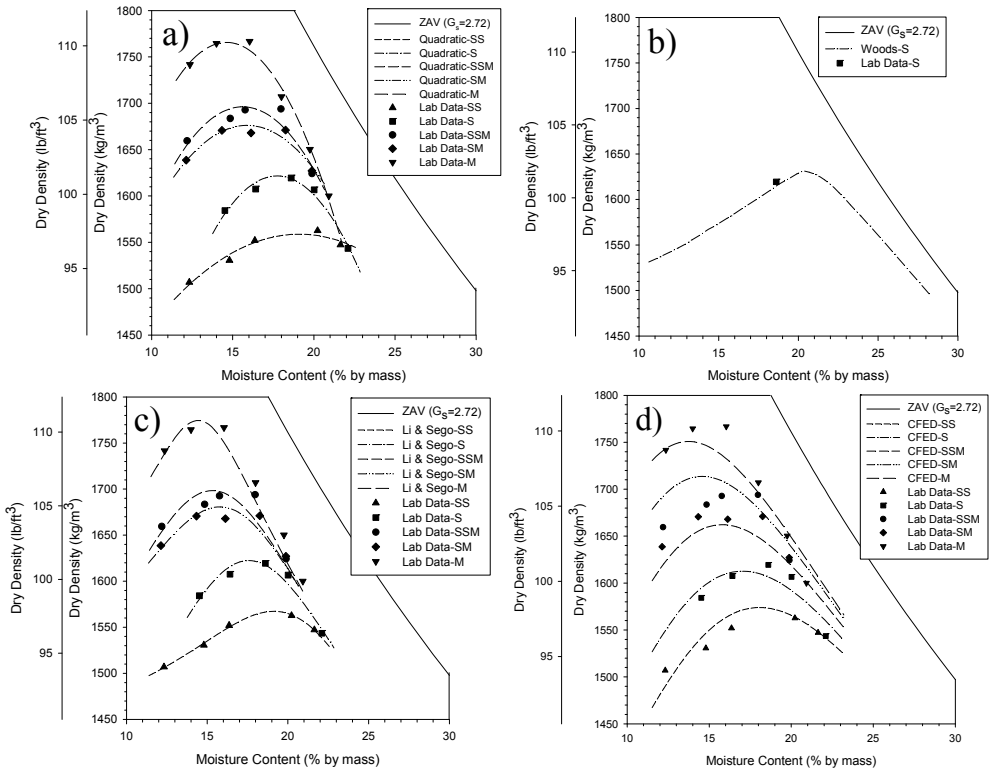


**Figure 128: Loess W. Iowa (Soil 1634) a) Quadratic, b) Woods, c) Li & Sego, d) CFED**

**Table 76: Soil 1634 Prediction Values**

| | | Quadratic | | | Woods | | | Blotz A | |
|---|---|---|---|---|---|---|---|---|---|
| Soil CFED # | Energy | $w_{opt}$ (%) | $\gamma_{d\ max}$ (lb/ft$^3$) | $R^2$ | $w_{opt}$ (%) | $\gamma_{d\ max}$ (lb/ft$^3$) | $R^2$ | $w_{opt}$ (%) | $\gamma_{d\ max}$ (lb/ft$^3$) |
| 1634 | SS | 19.1 | 97.3 | 0.95 | -- | -- | -- | 19.8 | 97.9 |
| | S | 17.7 | 101.2 | 0.97 | 20.3 | 102.4 | 1.00 | -- | -- |
| | SSM | 15.6 | 105.9 | 0.86 | -- | -- | -- | -- | -- |
| | SM | 15.9 | 104.6 | 0.88 | -- | -- | -- | -- | -- |
| | M | 14.6 | 110.2 | 0.99 | -- | -- | -- | 15.0 | 111.2 |

| | | Blotz B | | Li & Sego | | | | CFED | | |
|---|---|---|---|---|---|---|---|---|---|---|
| Soil CFED # | Energy | $w_{opt}$ (%) | $\gamma_{d\ max}$ (lb/ft$^3$) | $S_m$ | $w_{opt}$ (%) | $\gamma_{d\ max}$ (lb/ft$^3$) | $R^2$ | $w_{opt}$ (%) | $\gamma_{d\ max}$ (lb/ft$^3$) | $R^2$ |
| 1634 | SS | 14.7 | 87.2 | 80 | 19.1 | 97.8 | 0.99 | 18.0 | 98.1 | 0.94 |
| | S | 13.5 | 120.8 | 80 | 17.6 | 101.3 | 0.94 | 17.0 | 100.7 | |
| | SSM | -- | -- | 80 | 15.3 | 106.0 | 0.70 | 15.8 | 104.2 | |
| | SM | -- | -- | 80 | 15.8 | 104.9 | 0.68 | 14.5 | 107.1 | |
| | M | 9.9 | 130.8 | 80 | 14.4 | 110.8 | 0.94 | 13.7 | 109.2 | |

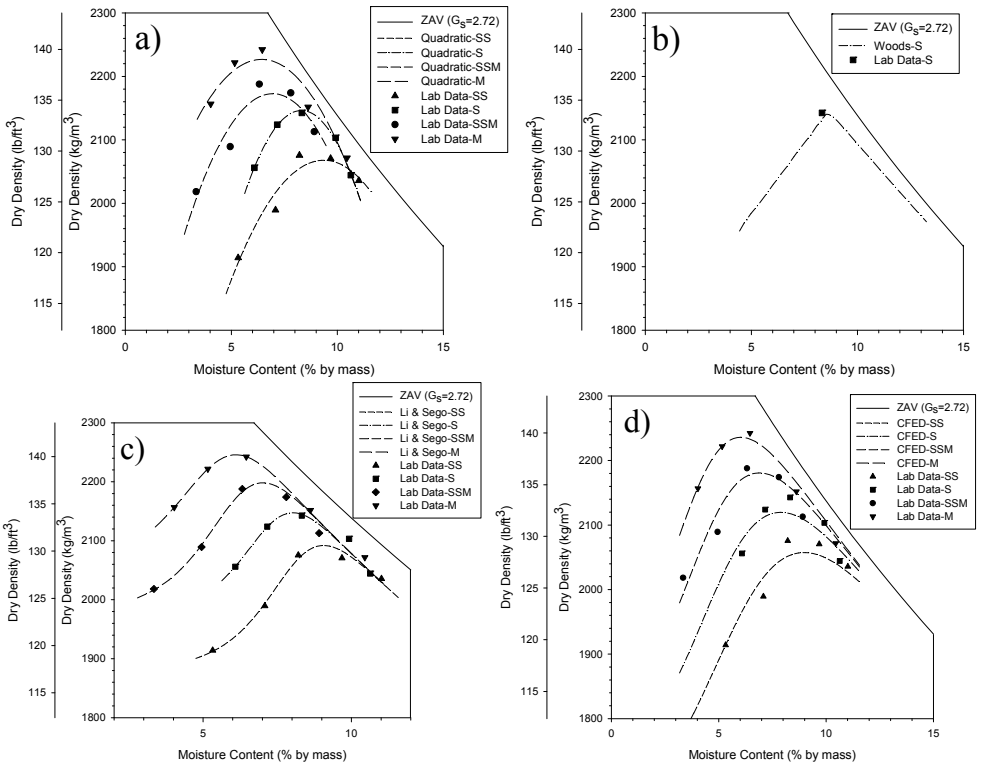


**Figure 129: Glacial Till W. Illinois (PPG) (Soil 1635) a) Quadratic, b) Woods, c) Li & Sego, d) CFED**

**Table 77: Soil 1635 Prediction Values**

| | | Quadratic | | | Woods | | | Blotz A | |
|---|---|---|---|---|---|---|---|---|---|
| Soil CFED # | Energy | $w_{opt}$ (%) | $\gamma_{d\,max}$ (lb/ft$^3$) | $R^2$ | $w_{opt}$ (%) | $\gamma_{d\,max}$ (lb/ft$^3$) | $R^2$ | $w_{opt}$ (%) | $\gamma_{d\,max}$ (lb/ft$^3$) |
| 1635 | SS | 9.4 | 129.1 | 0.93 | -- | -- | -- | 8.8 | 130.9 |
| | S | 8.3 | 134.0 | 0.99 | 8.5 | 134.2 | 0.99 | -- | -- |
| | SSM | 6.9 | 135.6 | 0.90 | -- | -- | -- | -- | -- |
| | M | 6.4 | 139.0 | 0.93 | -- | -- | -- | 6.0 | 141.9 |

| | | Blotz B | | Li & Sego | | | | CFED | | |
|---|---|---|---|---|---|---|---|---|---|---|
| Soil CFED # | Energy | $w_{opt}$ (%) | $\gamma_{d\,max}$ (lb/ft$^3$) | $S_m$ | $w_{opt}$ (%) | $\gamma_{d\,max}$ (lb/ft$^3$) | $R^2$ | $w_{opt}$ (%) | $\gamma_{d\,max}$ (lb/ft$^3$) | $R^2$ |
| 1635 | SS | 13.7 | 95.9 | 88 | 9.1 | 130.6 | 0.99 | 9.0 | 128.5 | 0.95 |
| | S | 13.0 | 123.6 | 88 | 8.0 | 134.1 | 0.93 | 7.9 | 132.3 | |
| | SSM | -- | -- | 88 | 7.0 | 137.2 | 0.97 | 6.9 | 136.1 | |
| | M | 10.9 | 131.9 | 88 | 6.1 | 140.2 | 0.99 | 6.0 | 139.6 | |

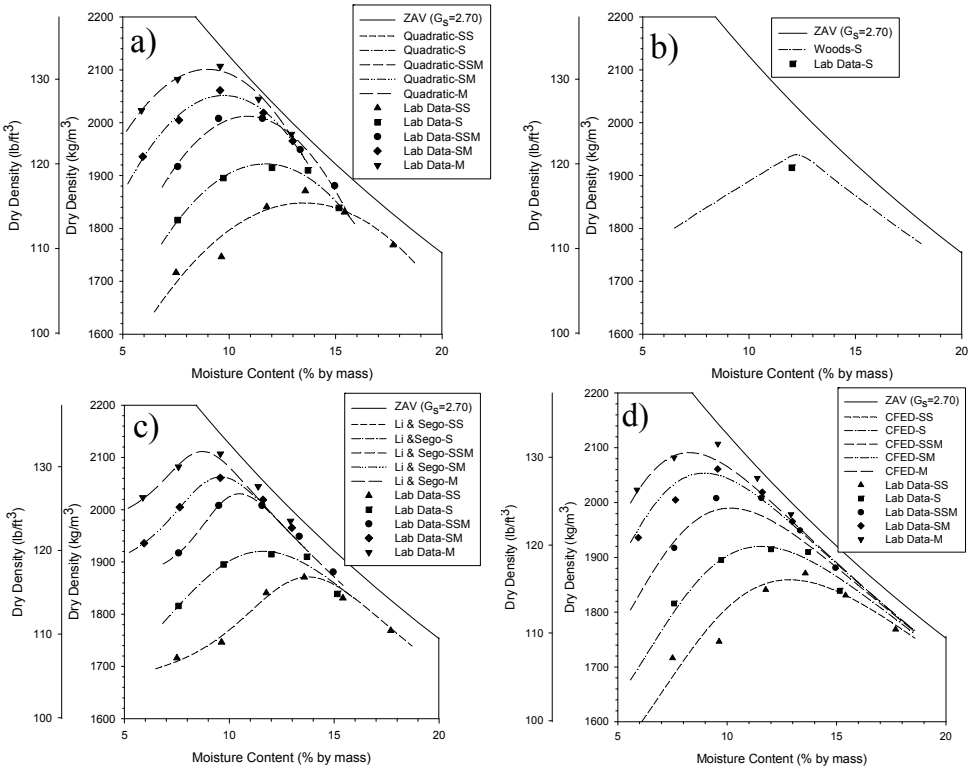


**Figure 130: Glacial Till W. Illinois (Edwards A) (Soil 1636) a) Quadratic, b) Woods, c) Li & Sego, d) CFED**

**Table 78: Soil 1636 Prediction Values**

| | | Quadratic | | | Woods | | | Blotz A | |
|---|---|---|---|---|---|---|---|---|---|
| Soil CFED # | Energy | $w_{opt}$ (%) | $\gamma_{d\,max}$ (lb/ft$^3$) | $R^2$ | $w_{opt}$ (%) | $\gamma_{d\,max}$ (lb/ft$^3$) | $R^2$ | $w_{opt}$ (%) | $\gamma_{d\,max}$ (lb/ft$^3$) |
| 1636 | SS | 13.5 | 115.4 | 0.87 | -- | -- | -- | 13.3 | 117.6 |
| | S | 11.7 | 120.0 | 0.96 | 11.9 | 121.7 | 0.93 | -- | -- |
| | SSM | 10.9 | 125.6 | 0.97 | -- | -- | -- | -- | -- |
| | SM | 9.7 | 128.1 | 0.98 | -- | -- | -- | -- | -- |
| | M | 9.0 | 131.2 | 0.98 | -- | -- | -- | 8.5 | 130.9 |

| | | Blotz B | | Li & Sego | | | | CFED | | |
|---|---|---|---|---|---|---|---|---|---|---|
| Soil CFED # | Energy | $w_{opt}$ (%) | $\gamma_{d\,max}$ (lb/ft$^3$) | $S_m$ | $w_{opt}$ (%) | $\gamma_{d\,max}$ (lb/ft$^3$) | $R^2$ | $w_{opt}$ (%) | $\gamma_{d\,max}$ (lb/ft$^3$) | $R^2$ |
| 1636 | SS | 14.7 | 87.2 | 91 | 13.8 | 116.8 | 0.97 | 12.8 | 116.1 | 0.96 |
| | S | 13.5 | 120.8 | 91 | 11.6 | 119.9 | 0.93 | 11.6 | 119.9 | |
| | SSM | -- | -- | 91 | 10.5 | 126.8 | 0.98 | 10.2 | 124.2 | |
| | SM | -- | -- | 91 | 9.6 | 128.8 | 0.97 | 8.9 | 128.1 | |
| | M | 9.9 | 130.8 | 91 | 8.7 | 131.8 | 0.88 | 8.3 | 130.5 | |

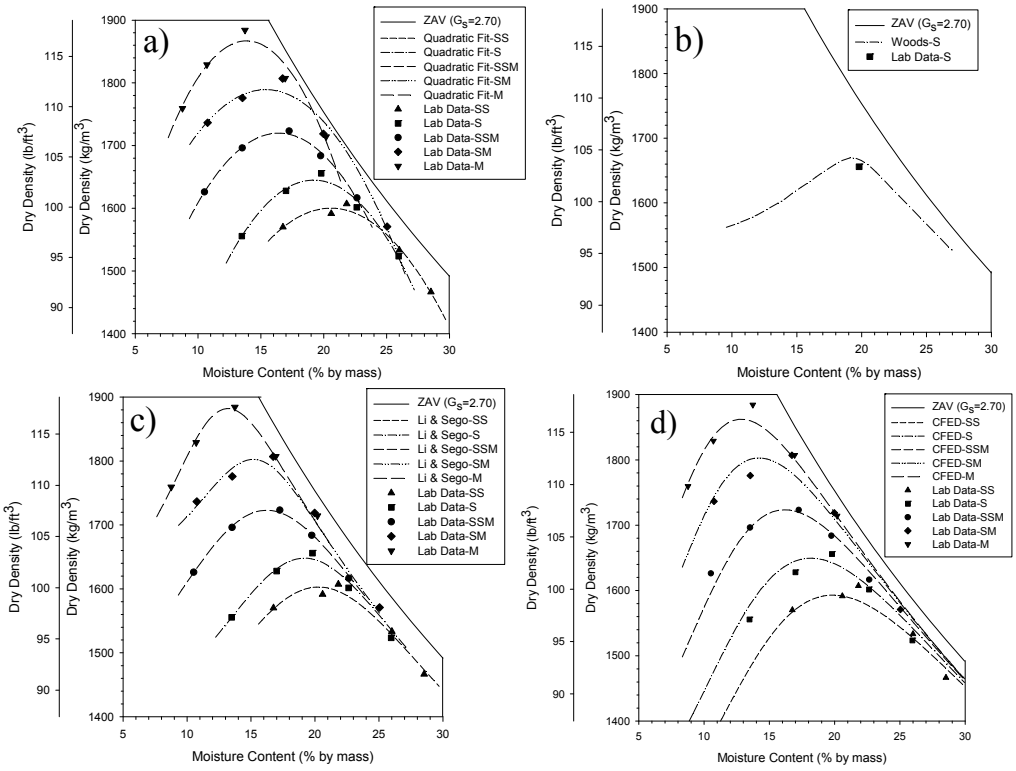


**Figure 131: Clay C. Iowa (728) (Soil 1637) a) Quadratic, b) Woods, c) Li & Sego, d) CFED**

**Table 79: Soil 1637 Prediction Values**

| | | Quadratic | | | Woods | | | Blotz A | |
|---|---|---|---|---|---|---|---|---|---|
| Soil CFED # | Energy | $w_{opt}$ (%) | $\gamma_{d\ max}$ (lb/ft$^3$) | $R^2$ | $w_{opt}$ (%) | $\gamma_{d\ max}$ (lb/ft$^3$) | $R^2$ | $w_{opt}$ (%) | $\gamma_{d\ max}$ (lb/ft$^3$) |
| 1637 | SS | 20.6 | 99.9 | 0.98 | -- | -- | -- | 21.2 | 99.9 |
| | S | 19.2 | 102.7 | 0.97 | 19.2 | 104.9 | 0.98 | -- | -- |
| | SSM | 16.4 | 107.4 | 0.99 | -- | -- | -- | -- | -- |
| | SM | 15.4 | 111.7 | 0.97 | -- | -- | -- | -- | -- |
| | M | 13.8 | 116.6 | 0.95 | -- | -- | -- | 14.7 | 115.3 |

| | | Blotz B | | Li & Sego | | | | CFED | | |
|---|---|---|---|---|---|---|---|---|---|---|
| Soil CFED # | Energy | $w_{opt}$ (%) | $\gamma_{d\ max}$ (lb/ft$^3$) | $S_m$ | $w_{opt}$ (%) | $\gamma_{d\ max}$ (lb/ft$^3$) | $R^2$ | $w_{opt}$ (%) | $\gamma_{d\ max}$ (lb/ft$^3$) | $R^2$ |
| 1637 | SS | 18.4 | 75.2 | 93 | 20.3 | 100.1 | 0.97 | 19.9 | 99.3 | 0.98 |
| | S | 16.8 | 114.0 | 93 | 19.2 | 102.9 | 0.97 | 18.2 | 103.0 | |
| | SSM | -- | -- | 93 | 16.2 | 107.6 | 1.00 | 16.1 | 107.5 | |
| | SM | -- | -- | 93 | 15.2 | 112.5 | 0.98 | 14.3 | 112.4 | |
| | M | 11.9 | 125.5 | 93 | 13.2 | 117.5 | 0.99 | 12.8 | 116.3 | |

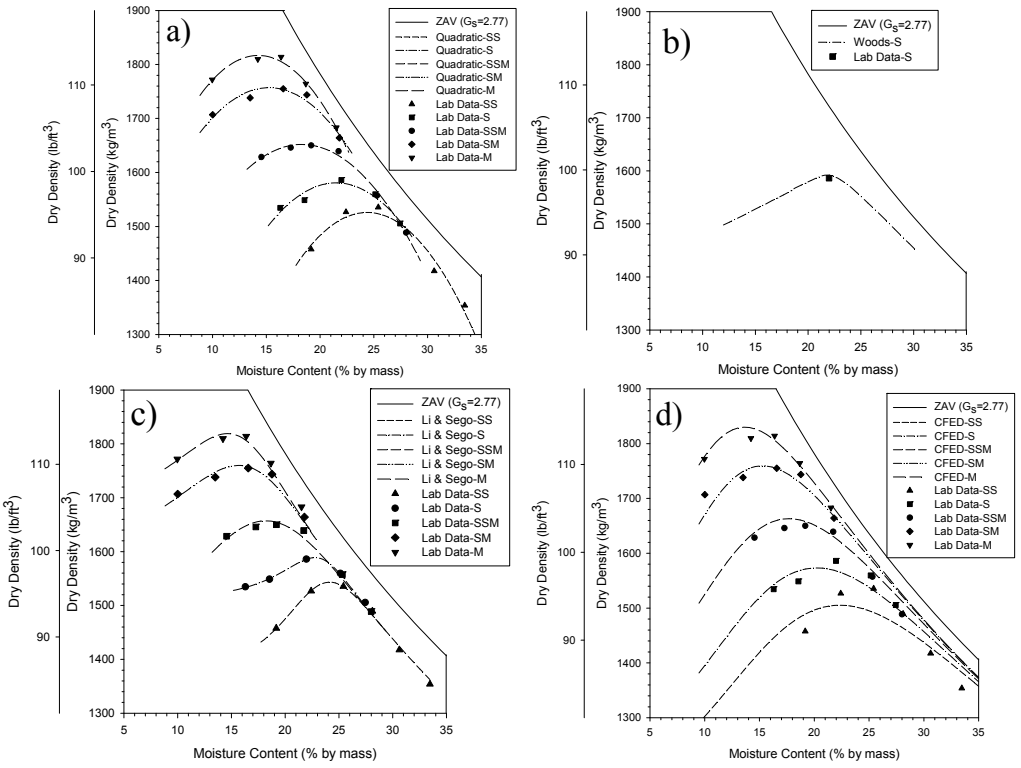


**Figure 132: Clay C. Iowa (GS) (Soil 1638) a) Quadratic, b) Woods, c) Li & Sego, d) CFED**

**Table 80: Soil 1638 Prediction Values**

| | | Quadratic | | | Woods | | | Blotz A | |
|---|---|---|---|---|---|---|---|---|---|
| Soil CFED # | Energy | $w_{opt}$ (%) | $\gamma_{d\,max}$ (lb/ft$^3$) | $R^2$ | $w_{opt}$ (%) | $\gamma_{d\,max}$ (lb/ft$^3$) | $R^2$ | $w_{opt}$ (%) | $\gamma_{d\,max}$ (lb/ft$^3$) |
| 1638 | SS | 24.4 | 95.3 | 0.96 | -- | -- | -- | 24.2 | 94.6 |
| | S | 21.5 | 98.7 | 0.90 | 21.5 | 99.9 | 1.00 | -- | -- |
| | SSM | 18.3 | 103.1 | 0.99 | -- | -- | -- | -- | -- |
| | SM | 15.2 | 109.7 | 0.93 | -- | -- | -- | -- | -- |
| | M | 14.2 | 113.4 | 0.99 | -- | -- | -- | 17.0 | 110.8 |

| | | Blotz B | | | Li & Sego | | | CFED | | |
|---|---|---|---|---|---|---|---|---|---|---|
| Soil CFED # | Energy | $w_{opt}$ (%) | $\gamma_{d\,max}$ (lb/ft$^3$) | $S_m$ | $w_{opt}$ (%) | $\gamma_{d\,max}$ (lb/ft$^3$) | $R^2$ | $w_{opt}$ (%) | $\gamma_{d\,max}$ (lb/ft$^3$) | $R^2$ |
| 1638 | SS | 21.0 | 68.6 | 89.7 | 24.1 | 96.3 | 0.99 | 22.4 | 94.0 | 0.98 |
| | S | 19.2 | 109.6 | 89.7 | 22.8 | 99.2 | 0.99 | 20.2 | 98.2 | |
| | SSM | -- | -- | 89.7 | 18.2 | 103.4 | 0.98 | 17.5 | 103.7 | |
| | SM | -- | -- | 89.7 | 15.7 | 109.9 | 0.92 | 15.4 | 109.9 | |
| | M | 13.8 | 121.7 | 89.7 | 14.6 | 113.6 | 0.94 | 13.7 | 114.2 | |

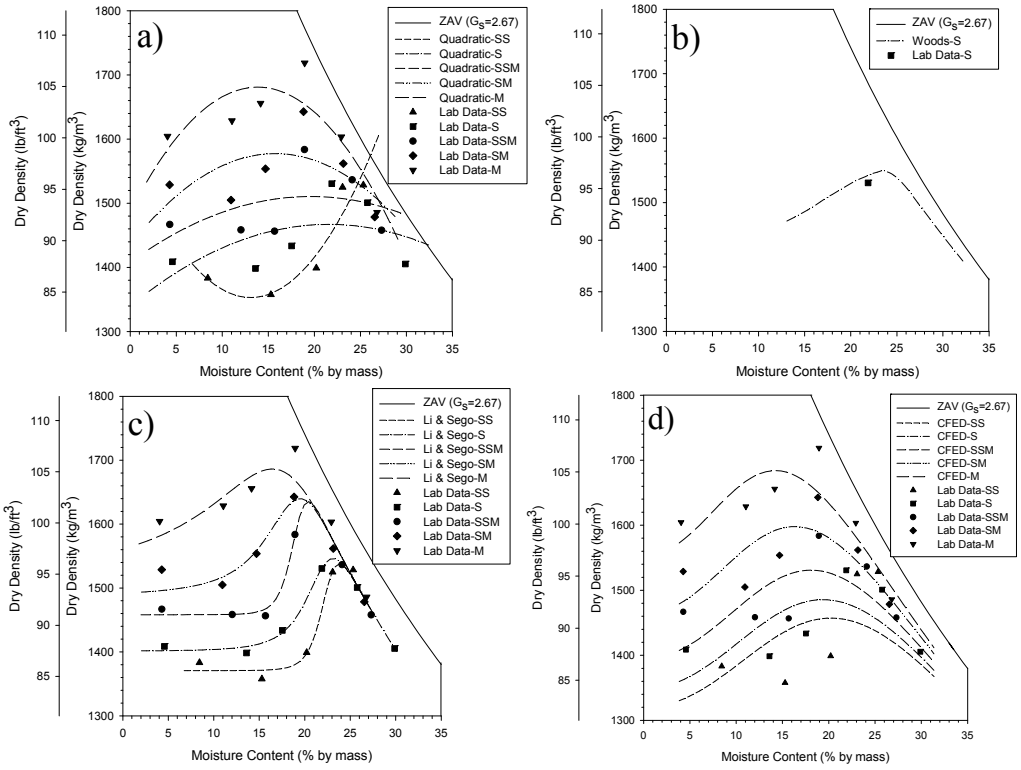


**Figure 133: Red Soil North Carolina (Soil 1640) a) Quadratic, b) Woods, c) Li & Sego, d) CFED**

**Table 81: Soil 1640 Prediction Values**

| | | Quadratic | | | Woods | | | Blotz A | |
|---|---|---|---|---|---|---|---|---|---|
| Soil CFED # | Energy | $w_{opt}$ (%) | $\gamma_{d\ max}$ (lb/ft$^3$) | $R^2$ | $w_{opt}$ (%) | $\gamma_{d\ max}$ (lb/ft$^3$) | $R^2$ | $w_{opt}$ (%) | $\gamma_{d\ max}$ (lb/ft$^3$) |
| 1640 | SS | 13.1 | 84.5 | 0.90 | -- | -- | -- | 23.8 | 92.2 |
| | S | 21.6 | 91.6 | 0.28 | 22.7 | 97.4 | 0.98 | -- | -- |
| | SSM | 19.6 | 94.3 | 0.18 | -- | -- | -- | -- | -- |
| | SM | 15.7 | 98.5 | 0.32 | -- | -- | -- | -- | -- |
| | M | 13.8 | 104.9 | 0.74 | -- | -- | -- | 17.0 | 107.9 |

| | | Blotz B | | Li & Sego | | | | CFED | | |
|---|---|---|---|---|---|---|---|---|---|---|
| Soil CFED # | Energy | $w_{opt}$ (%) | $\gamma_{d\ max}$ (lb/ft$^3$) | $S_m$ | $w_{opt}$ (%) | $\gamma_{d\ max}$ (lb/ft$^3$) | $R^2$ | $w_{opt}$ (%) | $\gamma_{d\ max}$ (lb/ft$^3$) | $R^2$ |
| 1640 | SS | 19.5 | 72.4 | 89 | 23.8 | 96.0 | 0.98 | 20.4 | 91.0 | 0.69 |
| | S | 17.8 | 112.2 | 89 | 23.1 | 96.5 | 0.99 | 19.4 | 92.7 | |
| | SSM | -- | -- | 89 | 20.4 | 102.1 | 0.97 | 18.0 | 95.5 | |
| | SM | -- | -- | 89 | 19.5 | 102.4 | 0.91 | 16.3 | 99.8 | |
| | M | 12.7 | 123.9 | 89 | 16.4 | 105.3 | 0.85 | 14.2 | 105.1 | |

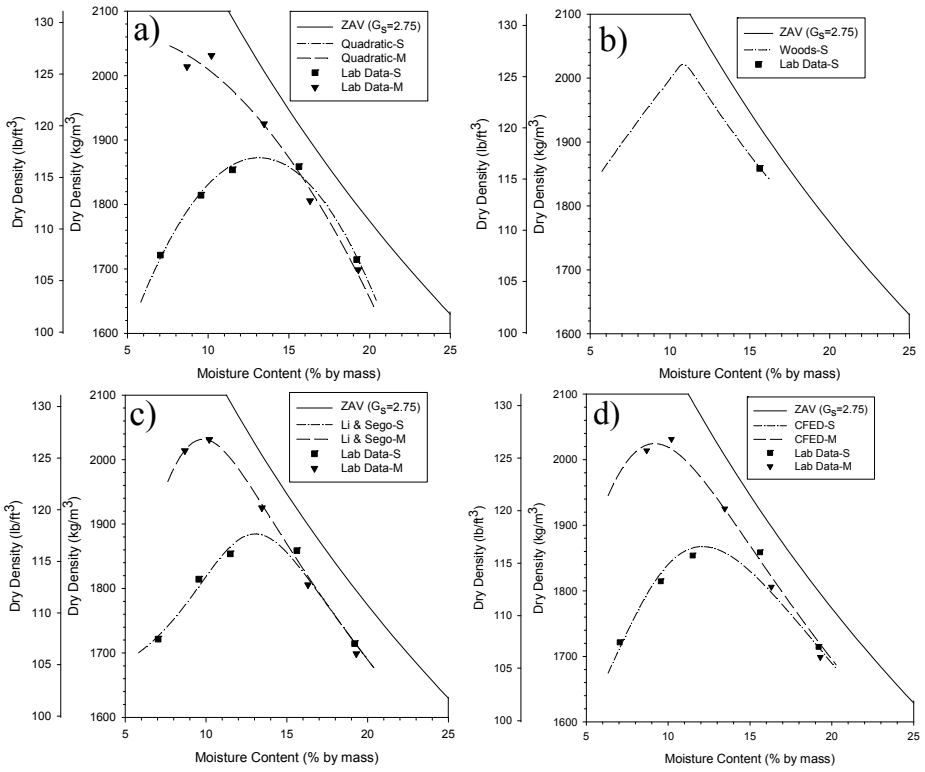


**Figure 134: Glacial Till W. Illinois (Edwards B) (Soil 2001) a) Quadratic, b) Woods, c) Li & Sego, d) CFED**

**Table 82: Soil 2001 Prediction Values**

| | | Quadratic | | | Woods | | | Blotz A | |
|---|---|---|---|---|---|---|---|---|---|
| Soil CFED # | Energy | $w_{opt}$ (%) | $\gamma_{d\ max}$ (lb/ft$^3$) | $R^2$ | $w_{opt}$ (%) | $\gamma_{d\ max}$ (lb/ft$^3$) | $R^2$ | $w_{opt}$ (%) | $\gamma_{d\ max}$ (lb/ft$^3$) |
| 2001 | S | 13.1 | 116.9 | 0.99 | 10.5 | 126.7 | 1.00 | -- | -- |
| | M | 4.0 | 129.0 | 0.98 | -- | -- | -- | 9.4 | 127.7 |

| | | Blotz B | | Li & Sego | | | | CFED | | |
|---|---|---|---|---|---|---|---|---|---|---|
| Soil CFED # | Energy | $w_{opt}$ (%) | $\gamma_{d\ max}$ (lb/ft$^3$) | $S_m$ | $w_{opt}$ (%) | $\gamma_{d\ max}$ (lb/ft$^3$) | $R^2$ | $w_{opt}$ (%) | $\gamma_{d\ max}$ (lb/ft$^3$) | $R^2$ |
| 2001 | S | 13.5 | 120.8 | 88 | 13.0 | 117.7 | 0.96 | 12.1 | 116.6 | 0.96 |
| | M | 9.9 | 130.8 | 88 | 9.8 | 126.8 | 1.00 | 9.2 | 126.4 | |

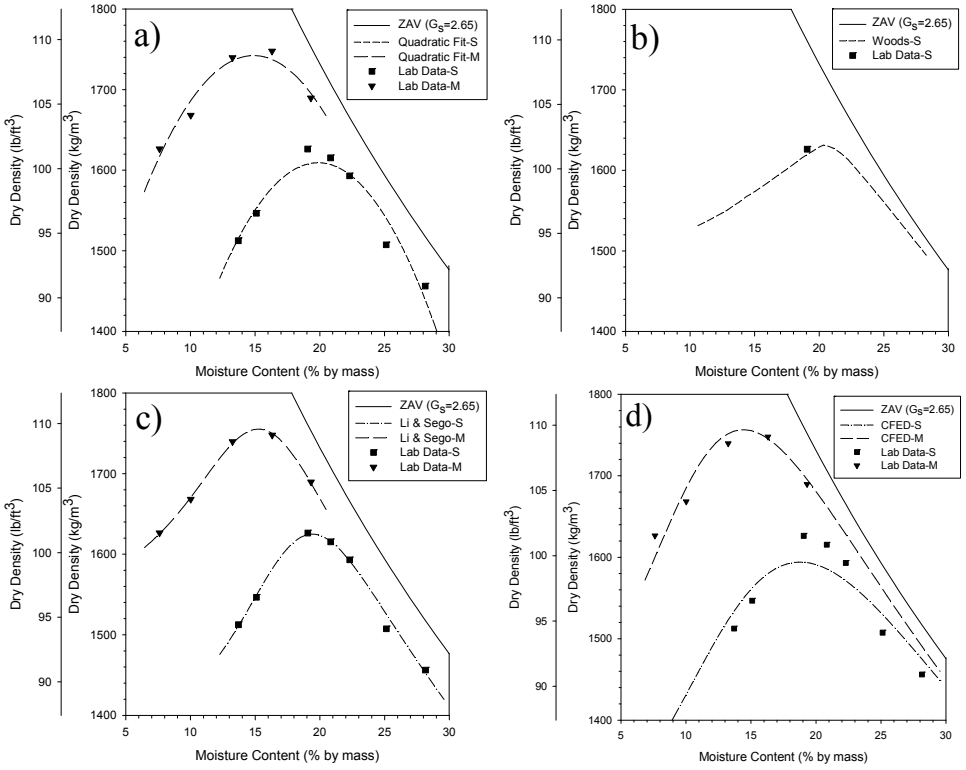


**Figure 135: Kickapoo Topsoil (Soil 2003) a) Quadratic, b) Woods, c) Li & Sego, d) CFED**

**Table 83: Soil 2003 Prediction Values**

| | | Quadratic | | | Woods | | | Blotz A | |
|---|---|---|---|---|---|---|---|---|---|
| Soil CFED # | Energy | $w_{opt}$ (%) | $\gamma_{d\ max}$ (lb/ft$^3$) | $R^2$ | $w_{opt}$ (%) | $\gamma_{d\ max}$ (lb/ft$^3$) | $R^2$ | $w_{opt}$ (%) | $\gamma_{d\ max}$ (lb/ft$^3$) |
| 2003 | S | 19.9 | 100.5 | 0.92 | 20.3 | 102.4 | 0.99 | -- | -- |
| | M | 14.9 | 108.8 | 0.94 | -- | -- | -- | 14.8 | 112.9 |

| | | Blotz B | | Li & Sego | | | | CFED | | |
|---|---|---|---|---|---|---|---|---|---|---|
| Soil CFED # | Energy | $w_{opt}$ (%) | $\gamma_{d\ max}$ (lb/ft$^3$) | $S_m$ | $w_{opt}$ (%) | $\gamma_{d\ max}$ (lb/ft$^3$) | $R^2$ | $w_{opt}$ (%) | $\gamma_{d\ max}$ (lb/ft$^3$) | $R^2$ |
| 2003 | S | 15.6 | 116.3 | 91 | 19.4 | 101.4 | 0.99 | 18.8 | 99.5 | 0.95 |
| | M | 11.1 | 127.4 | 91 | 15.3 | 109.6 | 1.00 | 14.4 | 109.7 | |

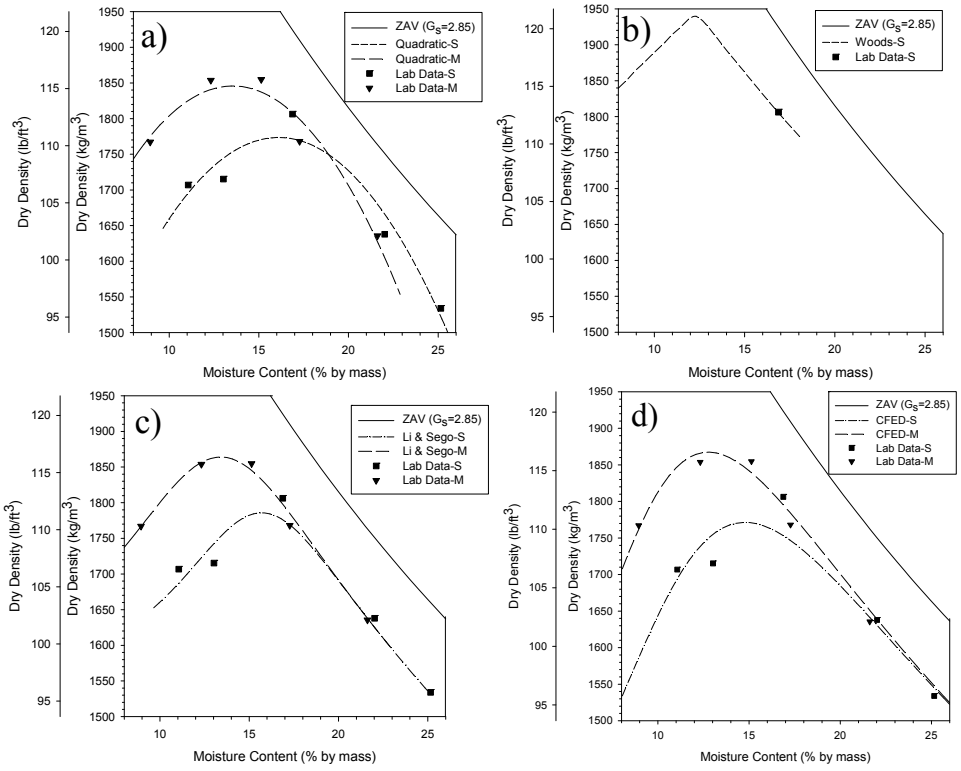


**Figure 136: Kickapoo Fill Clay (Soil 2004) a) Quadratic, b) Woods, c) Li & Sego, d) CFED**

**Table 84: Soil 2004 Prediction Values**

| | | Quadratic | | | Woods | | | Blotz A | |
|---|---|---|---|---|---|---|---|---|---|
| Soil CFED # | Energy | $w_{opt}$ (%) | $\gamma_{d\,max}$ (lb/ft$^3$) | $R^2$ | $w_{opt}$ (%) | $\gamma_{d\,max}$ (lb/ft$^3$) | $R^2$ | $w_{opt}$ (%) | $\gamma_{d\,max}$ (lb/ft$^3$) |
| 2004 | S | 16.1 | 110.7 | 0.92 | 11.9 | 121.7 | 1.00 | -- | -- |
| | M | 13.5 | 115.2 | 0.95 | -- | -- | -- | 11.6 | 125.3 |

| | | Blotz B | | Li & Sego | | | | CFED | | |
|---|---|---|---|---|---|---|---|---|---|---|
| Soil CFED # | Energy | $w_{opt}$ (%) | $\gamma_{d\,max}$ (lb/ft$^3$) | $S_m$ | $w_{opt}$ (%) | $\gamma_{d\,max}$ (lb/ft$^3$) | $R^2$ | $w_{opt}$ (%) | $\gamma_{d\,max}$ (lb/ft$^3$) | $R^2$ |
| 2004 | S | 18.5 | 110.9 | 83 | 15.7 | 111.5 | 0.95 | 14.8 | 110.6 | 0.94 |
| | M | 10.8 | 128.3 | 83 | 13.4 | 116.4 | 0.99 | 12.8 | 116.6 | |

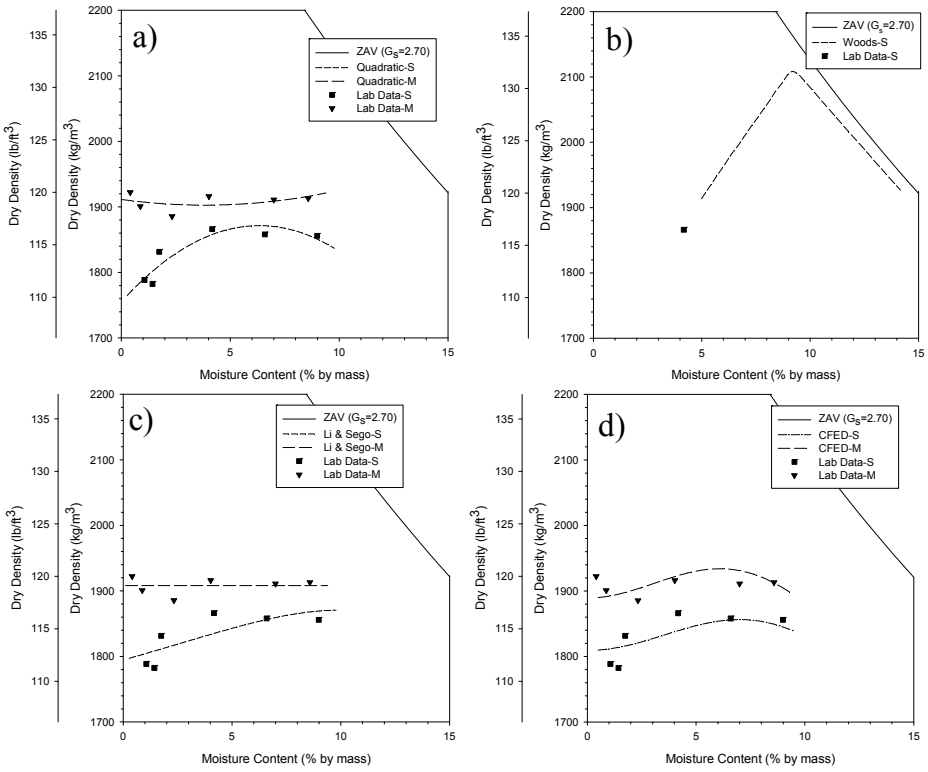


**Figure 137: Kickapoo Sand (Soil 2005) a) Quadratic, b) Woods, c) Li & Sego, d) CFED**

**Table 85: Soil 2005 Prediction Values**

| | | Quadratic | | | Woods | | | Blotz A | |
|---|---|---|---|---|---|---|---|---|---|
| Soil CFED # | Energy | $w_{opt}$ (%) | $\gamma_{d\ max}$ (lb/ft$^3$) | $R^2$ | $w_{opt}$ (%) | $\gamma_{d\ max}$ (lb/ft$^3$) | $R^2$ | $w_{opt}$ (%) | $\gamma_{d\ max}$ (lb/ft$^3$) |
| 2005 | S | 6.3 | 123.1 | 0.84 | 9.0 | 132.3 | 0.99 | NP | NP |
| | M | 3.8 | 118.8 | 0.13 | -- | -- | -- | NP | NP |

| | | Blotz B | | Li & Sego | | | | CFED | | |
|---|---|---|---|---|---|---|---|---|---|---|
| Soil CFED # | Energy | $w_{opt}$ (%) | $\gamma_{d\ max}$ (lb/ft$^3$) | $S_m$ | $w_{opt}$ (%) | $\gamma_{d\ max}$ (lb/ft$^3$) | $R^2$ | $w_{opt}$ (%) | $\gamma_{d\ max}$ (lb/ft$^3$) | $R^2$ |
| 2005 | S | NP | NP | 90 | 9.9 | 116.8 | 0.63 | 7.0 | 115.9 | 0.82 |
| | M | NP | NP | 90 | 0.1 | 119.1 | 0.00 | 6.1 | 120.7 | |

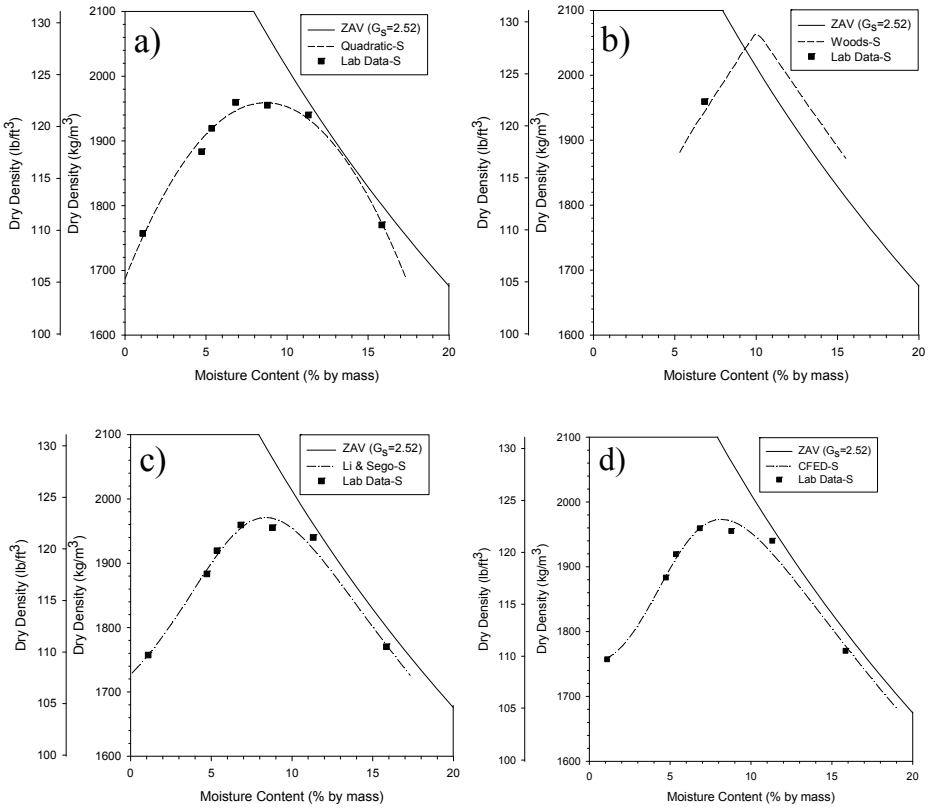


**Figure 138: RAP (Soil 2006) a) Quadratic, b) Woods, c) Li & Sego, d) CFED**

**Table 86: Soil 2006 Prediction Values**

| | | Quadratic | | | Woods | | | Blotz A | |
|---|---|---|---|---|---|---|---|---|---|
| Soil CFED # | Energy | $w_{opt}$ (%) | $\gamma_{d\,max}$ (lb/ft$^3$) | $R^2$ | $w_{opt}$ (%) | $\gamma_{d\,max}$ (lb/ft$^3$) | $R^2$ | $w_{opt}$ (%) | $\gamma_{d\,max}$ (lb/ft$^3$) |
| 2006 | S | 8.7 | 122.3 | 0.99 | 9.7 | 129.2 | 0.96 | -- | -- |

| | | Blotz B | | Li & Sego | | | | CFED | | |
|---|---|---|---|---|---|---|---|---|---|---|
| Soil CFED # | Energy | $w_{opt}$ (%) | $\gamma_{d\,max}$ (lb/ft$^3$) | $S_m$ | $w_{opt}$ (%) | $\gamma_{d\,max}$ (lb/ft$^3$) | $R^2$ | $w_{opt}$ (%) | $\gamma_{d\,max}$ (lb/ft$^3$) | $R^2$ |
| 2006 | S | 13.8 | 123.6 | 94.8 | 8.4 | 123.0 | 0.99 | 8.2 | 123.2 | 0.98 |

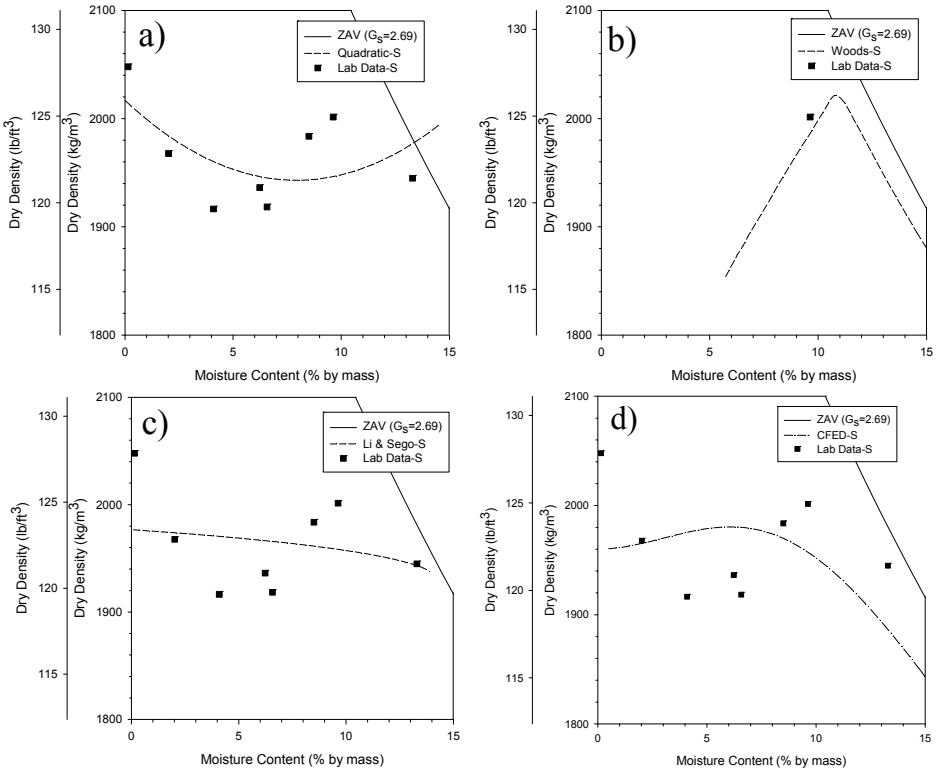


**Figure 139: CA6-C (Aug05) (Soil 2007) a) Quadratic, b) Woods, c) Li & Sego, d) CFED**

**Table 87: Soil 2007 Prediction Values**

| | | Quadratic | | | Woods | | | Blotz A | |
|---|---|---|---|---|---|---|---|---|---|
| Soil CFED # | Energy | $w_{opt}$ (%) | $\gamma_{d\ max}$ (lb/ft$^3$) | $R^2$ | $w_{opt}$ (%) | $\gamma_{d\ max}$ (lb/ft$^3$) | $R^2$ | $w_{opt}$ (%) | $\gamma_{d\ max}$ (lb/ft$^3$) |
| 2007 | S | 7.9 | 121.3 | 0.31 | 10.5 | 126.7 | 0.97 | -- | -- |

| | | Blotz B | | Li & Sego | | | | CFED | | |
|---|---|---|---|---|---|---|---|---|---|---|
| Soil CFED # | Energy | $w_{opt}$ (%) | $\gamma_{d\ max}$ (lb/ft$^3$) | $S_m$ | $w_{opt}$ (%) | $\gamma_{d\ max}$ (lb/ft$^3$) | $R^2$ | $w_{opt}$ (%) | $\gamma_{d\ max}$ (lb/ft$^3$) | $R^2$ |
| 2007 | S | 13.1 | 122.0 | 96 | 0.1 | 123.4 | 0.05 | 6.1 | 123.6 | -0.57 |

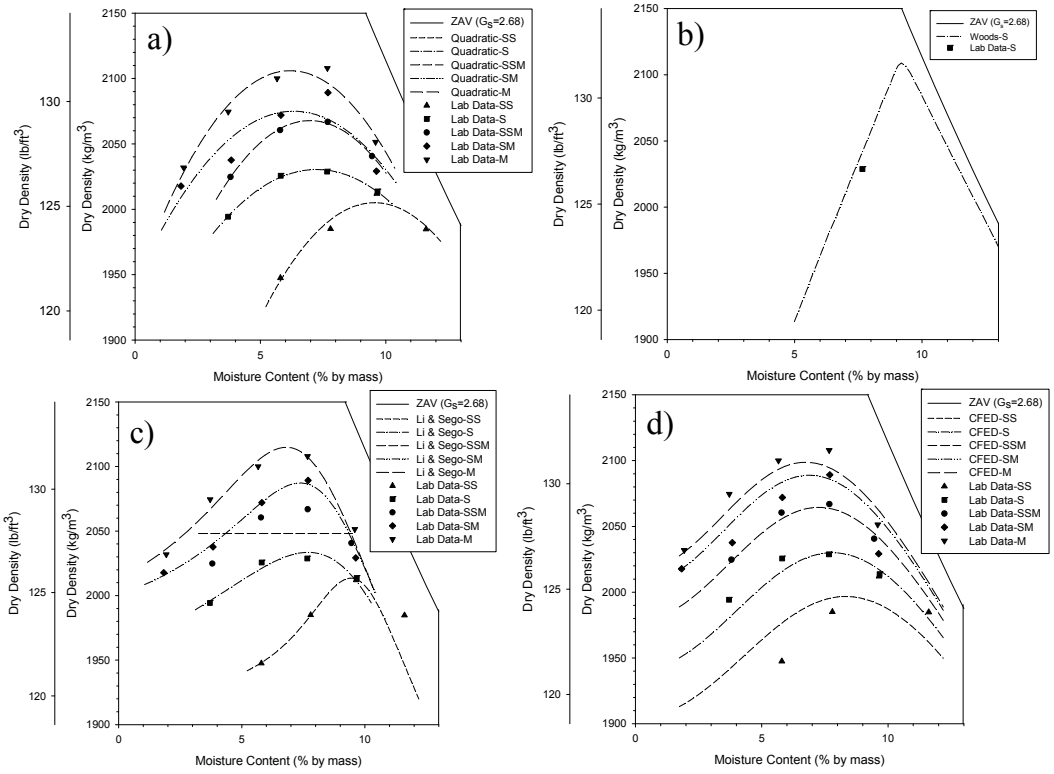


**Figure 140: FA6 (Soil 2008) a) Quadratic, b) Woods, c) Li & Sego, d) CFED**

**Table 88: Soil 2008 Prediction Values**

| | | Quadratic | | | Woods | | | Blotz A | |
|---|---|---|---|---|---|---|---|---|---|
| Soil CFED # | Energy | $w_{opt}$ (%) | $\gamma_{d\ max}$ (lb/ft$^3$) | $R^2$ | $w_{opt}$ (%) | $\gamma_{d\ max}$ (lb/ft$^3$) | $R^2$ | $w_{opt}$ (%) | $\gamma_{d\ max}$ (lb/ft$^3$) |
| 2008 | SS | 9.5 | 125.2 | 0.95 | -- | -- | -- | 8.5 | 124.1 |
| | S | 7.2 | 126.7 | 1.00 | 9.0 | 132.3 | 0.98 | -- | -- |
| | SSM | 7.0 | 129.1 | 1.00 | -- | -- | -- | -- | -- |
| | SM | 6.3 | 129.5 | 0.76 | -- | -- | -- | -- | -- |
| | M | 6.2 | 131.5 | 0.95 | -- | -- | -- | 6.2 | 134.4 |

| | | Blotz B | | Li & Sego | | | | CFED | | |
|---|---|---|---|---|---|---|---|---|---|---|
| Soil CFED # | Energy | $w_{opt}$ (%) | $\gamma_{d\ max}$ (lb/ft$^3$) | $S_m$ | $w_{opt}$ (%) | $\gamma_{d\ max}$ (lb/ft$^3$) | $R^2$ | $w_{opt}$ (%) | $\gamma_{d\ max}$ (lb/ft$^3$) | $R^2$ |
| 2008 | SS | 13.9 | 97.5 | 83 | 9.4 | 125.7 | 0.29 | 8.2 | 124.5 | 0.88 |
| | S | 13.3 | 123.7 | 83 | 7.7 | 126.9 | 0.93 | 7.8 | 126.7 | |
| | SSM | -- | -- | 83 | 0.1 | 127.9 | 0.00 | 7.5 | 128.2 | |
| | SM | -- | -- | 83 | 7.4 | 130.3 | 0.98 | 7.0 | 130.4 | |
| | M | 11.6 | 131.5 | 83 | 6.8 | 132.0 | 0.95 | 6.7 | 131.0 | |

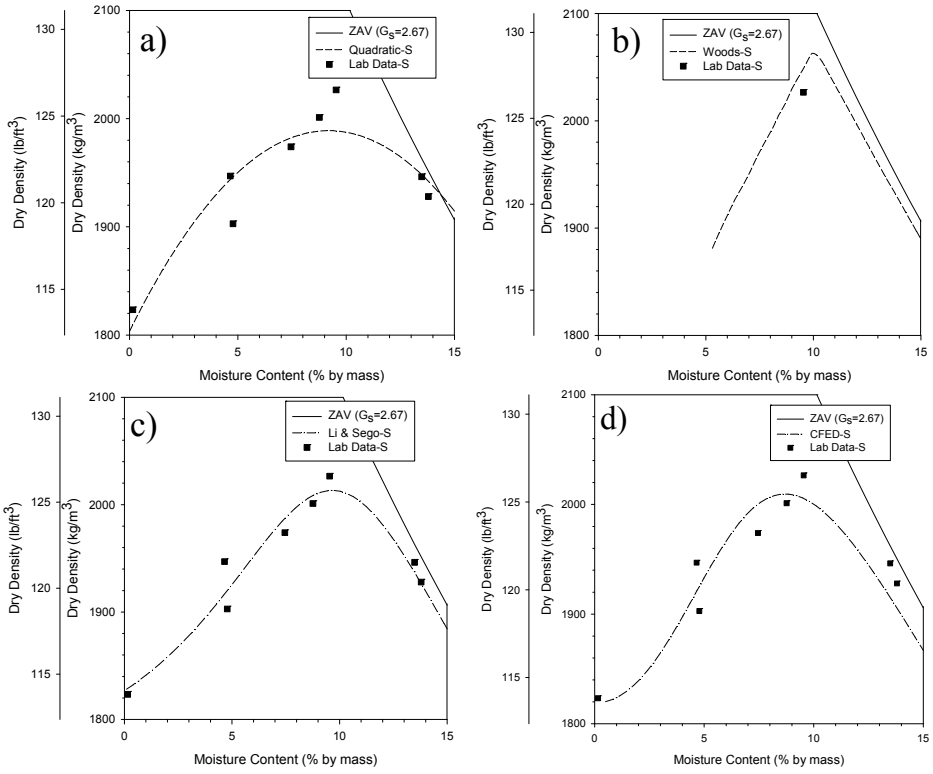


**Figure 141: CA6-G (Aug05) (Soil 2009) a) Quadratic, b) Woods, c) Li & Sego, d) CFED**

**Table 89: Soil 2009 Prediction Values**

| | | Quadratic | | | Woods | | | Blotz A | |
|---|---|---|---|---|---|---|---|---|---|
| Soil CFED # | Energy | $w_{opt}$ (%) | $\gamma_{d\ max}$ (lb/ft$^3$) | $R^2$ | $w_{opt}$ (%) | $\gamma_{d\ max}$ (lb/ft$^3$) | $R^2$ | $w_{opt}$ (%) | $\gamma_{d\ max}$ (lb/ft$^3$) |
| 2009 | S | 9.2 | 124.2 | 0.86 | 9.7 | 129.2 | 0.93 | -- | -- |

| | | Blotz B | | Li & Sego | | | | CFED | | |
|---|---|---|---|---|---|---|---|---|---|---|
| Soil CFED # | Energy | $w_{opt}$ (%) | $\gamma_{d\ max}$ (lb/ft$^3$) | $S_m$ | $w_{opt}$ (%) | $\gamma_{d\ max}$ (lb/ft$^3$) | $R^2$ | $w_{opt}$ (%) | $\gamma_{d\ max}$ (lb/ft$^3$) | $R^2$ |
| 2009 | S | 13.1 | 122.0 | 96 | 9.7 | 125.7 | 0.94 | 8.7 | 125.5 | 0.86 |

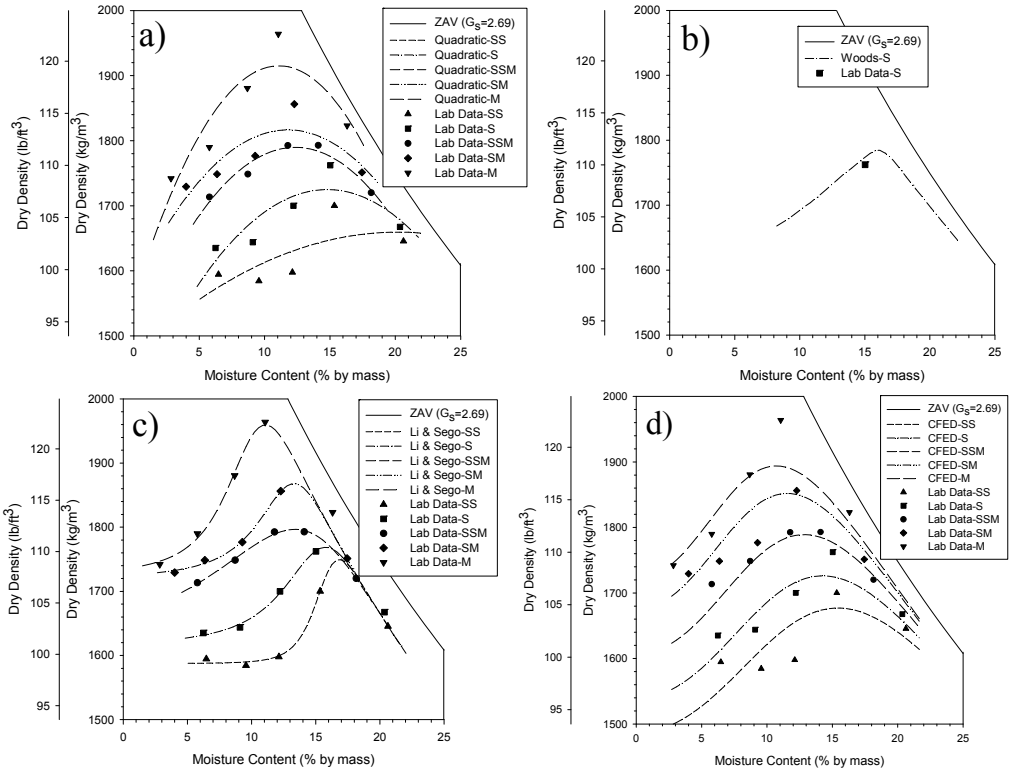


**Figure 142: MnRoad Glacial Till (Soil 2010) a) Quadratic, b) Woods, c) Li & Sego, d) CFED**

**Table 90: Soil 2010 Prediction Values**

| | | Quadratic | | | Woods | | | Blotz A | |
|---|---|---|---|---|---|---|---|---|---|
| Soil CFED # | Energy | $w_{opt}$ (%) | $\gamma_{d\,max}$ (lb/ft$^3$) | $R^2$ | $w_{opt}$ (%) | $\gamma_{d\,max}$ (lb/ft$^3$) | $R^2$ | $w_{opt}$ (%) | $\gamma_{d\,max}$ (lb/ft$^3$) |
| 2010 | SS | 20.2 | 103.6 | 0.48 | -- | -- | -- | 16.3 | 106.6 |
| | S | 14.8 | 107.7 | 0.70 | 15.8 | 111.7 | 0.98 | -- | -- |
| | SSM | 12.3 | 111.7 | 0.93 | -- | -- | -- | -- | -- |
| | SM | 11.8 | 113.4 | 0.68 | -- | -- | -- | -- | -- |
| | M | 11.1 | 119.5 | 0.82 | -- | -- | -- | 11.1 | 120.5 |

| | | Blotz B | | Li & Sego | | | | CFED | | |
|---|---|---|---|---|---|---|---|---|---|---|
| Soil CFED # | Energy | $w_{opt}$ (%) | $\gamma_{d\,max}$ (lb/ft$^3$) | $S_m$ | $w_{opt}$ (%) | $\gamma_{d\,max}$ (lb/ft$^3$) | $R^2$ | $w_{opt}$ (%) | $\gamma_{d\,max}$ (lb/ft$^3$) | $R^2$ |
| 2010 | SS | 15.4 | 84.4 | 87 | 16.8 | 109.2 | 0.99 | 15.4 | 104.8 | 0.90 |
| | S | 14.1 | 119.5 | 87 | 15.8 | 110.4 | 0.98 | 14.3 | 107.8 | |
| | SSM | -- | -- | 87 | 13.4 | 112.2 | 1.00 | 12.8 | 111.7 | |
| | SM | -- | -- | 87 | 13.3 | 116.6 | 1.00 | 11.7 | 115.6 | |
| | M | 10.2 | 129.8 | 87 | 11.1 | 122.3 | 0.96 | 10.7 | 118.2 | |

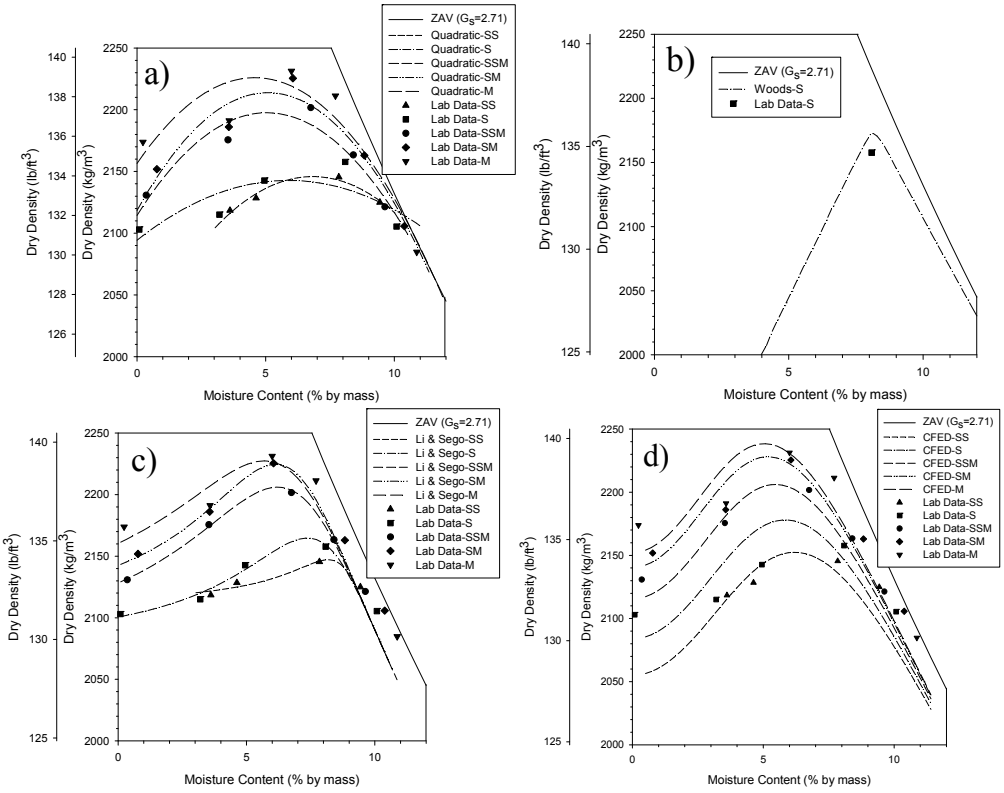


**Figure 143: MnRoad Class 5 Base (Soil 2011) a) Quadratic, b) Woods, c) Li & Sego, d) CFED**

**Table 91: Soil 2011 Prediction Values**

| | | Quadratic | | | Woods | | | Blotz A | |
|---|---|---|---|---|---|---|---|---|---|
| Soil CFED # | Energy | $w_{opt}$ (%) | $\gamma_{d\,max}$ (lb/ft$^3$) | $R^2$ | $w_{opt}$ (%) | $\gamma_{d\,max}$ (lb/ft$^3$) | $R^2$ | $w_{opt}$ (%) | $\gamma_{d\,max}$ (lb/ft$^3$) |
| 2011 | SS | 6.8 | 134.0 | 0.94 | -- | -- | -- | NP | NP |
| | S | 5.9 | 133.8 | 0.58 | 7.9 | 136.1 | 0.97 | NP | NP |
| | SSM | 5.0 | 137.2 | 0.89 | -- | -- | -- | NP | NP |
| | SM | 5.1 | 138.2 | 0.92 | -- | -- | -- | NP | NP |
| | M | 4.6 | 139.0 | 0.87 | -- | -- | -- | NP | NP |

| | | Blotz B | | Li & Sego | | | | CFED | | |
|---|---|---|---|---|---|---|---|---|---|---|
| Soil CFED # | Energy | $w_{opt}$ (%) | $\gamma_{d\,max}$ (lb/ft$^3$) | $S_m$ | $w_{opt}$ (%) | $\gamma_{d\,max}$ (lb/ft$^3$) | $R^2$ | $w_{opt}$ (%) | $\gamma_{d\,max}$ (lb/ft$^3$) | $R^2$ |
| 2011 | SS | NP | NP | 91 | 8.2 | 134.0 | 0.80 | 6.2 | 134.5 | 0.79 |
| | S | NP | NP | 91 | 7.4 | 135.1 | 0.83 | 5.8 | 136.0 | |
| | SSM | NP | NP | 91 | 6.2 | 137.7 | 0.95 | 5.5 | 138.0 | |
| | SM | NP | NP | 91 | 6.1 | 138.9 | 0.82 | 5.0 | 139.1 | |
| | M | NP | NP | 91 | 5.7 | 139.1 | 0.84 | 5.0 | 139.7 | |

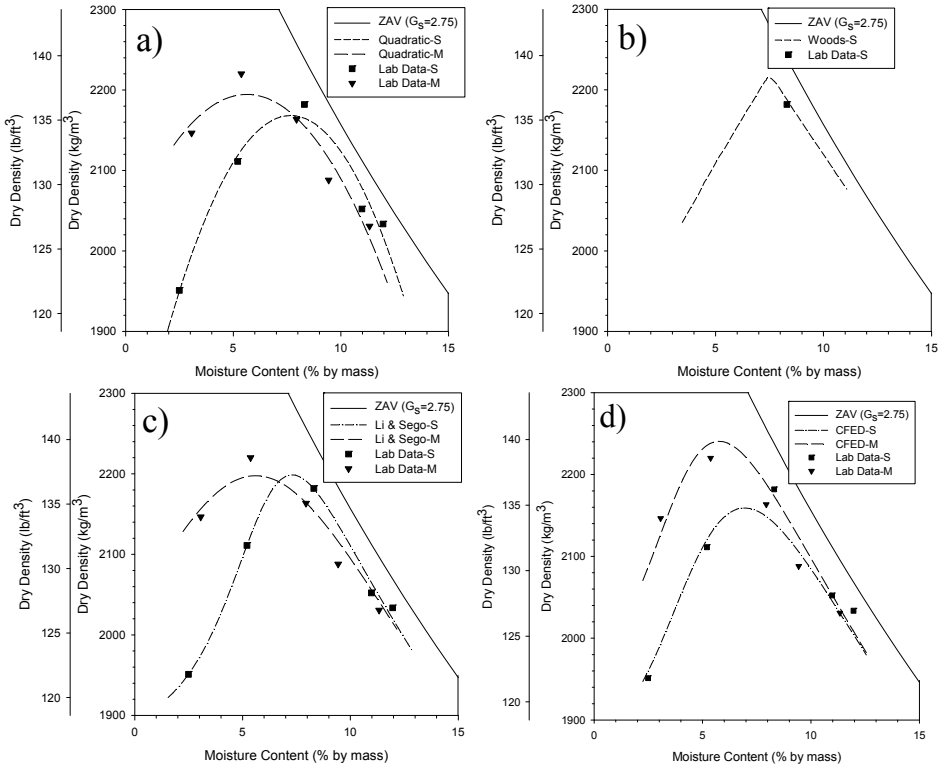


**Figure 144: CA6-G (June06) (Soil 2012) a) Quadratic, b) Woods, c) Li & Sego, d) CFED**

**Table 92: Soil 2012 Prediction Values**

| | | Quadratic | | | Woods | | | Blotz A | |
|---|---|---|---|---|---|---|---|---|---|
| Soil CFED # | Energy | $w_{opt}$ (%) | $\gamma_{d\,max}$ (lb/ft$^3$) | $R^2$ | $w_{opt}$ (%) | $\gamma_{d\,max}$ (lb/ft$^3$) | $R^2$ | $w_{opt}$ (%) | $\gamma_{d\,max}$ (lb/ft$^3$) |
| 2012 | S | 7.7 | 135.4 | 0.96 | 7.2 | 139.2 | 0.99 | NP | NP |
| | M | 5.6 | 137.0 | 0.92 | -- | -- | -- | NP | NP |

| | | Blotz B | | Li & Sego | | | | CFED | | |
|---|---|---|---|---|---|---|---|---|---|---|
| Soil CFED # | Energy | $w_{opt}$ (%) | $\gamma_{d\,max}$ (lb/ft$^3$) | $S_m$ | $w_{opt}$ (%) | $\gamma_{d\,max}$ (lb/ft$^3$) | $R^2$ | $w_{opt}$ (%) | $\gamma_{d\,max}$ (lb/ft$^3$) | $R^2$ |
| 2012 | S | NP | NP | 91 | 7.3 | 136.7 | 0.99 | 6.9 | 134.8 | 0.91 |
| | M | NP | NP | 91 | 5.6 | 137.2 | 0.93 | 5.8 | 139.9 | |

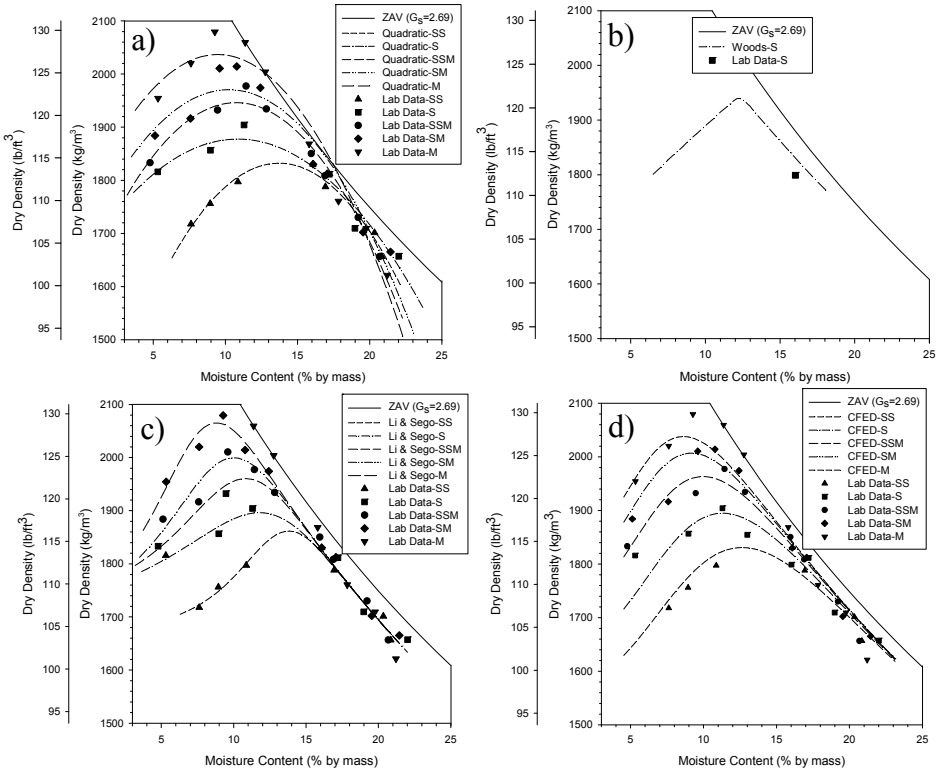


**Figure 145: TH60 Soil #1 (Soil 2013) a) Quadratic, b) Woods, c) Li & Sego, d) CFED**

**Table 93: Soil 2013 Prediction Values**

| | | Quadratic | | | Woods | | | Blotz A | |
|---|---|---|---|---|---|---|---|---|---|
| Soil CFED # | Energy | $w_{opt}$ (%) | $\gamma_{d\ max}$ (lb/ft$^3$) | $R^2$ | $w_{opt}$ (%) | $\gamma_{d\ max}$ (lb/ft$^3$) | $R^2$ | $w_{opt}$ (%) | $\gamma_{d\ max}$ (lb/ft$^3$) |
| 2013 | SS | 12.4 | 112.7 | 0.61 | -- | -- | -- | 12.8 | 115.8 |
| | S | 10.9 | 117.2 | 0.93 | 11.9 | 121.7 | 0.96 | -- | -- |
| | SSM | 11.1 | 120.7 | 0.92 | -- | -- | -- | -- | -- |
| | SM | 10.2 | 123.0 | 0.92 | -- | -- | -- | -- | -- |
| | M | 9.5 | 127.1 | 0.96 | -- | -- | -- | 8.4 | 128.7 |

| | | Blotz B | | Li & Sego | | | | CFED | | |
|---|---|---|---|---|---|---|---|---|---|---|
| Soil CFED # | Energy | $w_{opt}$ (%) | $\gamma_{d\ max}$ (lb/ft$^3$) | $S_m$ | $w_{opt}$ (%) | $\gamma_{d\ max}$ (lb/ft$^3$) | $R^2$ | $w_{opt}$ (%) | $\gamma_{d\ max}$ (lb/ft$^3$) | $R^2$ |
| 2013 | SS | 14.4 | 88.9 | 92 | 14.2 | 114.5 | 0.87 | 12.2 | 114.8 | 0.94 |
| | S | 13.2 | 121.6 | 92 | 11.8 | 118.4 | 0.96 | 11.3 | 118.3 | |
| | SSM | -- | -- | 92 | 11.2 | 121.8 | 0.95 | 10.0 | 122.5 | |
| | SM | -- | -- | 92 | 10.0 | 124.9 | 0.97 | 9.4 | 125.1 | |
| | M | 9.9 | 131.3 | 92 | 8.8 | 128.9 | 0.96 | 8.6 | 127.2 | |

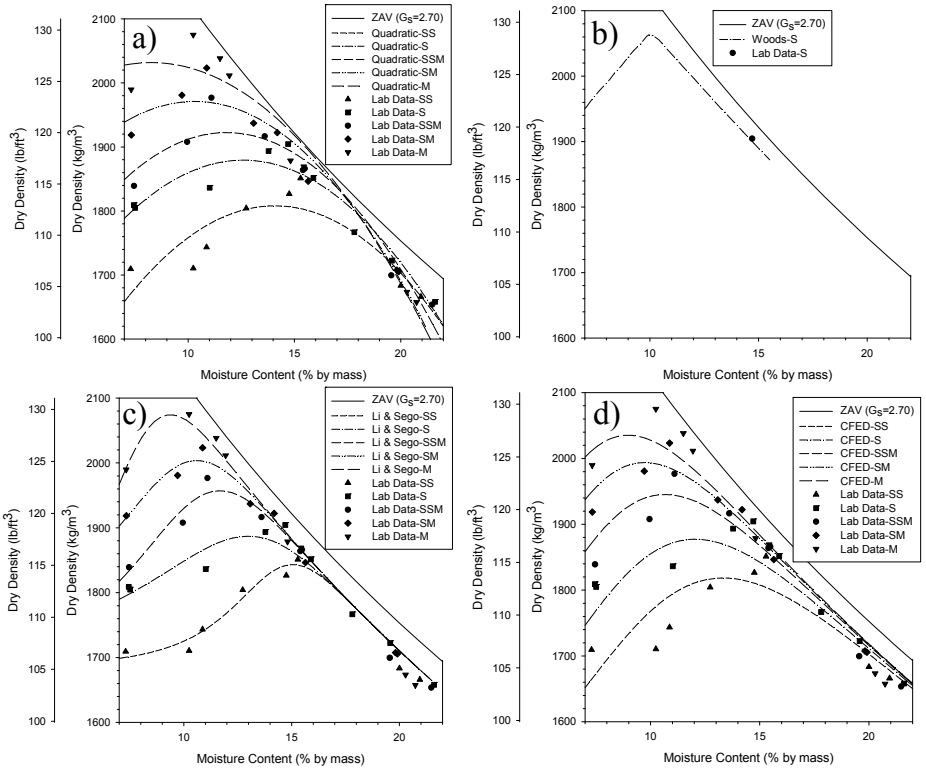


**Figure 146: TH60 Soil #2 (Soil 2014) a) Quadratic, b) Woods, c) Li & Sego, d) CFED**

**Table 94: Soil 2014 Prediction Values**

| | | Quadratic | | | Woods | | | Blotz A | |
|---|---|---|---|---|---|---|---|---|---|
| Soil CFED # | Energy | $w_{opt}$ (%) | $\gamma_{d\ max}$ (lb/ft$^3$) | $R^2$ | $w_{opt}$ (%) | $\gamma_{d\ max}$ (lb/ft$^3$) | $R^2$ | $w_{opt}$ (%) | $\gamma_{d\ max}$ (lb/ft$^3$) |
| 2014 | SS | 14.1 | 112.9 | 0.75 | -- | -- | -- | 14.6 | 115.0 |
| | S | 12.6 | 117.3 | 0.91 | 9.7 | 129.2 | 1.00 | -- | -- |
| | SSM | 11.8 | 120.0 | 0.93 | -- | -- | -- | -- | -- |
| | SM | 10.3 | 123.0 | 0.94 | -- | -- | -- | -- | -- |
| | M | 8.3 | 126.8 | 0.95 | -- | -- | -- | 9.6 | 128.5 |

| | | Blotz B | | Li & Sego | | | | CFED | | |
|---|---|---|---|---|---|---|---|---|---|---|
| Soil CFED # | Energy | $w_{opt}$ (%) | $\gamma_{d\ max}$ (lb/ft$^3$) | $S_m$ | $w_{opt}$ (%) | $\gamma_{d\ max}$ (lb/ft$^3$) | $R^2$ | $w_{opt}$ (%) | $\gamma_{d\ max}$ (lb/ft$^3$) | $R^2$ |
| 2014 | SS | 14.9 | 86.3 | 93 | 15.1 | 115.1 | 0.94 | 13.2 | 113.8 | 0.93 |
| | S | 13.7 | 120.4 | 93 | 13.0 | 117.8 | 0.94 | 12.0 | 117.2 | |
| | SSM | -- | -- | 93 | 11.7 | 122.2 | 0.98 | 10.6 | 121.5 | |
| | SM | -- | -- | 93 | 10.6 | 125.1 | 0.99 | 9.8 | 124.9 | |
| | M | 10.0 | 130.5 | 93 | 9.4 | 129.5 | 0.99 | 9.0 | 127.1 | |

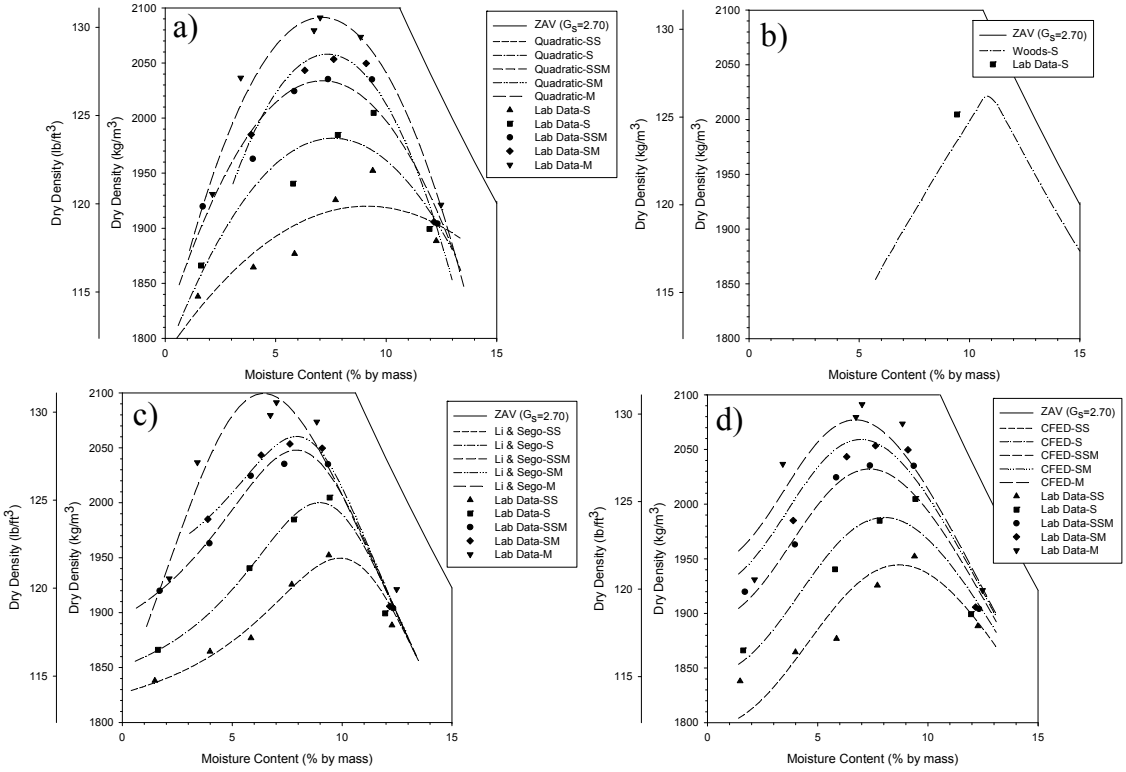


**Figure 147: US10-101 (Soil 2018) a) Quadratic, b) Woods, c) Li & Sego, d) CFED**

**Table 95: Soil 2018 Prediction Values**

| | | Quadratic | | | Woods | | | Blotz A | |
|---|---|---|---|---|---|---|---|---|---|
| Soil CFED # | Energy | $w_{opt}$ (%) | $\gamma_{d\ max}$ (lb/ft$^3$) | $R^2$ | $w_{opt}$ (%) | $\gamma_{d\ max}$ (lb/ft$^3$) | $R^2$ | $w_{opt}$ (%) | $\gamma_{d\ max}$ (lb/ft$^3$) |
| 2018 | SS | 9.1 | 119.9 | 0.7 | -- | -- | -- | NP | NP |
| | S | 7.6 | 123.7 | 0.8 | 10.5 | 126.7 | 0.9 | NP | NP |
| | SSM | 7.1 | 127.0 | 0.9 | -- | -- | -- | NP | NP |
| | SM | 7.3 | 128.5 | 1.0 | -- | -- | -- | NP | NP |
| | M | 7.1 | 130.6 | 1.0 | -- | -- | -- | NP | NP |

| | | Blotz B | | Li & Sego | | | | CFED | | |
|---|---|---|---|---|---|---|---|---|---|---|
| Soil CFED # | Energy | $w_{opt}$ (%) | $\gamma_{d\ max}$ (lb/ft$^3$) | $S_m$ | $w_{opt}$ (%) | $\gamma_{d\ max}$ (lb/ft$^3$) | $R^2$ | $w_{opt}$ (%) | $\gamma_{d\ max}$ (lb/ft$^3$) | $R^2$ |
| 2018 | SS | NP | NP | 80 | 9.9 | 121.7 | 0.95 | 8.7 | 121.8 | 0.93 |
| | S | NP | NP | 80 | 9.0 | 124.9 | 0.96 | 8.0 | 124.1 | |
| | SSM | NP | NP | 80 | 7.9 | 127.8 | 0.99 | 7.5 | 127.1 | |
| | SM | NP | NP | 80 | 7.9 | 128.6 | 0.99 | 7.0 | 128.5 | |
| | M | NP | NP | 80 | 6.4 | 131.1 | 0.93 | 6.7 | 129.7 | |

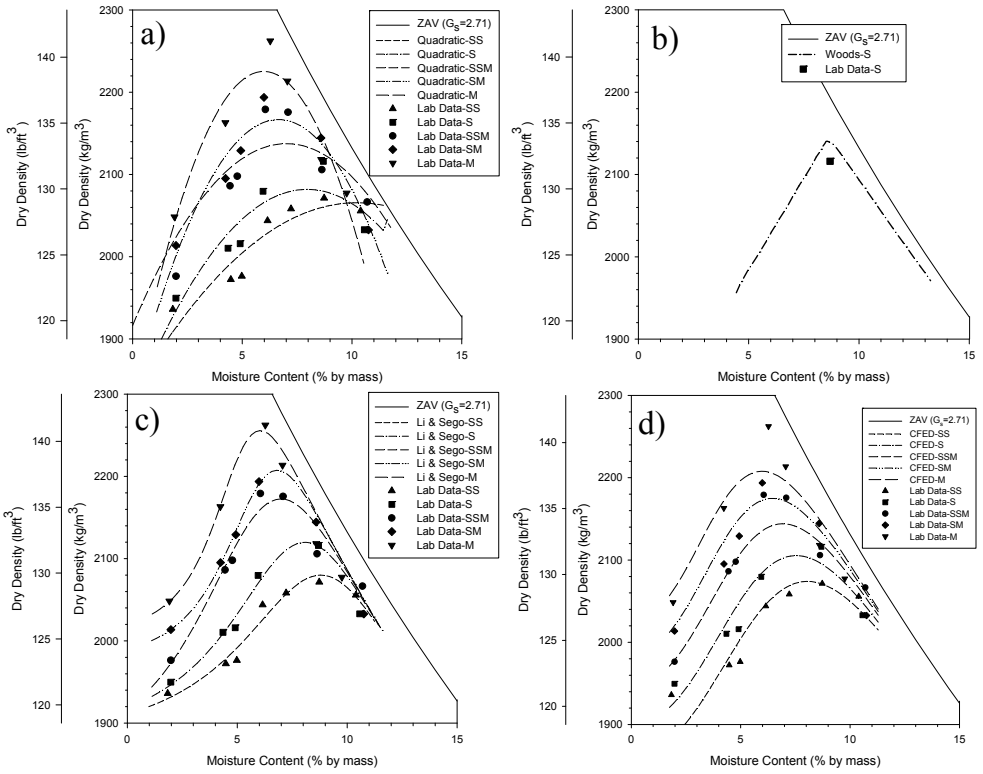


**Figure 148: TH36 Common (Soil 2020) a) Quadratic, b) Woods, c) Li & Sego, d) CFED**

**Table 96: Soil 2020 Prediction Values**

| | | Quadratic | | | Woods | | | Blotz A | |
|---|---|---|---|---|---|---|---|---|---|
| Soil CFED # | Energy | $w_{opt}$ (%) | $\gamma_{d\ max}$ (lb/ft$^3$) | $R^2$ | $w_{opt}$ (%) | $\gamma_{d\ max}$ (lb/ft$^3$) | $R^2$ | $w_{opt}$ (%) | $\gamma_{d\ max}$ (lb/ft$^3$) |
| 2020 | SS | 10.2 | 129.0 | 0.95 | -- | -- | -- | 7.7 | 130.2 |
| | S | 8.0 | 130.0 | 0.80 | 8.5 | 134.2 | 0.96 | -- | -- |
| | SSM | 7.0 | 133.4 | 0.83 | -- | -- | -- | -- | -- |
| | SM | 6.6 | 135.3 | 0.91 | -- | -- | -- | -- | -- |
| | M | 6.0 | 138.9 | 0.90 | -- | -- | -- | 6.6 | 139.1 |

| | | Blotz B | | Li & Sego | | | | CFED | | |
|---|---|---|---|---|---|---|---|---|---|---|
| Soil CFED # | Energy | $w_{opt}$ (%) | $\gamma_{d\ max}$ (lb/ft$^3$) | $S_m$ | $w_{opt}$ (%) | $\gamma_{d\ max}$ (lb/ft$^3$) | $R^2$ | $w_{opt}$ (%) | $\gamma_{d\ max}$ (lb/ft$^3$) | $R^2$ |
| 2020 | SS | 14.9 | 100.7 | 91 | 8.8 | 129.8 | 0.96 | 8.0 | 129.6 | 0.91 |
| | S | 14.6 | 123.1 | 91 | 8.1 | 132.3 | 0.95 | 7.5 | 131.4 | |
| | SSM | -- | -- | 91 | 7.0 | 135.6 | 0.93 | 7.0 | 134.0 | |
| | SM | -- | -- | 91 | 6.8 | 137.8 | 0.98 | 6.5 | 135.8 | |
| | M | 13.8 | 129.8 | 91 | 6.0 | 140.8 | 0.93 | 6.0 | 137.8 | |

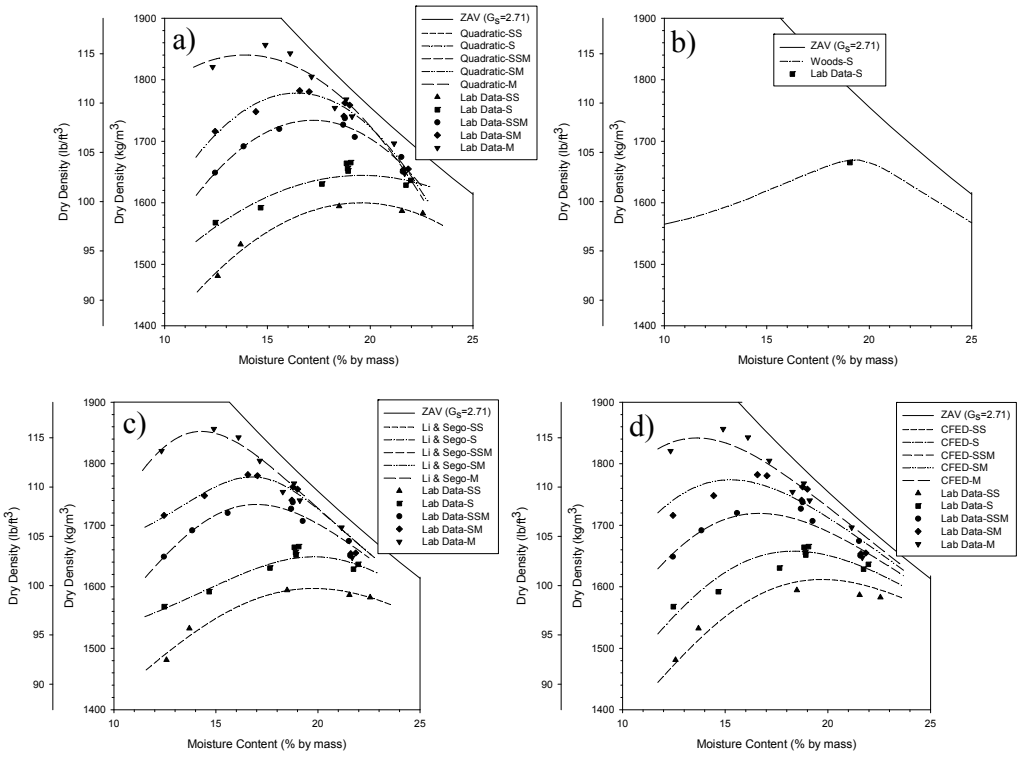


**Figure 149: TH60 Strip 2 (Soil 2021) a) Quadratic, b) Woods, c) Li and Sego, d) CFED**

**Table 97: Soil 2021 Prediction Values**

| | | Quadratic | | | Woods | | | Blotz A | |
|---|---|---|---|---|---|---|---|---|---|
| Soil CFED # | Energy | $w_{opt}$ (%) | $\gamma_{d\ max}$ (lb/ft$^3$) | $R^2$ | $w_{opt}$ (%) | $\gamma_{d\ max}$ (lb/ft$^3$) | $R^2$ | $w_{opt}$ (%) | $\gamma_{d\ max}$ (lb/ft$^3$) |
| 2021 | SS | 19.5 | 99.9 | 0.98 | -- | -- | -- | 20.4 | 99.9 |
| | S | 19.6 | 102.7 | 0.91 | 19.2 | 104.9 | 1.00 | -- | -- |
| | SSM | 17.2 | 108.3 | 0.93 | -- | -- | -- | -- | -- |
| | SM | 16.4 | 111.0 | 0.96 | -- | -- | -- | -- | -- |
| | M | 13.9 | 114.9 | 0.94 | -- | -- | -- | 13.7 | 115.4 |

| | | Blotz B | | Li & Sego | | | | CFED | | |
|---|---|---|---|---|---|---|---|---|---|---|
| Soil CFED # | Energy | $w_{opt}$ (%) | $\gamma_{d\ max}$ (lb/ft$^3$) | $S_m$ | $w_{opt}$ (%) | $\gamma_{d\ max}$ (lb/ft$^3$) | $R^2$ | $w_{opt}$ (%) | $\gamma_{d\ max}$ (lb/ft$^3$) | $R^2$ |
| 2021 | SS | 18.8 | 74.3 | 96 | 19.8 | 99.7 | 0.97 | 19.7 | 100.5 | 0.96 |
| | S | 17.1 | 113.4 | 96 | 19.8 | 102.9 | 0.95 | 18.4 | 103.5 | |
| | SSM | -- | -- | 96 | 17.0 | 108.2 | 0.91 | 16.7 | 106.8 | |
| | SM | -- | -- | 96 | 16.8 | 111.0 | 0.92 | 15.2 | 110.7 | |
| | M | 12.2 | 125.0 | 96 | 14.3 | 115.6 | 0.95 | 13.6 | 115.0 | |

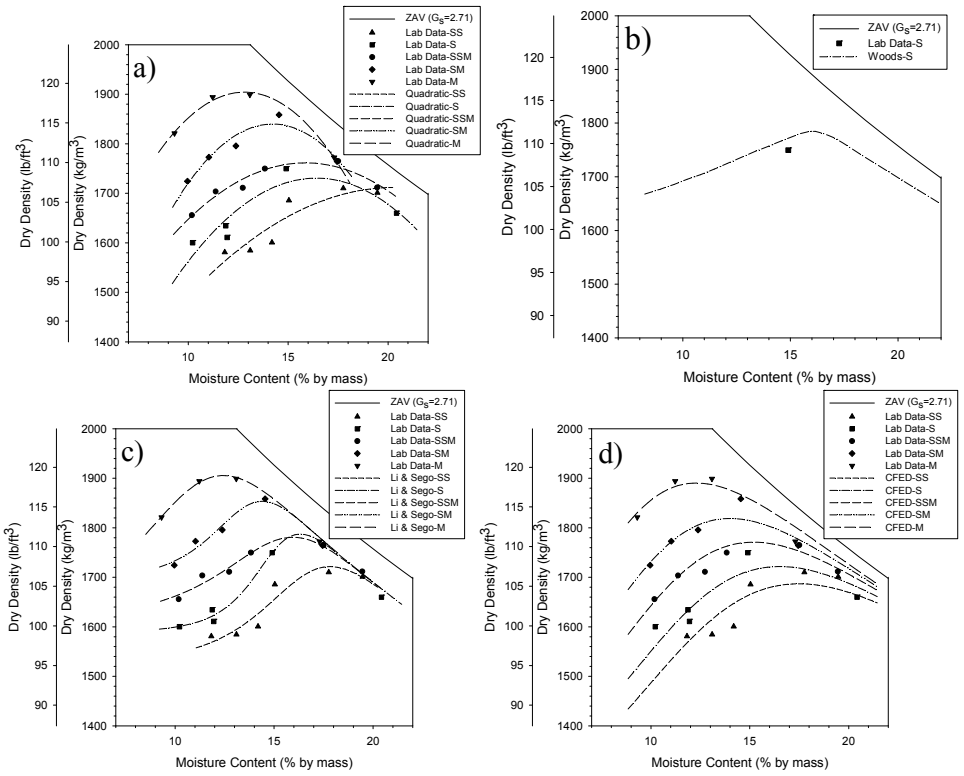


**Figure 150: China Red Clay (Soil 2022) a) Quadratic, b) Woods, c) Li and Sego, d) CFED**

**Table 98: Soil 2022 Prediction Values**

| | | Quadratic | | | Woods | | | Blotz A | |
|---|---|---|---|---|---|---|---|---|---|
| Soil CFED # | Energy | $w_{opt}$ (%) | $\gamma_{d\ max}$ (lb/ft$^3$) | $R^2$ | $w_{opt}$ (%) | $\gamma_{d\ max}$ (lb/ft$^3$) | $R^2$ | $w_{opt}$ (%) | $\gamma_{d\ max}$ (lb/ft$^3$) |
| 2022 | SS | 20.3 | 106.9 | 0.84 | -- | -- | -- | 16.0 | 109.0 |
| | S | 16.4 | 108.0 | 0.78 | 15.8 | 111.7 | 0.93 | -- | -- |
| | SSM | 15.9 | 110.0 | 0.92 | -- | -- | -- | -- | -- |
| | SM | 14.2 | 114.9 | 0.91 | -- | -- | -- | -- | -- |
| | M | 12.8 | 118.9 | 0.99 | -- | -- | -- | 10.2 | 111.7 |

| | | Blotz B | | Li & Sego | | | | CFED | | |
|---|---|---|---|---|---|---|---|---|---|---|
| Soil CFED # | Energy | $w_{opt}$ (%) | $\gamma_{d\ max}$ (lb/ft$^3$) | $S_m$ | $w_{opt}$ (%) | $\gamma_{d\ max}$ (lb/ft$^3$) | $R^2$ | $w_{opt}$ (%) | $\gamma_{d\ max}$ (lb/ft$^3$) | $R^2$ |
| 2022 | SS | 14.2 | 89.8 | 89.8 | 17.8 | 107.5 | 0.90 | 17.5 | 105.4 | 0.93 |
| | S | 13.1 | 122.0 | 89.8 | 16.3 | 111.6 | 0.96 | 16.5 | 107.5 | |
| | SSM | -- | -- | 89.8 | 15.9 | 111.2 | 0.94 | 15.2 | 110.6 | |
| | SM | -- | -- | 89.8 | 14.4 | 115.7 | 0.95 | 14.0 | 113.8 | |
| | M | 8.4 | 135.8 | 89.8 | 12.4 | 119.0 | 0.99 | 12.3 | 118.0 | |

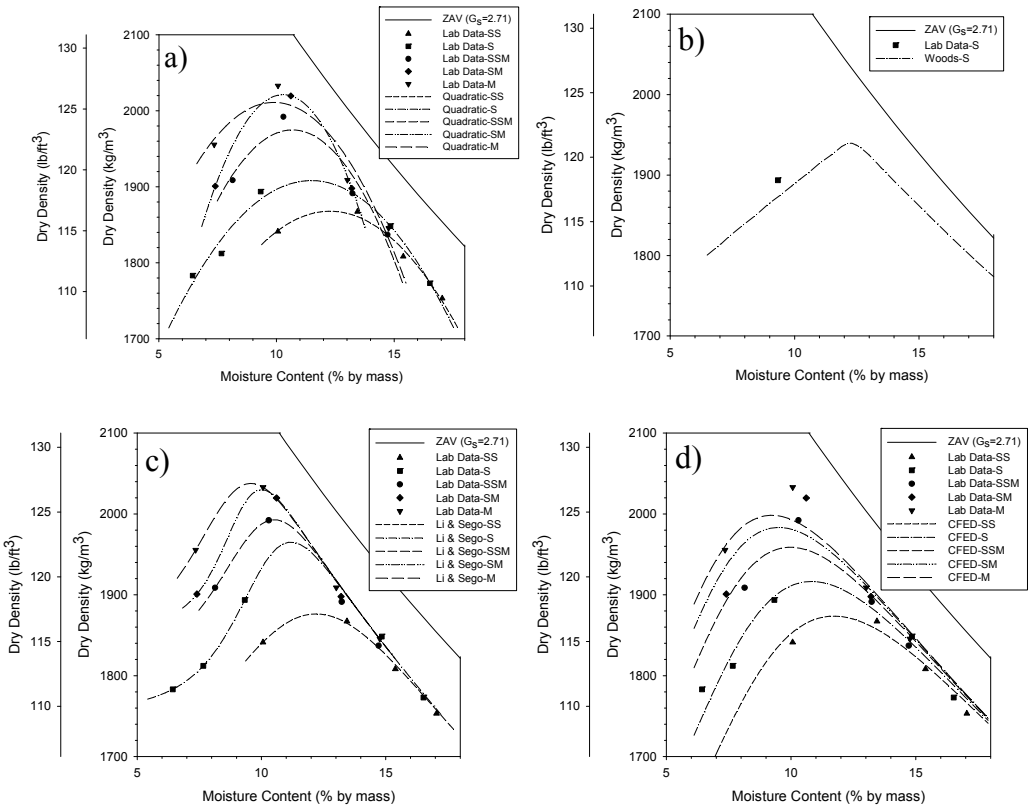


**Figure 151: China Yellow Clay (Soil 2023) a) Quadratic, b) Woods, c) Li and Sego, d) CFED**

**Table 99: Soil 2023 Prediction Values**

| | | Quadratic | | | Woods | | | Blotz A | |
|---|---|---|---|---|---|---|---|---|---|
| Soil CFED # | Energy | $w_{opt}$ (%) | $\gamma_{d\,max}$ (lb/ft$^3$) | $R^2$ | $w_{opt}$ (%) | $\gamma_{d\,max}$ (lb/ft$^3$) | $R^2$ | $w_{opt}$ (%) | $\gamma_{d\,max}$ (lb/ft$^3$) |
| 2023 | SS | 12.3 | 116.6 | 0.98 | -- | -- | -- | 11.7 | 119.3 |
| | S | 11.5 | 119.1 | 0.94 | 11.9 | 121.7 | 0.94 | -- | -- |
| | SSM | 10.7 | 123.3 | 0.91 | -- | -- | -- | -- | -- |
| | SM | 10.3 | 126.2 | 1.00 | -- | -- | -- | -- | -- |
| | M | 9.9 | 125.5 | 0.92 | -- | -- | -- | 7.9 | 121.6 |

| | | Blotz B | | Li & Sego | | | | CFED | | |
|---|---|---|---|---|---|---|---|---|---|---|
| Soil CFED # | Energy | $w_{opt}$ (%) | $\gamma_{d\,max}$ (lb/ft$^3$) | $S_m$ | $w_{opt}$ (%) | $\gamma_{d\,max}$ (lb/ft$^3$) | $R^2$ | $w_{opt}$ (%) | $\gamma_{d\,max}$ (lb/ft$^3$) | $R^2$ |
| 2023 | SS | 13.7 | 95.9 | 85.4 | 12.2 | 117.1 | 0.99 | 11.8 | 117.0 | 0.92 |
| | S | 13.0 | 123.6 | 85.4 | 11.2 | 122.7 | 0.99 | 10.8 | 119.6 | |
| | SSM | -- | -- | 85.4 | 10.5 | 124.4 | 0.97 | 9.9 | 122.2 | |
| | SM | -- | -- | 85.4 | 10.0 | 126.7 | 0.99 | 9.4 | 123.9 | |
| | M | 10.0 | 135.6 | 85.4 | 9.6 | 127.2 | 1.00 | 9.2 | 124.8 | |

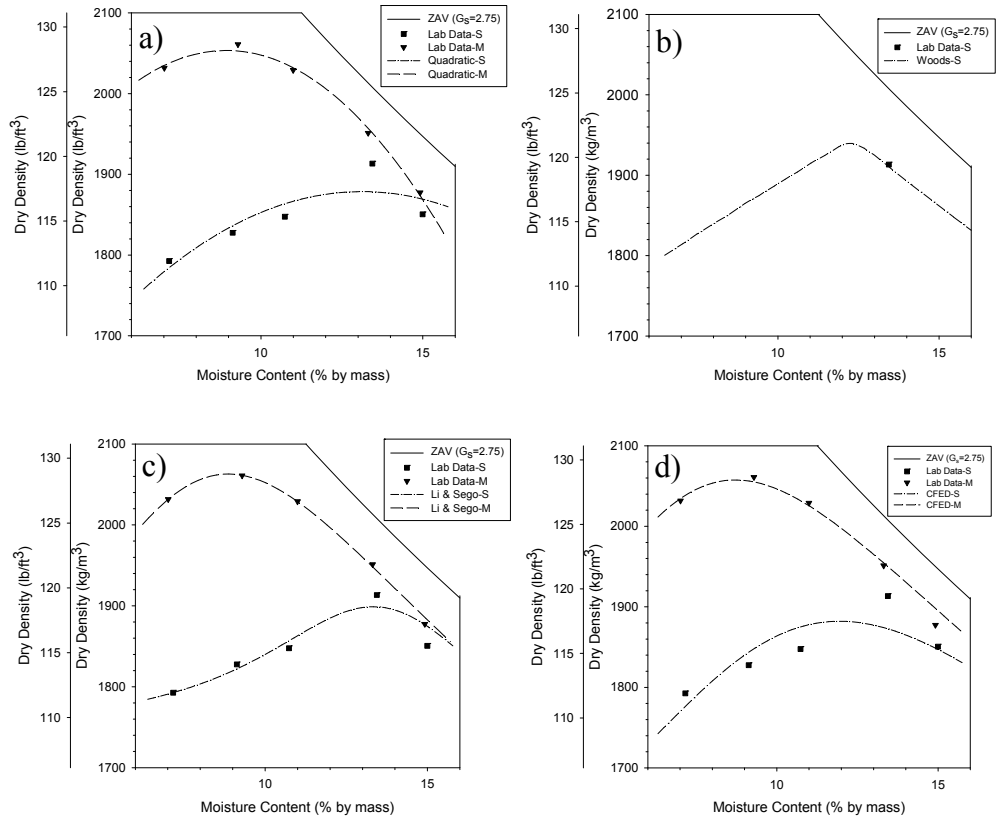


**Figure 152: Edwards Till 2008 (Soil 2024) a) Quadratic, b) Woods, c) Li and Sego, d) CFED**

**Table 100: Soil 2024 Prediction Values**

| | | Quadratic | | | Woods | | | Blotz A | |
|---|---|---|---|---|---|---|---|---|---|
| Soil CFED # | Energy | $w_{opt}$ (%) | $\gamma_{d\,max}$ (lb/ft$^3$) | $R^2$ | $w_{opt}$ (%) | $\gamma_{d\,max}$ (lb/ft$^3$) | $R^2$ | $w_{opt}$ (%) | $\gamma_{d\,max}$ (lb/ft$^3$) |
| 2024 | S | 13.1 | 117.3 | 0.75 | 11.9 | 121.7 | 1.00 | -- | -- |
| | M | 8.9 | 128.8 | 1.00 | -- | -- | -- | 7.6 | 121.9 |

| | | Blotz B | | Li & Sego | | | | CFED | | |
|---|---|---|---|---|---|---|---|---|---|---|
| Soil CFED # | Energy | $w_{opt}$ (%) | $\gamma_{d\,max}$ (lb/ft$^3$) | $S_m$ | $w_{opt}$ (%) | $\gamma_{d\,max}$ (lb/ft$^3$) | $R^2$ | $w_{opt}$ (%) | $\gamma_{d\,max}$ (lb/ft$^3$) | $R^2$ |
| 2024 | S | 14.1 | 119.5 | 89.7 | 13.3 | 118.5 | 0.88 | 11.9 | 117.5 | 0.96 |
| | M | 8.4 | 134.6 | 89.7 | 8.9 | 128.8 | 1.00 | 8.7 | 128.4 | |

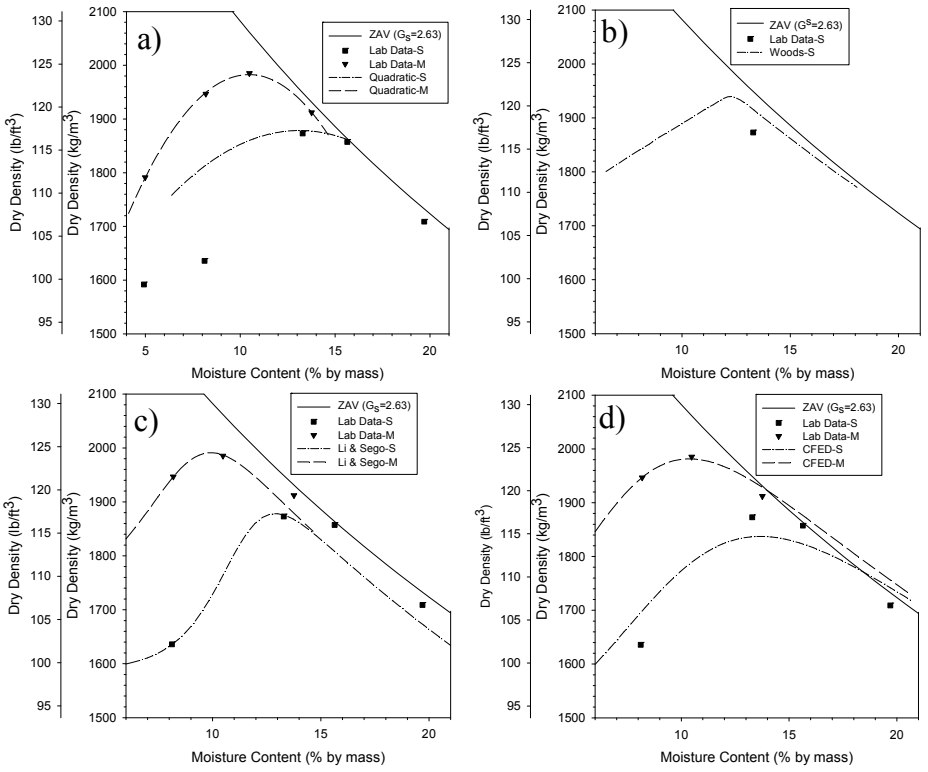


**Figure 153: CO Subgrade Clay 1 (Soil 2025) a) Quadratic, b) Woods, c) Li and Sego, d) CFED**

**Table 101: Soil 2025 Prediction Values**

| | | Quadratic | | | Woods | | | Blotz A | |
|---|---|---|---|---|---|---|---|---|---|
| Soil CFED # | Energy | $w_{opt}$ (%) | $\gamma_{d\,max}$ (lb/ft$^3$) | $R^2$ | $w_{opt}$ (%) | $\gamma_{d\,max}$ (lb/ft$^3$) | $R^2$ | $w_{opt}$ (%) | $\gamma_{d\,max}$ (lb/ft$^3$) |
| 2025 | S | 14.1 | 114.9 | 0.83 | 13.5 | 116.7 | 0.98 | -- | -- |
| | M | 10.5 | 123.8 | 1.00 | -- | -- | -- | 6.4 | 121.6 |

| | | Blotz B | | Li & Sego | | | | CFED | | |
|---|---|---|---|---|---|---|---|---|---|---|
| Soil CFED # | Energy | $w_{opt}$ (%) | $\gamma_{d\,max}$ (lb/ft$^3$) | $S_m$ | $w_{opt}$ (%) | $\gamma_{d\,max}$ (lb/ft$^3$) | $R^2$ | $w_{opt}$ (%) | $\gamma_{d\,max}$ (lb/ft$^3$) | $R^2$ |
| 2025 | S | 13.7 | 120.4 | 90.6 | 12.9 | 117.3 | 0.94 | 13.7 | 114.7 | 0.94 |
| | M | 8.3 | 135.1 | 90.6 | 9.9 | 124.3 | 0.95 | 10.4 | 123.7 | |

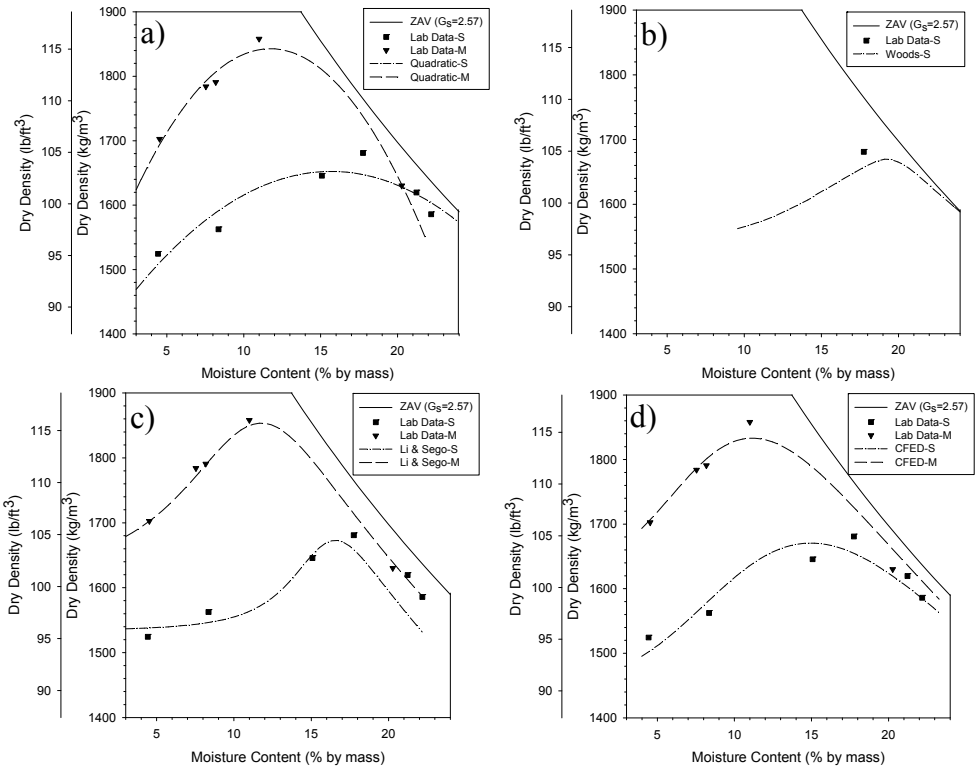


**Figure 154: CO Subgrade Clay 2 (Soil 2026) a) Quadratic, b) Woods, c) Li and Sego, d) CFED**

**Table 102: Soil 2026 Prediction Values**

| | | Quadratic | | | Woods | | | Blotz A | |
|---|---|---|---|---|---|---|---|---|---|
| Soil CFED # | Energy | $w_{opt}$ (%) | $\gamma_{d\ max}$ (lb/ft$^3$) | $R^2$ | $w_{opt}$ (%) | $\gamma_{d\ max}$ (lb/ft$^3$) | $R^2$ | $w_{opt}$ (%) | $\gamma_{d\ max}$ (lb/ft$^3$) |
| 2026 | S | 15.7 | 103.1 | 0.84 | 19.2 | 104.9 | 0.92 | -- | -- |
| | M | 11.7 | 115.0 | 0.98 | -- | -- | -- | 8.8 | 103.1 |

| | | Blotz B | | Li & Sego | | | | CFED | | |
|---|---|---|---|---|---|---|---|---|---|---|
| Soil CFED # | Energy | $w_{opt}$ (%) | $\gamma_{d\ max}$ (lb/ft$^3$) | $S_m$ | $w_{opt}$ (%) | $\gamma_{d\ max}$ (lb/ft$^3$) | $R^2$ | $w_{opt}$ (%) | $\gamma_{d\ max}$ (lb/ft$^3$) | $R^2$ |
| 2026 | S | 13.7 | 120.4 | 84.1 | 16.6 | 104.4 | 0.53 | 14.9 | 104.3 | 0.96 |
| | M | 8.3 | 135.1 | 84.1 | 11.0 | 115.7 | 0.94 | 11.2 | 114.4 | |

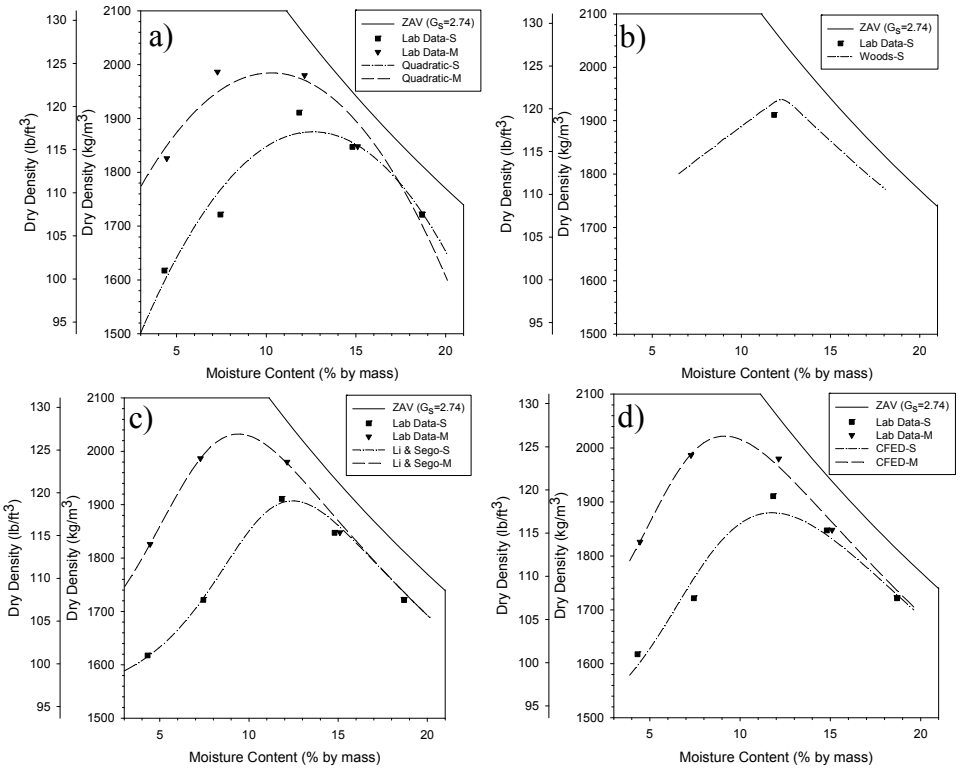


**Figure 155: CO Subgrade Clay 3 (Soil 2027) a) Quadratic, b) Woods, c) Li and Sego, d) CFED**

**Table 103: Soil 2027 Prediction Values**

| | | Quadratic | | | Woods | | | Blotz A | |
|---|---|---|---|---|---|---|---|---|---|
| Soil CFED # | Energy | $w_{opt}$ (%) | $\gamma_{d\,max}$ (lb/ft$^3$) | $R^2$ | $w_{opt}$ (%) | $\gamma_{d\,max}$ (lb/ft$^3$) | $R^2$ | $w_{opt}$ (%) | $\gamma_{d\,max}$ (lb/ft$^3$) |
| 2027 | S | 12.6 | 117.1 | 0.92 | 11.9 | 121.7 | 0.93 | -- | -- |
| | M | 10.3 | 123.9 | 0.91 | -- | -- | -- | 12.9 | 107.1 |

| | | Blotz B | | Li & Sego | | | | CFED | | |
|---|---|---|---|---|---|---|---|---|---|---|
| Soil CFED # | Energy | $w_{opt}$ (%) | $\gamma_{d\,max}$ (lb/ft$^3$) | $S_m$ | $w_{opt}$ (%) | $\gamma_{d\,max}$ (lb/ft$^3$) | $R^2$ | $w_{opt}$ (%) | $\gamma_{d\,max}$ (lb/ft$^3$) | $R^2$ |
| 2027 | S | 13.2 | 121.6 | 88.6 | 12.4 | 119.1 | 0.99 | 11.8 | 117.4 | 0.97 |
| | M | 8.4 | 135.7 | 88.6 | 9.4 | 126.9 | 0.99 | 9.1 | 126.2 | |

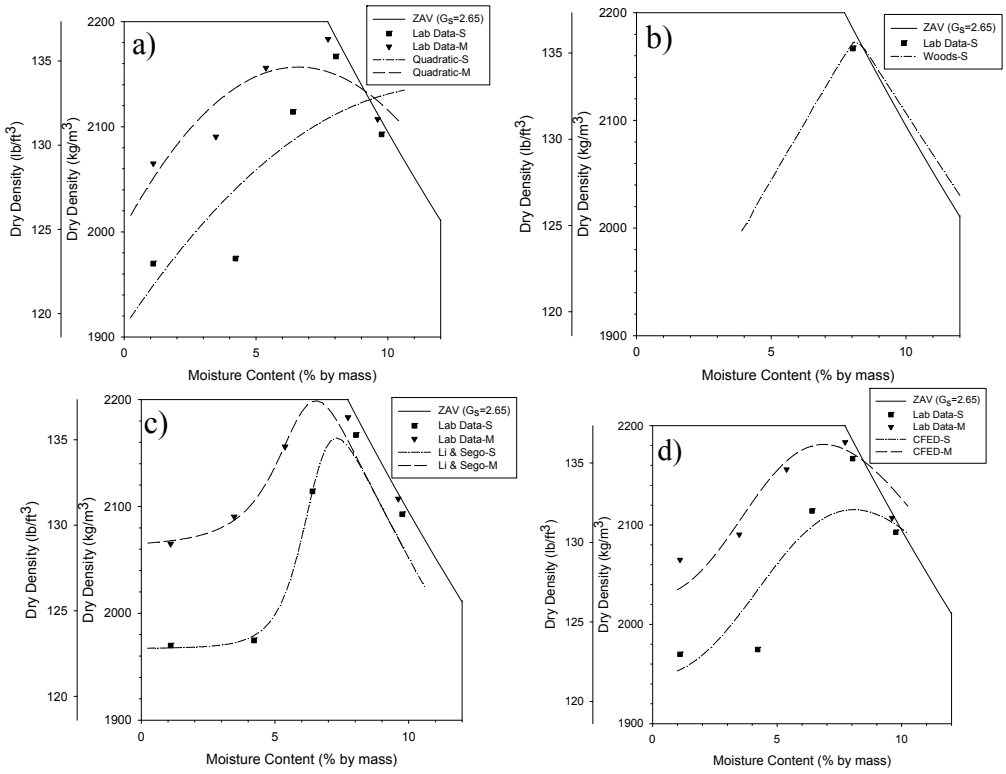


**Figure 156: CO Base Layer (Soil 2029) a) Quadratic, b) Woods, c) Li and Sego, d) CFED**

**Table 104: Soil 2029 Prediction Values**

| | | Quadratic | | | Woods | | | Blotz A | |
|---|---|---|---|---|---|---|---|---|---|
| Soil CFED # | Energy | $w_{opt}$ (%) | $\gamma_{d\,max}$ (lb/ft$^3$) | $R^2$ | $w_{opt}$ (%) | $\gamma_{d\,max}$ (lb/ft$^3$) | $R^2$ | $w_{opt}$ (%) | $\gamma_{d\,max}$ (lb/ft$^3$) |
| 2029 | S | 12.2 | 133.5 | 0.68 | 7.9 | 136.1 | 1.00 | NP | NP |
| | M | 6.6 | 134.6 | 0.73 | -- | -- | -- | NP | NP |

| | | Blotz B | | Li & Sego | | | | CFED | | |
|---|---|---|---|---|---|---|---|---|---|---|
| Soil CFED # | Energy | $w_{opt}$ (%) | $\gamma_{d\,max}$ (lb/ft$^3$) | $S_m$ | $w_{opt}$ (%) | $\gamma_{d\,max}$ (lb/ft$^3$) | $R^2$ | $w_{opt}$ (%) | $\gamma_{d\,max}$ (lb/ft$^3$) | $R^2$ |
| 2029 | S | NP | NP | 90.9 | 7.3 | 135.1 | 0.96 | 8.1 | 132.1 | 0.82 |
| | M | NP | NP | 90.9 | 6.5 | 137.3 | 0.80 | 6.9 | 136.2 | |

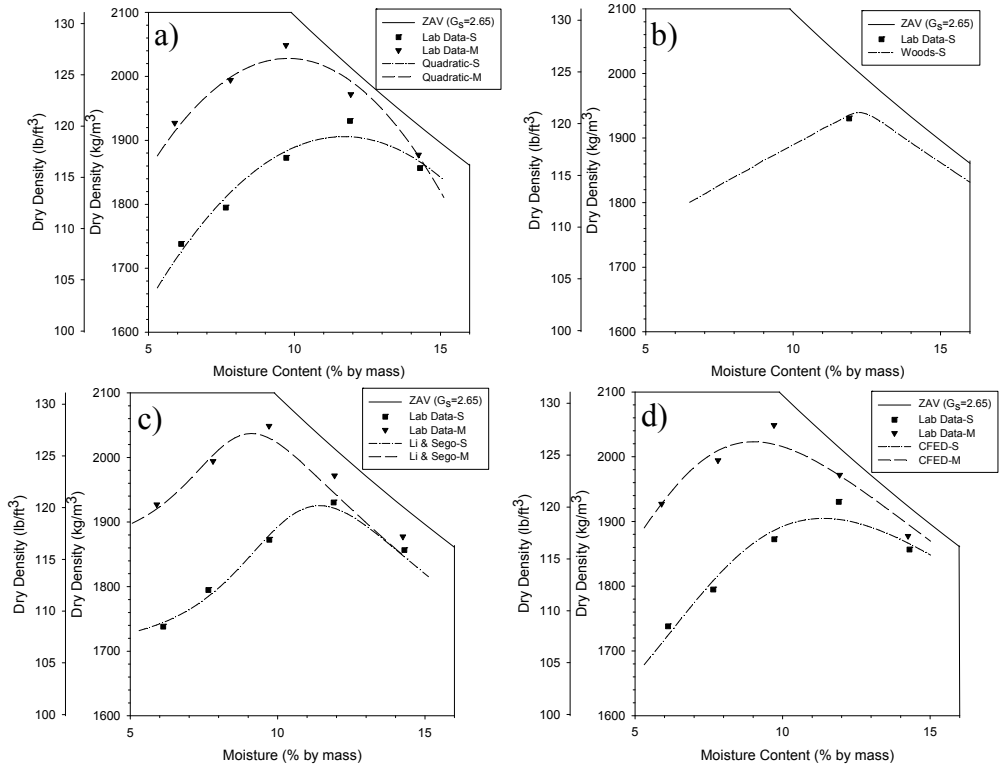


**Figure 157: MD Subgrade clay (Soil 2030) a) Quadratic, b) Woods, c) Li and Sego, d) CFED**

**Table 105: Soil 2030 Prediction Values**

| | | Quadratic | | | Woods | | | Blotz A | |
|---|---|---|---|---|---|---|---|---|---|
| Soil CFED # | Energy | $w_{opt}$ (%) | $\gamma_{d\,max}$ (lb/ft$^3$) | $R^2$ | $w_{opt}$ (%) | $\gamma_{d\,max}$ (lb/ft$^3$) | $R^2$ | $w_{opt}$ (%) | $\gamma_{d\,max}$ (lb/ft$^3$) |
| 2030 | S | 11.7 | 119.0 | 0.94 | 11.9 | 121.7 | 1.00 | -- | -- |
| | M | 9.6 | 126.6 | 0.95 | -- | -- | -- | 8.1 | 122.5 |

| | | Blotz B | | Li & Sego | | | | CFED | | |
|---|---|---|---|---|---|---|---|---|---|---|
| Soil CFED # | Energy | $w_{opt}$ (%) | $\gamma_{d\,max}$ (lb/ft$^3$) | $S_m$ | $w_{opt}$ (%) | $\gamma_{d\,max}$ (lb/ft$^3$) | $R^2$ | $w_{opt}$ (%) | $\gamma_{d\,max}$ (lb/ft$^3$) | $R^2$ |
| 2030 | S | 12.9 | 123.1 | 87.1 | 11.4 | 120.2 | 0.98 | 11.4 | 118.9 | 0.96 |
| | M | 9.1 | 136.0 | 87.1 | 9.1 | 127.2 | 0.88 | 9.0 | 126.3 | |

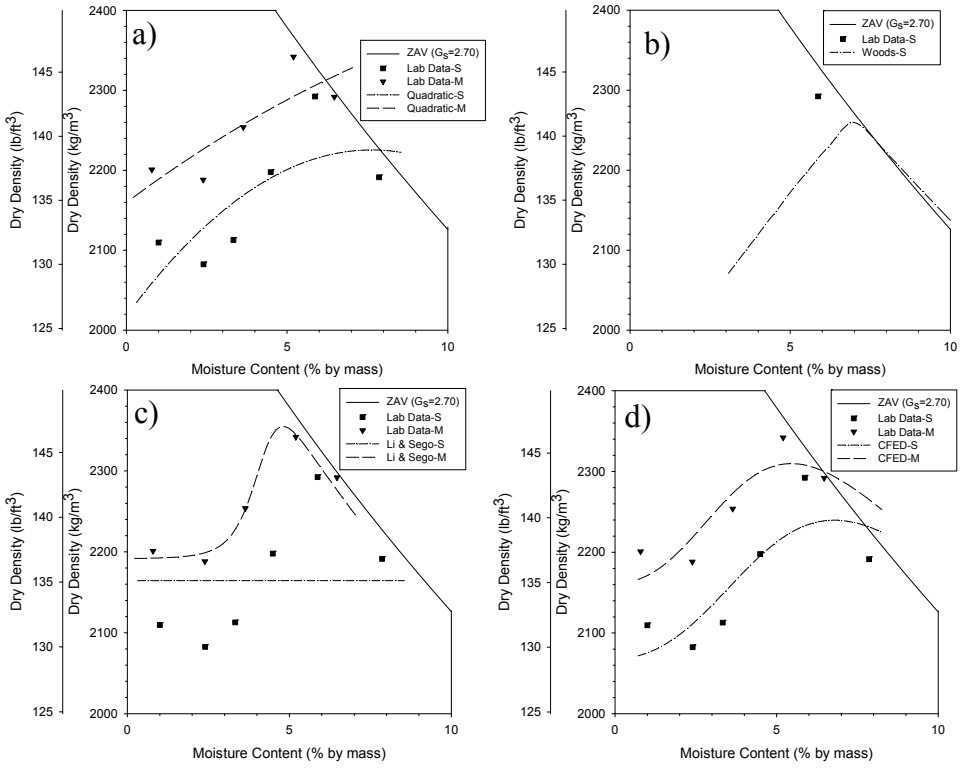


**Figure 158: MD Base Material (Soil 2031) a) Quadratic, b) Woods, c) Li and Sego, d) CFED**

**Table 106: Soil 2031 Prediction Values**

| | | Quadratic | | | Woods | | | Blotz A | |
|---|---|---|---|---|---|---|---|---|---|
| Soil CFED # | Energy | $w_{opt}$ (%) | $\gamma_{d\ max}$ (lb/ft$^3$) | $R^2$ | $w_{opt}$ (%) | $\gamma_{d\ max}$ (lb/ft$^3$) | $R^2$ | $w_{opt}$ (%) | $\gamma_{d\ max}$ (lb/ft$^3$) |
| 2031 | S | 7.6 | 138.9 | 0.57 | 6.6 | 141.7 | 0.19 | NP | NP |
| | M | 17.7 | 151.4 | 0.70 | -- | -- | -- | NP | NP |

| | | Blotz B | | Li & Sego | | | | CFED | | |
|---|---|---|---|---|---|---|---|---|---|---|
| Soil CFED # | Energy | $w_{opt}$ (%) | $\gamma_{d\ max}$ (lb/ft$^3$) | $S_m$ | $w_{opt}$ (%) | $\gamma_{d\ max}$ (lb/ft$^3$) | $R^2$ | $w_{opt}$ (%) | $\gamma_{d\ max}$ (lb/ft$^3$) | $R^2$ |
| 2031 | S | NP | NP | 93.9 | 0.1 | 135.1 | 0.00 | 6.8 | 139.8 | 0.83 |
| | M | NP | NP | 93.9 | 4.8 | 147.0 | 0.97 | 5.5 | 144.2 | |

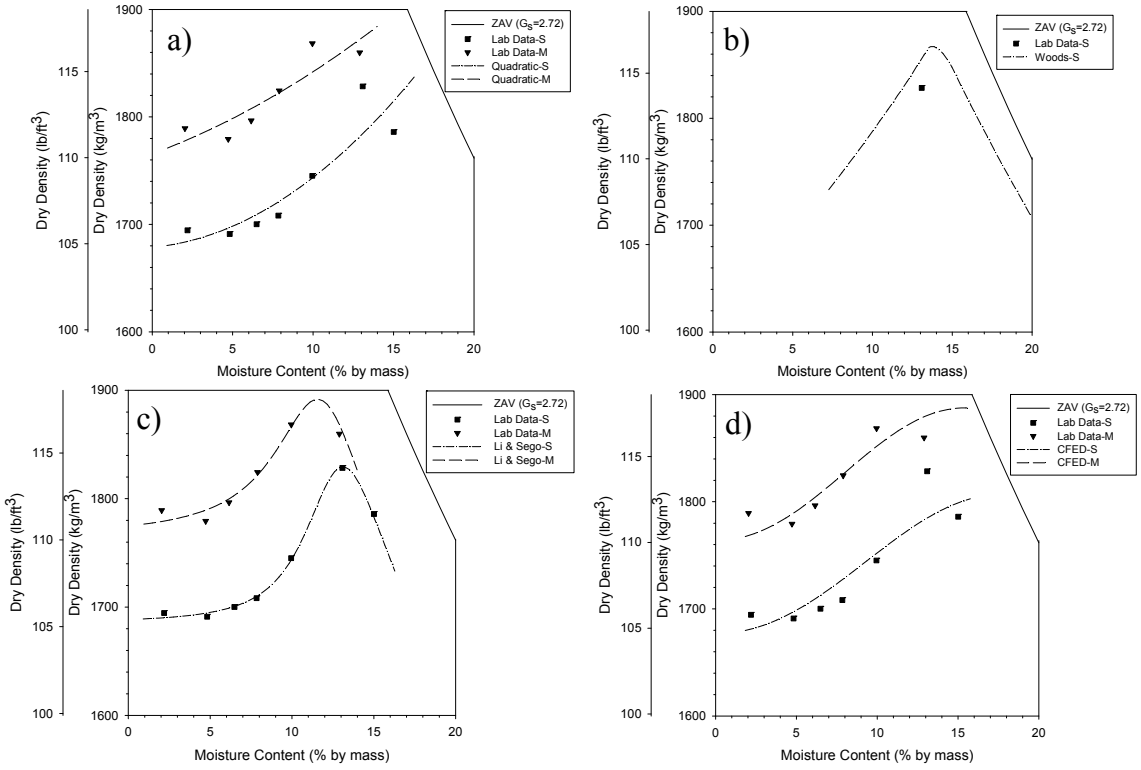


**Figure 159: FLA FL19 (Soil 2032) a) Quadratic, b) Woods, c) Li and Sego, d) CFED**

**Table 107: Soil 2032 Prediction Values**

| | | Quadratic | | | Woods | | | Blotz A | |
|---|---|---|---|---|---|---|---|---|---|
| Soil CFED # | Energy | $w_{opt}$ (%) | $\gamma_{d\ max}$ (lb/ft$^3$) | $R^2$ | $w_{opt}$ (%) | $\gamma_{d\ max}$ (lb/ft$^3$) | $R^2$ | $w_{opt}$ (%) | $\gamma_{d\ max}$ (lb/ft$^3$) |
| 2032 | S | 0.0 | 104.8 | 0.81 | 13.5 | 116.7 | 0.90 | NP | NP |
| | M | 0.0 | 110.2 | 0.80 | -- | -- | -- | NP | NP |

| | | Blotz B | | Li & Sego | | | | CFED | | |
|---|---|---|---|---|---|---|---|---|---|---|
| Soil CFED # | Energy | $w_{opt}$ (%) | $\gamma_{d\ max}$ (lb/ft$^3$) | $S_m$ | $w_{opt}$ (%) | $\gamma_{d\ max}$ (lb/ft$^3$) | $R^2$ | $w_{opt}$ (%) | $\gamma_{d\ max}$ (lb/ft$^3$) | $R^2$ |
| 2032 | S | NP | NP | 77.8 | 13.1 | 114.2 | 1.00 | 17.8 | 112.8 | 0.91 |
| | M | NP | NP | 77.8 | 11.6 | 118.1 | 0.96 | 15.4 | 117.8 | |

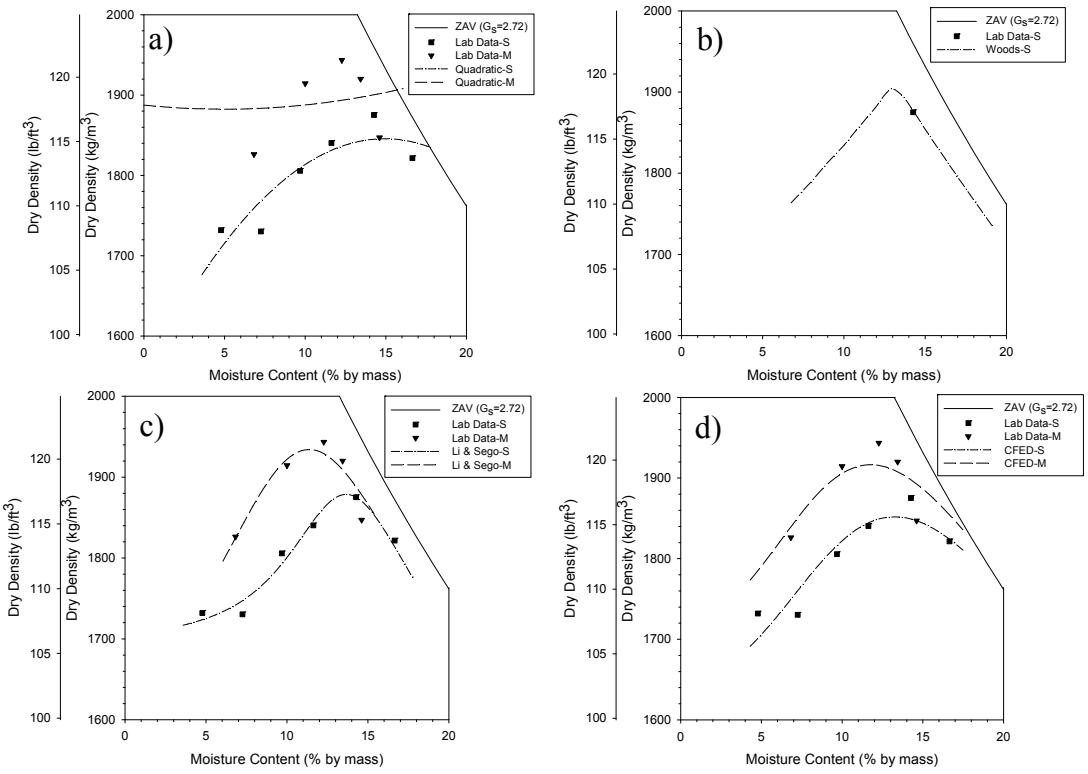


**Figure 160: FLA FL20-22 (Soil 2033) a) Quadratic, b) Woods, c) Li and Sego, d) CFED**

**Table 108: Soil 2033 Prediction Values**

| | | Quadratic | | | Woods | | | Blotz A | |
|---|---|---|---|---|---|---|---|---|---|
| Soil CFED # | Energy | $w_{opt}$ (%) | $\gamma_{d\ max}$ (lb/ft$^3$) | $R^2$ | $w_{opt}$ (%) | $\gamma_{d\ max}$ (lb/ft$^3$) | $R^2$ | $w_{opt}$ (%) | $\gamma_{d\ max}$ (lb/ft$^3$) |
| 2033 | S | 14.9 | 115.2 | 0.81 | 12.7 | 119.2 | 1.00 | NP | NP |
| | M | 5.0 | 117.5 | 0.02 | -- | -- | -- | NP | NP |

| | | Blotz B | | Li & Sego | | | | CFED | | |
|---|---|---|---|---|---|---|---|---|---|---|
| Soil CFED # | Energy | $w_{opt}$ (%) | $\gamma_{d\ max}$ (lb/ft$^3$) | $S_m$ | $w_{opt}$ (%) | $\gamma_{d\ max}$ (lb/ft$^3$) | $R^2$ | $w_{opt}$ (%) | $\gamma_{d\ max}$ (lb/ft$^3$) | $R^2$ |
| 2033 | S | NP | NP | 90.9 | 13.7 | 117.3 | 0.96 | 13.3 | 115.6 | 0.88 |
| | M | NP | NP | 90.9 | 11.4 | 120.7 | 0.87 | 11.8 | 119.6 | |

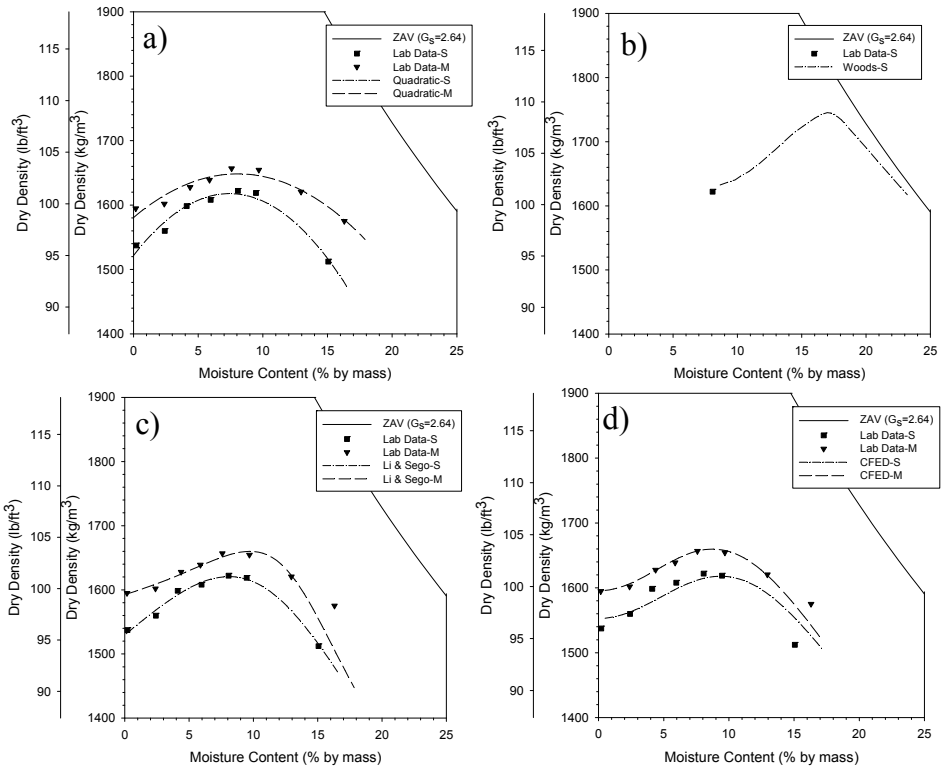


**Figure 161: FLA FL23 (Soil 2034) a) Quadratic, b) Woods, c) Li and Sego, d) CFED**

**Table 109: Soil 2034 Prediction Values**

| | | Quadratic | | | Woods | | | Blotz A | |
|---|---|---|---|---|---|---|---|---|---|
| Soil CFED # | Energy | $w_{opt}$ (%) | $\gamma_{d\ max}$ (lb/ft$^3$) | $R^2$ | $w_{opt}$ (%) | $\gamma_{d\ max}$ (lb/ft$^3$) | $R^2$ | $w_{opt}$ (%) | $\gamma_{d\ max}$ (lb/ft$^3$) |
| 2034 | S | 7.4 | 101.0 | 0.96 | 16.9 | 109.9 | 0.99 | NP | NP |
| | M | 8.0 | 102.9 | 0.91 | -- | -- | -- | NP | NP |

| | | Blotz B | | Li & Sego | | | | CFED | | |
|---|---|---|---|---|---|---|---|---|---|---|
| Soil CFED # | Energy | $w_{opt}$ (%) | $\gamma_{d\ max}$ (lb/ft$^3$) | $S_m$ | $w_{opt}$ (%) | $\gamma_{d\ max}$ (lb/ft$^3$) | $R^2$ | $w_{opt}$ (%) | $\gamma_{d\ max}$ (lb/ft$^3$) | $R^2$ |
| 2034 | S | NP | NP | 56.9 | 8.1 | 101.2 | 1.0 | 9.4 | 101.0 | 0.85 |
| | M | NP | NP | 56.9 | 9.7 | 103.6 | 0.17 | 8.8 | 103.6 | |

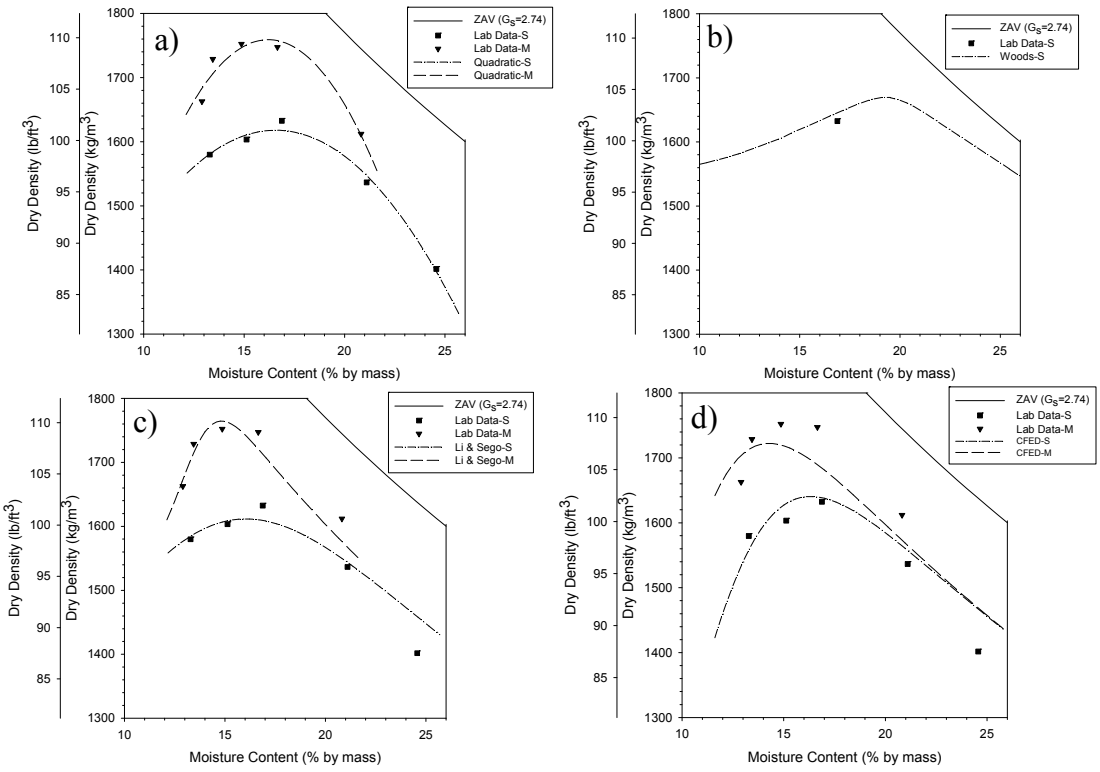


**Figure 162: FLA FL24 (Soil 2035) a) Quadratic, b) Woods, c) Li and Sego, d) CFED**

**Table 110: Soil 2035 Prediction Values**

| | | Quadratic | | | Woods | | | Blotz A | |
|---|---|---|---|---|---|---|---|---|---|
| Soil CFED # | Energy | $w_{opt}$ (%) | $\gamma_{d\ max}$ (lb/ft$^3$) | $R^2$ | $w_{opt}$ (%) | $\gamma_{d\ max}$ (lb/ft$^3$) | $R^2$ | $w_{opt}$ (%) | $\gamma_{d\ max}$ (lb/ft$^3$) |
| 2035 | S | 16.6 | 101.0 | 0.99 | 19.2 | 104.9 | 0.98 | NP | NP |
| | M | 16.2 | 109.8 | 0.93 | -- | -- | -- | NP | NP |

| | | Blotz B | | Li & Sego | | | | CFED | | |
|---|---|---|---|---|---|---|---|---|---|---|
| Soil CFED # | Energy | $w_{opt}$ (%) | $\gamma_{d\ max}$ (lb/ft$^3$) | $S_m$ | $w_{opt}$ (%) | $\gamma_{d\ max}$ (lb/ft$^3$) | $R^2$ | $w_{opt}$ (%) | $\gamma_{d\ max}$ (lb/ft$^3$) | $R^2$ |
| 2035 | S | NP | NP | 77.3 | 16.0 | 100.6 | 0.88 | 16.3 | 102.4 | 0.87 |
| | M | NP | NP | 77.3 | 14.8 | 110.2 | 0.84 | 14.3 | 107.5 | |

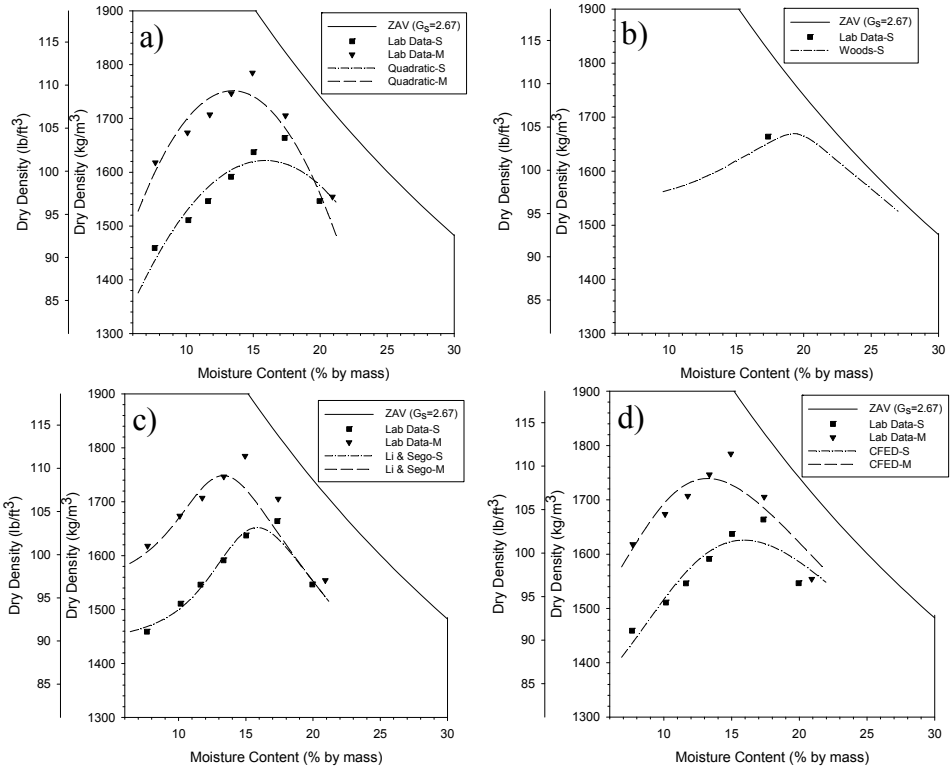


**Figure 163: FLA FL25-1 (Soil 2036) a) Quadratic, b) Woods, c) Li and Sego, d) CFED**

**Table 111: Soil 2036 Prediction Values**

| | | Quadratic | | | Woods | | | Blotz A | |
|---|---|---|---|---|---|---|---|---|---|
| Soil CFED # | Energy | $w_{opt}$ (%) | $\gamma_{d\ max}$ (lb/ft$^3$) | $R^2$ | $w_{opt}$ (%) | $\gamma_{d\ max}$ (lb/ft$^3$) | $R^2$ | $w_{opt}$ (%) | $\gamma_{d\ max}$ (lb/ft$^3$) |
| 2036 | S | 15.9 | 101.2 | 0.83 | 19.2 | 104.9 | 0.98 | NP | NP |
| | M | 13.9 | 109.3 | 0.92 | -- | -- | -- | NP | NP |

| | | Blotz B | | Li & Sego | | | | CFED | | |
|---|---|---|---|---|---|---|---|---|---|---|
| Soil CFED # | Energy | $w_{opt}$ (%) | $\gamma_{d\ max}$ (lb/ft$^3$) | $S_m$ | $w_{opt}$ (%) | $\gamma_{d\ max}$ (lb/ft$^3$) | $R^2$ | $w_{opt}$ (%) | $\gamma_{d\ max}$ (lb/ft$^3$) | $R^2$ |
| 2036 | S | NP | NP | 74.2 | 15.8 | 103.1 | 0.96 | 15.9 | 101.5 | 0.90 |
| | M | NP | NP | 74.2 | 13.3 | 109.2 | 0.75 | 13.2 | 108.6 | |

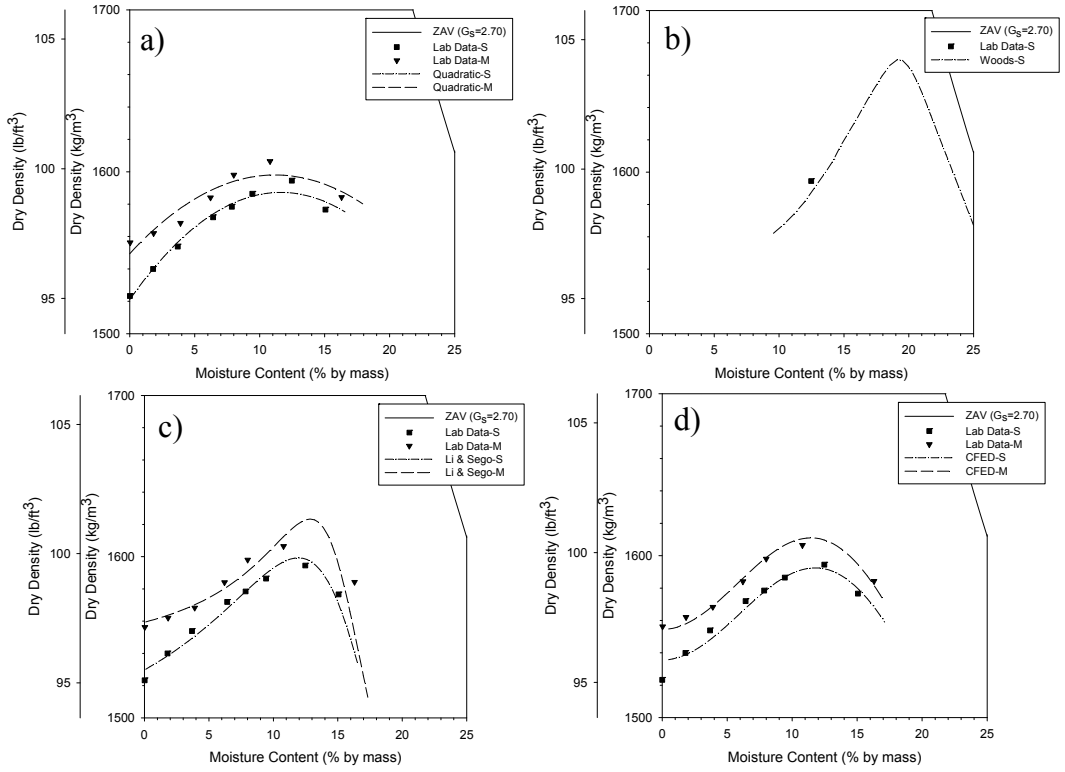


**Figure 164: FLA FL25-2 (Soil 2037) a) Quadratic, b) Woods, c) Li and Sego, d) CFED**

**Table 112: Soil 2037 Prediction Values**

| | | Quadratic | | | Woods | | | Blotz A | |
|---|---|---|---|---|---|---|---|---|---|
| Soil CFED # | Energy | $w_{opt}$ (%) | $\gamma_{d\ max}$ (lb/ft$^3$) | $R^2$ | $w_{opt}$ (%) | $\gamma_{d\ max}$ (lb/ft$^3$) | $R^2$ | $w_{opt}$ (%) | $\gamma_{d\ max}$ (lb/ft$^3$) |
| 2037 | S | 11.6 | 99.1 | 0.98 | 19.2 | 104.9 | 0.99 | NP | NP |
| | M | 11.2 | 99.8 | 0.88 | -- | -- | -- | NP | NP |

| | | Blotz B | | Li & Sego | | | | CFED | | |
|---|---|---|---|---|---|---|---|---|---|---|
| Soil CFED # | Energy | $w_{opt}$ (%) | $\gamma_{d\ max}$ (lb/ft$^3$) | $S_m$ | $w_{opt}$ (%) | $\gamma_{d\ max}$ (lb/ft$^3$) | $R^2$ | $w_{opt}$ (%) | $\gamma_{d\ max}$ (lb/ft$^3$) | $R^2$ |
| 2037 | S | NP | NP | 59.6 | 11.9 | 99.8 | 0.97 | 11.8 | 99.4 | 0.96 |
| | M | NP | NP | 59.6 | 12.9 | 101.3 | 0.47 | 11.4 | 100.6 | |

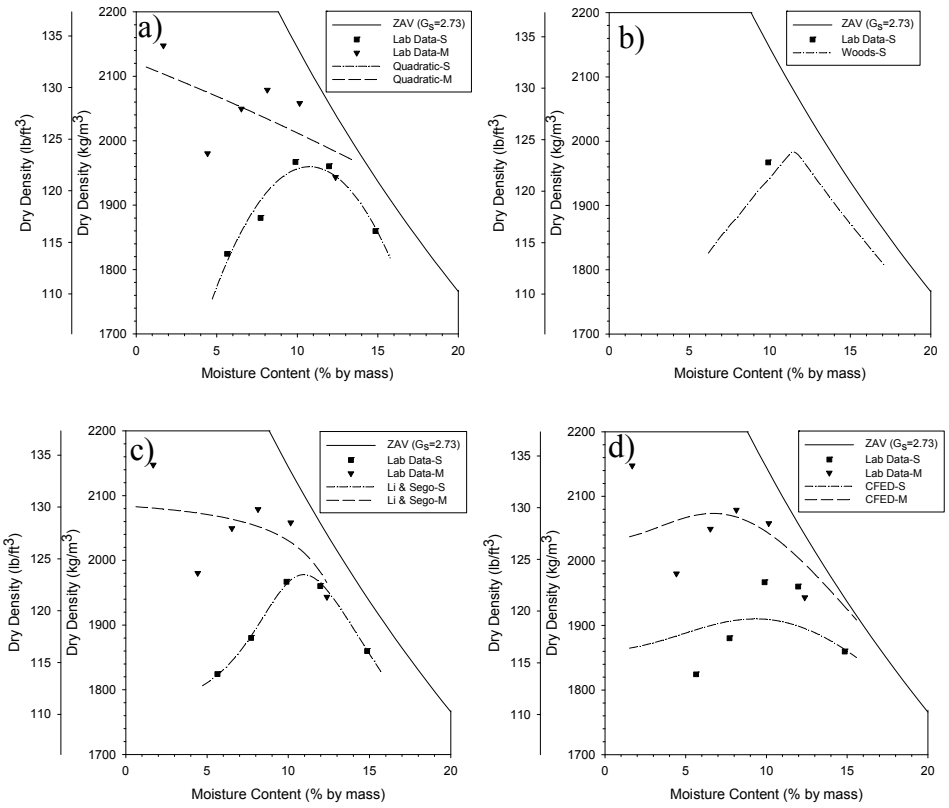


**Figure 165: NC1 (Soil 2038) a) Quadratic, b) Woods, c) Li and Sego, d) CFED**

**Table 113: Soil 2038 Prediction Values**

| | | Quadratic | | | Woods | | | Blotz A | |
|---|---|---|---|---|---|---|---|---|---|
| Soil CFED # | Energy | $w_{opt}$ (%) | $\gamma_{d\,max}$ (lb/ft$^3$) | $R^2$ | $w_{opt}$ (%) | $\gamma_{d\,max}$ (lb/ft$^3$) | $R^2$ | $w_{opt}$ (%) | $\gamma_{d\,max}$ (lb/ft$^3$) |
| 2038 | S | 10.8 | 122.3 | 0.93 | 11.2 | 124.2 | 0.90 | -- | -- |
| | M | 0.0 | 132.4 | 0.36 | -- | -- | -- | 7.6 | 123.7 |

| | | Blotz B | | Li & Sego | | | | CFED | | |
|---|---|---|---|---|---|---|---|---|---|---|
| Soil CFED # | Energy | $w_{opt}$ (%) | $\gamma_{d\,max}$ (lb/ft$^3$) | $S_m$ | $w_{opt}$ (%) | $\gamma_{d\,max}$ (lb/ft$^3$) | $R^2$ | $w_{opt}$ (%) | $\gamma_{d\,max}$ (lb/ft$^3$) | $R^2$ |
| 2038 | S | 13.0 | 123.5 | 86.9 | 11.0 | 123.5 | 1.00 | 9.3 | 119.3 | 0.65 |
| | M | 9.6 | 135.8 | 86.9 | 0.1 | 130.1 | 0.42 | 6.7 | 129.4 | |

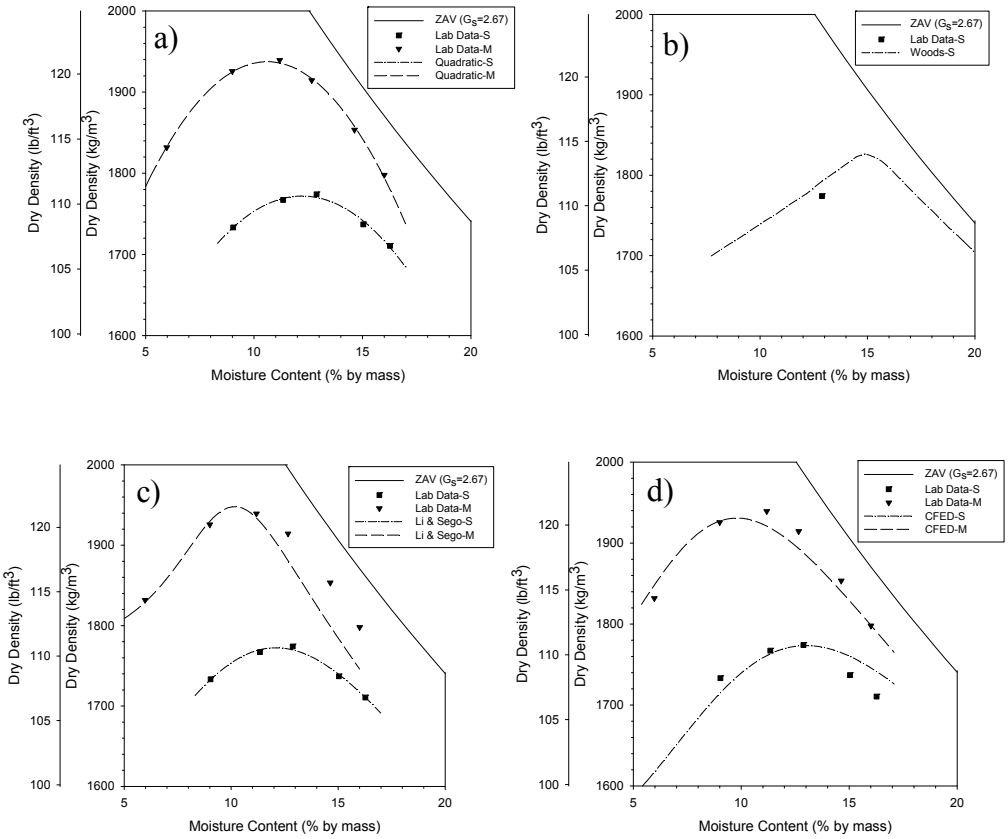


**Figure 166: NC2 (Soil 2039) a) Quadratic, b) Woods, c) Li and Sego, d) CFED**

**Table 114: Soil 2039 Prediction Values**

| | | Quadratic | | | Woods | | | Blotz A | |
|---|---|---|---|---|---|---|---|---|---|
| Soil CFED # | Energy | $w_{opt}$ (%) | $\gamma_{d\,max}$ (lb/ft$^3$) | $R^2$ | $w_{opt}$ (%) | $\gamma_{d\,max}$ (lb/ft$^3$) | $R^2$ | $w_{opt}$ (%) | $\gamma_{d\,max}$ (lb/ft$^3$) |
| 2039 | S | 12.2 | 110.6 | 0.99 | 14.6 | 114.2 | 0.95 | -- | -- |
| | M | 10.6 | 120.9 | 1.00 | -- | -- | -- | 7.7 | 112.9 |

| | | Blotz B | | Li & Sego | | | | CFED | | |
|---|---|---|---|---|---|---|---|---|---|---|
| Soil CFED # | Energy | $w_{opt}$ (%) | $\gamma_{d\,max}$ (lb/ft$^3$) | $S_m$ | $w_{opt}$ (%) | $\gamma_{d\,max}$ (lb/ft$^3$) | $R^2$ | $w_{opt}$ (%) | $\gamma_{d\,max}$ (lb/ft$^3$) | $R^2$ |
| 2039 | S | 13.4 | 121.2 | 80.7 | 12.1 | 110.6 | 0.99 | 13.0 | 110.7 | 0.95 |
| | M | 8.3 | 135.5 | 80.7 | 10.2 | 121.6 | 0.59 | 9.8 | 120.5 | |

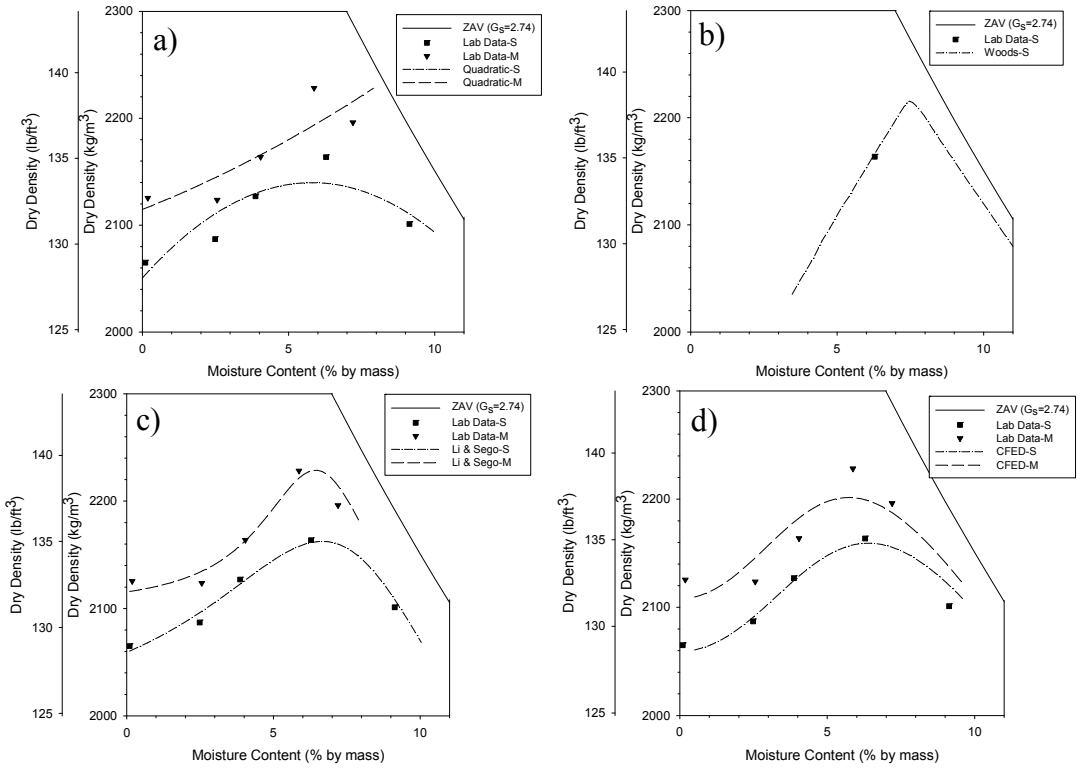


**Figure 167: NC4 (Soil 2040) a) Quadratic, b) Woods, c) Li and Sego, d) CFED**

**Table 115: Soil 2040 Prediction Values**

| | | Quadratic | | | Woods | | | Blotz A | |
|---|---|---|---|---|---|---|---|---|---|
| Soil CFED # | Energy | $w_{opt}$ (%) | $\gamma_{d\ max}$ (lb/ft$^3$) | $R^2$ | $w_{opt}$ (%) | $\gamma_{d\ max}$ (lb/ft$^3$) | $R^2$ | $w_{opt}$ (%) | $\gamma_{d\ max}$ (lb/ft$^3$) |
| 2040 | S | 5.8 | 133.6 | 0.76 | 7.2 | 139.2 | 1.00 | NP | NP |
| | M | 0.0 | 132.0 | 0.74 | -- | -- | -- | NP | NP |

| | | Blotz B | | Li & Sego | | | | CFED | | |
|---|---|---|---|---|---|---|---|---|---|---|
| Soil CFED # | Energy | $w_{opt}$ (%) | $\gamma_{d\ max}$ (lb/ft$^3$) | $S_m$ | $w_{opt}$ (%) | $\gamma_{d\ max}$ (lb/ft$^3$) | $R^2$ | $w_{opt}$ (%) | $\gamma_{d\ max}$ (lb/ft$^3$) | $R^2$ |
| 2039 | S | NP | NP | 85.0 | 6.7 | 135.0 | 0.97 | 6.4 | 134.8 | 0.89 |
| | M | NP | NP | 85.0 | 6.4 | 139.1 | 0.93 | 5.7 | 137.4 | |

**Mean Square Error**

Because CFED and Li and Sego (1999, 2000a, 2000b) models have different numbers of prediction parameters they should not be compared by regression coefficient alone. A statistical method, referred to as "mean square error" is available to determine the error associated with each model such that they may be compared by proper statistical means. This method accounts for the number of parameters used in the model and is therefore a valid mode of comparison.

The difference between CFED and Li and Sego (1999, 2000a, 2000b) models is in how each model predicts the entire data set. Li and Sego (1999, 2000a, 2000b) constructs a model for each individual energy level where CFED creates the family of curves based upon the entire dataset. If the ratio of prediction parameters to data set is high, the model may simply be following trends in the data. In this case, a model may produce incorrect results which can be attributed to random testing error. If the ratio is low, the model should produce a similar prediction, regardless of small changes in the data set.

Mean square error is the sum of the squares of the differences between actual and predicted values ($SS_E$) divided by the number of fit parameters (p) subtracted from the sample size (N). The general form of the mean square error (MSE) from Kutner (2003) equation is:

$$MSE=\frac{SS_E}{N-p} \tag{30}$$

Error sum of squares is defined in Equation 34.

$$SS_E=\sum_{i=1}^{n}(y_i-f(x_i))^2 \tag{31}$$

Where $y_i$ is the actual value from laboratory testing and $f(x_i)$ is the value predicted by the model.

The square root of the mean square error can be taken to display the error in units of $y_i$ or in this case, density. The comparison of mean square error values is not on an absolute scale (i.e 0 to 1). The value is a relative measurement; the lower the mean square error, the better the fit.

For the MSE of CFED, the form of Equation 30 was used. However, because Li and Sego predicts each curve independently, the number of parameters becomes a summation of all parameters. For example, Li and Sego uses four parameters per curve, for five curves the value of p becomes 20. Figure 168 summarizes the method of the analysis.

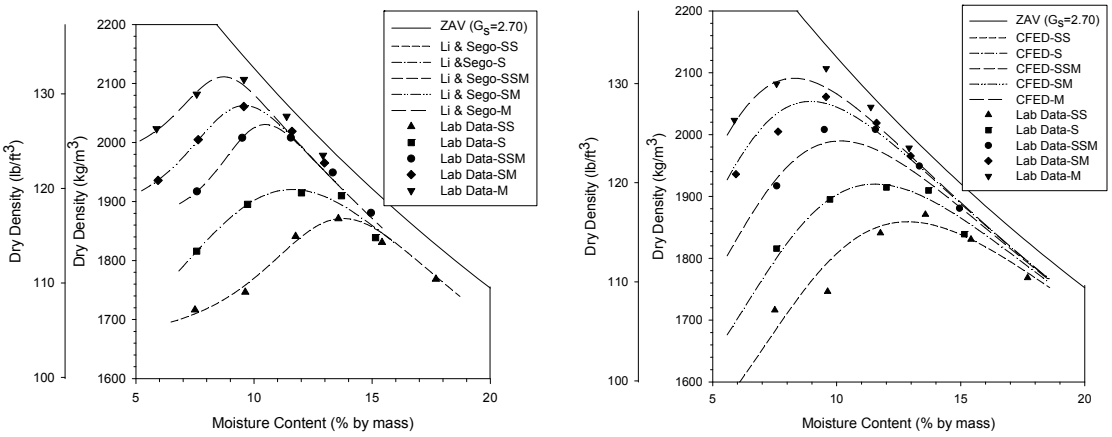


$$MSE=\frac{SS_{E_1}+SS_{E_2}+SS_{E_n}+\dots}{N-p_1-p_2-p_n-\dots} \qquad MSE=\frac{SS_E}{N-p}$$

**Figure 168: Mean square error**

**Sensitivity of CFED**

A sample soil was input into CFED to determine the sensitivity of the model to changes in the data. TH60 Soil #1 (CFED # 2013) was used in this analysis. The purpose was to determine how many points are required to create the family of curves for a given soil. Also, it was desired to determine how the distribution of points affects the model. This data consists of 44 points, many of which are on the wet-side of optimum. Figure 169 shows this

data prior to any analyses. Figure 170 is the CFED predicted model for the entire set of data. The original prediction values are shown in Table 116.

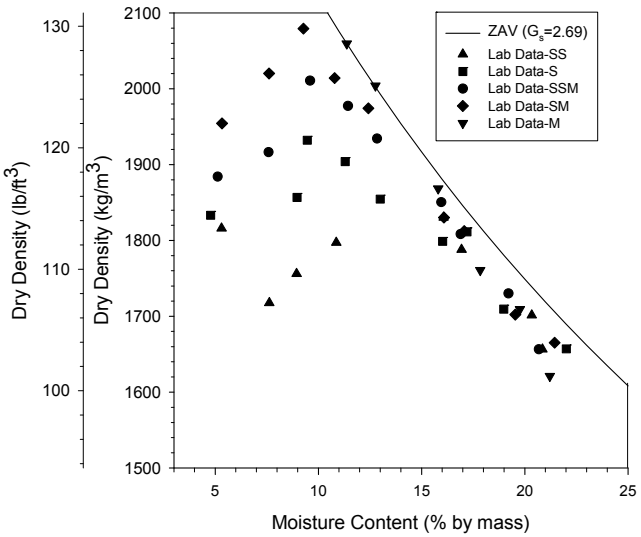


**Figure 169: TH60 Soil #1 Laboratory compaction data**

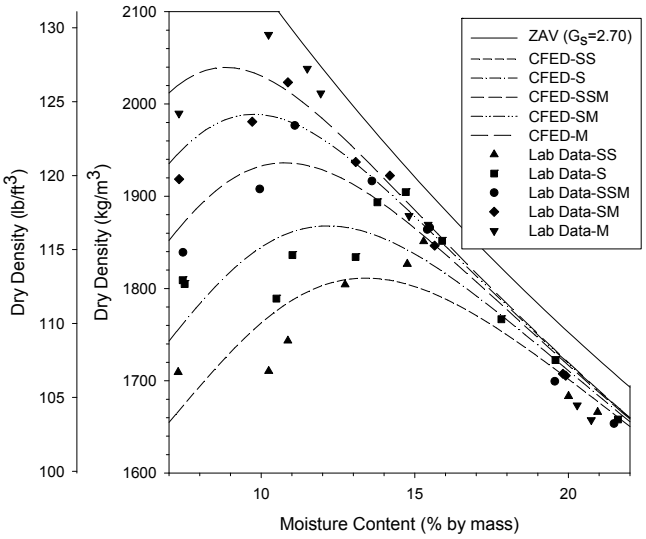


**Figure 170: CFED Soil 2013 Prediction for all data**

**Table 116: CFED Soil 2013 Predicted values**

| | | CFED | | |
|---|---|---|---|---|
| Soil CFED # | Energy | $w_{opt}$ (%) | $\gamma_{d\ max}$ (lb/ft$^3$) | $R^2$ |
| 2013 | SS | 12.1 | 114.9 | 0.92 |
| | S | 11.2 | 117.6 | |
| | SSM | 10.1 | 121.1 | |
| | SM | 9.3 | 124.2 | |
| | M | 8.4 | 127.3 | |

The first step in the analysis was the removal of the point with the highest moisture content from each energy level. The only change in the model prediction from this was a reduction of the regression coefficient to 0.89. A second time, the point with the highest moisture content for each energy level was removed with little change in the model other than a reduction in the regression coefficient. A third time, points were removed from the wet side of optimum such that each energy level had only one point lying near the zero-air-void curve. Points were continually removed without any significant variance of the model. The model showed no significant change in shape or predicted values until enough points were removed so that no points were left wet of optimum.

All data points were re-input into CFED so that another sensitivity analysis may be performed. Caterpillar engineers suggested that a more efficient method of lab testing may exist for soils to be used in CFED. Rather than compact the soil at all energy levels for all moisture contents, the energies should be selected on the basis of energy-density relationships. As the compaction energy increases for a given soil, the curves will move up and to the left on the moisture content vs. density plot. Therefore, lab compaction testing should be skewed so that the lab time/effort may be minimized. In Figure 171 the points within the parallelogram are those which would be included in testing and the outliers would be excluded.

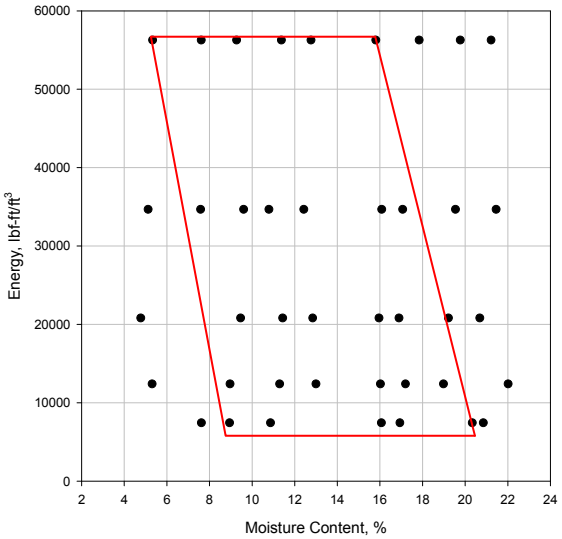


**Figure 171: Suggested lab compaction method**

This was tested, but no significant variation in the model occurred. A decrease in the regression coefficient to 0.90 and a slight increase (0.1 pcf) of the predicted value for modified maximum density. While this change in testing would undoubtedly decrease lab work, it is does not appear to affect the accuracy of the model.

The model was again tested, this time to determine the minimum number of points required to create a valuable model. Initially, all points were removed from the data set so that only the point nearest to optimum remained. However, CFED was unable to generate a model from so few data. Several different attempts were made and it was determined that the minimum number of points to generate a model is three points per energy level. These points should consist of one point near optimum moisture content and one point each other either side of optimum. Points spread across the data set will not provide a sufficient model for prediction. A larger number of points should be expected to increase the accuracy of the CFED prediction, but it is ultimately the discretion of the user as to the applicability of a model using a given number of points. Figure 172, Figure 173, Table 117, and Table 118 show these predictions and their results.

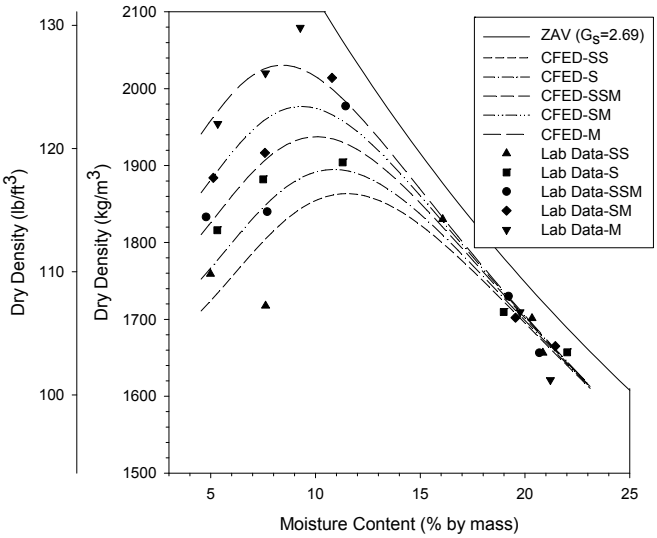


**Figure 172: CFED 5 Point prediction**

**Table 117: CFED 5 Point prediction results**

| | | CFED | | |
|---|---|---|---|---|
| Soil CFED # | Energy | $w_{opt}$ (%) | $\gamma_{d\ max}$ (lb/ft$^3$) | $R^2$ |
| 2013 | SS | 11.5 | 116.0 | 0.93 |
| | S | 10.9 | 118.3 | |
| | SSM | 10. | 121.8 | |
| | SM | 9.0 | 123.1 | |
| | M | 8.4 | 126.8 | |

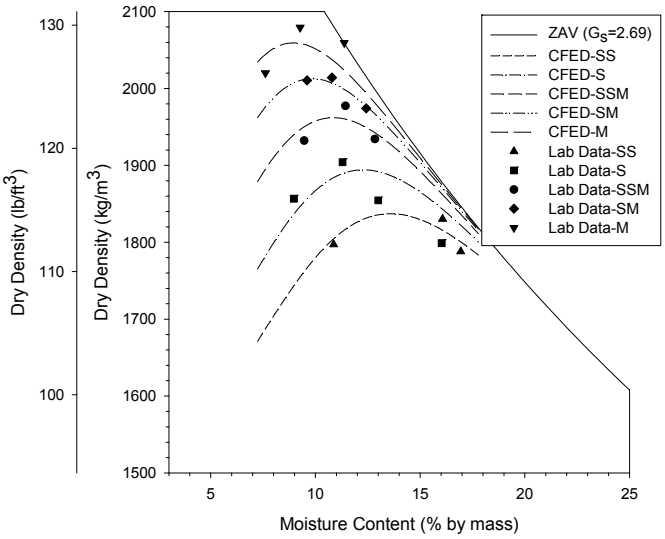


**Figure 173: CFED 3 Point prediction**

**Table 118: CFED 3 Point prediction results**

| | | CFED | | |
|---|---|---|---|---|
| Soil CFED # | Energy | $w_{opt}$ (%) | $\gamma_{d\ max}$ (lb/ft$^3$) | $R^2$ |
| 2013 | SS | 13.0 | 114.9 | 0.96 |
| | S | 12.3 | 118.3 | |
| | SSM | 10.8 | 122.8 | |
| | SM | 9.5 | 126.0 | |
| | M | 9.0 | 128.6 | |

**Field Compaction Results**

Field compaction data has been collected and stored for some soils in CFED. A variety of machines were used with varying settings to compact each soil. Data was collected at given intervals to establish relationships between machine passes, soil index properties and machine parameters.

For some field data, moisture content and density measurements were taken with the nuclear

gauge on loose material at zero passes. Because of the significant voids in the material this test will give abnormally low moisture contents and abnormally high densities. This error in measurement was normalized by averaging the moisture content reading for the first two passes (typically 0 and 1 pass). The moisture content data from the 0 pass reading was increased by the difference between two averages such that the average moisture content was equal for the first two measurements (again, typically 0 and 1 pass). The equations below describe this process.

$$A = w\%_{avg,pass1} - w\%_{avg,pass0} \tag{32}$$

$$w\%_{corrected\ pass0} = w\%_{pass0} + A \tag{33}$$

Lab density values were superimposed on field density curves to evaluate the correlation between lab and field compaction. As soil is compacted by machine, the density of the soil is expected to increase toward an asymptotic value as the number of passes increase. The purpose of comparing laboratory to field compaction data is to determine at what lab compaction energy this asymptotic value lies; the ultimate goal being to find a correlation between lab compaction energy and machine pass. For some soils, laboratory compaction was only performed at one or two energy levels (Standard and Modified Proctor). Therefore, it is not possible to create a laboratory compaction curve. For these soils, reference lines are plotted which show the maximum densities for Standard and Modified laboratory compaction effort.

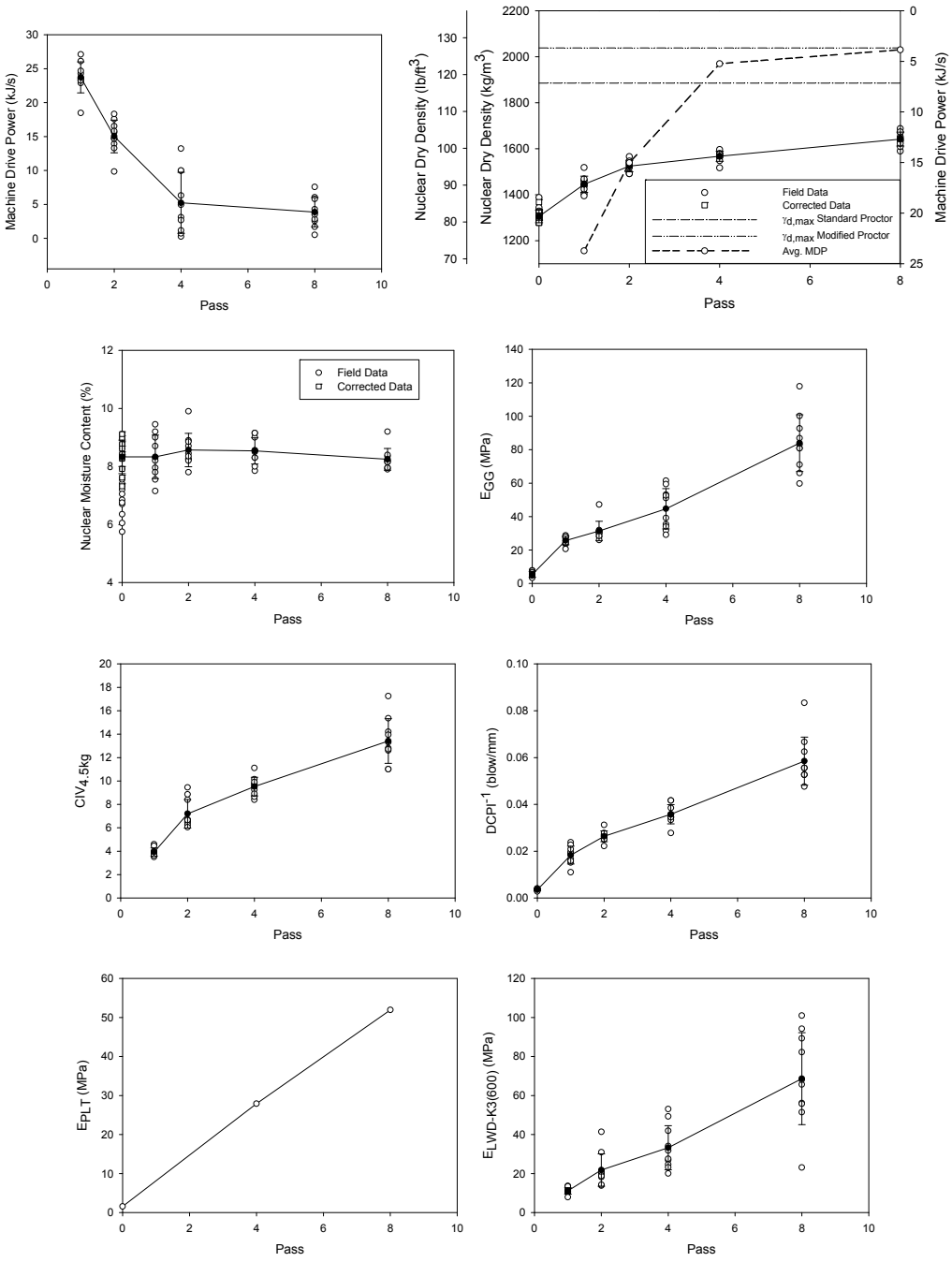


**Figure 174: CP533 Static Padfoot Edwards Till B (Soil 2001) - Strip 1 ($wc_{avg}$=8.4%)**

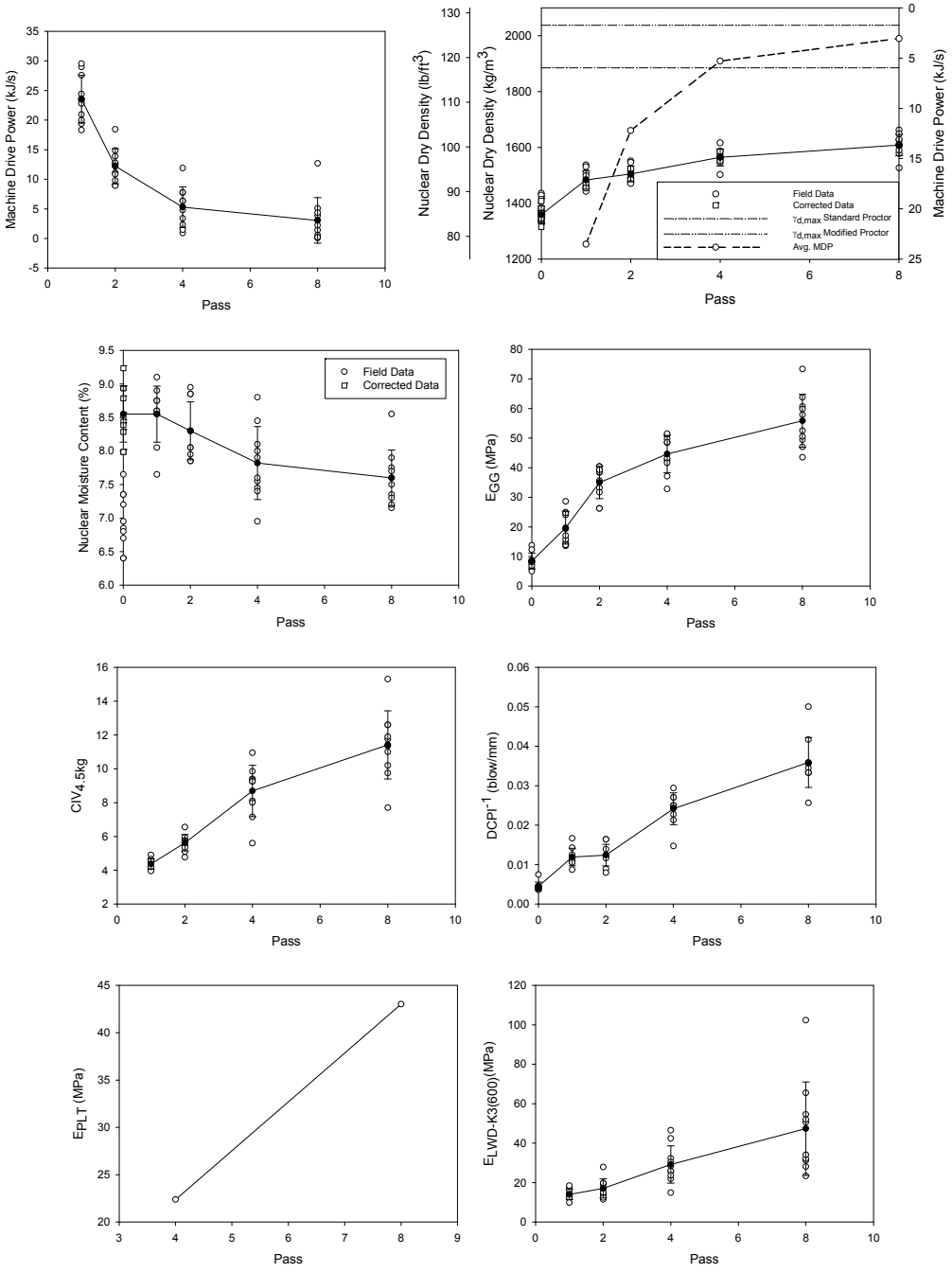


**Figure 175: CP533 Static Padfoot Edwards Till B (Soil 2001) - Strip 2 ($wc_{avg}$=8.2%)**

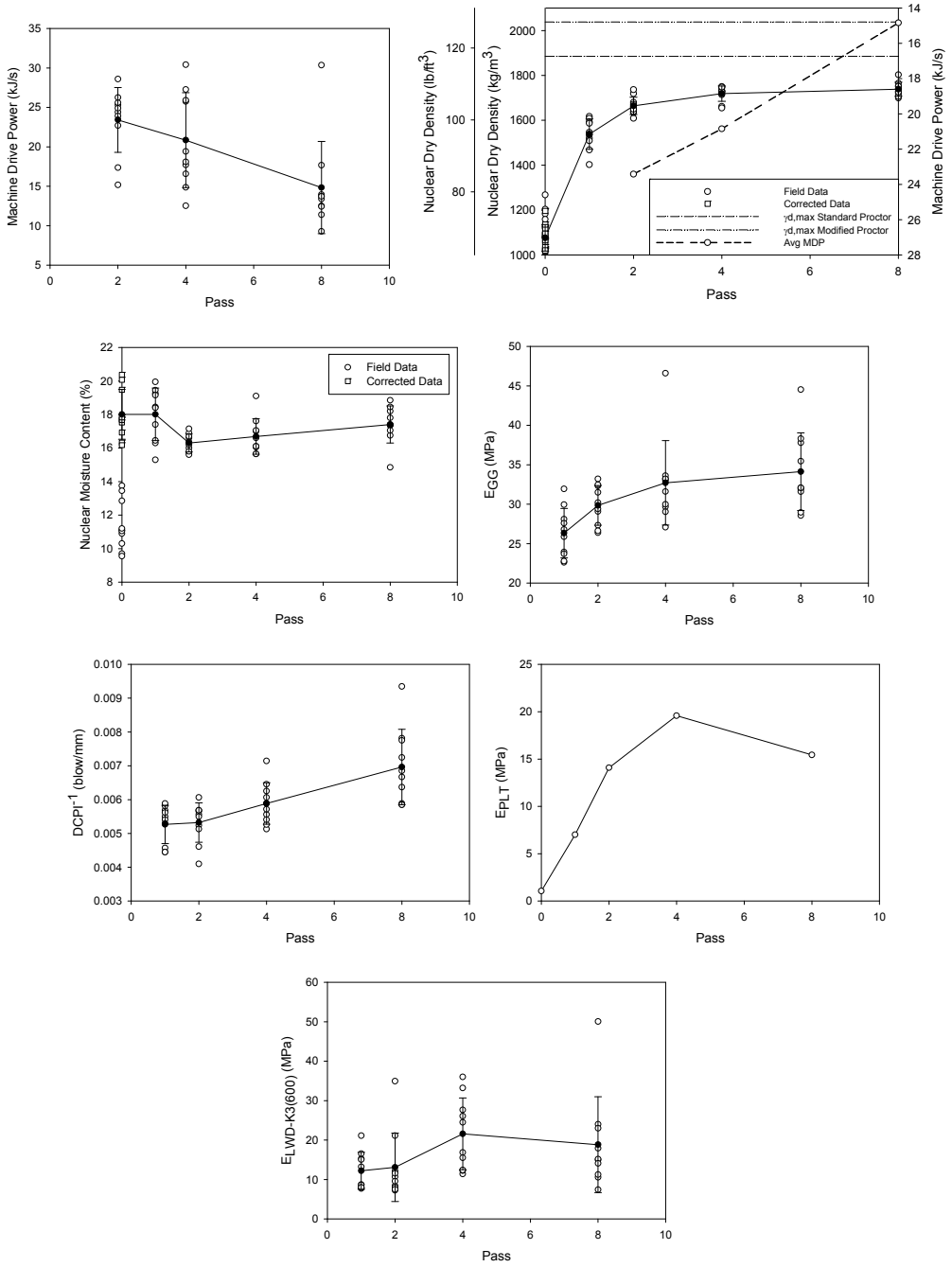


**Figure 176: CP533 Static Padfoot Edwards Till B (Soil 2001) - Strip 3 ($wc_{avg}$=17.3%)**

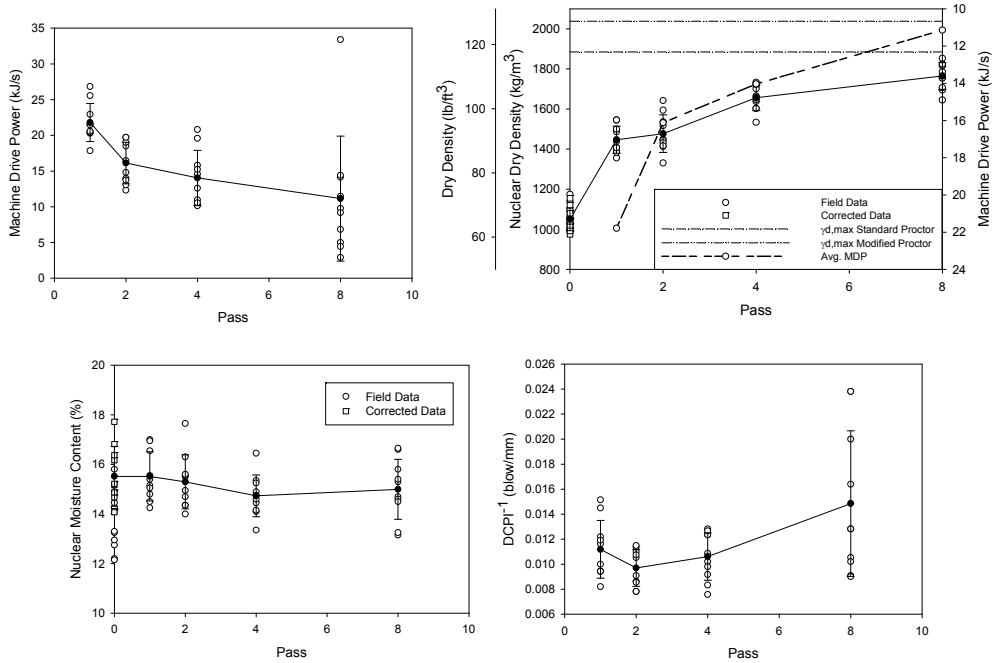


**Figure 177: CP533 Static Padfoot Edwards Till B (Soil 2001) - Strip 4 ($wc_{avg}$=15.2%)**

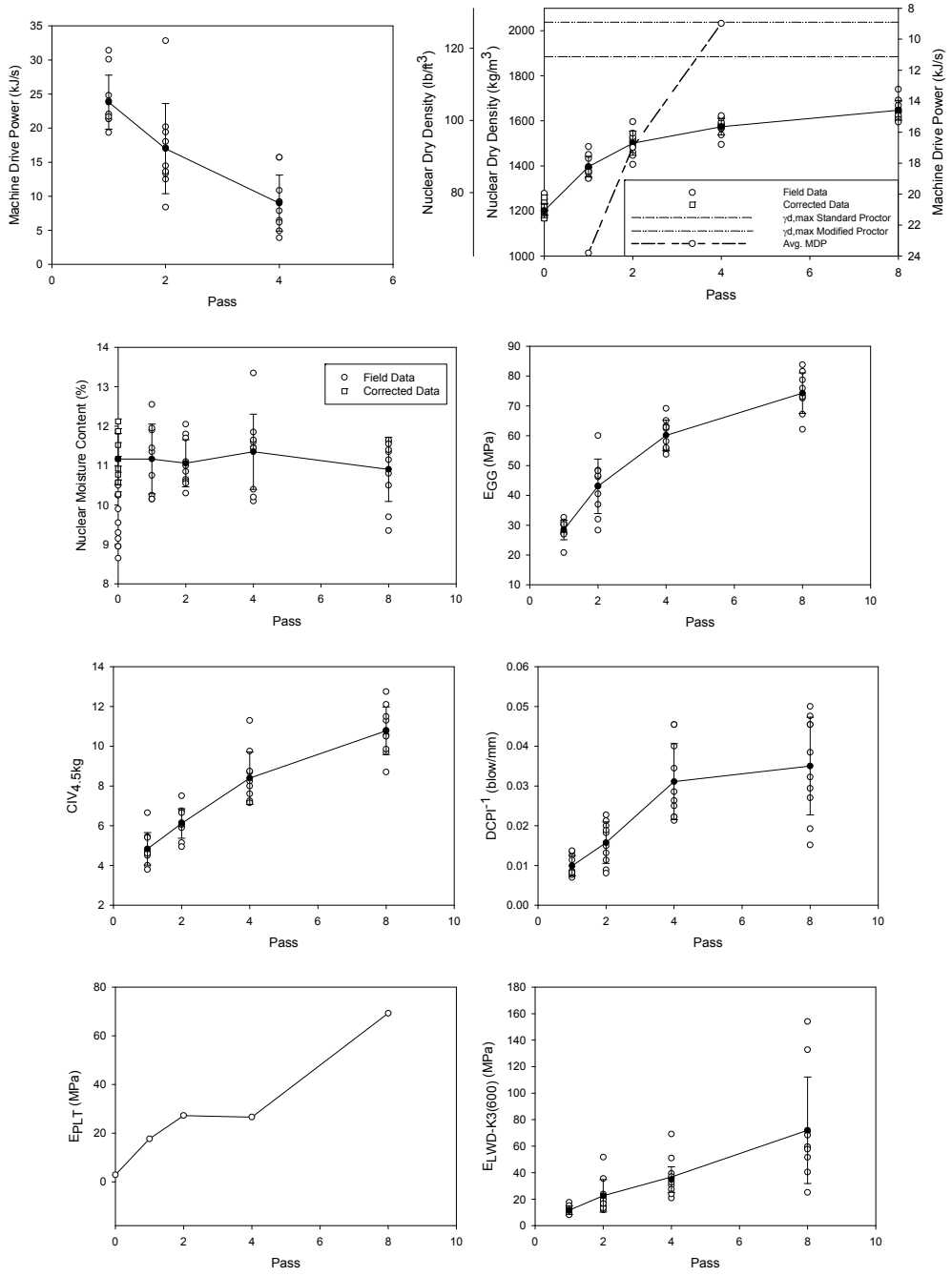


**Figure 178: CP533 Static Padfoot Edwards Till B (Soil 2001) - Strip 5 ($wc_{avg}$=11.1%)**

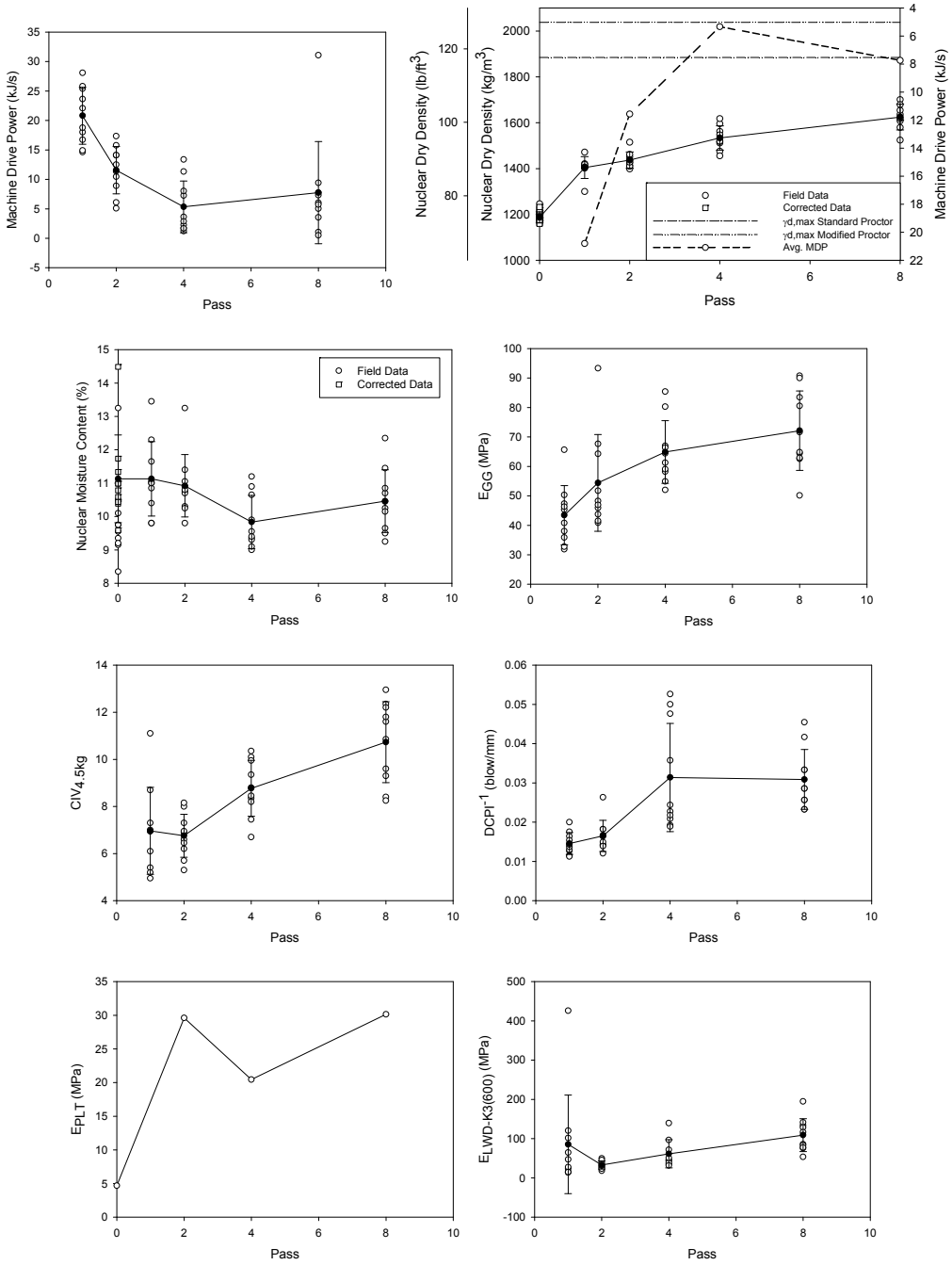


**Figure 179: CP533 Static Padfoot Edwards Till B (Soil 2001) - Strip 6 ($wc_{avg}$=10.7%)**

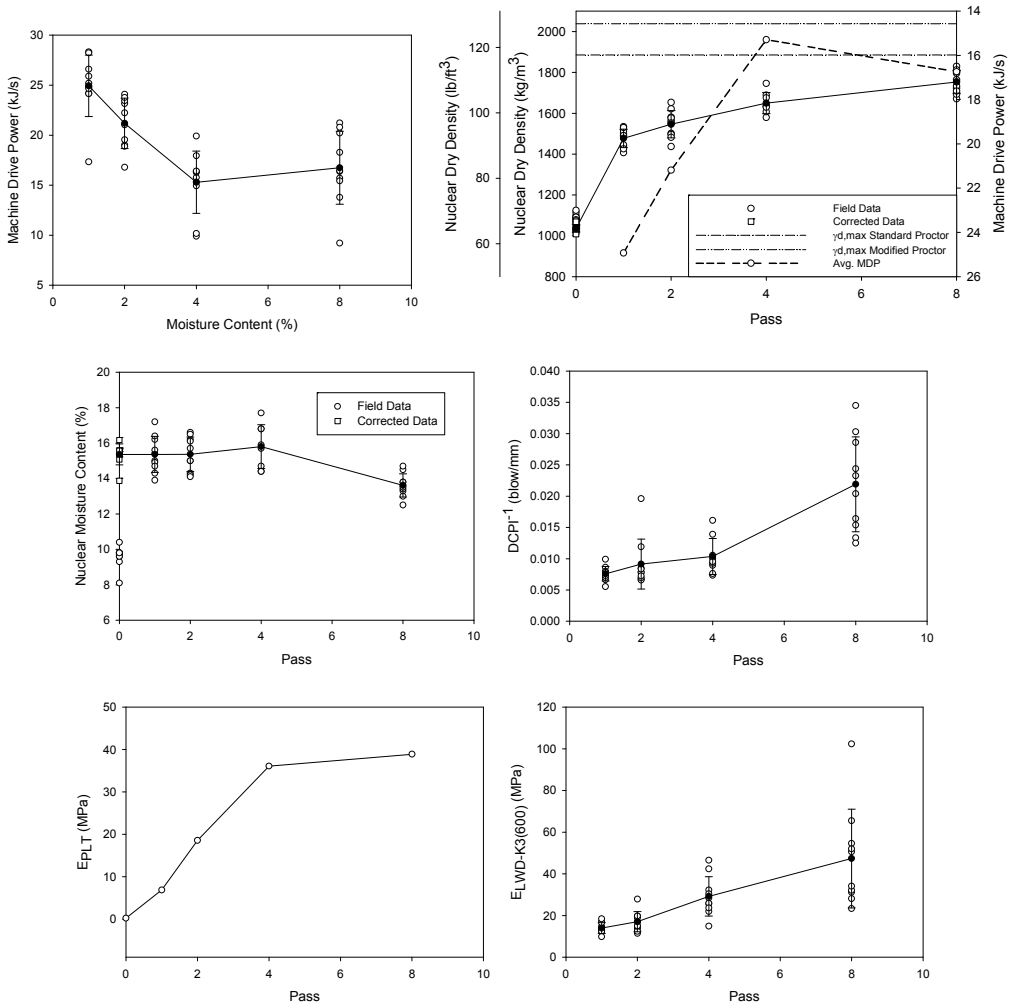


**Figure 180: CP533 Vibratory Padfoot Edwards Till B (Soil 2001) - Strip 1 ($wc_{avg}$=15.1%)**

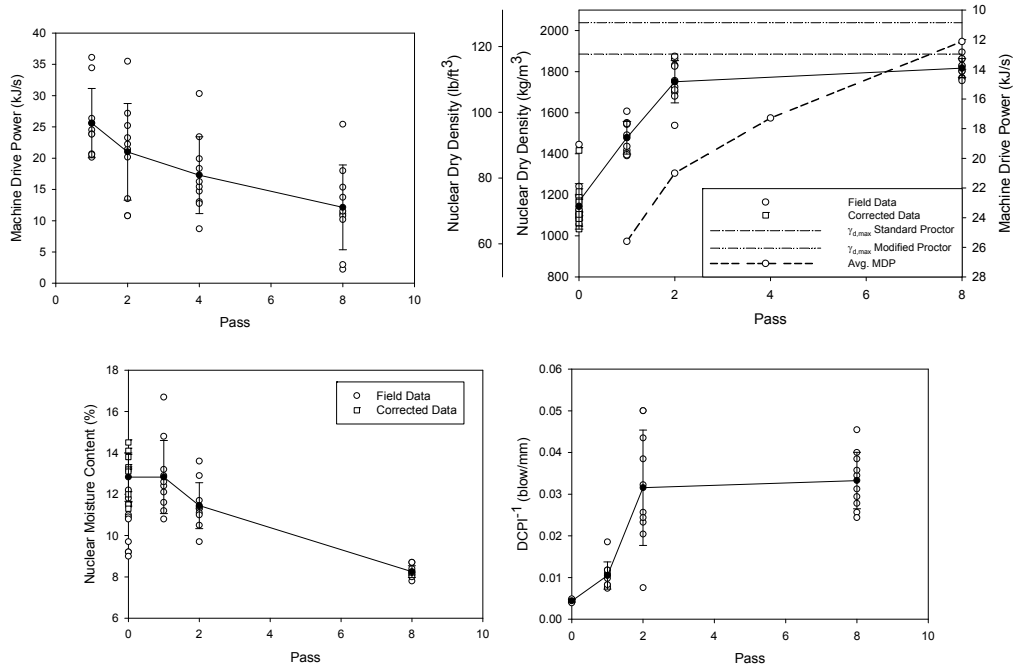


**Figure 181: CP 533 Vibratory Padfoot Edwards Till B (Soil 2001) - Strip 2 ($wc_{avg}$=11.3%)**

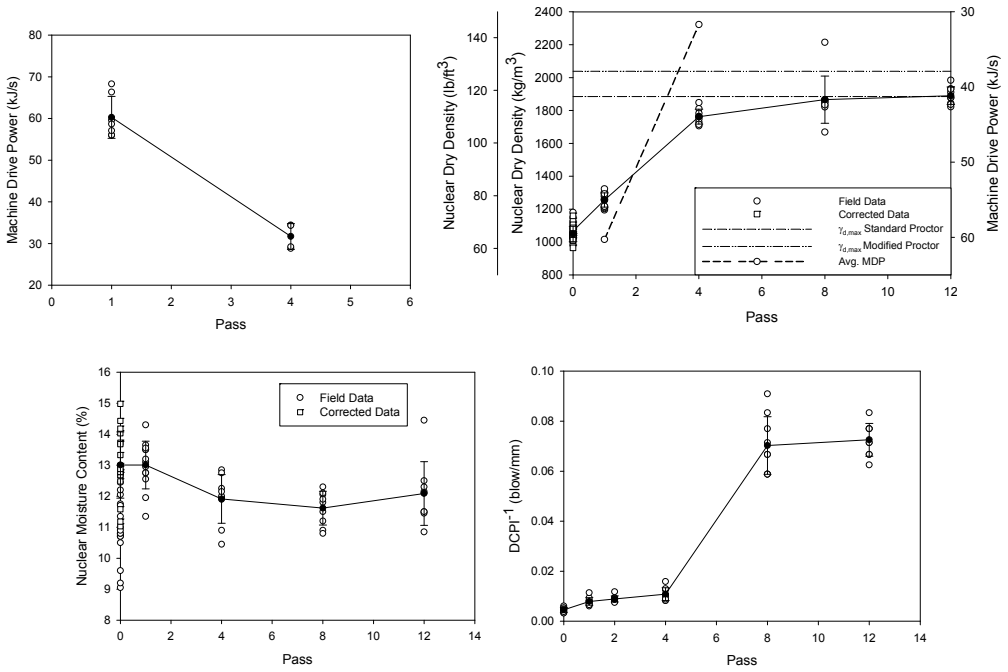


**Figure 182: CAT825 Static Padfoot Edwards Till B (Soil 2001) - Strip 1 ($wc_{avg}$=12.1%)**

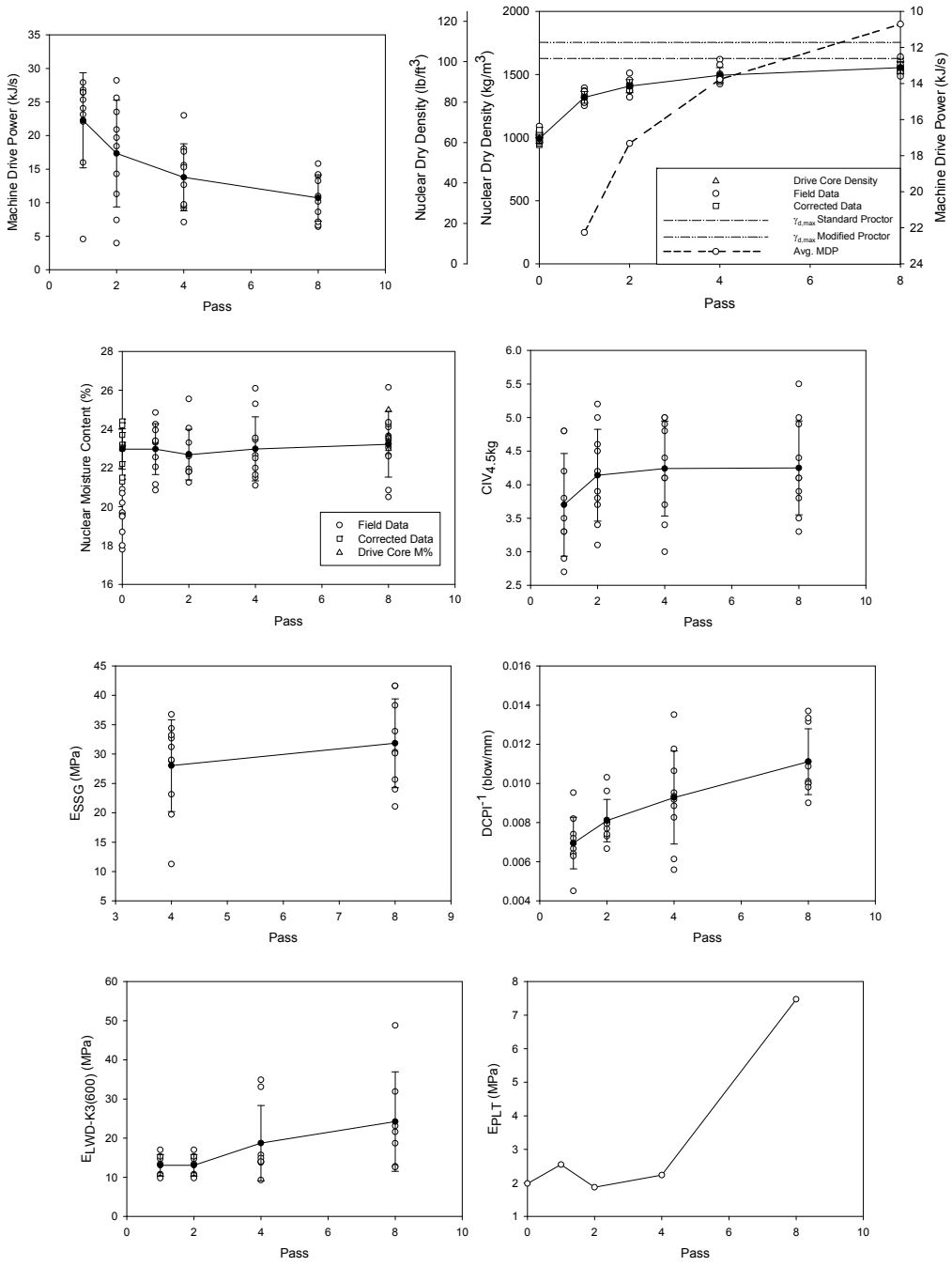


**Figure 183: CP533 Static Padfoot Kickapoo Topsoil (Soil 2003) - Strip 1 ($wc_{avg}$=23.0%**

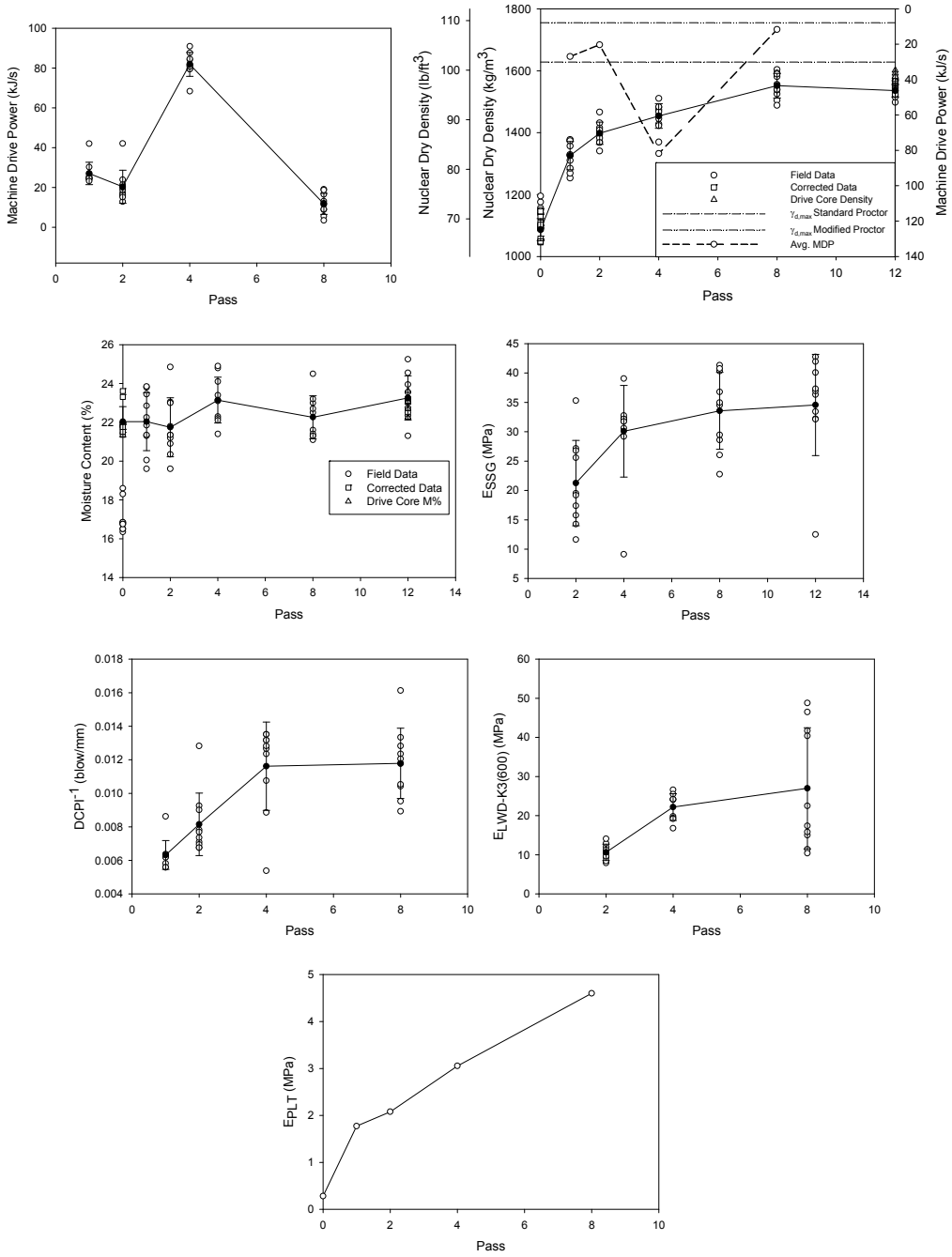


**Figure 184: CP533 Static Padfoot Kickapoo Topsoil (Soil 2003) - Strip 2 ($wc_{avg}$=22.4%)**

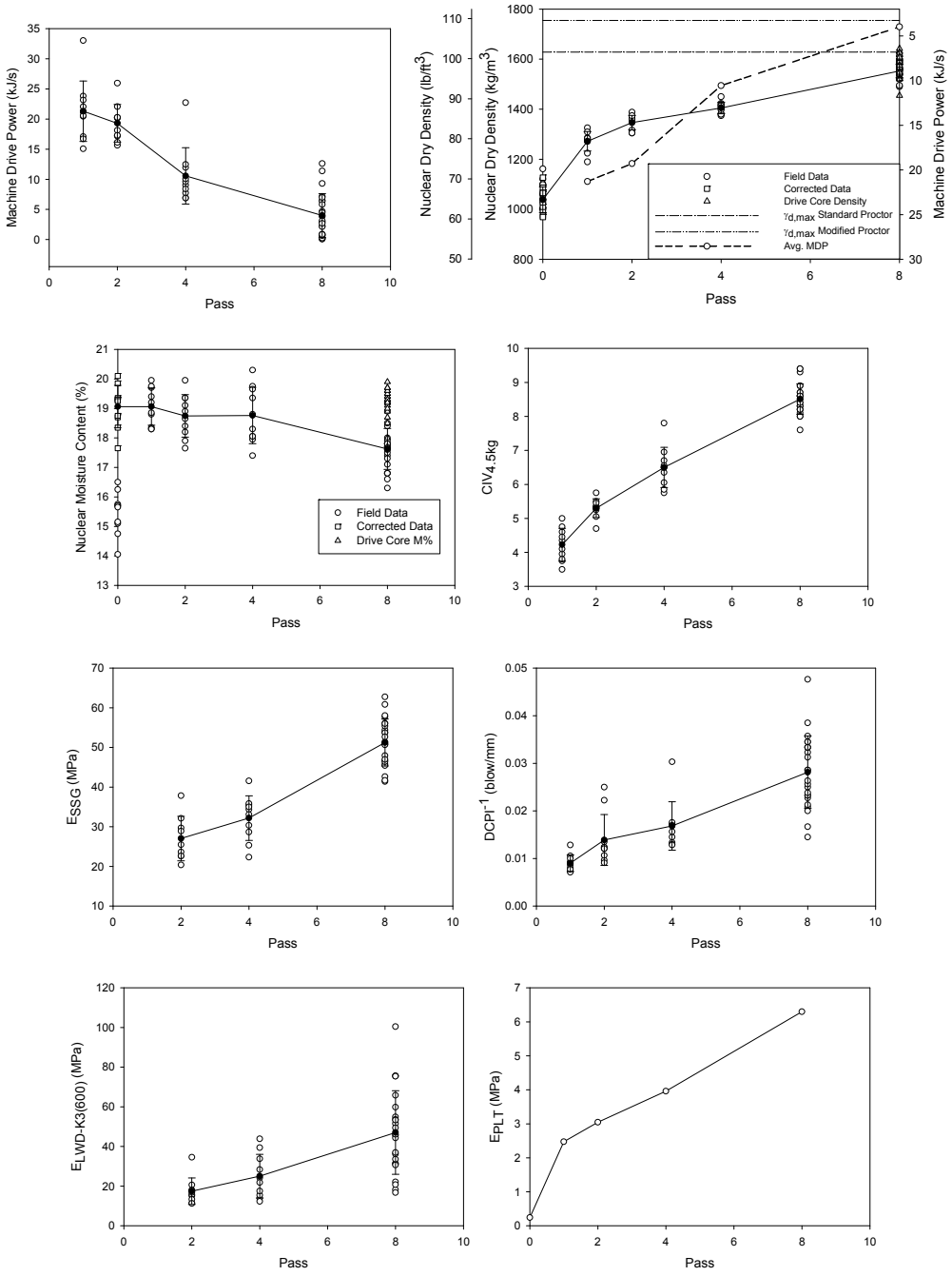


**Figure 185: CP533 Static Padfoot Kickapoo Topsoil (Soil 2003) - Strip 3 ($wc_{avg}$=18.4%)**

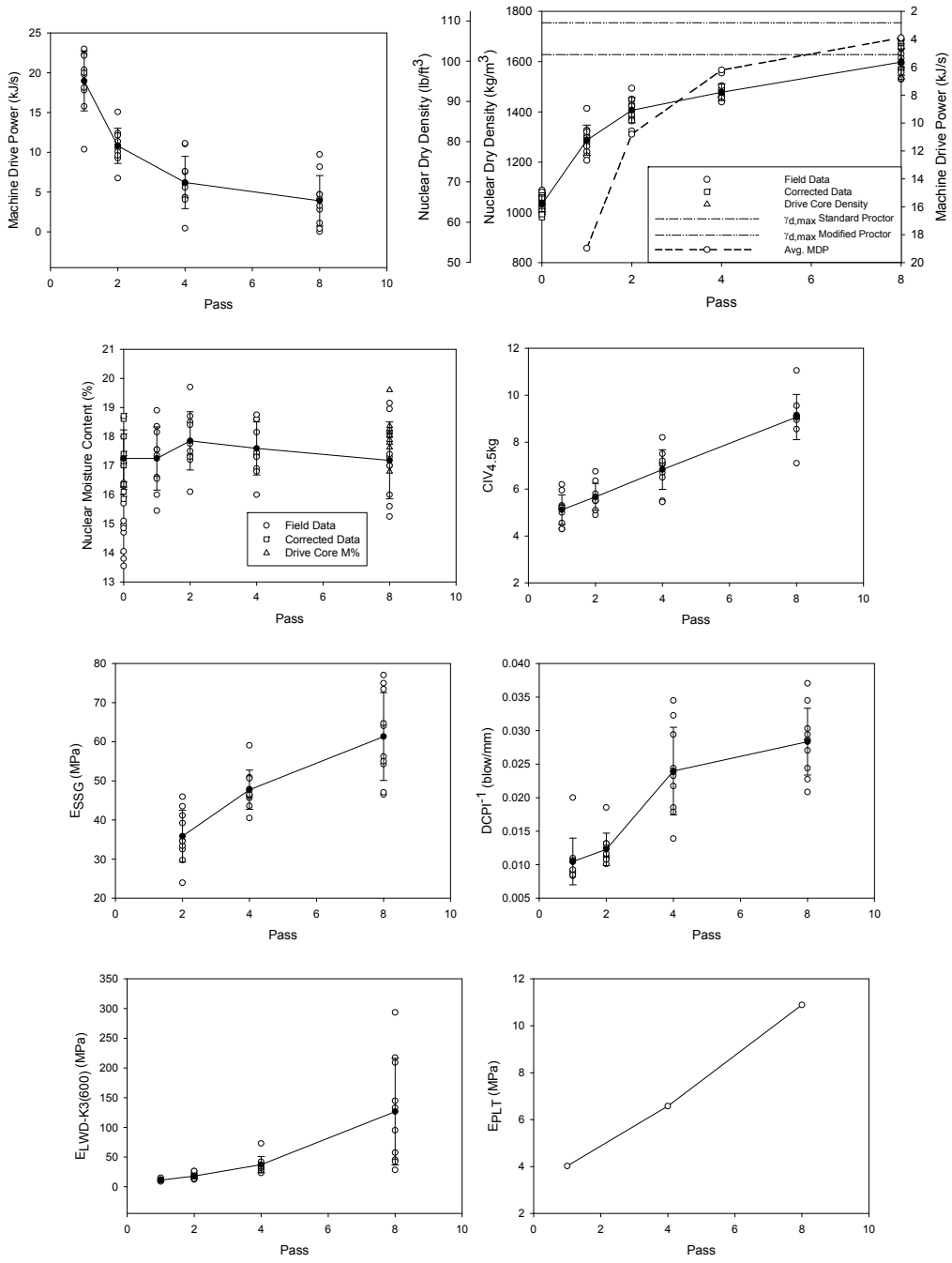


**Figure 186: CP533 Static Padfoot Kickapoo Topsoil (Soil 2003) - Strip 4 ($wc_{avg}$=17.4%)**

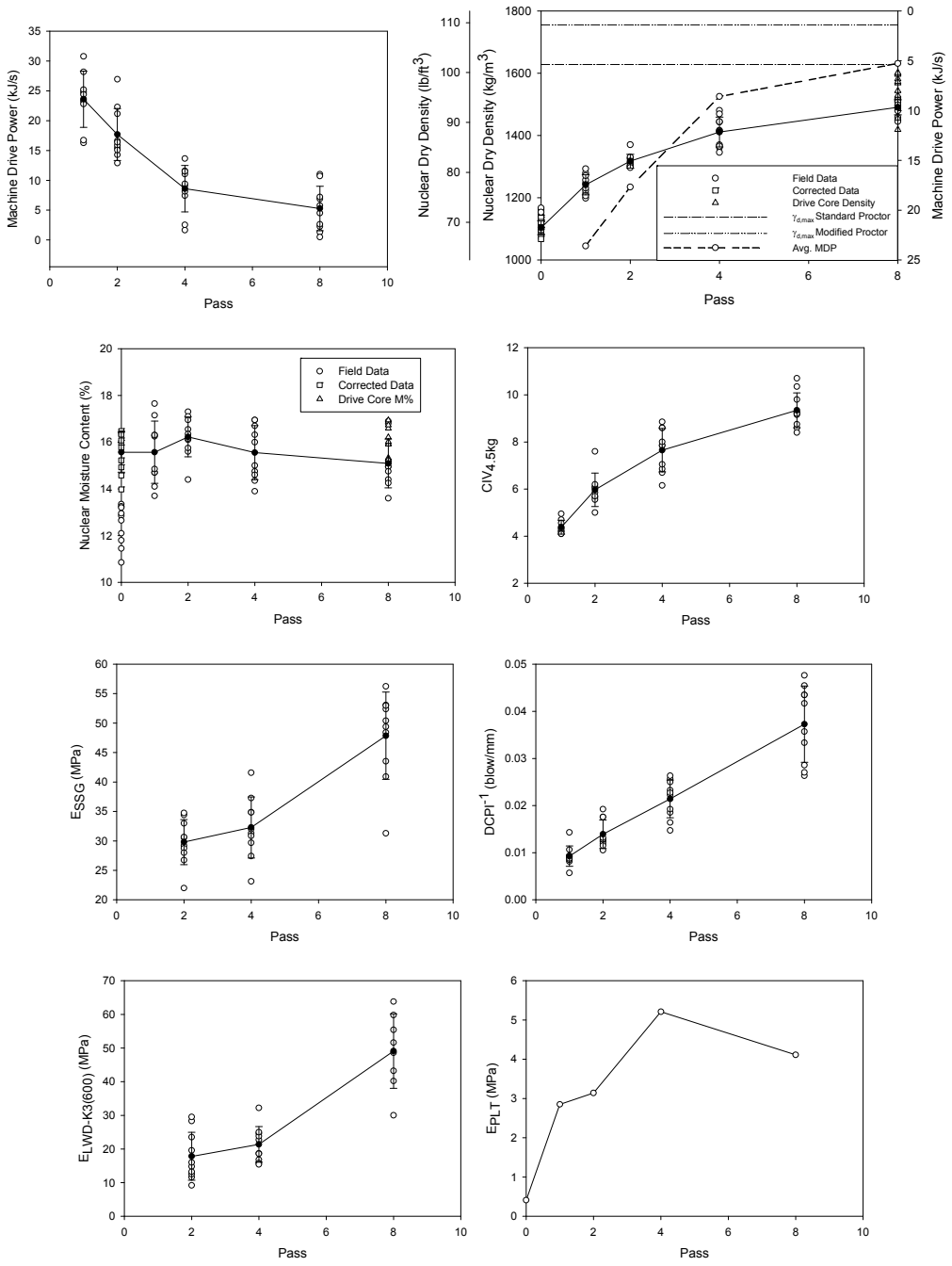


**Figure 187: CP533 Static Padfoot Kickapoo Topsoil (Soil 2003) - Strip 5 ($wc_{avg}$=15.6%)**

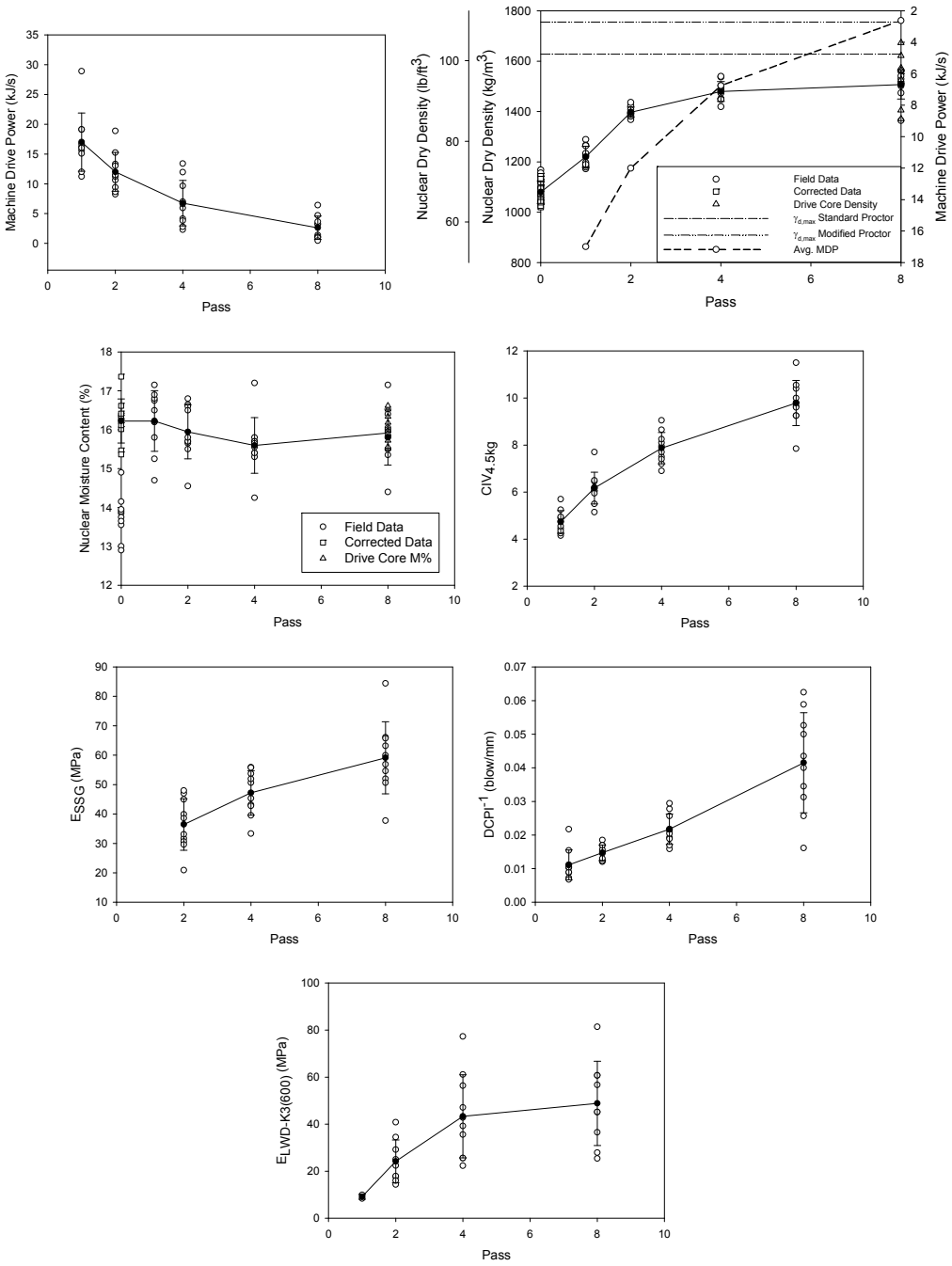


**Figure 188: CP533 Static Padfoot Kickapoo Topsoil (Soil 2003) - Strip 6 ($wc_{avg}$=16.0%)**

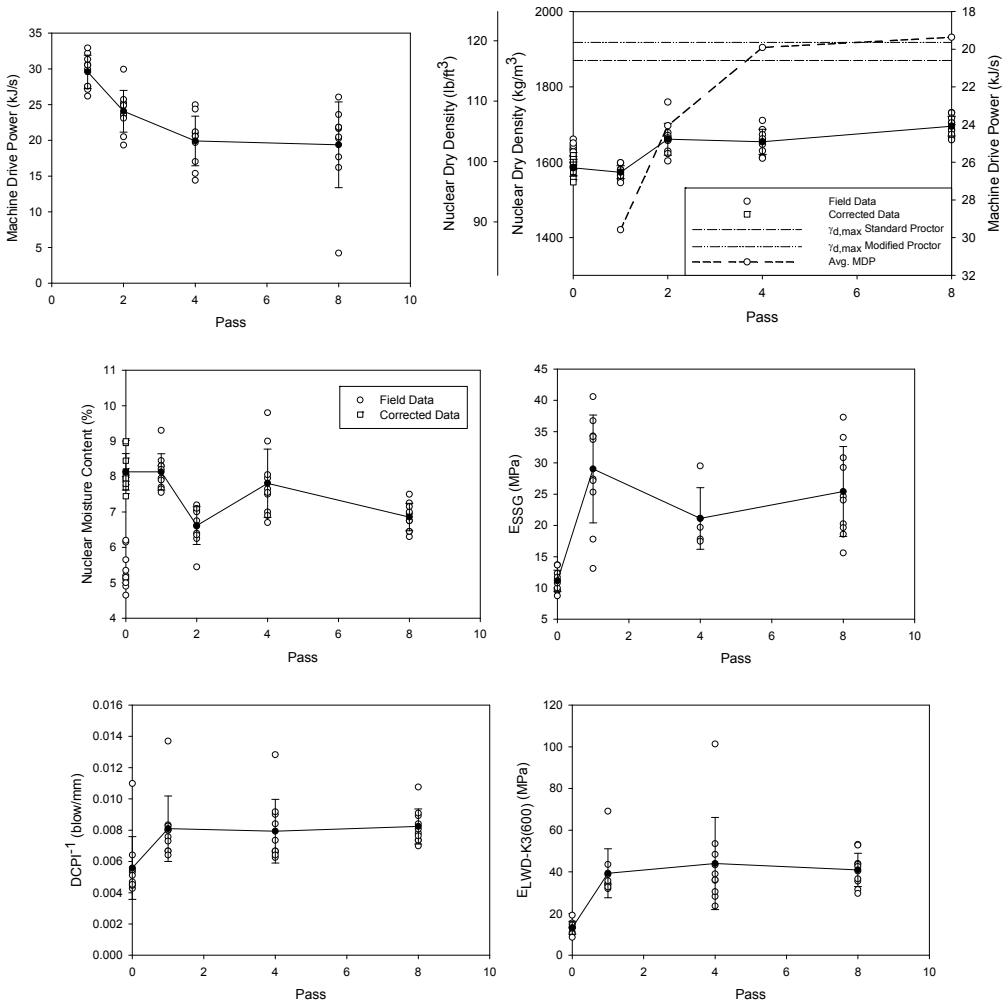


**Figure 189: CP533 Static Padfoot Kickapoo Sand (Soil 2005) - Strip 1 ($wc_{avg}$=7.5%)**

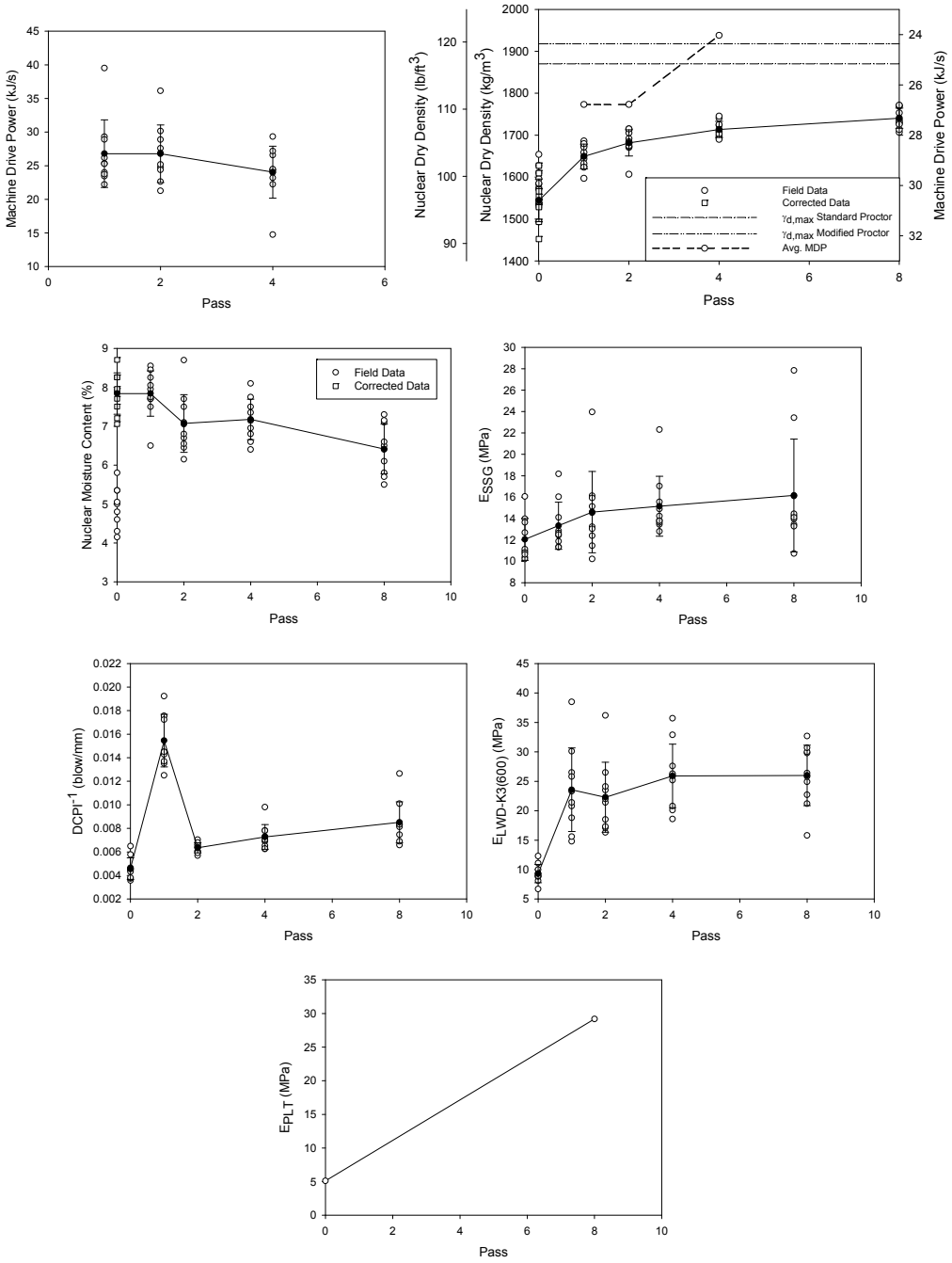


**Figure 190: CP533 Static Padfoot Kickapoo Sand (Soil 2005) - Strip 2 ($wc_{avg}$=7.3%)**

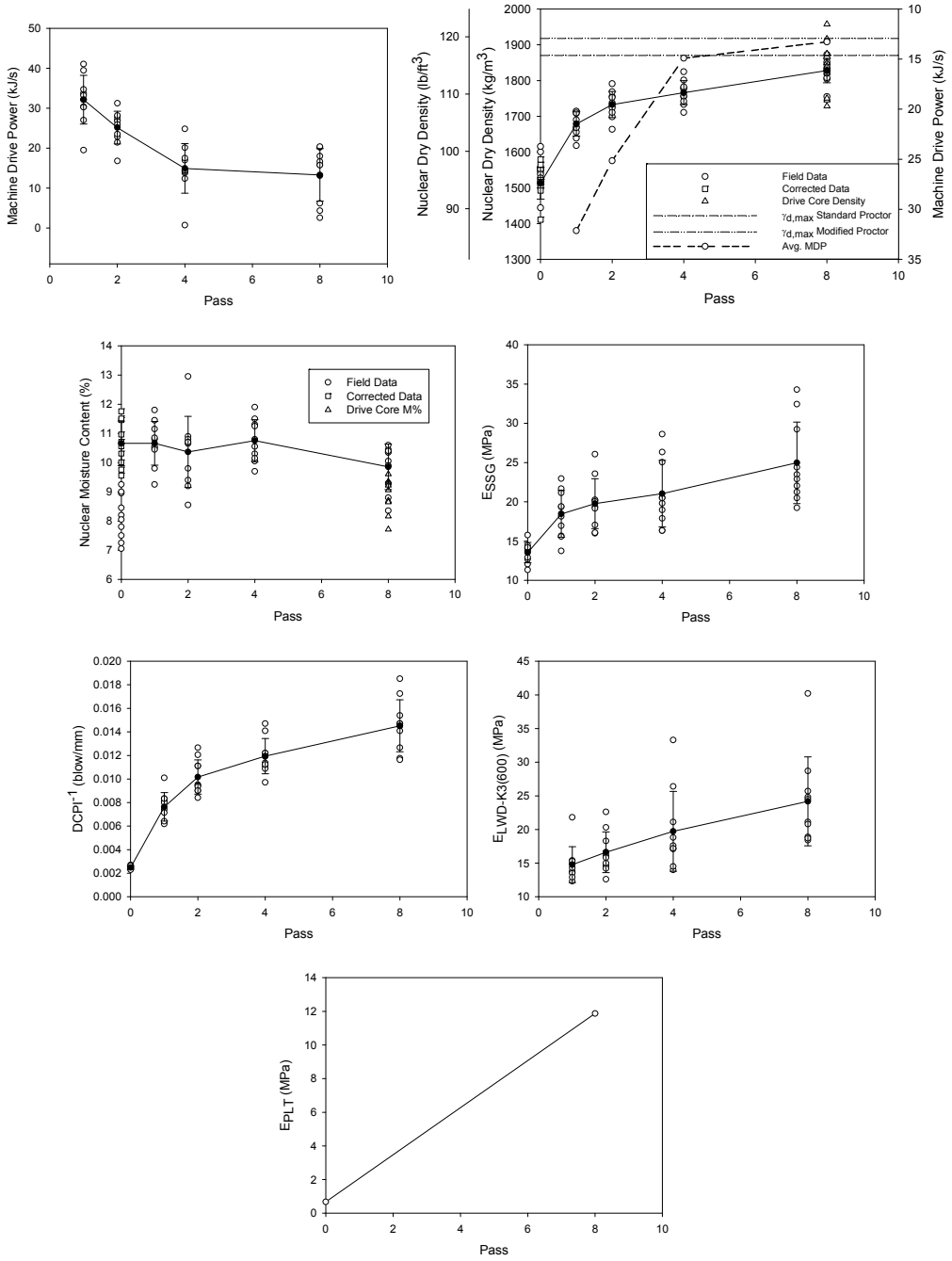


**Figure 191: CP533 Static Padfoot Kickapoo Sand (Soil 2005) - Strip 3 ($wc_{avg}$=10.5%)**

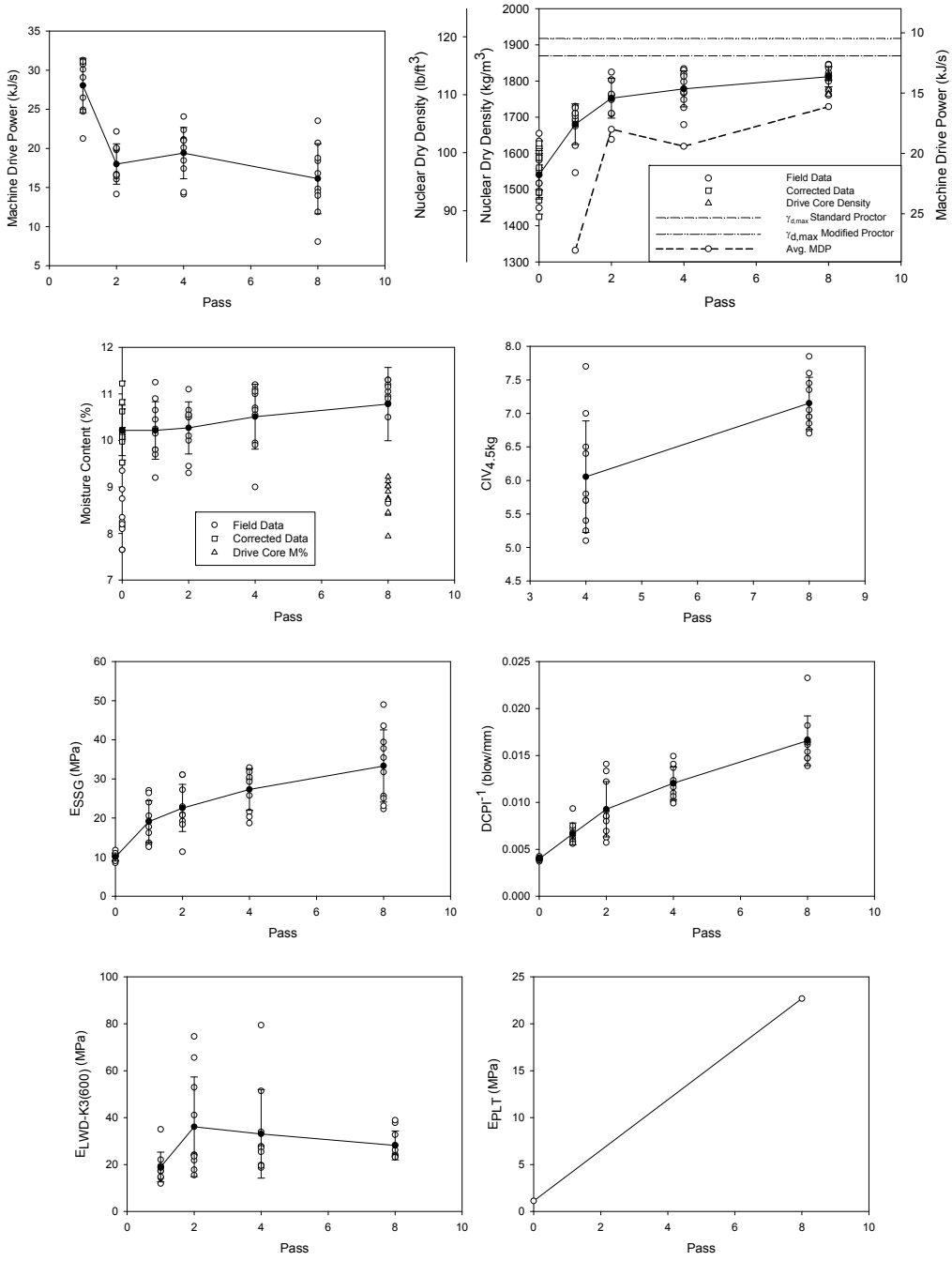


**Figure 192: CP533 Static Padfoot Kickapoo Sand (Soil 2005) - Strip 4 ($wc_{avg}$=10.4%)**

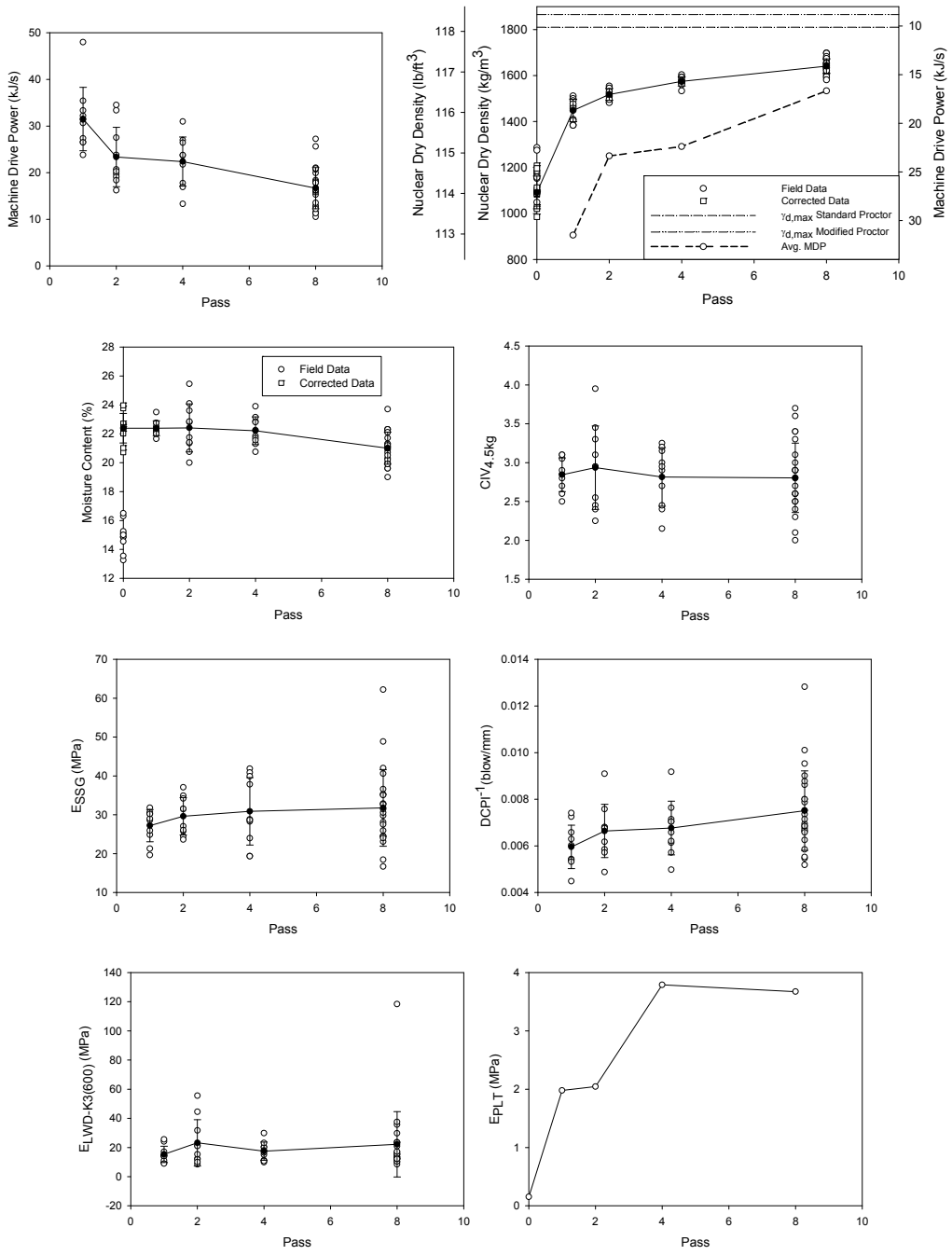


**Figure 193: CP533 Static Padfoot Kickapoo Fill Clay (Soil 2004) - Strip 1 ($wc_{avg}$=21.7%)**

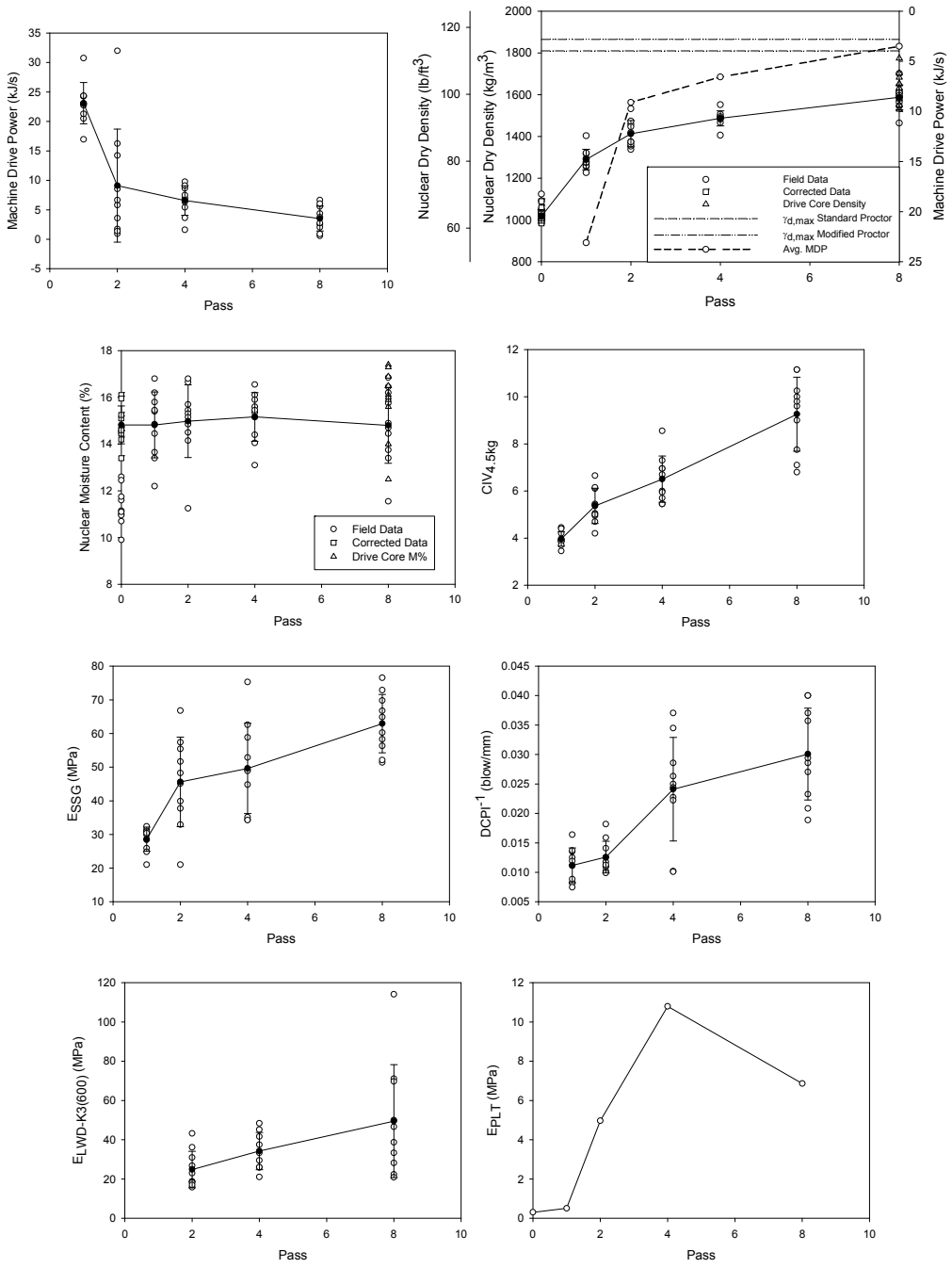


**Figure 194: CP533 Static Padfoot Kickapoo Fill Clay (Soil 2004) - Strip 2 ($wc_{avg}$=14.9%)**

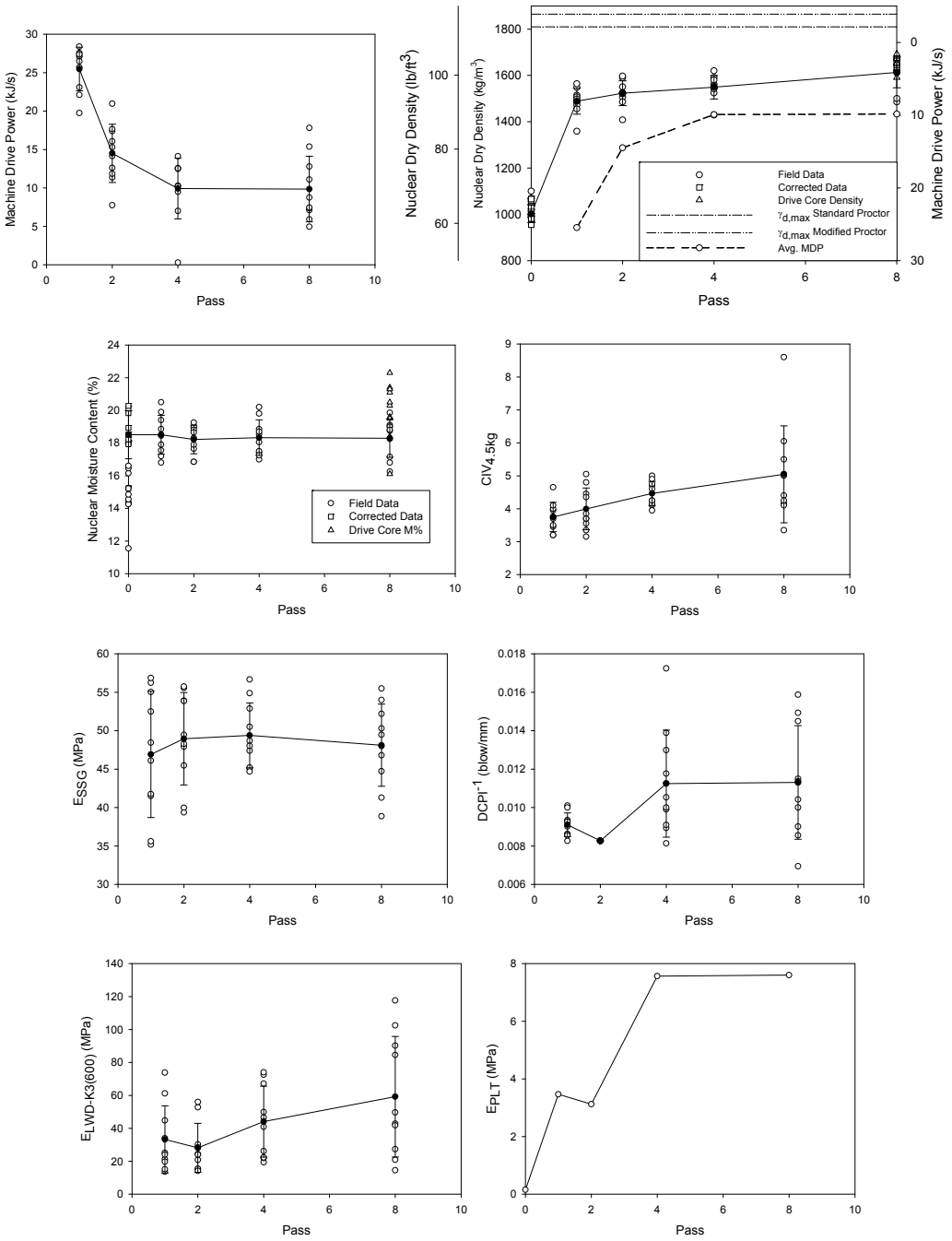


**Figure 195: CP533 Static Padfoot Kickapoo Fill Clay (Soil 2004) - Strip 3 ($wc_{avg}$=18.4%)**

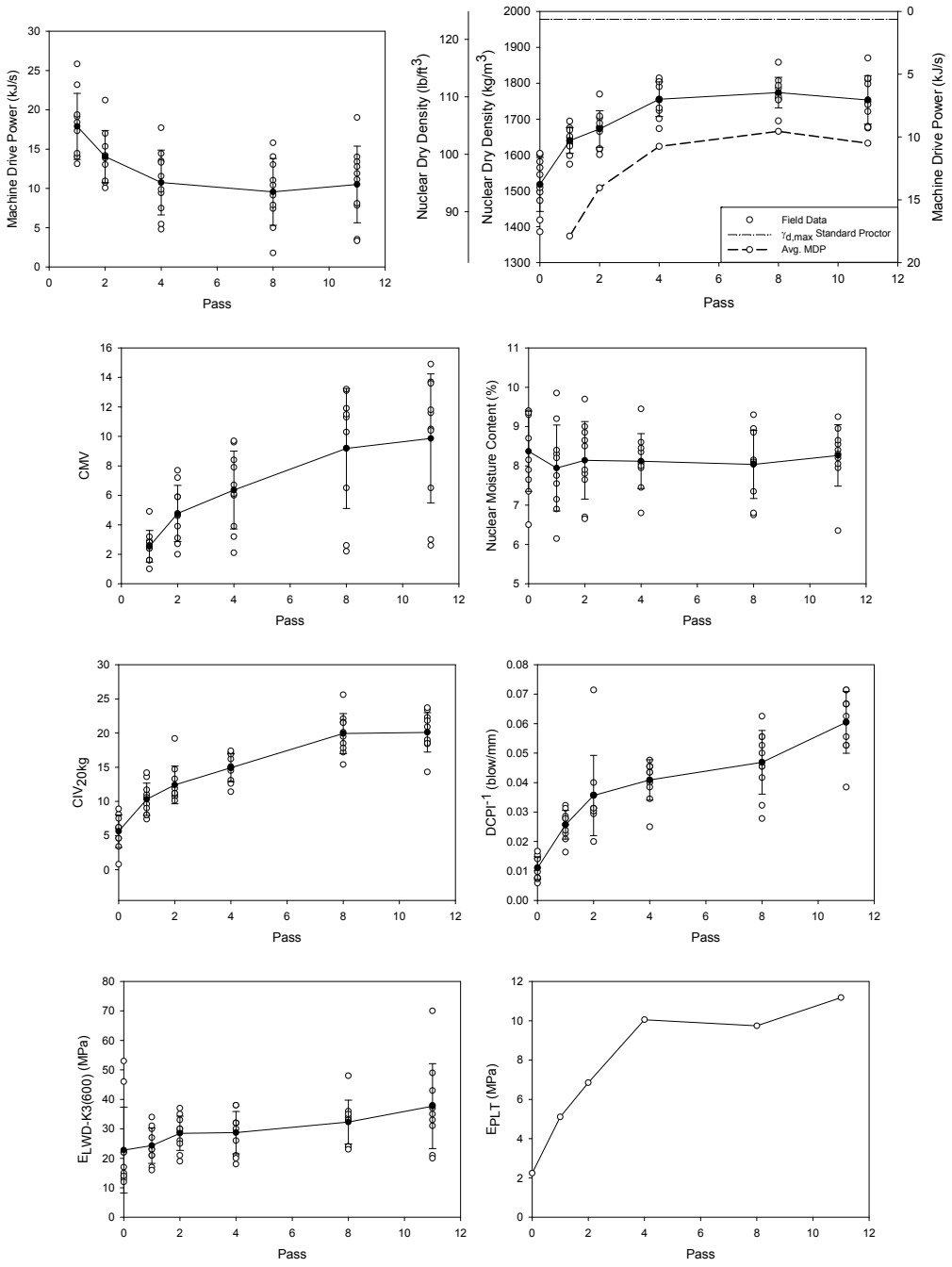


**Figure 196: CS533 Vibratory Smooth Drum RAP (Soil 2006) ($wc_{avg}$=8.1%)**

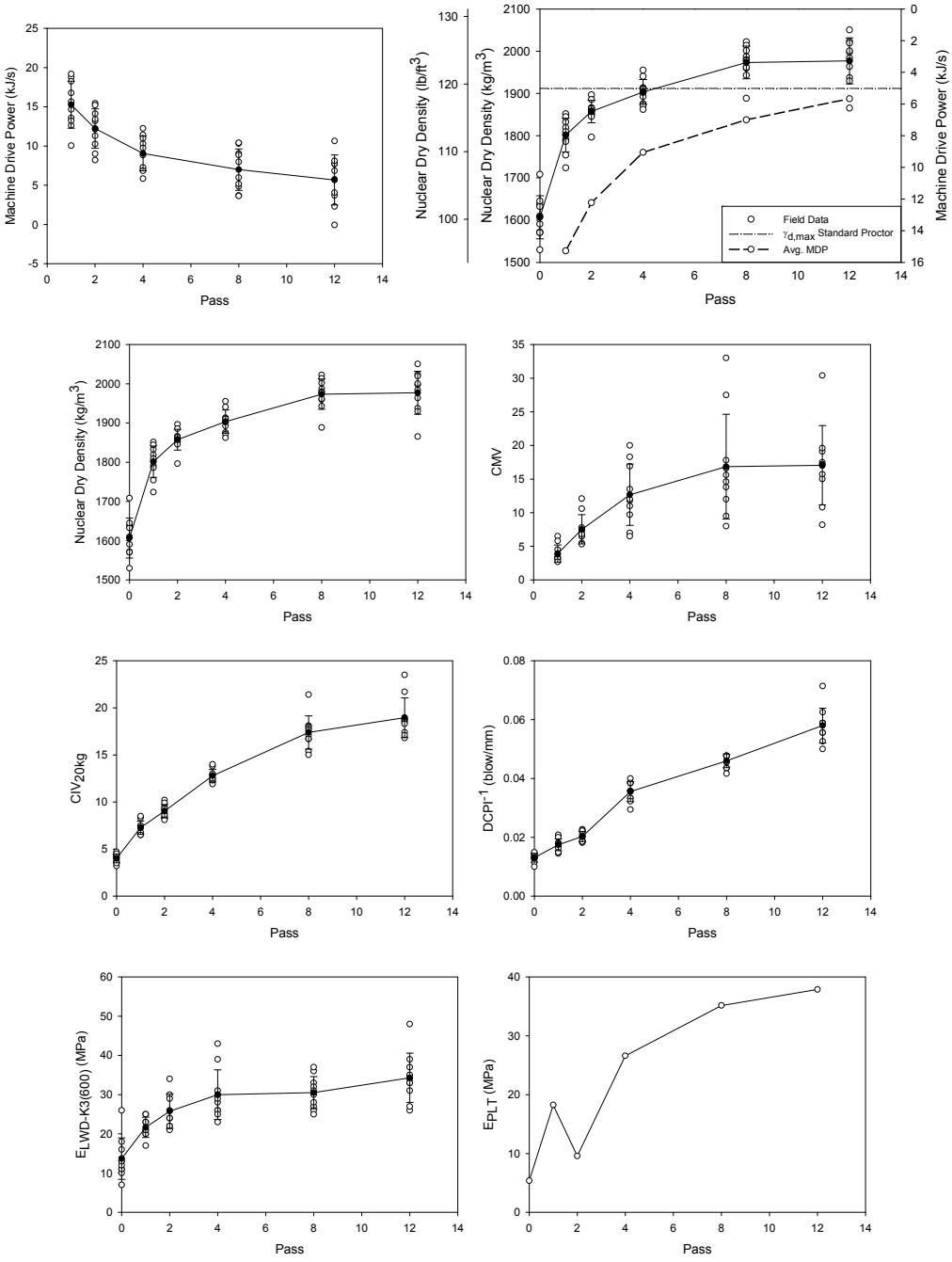


**Figure 197: CS533 Vibratory Smooth Drum CA6-C (Soil 2007)**

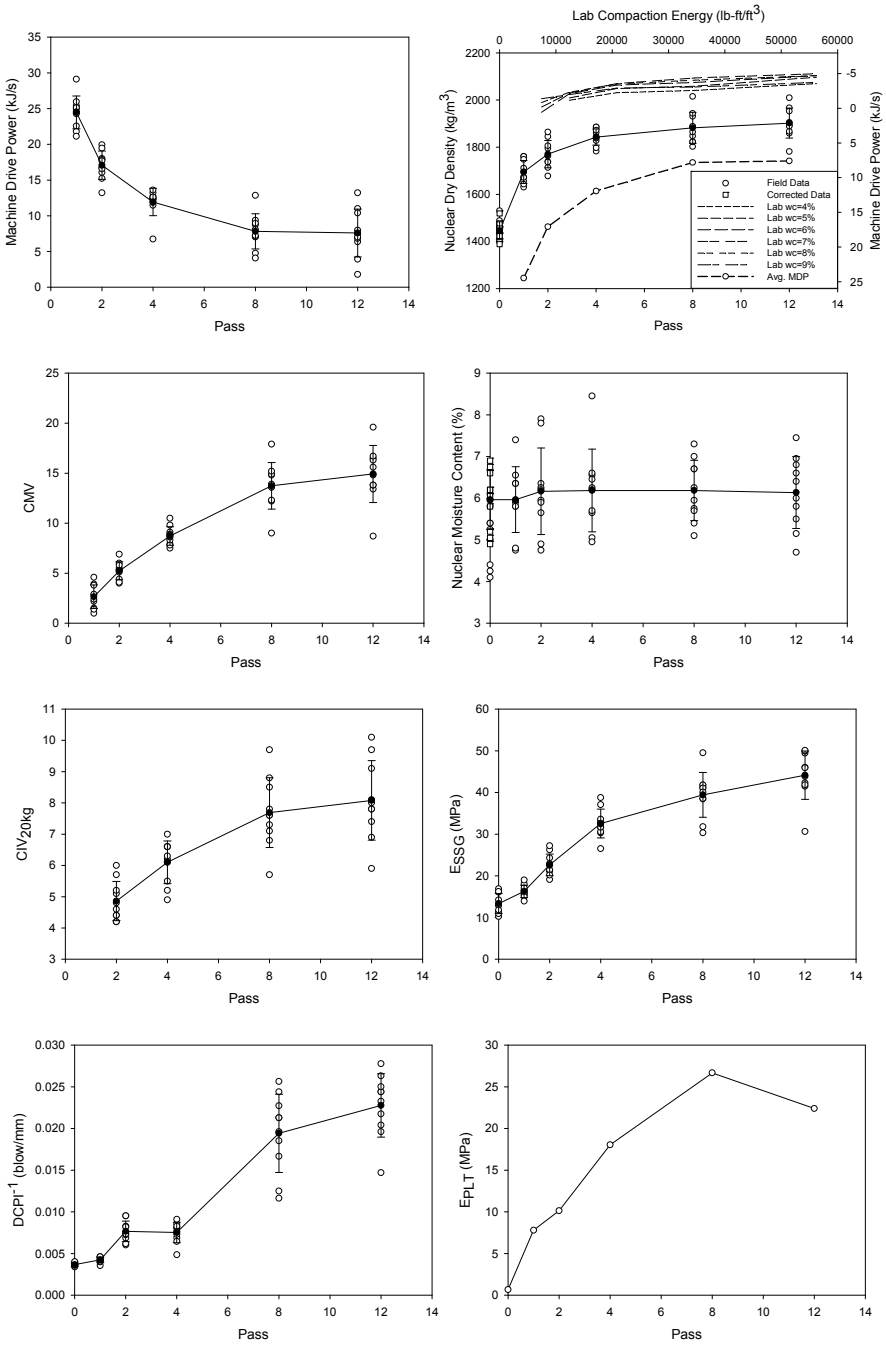


**Figure 198: CS533 Vibratory Smooth Drum FA6 (Soil 2008) ($wc_{avg}$=6.1%)**

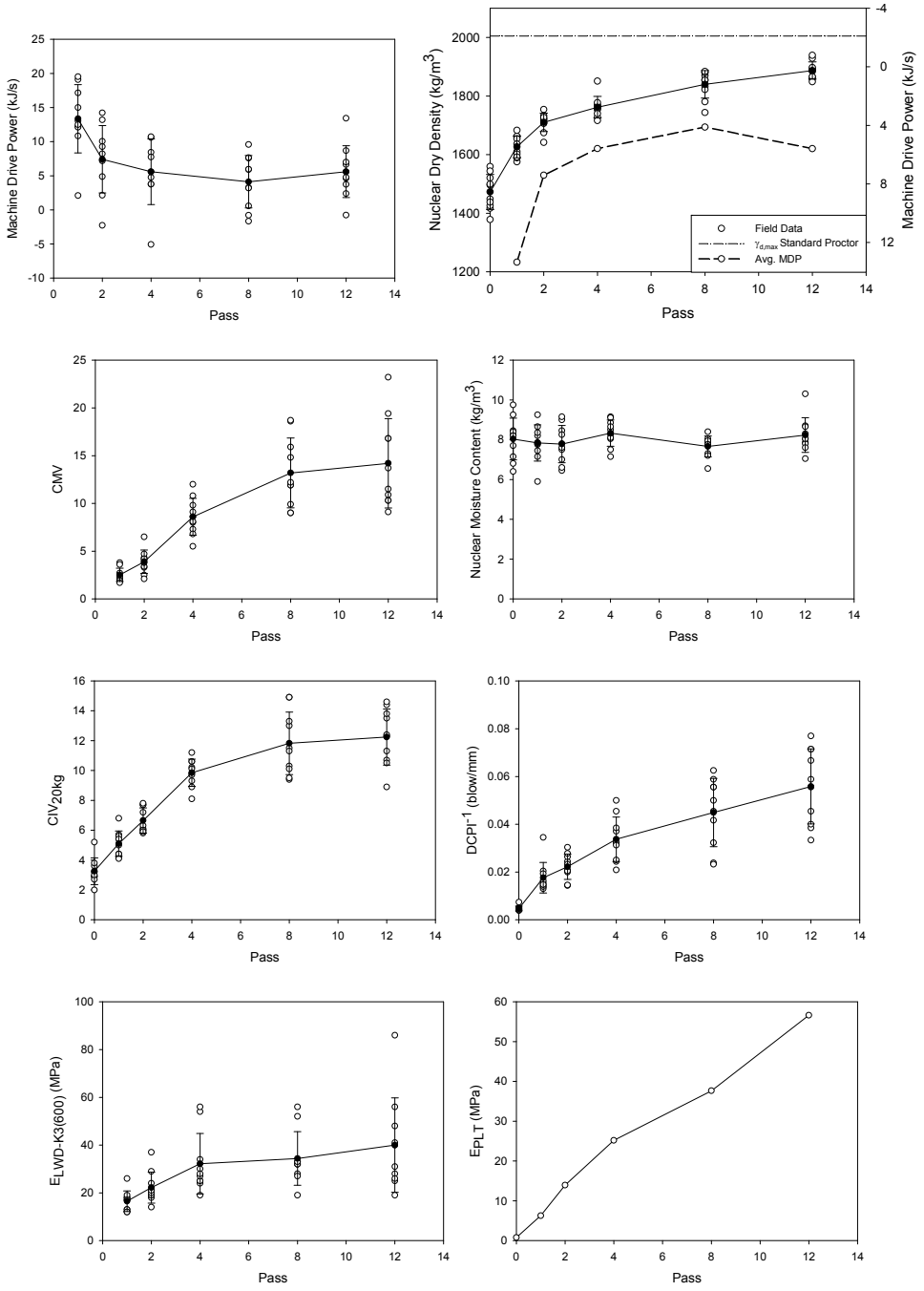


**Figure 199: CS533 Vibratory Smooth Drum CA6-G (Soil 2009) ($wc_{ave}$=8.0%)**

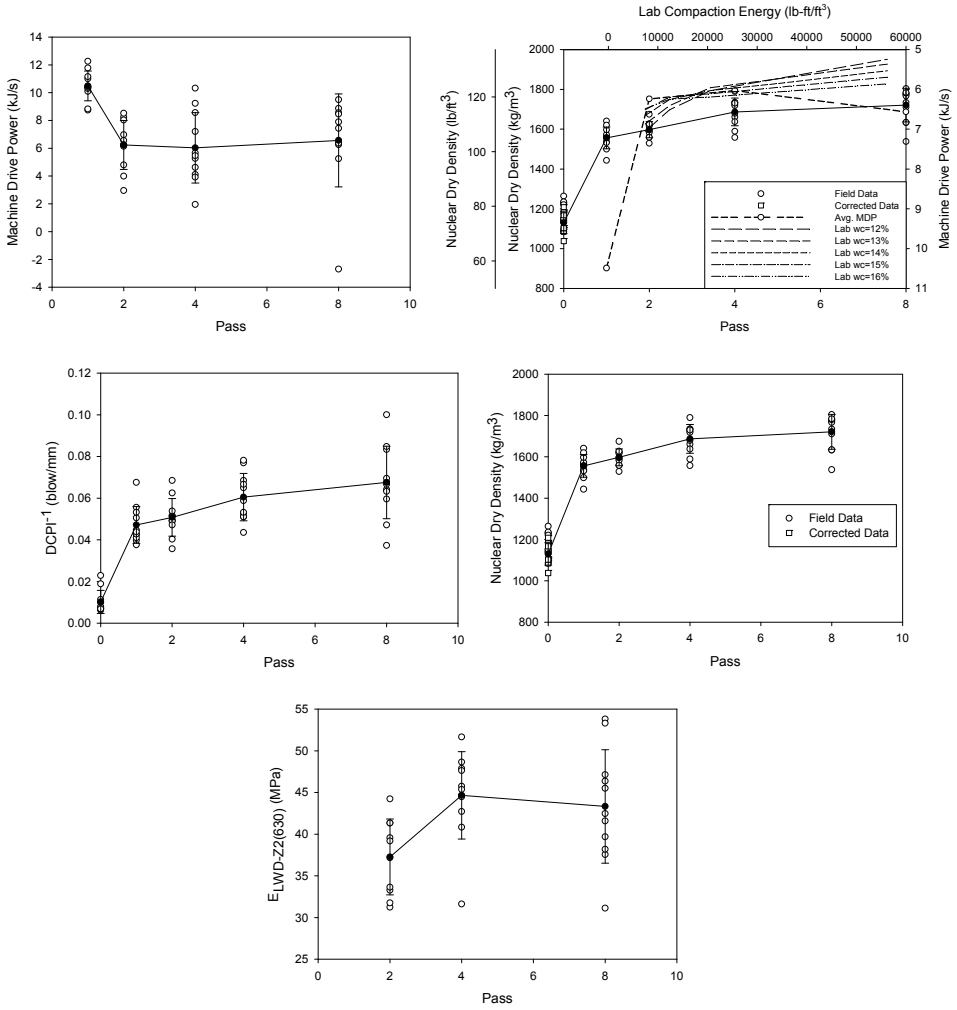


**Figure 200: CP533 Vibratory Smooth Drum MnRoad Glacial Till (Soil 2010) - Test Bed 5 ($wc_{avg}$=15.5%)**

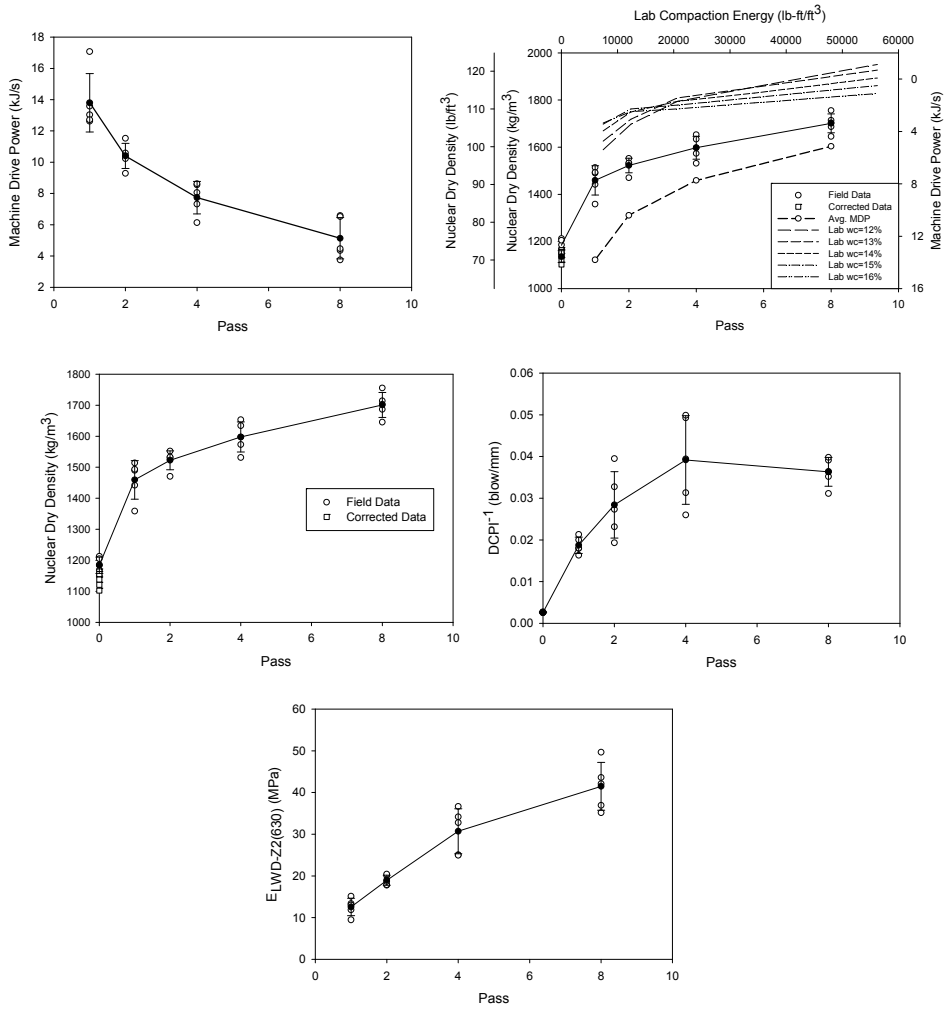


**Figure 201: CP533 Vibratory Padfoot MnRoad Glacial Till (Soil 2010) - Test Bed 7(1) ($wc_{avg}$=14.1%)**

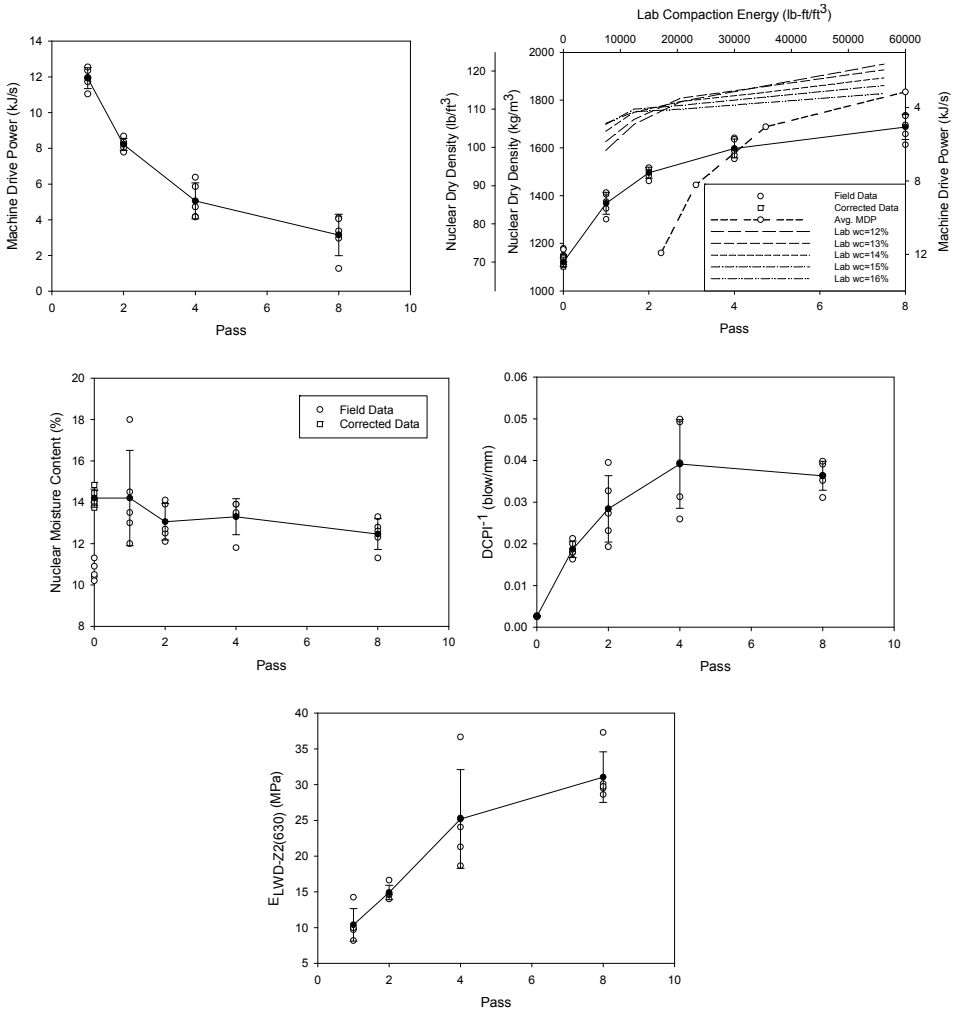


**Figure 202: CP533 Vibratory Padfoot MnRoad Glacial Till (Soil 2010) - Test Bed 7(2) ($wc_{avg}$=13.4%)**

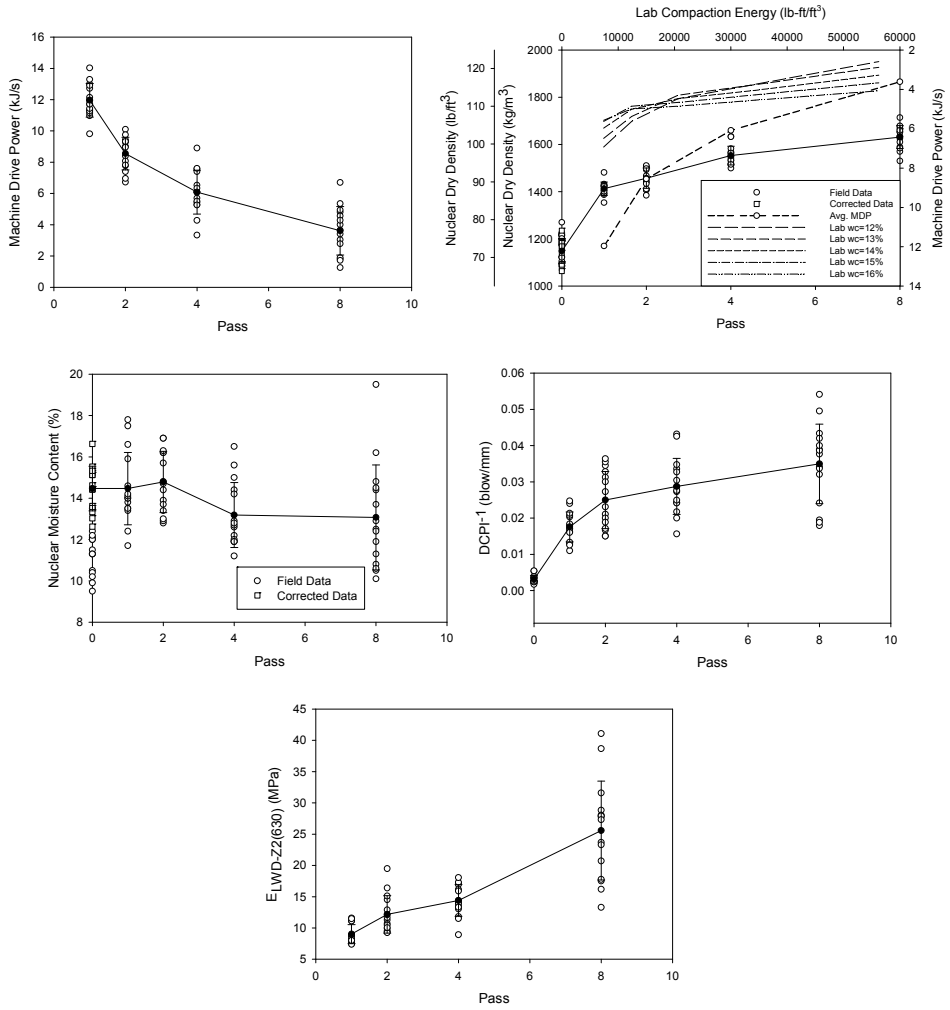


**Figure 203: CP533 Vibratory Padfoot MnRoad Glacial Till (Soil 2010) - Test Bed 11 ($wc_{avg}$=14.0%)**

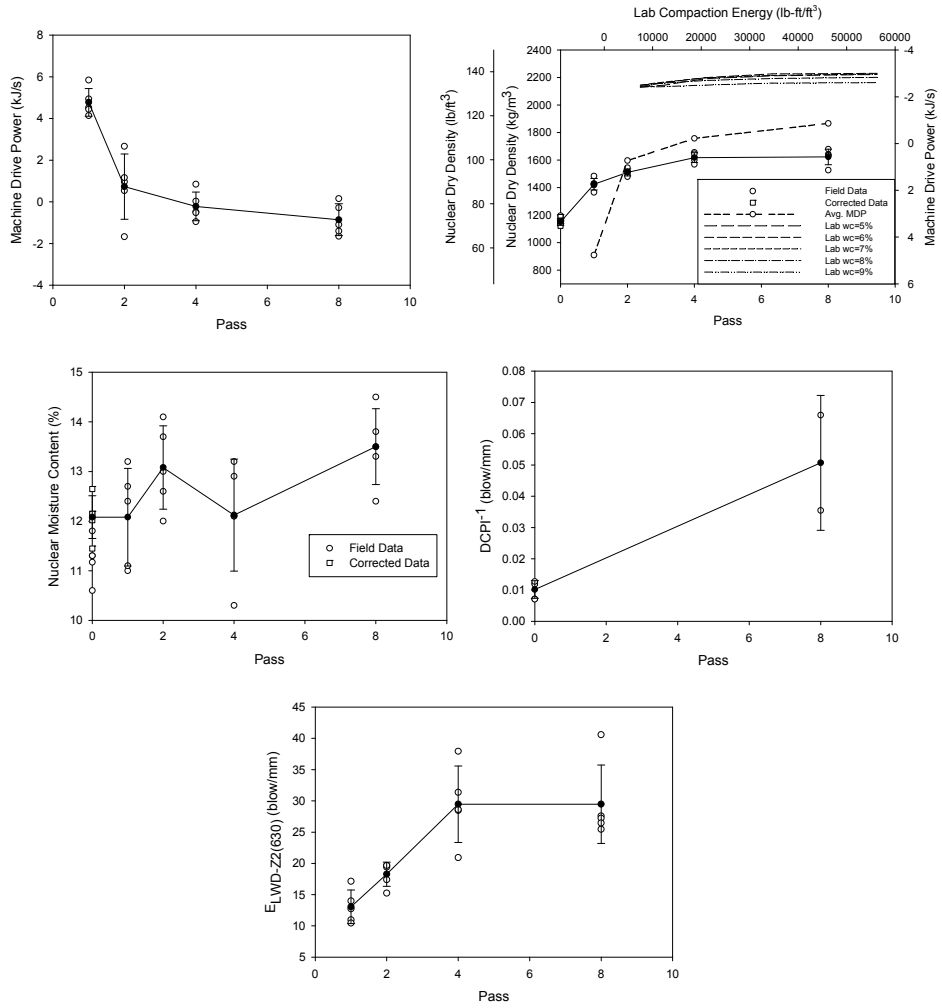


**Figure 204: CP533 Vibratory Smooth Drum MnRoad Class 5 Base – Test Bed 21 Low Amplitude ($wc_{avg}$=12.6%)**

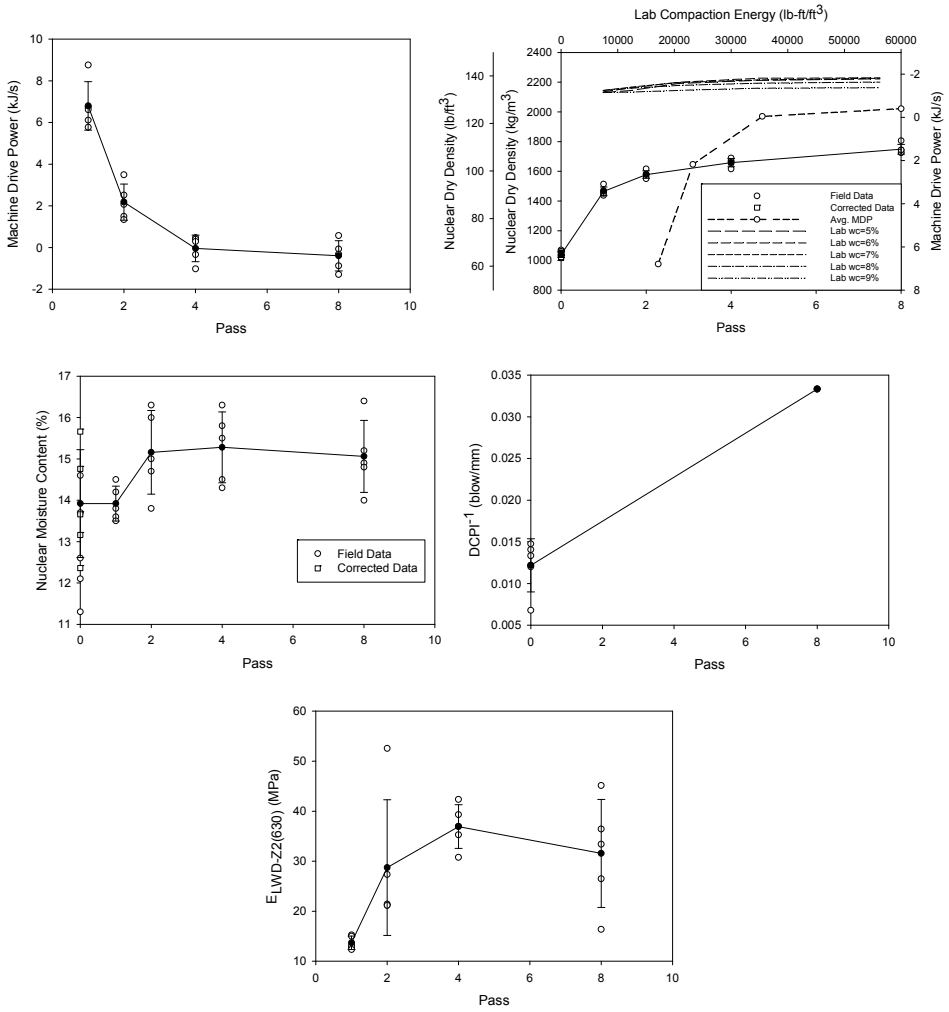


**Figure 205: CS533 Vibratory Smooth Drum MnRoad Class 5 Base (Soil 2011) - Test Bed 21 Med. Amplitude ($wc_{avg}$=14.7%)**

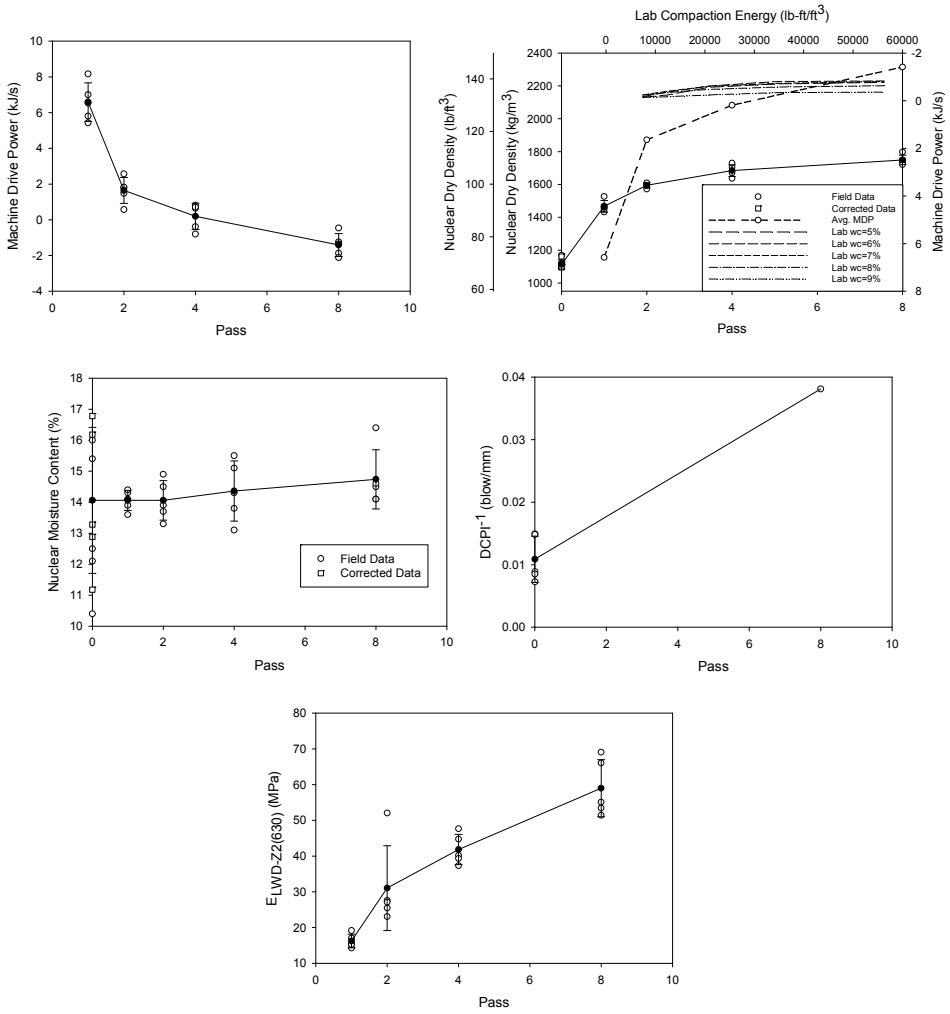


**Figure 206: CS533 Vibratory Smooth Drum MnRoad Class 5 Base (Soil 2011) - Test Bed 21 High Amplitude ($wc_{avg}$=14.3%)**

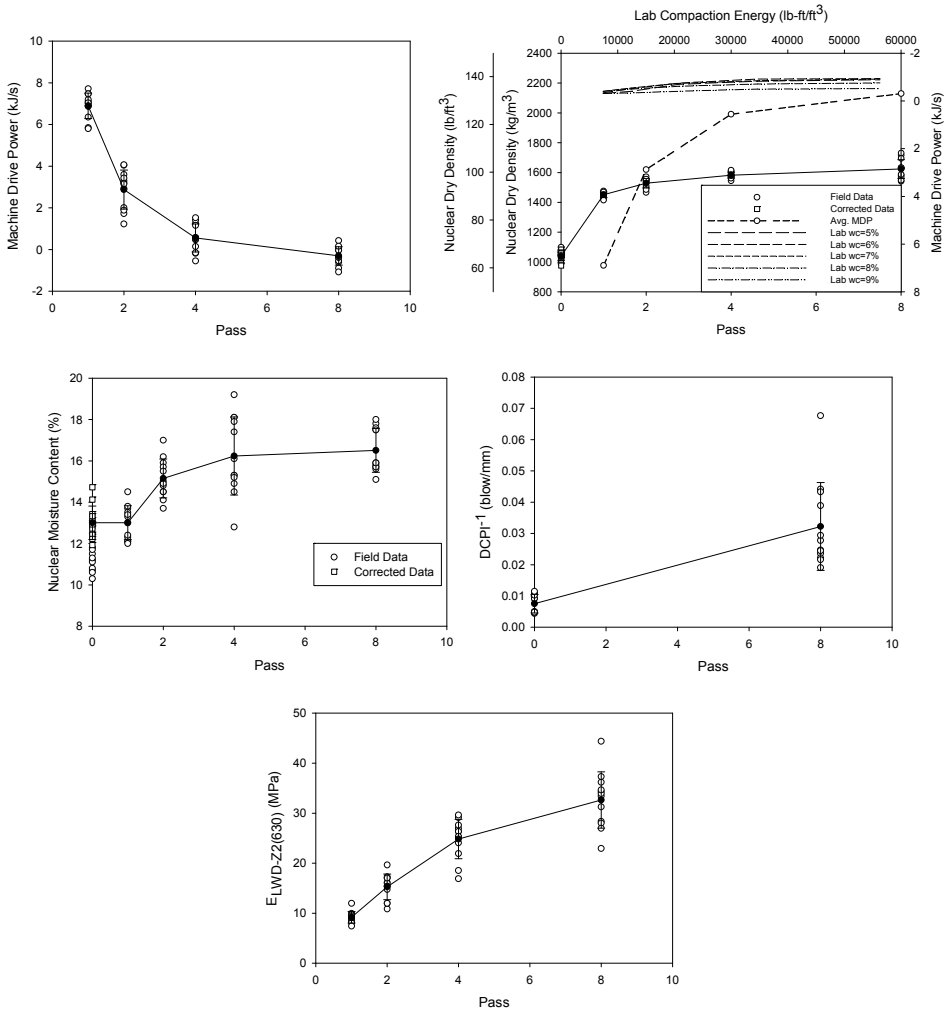


**Figure 207: CS533 Vibratory Smooth Drum MnRoad Class 5 Base (Soil 2011) - Test Bed 24 ($wc_{avg}$=14.8%)**

**Comparison of Laboratory and Field Compaction Curves**

Of the 33 test strips which were evaluated, nearly all test strips did not reach densities achieved with laboratory testing. With the exception of a few test strips, soils in the field were not able to achieve laboratory densities of 100% Standard Proctor effort. Several factors can inhibit the ability for a soil to be compacted in the field. It is possible that for most of the test strips, the compacting machine was simply too light to properly compact the soil. Also, some test strips were compacted well wet of optimum, which can also hinder field compaction.

**Laboratory and Field Curve Fit Methods**

The current version of CFED applies an exponential fit to field compaction data. This fit is used as part of the prediction algorithm for the suggested number of machine passes in field compaction. Therefore, an analysis was performed on a small data set to determine if the use of an exponential fit is the most appropriate. Three fitting techniques were used: the first order rate equation (FORE), two-parameter hyperbolic, and three-parameter exponential.

Handy (2002) applied first-order rate equations from chemical kinetics to geotechnical engineering relationships. Handy stated that a first order rate equation is applicable to modeling a physical process where the rate of approach to an equilibrium condition is proportional to the departure from that condition. The first order rate equation requires an asymptotic approach to an end condition. As was previously stated, when soils are compacted in the laboratory and in the field, the curves approach an asymptotic end condition with increasing compaction energy and/or machine pass. Therefore, it is pertinent to apply the first order rate equation to this case. The first-order rate equation could be useful to earthwork compaction projects because of its ability to predict values of field compaction (eg field density, CMV, MDP, etc).

The general form of the first-order rate equation is:

$$-\frac{dD}{dt}=kD \tag{34}$$

Where D represents departure from an end condition that may or may not be known: and dD/dt=change in D per unit of time t. The negative sign indicates that the rate is decreasing as it approaches the end condition.

The equation can be rearranged so that it becomes the form of:

$$\log D=-k_{10}t+C_{10} \tag{35}$$

where the subscripts indicate conversion to a logarithm to base 10.

This form of the equation can be applied to both laboratory and field compaction:

$$\gamma_{d_i}=\gamma_{d_0}+F^{*}\log\frac{E_i}{E_0} \tag{36}$$

Where $\boldsymbol{\gamma}_{di}$ is the dry density at lab compaction energy $E_i$ and $\boldsymbol{\gamma}_{do}$ is the known dry density at compaction energy $E_0$.

$$\gamma_{d_i}=\gamma_{d_0}+F^{*}\log\frac{P_i}{P_0} \tag{37}$$

Where $\boldsymbol{\gamma}_{di}$ is the dry density at machine pass $P_i$ and $\boldsymbol{\gamma}_{do}$ is the known dry density at machine pass $P_0$.

For Equation 36 and 37, F is a coefficient of compaction which determines the shape of the predicted curve.

This first-order rate equation was applied to soils where lab and field data were available. However, the equation did not appear to perform as was hoped. Figure 208 shows the first-order rate equation applied to the laboratory compaction curve for Edwards till. Because the

curves are created using the first and last laboratory compaction points, the equation fits these two points very well. However, it does not account for any of the points in between. Therefore, it misses the intermediate points significantly. This was the case for all soils and their laboratory compaction curves. Figure 209 shows the first-order rate equation applied to the same soil and its field data. Although it appears that the equation fits this data better, it is still unable to fit points in between the initial and final measurements.

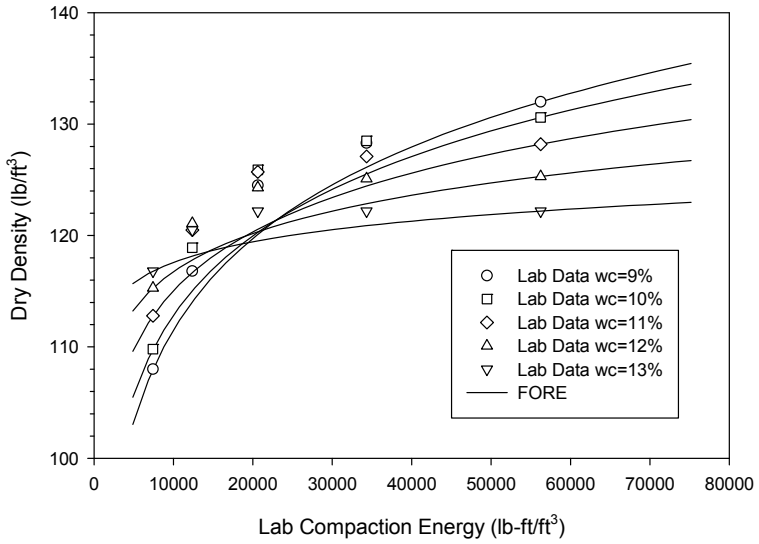


**Figure 208: First-order rate equation applied to Edwards Till A (Standard Proctor optimum=12.1%)**

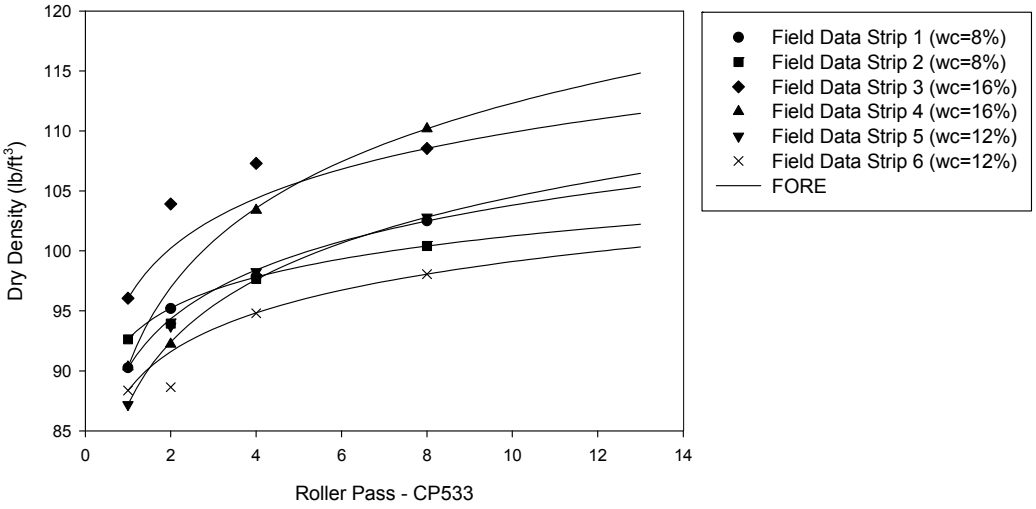


**Figure 209: First-order rate equation applied to Edwards Till A field data**

Figure 210 and Figure 211 show a standard hyperbolic fit for the same data set. It appears that the hyperbolic fit matches the data better than the first-order rate equation for both laboratory and field compaction. The hyperbolic fit better captures the entire data set rather than simply the first and last point; as is the case with the first order rate equation. The general form of the hyperbola is:

$$y=\frac{ax}{b+x} \tag{38}$$

where a and b are fitting parameters.

For the laboratory, where E is laboratory compaction energy:

$$\gamma_d=\frac{aE}{b+E} \tag{39}$$

For the field, where P is machine pass:

$$\gamma_d=\frac{aP}{b+P} \tag{40}$$

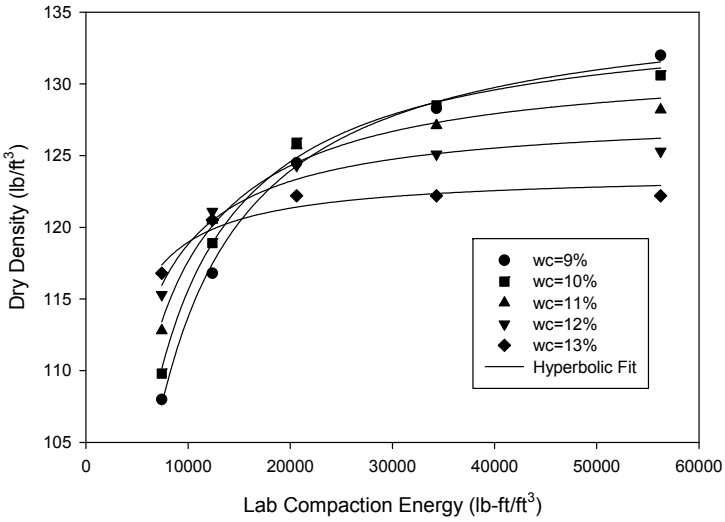


**Figure 210: Hyperbolic fit applied to Edwards A laboratory compaction data**

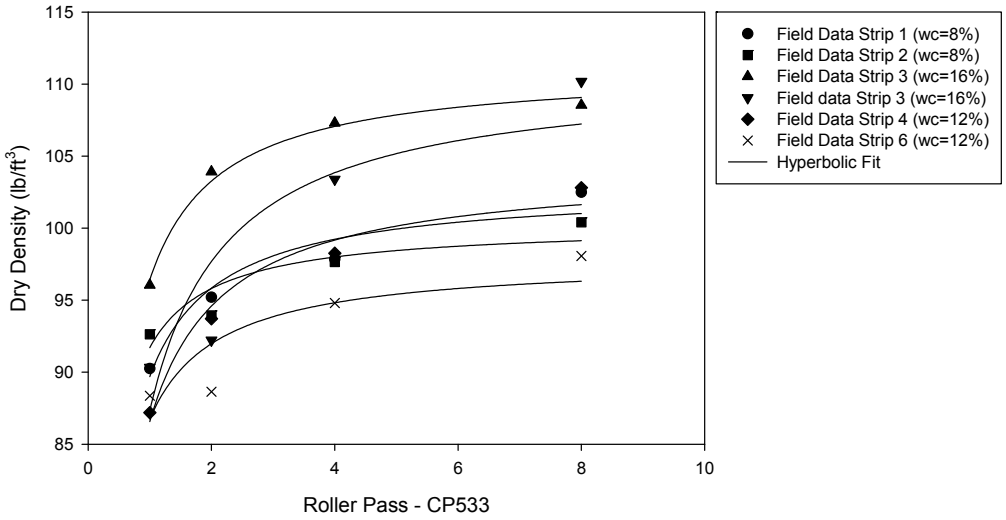


**Figure 211: Hyperbolic fit applied to Edwards A field compaction data**

Finally, a three-parameter exponential fit was applied to both lab and field data sets. The performance of the exponential fit is very similar compared to the hyperbolic fit for lab compaction data. There methods do differ in their prediction of the field data, however. The

hyperbolic fit curves are more representative of what is expected in the field. The exponential curves are nearly linear for some data sets which is not as would be expected in the field. However, these differences are subtle and may be due simply to scatter in the data. The exponential fit of the data sets are shown in Figure 212 and Figure 213.

The general form of the exponential equation is:

$$y=y_o+a(1+e^{-bx}) \quad (41)$$

For the laboratory condition, the form of the equation becomes:

$$\gamma=\gamma_o+a(1+e^{-bE}) \quad (42)$$

For the field condition, the form of the equation becomes:

$$\gamma=\gamma_o+a(1+e^{-bP}) \quad (43)$$

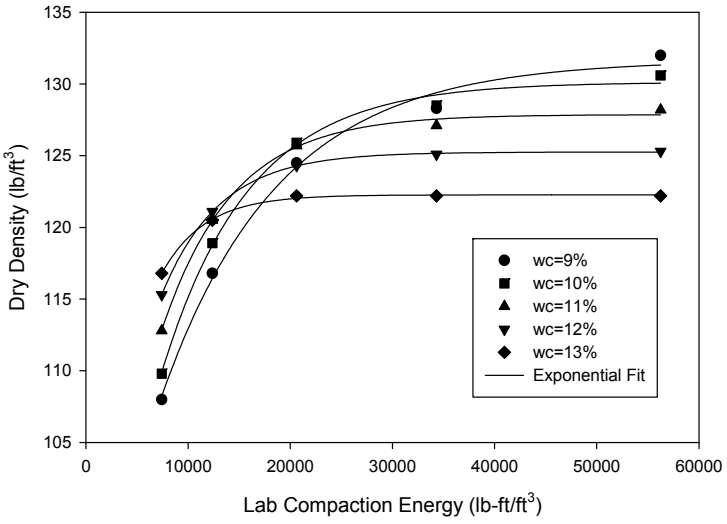


**Figure 212: Exponential fit applied to Edwards A lab compaction data**

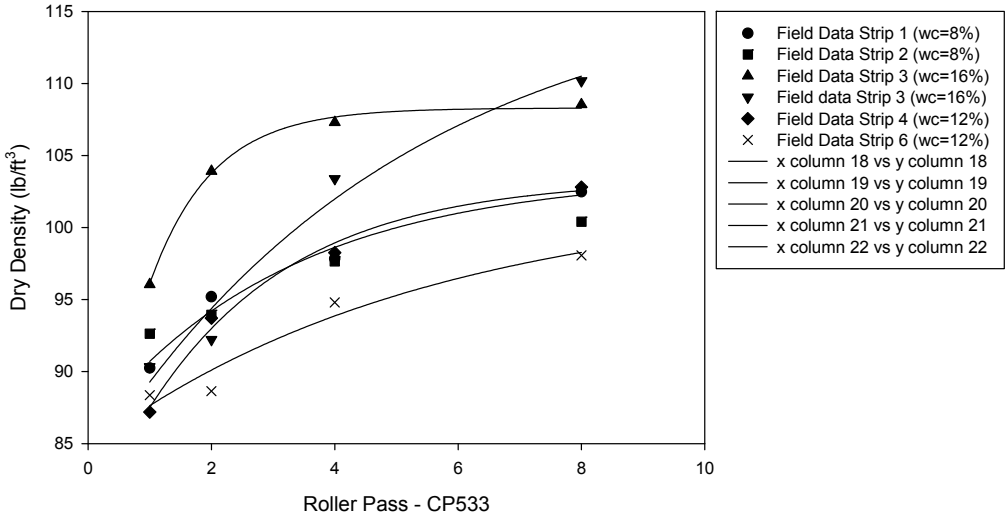


**Figure 213: Exponential fit applied to Edwards A field compaction data**

More investigation is needed to determine how well the hyperbolic and exponential fits apply to a broad range of field and laboratory data. However, at this time it appears that either of these methods is adequate to fit field and lab compaction curves. The first order rate equation, however, does not fit the entire data set adequately enough to be used in compaction prediction. Further investigations should determine what, if any, are the correlation between hyperbolic or exponential fit parameters a and b for laboratory and field compaction. This may be one method by which field compaction could be predicted from laboratory compaction.

# CHAPTER 7. DISCUSSION OF RESULTS

## Deviation from Hand Curve

Once all lab prediction methods were completed, each method was compared against the values determined by manually drawing the laboratory compaction curve. The average deviation column displays the average of the differences for both optimum moisture content and maximum density; these values were calculated by subtracting the predicted value from the hand drawn value. If the models are performing perfectly, these values should be expected to be zero. However, all models tend to over-predict optimum moisture content and (with the exception of Woods 1938) tend to over-predict maximum density as well.

For each model, the difference between the actual lab data and predicted curves was determined for the density predictions. Lab data was matched to the output curves from SoilVision 4.0 (2006) for Li and Sego (1999, 2000a, 2000b) and CFED. The lab point was matched to the curve predicted point with the nearest moisture content within 0.1% (+/-). Where curve points were not within 0.1% of lab points, linear interpolation was used to determine the predicted point within 0.1% moisture. Again, if the models are performing perfectly, these differences should sum to zero. In general, each model over-predicts the density of the lab data. However, the average differences are typically small (less than 0.2 $lb/ft^3$) in most cases. The average difference for all data points (763 total) included in this study was 0.2 $lb/ft^3$ for Li and Sego and 0.1 $lb/ft^3$ for CFED.

Table 119 shows statistical measurements of the range of deviations from the values determined by the hand drawn curves. The values in Table 119 were determined by subtracting the predicted value of the model from the actual value of the hand curve. These are values over all five energy levels. It should be noted that for the Blotz Method A, the value of maximum density ($\gamma_{d,max}$) and optimum moisture content ($w_{opt}$) for the Standard Proctor are entered into the prediction equation. Theoretically, this method should always correctly determine these values for the Standard Proctor Data. Also note that these numbers

do reflect the prediction methods' values determined for granular materials, which the models were not intended to predict. This explains some of the abnormally high deviations from the hand curves. The average deviation column displays the average of the differences for both optimum moisture content and maximum density. If the models are performing perfectly, these values should be expected to be zero.

**Table 119: Prediction method performance for all soils**

| | Range of Deviation | | Average Deviation | | Standard Deviation | |
|---|---|---|---|---|---|---|
| **Prediction Method** | $w_{opt}$ (%) | $\gamma_{d,max}$ (lb/ft$^3$) | $w_{opt}$ (%) | $\gamma_{d,max}$ (lb/ft$^3$) | $w_{opt}$ (%) | $\gamma_{d,max}$ (lb/ft$^3$) |
| Quadratic | -12.5 to 13.0 | -7.5 to 10.7 | 0.6 | 1.3 | 2.5 | 2.1 |
| Woods | -8.3 to 5.0 | -15.6 to 1.4 | -0.4 | -2.8 | 2.3 | 3.3 |
| Blotz A | -3.5 to 4.1 | -8.9 to 19.9 | 0.4 | 1.6 | 1.3 | 4.6 |
| Blotz B | -7.9 to 5.2 | -20.2 to 34.5 | 0.3 | 0.8 | 3.1 | 14.6 |
| Li & Sego | -5.1 to 9.7 | -7.4 to 8.0 | 0.4 | 0.1 | 1.5 | 1.3 |
| CFED | -4.8 to 3.7 | -6.8 to 4.4 | 0.8 | 1.0 | 1.2 | 1.4 |

Because these methods were specifically developed to predict for fine-grained soils, the preceding analysis was performed again on soils separated by soil type. Table 120 shows the range of deviations for coarse-grained soils while Table 121 shows the range of deviations for fine-grained soils. With the exception of Blotz's methods, each model performs better for fine-grained soils than for coarse-grained; as should be the case. CFED and Li and Sego, especially, perform much better for fine-grained soils than for coarse-grained.

**Table 120: Prediction method performance for coarse-grained soils**

| | Range of Deviation | | Average Deviation | | Standard Deviation | |
|---|---|---|---|---|---|---|
| **Prediction Method** | $w_{opt}$ (%) | $\gamma_{d,max}$ (lb/ft$^3$) | $w_{opt}$ (%) | $\gamma_{d,max}$ (lb/ft$^3$) | $w_{opt}$ (%) | $\gamma_{d,max}$ (lb/ft$^3$) |
| Quadratic | -12.5 to 13.0 | -7.5 to 9.4 | 0.6 | 1.2 | 3.2 | 2.5 |
| Woods | -8.3 to 1.4 | -15.6 to 1.4 | -1.3 | -2.9 | 2.1 | 3.4 |
| Blotz A | -1.1 to 3.0 | -2.5 to 13.0 | 1.0 | 3.5 | 1.3 | 4.6 |
| Blotz B | -7.9 to 4.1 | -19.0 to 28.8 | -0.9 | -0.4 | 3.6 | 13.5 |
| Li & Sego | -5.1 to 9.7 | -7.4 to 8.0 | 0.5 | 0.1 | 2.0 | 1.5 |
| CFED | -4.8 to 3.7 | -6.8 to 4.4 | 0.4 | 0.9 | 1.3 | 1.6 |

**Table 121: Prediction method performance for fine-grained soils**

| | Range of Deviation | | Average Deviation | | Standard Deviation | |
|---|---|---|---|---|---|---|
| **Prediction Method** | $w_{opt}$ (%) | $\gamma_{d,max}$ (lb/ft$^3$) | $w_{opt}$ (%) | $\gamma_{d,max}$ (lb/ft$^3$) | $w_{opt}$ (%) | $\gamma_{d,max}$ (lb/ft$^3$) |
| Quadratic | -4.6 to 10.0 | -2.5 to 10.7 | 0.5 | 1.4 | 1.6 | 1.7 |
| Woods | -1.7 to 5.0 | -10.6 to 0.1 | 0.7 | -2.6 | 1.7 | 3.1 |
| Blotz A | -3.5 to 4.1 | -8.9 to 19.9 | 0.3 | 1.2 | 1.3 | 4.5 |
| Blotz B | -4.9 to 5.2 | -20.2 to 34.5 | 1.1 | 1.2 | 2.4 | 15.4 |
| Li & Sego | -1.2 to 2.1 | -3.1 to 2.7 | 0.2 | 0.2 | 0.7 | 0.9 |
| CFED | -0.4 to 3.7 | -0.6 to 4.3 | 1.0 | 1.2 | 0.9 | 1.1 |

Li and Sego and CFED are able to predict the maximum density and optimum moisture content with more regularity than any of the other models. Therefore, a further analysis was performed on these two models. This analysis is discussed in the section titled "Mean Square Error."

**Limitations of Each Model**

A major limitation common among all methods investigated is their inability to predict the compaction curve for granular soils. In the literature each method states that it is to be used explicitly for fine-grained materials. This statement was reinforced by the research. When moving along the laboratory compaction curve of a granular soil from optimum toward zero the soil density will decrease to a point (commonly referred to as the bulking moisture content) at which point it will begin to increase until reaching zero moisture content. To date, no model has been created to account for this bulking moisture content in granular soils.

*Quadratic*

The main limitation to the Quadratic model is the shape of the curve. While the curve may be adequate in predicting optimum moisture content and maximum dry density, it does not adequately predict other points. Also, there are cases where the quadratic model predicts curves which are otherwise impossible. For some soils, the quadratic model predicted curves

which were concave up, rather than down (CFED #1640, 2005, 2007, 2032, 2033, 2040) and others where it predicted curves beyond the zero-air-void curve (CFED #2011, 2013, 2029, 2031); both of which are not possible. Also, because the prediction equation does not include energy predicted curves for energy levels intersect in some cases, which is theoretically impossible. This method should not be used as a basis for predicting the complete compaction curve.

*Blotz Atterberg Method*

Obviously, one limitation of the Blotz prediction method is that it is unable to predict soils that do not have a liquid limit. It is important for any prediction model to be able to at least produce a curve for granular soils. Also, these methods only predict the optimum moisture content and maximum dry density for a soil. This method is not useful in predicting the complete compaction curve. As stated previously, this method is only applicable to certain energy levels. This method appears to be the most erratic of all the models because it had the widest range of predictions for both optimum moisture content and maximum density. Therefore, this method would not be applicable for predicting the full compaction curve.

*Woods*

As with the Quadratic model, the major limitation of the Woods (1938) model is its shape. This method is not sufficient to predict the entire compaction curve. Also, these curves are site specific. Several states have created their own set of curves in accordance with AASHTO T272 and much time would be required to develop a family of curves for each state or region.

Because these curves are developed using the standard Proctor testing method, they are only valid for this lab compaction energy. They cannot be used to predict compaction curves at other compaction energies. This hinders the possibility of relating these energies to machine compaction data. Also, it is difficult to distinguish curves on the wet side of optimum (see Figure 54). Therefore, if a point on the wet side of optimum is used in a prediction, several

curves may be selected with low accuracy to determine the actual curve which best represents the compaction curve for that soil.

*Li and Sego*

It has been determined that the maximum saturation ($S_m$) parameter in Li and Sego's model can greatly affect the ability of the model to predict the compaction curve. For a given soil, the compaction curve was predicted using $S_m$ at 100%, 95%, 90%, and the actual calculated value for the soil. The value of $S_m$ was calculated from the laboratory compaction data curves. Figure 214 showed a method of determining $S_m$ from the compaction curve. The relationship between moisture content (w%), $\gamma_d$, void ratio ($e$), and Saturation ($S$) shown in Equations 44 and 45 can be employed to determine the saturation of points on the $S_m$ line.

$$e = \frac{G_s * \gamma_w}{\gamma_d} - 1 \tag{44}$$

$$S\% = \frac{\frac{w\%}{100} * G_s}{e} * 100 \tag{45}$$

For each soil, two points were selected on the line and their respective saturations determined. These were then averaged to obtain an average $S_m$ for the soil. Figure 214 shows this influence graphically for Glacial Till Western Illinois (PPG) soil.

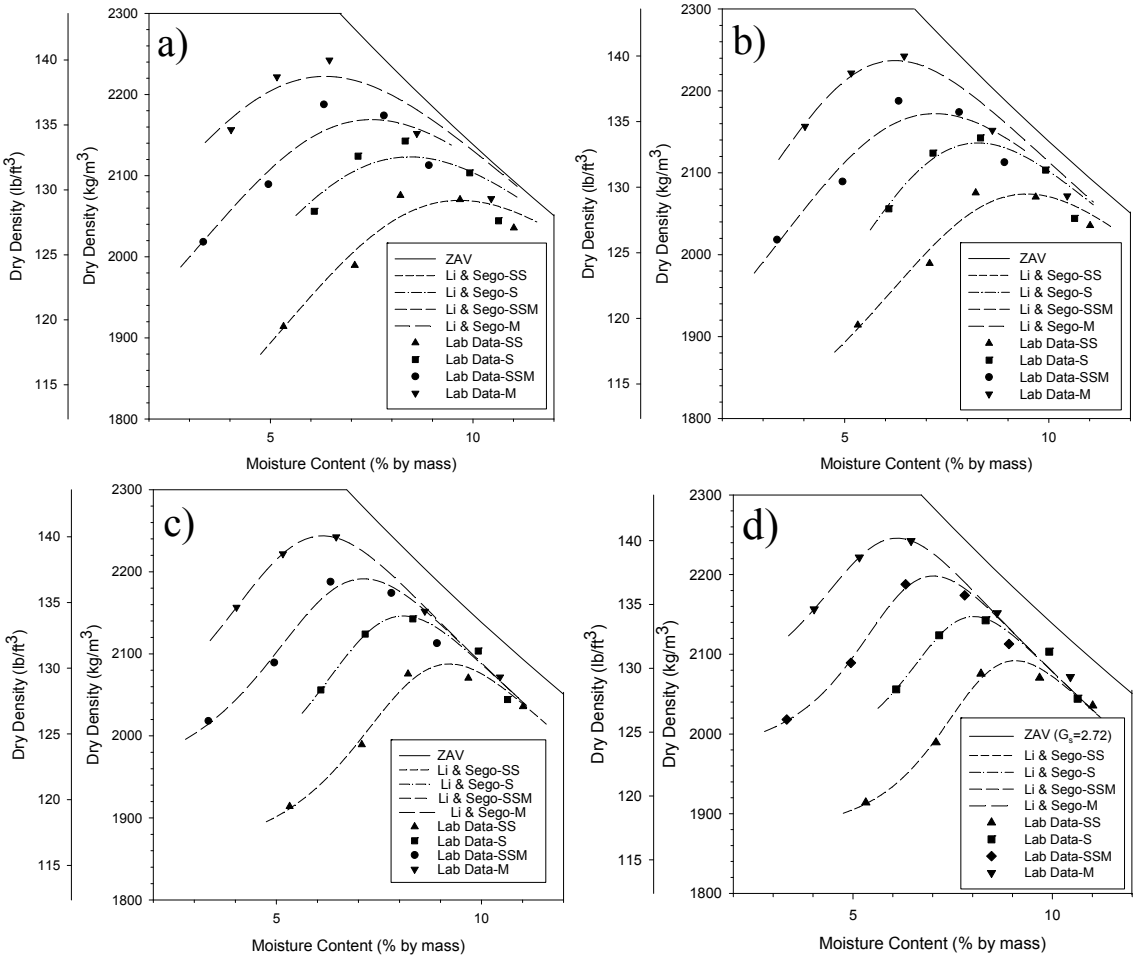


**Figure 214: Influence of $S_m$ a) $S_m$=100%, b) $S_m$=95%, c) $S_m$=90% and d) $S_m$=88%**

**Table 122: Influence of $S_m$ on predicted soil properties**

| *Energy Level* | $S_m$ (%) | $w_{opt}$ (%) | $\gamma_{d,max}$ (lb/ft$^3$) | $R^2$ |
|---|---|---|---|---|
| SS | 100 | 9.7 | 129.2 | 0.92 |
| | 95 | 9.5 | 129.5 | 0.95 |
| | 90 | 9.2 | 130.3 | 0.98 |
| | 88 | 9.1 | 130.6 | 0.99 |
| S | 100 | 8.4 | 132.5 | 0.62 |
| | 95 | 8.3 | 133.4 | 0.82 |
| | 90 | 8.1 | 134.0 | 0.95 |
| | 88 | 8.0 | 134.1 | 0.93 |
| SSM | 100 | 7.5 | 135.4 | 0.85 |
| | 95 | 7.2 | 135.6 | 0.89 |
| | 90 | 7.1 | 136.8 | 0.95 |
| | 88 | 7.0 | 137.2 | 0.97 |
| SM | 100 | 6.3 | 138.7 | 0.82 |
| | 95 | 6.2 | 139.6 | 0.94 |
| | 90 | 6.1 | 140.2 | 0.99 |
| | 88 | 6.1 | 140.2 | 0.99 |
| M | 100 | 9.7 | 129.2 | 0.92 |
| | 95 | 9.5 | 129.5 | 0.95 |
| | 90 | 9.2 | 130.3 | 0.98 |
| | 88 | 9.1 | 130.6 | 0.99 |

Table 122 shows the changes in $w_{opt}$, $\gamma_{d,max}$, and $R^2$ for each energy level and each $S_m$. In nearly all energy levels, as the $S_m$ approaches the calculated value, $w_{opt}$ decreases, $\gamma_{d,max}$ increases, and $R^2$ increases. The change in $w_{opt}$ and $\gamma_{d,max}$ differ by a maximum of 0.6% and 1.83 pcf (29.3 kg/m$^3$), respectively between $S_m$=100% and $S_m$=88%. Although these differences are not great, the $R^2$ values do differ at a maximum of 0.17 between the same two saturations.

By calculating the $S_m$ value rather than using it as a fitting parameter or arbitrarily selecting a value the $w_{opt}$ and $\gamma_{d,max}$ will not differ greatly. However, because the $R^2$ values can vary significantly using any other portion of the plot beyond the maximum values may be problematic if a maximum saturation is not determined for a given soil.

The Li and Sego (1999, 2000a, 2000b) model was shown to be limited in its ability to predict for coarse-grained soils. Specifically, the model could not properly predict for soils with a bulking condition. However, when compared to previous models, Li and Sego performed

best at predicting the family of compaction curves for a given soil. This method also has a high parameter to sample ratio. In most cases of this study, it used four parameters to predict four or five compaction points. Therefore, this method can be subject to variance in the data.

*CFED*

The CFED prediction model exhibits some inability to capture outlying points. The model selects the best fit curve for the data and then reflects this curve to different compaction energies. However, this causes it to miss outlying points which may be important to the data set.

One advantage of CFED that sets it apart from all the other models is that it develops a prediction for an entire set of data, rather than level by level. This makes it more applicable to predictions with limited testing because it is able to overcome large variances in the data. The ability of CFED to use compaction energy to develop the model makes it unique from all other models. Where the other models predict based upon a given set of data at a given energy level, CFED predicts the entirety of the family of curves considering all data from lab testing.

Of all the models, CFED shows the best ability to predict the compaction curves for granular soils. Modifications to the model may be able to improve upon this. Developers of the software should view prediction of compaction curves for granular soils as an opportunity to excel where others have not.

**Mean Square Error**

Table 123 and Table 124 show the results of the mean square error analysis for all soils investigated in this study. An absolute comparison of the two methods using mean square error would give the advantage to Li and Sego. Of the forty-two soils investigated, Li and Sego had a lower mean square error for 22 of the soils while 17 of the soils had lower mean

square error for CFED and 2 had equal values. However, these differences are subtle; on the order of tenths of lb/ft$^3$. Therefore, the methods appear to be similar in predicting the data. The largest deviation in the mean square error for the entire set of data was 3.6 lb/ft$^3$(Soil 2031) which was a granular soil. The average mean square error, for all soils was 2.0 lb/ft$^3$ and 1.8 lb/ft$^3$ for Li and Sego and CFED, respectively.

**Table 123: Mean square error results**

| | | N | p | MSE (lb/ft$^3$) | | | N | p | MSE (lb/ft$^3$) |
|---|---|---|---|---|---|---|---|---|---|
| 1632 | Li & Sego | 24 | 20 | 1.5 | 2018 | Li & Sego | 27 | 20 | 1.3 |
| | CFED | | 5 | 1.2 | | CFED | | 5 | 1.3 |
| 1633 | Li & Sego | 23 | 20 | 1.0 | 2020 | Li & Sego | 32 | 20 | 1.4 |
| | CFED | | 5 | 0.9 | | CFED | | 5 | 1.6 |
| 1634 | Li & Sego | 27 | 20 | 1.4 | 2021 | Li & Sego | 38 | 20 | 1.2 |
| | CFED | | 5 | 1.7 | | CFED | | 5 | 0.3 |
| 1635 | Li & Sego | 20 | 16 | 1.2 | 2022 | Li & Sego | 36 | 20 | 1.5 |
| | CFED | | 5 | 1.3 | | CFED | | 5 | 1.6 |
| 1636 | Li & Sego | 26 | 20 | 1.4 | 2023** | Li & Sego | 20 | 20 | -- |
| | CFED | | 5 | 1.3 | | CFED | | 5 | 1.6 |
| 1637 | Li & Sego | 25 | 20 | 1.1 | 2024 | Li & Sego | 10 | 8 | 1.3 |
| | CFED | | 5 | 1.0 | | CFED | | 5 | 1.6 |
| 1638 | Li & Sego | 27 | 20 | 1.0 | 2025 | Li & Sego | 9 | 8 | 6.0 |
| | CFED | | 5 | 1.3 | | CFED | | 5 | 2.9 |
| 1640 | Li & Sego | 29 | 20 | 1.8 | 2026 | Li & Sego | 11 | 8 | 3.5 |
| | CFED | | 5 | 3.4 | | CFED | | 5 | 1.7 |
| 2001 | Li & Sego | 10 | 8 | 1.4 | 2027 | Li & Sego | 10 | 8 | 1.5 |
| | CFED | | 5 | 1.5 | | CFED | | 5 | 1.6 |
| 2003 | Li & Sego | 12 | 8 | 0.9 | 2029 | Li & Sego | 10 | 8 | 2.6 |
| | CFED | | 5 | 2.0 | | CFED | | 5 | 2.5 |
| 2004 | Li & Sego | 10 | 8 | 0.2 | 2030 | Li & Sego | 10 | 8 | 2.1 |
| | CFED | | 5 | 0.0 | | CFED | | 5 | 1.5 |

**For soil 2023, the number of prediction parameters was equal to the sample size for Li & Sego, therefore the MSE was undefined.

**Table 124: Mean square error results (cont.)**

| | | N | p | MSE ($lb/ft^3$) | | | N | p | MSE ($lb/ft^3$) |
|---|---|---|---|---|---|---|---|---|---|
| 2005 | Li & Sego | 12 | 8 | 1.8 | 2031 | Li & Sego | 11 | 8 | 6.3 |
| | CFED | | 5 | 1.6 | | CFED | | 5 | 2.8 |
| 2006 | Li & Sego | 7 | 4 | 1.0 | 2032 | Li & Sego | 13 | 8 | 0.5 |
| | CFED | | 5 | 1.3 | | CFED | | 5 | 1.4 |
| 2007 | Li & Sego | 8 | 4 | 3.6 | 2033 | Li & Sego | 11 | 8 | 1.6 |
| | CFED | | 5 | 5.3 | | CFED | | 5 | 1.9 |
| 2008 | Li & Sego | 22 | 20 | 2.4 | 2034 | Li & Sego | 15 | 8 | 1.7 |
| | CFED | | 5 | 0.9 | | CFED | | 5 | 1.2 |
| 2009 | Li & Sego | 8 | 4 | 1.4 | 2035 | Li & Sego | 10 | 8 | 3.5 |
| | CFED | | 5 | 2.3 | | CFED | | 5 | 2.7 |
| 2010 | Li & Sego | 25 | 20 | 1.2 | 2036 | Li & Sego | 14 | 8 | 2.6 |
| | CFED | | 5 | 2.0 | | CFED | | 5 | 2.3 |
| 2011 | Li & Sego | 24 | 20 | 2.0 | 2037 | Li & Sego | 15 | 8 | 0.9 |
| | CFED | | 5 | 1.3 | | CFED | | 5 | 0.3 |
| 2012 | Li & Sego | 10 | 8 | 2.0 | 2038 | Li & Sego | 11 | 8 | 4.7 |
| | CFED | | 5 | 1.9 | | CFED | | 5 | 4.8 |
| 2013 | Li & Sego | 39 | 20 | 1.9 | 2039 | Li & Sego | 11 | 8 | 3.0 |
| | CFED | | 5 | 1.9 | | CFED | | 5 | 1.4 |
| 2014 | Li & Sego | 41 | 20 | 1.5 | 2040 | Li & Sego | 10 | 8 | 1.2 |
| | CFED | | 5 | 2.0 | | CFED | | 5 | 1.3 |

# CHAPTER 8. CONCLUSIONS AND RECOMMENDATIONS

Of all the prediction methods, Li and Sego (1999, 2000a, 2000b) and CFED appear to most accurately predict the complete compaction curves for a given soil. The performance of these two would be expected to be somewhat related because CFED integrates the basic equations from Li and Sego for its analysis.

CFED provides an adequate method by which to predict the complete compaction curves for a given soil. A mean square error analysis on the two methods determined that average mean square error over a range of 41 soils of varying classification was nearly equal for the two methods (2.0 $lb/ft^3$ for Li and Sego and 1.8 $lb/ft^3$ for CFED).

More research is needed to determine the applicability of CFED. Some suggestions for future research are:

- Continue to expand the CFED database and evaluate its performance for various soil types. Efforts should be made to collect data for soils from various regions around the globe where there is potential for soil compaction by Caterpillar machinery. This data is essential if CFED is to be applied to earthwork projects across the United States and/or world. Soils from different geographic regions will provide the database with reference soils to be used in compaction prediction.
- Perform a repeatability study on a select number of soil types. This study will evaluate each model's ability to reproduce given what should be the same data set. A sensitivity analysis will provide insight into how the models are affected by random testing errors in laboratory compaction.
- Investigate ability of CFED to predict number of machine passes based upon laboratory compaction curves. This report includes several analyses for the laboratory prediction methods, but more investigation is need into the ability of CFED to apply these predictions to field compaction.
- Development of other laboratory compaction methods. Some investigations (not included in this study) have been made with respect to the applicability of laboratory

gyratory and kneading compaction. These methods of lab compaction should be pursued to determine what, if any, is their relationship to machine field compaction.

- Perform an elaborate field study to establish a relationship between laboratory and field compaction. This study would include several machine types compacting one soil type at varying lift thicknesses and moisture contents.

As is true for any automated software in engineering, CFED should always be subject to review by a professional in the field of construction and/or earthwork engineering. The software, even when deemed applicable, cannot be used as a "black box," meaning, the results of such software should not be blindly accepted. The engineer or resident professional who may use CFED in an earthworks project must always determine if the results produced by the software are within reasonable expectations for a given project. It would be erroneous for one to apply the software predictions to any project without first considering their validity.

With that said, CFED has high potential to provide a unique tool to earthwork professionals. In the author's experience, there is yet to be developed software which can accurately predict compaction characteristics of soils and aid in selection of required machinery to achieve those characteristics.

**REFERENCES**

Adam, D. (1997). "Continuous compaction control (CCC) with vibratory rollers." *Proceedings of 1st Australia-New Zealand Conference on Environmental Geotechnics – GeoEnvironment 97*, Melbourne, p. 245-250.

Amini, F. (2004). "Dynamic cone penetrometer in quality control of compaction, state-of-the-art report." *Proc., Geo-Trans 2004 – Geotechnical Engineering for Transportation Projects*, Geotechnical Special Publication No. 126, Yegian and Kavazanjan, eds., ASCE, Los Angeles, Ca., 1023-1031.

Ampadu, S., and Arthur, T (2006). "The dynamic cone penetrometer in compaction verification on a model road pavement." *Geotech. Test. J.*, ASTM, 29(1), 70-79.

ASTM D422-63(2002). "Standard Test Method for Particle-Size Analysis of Soils." Copyright ASTM International, West Conshohocken, PA.

ASTM D4318-05. "Liquid Limit, Plastic Limit, and Plasticity Index of Soils." Copyright ASTM International, West Conshohocken, PA.

ASTM D854-06. "Standard Test Methods for Specific Gravity of Soil Solids by Water Pycnometer." Copyright ASTM International, West Conshohocken, PA.

ASTM D698-00. "Standard Test Methods for Laboratory Compaction Characteristics of Soil Using Standard Effort." Copyright ASTM International, West Conshohocken, PA.

ASTM WK218. "Test Method for In-Place Density and Water (Moisture) Content of Soil and Soil-Aggregate by Nuclear Methods (Shallow Depth)." Copyright ASTM International, West Conshohocken, PA.

Bekker, M. (1969). *Introduction to Terrain-Vehicle Systems*. The University of Michigan Press: Ann Arbor, MI.

Blotz, L.R., Benson, C.H., and Boutwell, G.P. (1998). "Estimating Optimum Water Content and Maximum Dry Unit Weight For Compacted Clays." *Journal of Geotechnical and Geoenvironmental Engineering* Vol 124, No. 9, New York, NY, p. 907-912.

Burnham, T., and Johnson, D. (1993). "In-Situ foundation characterization using the dynamic cone penetrometer," Final report MN/RD-93/05, Minnesota Department of Transportation, St. Paul, Mn.

Caterpillar (2000). *Soil and Asphalt Compaction Manual.* Manual No. QECB9729 (01/00), Copyright 2000, Caterpillar.

Caterpillar (2001). *United States Patent No. US 6,188,942 B1.* Feb. 13.

Caterpillar (2003). *Caterpillar Performance Handbook 34th Edition.* Caterpillar Incorporated, Peoria, Illinois.

Clegg, B. (1986). "Correlation with California bearing ratio." *News Letter 2*, <http://www.clegg.com.au/information_list12.asp > (Mar. 1, 2007).

Fang, Hsai-Yang (1991). *Foundation Engineering Handbook*, 2nd Edition, VanNostrand Reinhold, N.Y., NY.

Forssblad, L. (1980). "Compaction meter on vibrating rollers for improved compaction control." *Proceedings of the International Conference on Compaction*, Vol. II, Paris, p. 541-546.

Gabr, M., Hopkins, K., Coonse, J., and Hearne, T. (2000). "DCP criteria for performance evaluation of pavement layers." *J. Perf. of Constr. Facil.*, ASCE, 14(4), 141-148.

Gabr, M. A., Coonse, J., and Lambe, P.C. (2001). "A potential model for compaction evaluation of piedmont soils using dynamic cone penetrometer (DCP)." *Geotech. Test. J.*, 24(3), 308-313.

Hall, J.W. (1968). "Evaluation of Vibratory Rollers on Three Types of Soils." *U.S. Army Engineer Waterways Experiment Station Soil Compaction Investigation,* Report 10, Vicksburg, MI.

Handy, R.L. (2002). "First-Order Rate Equations in Geotechnical Engineering." *Journal of Geotechnical and Geoenvironmental Engineering,* Vol. 128, No. 5, May 2002, pp. 416-425.

Humboldt Mfg. Co. (2000). *Geogauge (soil stiffness/modulus) user guide*. Ver. 3.8.

ISSMGE. 2005. Roller-Integrated continuous compaction control (CCC): Technical Contractual Provisions, Recommendations. *TC3: Geotechnics for Pavements in Transportation Infrastructure.* International Society for Soil Mechanics and Geotechnical Engineering. http://egweb.mines.edu/IntelligentCompaction/files/ISSMGE1.pdf

Johnson, A.W. and Sallberg, J.R. (1960). "Factors That Influence Field Compaction of Soils." *Highway Research Board Bulletin, No. 272.*

Konrad, J. and Lachance, D. (2001). "Use of in-situ penetration tests in pavement evaluation." *Can. Geotech. J.*, 38: 924-935.

Krebs, R.D., and Walker, R.D. (1971). "Highway Materials." *McGraw-Hill, Inc.* USA.

Kutner, Michael H, Christopher J. Nachtsheim, John Neter, *Applied Linear Regression Models*, 2003, McGraw-Hill/Irwin.

Lee, K. L. and Haley, S.C. (1968). "Strength of compacted clay and high pressure." *Journal of Soil Mechanics and Foundation Division.* ASCE, Vol. 94, No. 1, pp. 1303-1332.

Li, H., and Sego, D.C. (1999). "Soil Compaction Parameters and Their Relationship With Soil Physical Properties." *52nd Canadian Geotechnical Conference* Regina, Saskatchewan, Canada, p. 517-524.

Li. H., and Sego. D.C. (2000a). "Equation for Complete Compaction Curve of Fine-grained Soils and Its Applications." *Constructing and Controlling Compaction of Earth Fills, ASTM STP 1384* pg. 113-125.

Li. H., and Sego, D.C. (2000b). "The Strength Behavior Along Complete Compaction Curves." *53rd Canadian Geotechnical Conference* Montreal, 8, pg. 1195-1202.

Livneh, M., Livneh, N., and Ishai, I. (2000). "The Israeli experience with the regular and extended dynamic cone penetrometer for pavement and subsoil-strength evaluation." *Nondestructive Testing of Pavements and Backcalculation of Moduli: Third Volume*, ASTM STP 1375, Tayabji and Lukanen, eds., American Society of Testing and Materials, West Conshohocken, Pa., 189-213

Natrajan, S. (1983). "Study of the performace of different types of rollers in compacting different types of soils." *Indian Highways*, Vol. 11, No. 11, p. 14-24.

Parsons, A.W. (1992). "Compaction of soils and granular materials. TRL State of the Art Report." *Her Majesty's Stationery Office*. London.

Proctor, R.R. (1933a). "Fundamental Principles of Soil Compaction." *Engineering News-Record*, 111, 245-248.

Proctor, R.R. (1933b). "Description of Field and Laboratory Methods." *Engineering News-Record,* 111, 289.

Proctor, R.R. (1933d). "Field and Laboratory Verification of Soil Suitability." *Engineering News-Record,* 111, 372-376.

Proctor, R.R. (1948b). "Laboratory Soil Compaction Methods, Penetration Resistance Measurements and the Indicated Saturated Penetration Resistance." *Proceedings of the 2nd International Conference on Soil Mechanics and Foundation Engineering,*5, 242-247.

Rodriguez, A.R. (1988). *Soil Mechanics in Highway Engineering,* pp. 117-185.

Sandström, A. and C. Pettersson (2004). "Intelligent systems for QA/QC in soil compaction." *Proceedings of the Annual Transportation Research Board Meeting*, January, Washington, D.C., CD-ROM.

Seed, H.B. et. al (1960). "The strength of compacted cohesive soils." *Research Conference on Shear Strength of Cohesive Soils.* ASCE, pp. 877-964.

Selig, E.T. (1971). "Unified System for Compactor Performance Specification." *Society of Automotive Engineers National Farm, Contruction & Industrial Machinery Meeting.* Milwaukee, Wis.

Siekmeier, J.A., Young, D., and Beberg, D. (2000). "Comparison of the dynamic cone penetrometer with other tests during subgrade and granular base characterization in Minnesota." *Nondestructive Testing of Pavements and Backcalculation of Moduli: Third Volume*, ASTM STP 1375, Tayabji and Lukanen, eds., ASTM, West Conshohocken, Pa., 175188.

SoilVision 4.0 (2006). SoilVision Systems Ltd. Copyright 2006, Saskatoon, Sasketchewan, Canada.

Thurner, H. and A. Sandström (1980). "A new device for instant compaction control." *Proceedings of International Conference on Compaction*, Vol. II, Paris, p. 611-614.

Trenter, N. A. (2001). "Earthworks: a guide." *Thomas Telford Publishing,* London, England.

Turnbull, W.J., and Foster, C.R., "Effect of Tire Pressure and Lift Thicknesses on Compaction of Soil with Rubber Tire Rollers." *American Society for Testing Materials, Special Technical Pbulication STP,* No. 232, pp. 102-121.

Waterways Experiment Station (1956). "Effect on soil compaction of tire pressure and number of coverages of rubber-tired rollers and foot-contact pressure of sheepsfoot rollers." *Army Corps of Engineers Soil Compaction Investigation Report No.7*, No. 3-271.

White, D.J, Jaselskis, E., Schaefer, V., Cackler, T., Drew, I., and Li, L. (2004). *Field Evaluation of Compaction Monitoring Technology: Phase I,* Final Report, Iowa DOT Project TR-495, Iowa State University, Ames, Ia.

White, D., Jaselskis, E., Schaefer, V. and E. Cackler (2005). "Real-time compaction monitoring in cohesive soils from machine response." *Transportation Research Record: Journal of the Transportation Research Board*, National Academy Press, No. 1936, p. 173-180.

White, D. J., Thompson, M. T., Morris, M. (2006). "Power-Based Compaction Monitoring using Vibratory Padfoot Roller." *Proceedings of GeoCongress 2006 – Geotechnical Engineering in the Information Technology Age, CD-ROM, February*. Atlanta, GA USA

White, D.J., Thompson, M.J., and Jovaag, K.(2007a). "Field Evaluation of Compaction Monitoring Technology: Phase II." *Center for Transportation and Research Education,* Ames, IA.

White, D.J., and Thompson, M.J. (2007b). "Relationships Between In-Situ and Roller-Integrated Compaction Measurements for Granular Soils." *Department of Civil, Construction and Environmental Engineering Iowa State University* Ames, IA, pg. 3-5.

White, D.J., Thompson, M.J., and Vennapusa, P.K. (2007c). "Field Study of Compaction Monitoring Systems: Self-Propelled Non-Vibratory 825G and Vibratory Smooth Drum CS-533E Rollers." *Center for Transportation and Research Education,* Ames, IA.

White, D.J., Thompson, M.J., and Vennapusa, P.K. (2007d). "Field Validation of Intelligent Compaction Monitoring Technology for Unbound Materials." Minnesota Department of Transportation, St. Paul, MN.

White, D.J., Vennapusa, P.K., Enz, D., and Puls, J.P. (2007e). "Implementation of Intelligent Compaction Performance Based Specifications in Minnesota – Project Report." Minnesota Department of Transportation, St. Paul, MN.

Woods, K.B. (1938). "Soil Mechanics Applied to Highway Engineering In Ohio." *The Ohio State University The Engineering Experiment Station,* No. 99, Columbus, OH, p. 14-25.

# APPENDIX: ALL CFED OUTPUTS

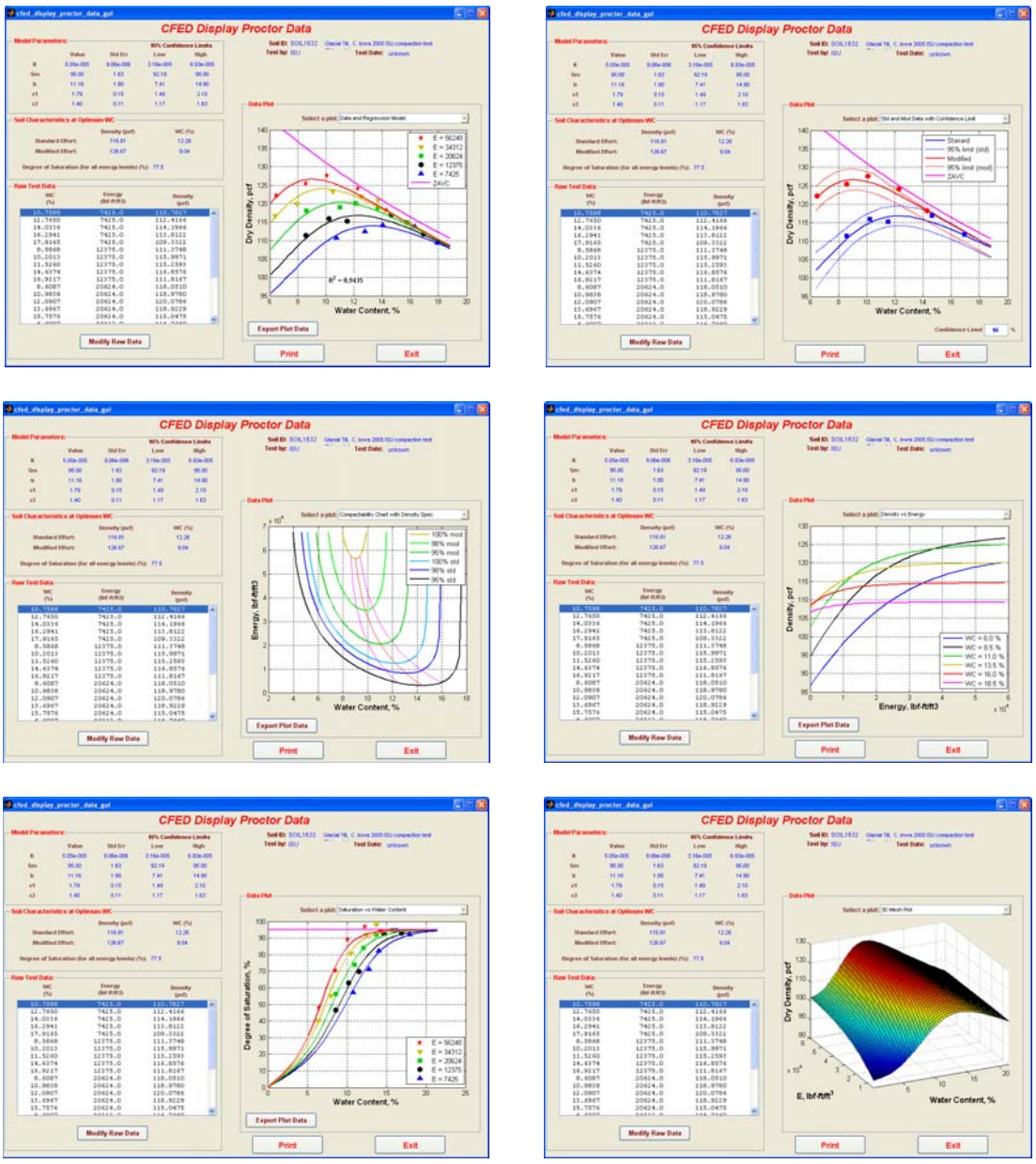


**Figure 215: Soil 1632 CFED outputs**

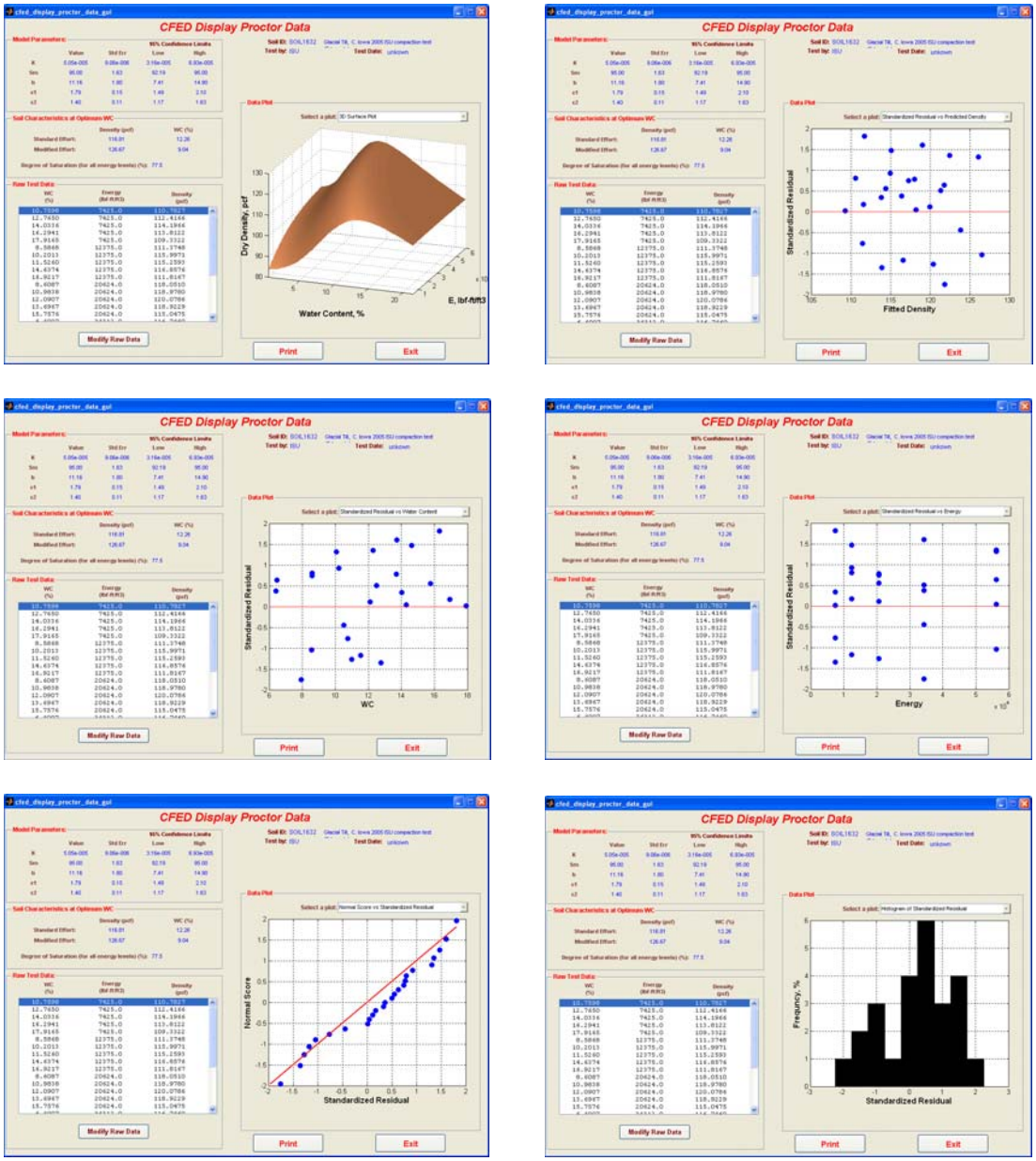


**Figure 215: Continued**

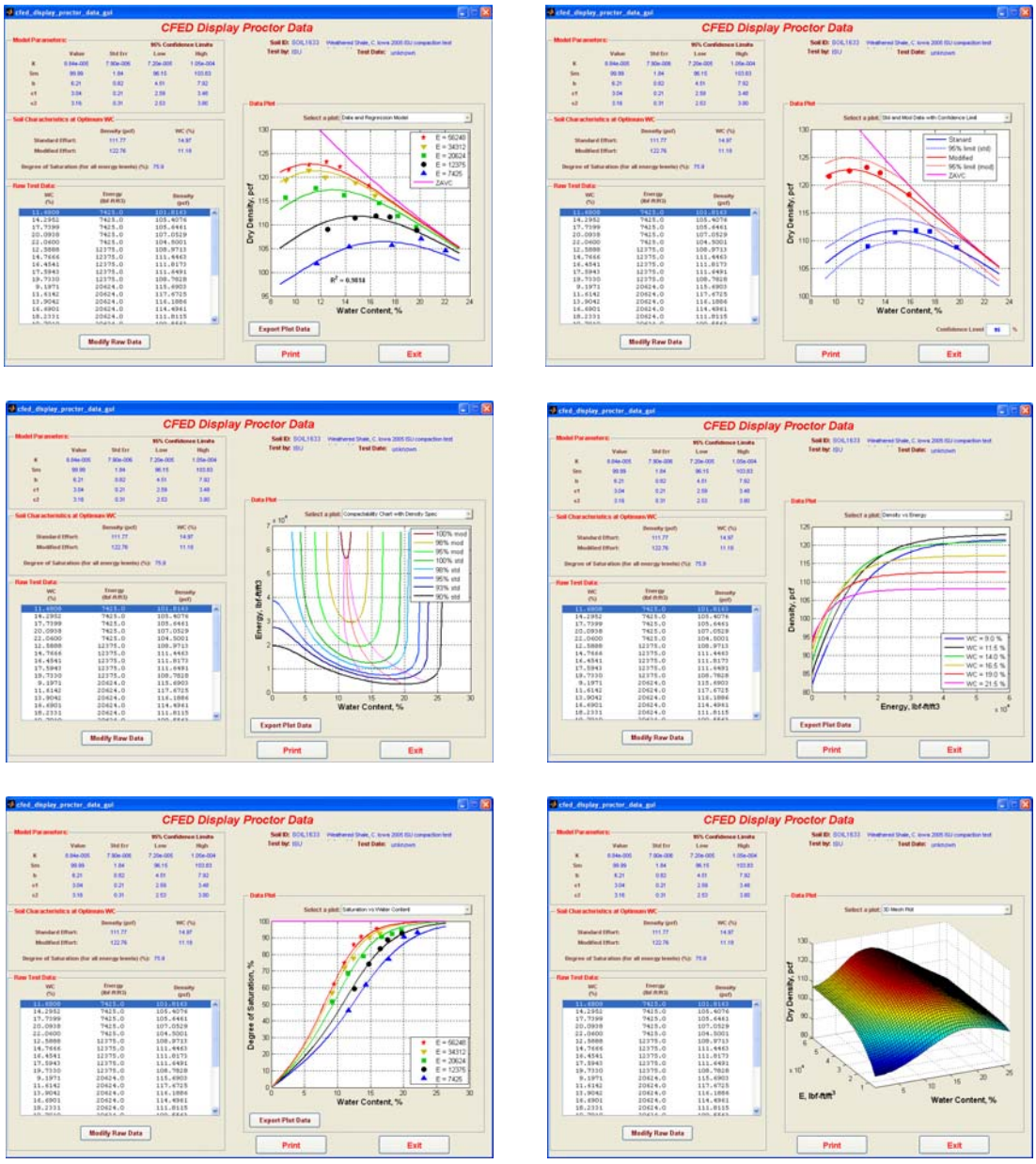


**Figure 216: Soil 1633 CFED outputs**

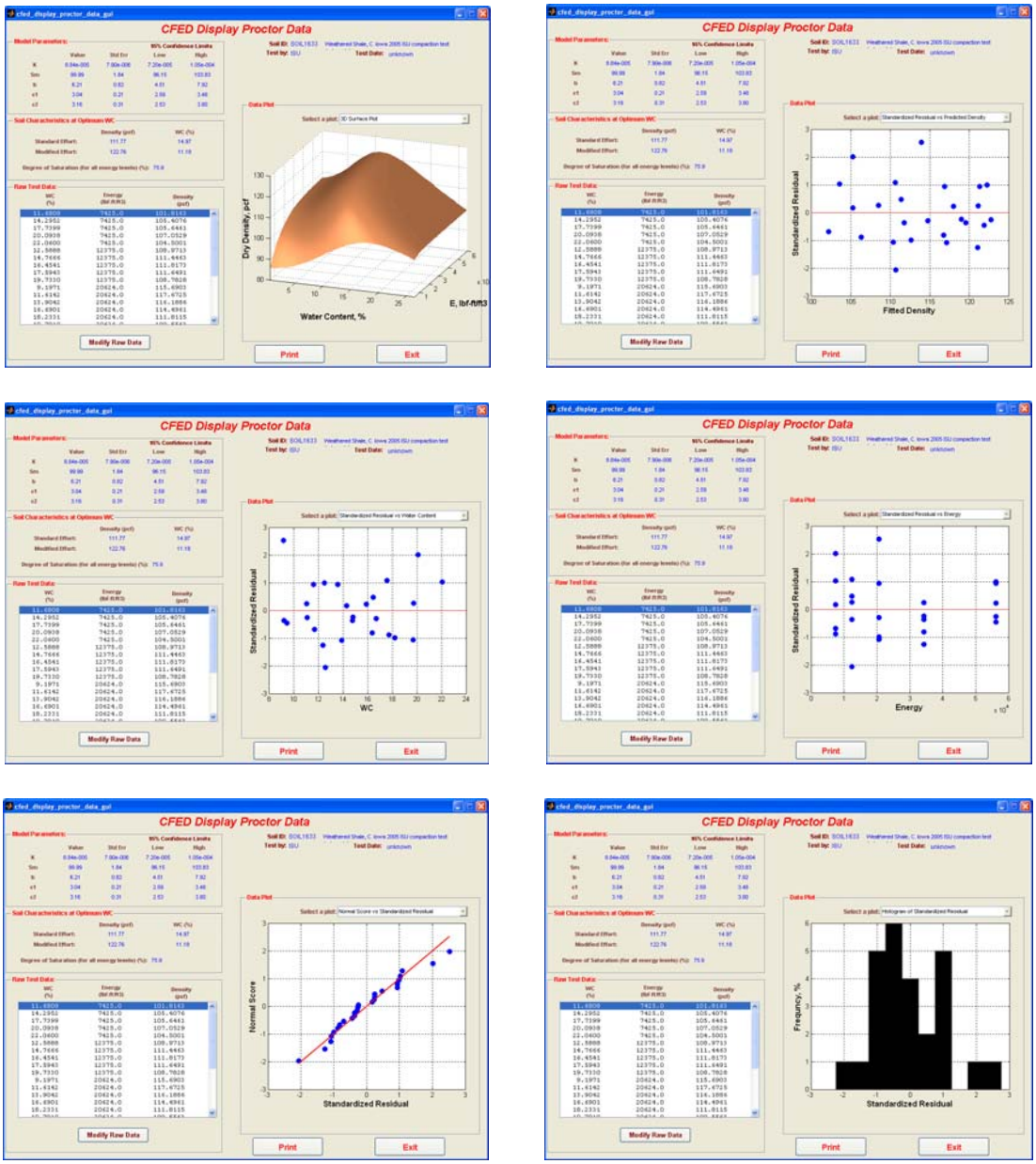


**Figure 216: Continued**

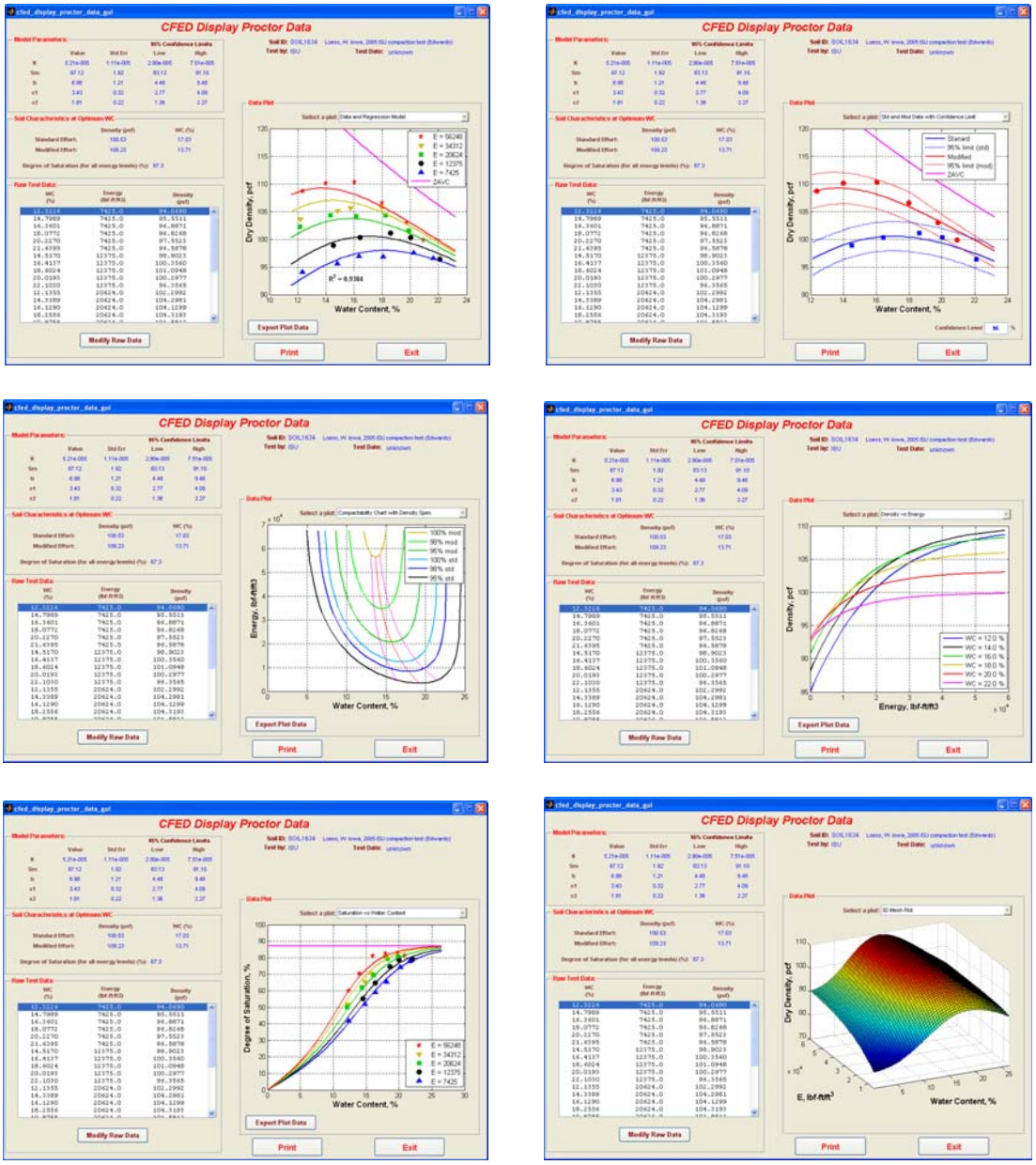


**Figure 217: Soil 1634 CFED outputs**

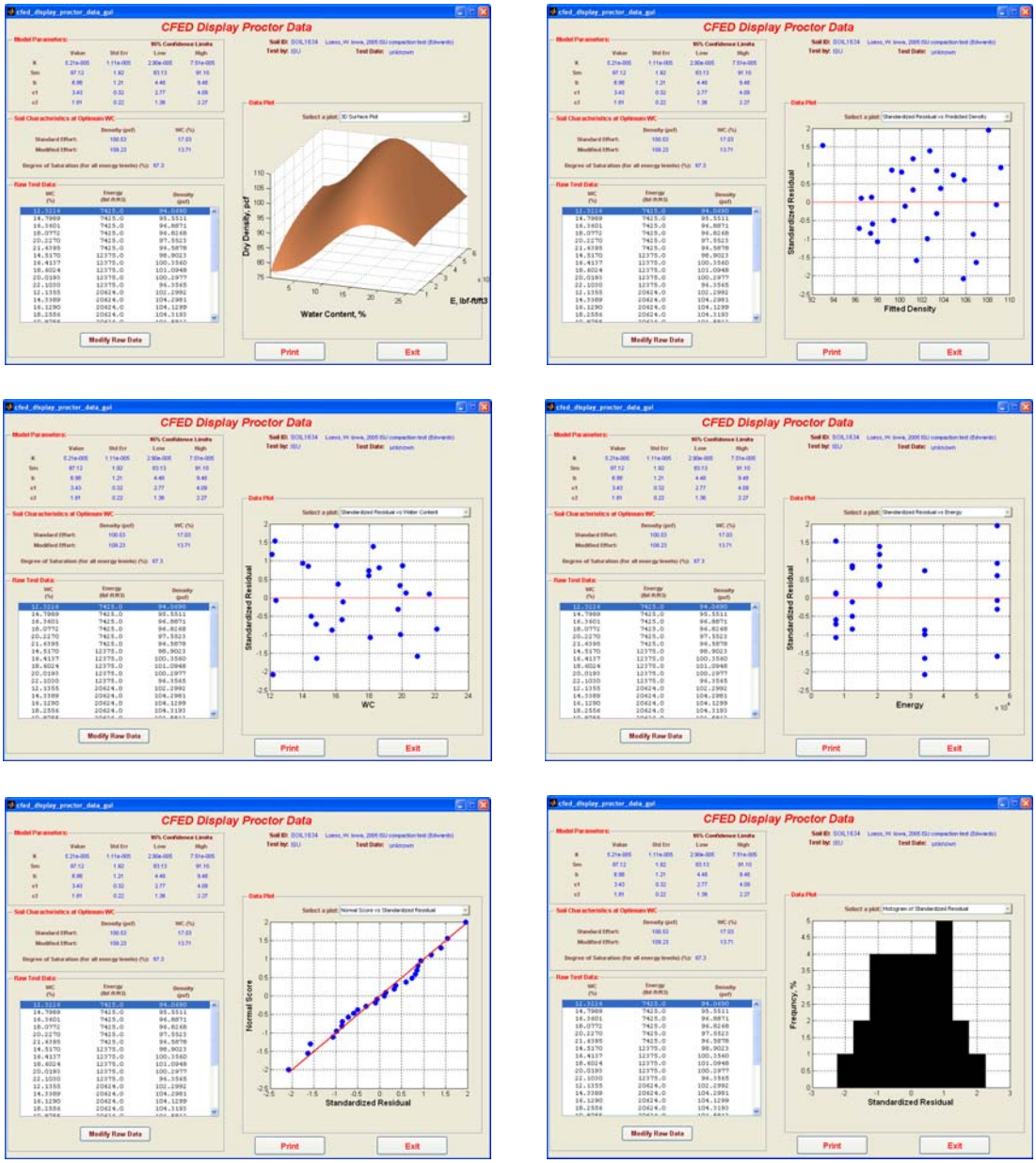


**Figure 217: Continued**

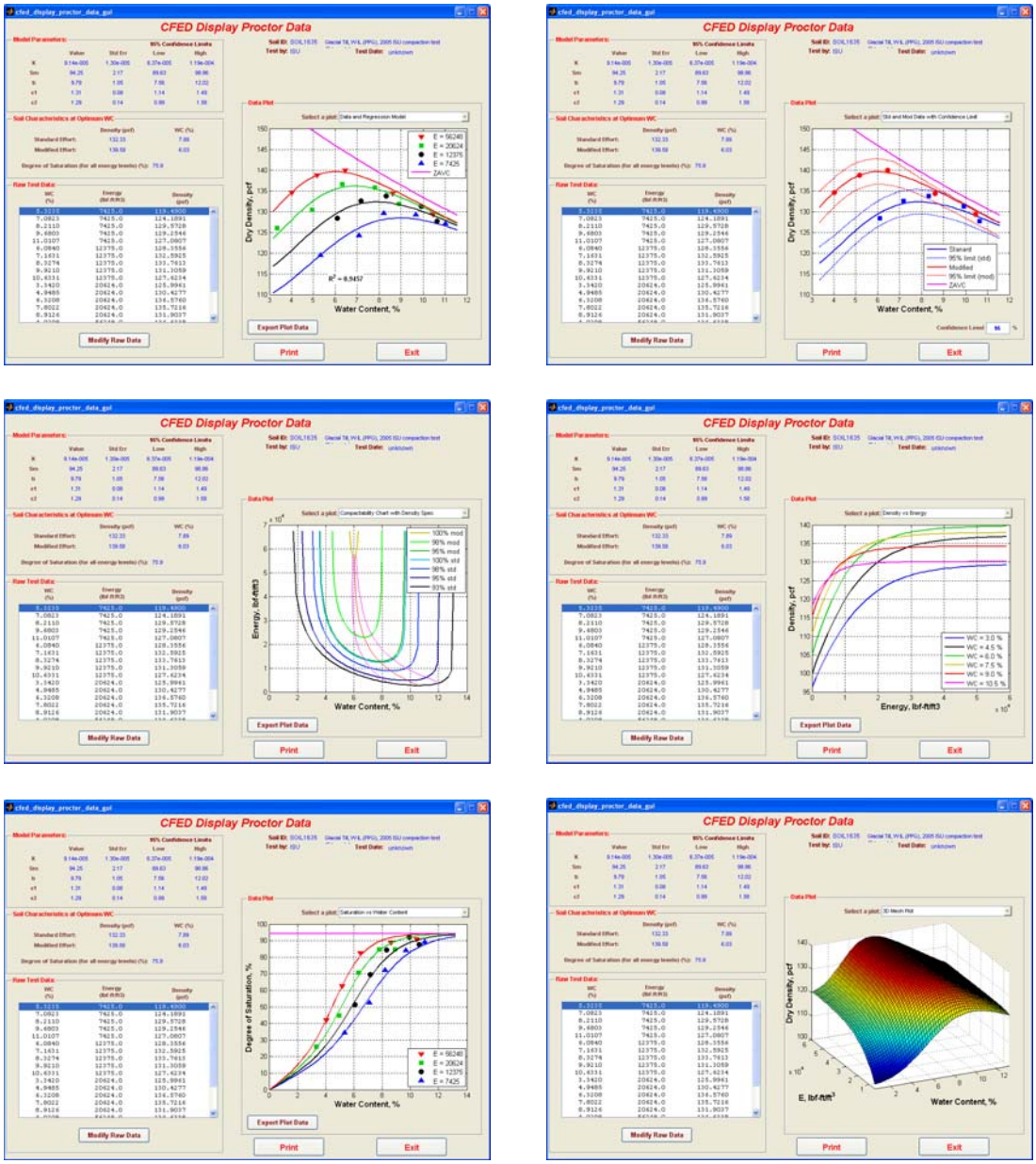


**Figure 218: Soil 1635 CFED outputs**

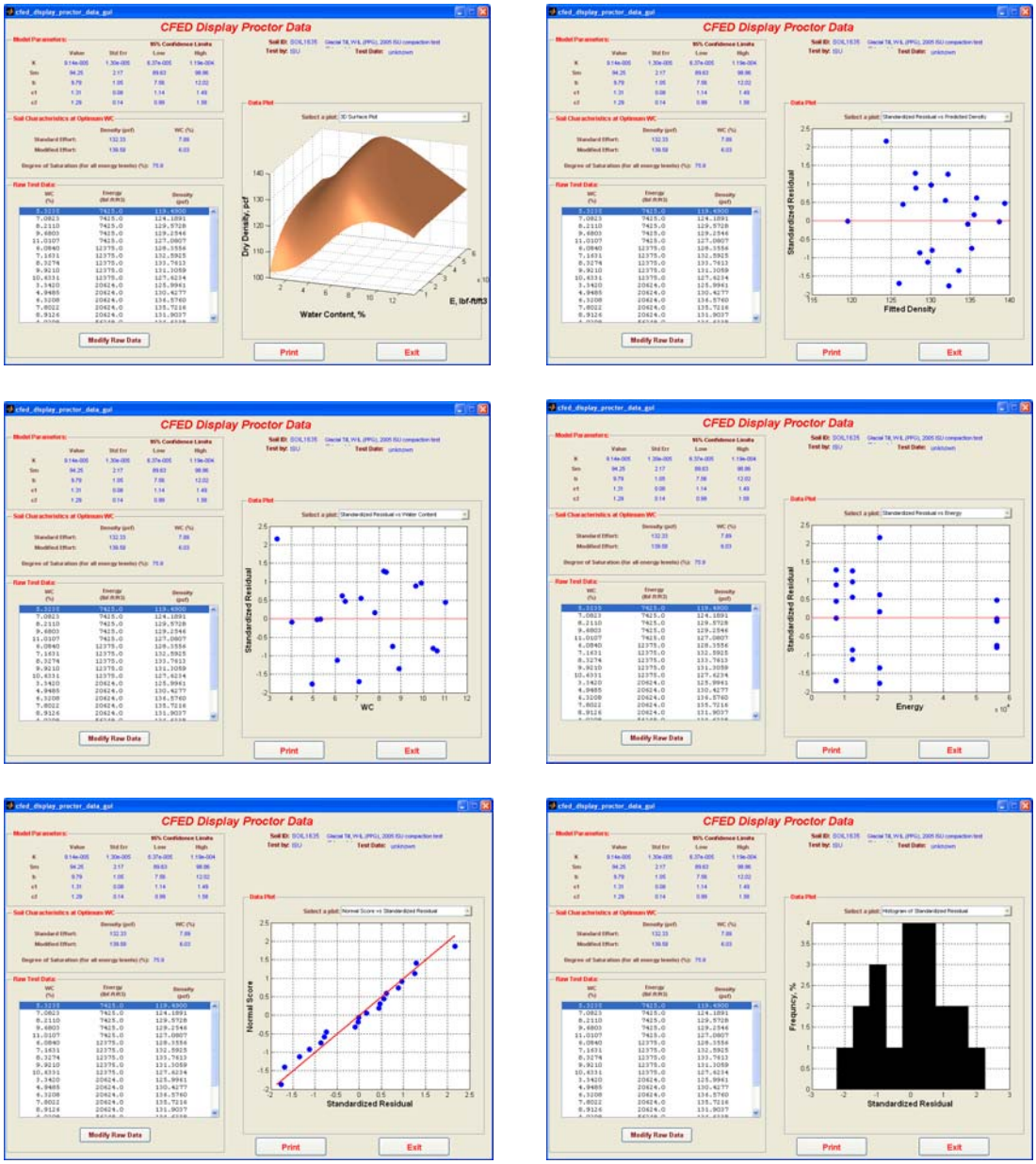


**Figure 218: Continued**

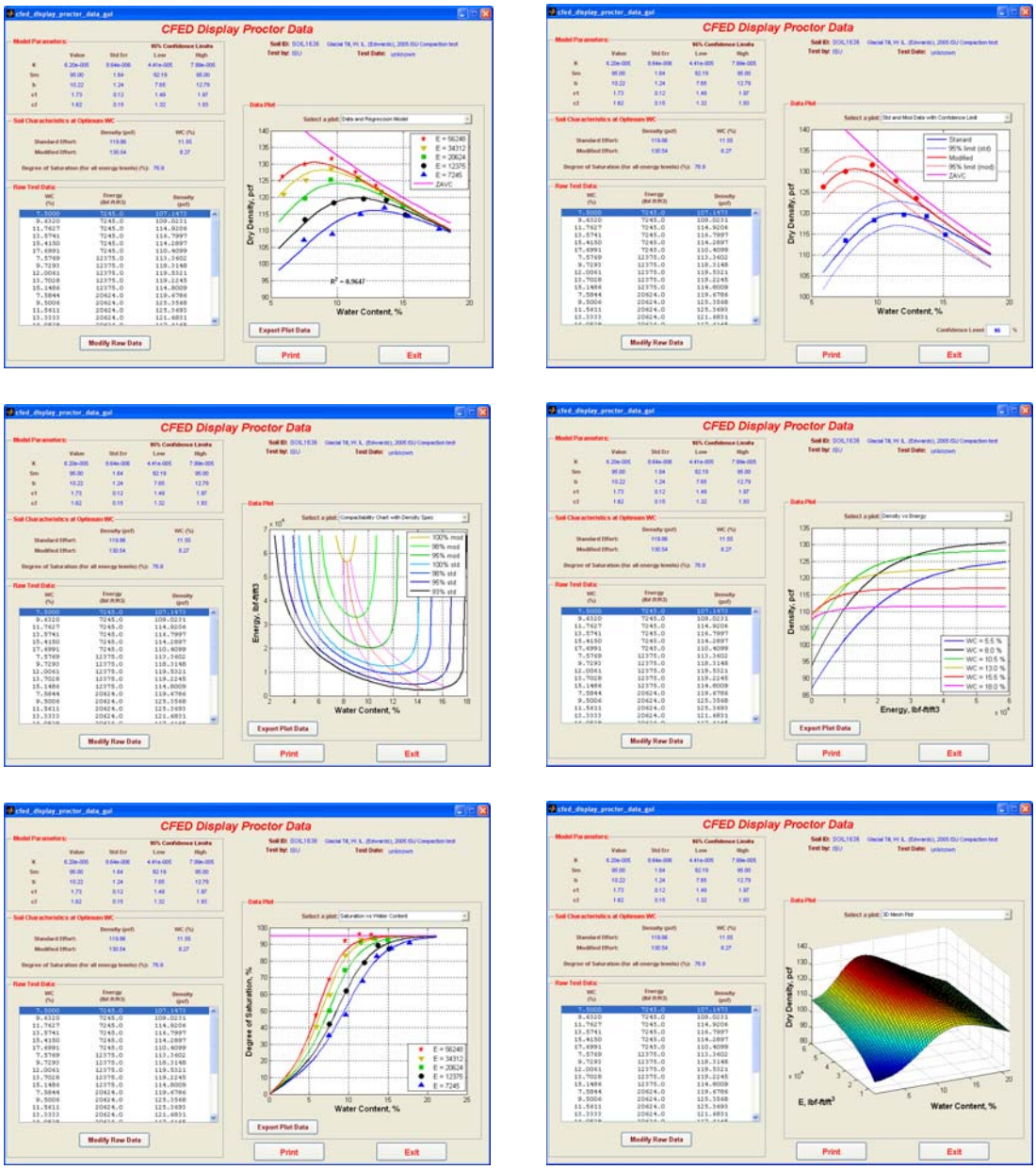


**Figure 219: Soil 1636 CFED outputs**

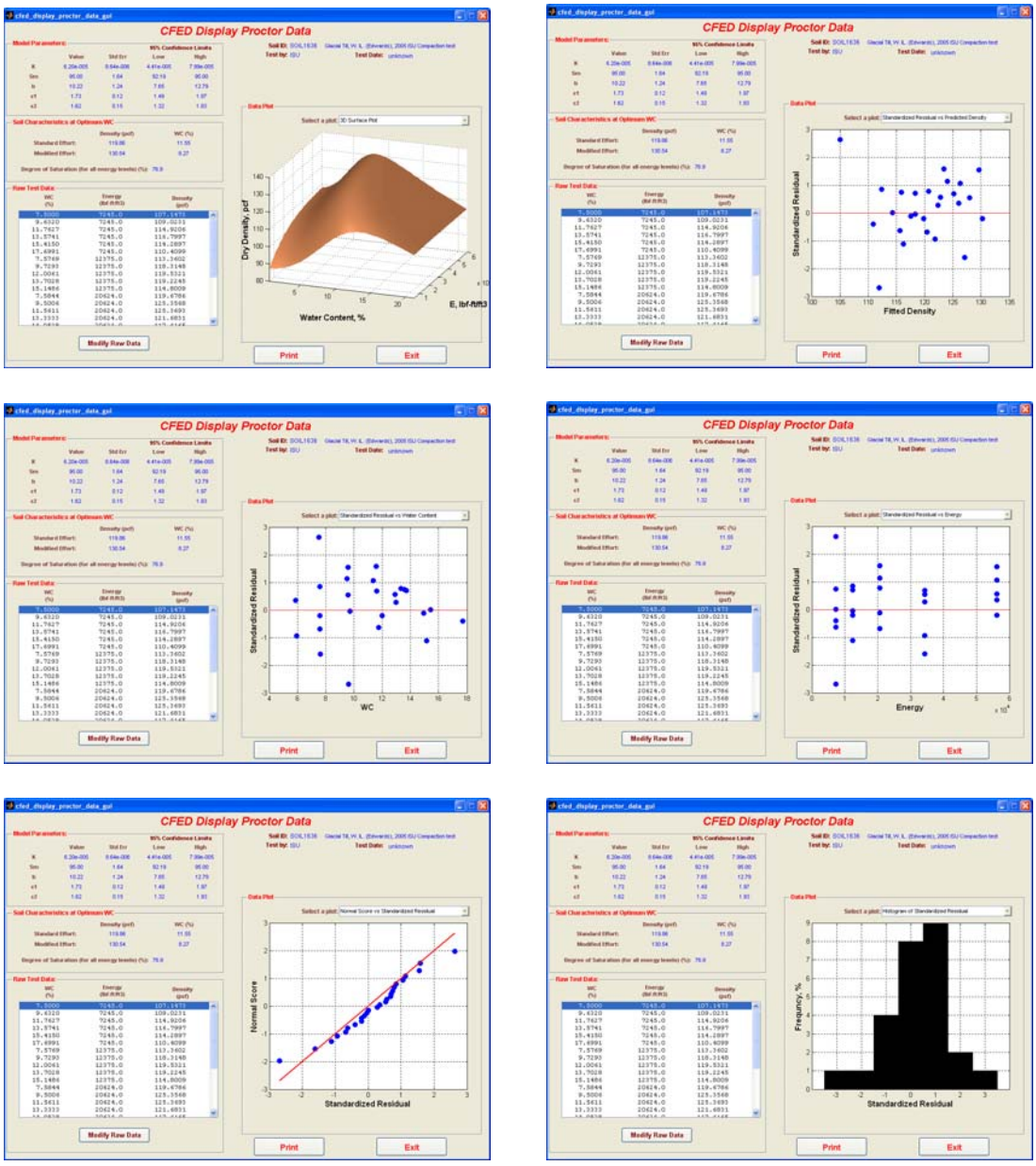


**Figure 219: Continued**

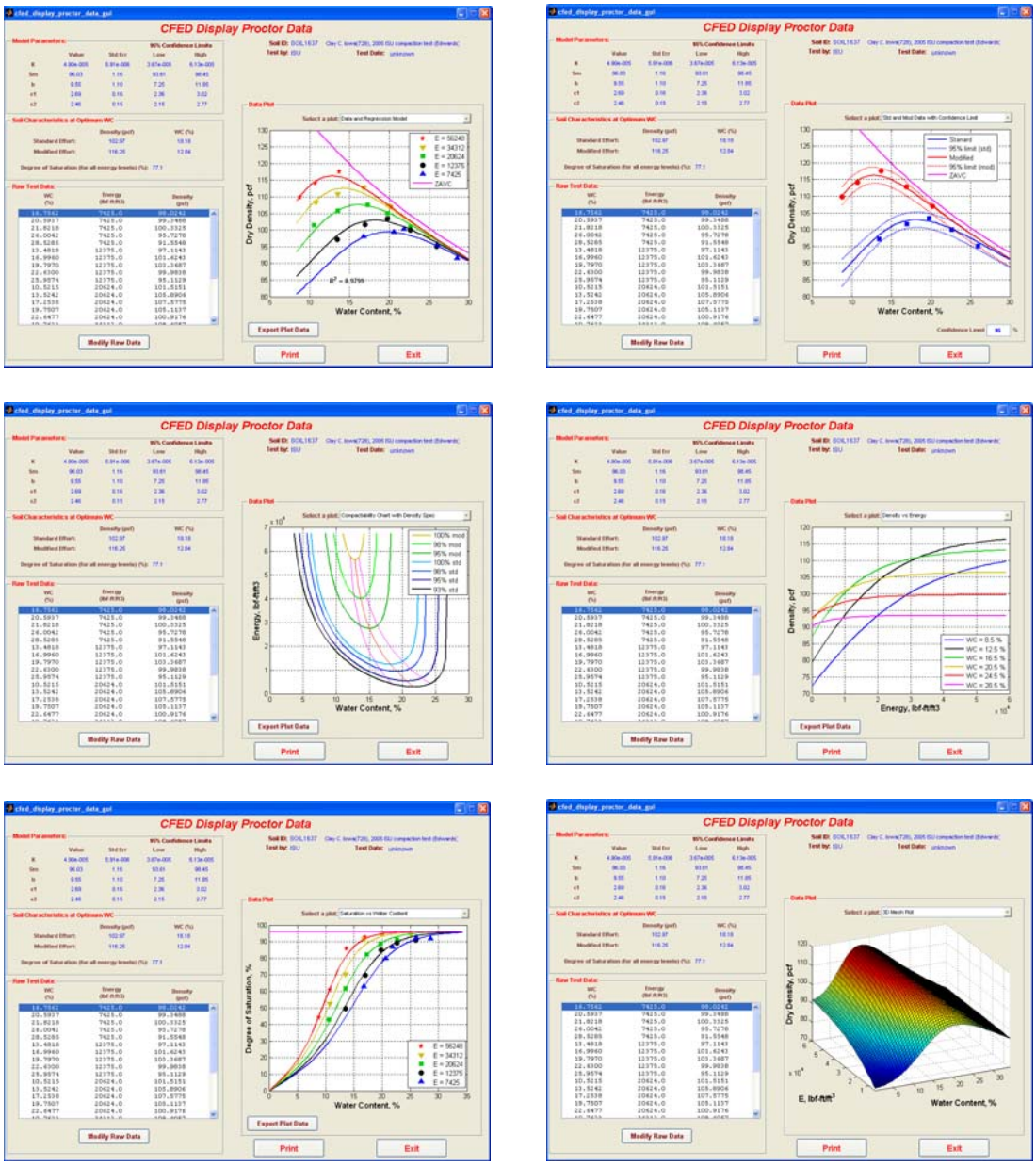


**Figure 220: Soil 1637 CFED outputs**

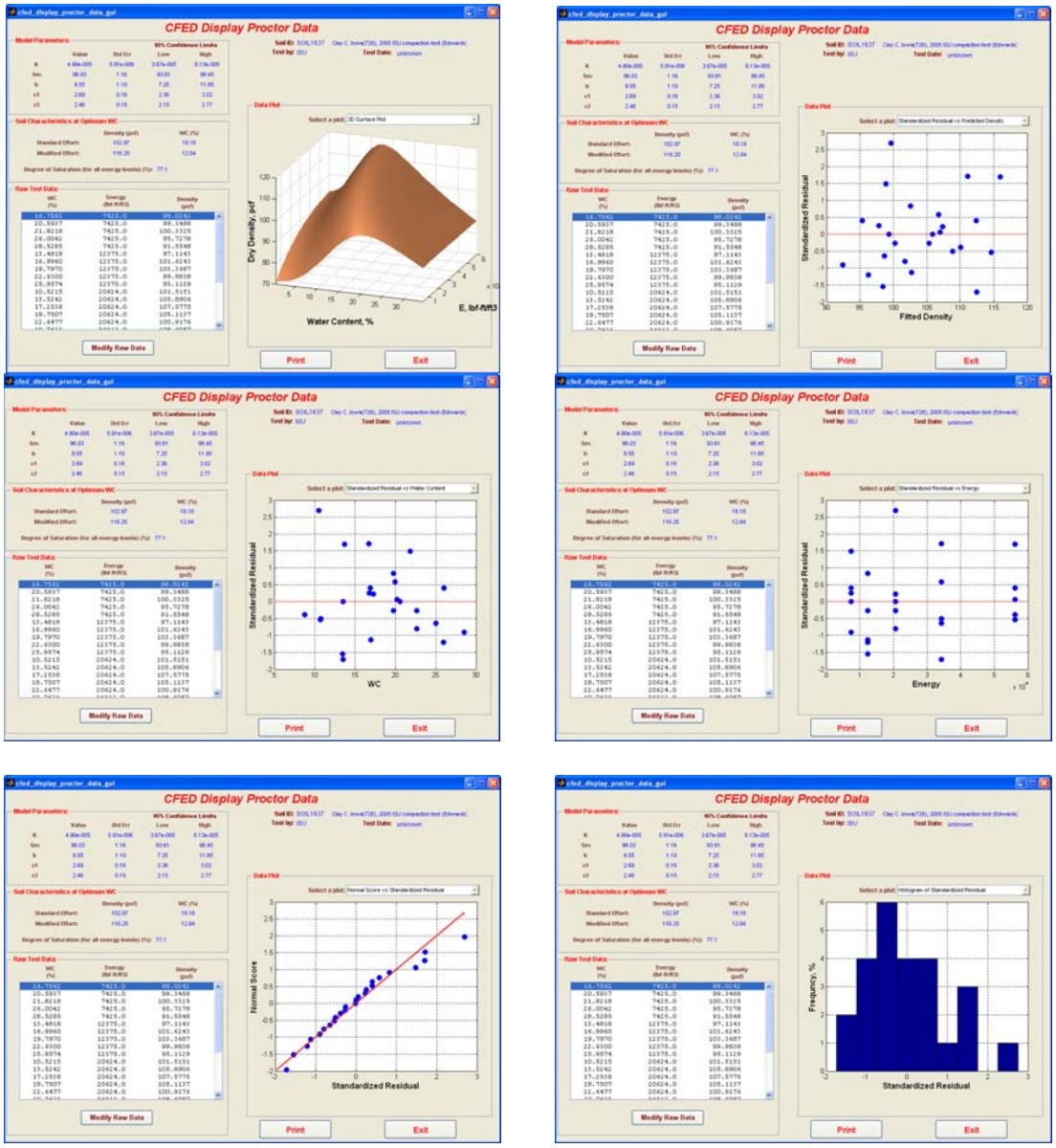


**Figure 220: Continued**

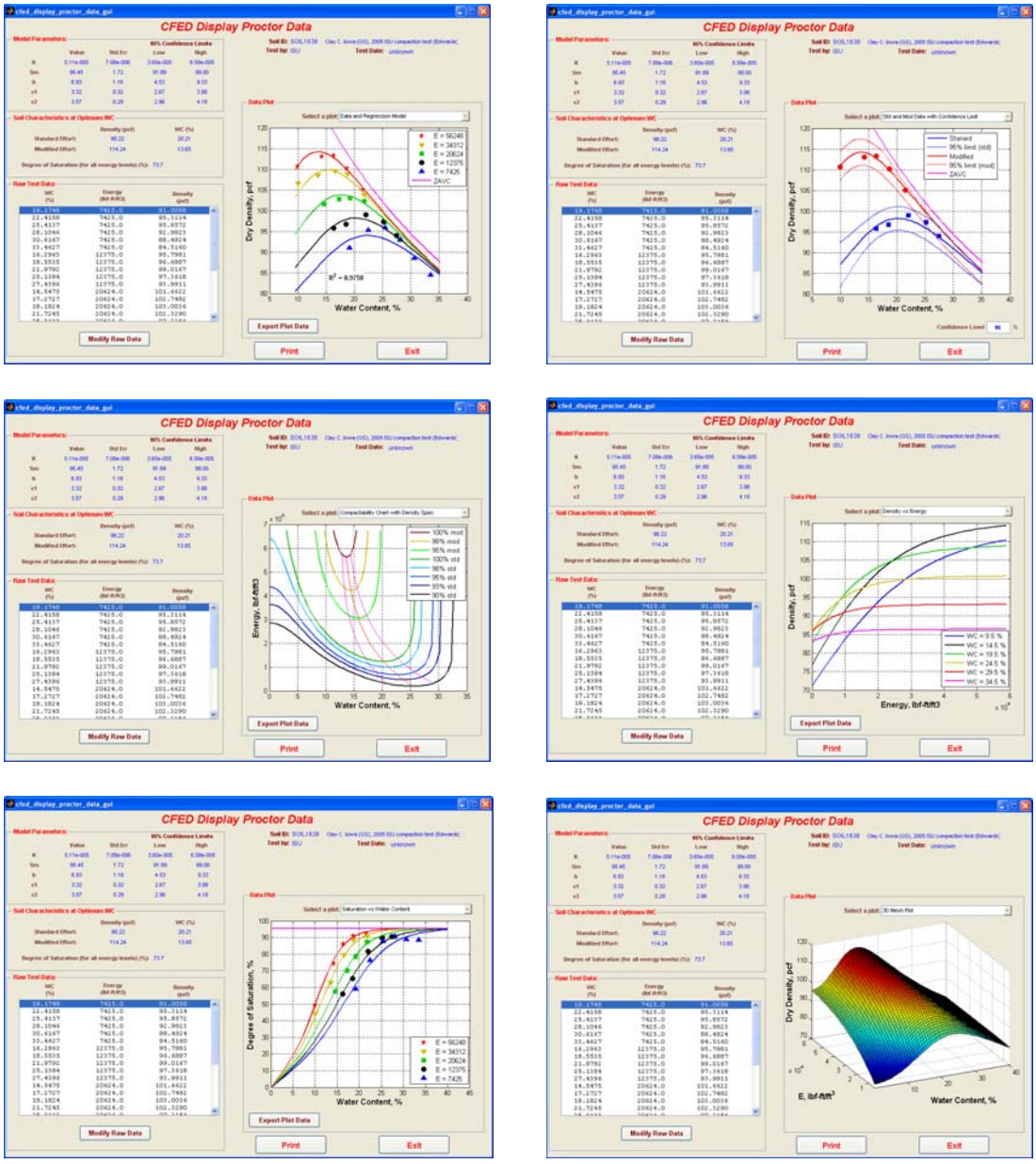


**Figure 221: Soil 1638 CFED outputs**

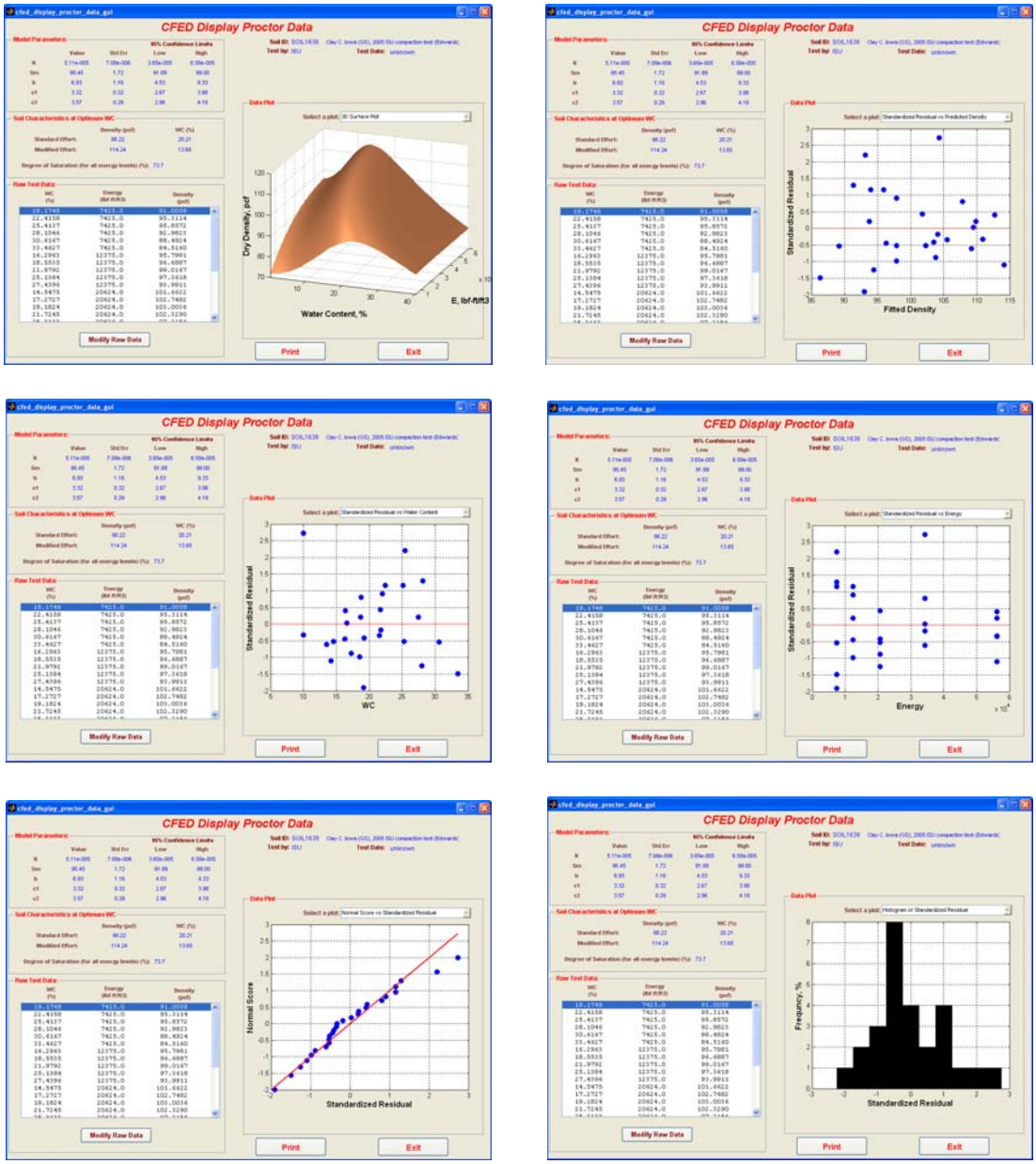


**Figure 221: Continued**

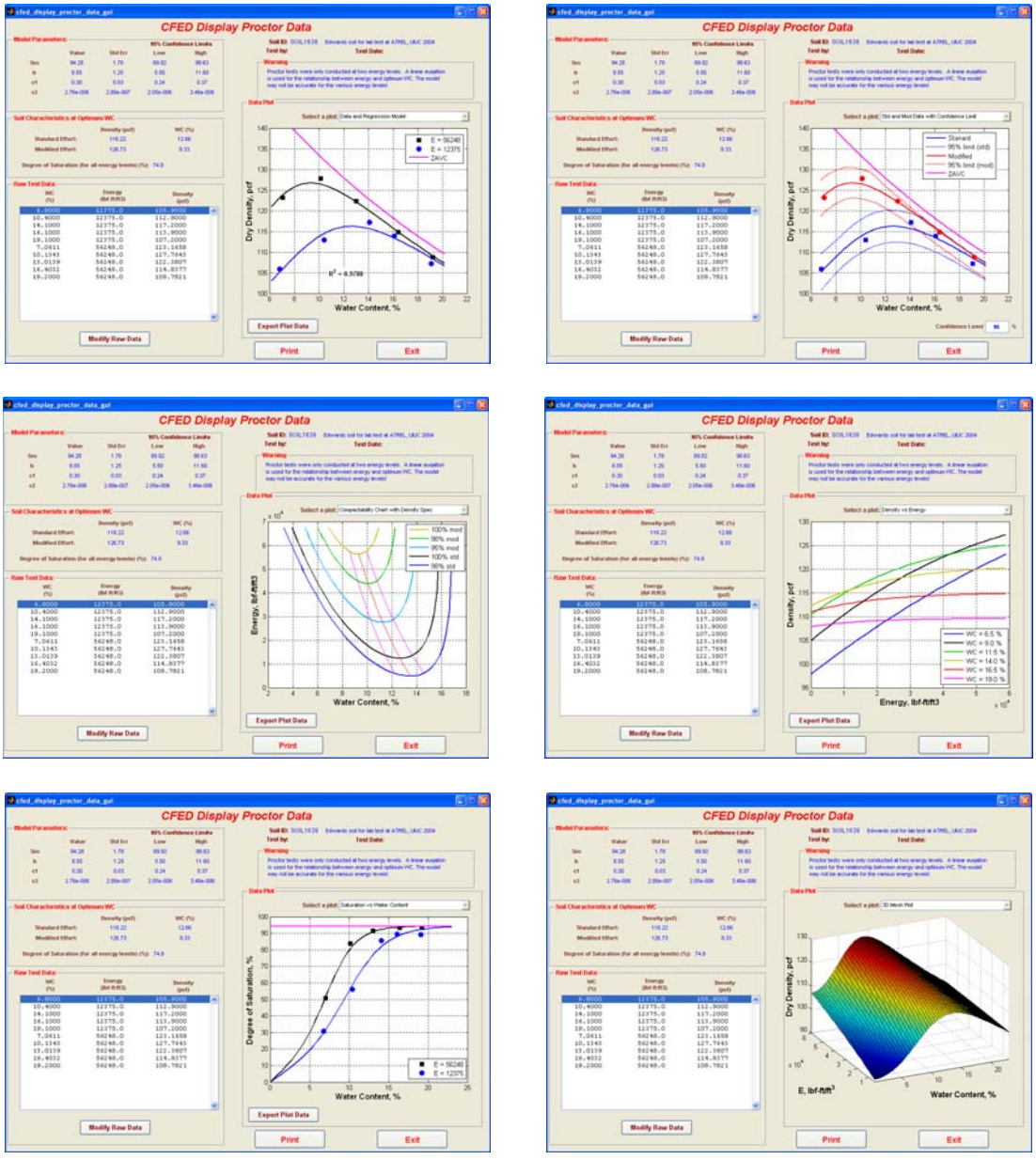


**Figure 222: Soil 1639 CFED outputs**

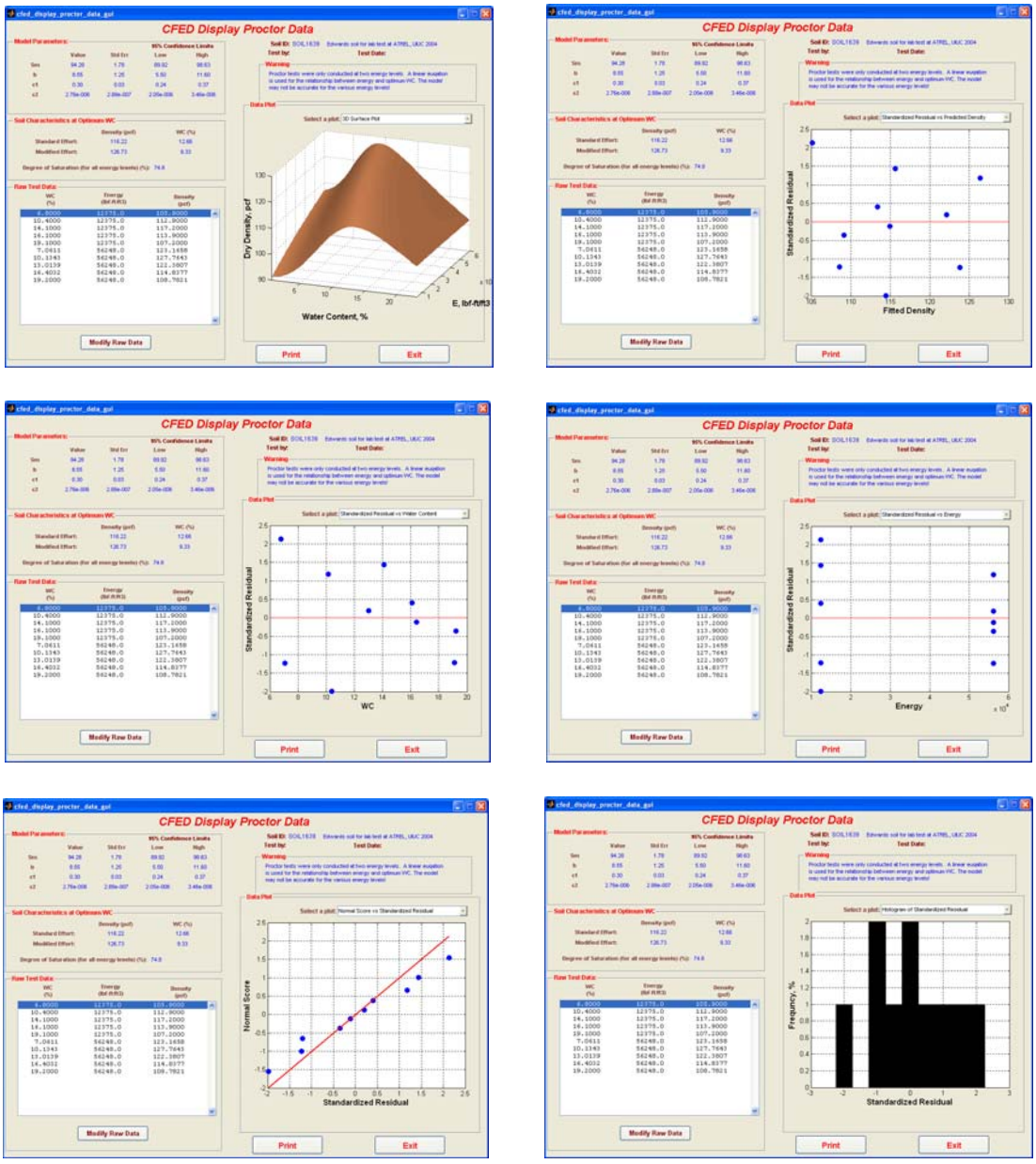


**Figure 222: Continued**

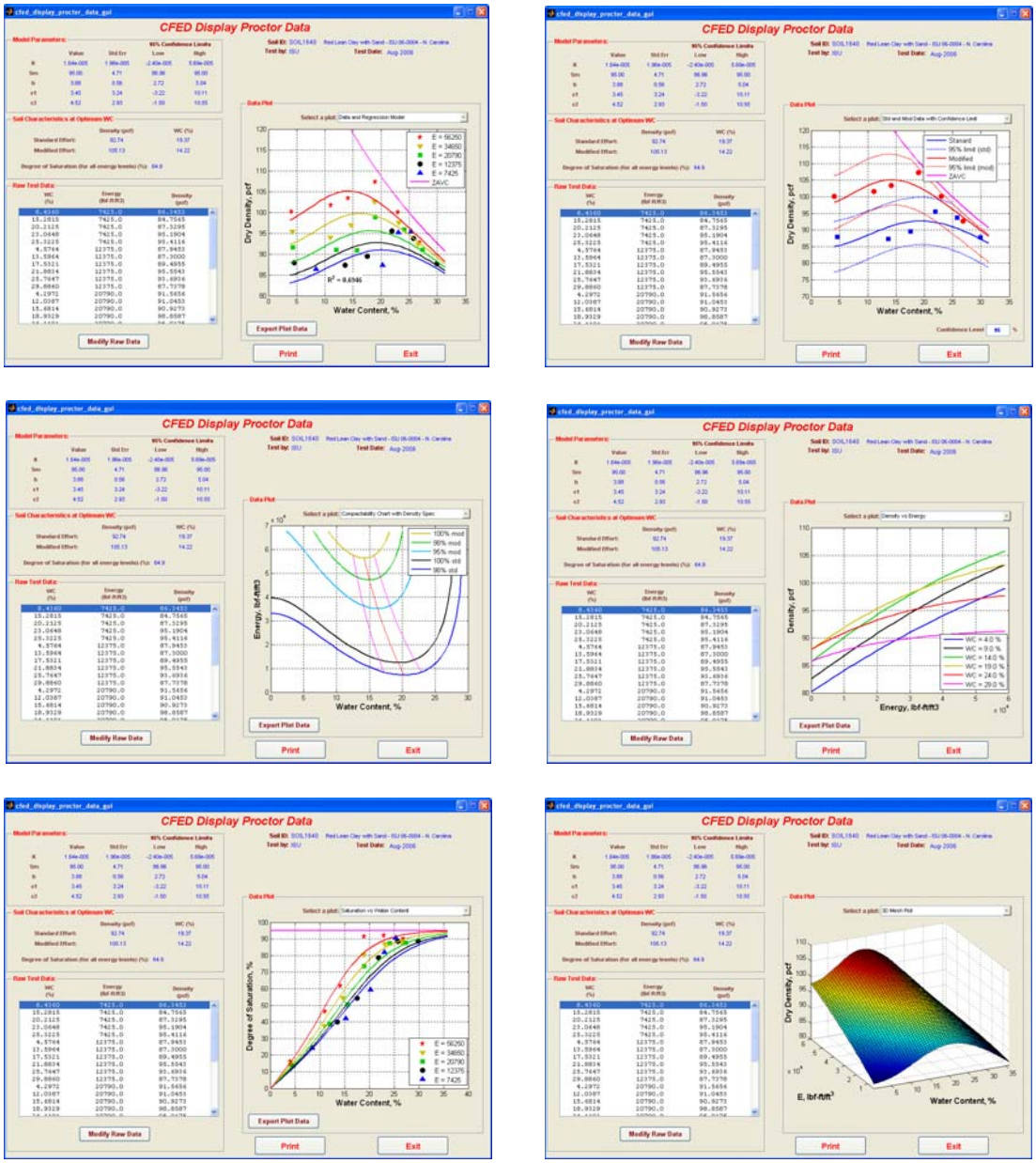


**Figure 223: Soil 1640 CFED outputs**

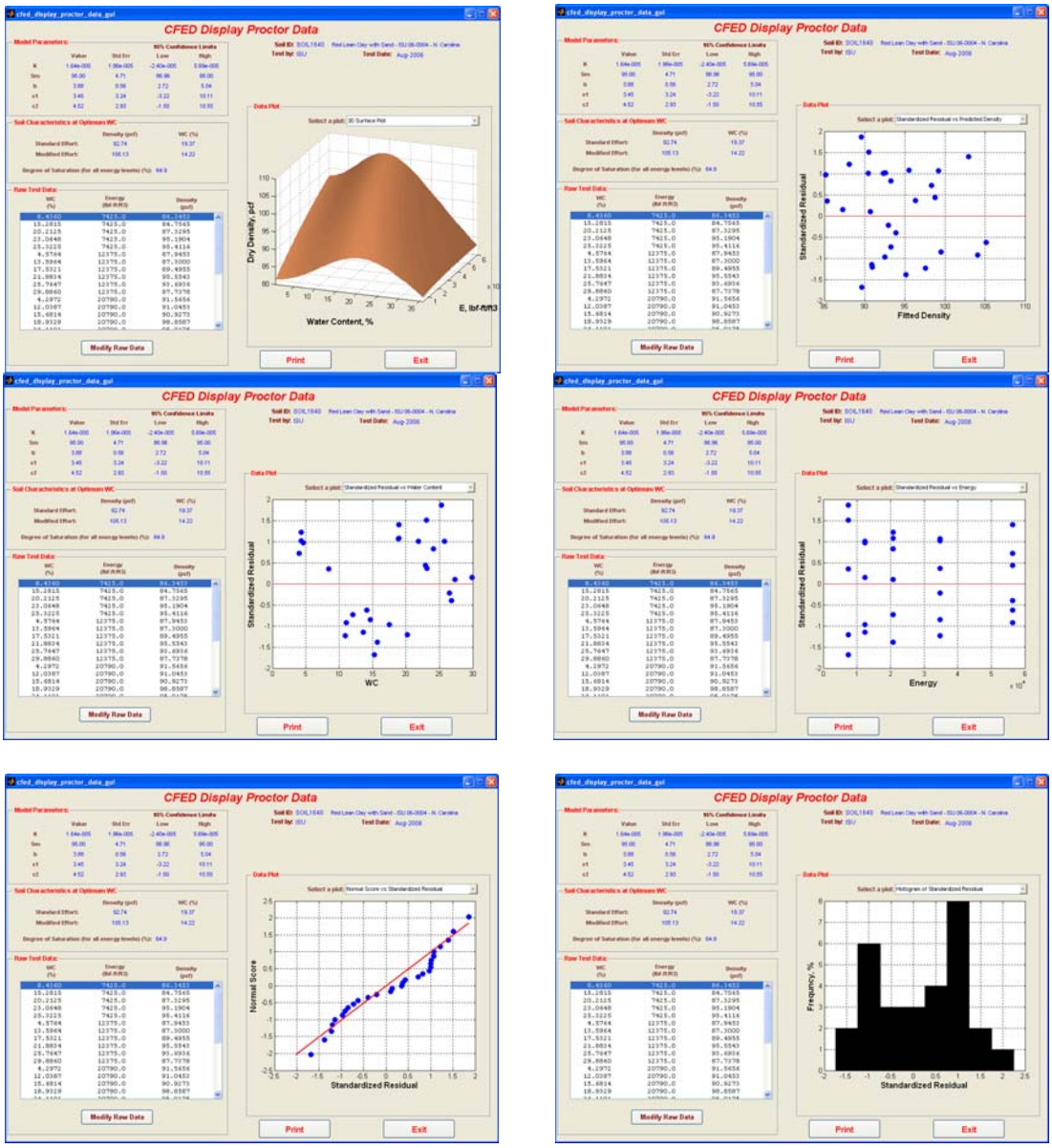


**Figure 223: Continued**

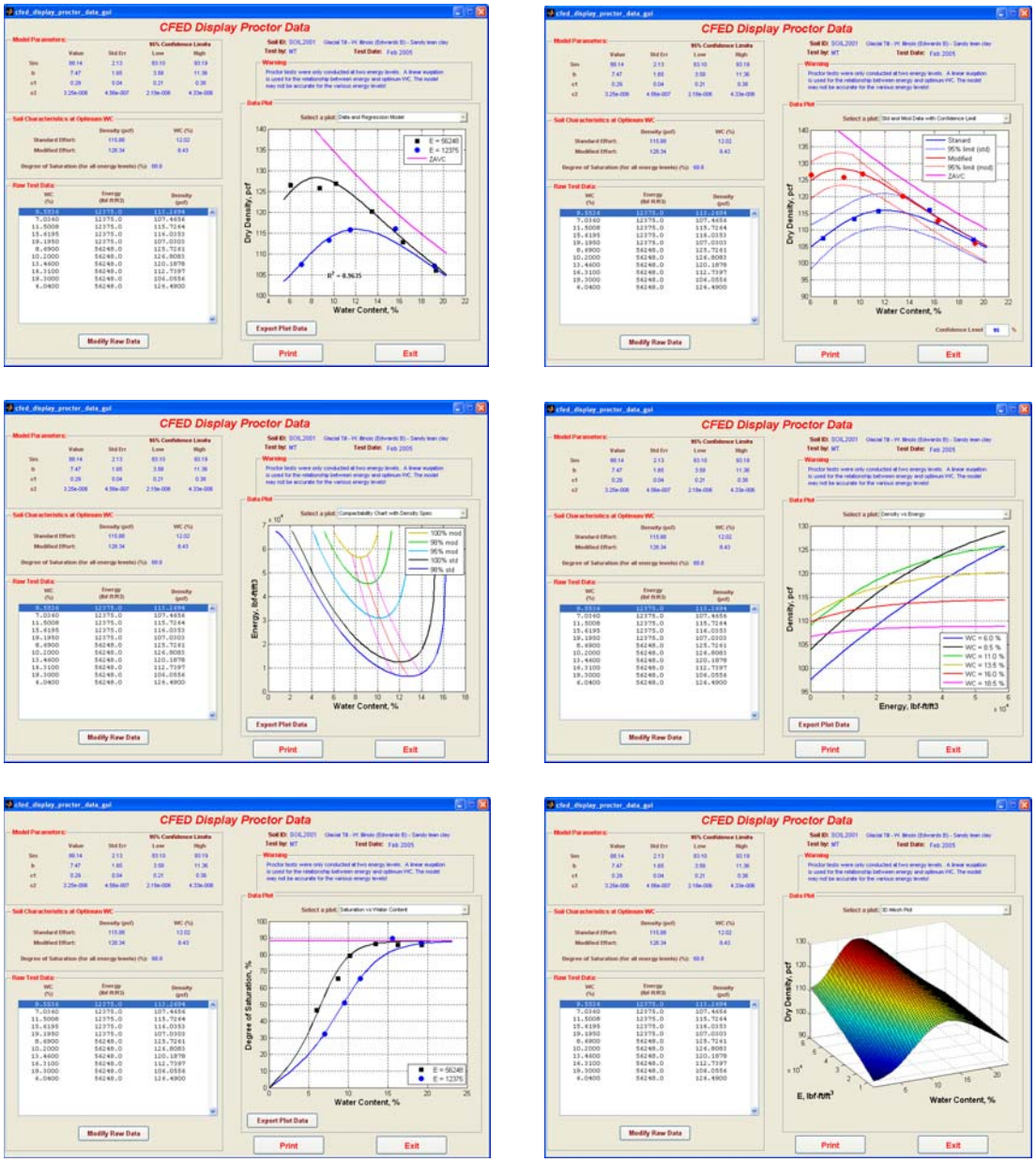


**Figure 224: Soil 2001 CFED outputs**

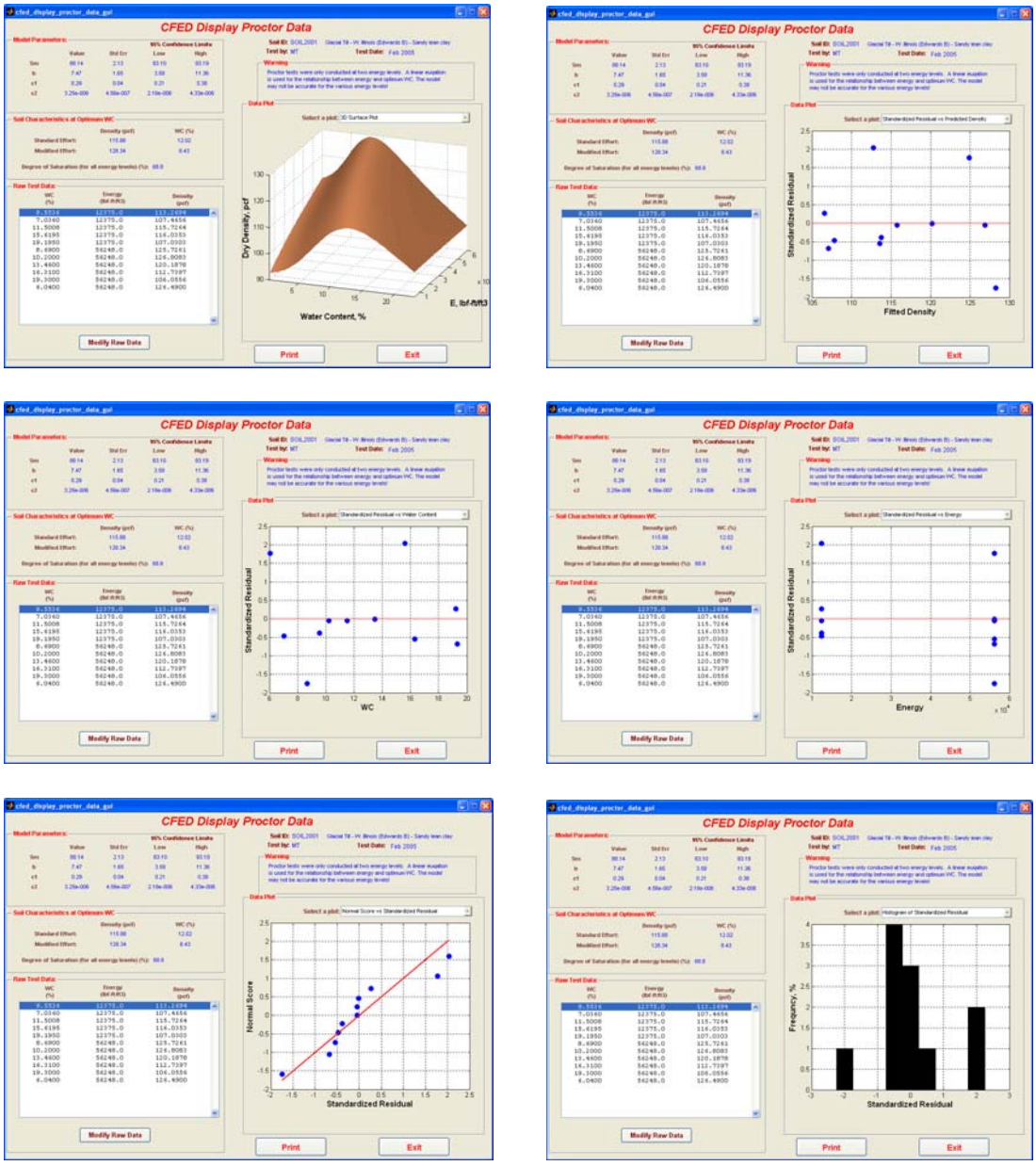


**Figure 224: Continued**

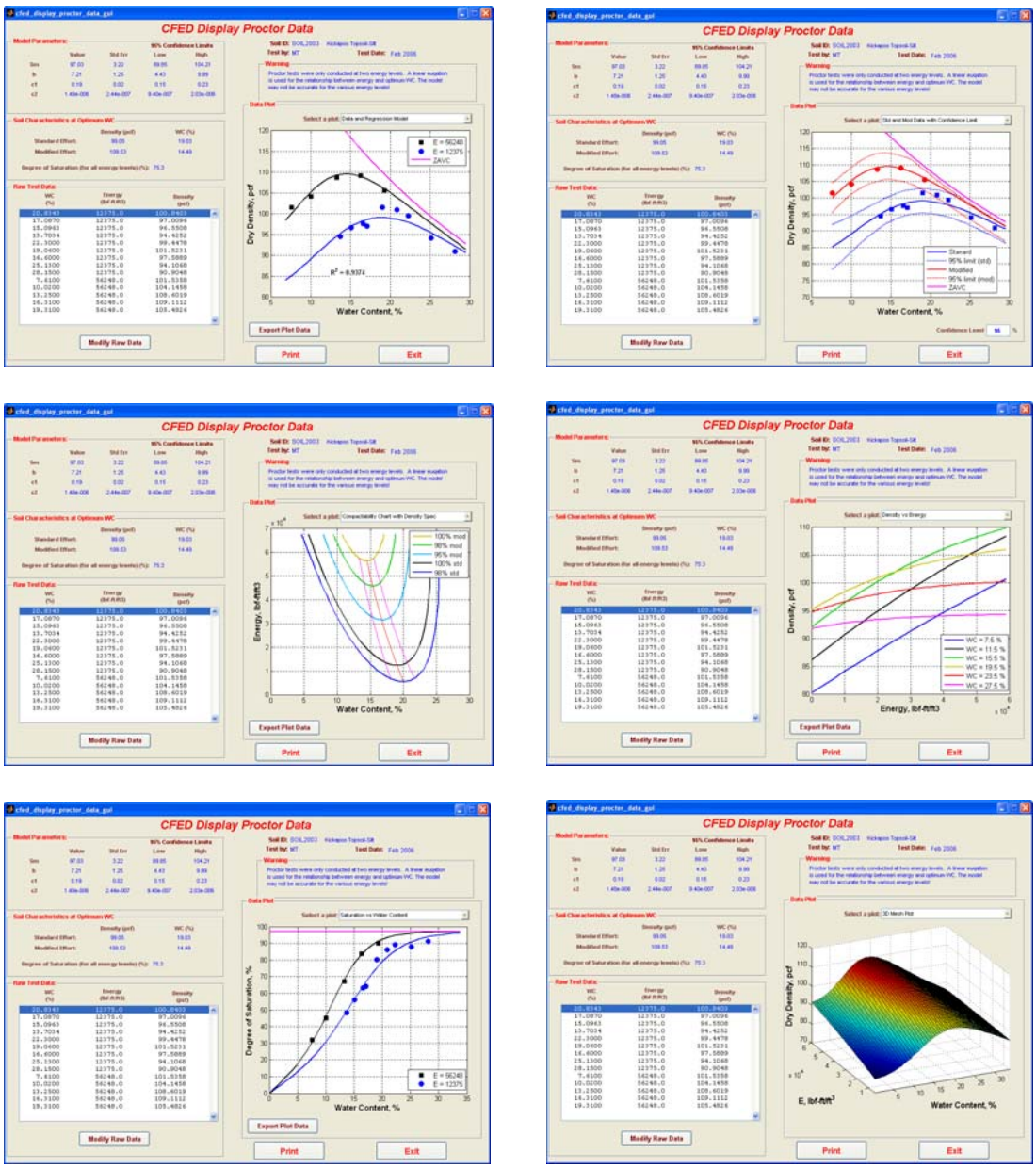


**Figure 225: Soil 2003 CFED outputs**

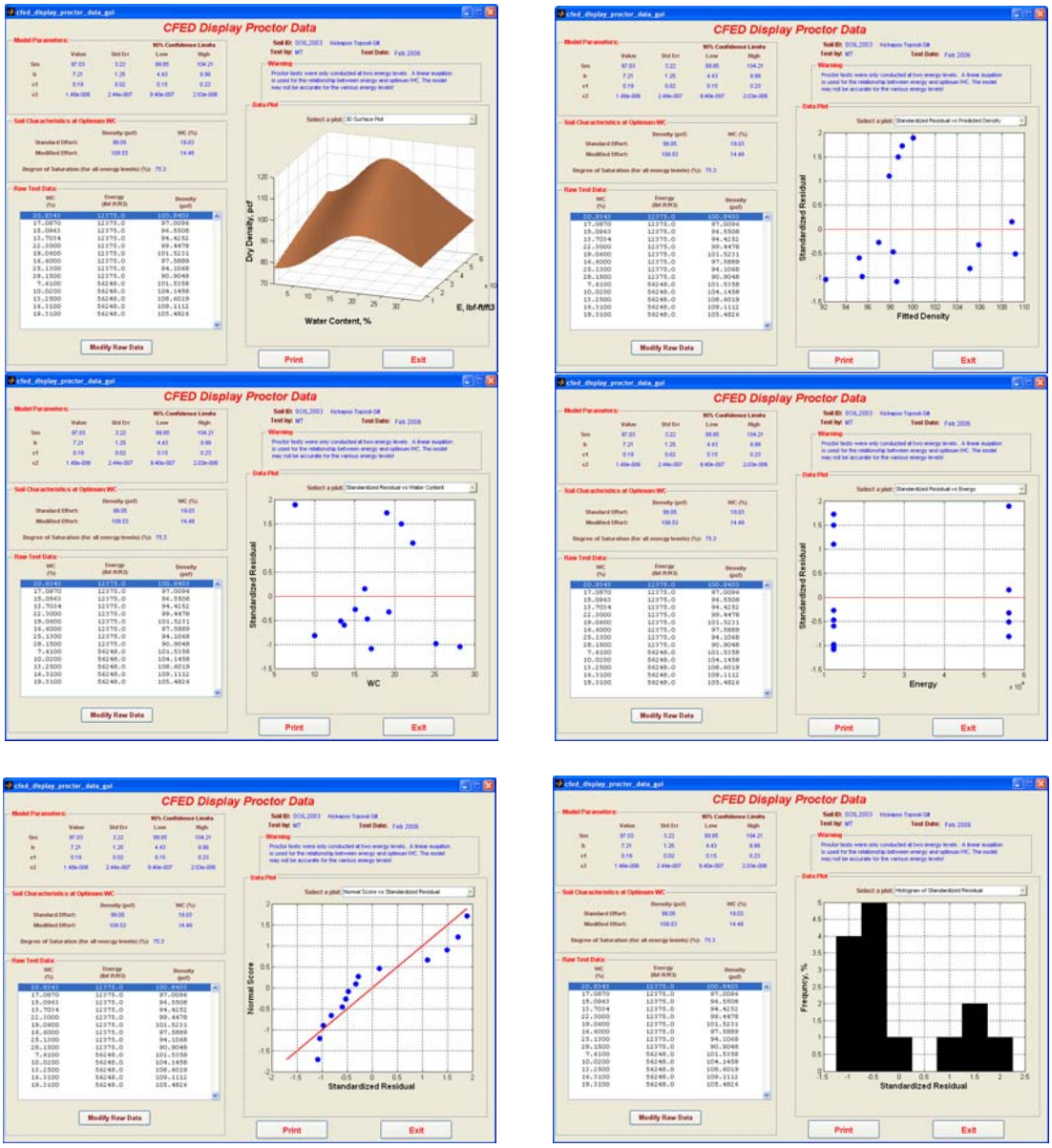


**Figure 225: Continued**

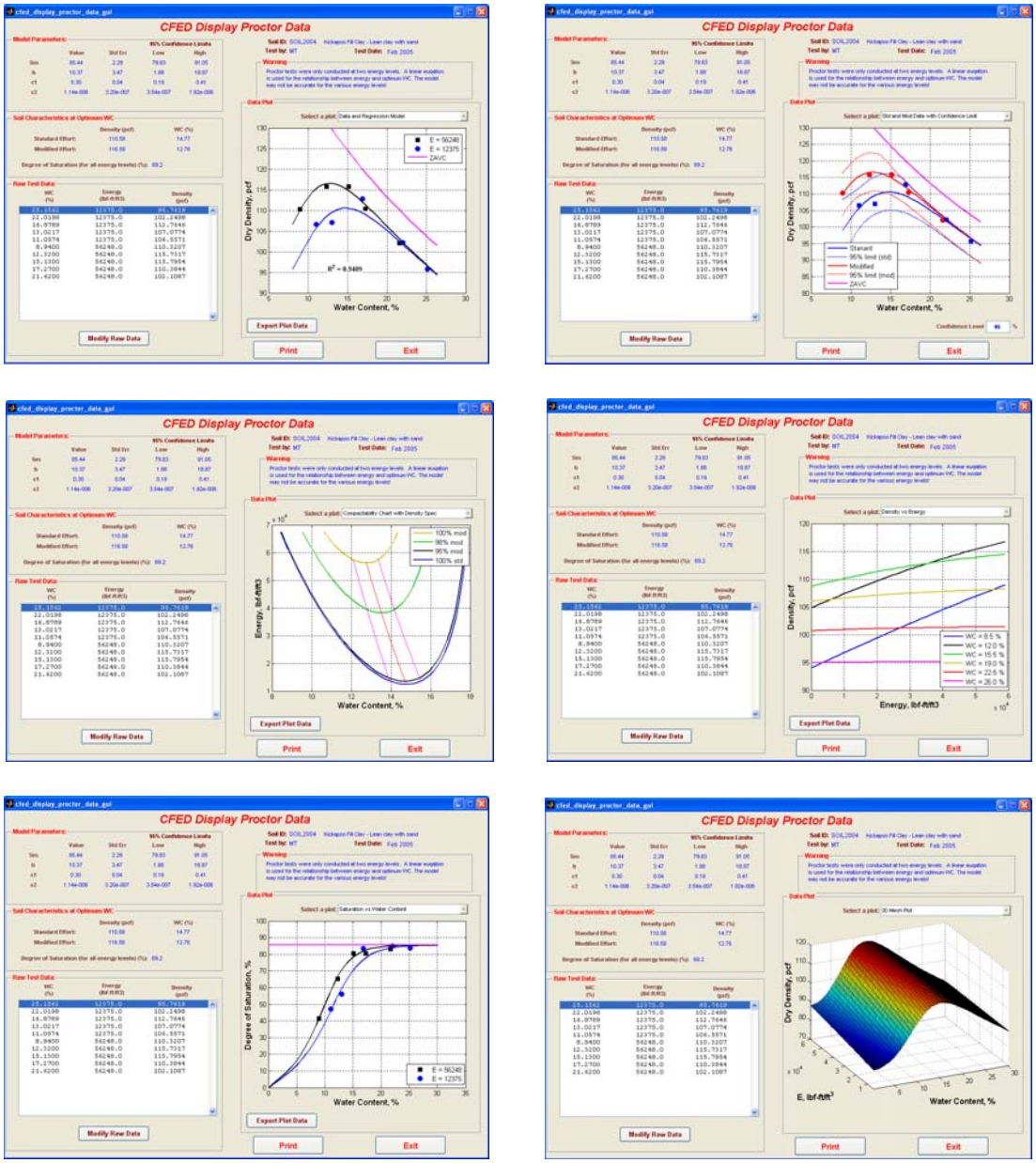


**Figure 226: Soil 2004 CFED outputs**

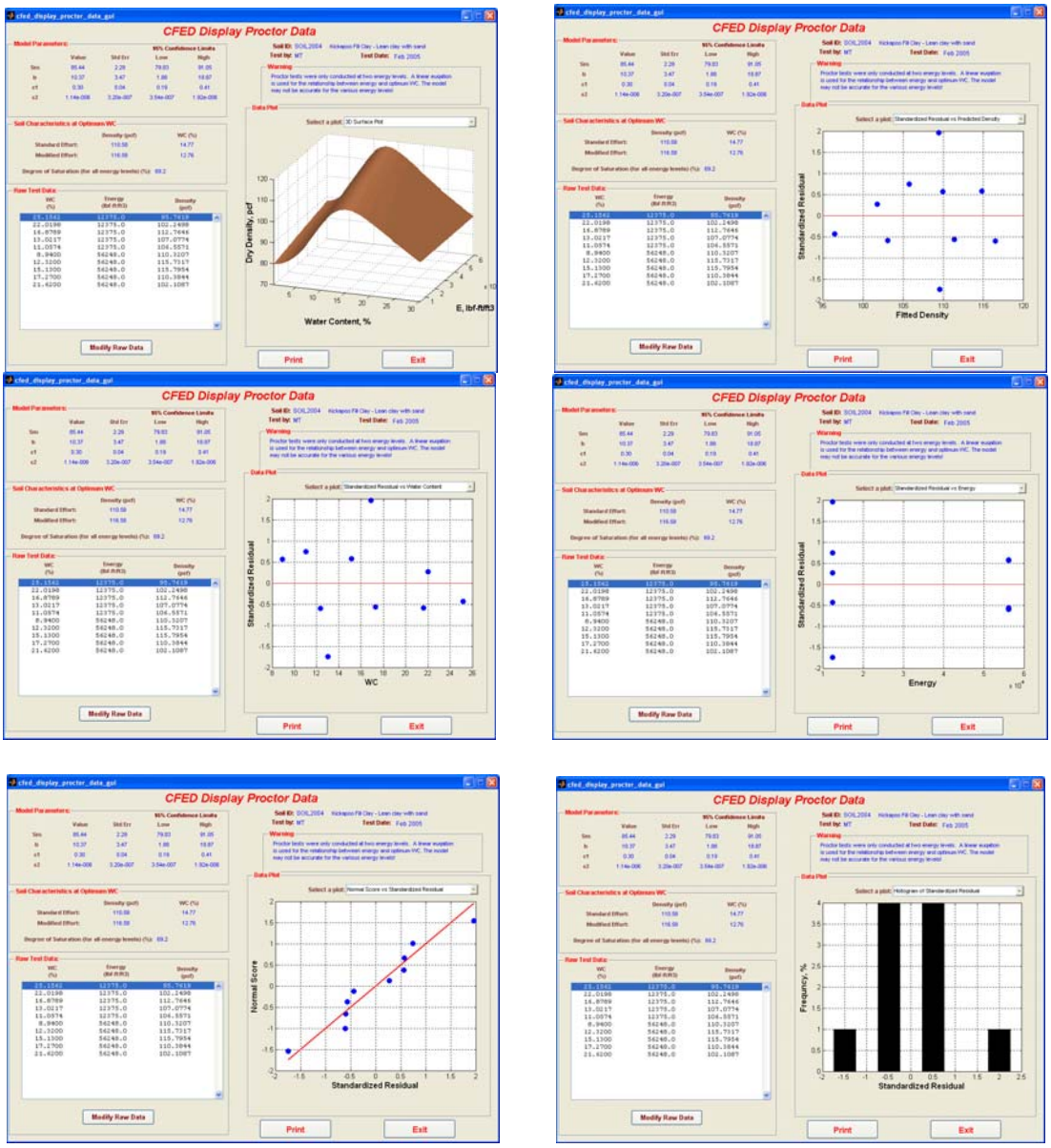


**Figure 226: Continued**

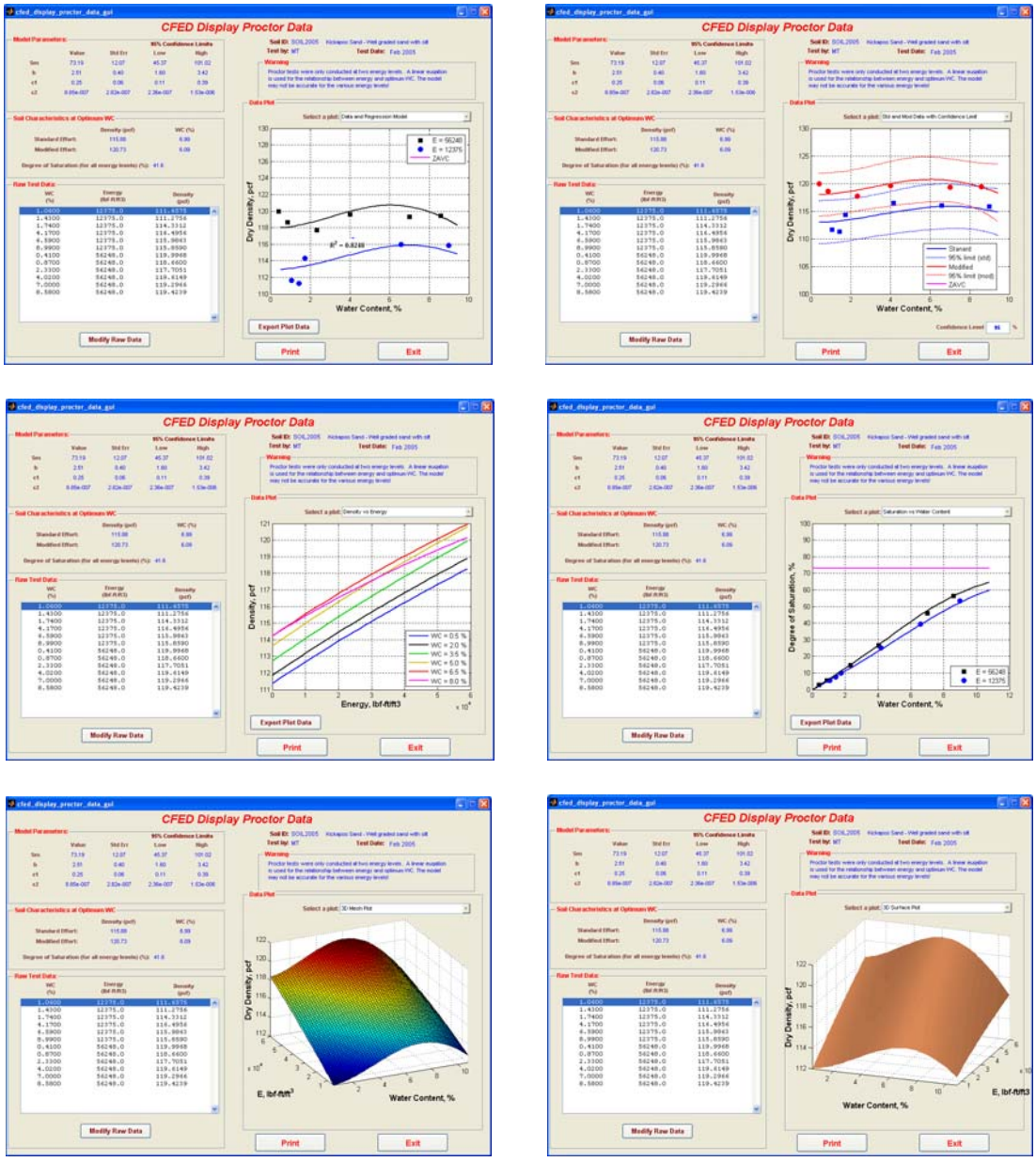


**Figure 227: Soil 2005 CFED outputs**

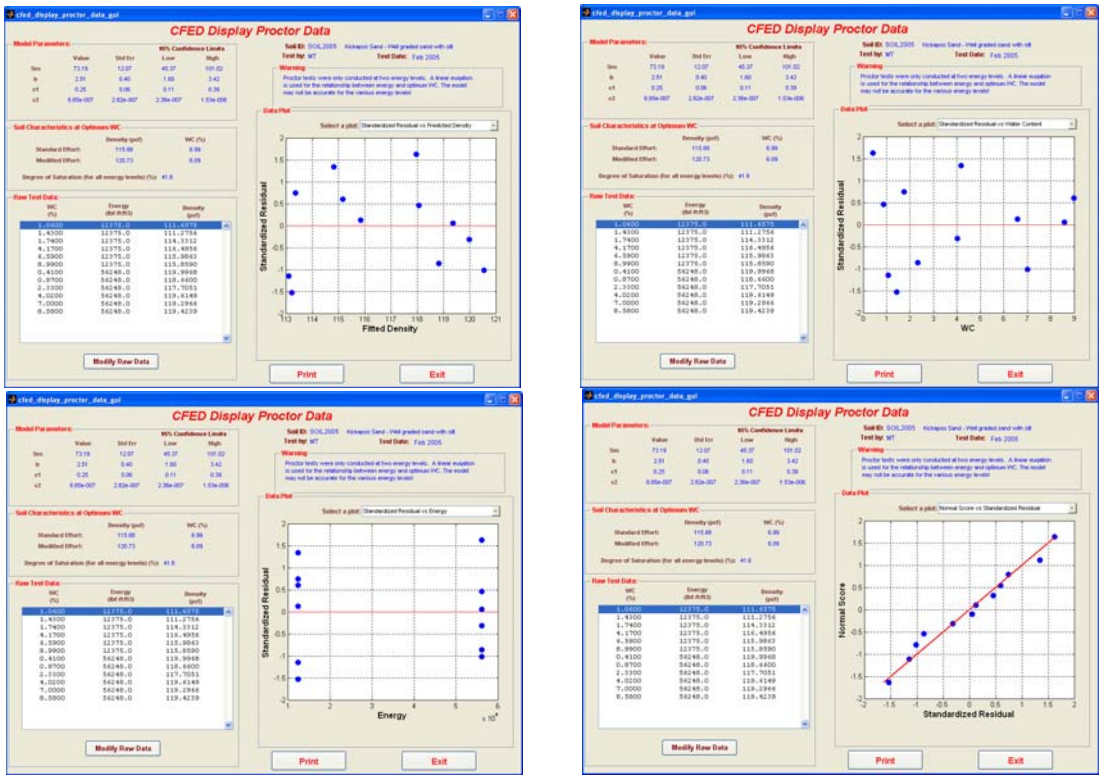


**Figure 227: Continued**

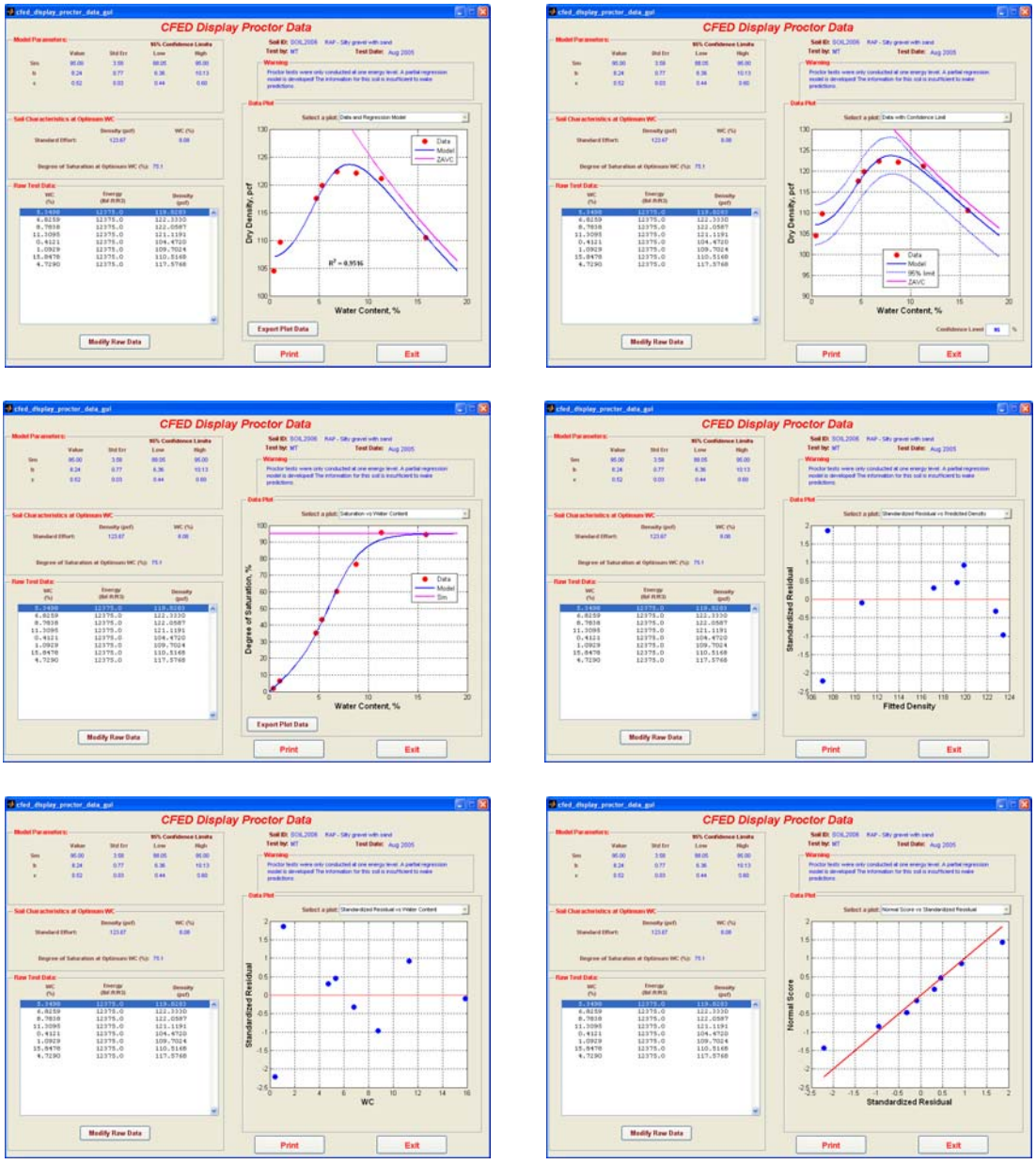


**Figure 228: Soil 2006 CFED outputs**

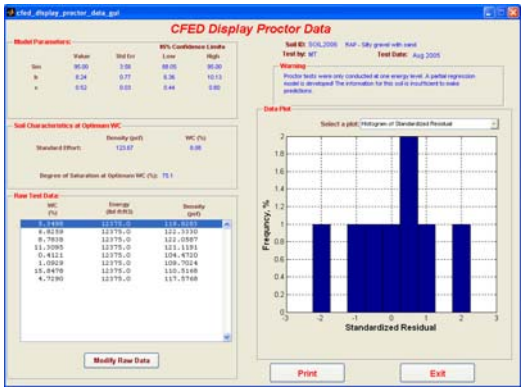


**Figure 228: Continued**

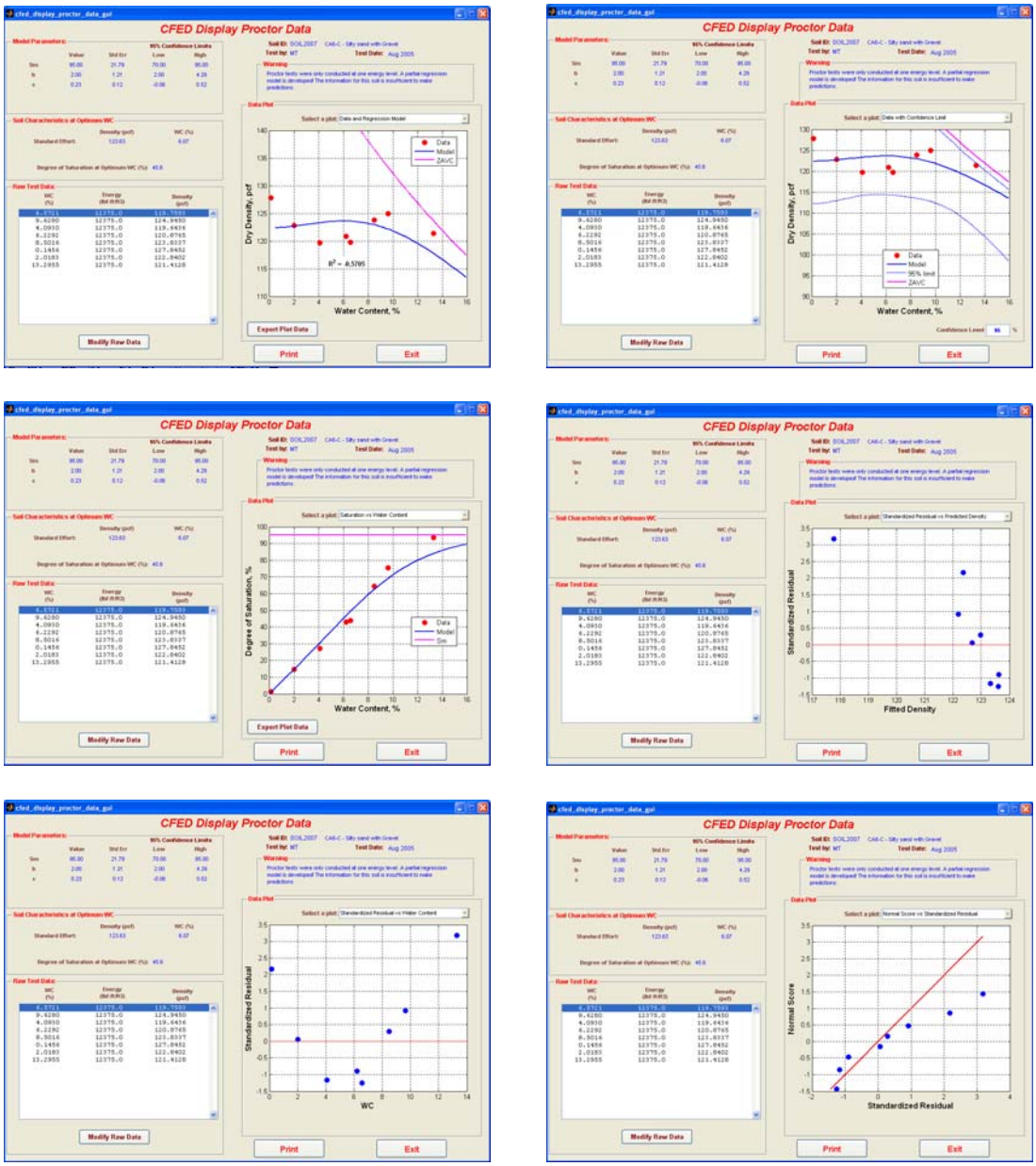


**Figure 229: Soil 2007 CFED outputs**

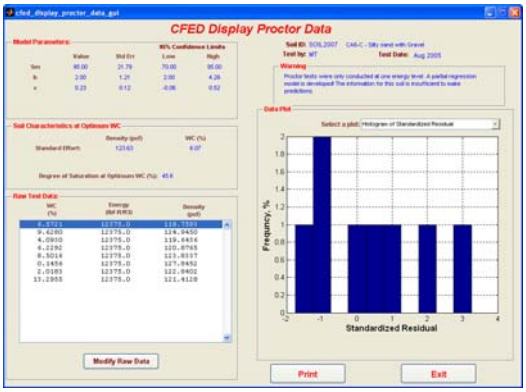


**Figure 229: Continued**

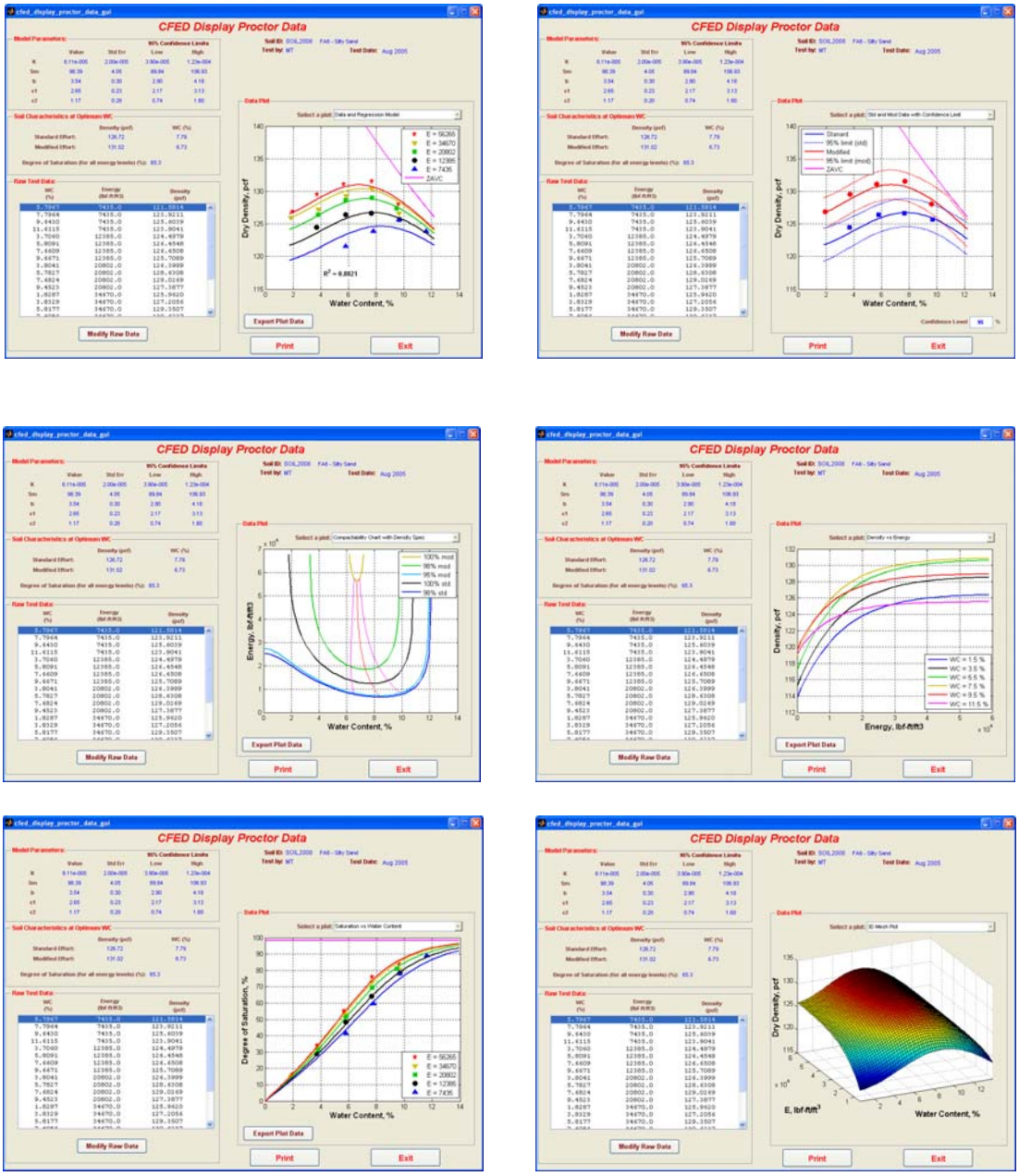


**Figure 230: Soil 2008 CFED outputs**

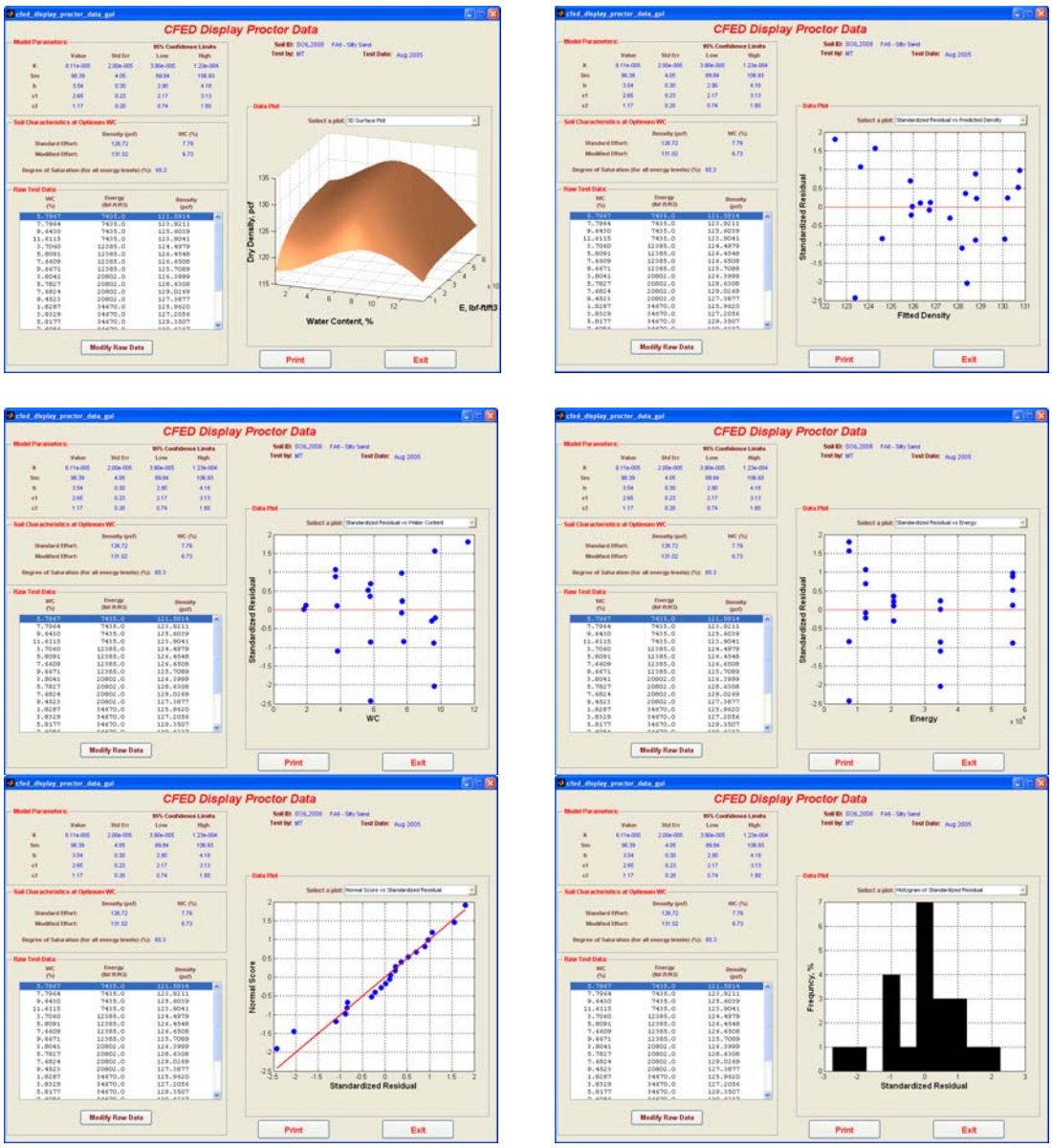


**Figure 230: Continued**

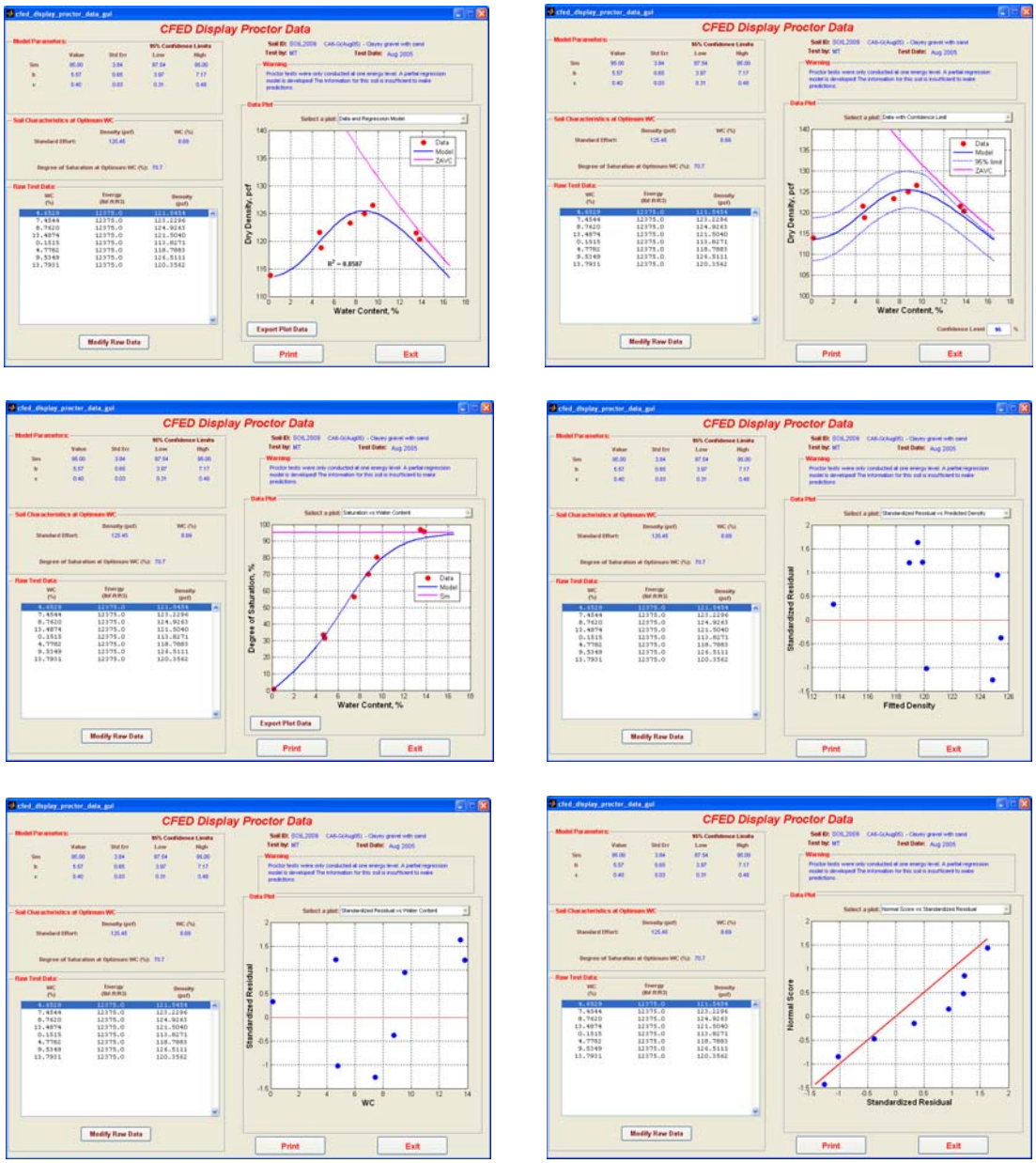


**Figure 231: Soil 2009 CFED outputs**

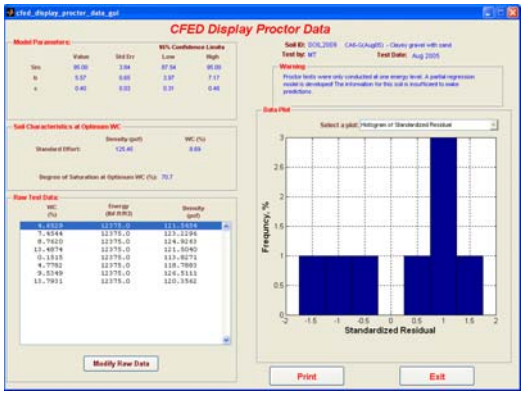


**Figure 231: Continued**

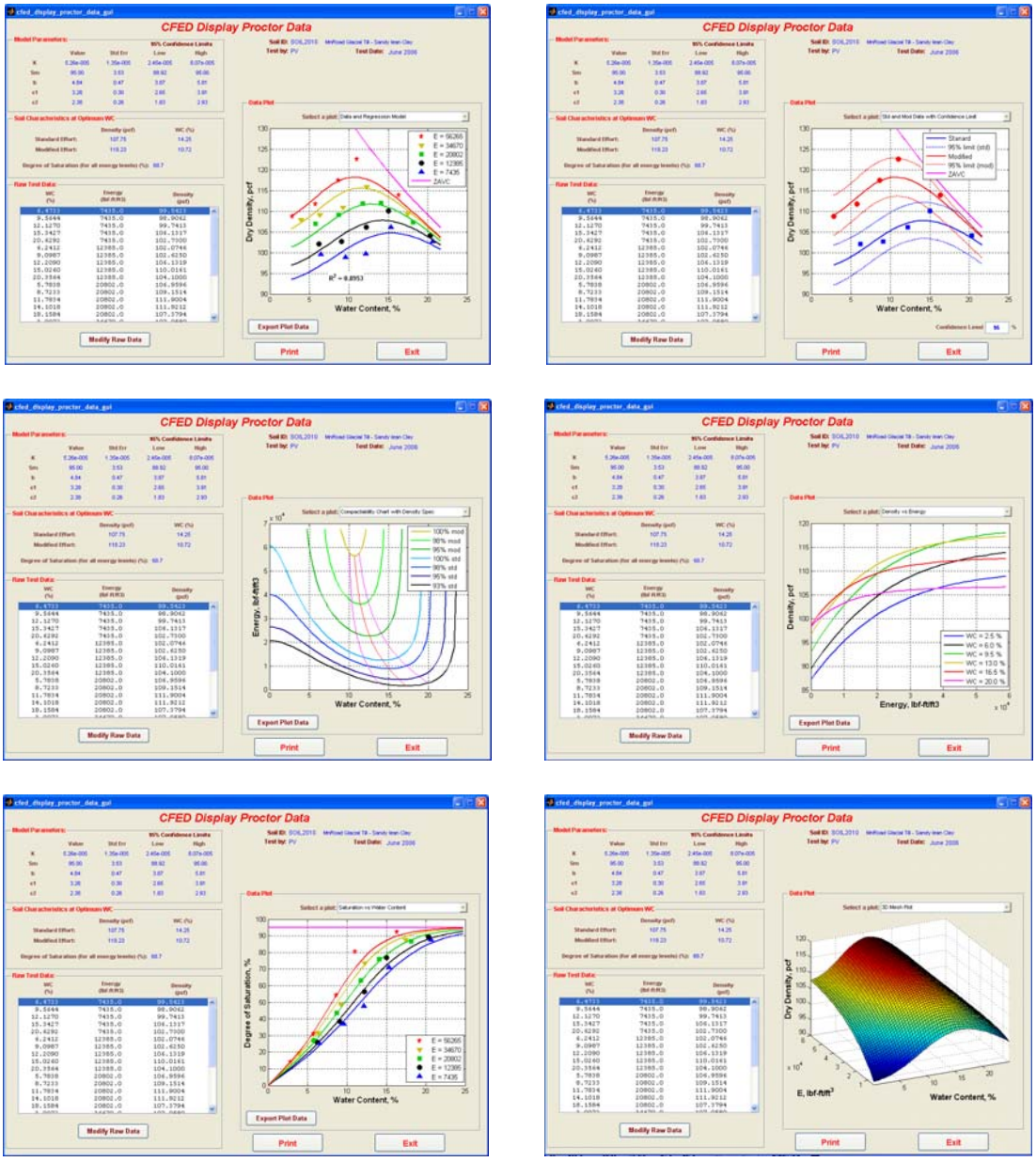


**Figure 232: Soil 2010 CFED outputs**

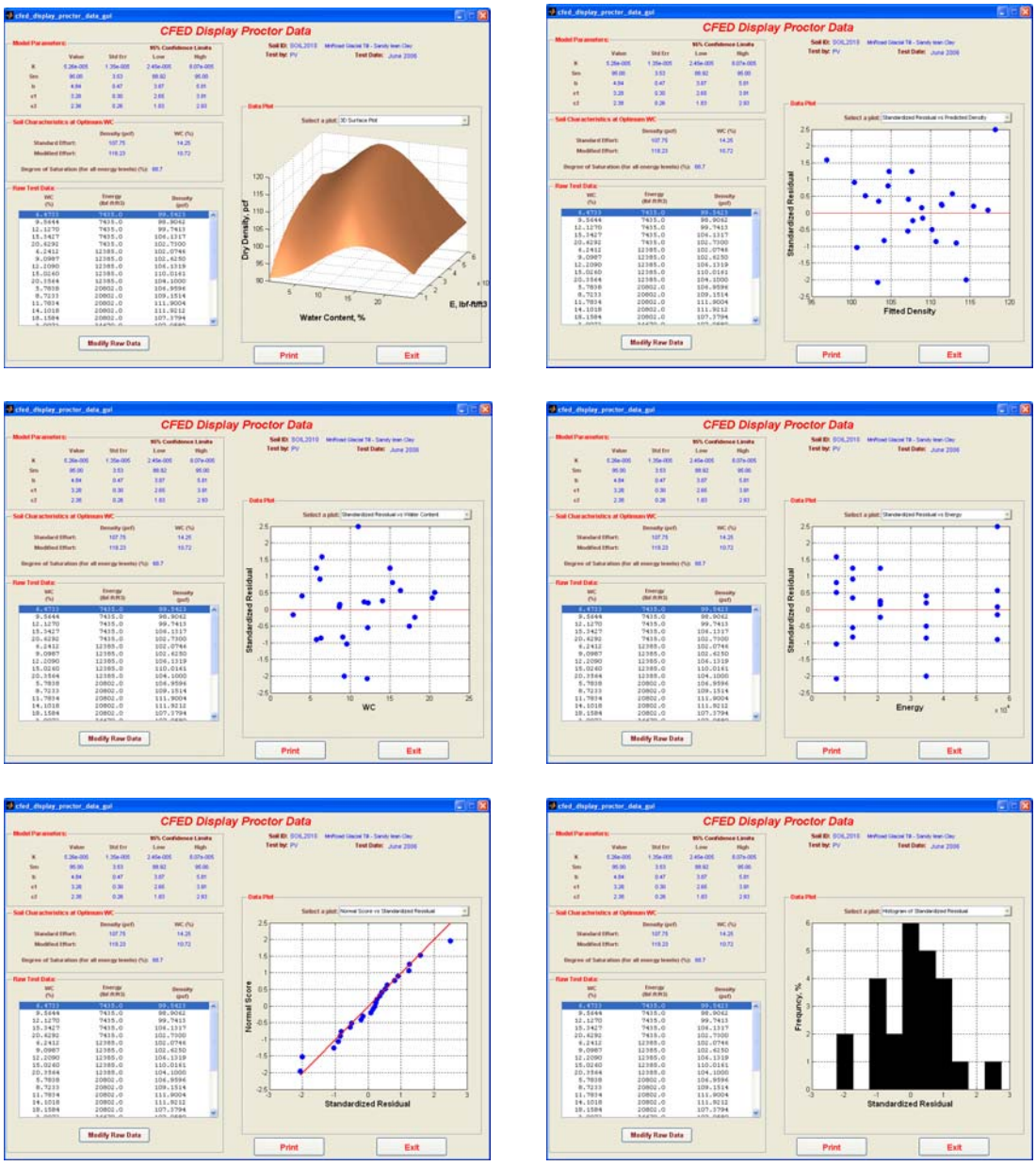


**Figure 232: Continued**

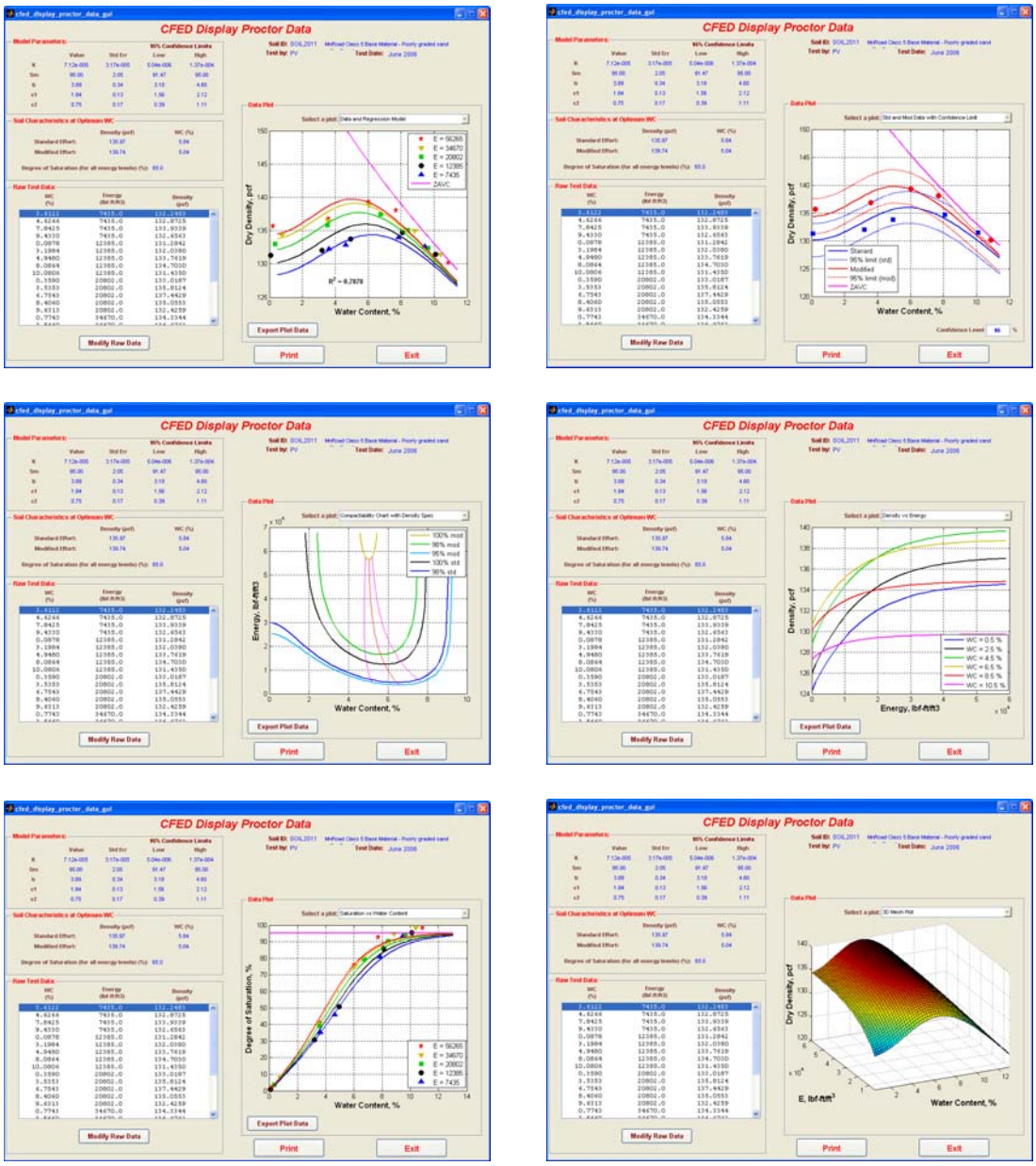


**Figure 233: Soil 2011 CFED outputs**

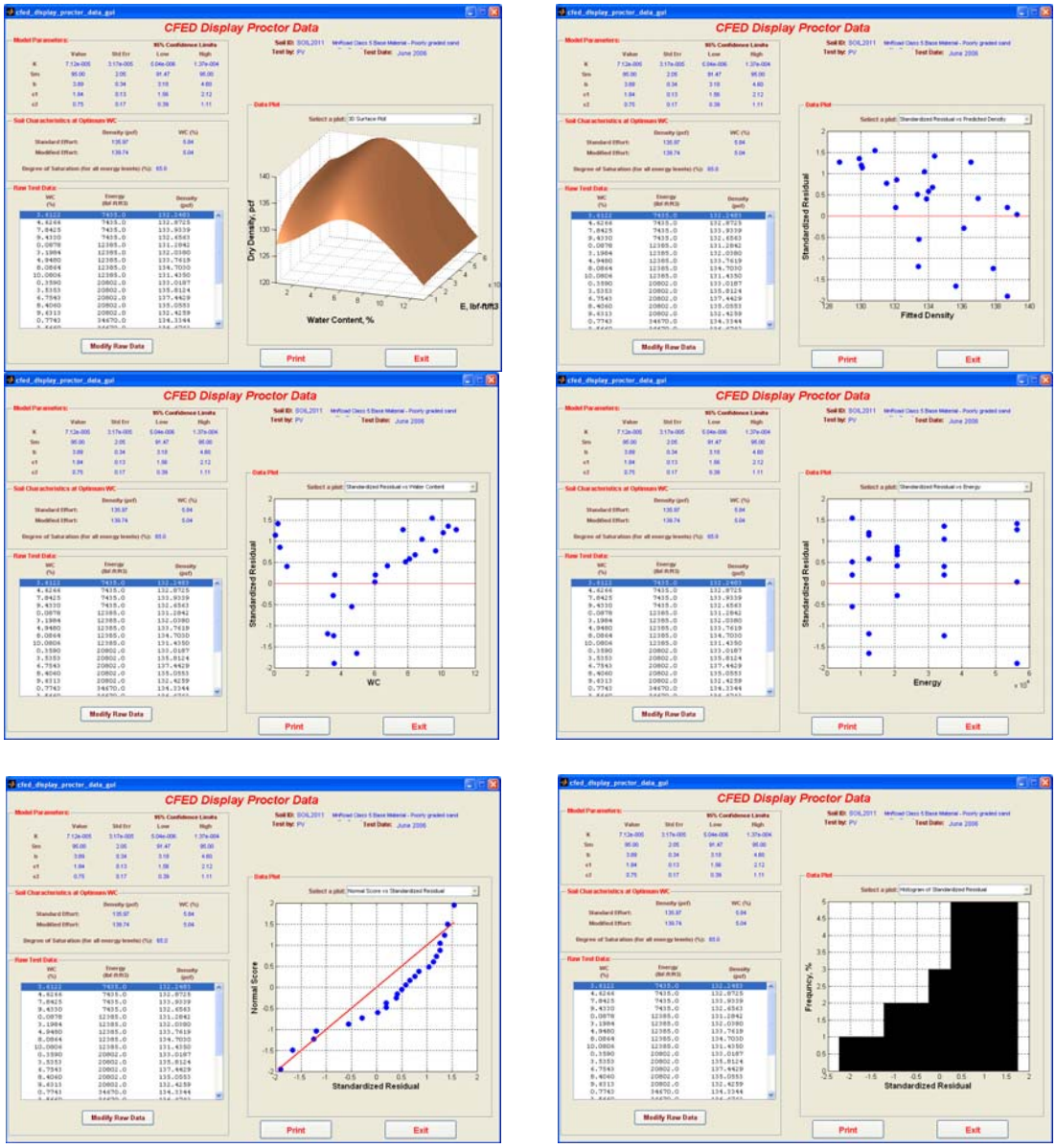


**Figure 233: Continued**

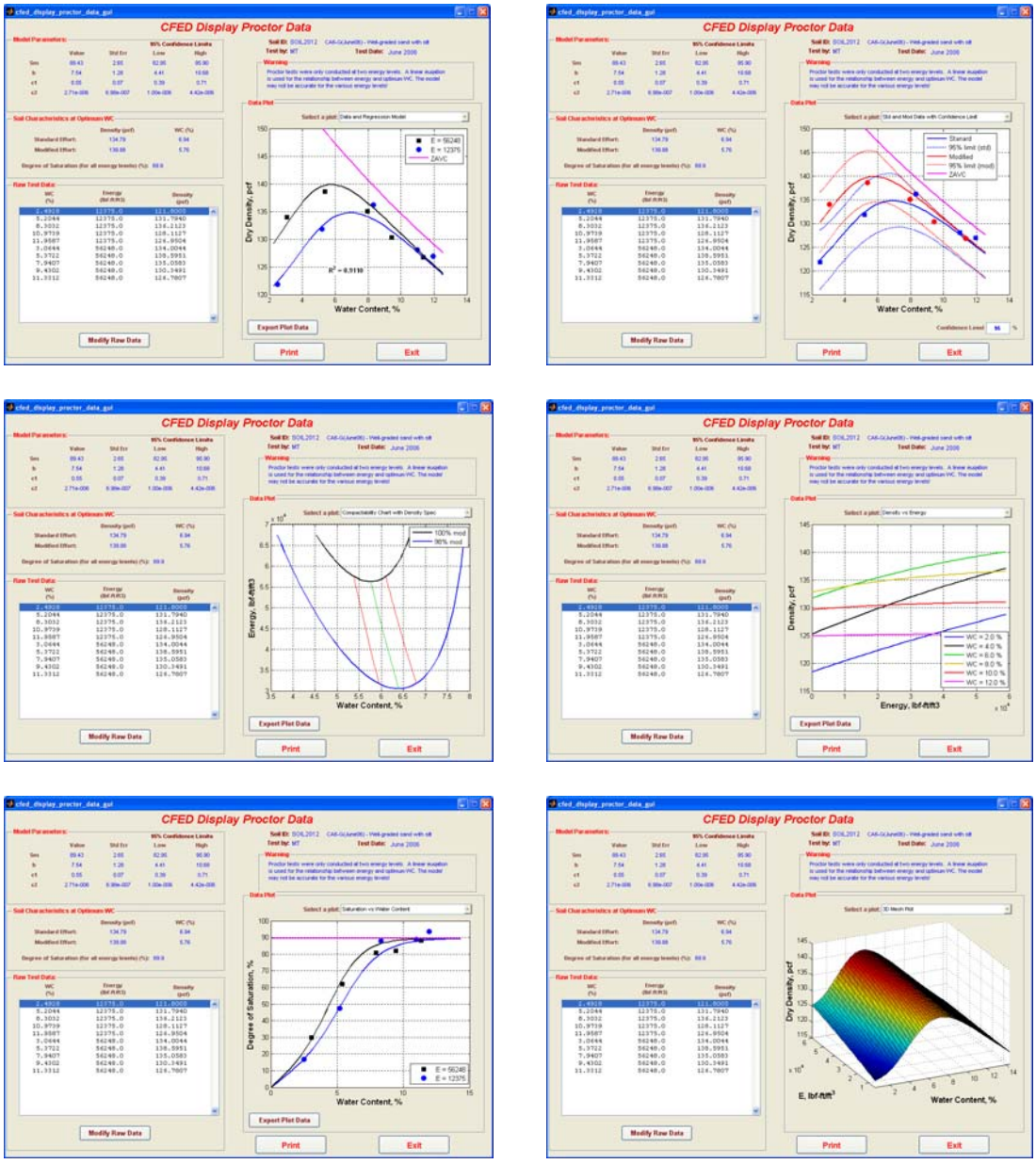


**Figure 234: Soil 2012 CFED outputs**

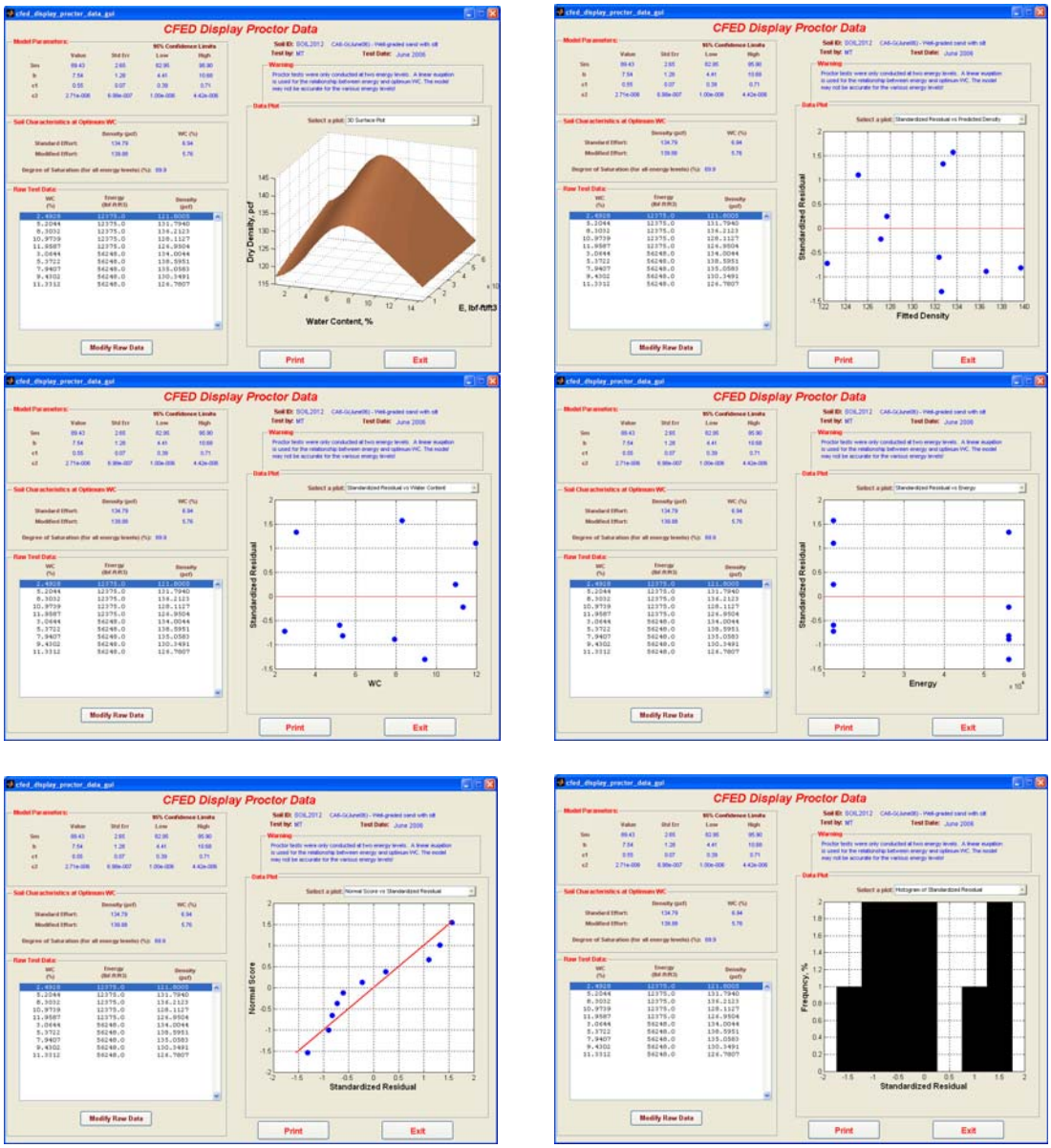


**Figure 234: Continued**

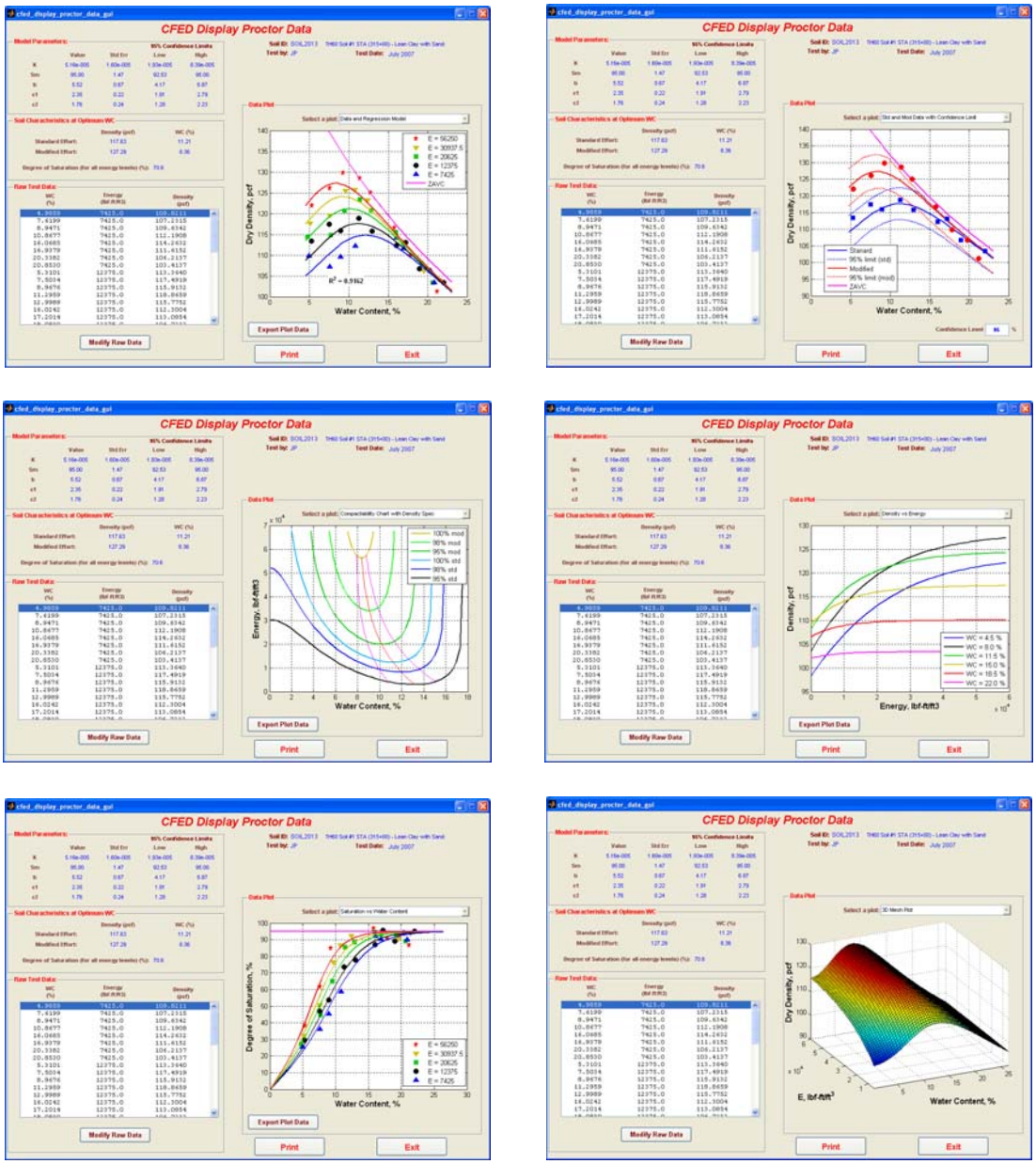


**Figure 235: Soil 2013 CFED outputs**

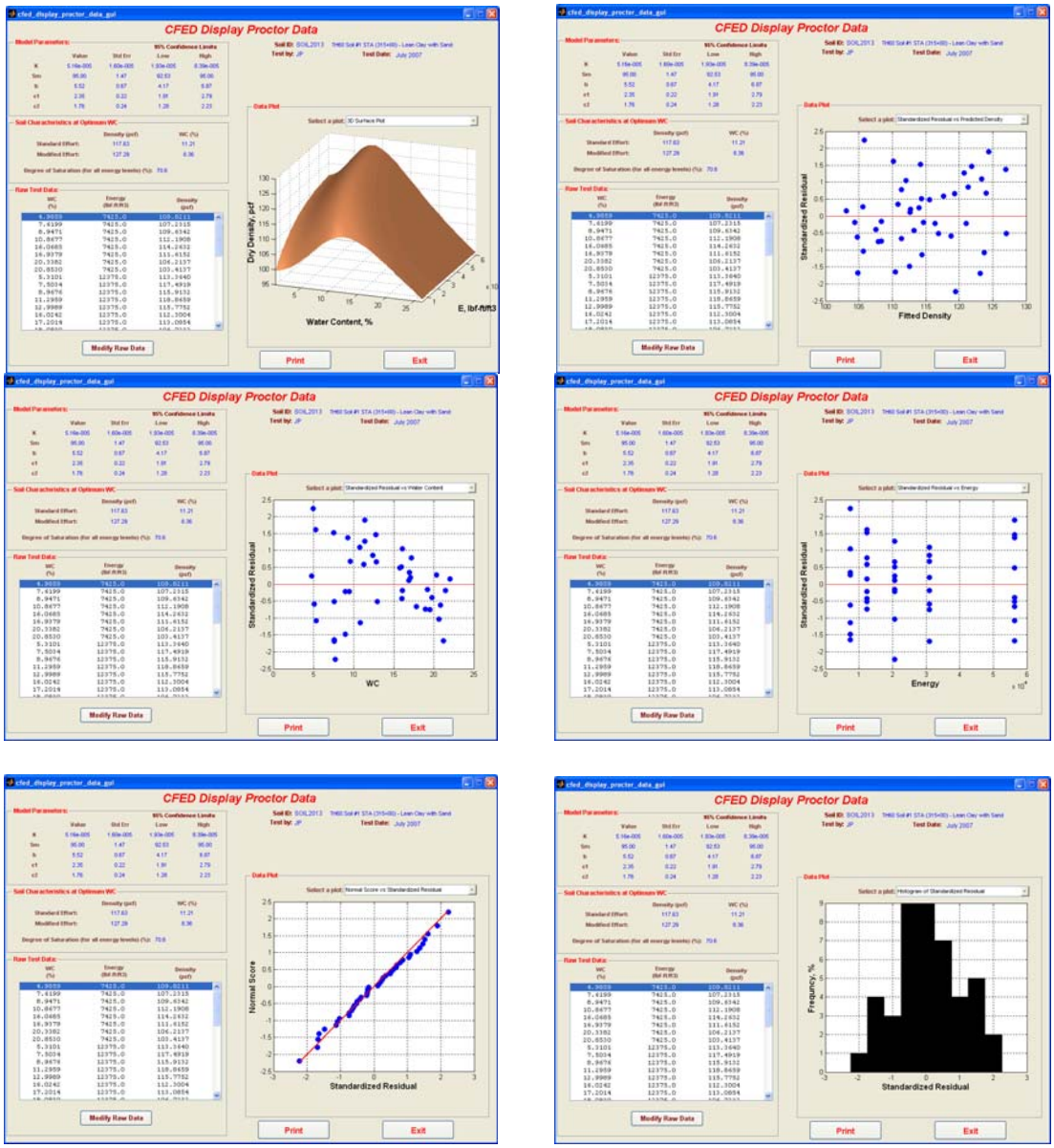


**Figure 235: Continued**

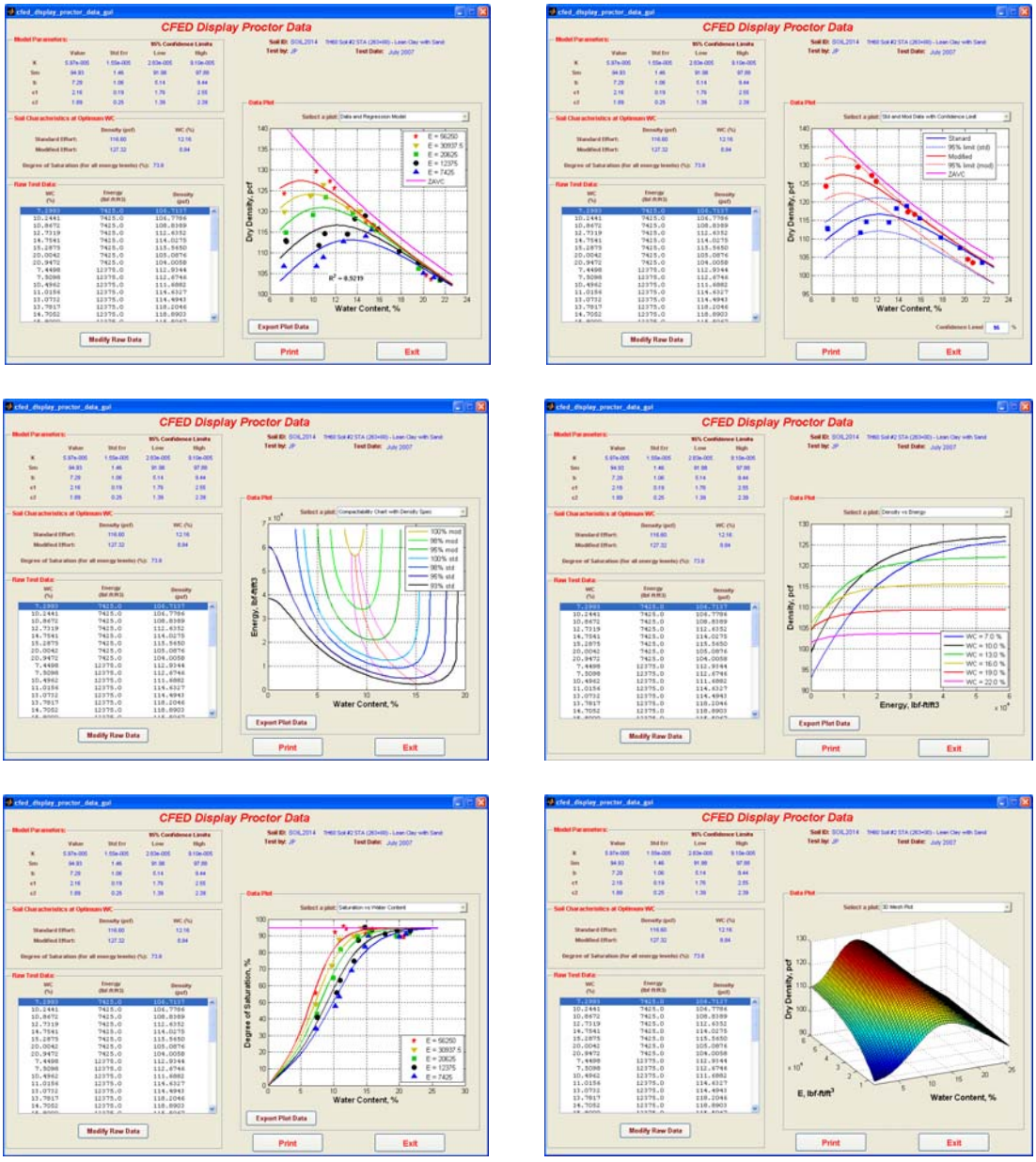


**Figure 236: Soil 2014 CFED outputs**

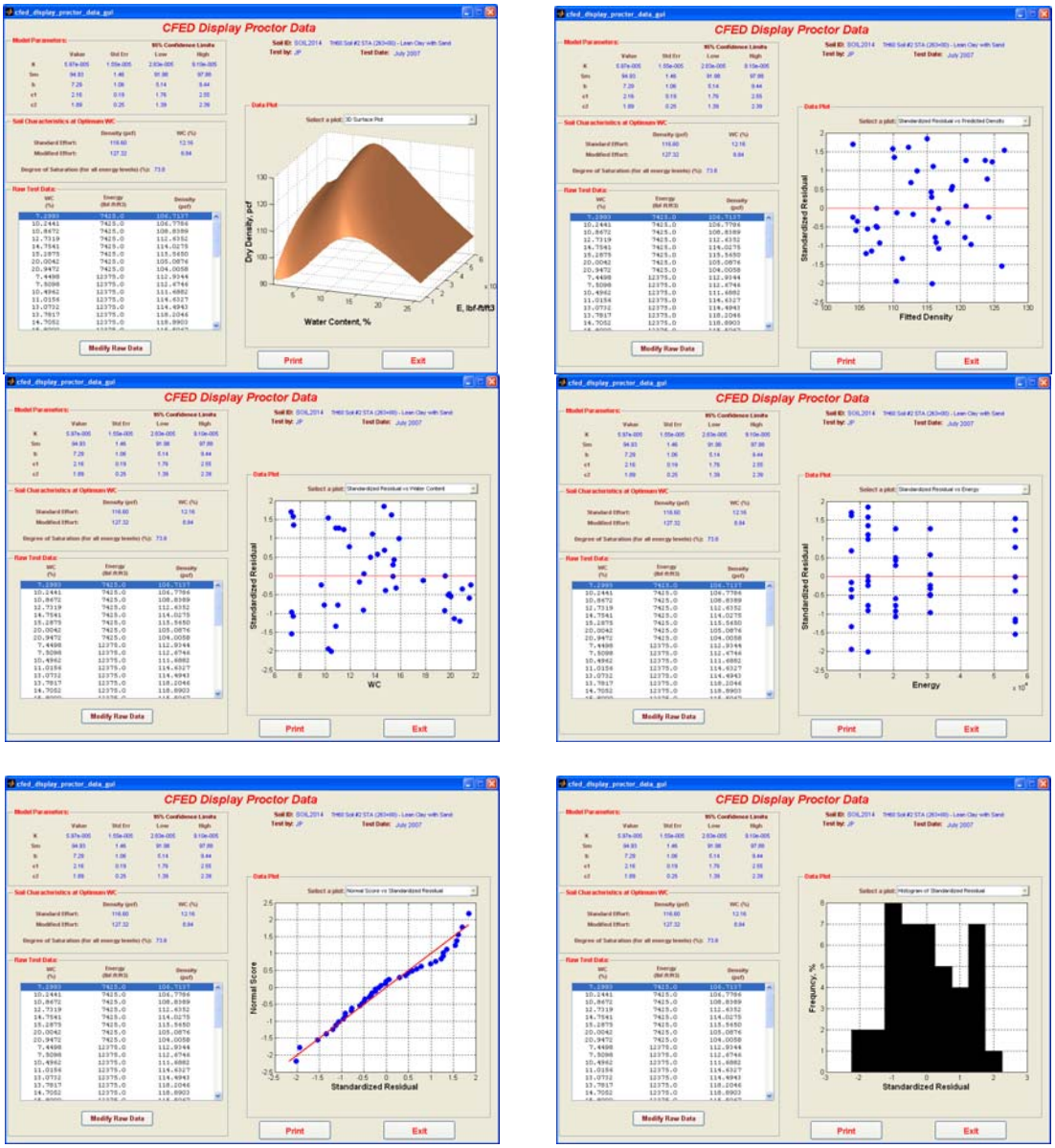


**Figure 236: Continued**

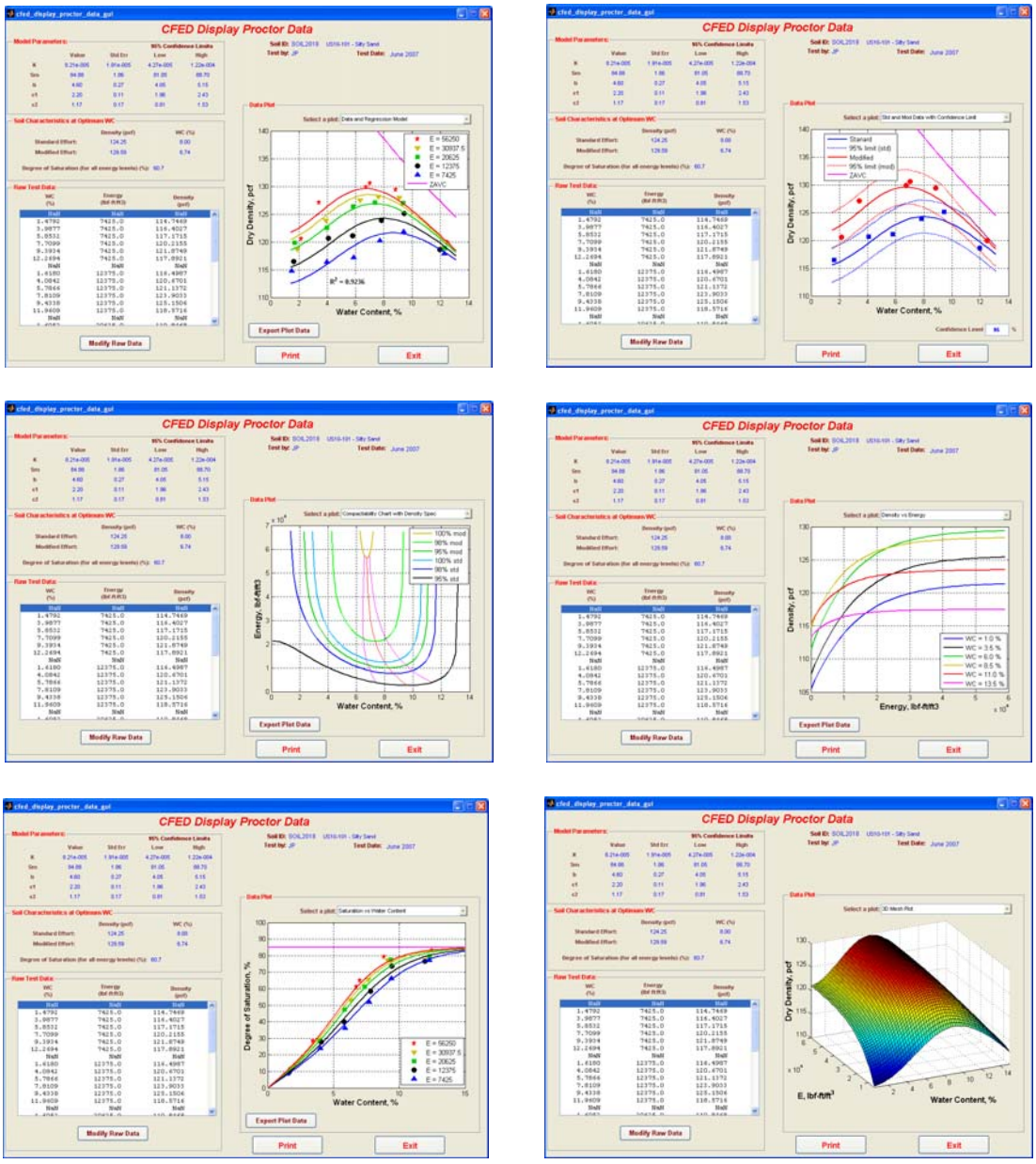


**Figure 237: Soil 2018 CFED outputs**

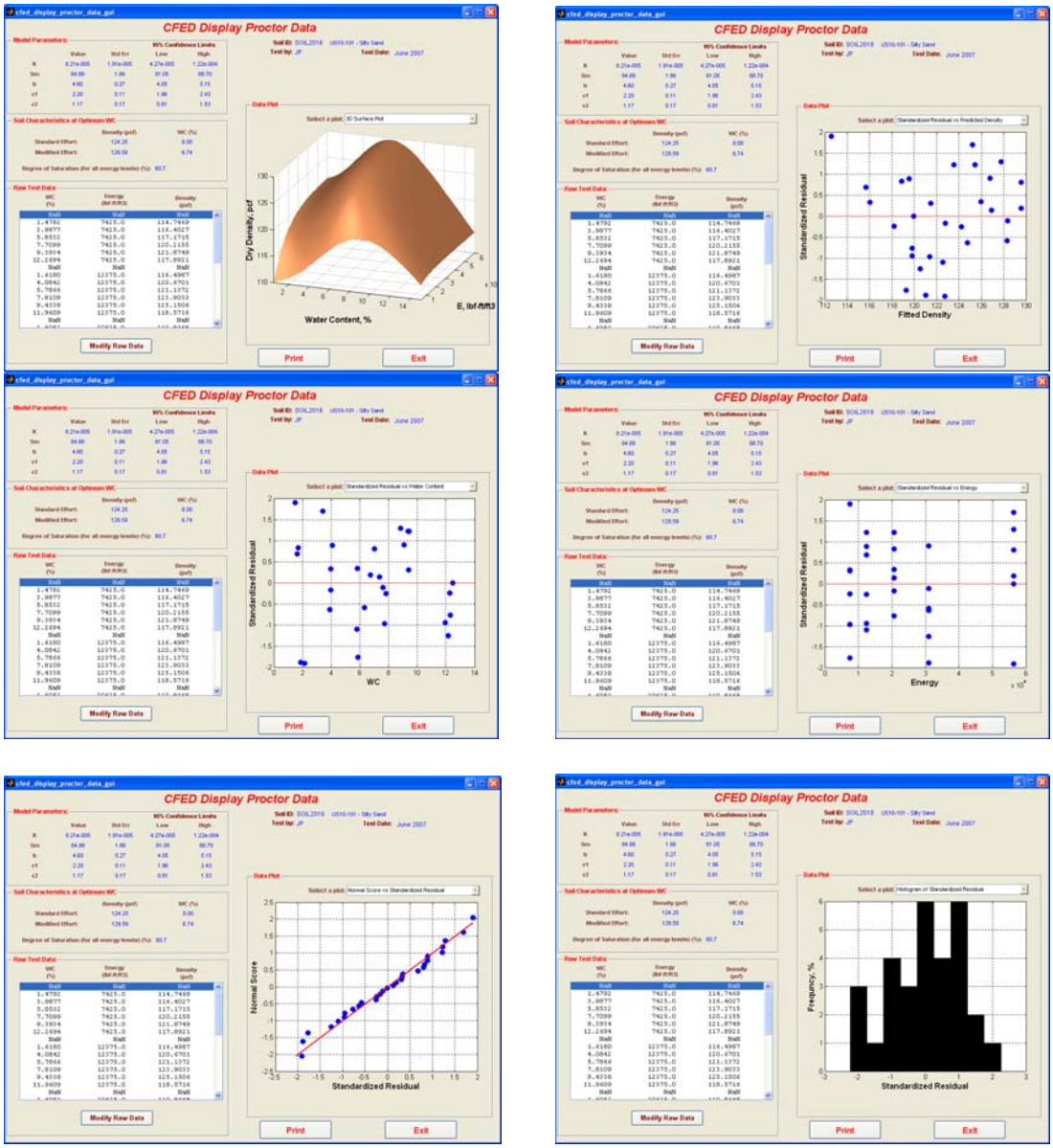


**Figure 237: Continued**

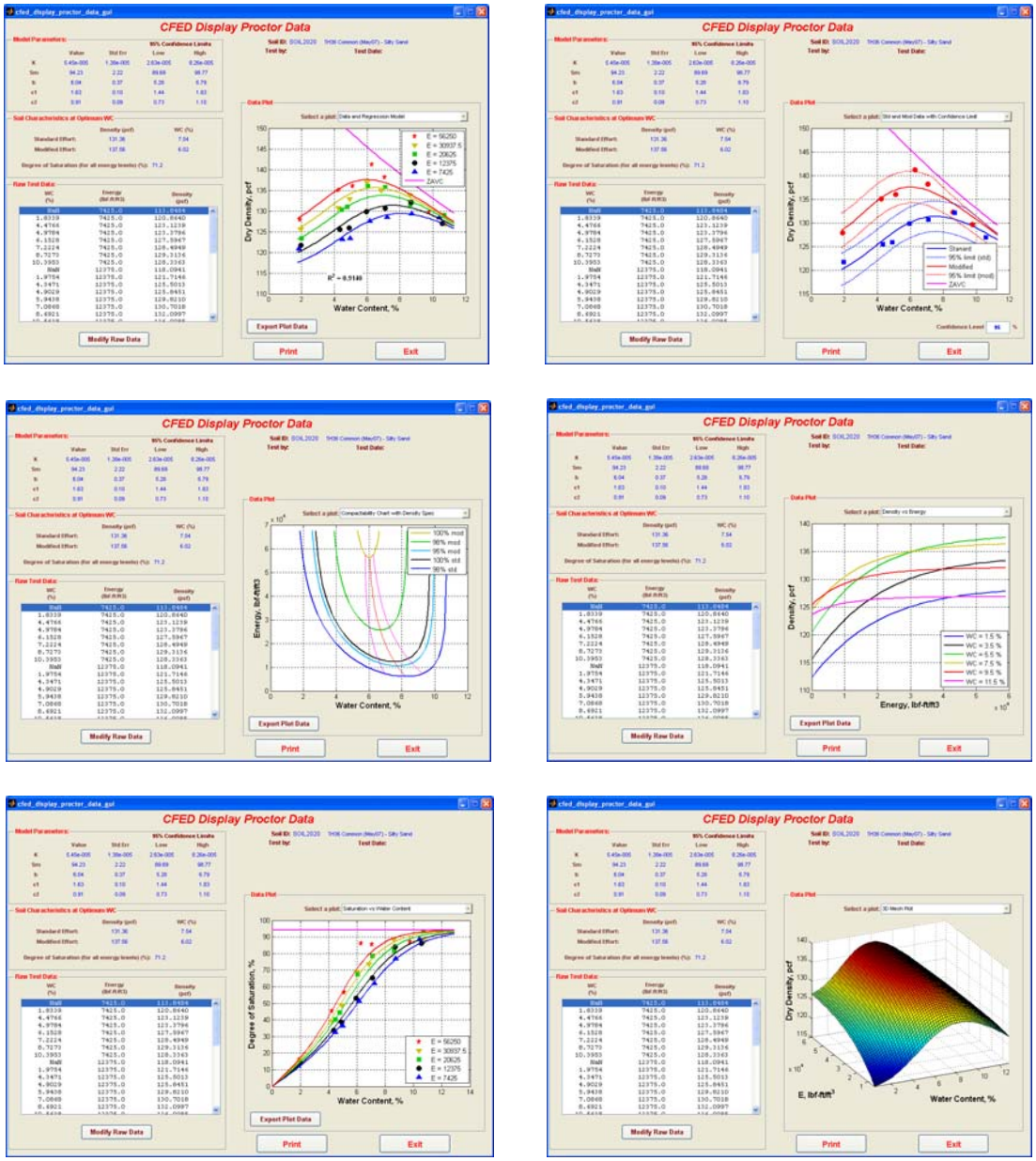


**Figure 238: Soil 2020 CFED outputs**

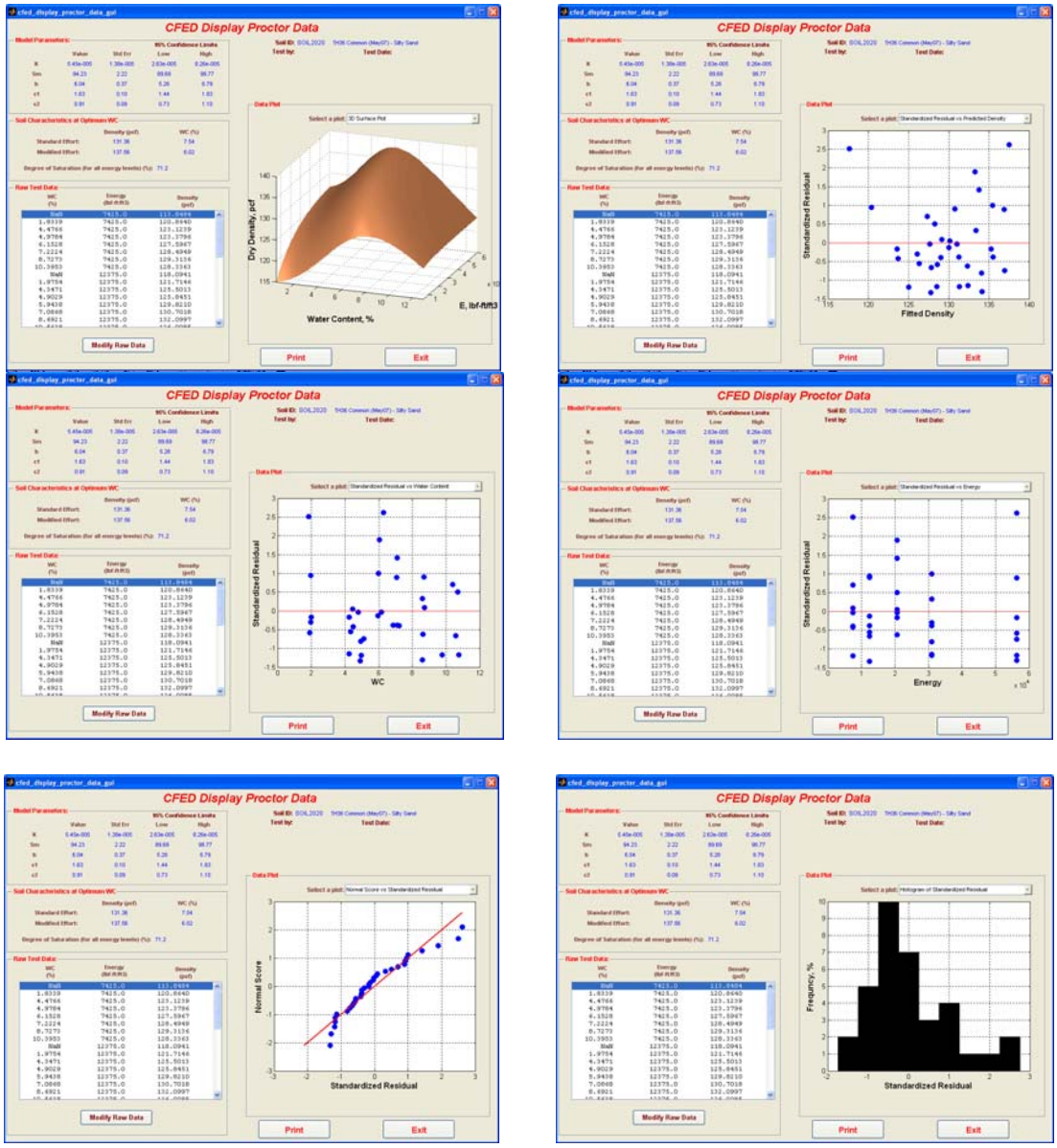


**Figure 238: Continued**

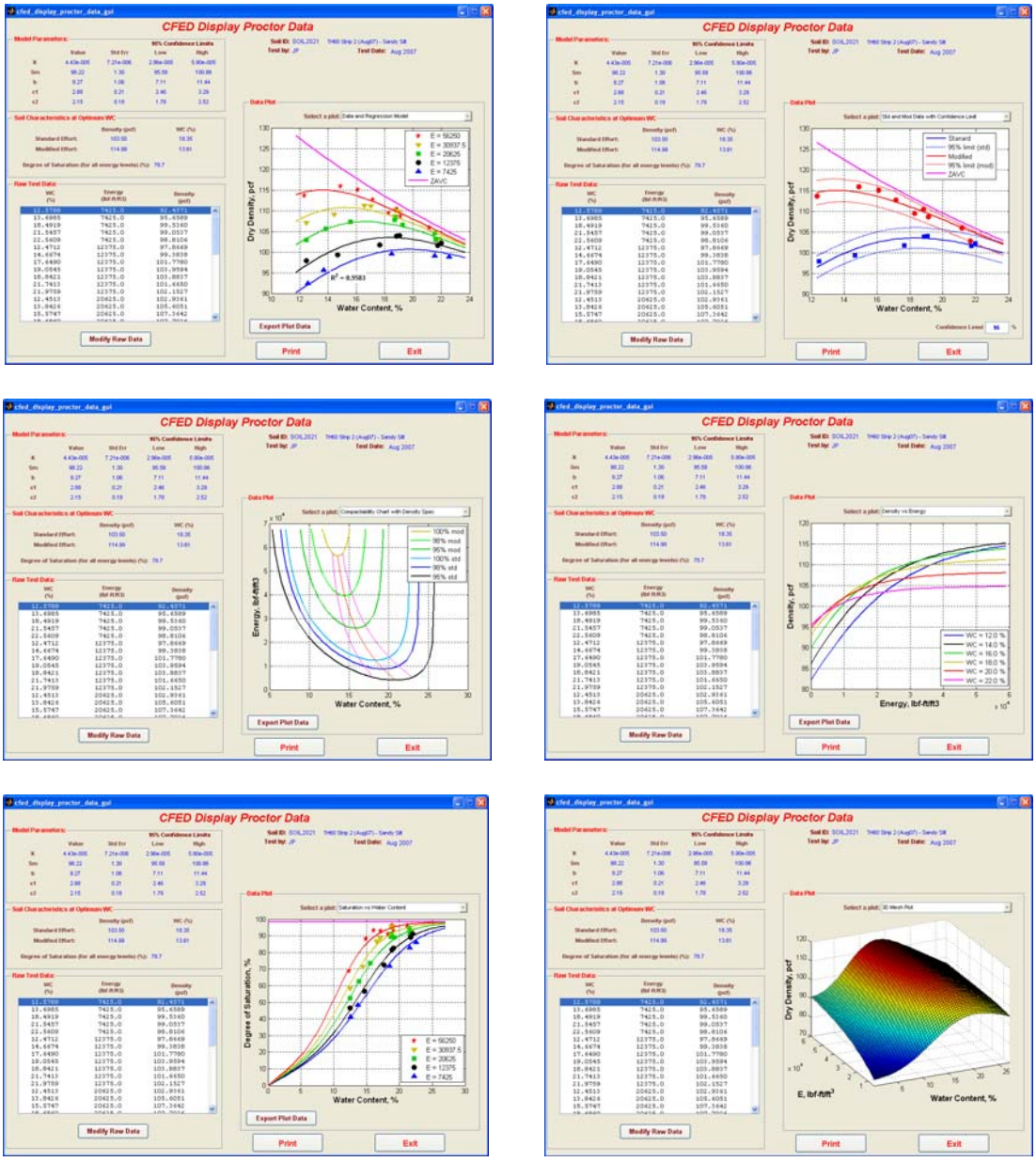


**Figure 239: Soil 2021 CFED outputs**

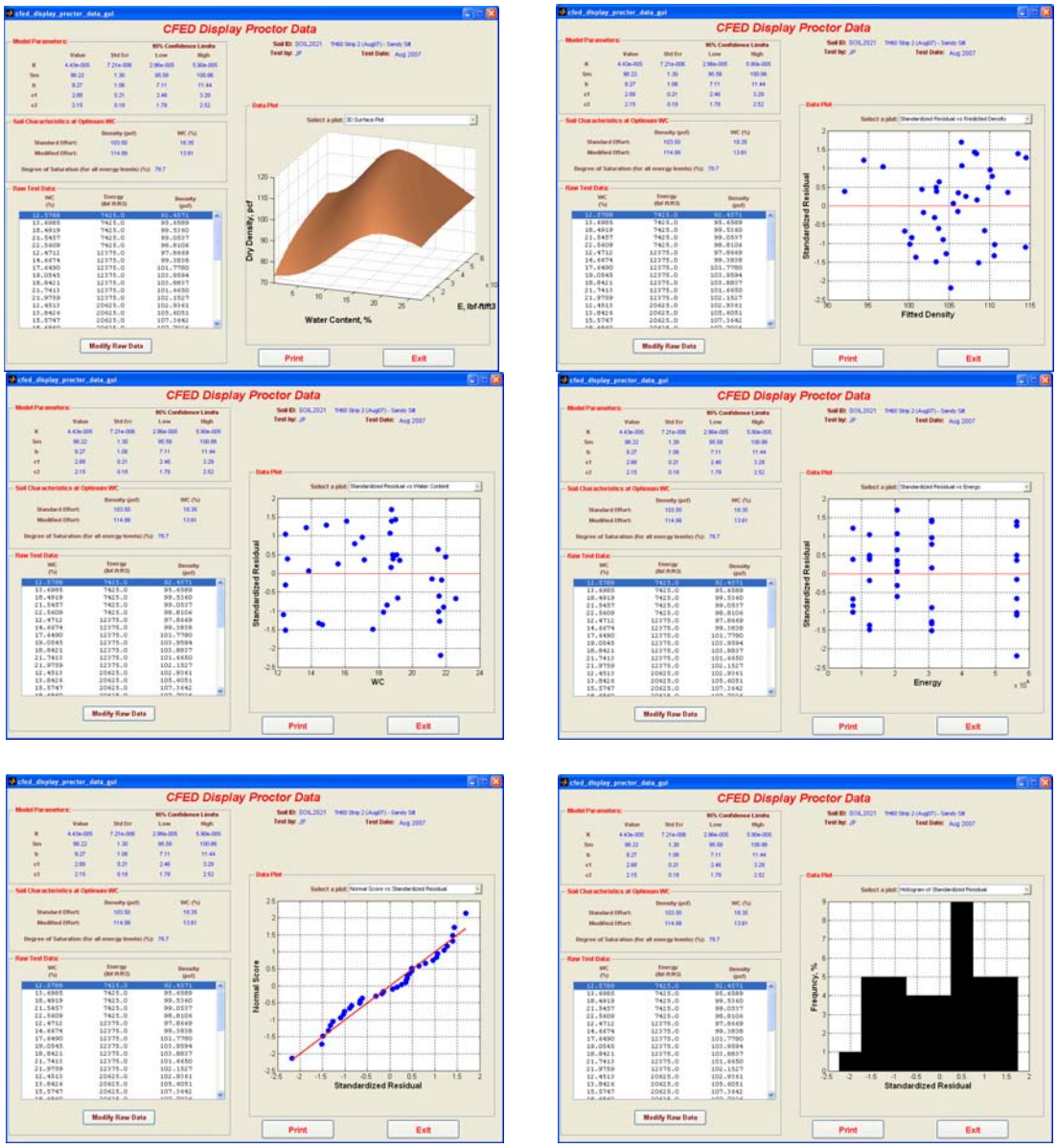


**Figure 239: Continued**

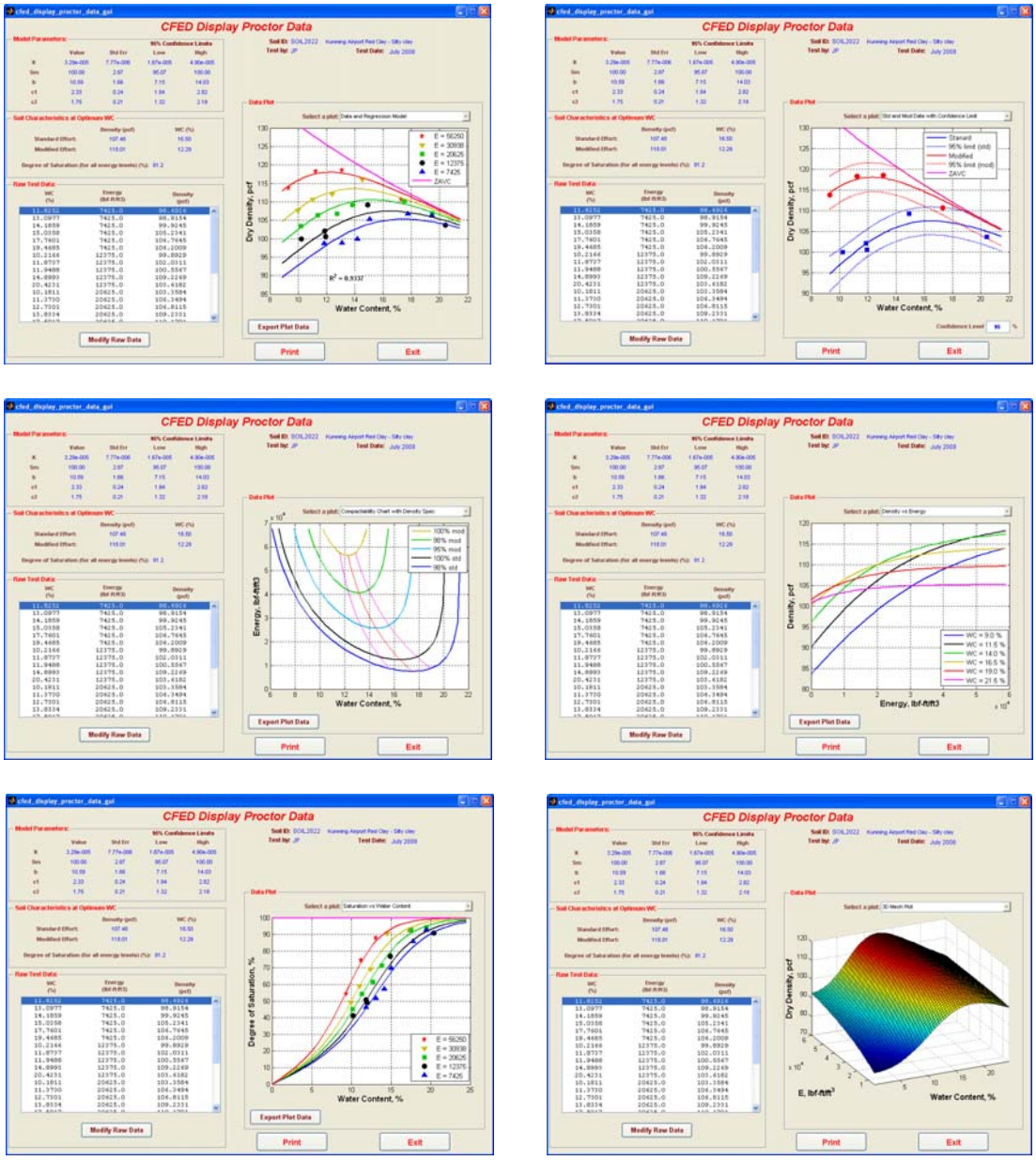


**Figure 240: Soil 2022 CFED outputs**

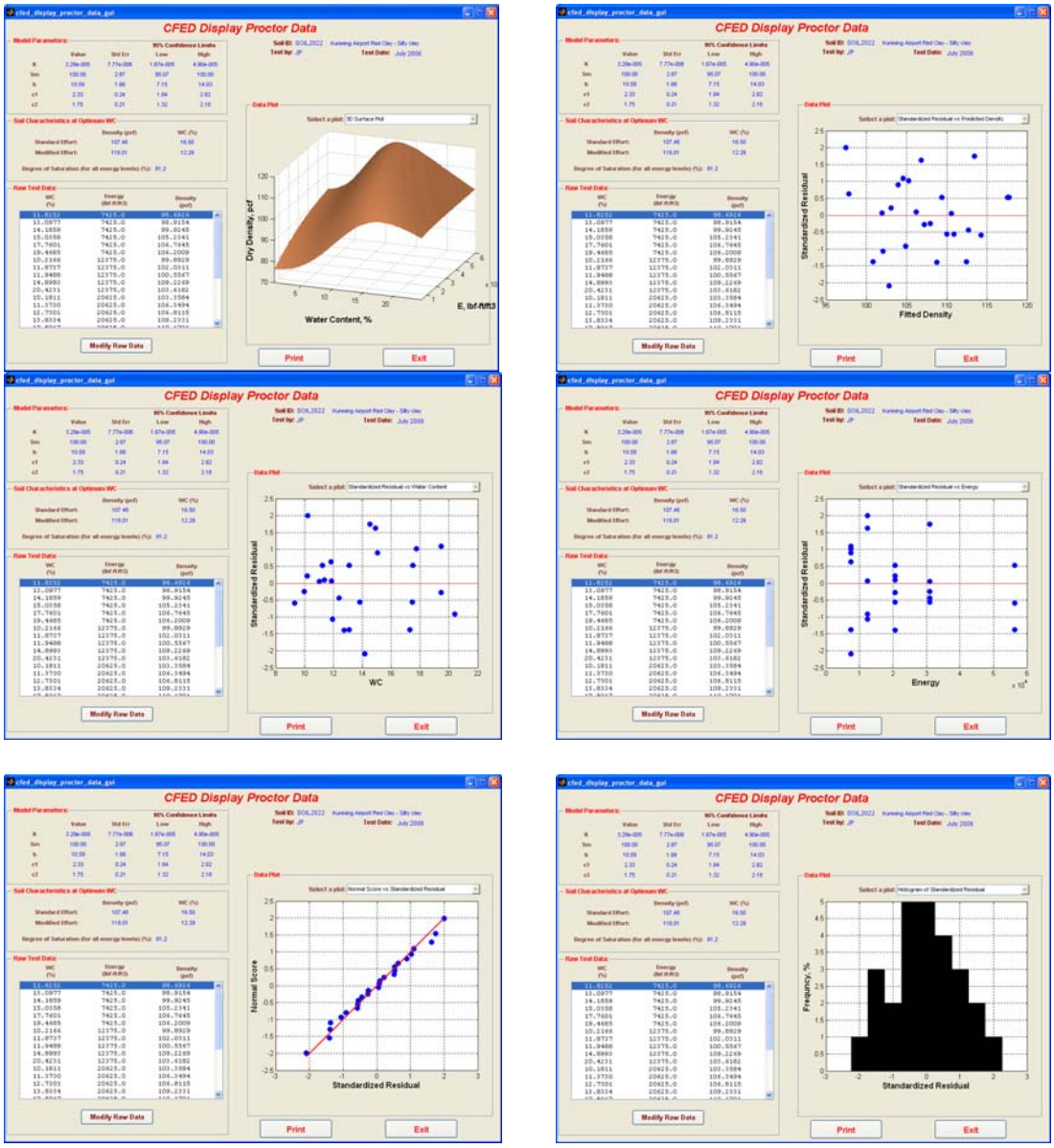


**Figure 240: Continued**

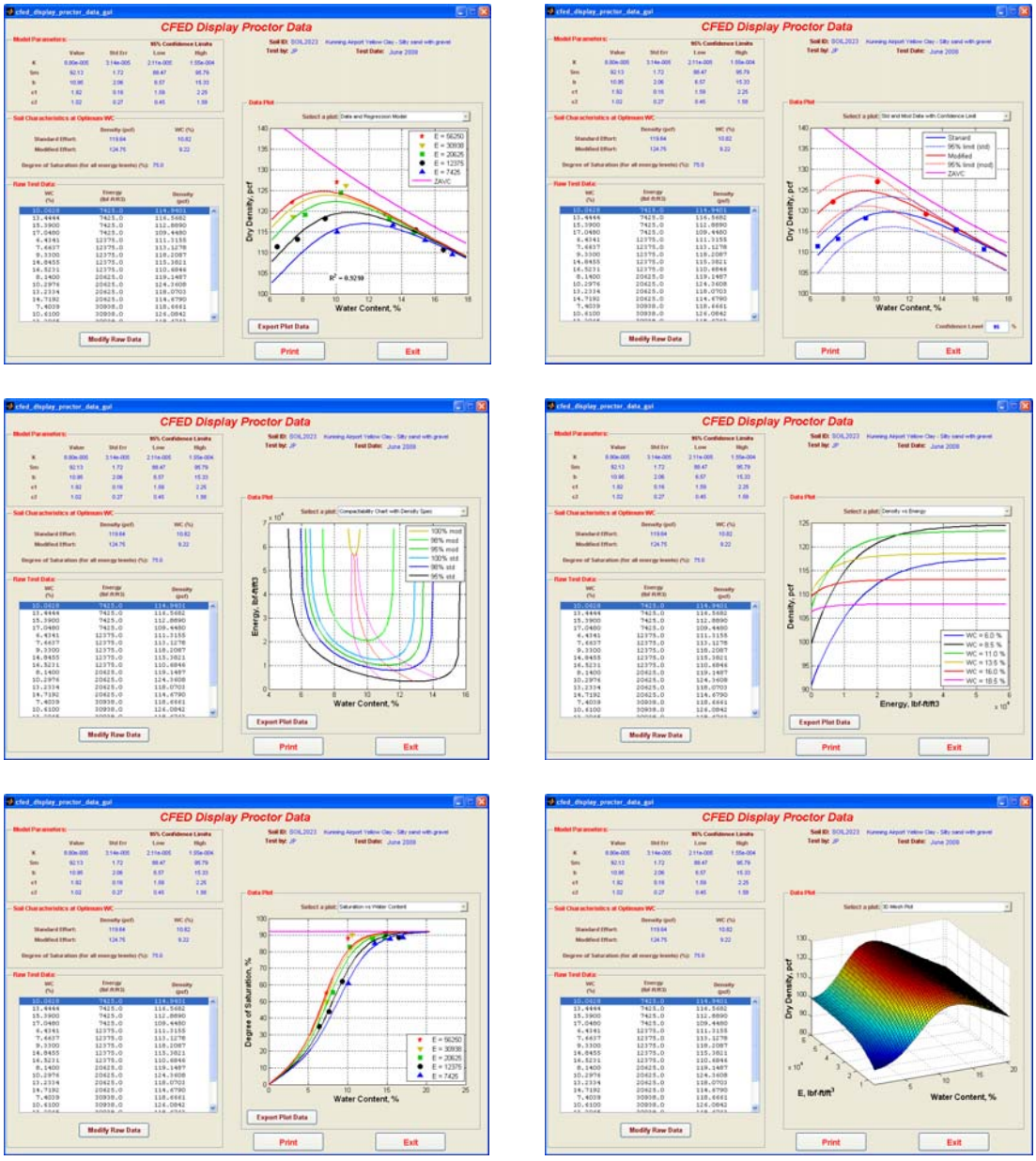


**Figure 241: Soil 2023 CFED outputs**

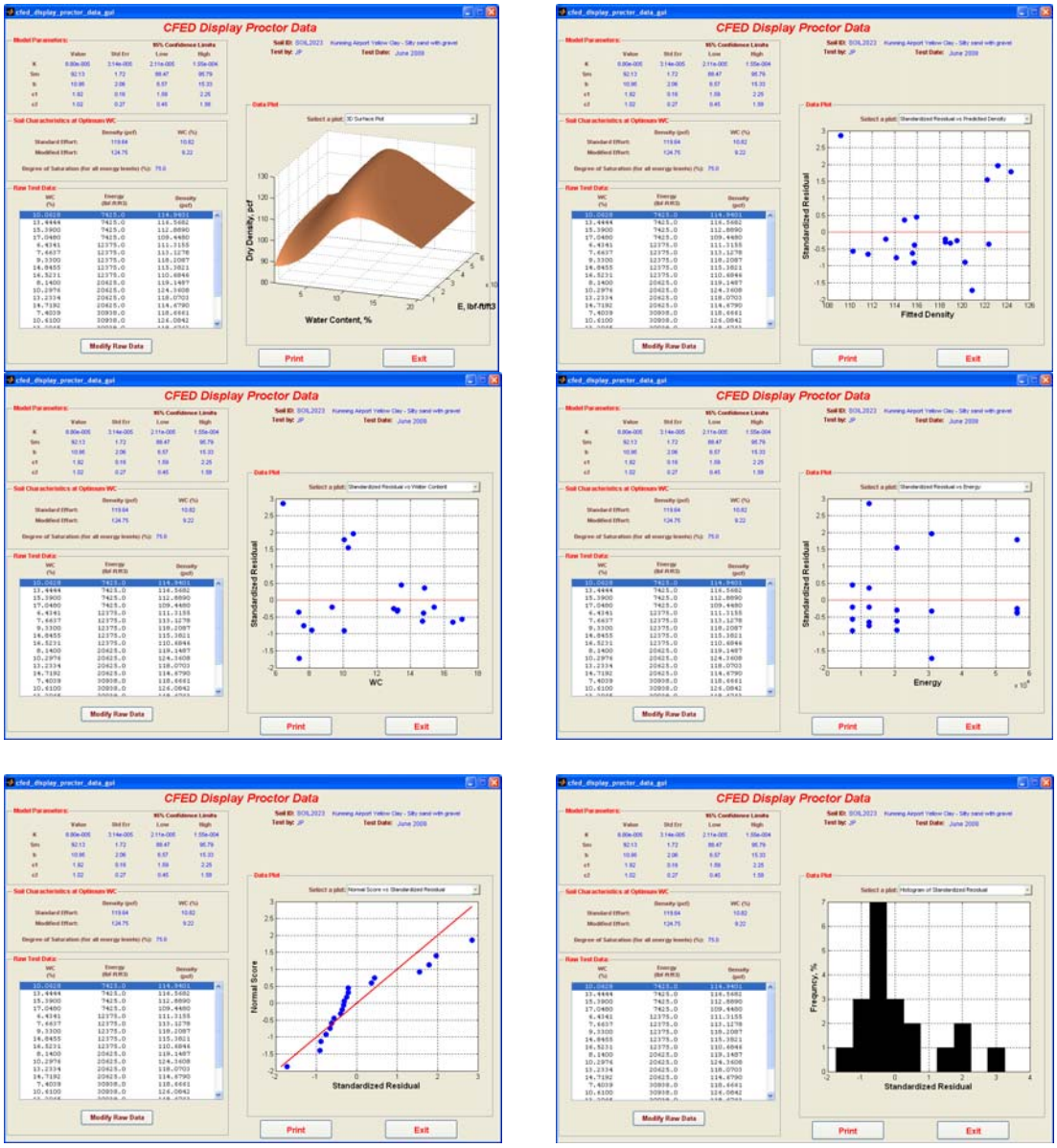


**Figure 241: Continued**

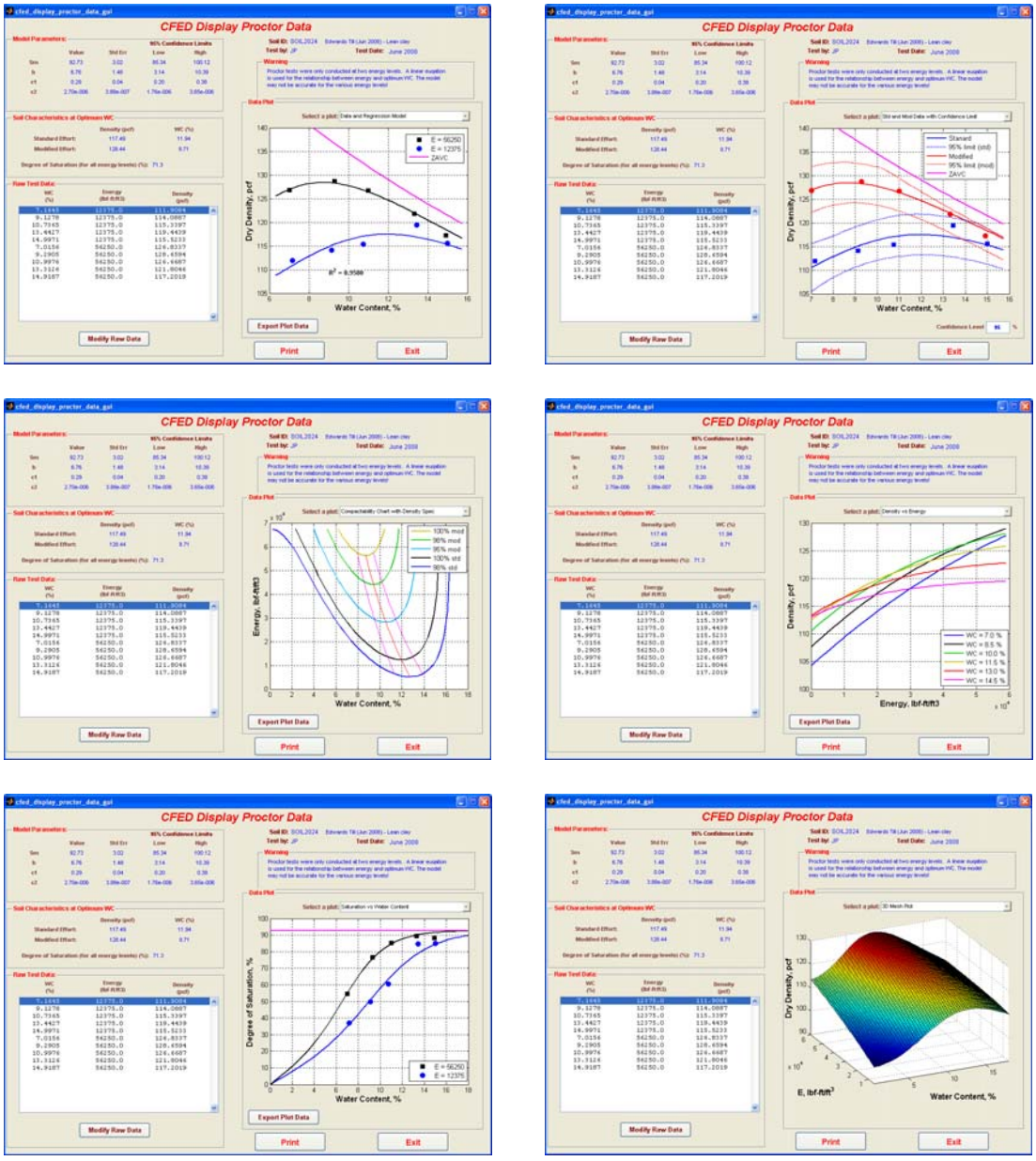


**Figure 242: Soil 2024 CFED outputs**

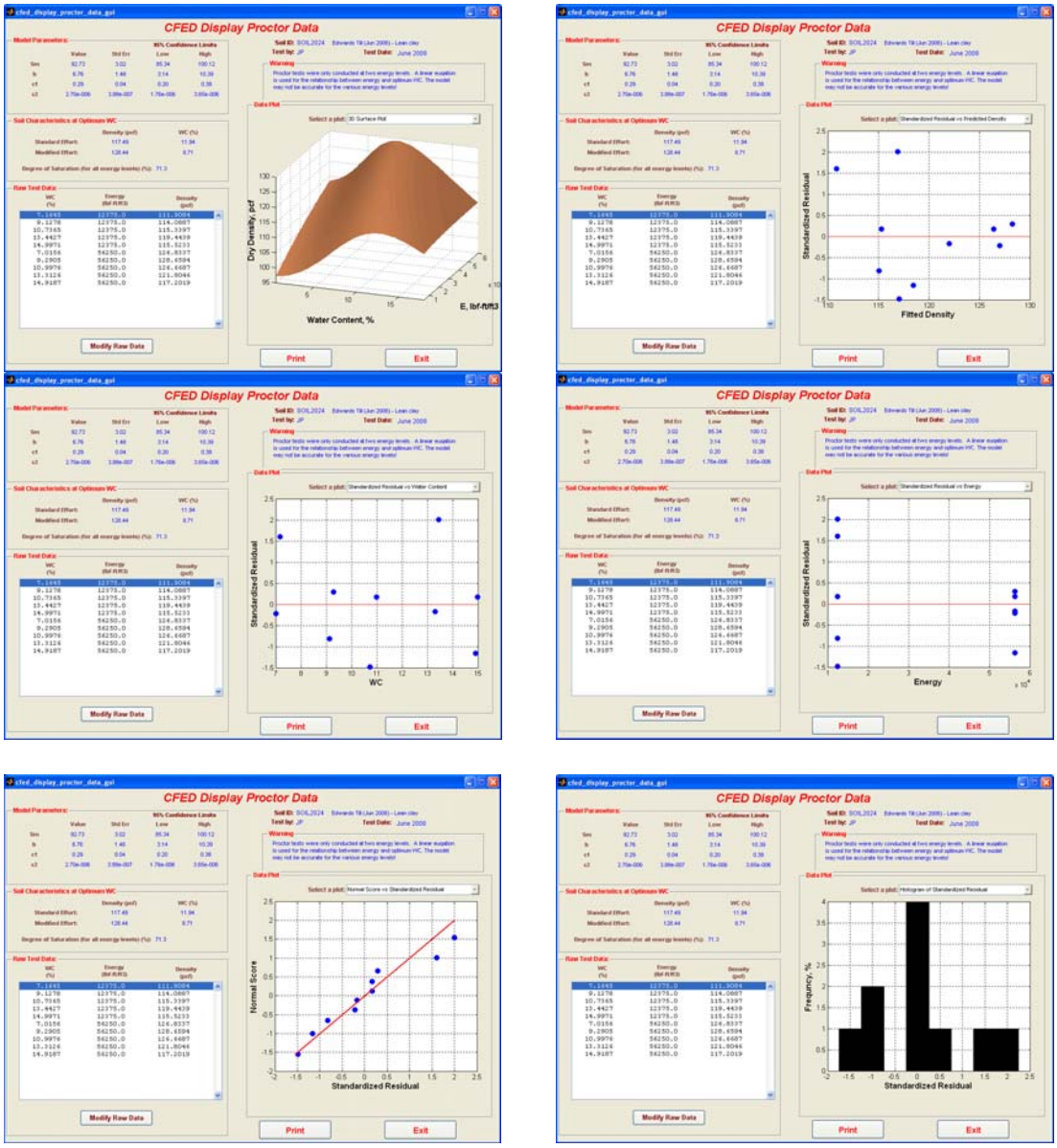


**Figure 242: Continued**

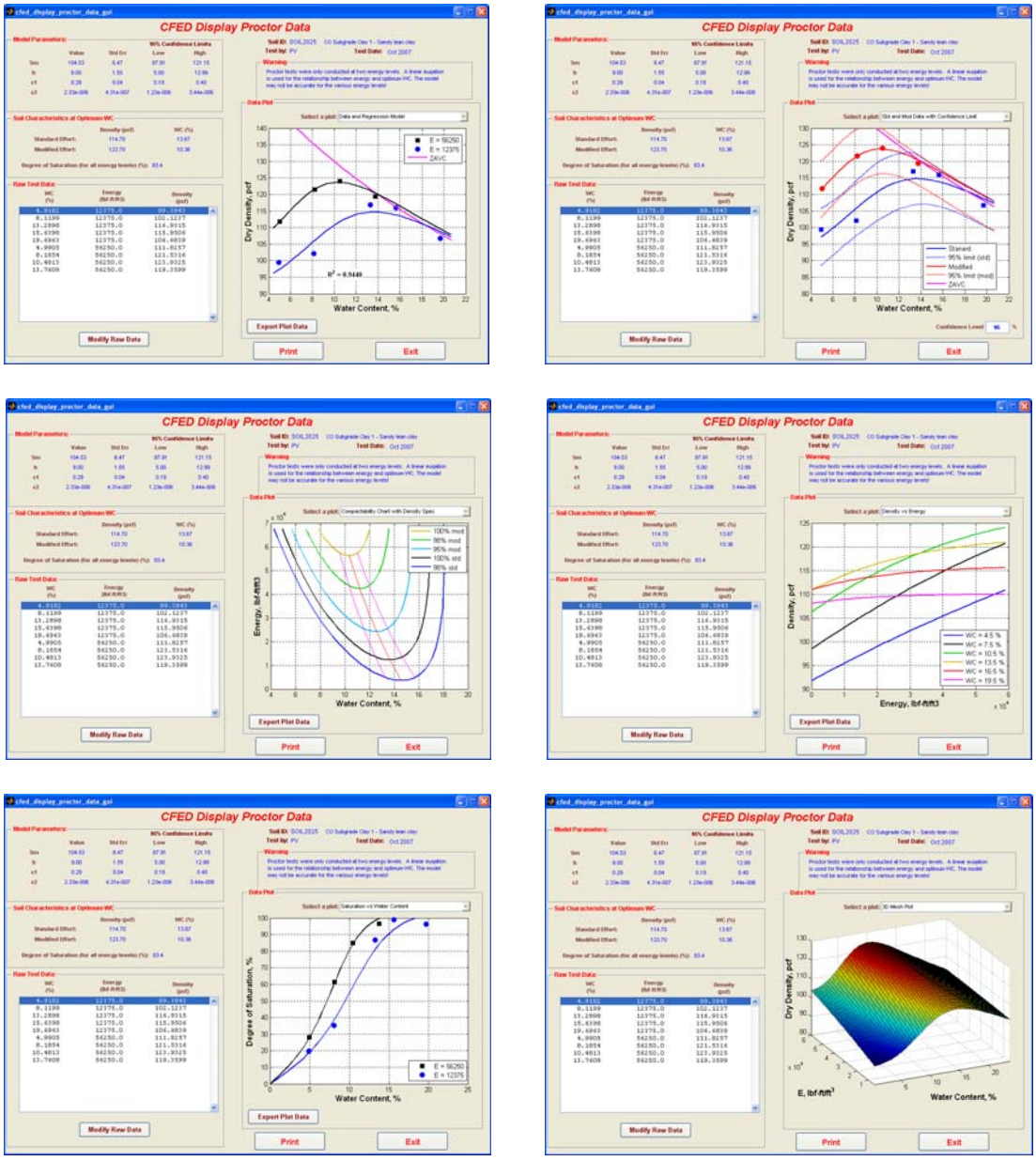


**Figure 243: Soil 2025 CFED outputs**

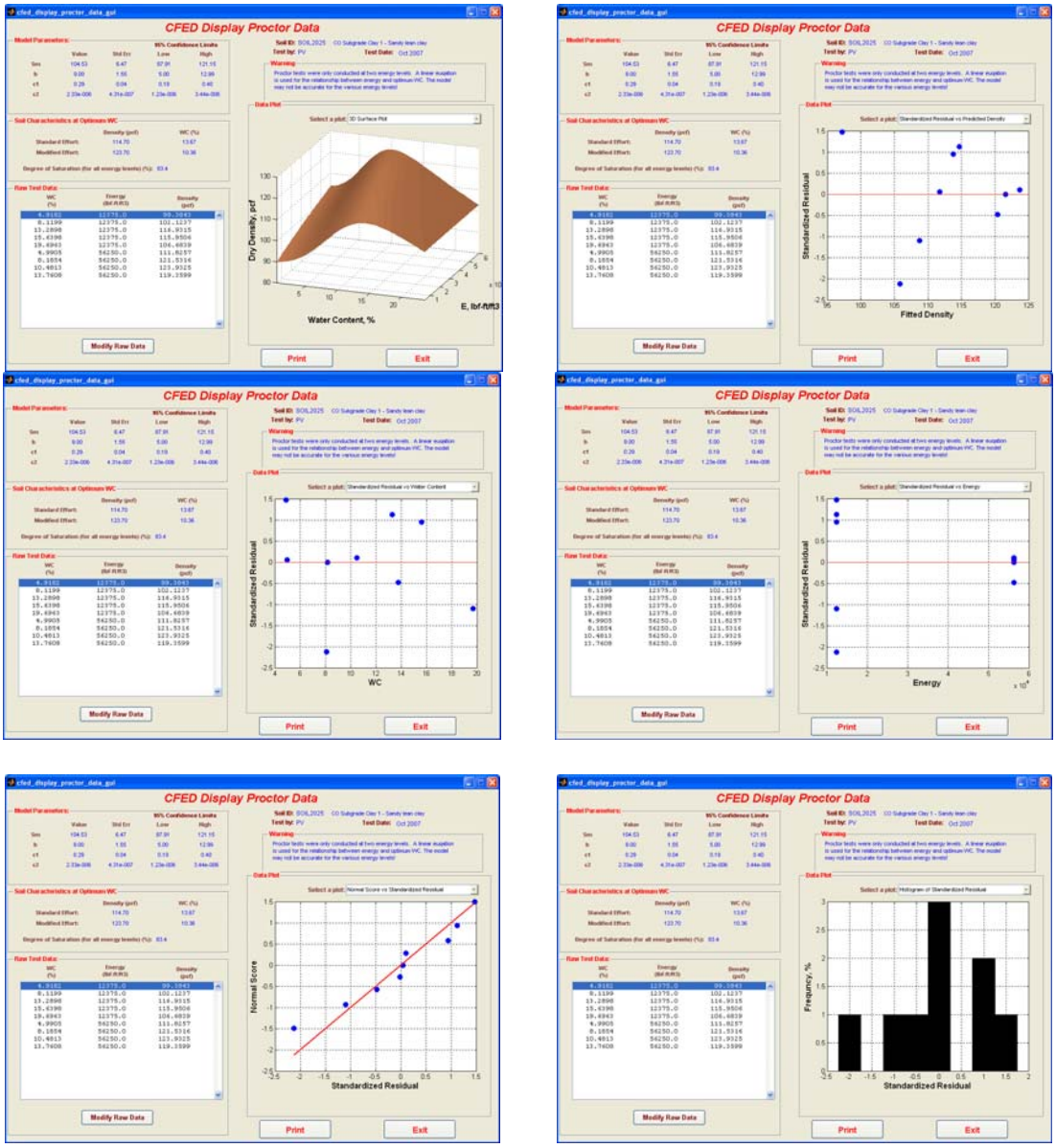


**Figure 243: Continued**

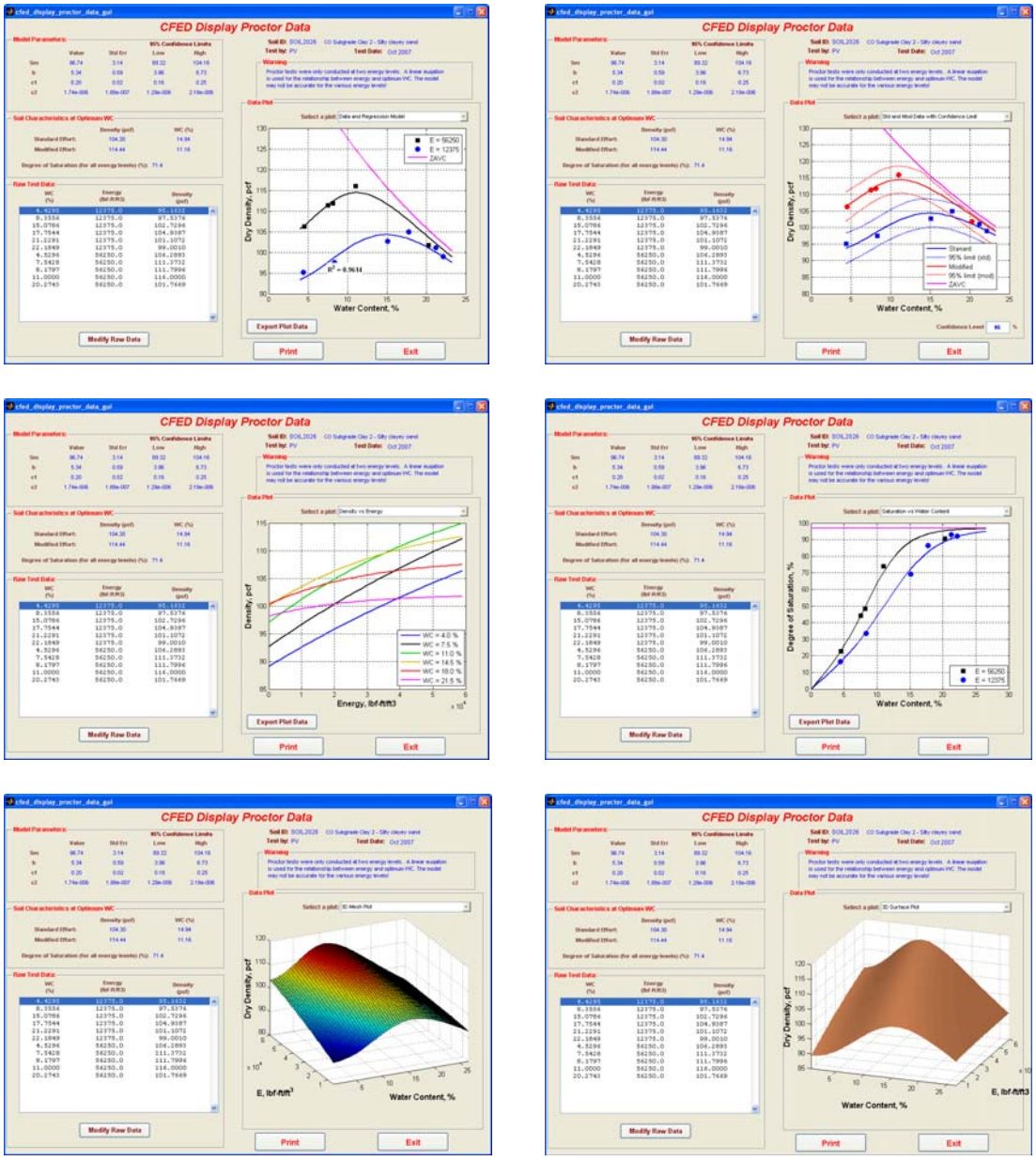


**Figure 244: Soil 2026 CFED outputs**

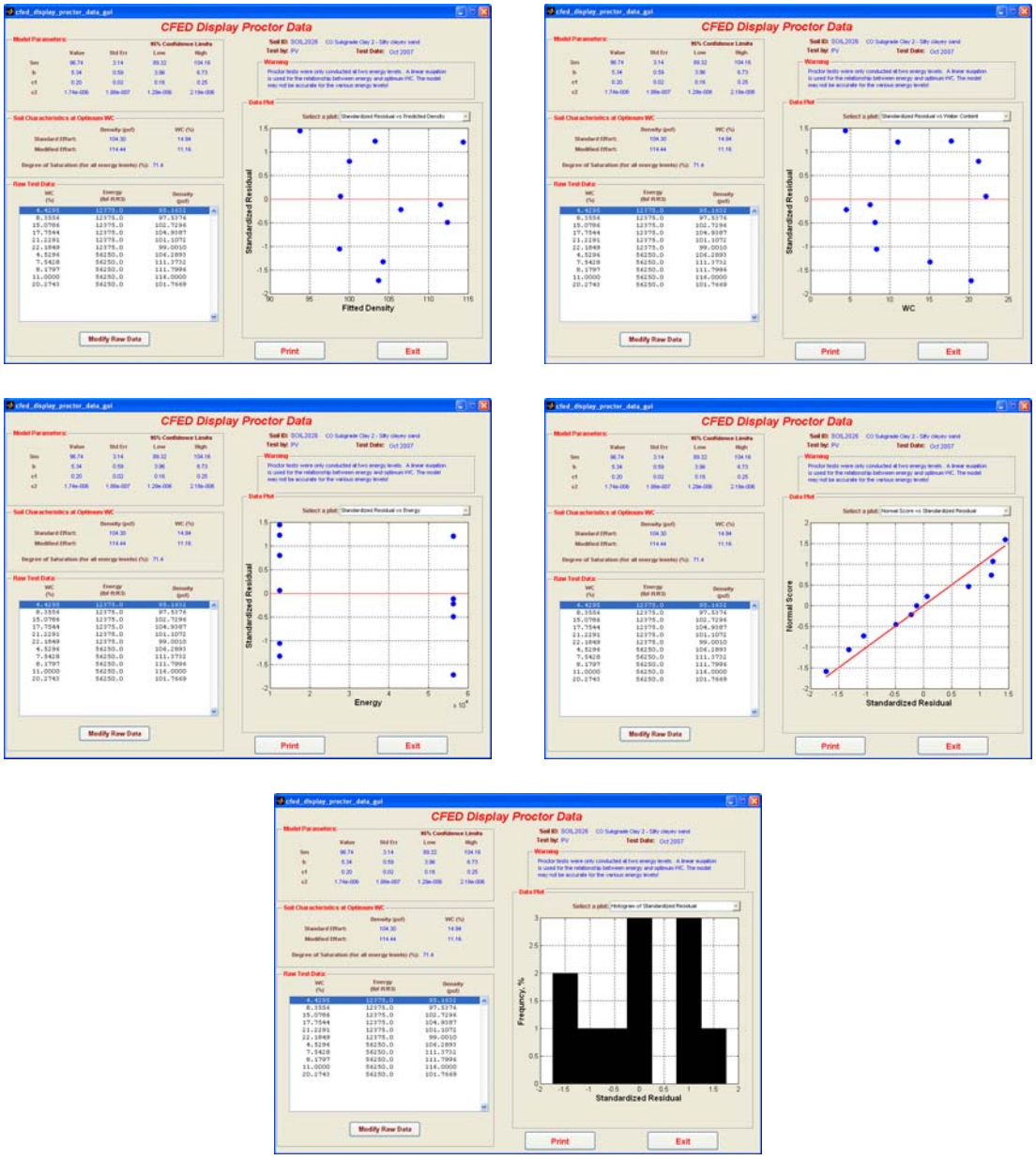


**Figure 244: Continued**

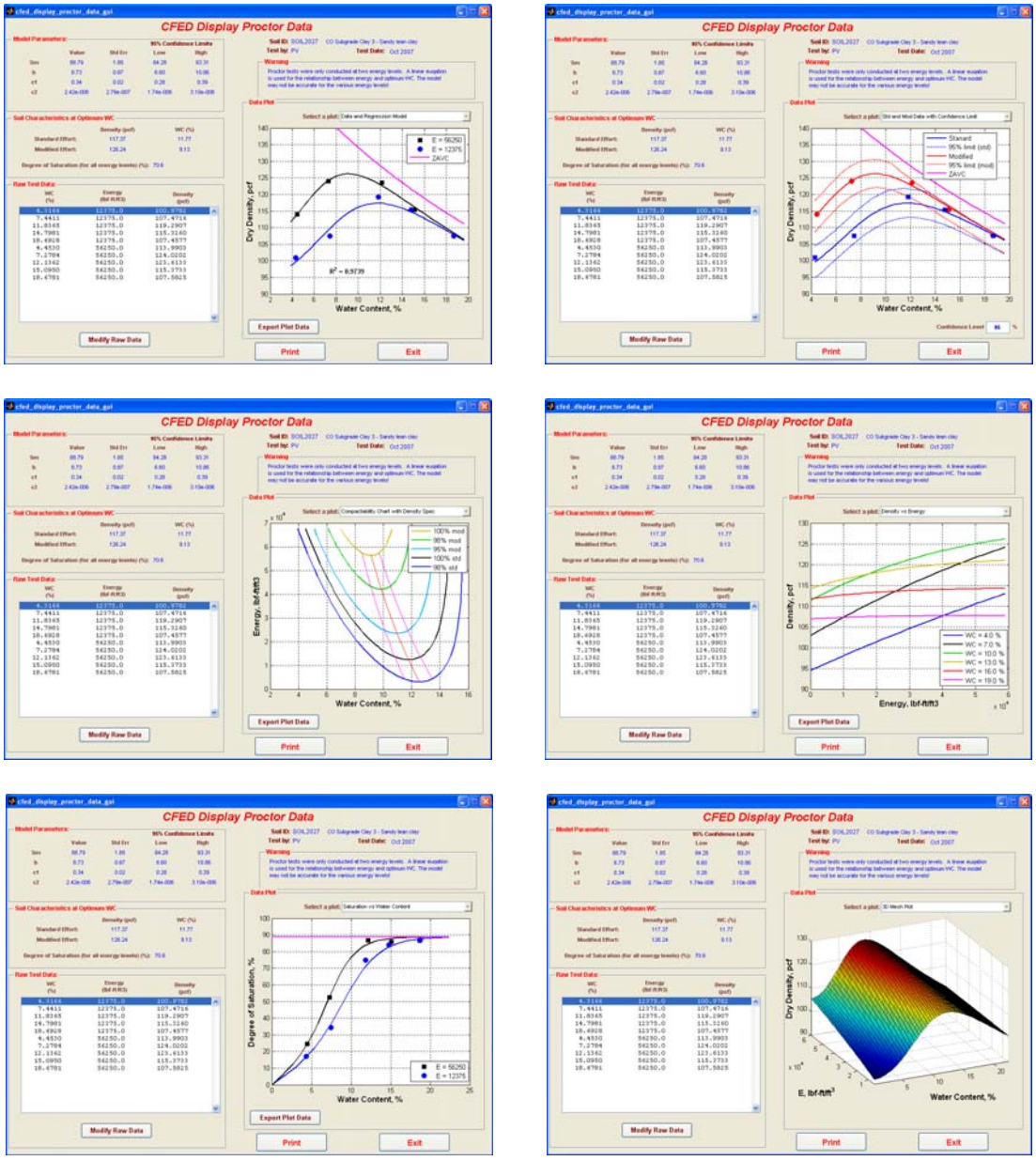


**Figure 245: Soil 2027 CFED outputs**

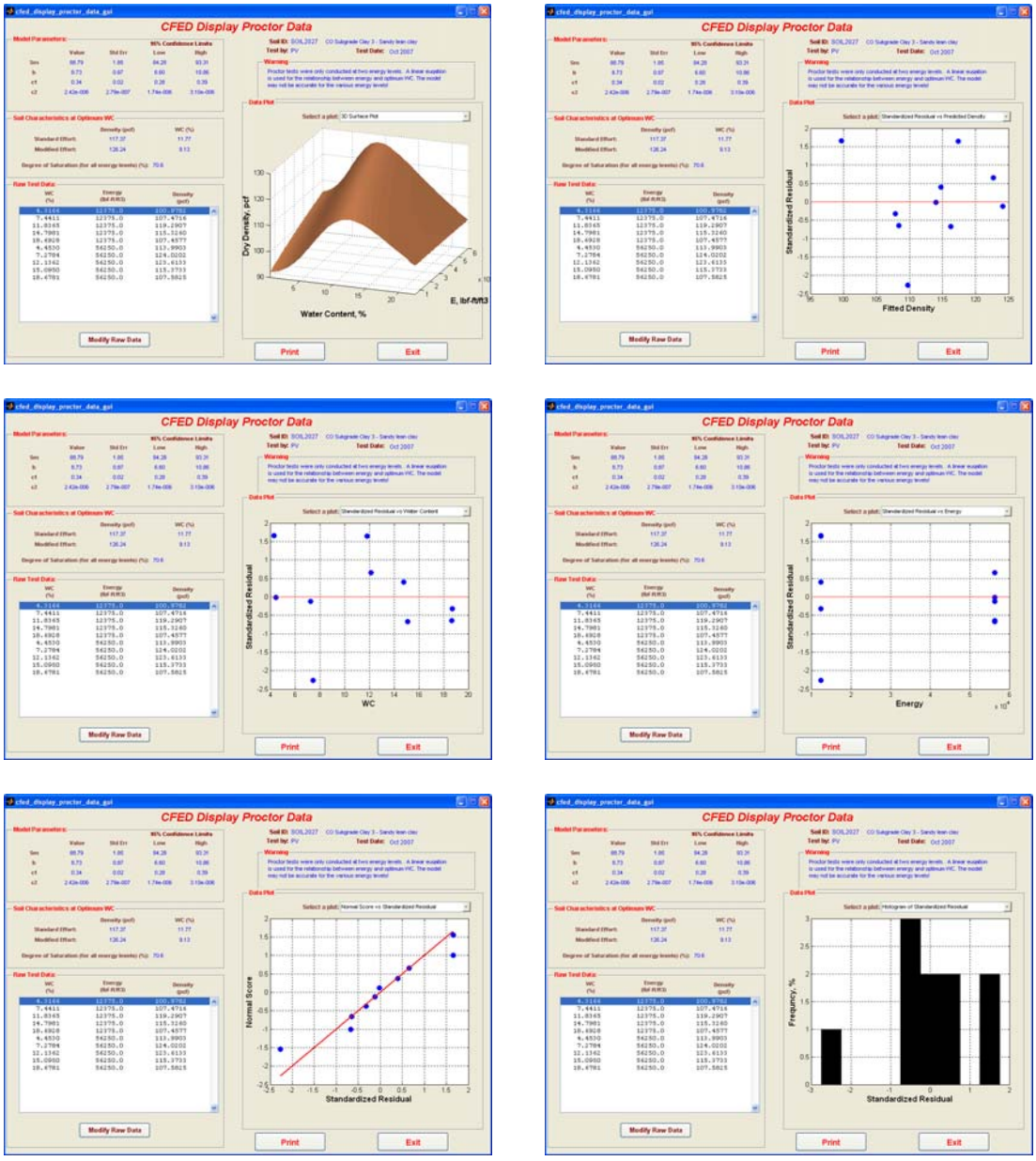


**Figure 245: Continued**

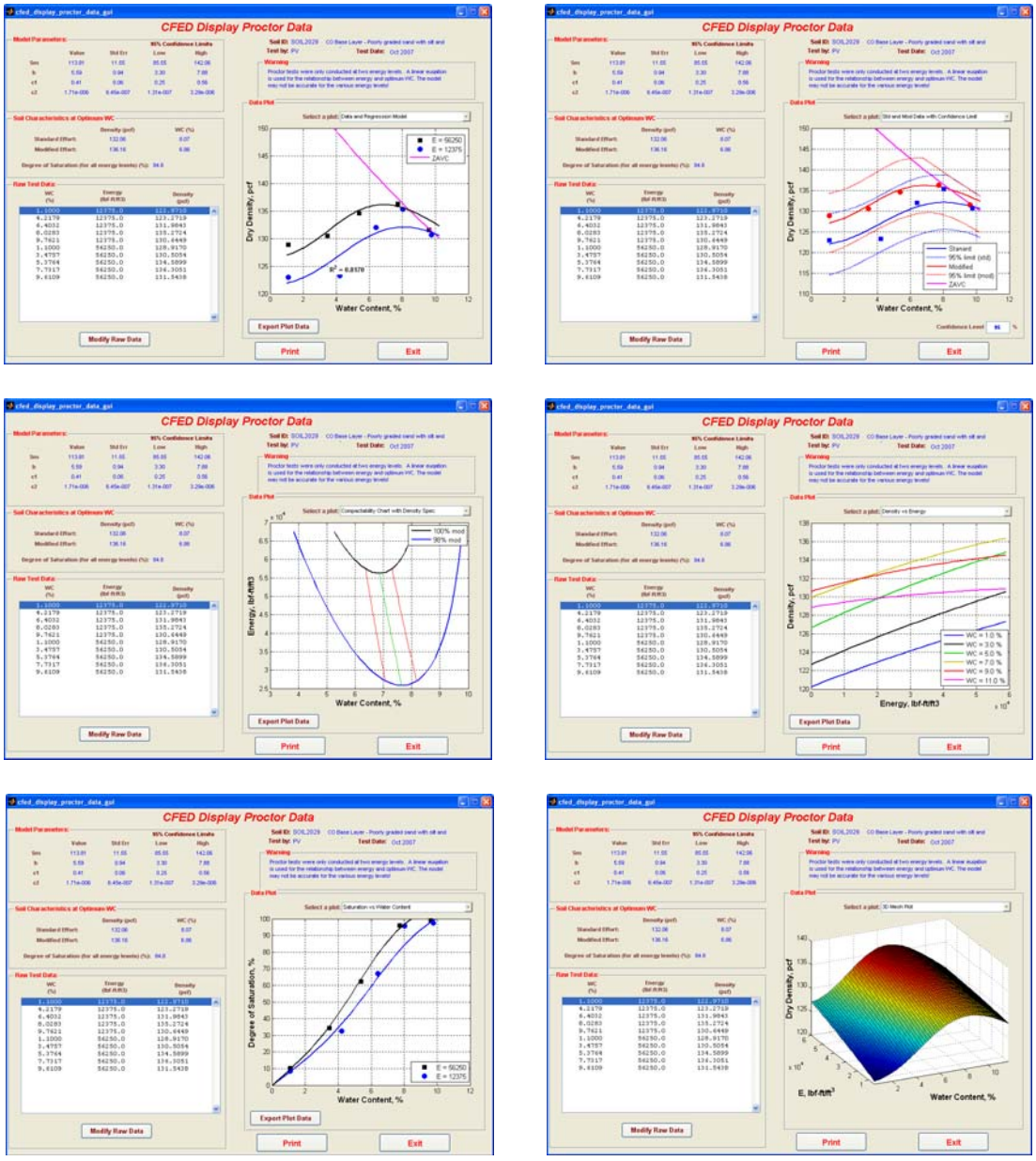


**Figure 246: Soil 2029 CFED outputs**

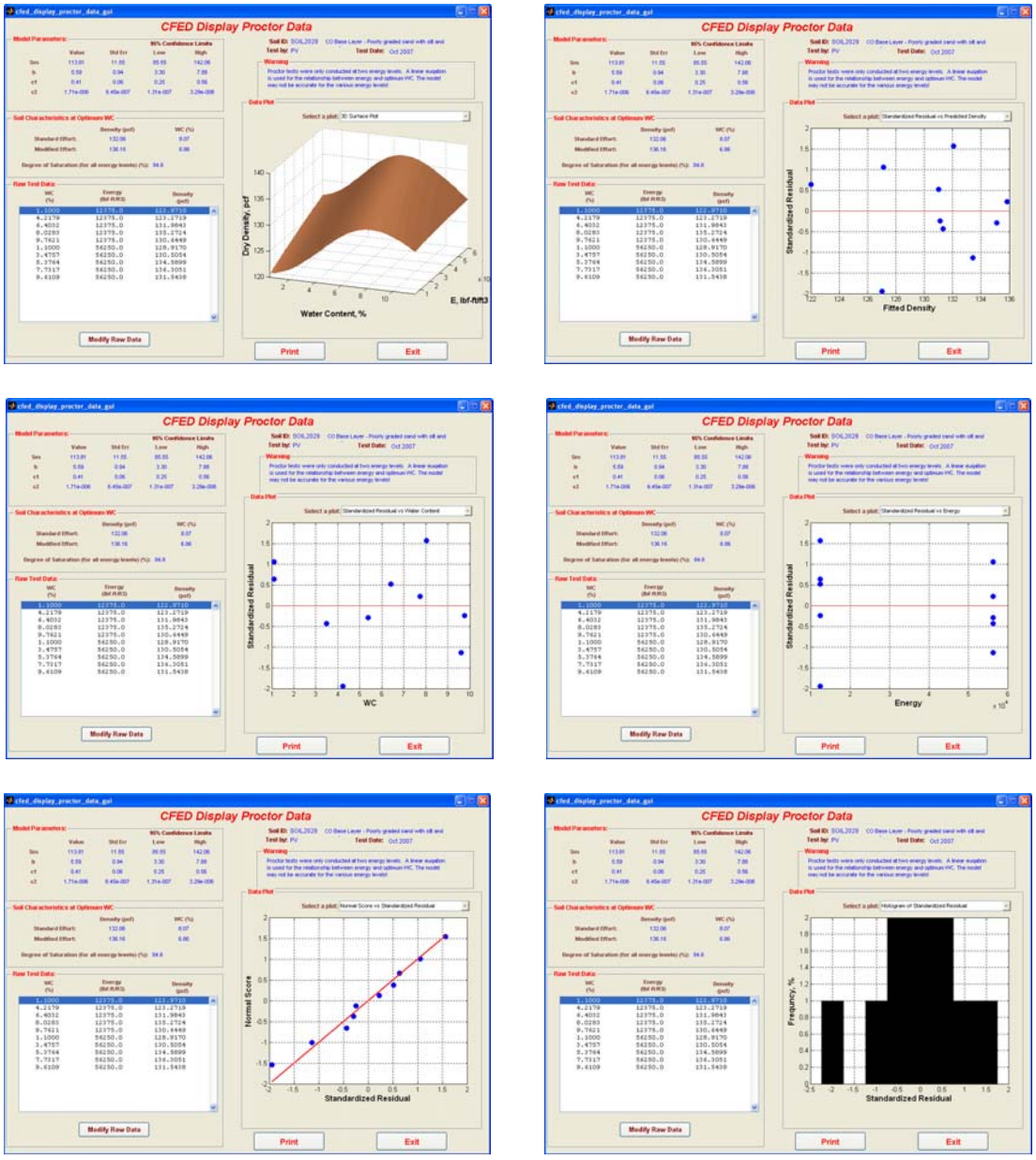


**Figure 246: Continued**

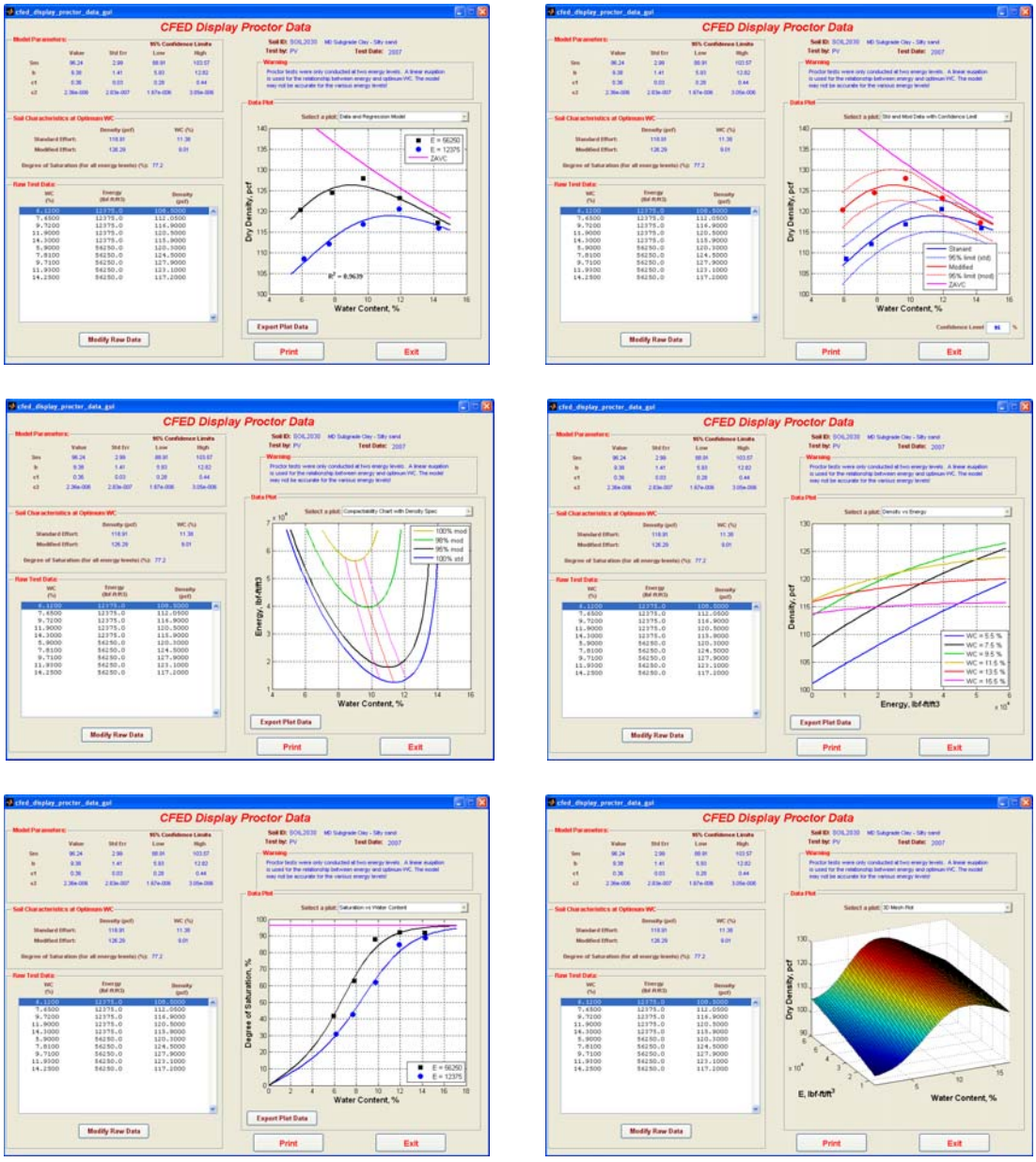


**Figure 247: Soil 2030 CFED outputs**

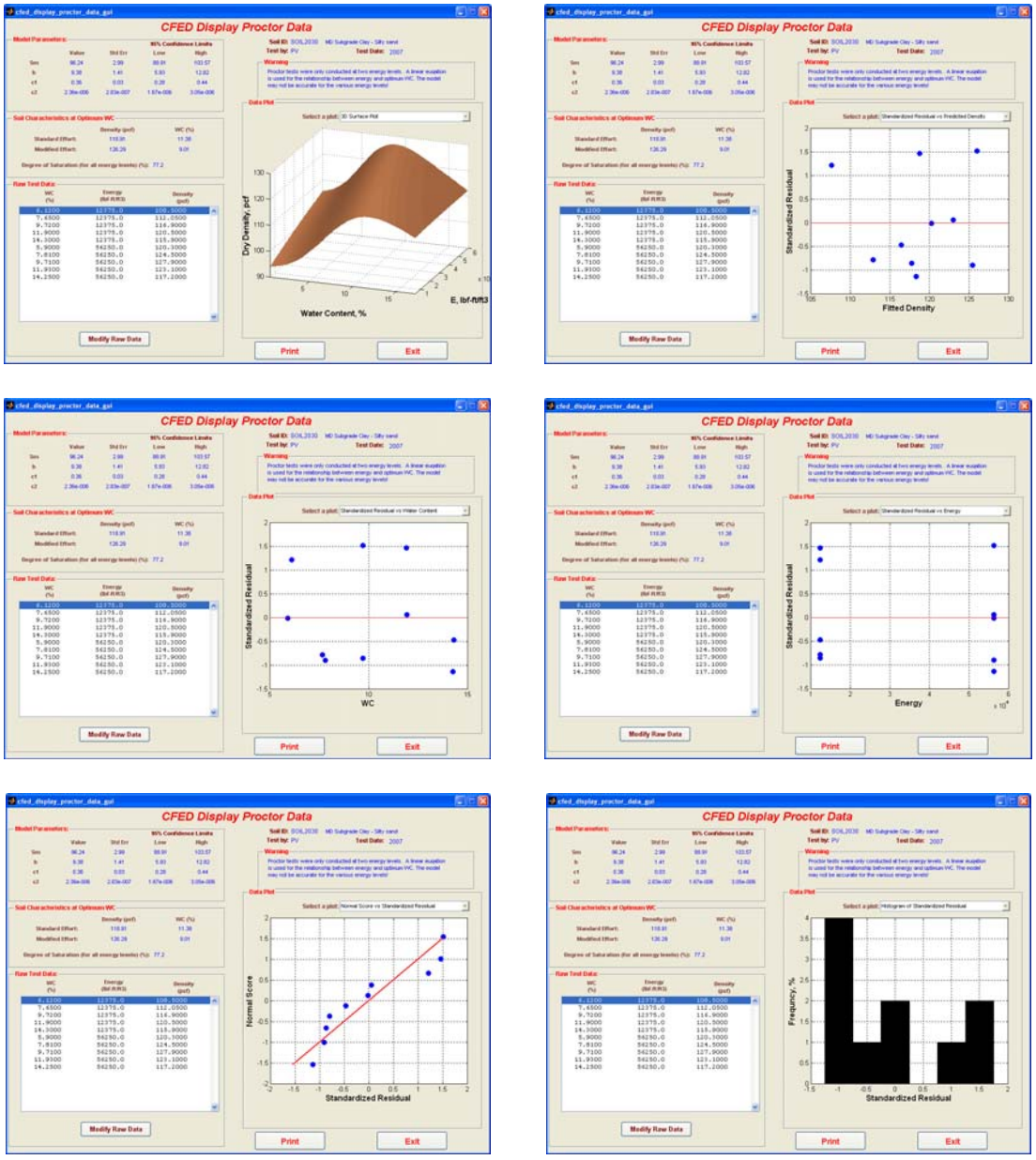


**Figure 247: Continued**

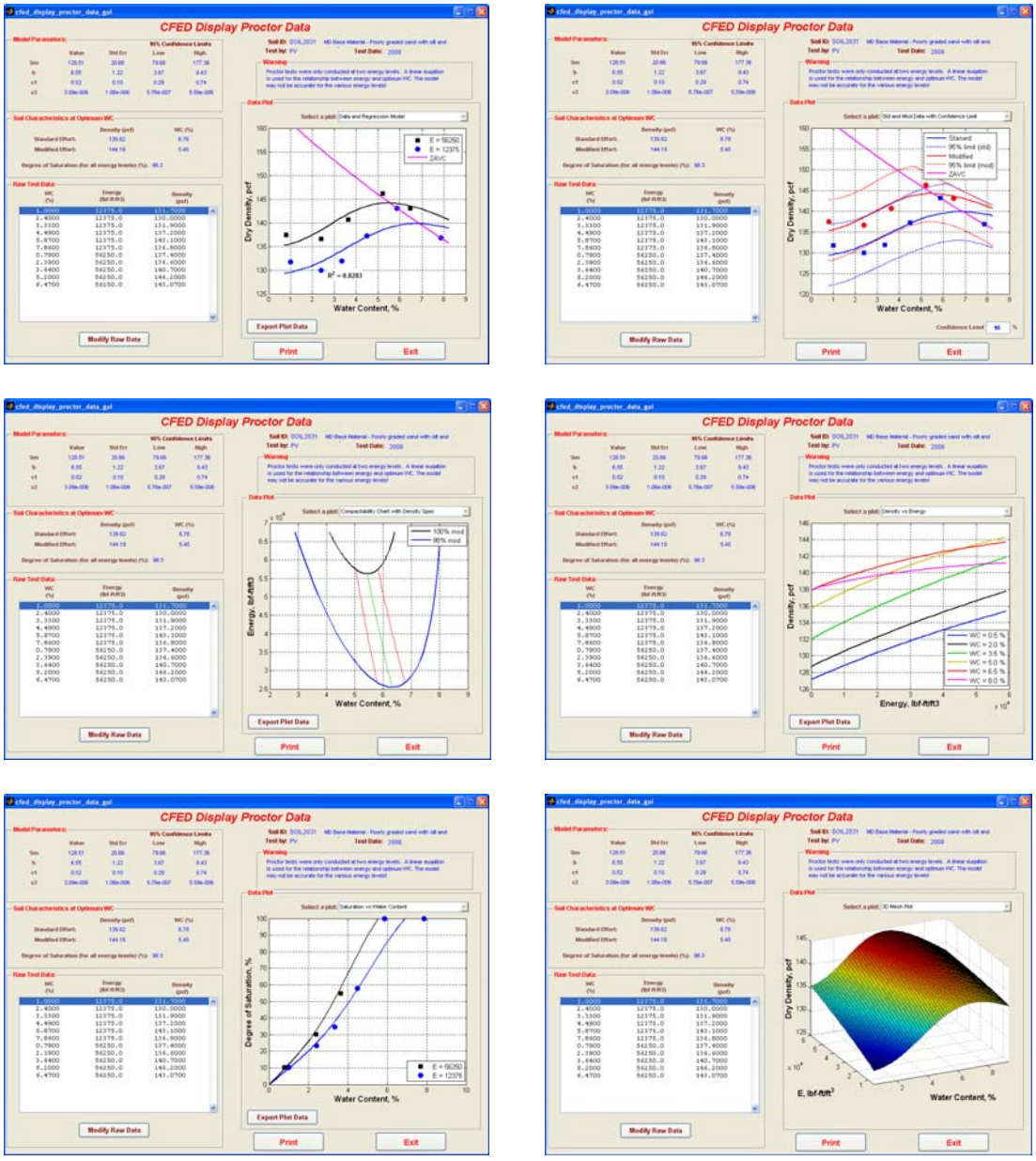


**Figure 248: Soil 2031 CFED outputs**

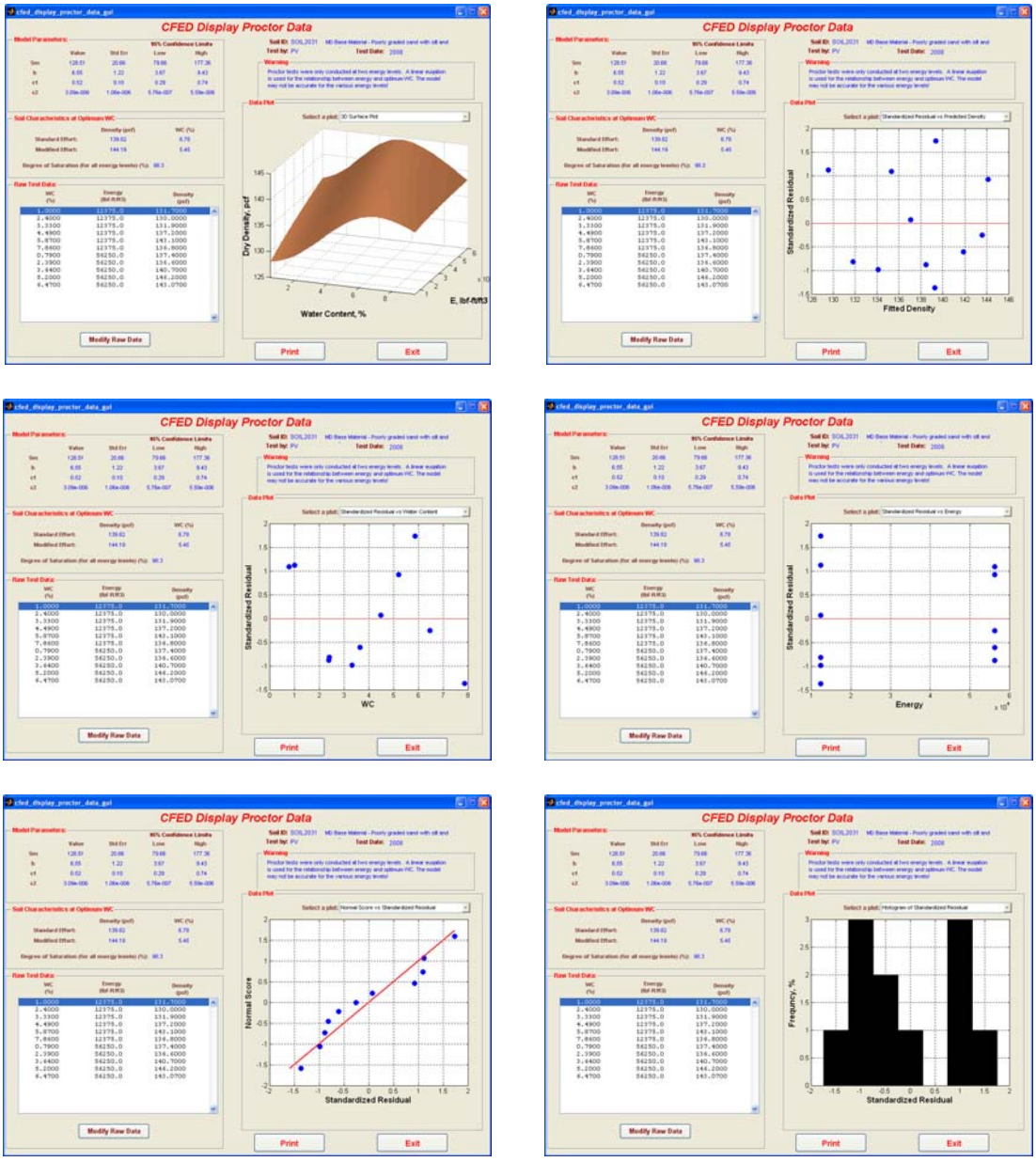


**Figure 248: Continued**

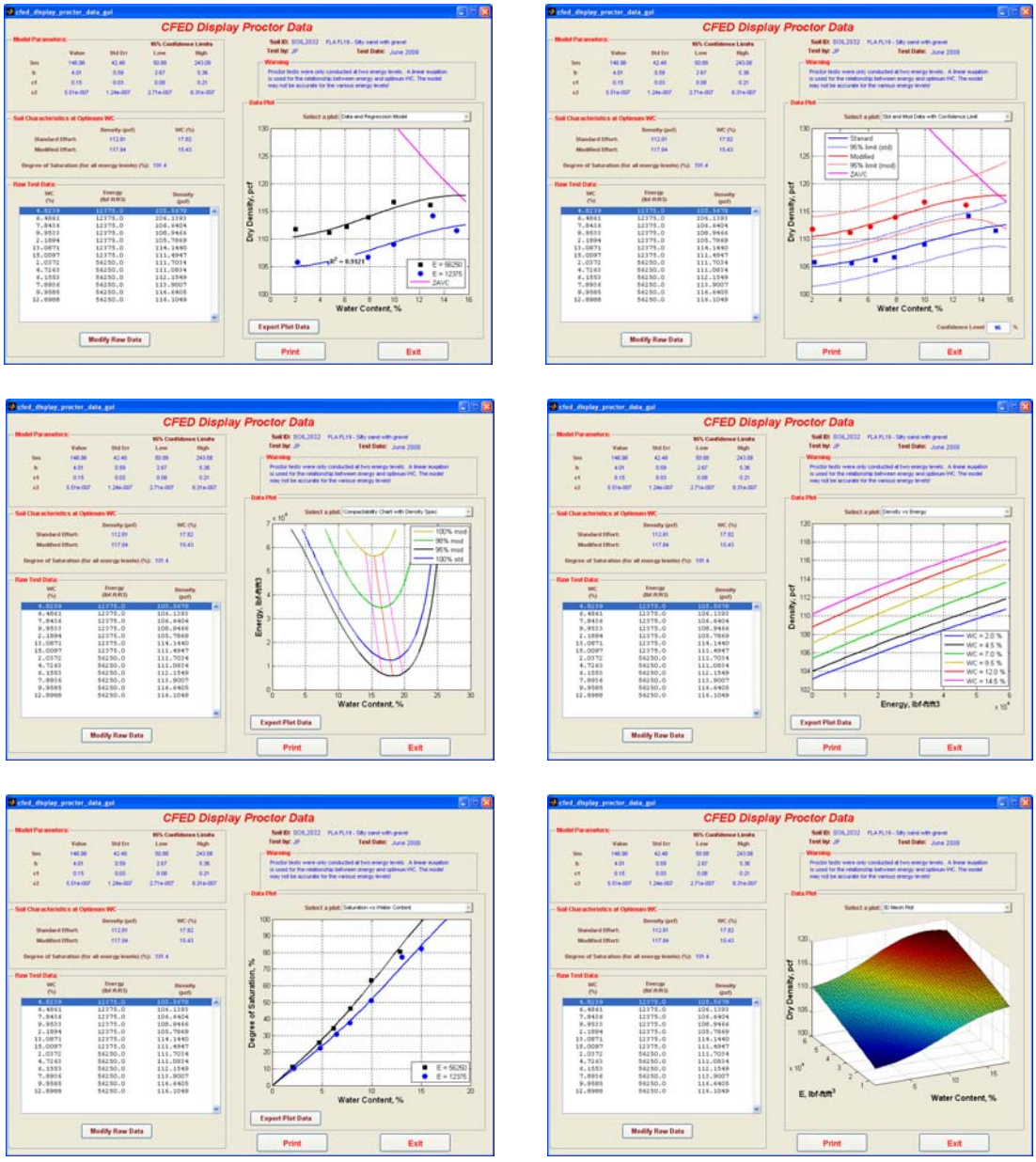


**Figure 249: Soil 2032 CFED outputs**

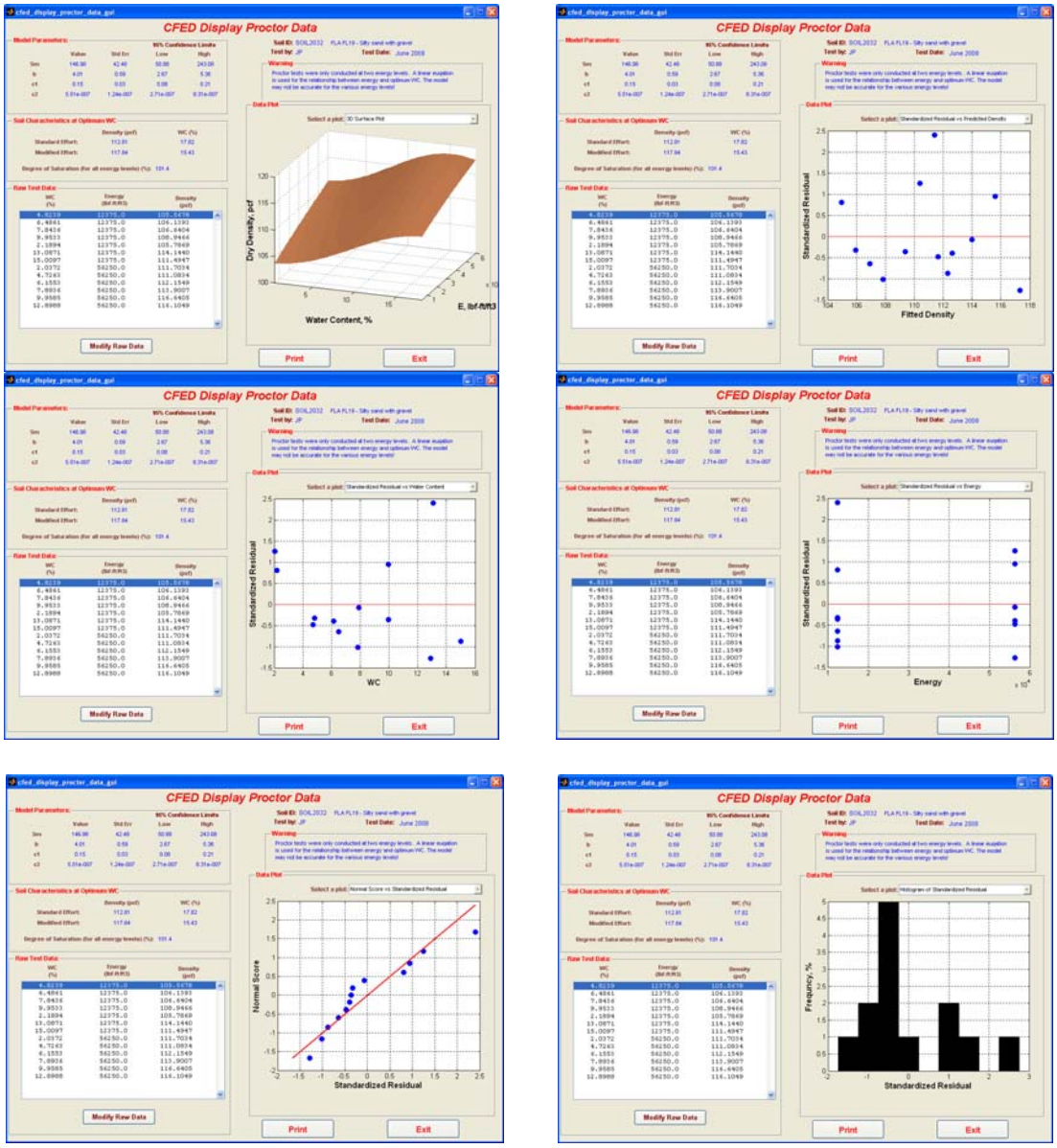


**Figure 249: Continued**

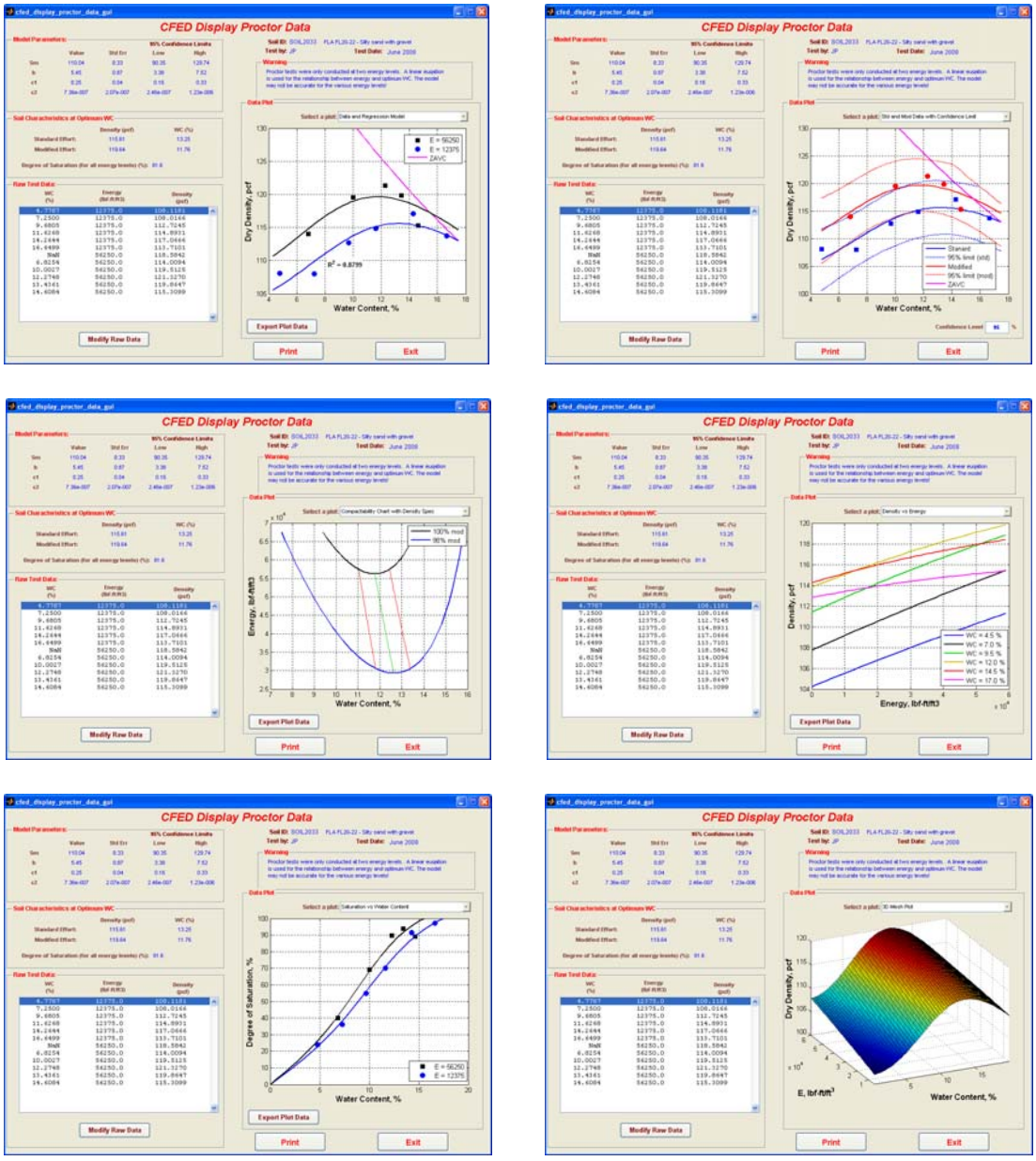


**Figure 250: Soil 2033 CFED outputs**

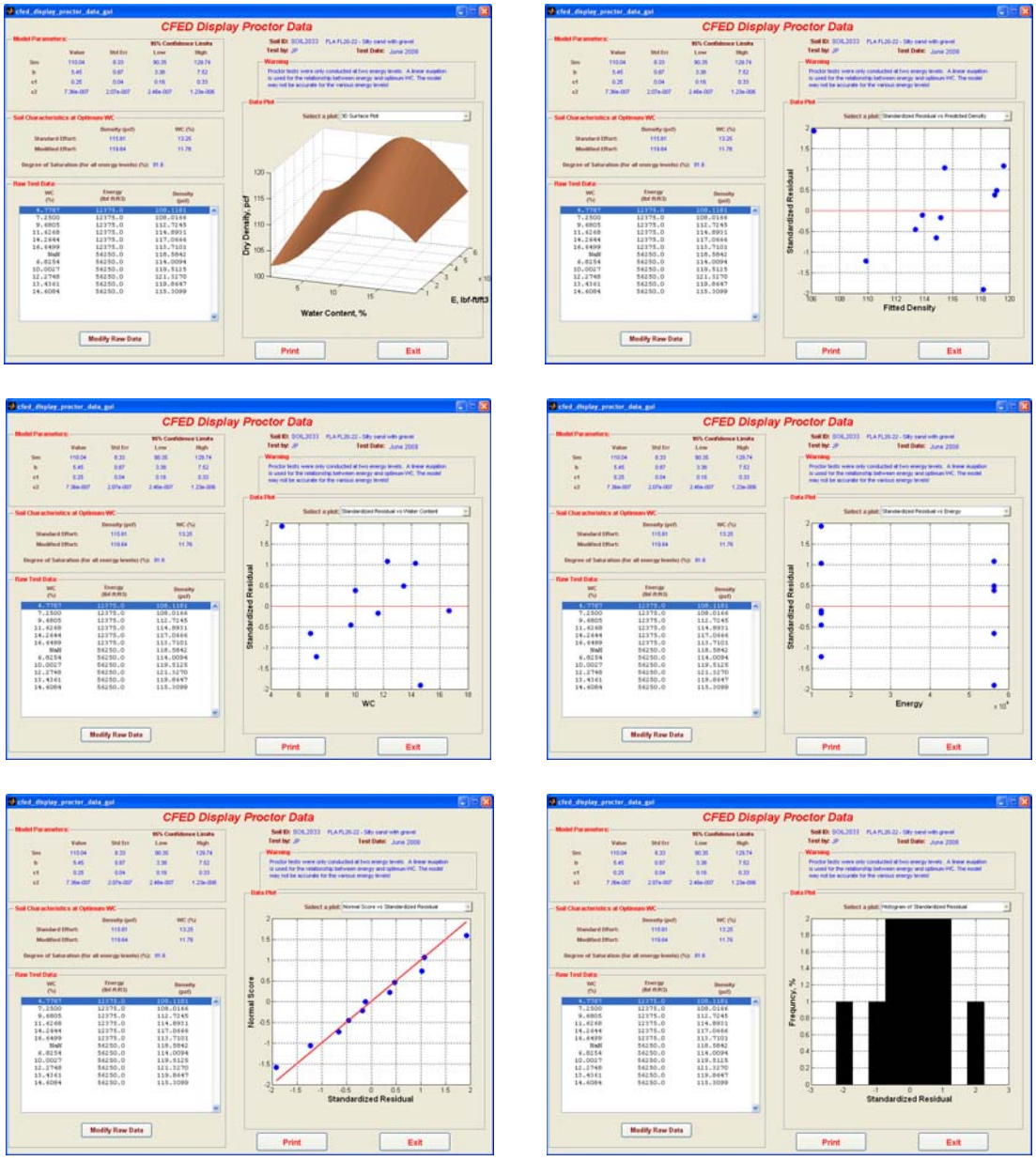


**Figure 250: Continued**

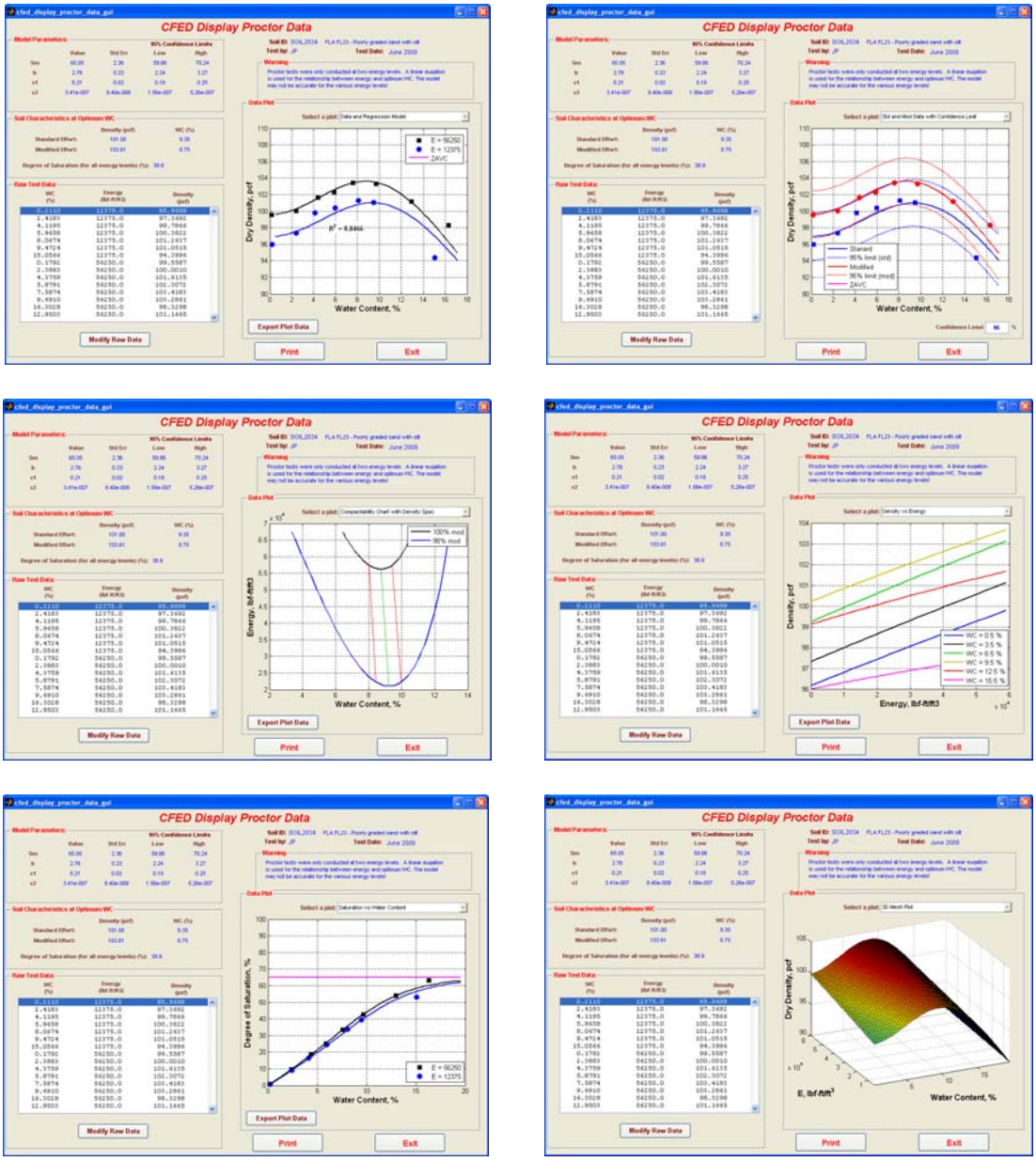


**Figure 251: Soil 2034 CFED outputs**

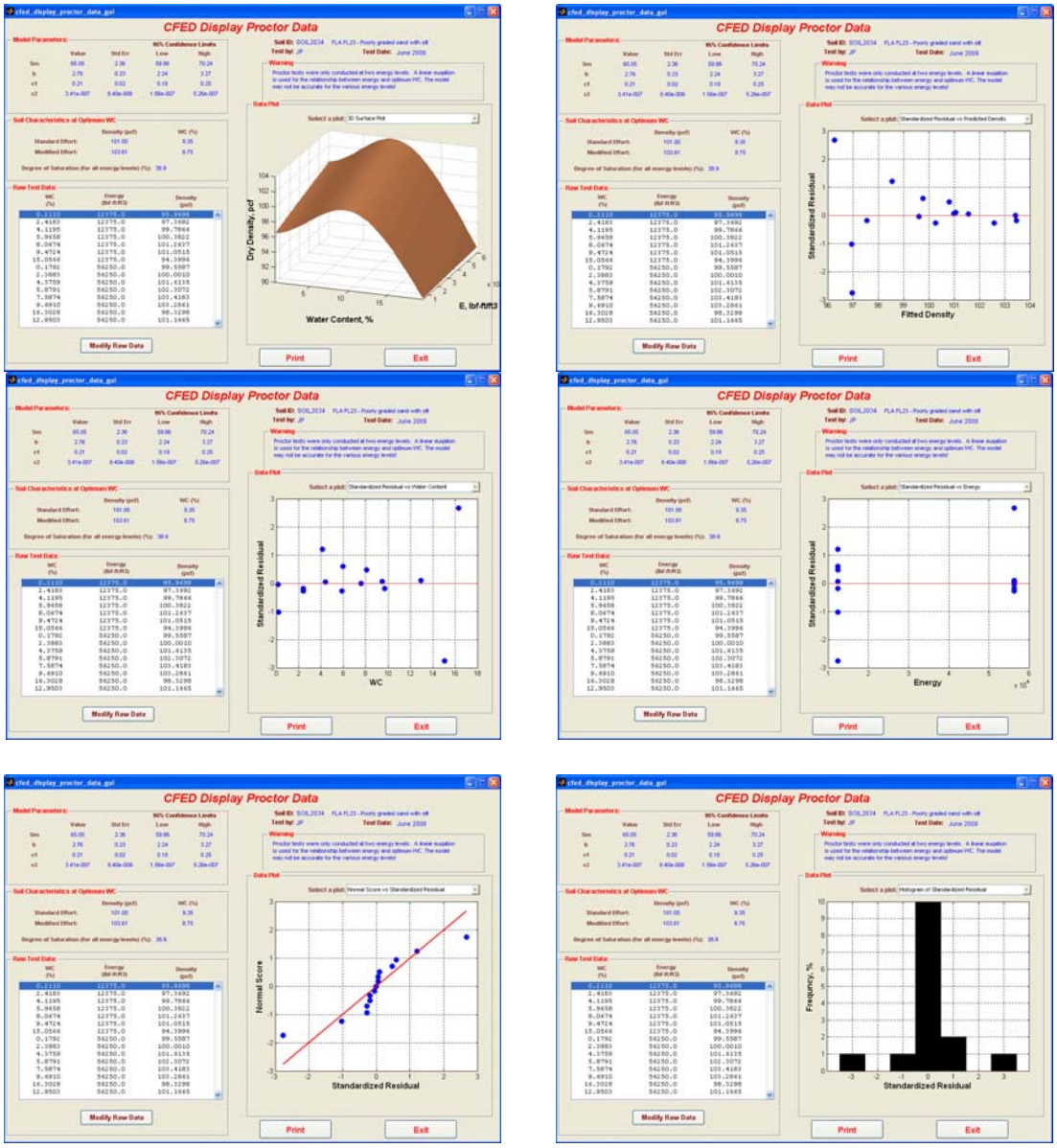


**Figure 251: Continued**

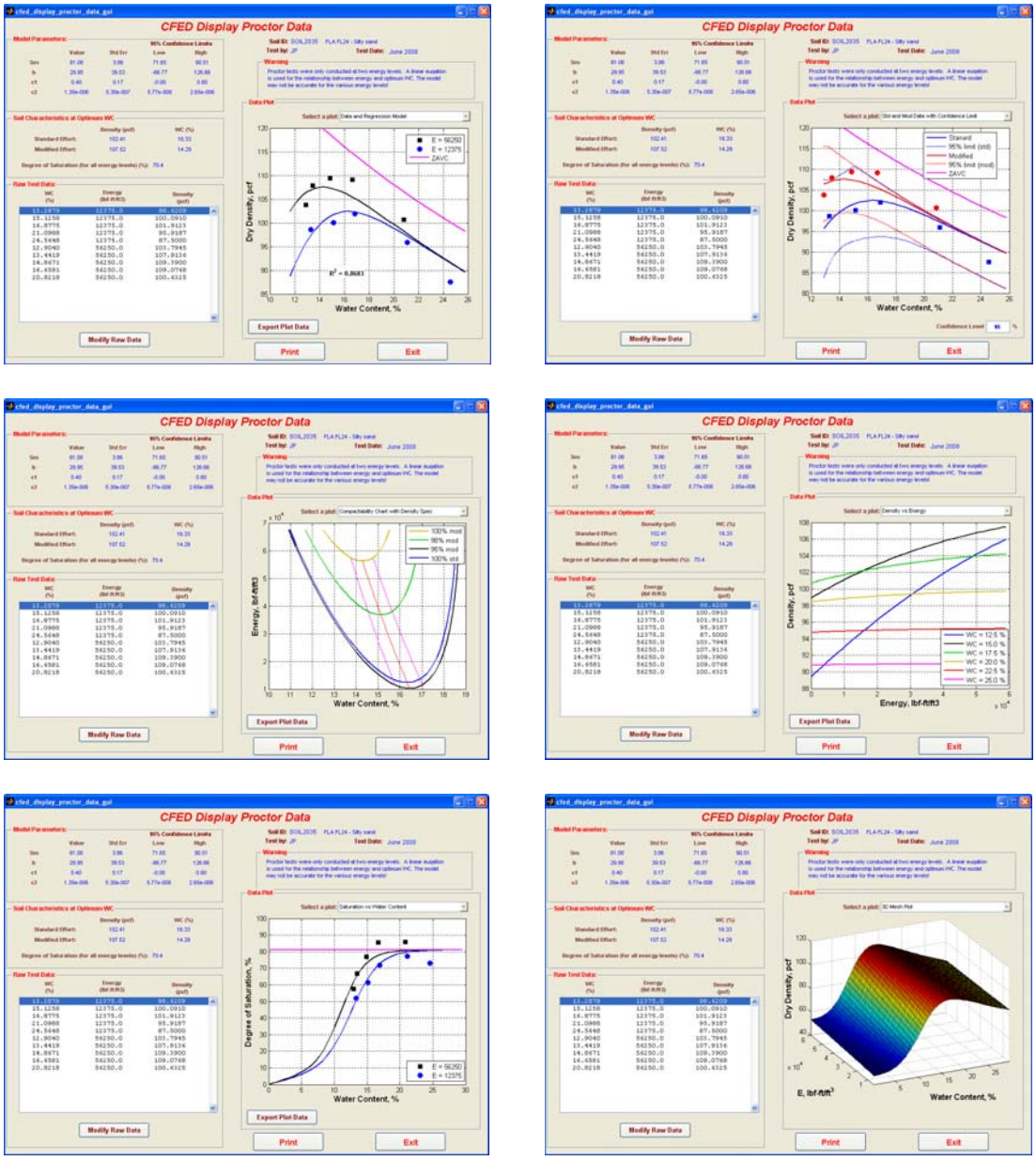


**Figure 252: Soil 2035 CFED outputs**

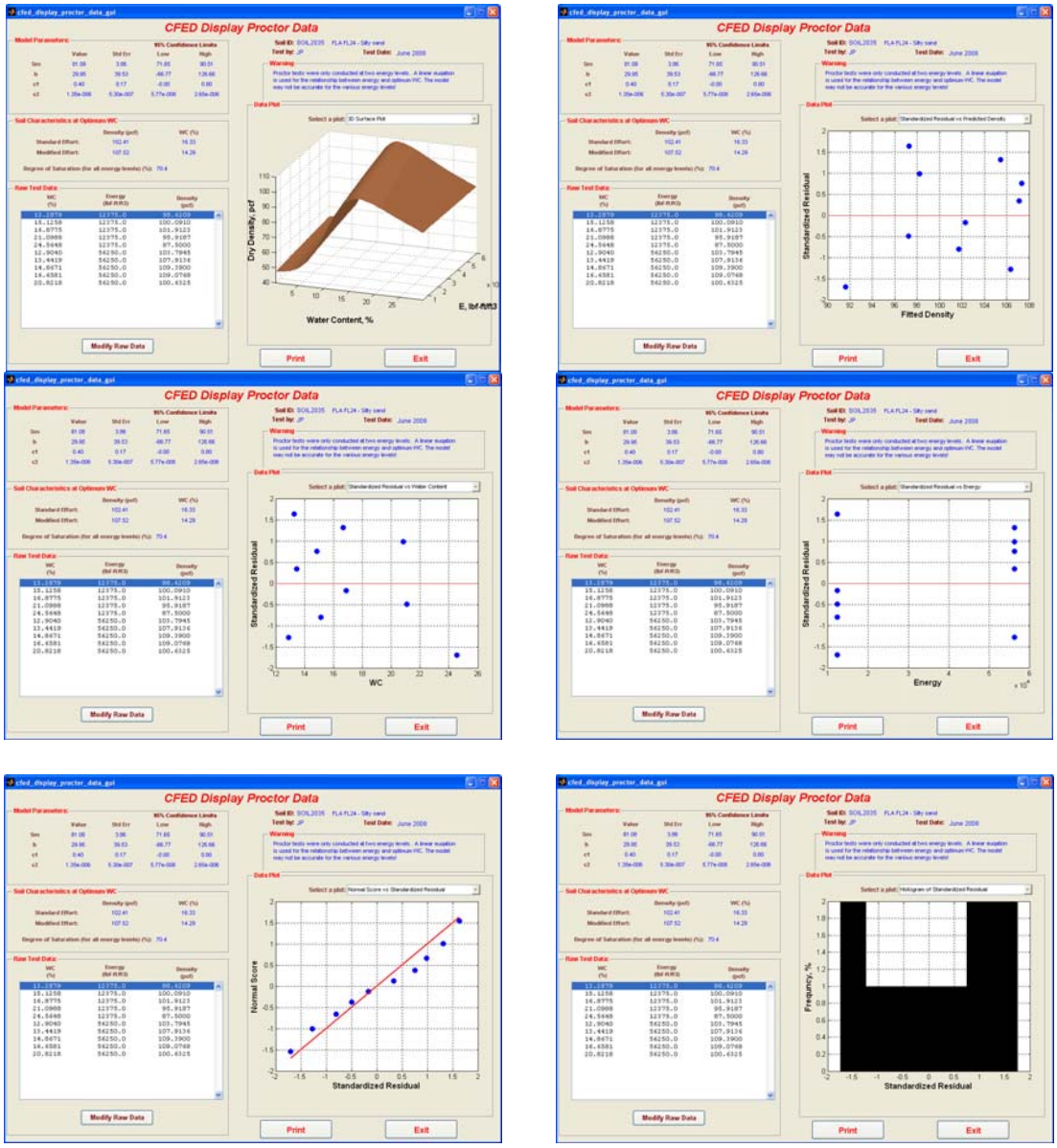


**Figure 252: Continued**

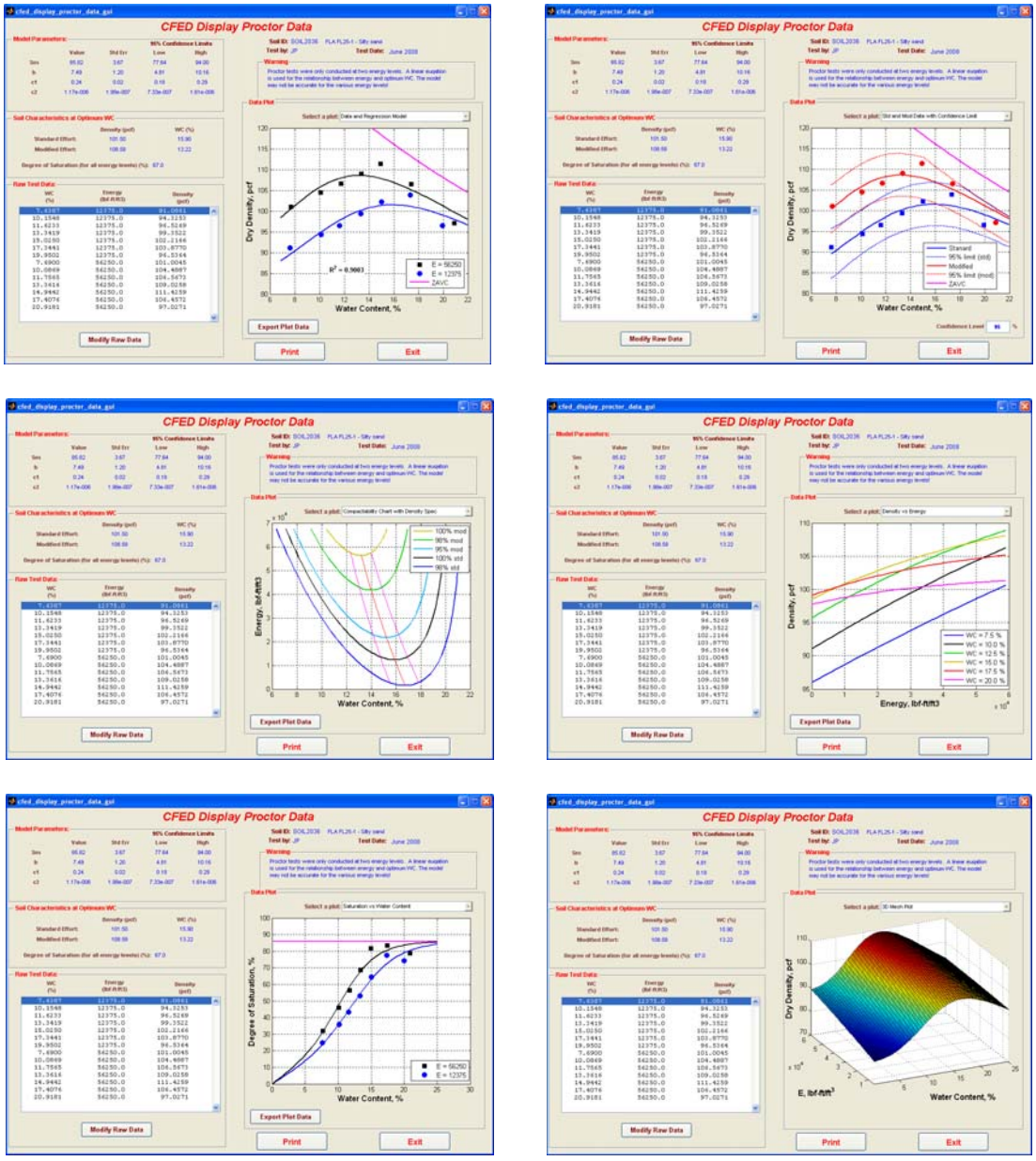


**Figure 253: Soil 2036 CFED outputs**

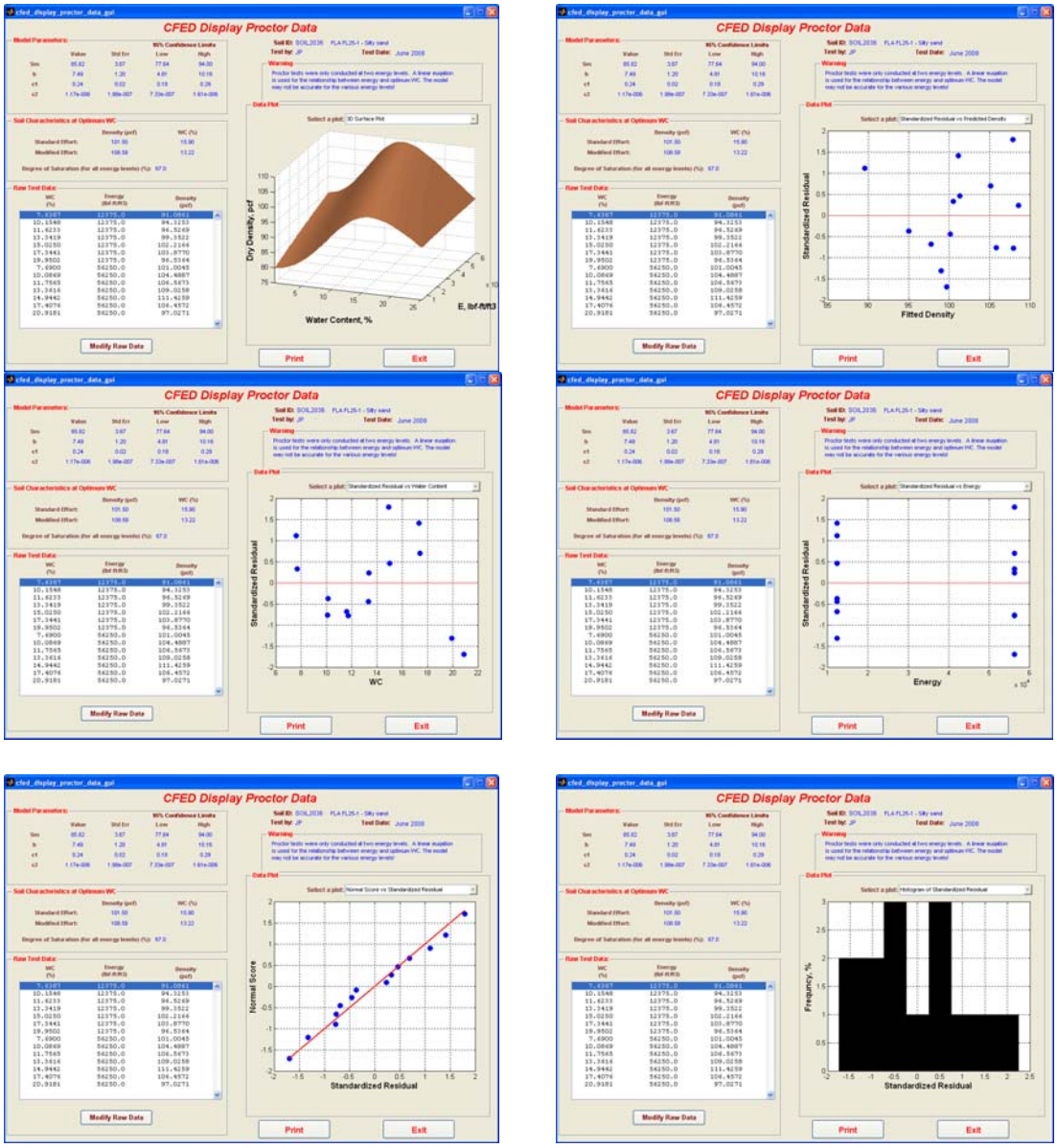


**Figure 253: Continued**

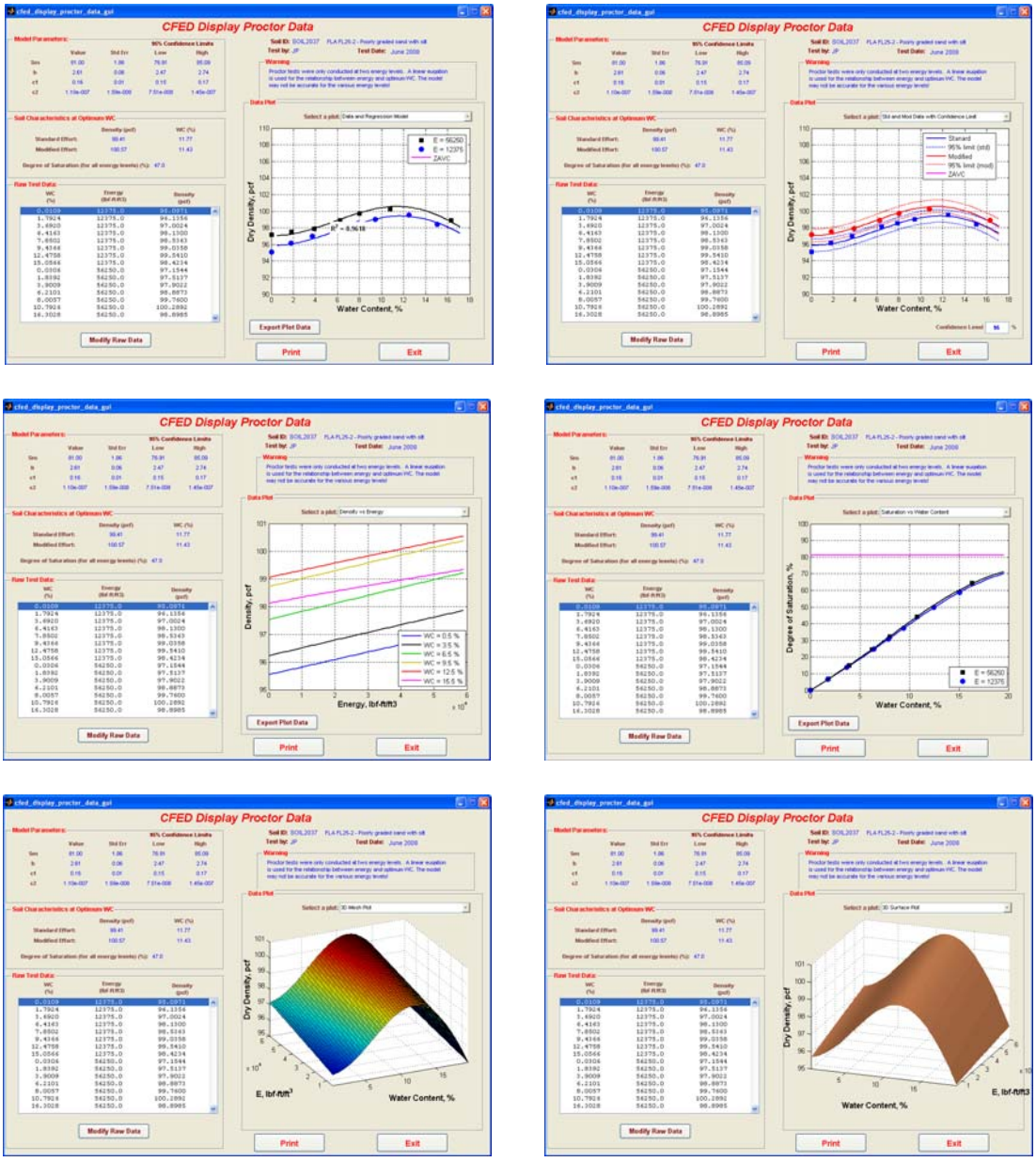


**Figure 254: Soil 2036 CFED outputs**

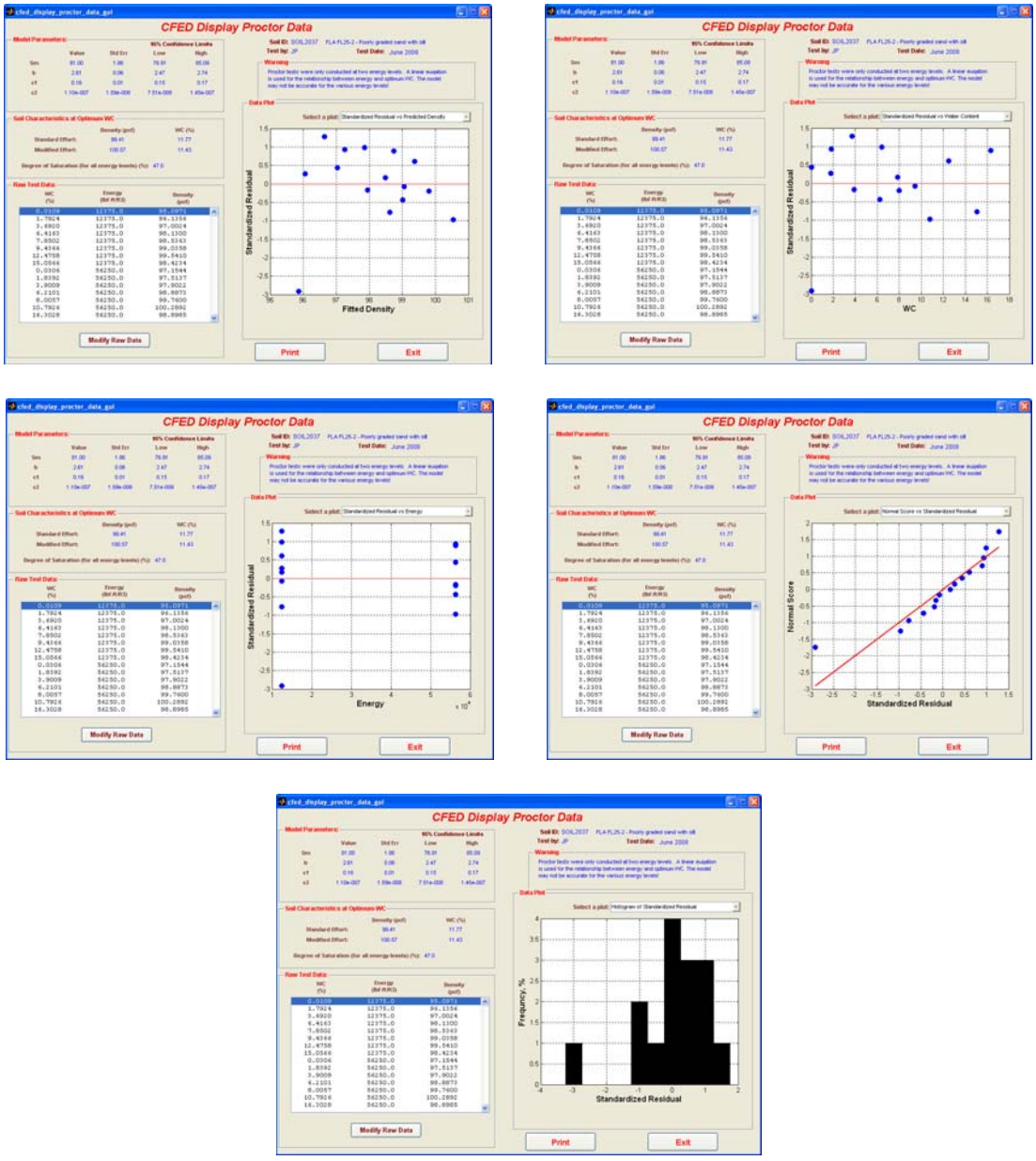


**Figure 254: Continued**

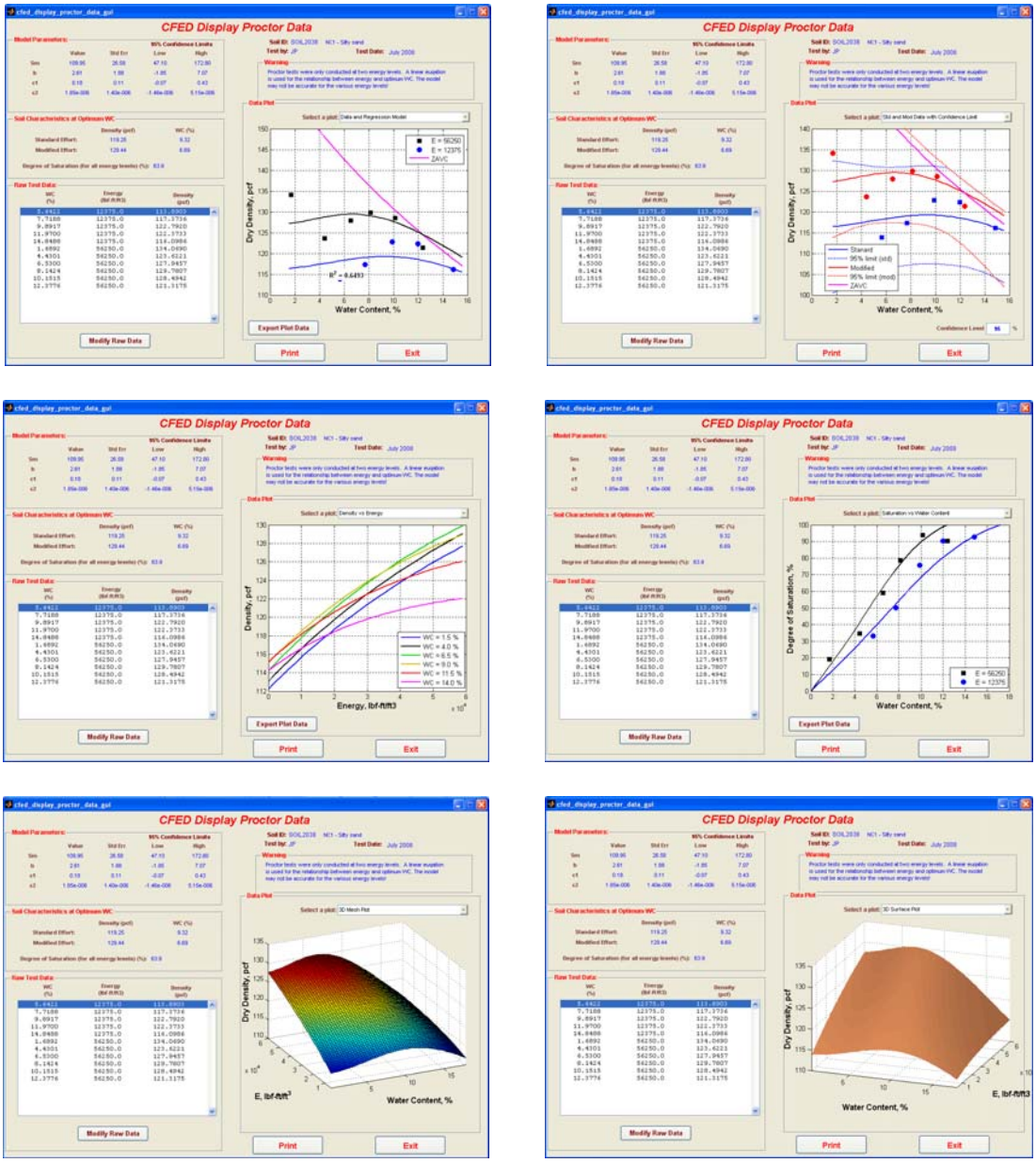


**Figure 255: Soil 2038 CFED outputs**

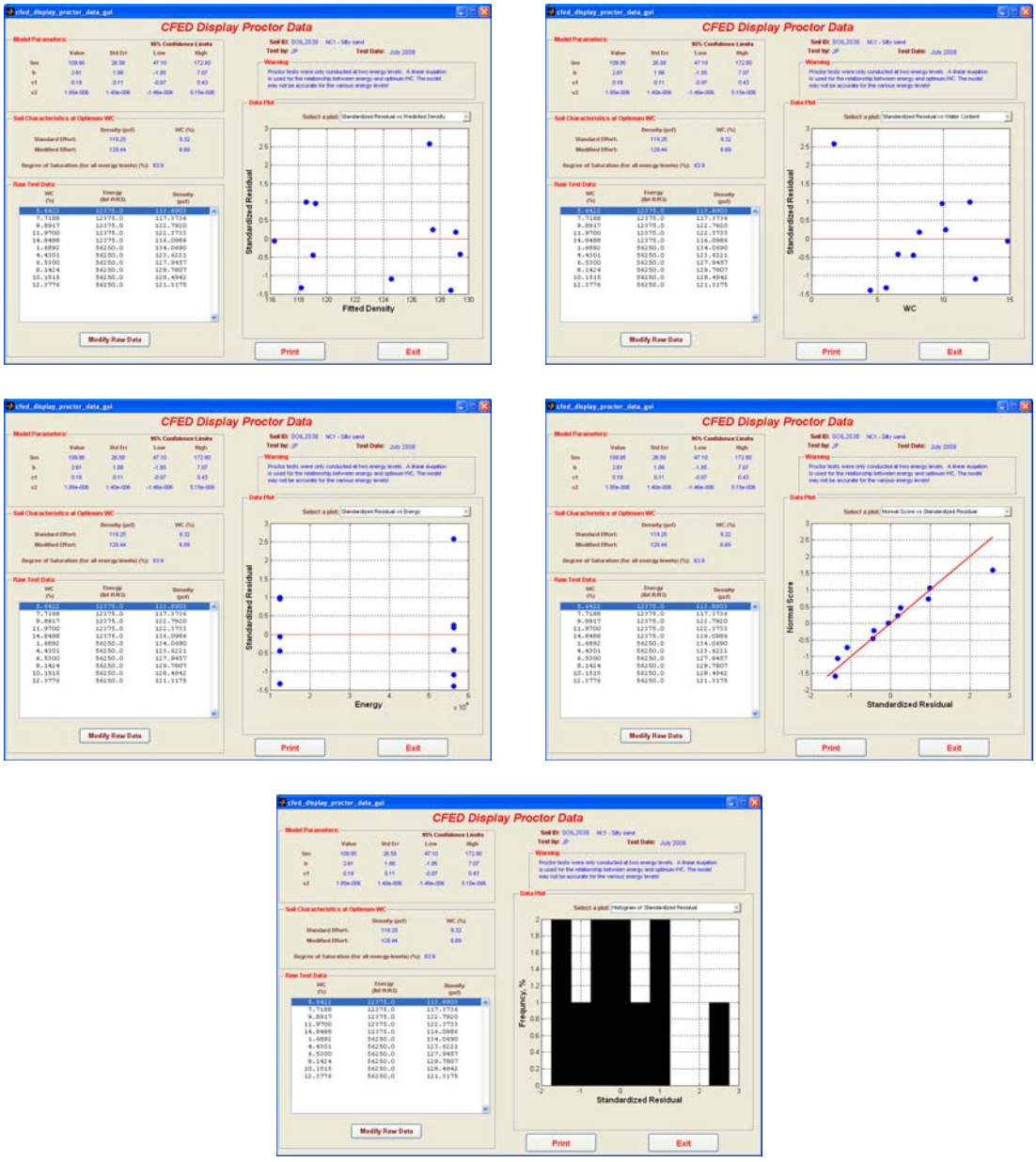


**Figure 255: Continued**

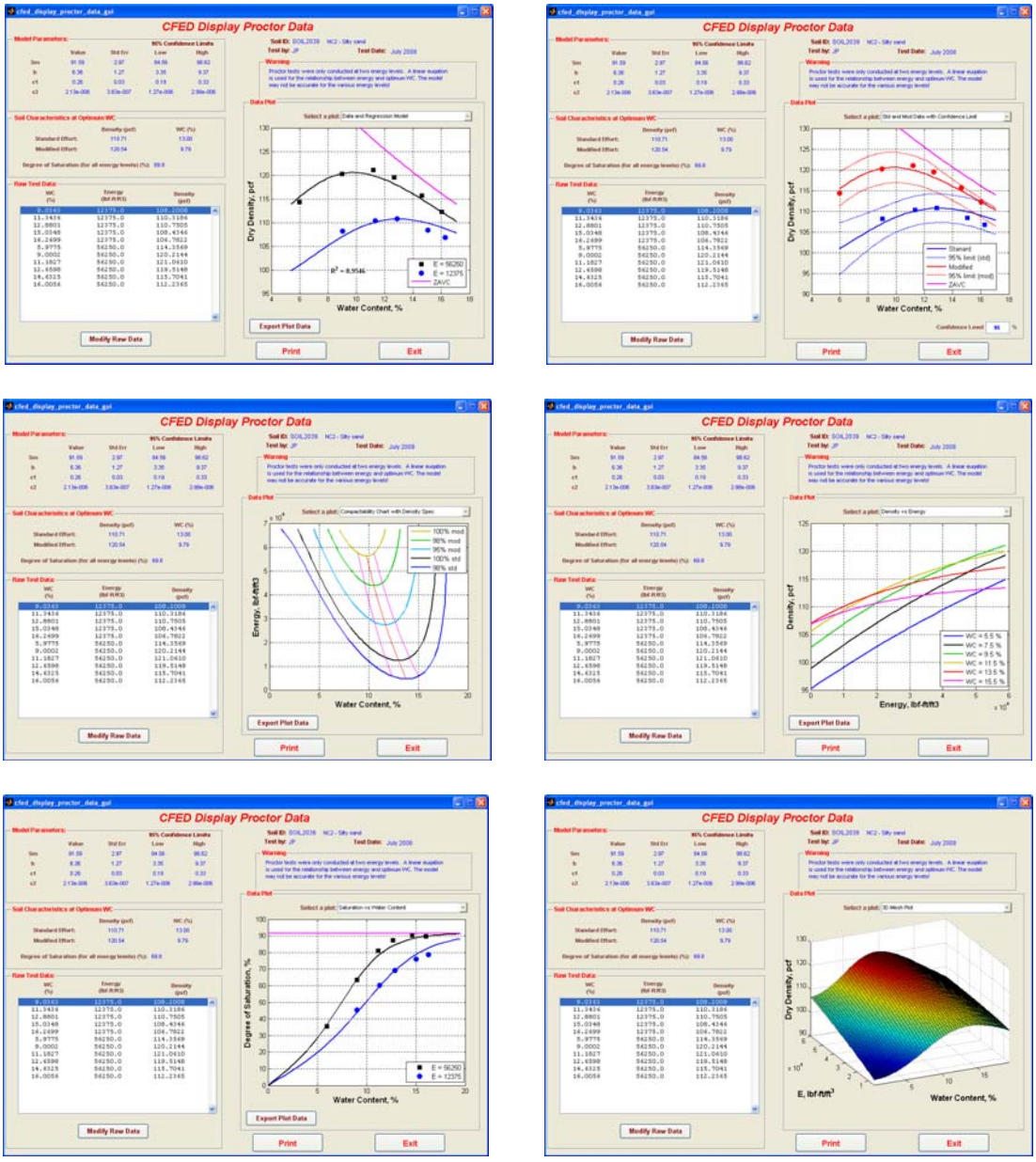


**Figure 256: Soil 2039 CFED outputs**

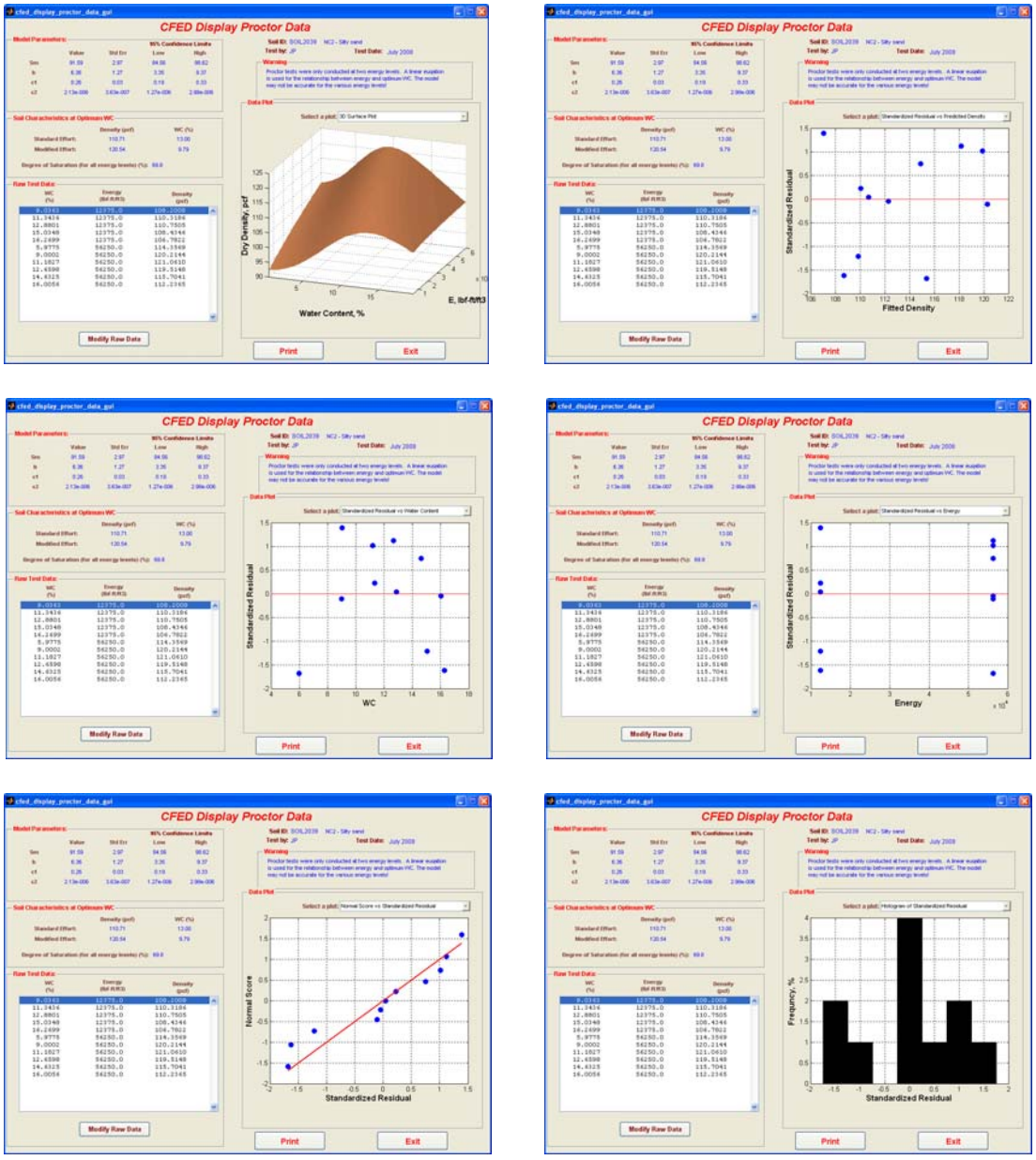


**Figure 256: Continued**

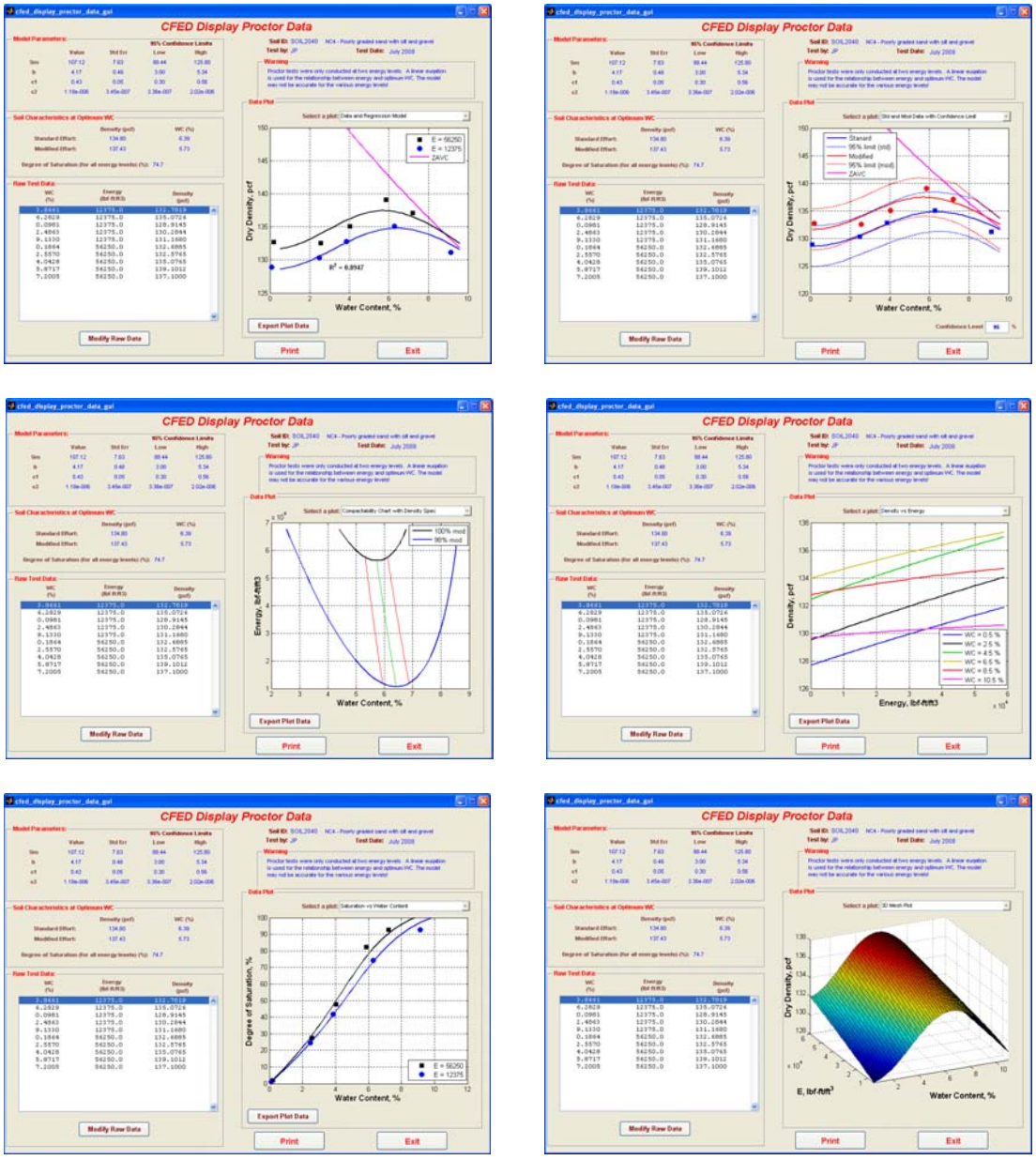


**Figure 257: Soil 2040 CFED outputs**

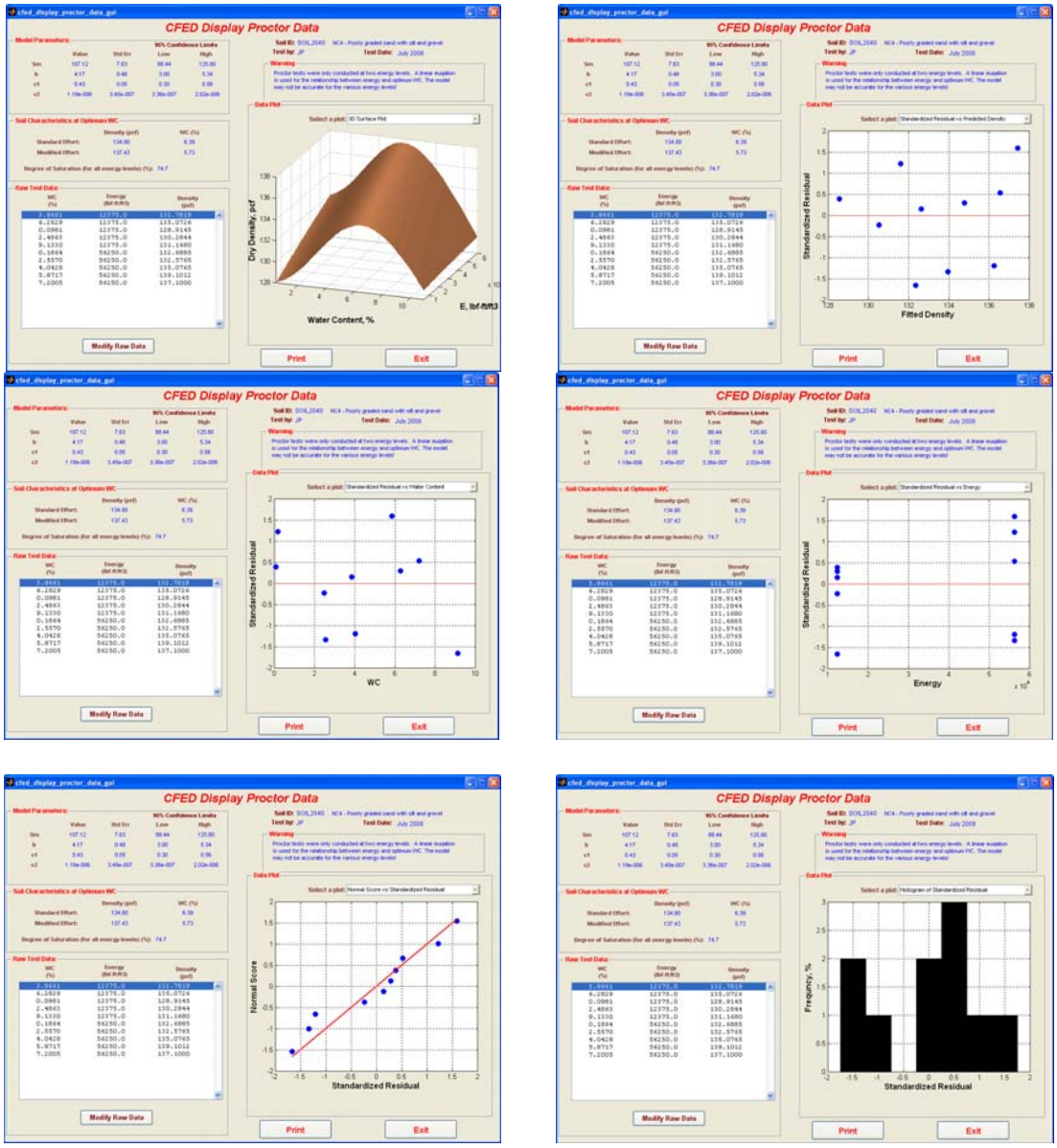


**Figure 257: Continued**

**ACKNOWLEDGMENTS**

There are far too many whom deserve my deepest gratitude to express in so few words. I would like to first thank Caterpillar, Inc. and the geo-construction engineering program for providing funding and resources to complete my research. Other members of the committee, Iowa State faculty and staff, I am grateful to you for all your support, both direct and indirect.

I would like to thank Dr. David White for providing me with the opportunity to work with and learn from his expansive knowledge of geotechnical engineering. He has helped me set the foundation for what I hope will be a long and successful career. I am truly grateful for all the opportunities he has given me and those which I will be given as a result of his mentoring.

Special thanks go to Pavana Vennapusa, Heath Gieselman and all other members of Dr. White's research team, both past and present. This work would have not been possible without the determination, assistance and kindness of several members of the research team. Your tireless hours of work and dedication to the quality of research have inspired me to always strive for the best in myself and in my work.

Finally, my deepest love and gratitude belong to my family and friends who have supported me both professionally and personally. I owe all that I am today to each and every family member and friend who has taken part in shaping the person I have become. Without you, my life would not have been possible.

I would once again like to thank each and every person I have worked with during my time at Iowa State. I appreciate all that each of you have done and I will miss you all dearly. I wish you all the best in everything that you do and I can only hope and pray that our paths will cross again.